

**The relationship between diatoms and climate in a European mountain
lake training set: Implications for detecting the Little Ice Age in lake
sediments from Central Norway**

**Thesis submitted for the degree of
Doctor of Philosophy
in the
University College London
by
Gina Clarke**

**University College London
December 2003**

UMI Number: U602533

All rights reserved

INFORMATION TO ALL USERS

The quality of this reproduction is dependent upon the quality of the copy submitted.

In the unlikely event that the author did not send a complete manuscript and there are missing pages, these will be noted. Also, if material had to be removed, a note will indicate the deletion.



UMI U602533

Published by ProQuest LLC 2014. Copyright in the Dissertation held by the Author.
Microform Edition © ProQuest LLC.

All rights reserved. This work is protected against
unauthorized copying under Title 17, United States Code.



ProQuest LLC
789 East Eisenhower Parkway
P.O. Box 1346
Ann Arbor, MI 48106-1346

Abstract

This study evaluates the use of fresh water diatoms, from lacustrine sediments, to infer past changes in climate. The main aim of the thesis is to reconstruct changes in climate over the past 500 years, including the Little Ice Age event, using lake sediments from Central Southern Norway.

The relationship between surficial high altitude lake sediment diatom species and measured environmental variables is explored in 80 lakes from Central Southern Norway and North West Scotland through the creation of a 'surface sample training set'. 40 of these lakes have ice-cover duration data and diatom assemblages from these are examined to determine their relationship with measured environmental parameters. Multivariate statistical techniques demonstrate that ice-cover duration accounts for a statistically significant proportion of the diatom variance, and an ice-cover transfer function using weighted- averaging- tolerance- down- weighted (WA(tol)) techniques is developed. Unfortunately, large errors are incurred with the resulting model. For this reason diatom assemblages from all 80 lakes are explored in conjunction with the available environmental parameters. Canonical correspondence analysis with forward selection and Monte Carlo permutation tests reveal that three environmental variables independently explain significant proportions of the diatom variance. These variables are January temperature, TOC and pH. A January temperature transfer function is produced using weighted- averaging- partial- least-squares (WA-PLS) techniques and a pH transfer function is produced using WA(tol) methods.

These quantitative inference models are used to help identify changes in climate for two high altitude Norwegian lakes (Gåvålivatnet and Hornsjøen). Few changes occur in the diatom inferred pH reconstructions and few linkages are, therefore, made between pH and climate. The January temperature transfer function was applied and its performance is directly compared with measured values of century- long meteorological records. It appears to perform well at Hornsjøen and infers successfully the recent climatic warming. The reconstruction at Gåvålivatnet does not reflect the extent of recent climatic warming suggesting that the method is not so robust for this site.

Inferences about the changes in the Norwegian climate during the LIA are made using a combination of diatom inferred reconstructed temperatures, lithostratigraphic changes, chrysophyte cyst production and diatom species shifts. Several trends are evident within the proxy records of the lakes which can be linked with the climatic changes associated with the Little Ice Age and recent climatic warming. It is concluded, however, that although changes in the lake biota could be related to climatic fluctuations the signal is complex and multi-faceted. It is proposed that the two lakes respond individually to climatic changes, due to differing lake chemistry and bathymetry, despite being exposed to similar driving macroclimate variables.

Acknowledgements

I would like to thank Dr. Viv Jones and Professor Rick Battarbee for their suggestions, encouragement and motivation throughout the completion of this research. Their help, advice and supervision were invaluable. I would also like to thank my third supervisor Professor John Birks for data and surface-sediment material from Norway, his patience and help with the various numerical difficulties that arose, and his assistance during midnight water sampling expeditions in Norway.

My thanks also goes to Alex Kirika who provided much of the nutrient data for the training set samples and to Øyvind Nordli for providing the temperature series and access to the various Norwegian farmer's diaries for the area near Gåvålivatnet and Hornsjøen.

I would also like to thank the members of the Botanical Institute in Bergen, Norway, for making me feel so welcome throughout my stay as a Marie Curie Fellow. In particular my thanks goes to Anne Bjune, Jorunn Larsen, Wenche Eide, Silvia Peglar, Torbjørg Bjelland and to Jim Clarke for his help with transportation.

I am eternally grateful to my friends at UCL and especially to; Andy Henderson, Sally Luckes, Sam Mendelson, Ben Goldsmith, Carl Sayer, Tom Davidson, Kira Larsen, Patrick Rioual, Sophie Evitt, Helen Bennion, Martin Kernan, Andrew McGovern, Mike Hughes, Gavin Simpson and Ewan Shilland for their help with fieldwork, taxonomic guidance, assistance with numerical analyses, lessons regarding withholding data and continual entertainment whilst counting. I would also like to thank my family for being so supportive of my chosen career path over the last four years.

This research was sponsored by the UCL Graduate School and the fieldwork was part funded by the EU EMERGE mountain lake project.

Table of Contents

Title page	1
Abstract	2
Acknowledgements	3
Table of contents	4
List of tables	9
List of figures	12
List of plates	20
List of appendices	20

Chapter 1

Introduction- The use of palaeolimnology for climatic reconstruction and research rationale	21
1.1 The relationship between air temperature, lake temperature and ice-cover	23
1.2 Stratification patterns, lake mixing and ice-cover in high altitude lakes	24
1.3 The relationship between diatoms and climate	26
1.3.1 The diatoms	26
1.3.2 The direct effects of climate on diatom growth	28
1.3.3 The indirect effects of climate on diatom growth	31
1.3.3.1 Changes in lake ice-cover and its relationship to diatom assemblages	31
1.3.3.2 The relationship between climate, water column mixing and diatom growth	36
1.3.3.3 Changes in lake nutrient dynamics due to climate and the effect this has on diatom growth	37
1.4 The detection of climatic change using palaeolimnology	41
1.4.1 Using the fossil diatom record to detect climate change	42
1.4.1.1 Diatom frustule preservation and habitat representation within the sediment record	42
1.4.1.2 Qualitative inferences	43
1.4.1.3 Quantitative inferences	49
1.4.2 The use of lithostratigraphic analyses to detect changes in climate	54
1.5 Climatic changes in Europe over the last 800 years	56
1.5.1 Climatic changes in Norway over the last 800 years	57
1.6 Research rationale, study aims and thesis structure	61

Chapter 2

Site selection and description	63
2.1 Introduction	63
2.2 Training set site selection rationale	63
2.2.1 Scotland ('EMERGE' sites)	64
2.2.2 Norway 1	67
2.2.3 Norway 2 ('EMERGE' sites)	68
2.2.4 The 80 lake set	73
2.3 Lakes selected for sediment coring	75
2.3.1 The six cored lakes	76
2.3.2 Rasletjernet, Code 98-20	77

2.3.3	Leirvatn, Code 98-6	79
2.3.4	Davialec, Code 98-9	81
2.3.5	Hornsvatnet, Code 98-2	83
2.3.6	Gåvålivatnet, Code 01-03	85
2.3.7	Hornsjøen, Code 98-18	88
2.3.8	The selection of cores for further palaeolimnological analyses	90
2.4	Conclusion	91

Chapter 3

Methods	92
3.1	Field methods
3.1.1	Surface sediment retrieval, sediment core sampling and water sample collection
3.1.2	Ice-cover measurements- surface water thermistor installation
3.2	Laboratory methods
3.2.1	Environmental data and water sample analyses
3.2.1.1	Problems with nutrient analyses: detection limits and inter comparisons
3.2.2	Ice-cover modelling
3.2.2.1	The accuracy of the ice-cover estimates from the empirical model
3.2.3	Selection of the transfer function training sets
3.2.4	Diatom preparation and counting
3.2.5	Diatom taxonomy and classification/nomenclature
3.2.6	Down core diatom analysis
3.2.7	% Loss on Ignition and % Dry Weight analyses
3.2.8	Core chronologies
3.3	Numerical methods
3.3.1	Transformation of data prior to analyses
3.3.2	Gradient analysis- Ordination and constrained ordination
3.3.2.1	PCA- Principal components analysis
3.3.2.2	Correspondence Analysis (CA), Detrended Correspondence Analysis (DCA)
3.3.2.3	RDA - Redundancy analysis
3.3.2.4	CCA - Canonical Correspondence analysis
3.3.2.5	Species response models
3.3.3	Inference models
3.3.4	Down core reconstruction of environmental variables
3.3.5	Analogue matching techniques
3.3.6	Down core ordination and zonation
3.3.7	Summary of numerical methods
3.4	The use of older surface sediment in data set 'Norway 1'
3.5	Instrumental records of climate for Gåvålivatnet and Hornsjøen
3.6	Conclusion

Chapter 4

Analysis of the 40 lake modern sample training set	140
4.1 Results	141
4.1.1 Environmental data	141
4.1.1.1 Summary environmental statistics	142
4.1.1.2 Relationships between environmental variables	153
4.2 Biological data analysis	159
4.2.1 Exploration of the dominant and most abundant taxa	159
4.2.2 Indirect ordination analysis of the surface sediment diatom assemblages	163
4.3 The relationship between the environmental and species data	167
4.3.1 Indirect gradient analysis	167
4.3.2 Identification of the most important environmental variables	169
4.4 The relationship between diatoms and ice-cover duration	177
4.4.1 Individual species responses to ice-cover duration in relation to other environmental variables	178
4.4.2 The relationship between planktonic diatoms and ice-cover duration	180
4.4.3 The relationship between ice-cover duration and non planktonic diatom species	184
4.4.4 The identification of ice-cover indicator species	203
4.4.5 The feasibility of creating an ice-cover transfer function for down core climate reconstruction	207
4.5 Discussion	213
4.6 The main environmental variables determining the diatom variance within the data set	213
4.6.1 The Ca ²⁺ / pH/ Alkalinity gradient	213
4.6.2 The TOC gradient	214
4.6.3 The Na ⁺ gradient	215
4.7 Conclusion	217

Chapter 5

Analysis of the 80 lake modern sample training set	219
5.1 Environmental data	219
5.1.1 Summary environmental statistics	221
5.1.2 Identification of outliers and the transformation of environmental variables	231
5.1.3 Relationship between environmental variables	233
5.2 Biological data analysis	237
5.2.1 Exploration of the common and most abundant taxa	237
5.2.2 Indirect ordination analysis of the surface sediment diatom assemblages	241
5.3 The relationship between the environmental and species data	246
5.3.1 Indirect gradient analysis	246
5.3.2 The identification of the most important environmental variables	250
5.4 The development of an appropriate transfer function for climate interpretation	255
5.4.1 The feasibility of creating a pH transfer function	257
5.4.1.1 Variance partitioning of the main explanatory variables	257
5.4.1.2 Constrained RDA using only pH as the explanatory variable	260
5.4.2 The pH transfer function	260

5.4.2.1	A comparison of pH inference models	263
5.4.2.2	Individual species responses to pH	264
5.4.3	The feasibility of creating a January air temperature transfer function	270
5.4.3.1	The January air temperature transfer function and comparison with other air temperature transfer functions	270
5.4.3.2	The individual response of species to January air temperature	273
5.5	Conclusion	276

Chapter 6

Palaeolimnological analysis of Lake Hornsjøen (core 98-18)		278
6.1	Results	278
6.1.1	Water chemistry and site details	278
6.1.2	Lithostratigraphy	278
6.1.3	Dating	280
6.1.4	Diatom analysis	281
6.1.5	The reconstruction of environmental variables	286
6.1.5.1	pH reconstruction	288
6.1.5.2	TP reconstruction	289
6.1.5.3	Diatom inferred ice-cover and diatom inferred January temperature reconstructions	290
6.2	Discussion	295
6.2.1	Summary results and synthesis	295
6.2.2	Diatom zone three, covering the period from <i>ca.</i> 1740 (27.5 cm) to <i>ca.</i> 1622 (18.5 cm)	298
6.2.3	Diatom zone two, covering the period from <i>ca.</i> 1910 (7cm) to <i>ca.</i> 1740 (18.5cm)	301
6.2.4	Diatom zone one, covering the period from <i>ca.</i> 1910 (7cm) to 2001 (surface sediments)	303
6.3	How faithfully are known climatic changes occurring over the last 500 years recorded by the palaeolimnological record at Lake Hornsjøen	305
6.3.1	The detection of recent climatic change using the palaeolimnological record at Lake Hornsjøen	305
6.3.1.1	Does the January temperature transfer function reflect the increase in temperature occurring over the period of the instrumental record?	306
6.3.1.2	Do changes in species abundance reflect recent climate warming?	309
6.3.1.3	Do changes in habitat availability reflect recent climatic change?	310
6.3.1.4.	Do changes in lake productivity indicate recent climate warming?	311
6.3.1.5	Summary of evidence reflecting recent climate warming	312
6.3.2	The detection of climatic changes associated with the LIA at Lake Hornsjøen	313
6.3.2.1	Does the January temperature transfer function record LIA cooling?	313
6.3.2.2	Changes in diatom species related to the LIA	313
6.3.2.3	The detection of the LIA using lake habitat availability shifts	315
6.3.2.4	Detecting the LIA using patterns of lake/ catchment productivity	316
6.3.3	Dating caveat	316
6.4	Summary and conclusions	317

Chapter 7

Palaeolimnological analysis of Lake Gåvålivatnet (core 01-03)	319
7.1 Results	319
7.1.1 Water chemistry and site details	319
7.1.2 Lithostratigraphy	320
7.1.3 Dating	320
7.1.4 Diatom analysis	322
7.1.5 The reconstruction of environmental variables	328
7.1.5.1 pH reconstruction	328
7.1.5.2 TP reconstruction	330
7.1.5.3 Ice-cover and January temperature reconstructions	331
7.2 Discussion	335
7.2.1 Summary results and synthesis	336
7.2.2 Diatom zone four, covering the period from <i>ca.</i> 1653 (29cm) to <i>ca.</i> 1830 (14cm)	336
7.2.3 Diatom zone three, covering the period from <i>ca.</i> 1830 (14cm) to <i>ca.</i> 1860 (12.5cm)	340
7.2.4 Diatom zone two, covering the period from <i>ca.</i> 1860 (12.5cm) to <i>ca.</i> 1997 (1.5cm)	342
7.2.5 Diatom zone one, covering the period from <i>ca.</i> 1997 (1.5cm) to <i>ca.</i> 2001 (surface sediments)	343
7.2.6 Summary	344
7.3 How faithfully are known climatic changes occurring over the last 500 years recorded by the palaeolimnological record at Gåvålivatnet	344
7.3.1 The detection of recent climate change using the palaeolimnological record at Lake Gåvålivatnet	345
7.3.1.1 Do the diatom inferred January temperatures reflect recent climate warming?	346
7.3.1.2 Do changes in species abundance and within lake habitat reflect recent climate warming?	350
7.3.1.3 Do changes in lake productivity reflect recent climate warming?	351
7.3.1.4 Summary of evidence reflecting recent climate warming	351
7.3.2 The detection of climatic change associated with the LIA at Lake Gåvålivatnet	352
7.3.2.1 Changes in diatom species and within lake habitat related to the LIA	352
7.3.2.2 Detecting the LIA using patterns of lake/ catchment productivity	353
7.3.2.3 Summary of the palaeolimnological evidence of the LIA	354
7.4 Summary and conclusions	354

Chapter 8

Summary and Conclusions	356
8.1 Introduction	356
8.2 The relationship between ice-cover and diatom species, and the development of the ice-cover transfer function	356
8.3 The January temperature transfer function	359
8.4 The pH transfer function	360
8.5 The detection of climate change over the past 500 years in Norway using the palaeolimnological record	361
8.6 Key contributions of the current research and future work	368

References

371

Appendices

393

List of Tables

Table 1.1	The main stages of annual ice formation and mixing in a typical European high altitude lake.	26
Table 1.2	Measurements for various wavelengths of the visible spectrum (given as percentile transmission per metre).	33
Table 1.3	Climatic changes and the corresponding response in the diatom community.	45
Table 1.4	Shifts in the main planktonic diatoms species in Elk Lake and the suggested climatic reasons for the changes in abundance throughout the core.	48
Table 2.1	Lake code, Lake name, Longitude, Latitude, Altitude and lake area measurements for each of the 80 lakes within the training set.	72
Table 2.2	Summary table of the six lakes cored.	76
Table 3.1	Environmental and chemical variables available for each data set.	112
Table 3.2	Summary of DCA ordination, eigenvalues and cumulative % variance, of the 8 surface samples taken from 4 lakes.	137
Table 3.3	Summary of PCA ordination, eigenvalues and cumulative % variance, of the 8 surface samples taken from 4 lakes.	137
Table 4.1	Lake code, Longitude, Latitude, Altitude and lake area measurements for each of the 40 lakes within the training set.	142
Table 4.2	Selected descriptive statistics for the environmental parameters in the 'ice-cover' training set.	143
Table 4.3	Pearson product moment correlation matrix between 26 chemical determinands for 40 sites.	156
Table 4.4	Summary of PCA ordination, eigenvalues and cumulative % variance, of the 25 environmental variables and 40 sites, with centering and standardisation by species.	157
Table 4.5	PCA scores for the 23 environmental variables on the first four axes.	158
Table 4.6	A list of the most abundant species (in terms of % sum abundance from all 40 samples), minimum and maximum abundance for the species, and the number of samples that the species occurs in.	160
Table 4.7	Results of DCA analysis with different transformation options for the species data.	164
Table 4.8	Summary of PCA ordination results of 152 species in 40 samples, eigenvalues and cumulative % variance are displayed.	164

Table 4.9	Species ranking, based on their PCA ordination scores, for ordination axes 1-4.	166
Table 4.10	Summary results from the DCCA of 25 environmental variables, 40 sites and 152 species, with square root transformation of species data.	167
Table 4.11	Summary results of the RDA conducted on 40 samples, 152 species and 25 environmental variables, with square root transformation of species data.	168
Table 4.12	VIF values for the RDA with 25 environmental variables.	170
Table 4.13	Results of the RDA of diatom data constrained against each environmental variable independently.	170
Table 4.14	RDA of 40 sites, 152 species, and 22 environmental variables with square root transformation of species data.	171
Table 4.15	VIF values generated by the RDA analysis of 18 environmental variables.	172
Table 4.16	Reasons for inclusion or deletion of environmental variables within the ordination analyses.	173
Table 4.17	VIF values and RDA biplot scores for axes 1-4 for the RDA of 17 environmental variables and 152 species.	173
Table 4.18	RDA of 40 samples, 17 environmental variables and 152 species with square root transformation.	174
Table 4.19	Forward selection of environmental variables using RDA of 25 environmental variables.	177
Table 4.20	RDA of 40 samples, 3 environmental variables and 152 species, with square root transformation of species data.	177
Table 4.21	Results using the HOF programme for 128 species in the data set.	178
Table 4.22	The planktonic diatoms found with the 40 lake training set, their N ₂ values and their maximum abundances are listed.	181
Table 4.23	WA optima and tolerances for ice-cover and altitude for the planktonic species occurring within the 40 samples.	181
Table 4.24	WA optima and tolerances for pH, Ca ²⁺ , TOC, Na ⁺ and TN for the planktonic species occurring within the 40 samples.	183
Table 4.25	RDA of ice-cover duration with 152 species. Species data are square root transformed.	208
Table 4.26	A comparison of WA and WA(tol) calibration and prediction techniques for ice-cover duration for the 40 lakes training set.	209
Table 4.27	The results of the PLS and WA-PLS calibration and prediction techniques for ice-cover duration for the 40 lakes training set.	209
Table 4.28	A comparison of WA and WA(tol) calibration and prediction techniques for ice-cover duration for the 40 lakes training set using only the 59 species that had a significant relationship with ice-cover.	212

Table 4.29	Results of the WA-PLS calibration and prediction techniques for ice-cover duration for the 40 lakes training set using only the 59 species that had a significant relationship with ice-cover.	212
Table 5.1	Lake code, Longitude, Latitude, Altitude and lake area measurements for each of the 80 lakes within the training set.	220
Table 5.2	Selected descriptive statistics of the environmental parameters for the 80 lake training set.	222
Table 5.3	Summary of PCA ordination, eigenvalues and cumulative % variance, of the 22 environmental variables and 79 sites, with centering and standardisation by species.	232
Table 5.4	Pearson product moment correlation matrix between 22 environmental variables (after transformation) for the 79 sites.	235
Table 5.5	PCA scores for the 22 environmental variables on the first four axes.	237
Table 5.6	A list of the most abundant species, maximum abundance for the species, the number of samples that the species occurs in and the species N2 value.	238
Table 5.7	Results of the DCA analyses with different transformation options for the species data in the 79 samples, with 187 species.	242
Table 5.8	Summary of DCA ordination, eigenvalues and cumulative % variance, of the 22 environmental variables and 79 sites, with square root transformation and down weighting of rare species.	242
Table 5.9	Species ranking, based on their DCA ordination scores, for ordination axes 1-4.	245
Table 5.10	Summary results from the DCCA of 22 environmental variables, 79 sites and 187 species, with square root transformation of species data.	247
Table 5.11	Summary of RDA ordination results of 187 species in 79 samples, eigenvalues and cumulative % variance are displayed.	247
Table 5.12	Species with the highest species scores associated with axes 1 and 2 of the RDA of 79 samples and 22 environmental variables.	248
Table 5.13	Results of the RDA of diatom data for all the 79 samples constrained against each environmental variable independently.	253
Table 5.14	The Variance Inflation Factors for the RDA of 22 environmental variables.	253
Table 5.15	Forward selection of environmental variables using RDA of 22 environmental variables.	254
Table 5.16	RDA of 79 samples, 6 environmental variables and 187 species, with square root transformation of species data.	254
Table 5.17	Results using the HOF programme for 171 species in the data set.	255
Table 5.18	RDA of 79 samples, 3 environmental variables and 187 species, with square root transformation of species data.	258
Table 5.19	The various CANOCO options involved in the calculation of the variance for each section using partial RDA (T=TOC, P=pH, J=JanT).	259

Table 5.20	The equations used for the calculation of the variance for each section displayed in Figure 5.30.	259
Table 5.21	The results of the RDA of pH with 187 species and 79 samples.	260
Table 5.22	A comparison of WA and WA(tol) calibration and prediction techniques for pH for the 79 lake training set.	261
Table 5.23	The results of the PLS and WA-PLS calibration and prediction techniques for pH for the 79 lake training set.	262
Table 5.24	A comparison of WA and WA(tol) calibration and prediction techniques for pH for the 79 lake training set.	263
Table 5.25	Summary of selected pH calibration transfer functions in comparison to the one generated from the 79 lake training set used in this study.	264
Table 5.26	Species pH optima generated for the 25 most abundant species within this data set using the 79 data set presented (current study) in comparison with similar studies within the current literature also using the WA technique.	269
Table 5.27	The results of the RDA of January temperature with 187 species and 79 samples.	270
Table 5.28	A comparison of WA and WA(tol) calibration and prediction techniques for January air temperature for the 79 lake training set.	271
Table 5.29	The results of the PLS and WA-PLS calibration and prediction techniques for January air temperature for the 79 lake training set.	271
Table 5.30	Summary of selected diatom air/ water temperature calibration transfer functions in comparison to the one generated from the 79 lake training set used in this study.	273
Table 6.1	Summary of the environmental data for Hornsjøen.	279
Table 6.2	Fallout radionuclide concentration in Hornsjøen core 98-18.	280
Table 6.3	The main changes in diatom species assemblage for Hornsjøen, core 98-18.	282
Table 6.4	Summary statistics for the first four axes of the DCA of Lake Hornsjøen, core 98-18.	284
Table 6.5	Summary statistics for the first four axes of the PCA of Lake Hornsjøen, core 98-18.	284
Table 7.1	Summary of the environmental data for Gåvålivatnet.	320
Table 7.2	Fallout radionuclide concentration in Gåvålivatnet, core 01-03.	321
Table 7.3	The main changes in diatom assemblage in the core from Lake Gåvålivatnet.	323
Table 7.4	Summary statistics for the first four axes of the DCA for Lake Gåvålivatnet.	325
Table 7.5	Summary statistics for the first four axes of the PCA for Lake Gåvålivatnet.	326

List of Figures

Figure 1.1	Summary diagram highlighting the inter-linking variables which might affect diatom growth and composition within a lake and its catchment.	29
-------------------	--	----

Figure 1.2	Summary diagram illustrating evidence of climate changes during the LIA in Norway.	59
Figure 2.1	Map of sites in the Scotland data set.	65
Figure 2.2	Geology map of Scotland.	66
Figure 2.3	A selection of sites within the Scotland data set, a) Lochnagar (Code SC0399) b) Unnamed (Code SC0108) c) Loch Bealach na h-Uidhe (Code SC0211) d) Loch an Fhuar-thuill Mhoir (Code SC0189) e) Lochan Bac an Lochain (Code SC0010) f) Loch Coire na Caime (Code SC0067)	66
Figure 2.4	Sampled sites map for lakes in the 'Norway 1' data set.	68
Figure 2.5	Sampled sites map for lakes in the 'Norway 2' data set.	69
Figure 2.6	Geology map of Norway.	70
Figure 2.7	A selection of training set sites located within Norway, a) Råtasjøen (Code 98-15) b) Langrumpa (Code 99-43) c) Reinstjønn (Code 96-78) d) Nøglavatnet (Code 96-10) e) Gryta (Code 98-8)	70
Figure 2.8	The altitudinal gradient for the 80 lake training set.	74
Figure 2.9	The location of the six cored lakes within Norway.	77
Figure 2.10	a) Rasletjernet, Code 98-20. b) Topographic map of Rasletjernet (circled), Code 98-20.	78
Figure 2.11	Percentage dry weight, percentage loss on ignition graphs and diatom profile for Rasletjernet.	79
Figure 2.12	a) Leirvatn, Code 98-6. b) Topographic map of Leirvatn (circled), Code 98-6.	80
Figure 2.13	Percentage dry weight, percentage loss on ignition graphs and diatom profile for Leirvatn.	81
Figure 2.14	a) Davialec (unofficial name), Code 98-9. b) Topographic map of Davialec (circled), Code 98-9.	82
Figure 2.15	Percentage dry weight, percentage loss on ignition graphs and diatom profile for Davialec.	83
Figure 2.16	a) Hornsvatnet, Code 98-2. b) Topographic map of Hornsvatnet (circled), Code 98-2.	84
Figure 2.17	Percentage dry weight, percentage loss on ignition graphs and diatom profile for Hornsvatnet.	85
Figure 2.18	a) Gåvålivatnet, Code 01-03. b) Topographic map of Gåvålivatnet (circled), Code 01-03.	86

Figure 2.19	Percentage dry weight, percentage loss on ignition graphs and diatom profile for Gåvålivatnet.	88
Figure 2.20	a) Hornsjøen, Code 98-18. b) Topographic map of Hornsjøen (circled), Code 98-18.	89
Figure 2.21	Percentage dry weight, percentage loss on ignition graphs and diatom profile for Hornsjøen.	90
Figure 3.1	a) The 'TP gradient' for the Scotland data set. b) The 'TP gradient' for the Norway 2 sites, four sites have TP data missing. c) The 'TP gradient' for the Scotland and Norway 2 data set.	100 101 101
Figure 3.2	Graph comparing TP and chl <i>a</i> for Norway 1 data set.	103
Figure 3.3	TP results for Norway 1 data set.	103
Figure 3.4	SRP results for Norway 1 data set.	104
Figure 3.5	Comparison of TP ($\mu\text{g/l}$) for five Norway 1 sites.	104
Figure 3.6	Comparison of SRP ($\mu\text{g/l}$) values for five Norway 1 sites.	105
Figure 3.7	The components of the empirical ice-cover model.	108
Figure 3.8	A comparison of the thermistor ice-cover duration (days) with the modelled ice-cover duration (days) for 7 sites within the 80 lake training set.	109
Figure 3.9	A comparison between thermistor ice-cover duration and modelled ice-cover duration for 58 EMERGE sites across Europe.	110
Figure 3.10	A comparison of the thermistor ice-cover duration (days) and the modelled ice-cover duration (days) for 58 EMERGE sites.	111
Figure 3.11	The relationship between species number and valve count for Hornsjøen.	119
Figure 3.12	The relationship between species number and valve count for Gåvålivatnet.	120
Figure 3.13	Diagram explaining the various steps involved in the selection of an ordination model to explore species response data.	124
Figure 3.14	PCA biplot on axis 1 and 2, of 8 surface samples taken from four lakes.	138
Figures 4.1, 4.2	Box plots of maximum lake area and maximum lake depth for the Norway and Scotland lake classes.	144
Figure 4.3	Box plot of lake altitude for both the Norway and Scotland lake classes.	145
Figures 4.4, 4.5	Box plots of pH and Ca^{2+} , with means and 25 percentile ranges shown, for both the Norway and Scotland lake classes.	146
Figure 4.6	Box plot of Alkalinity for the Scotland and Norway lakes with means and 25 percentile ranges displayed.	146
Figure 4.7	Conductivity box plot for the Norway and Scotland lakes with means and 25 percentile ranges plotted.	147
Figures 4.8-4.13	Box plots, with means and 25 percentiles plotted, for the major ions (excluding Ca^{2+}), Mg^{2+} , K^+ , Na^+ , SO_4^{2-} , NO_3^- , Cl^- for the Norway and Scotland lake classes.	149

Figures 4.14, 4.15	Box plots for NH_4^+ and TP, with means and 25 percentile ranges plotted, for the Norway and Scotland lake classes.	150
Figure 4.16	Box plots, with means and 25 percentiles ranges, plotted for TN for the Norway and Scotland lake classes.	150
Figures 4.17-4.19	Box plots, with means and 25 percentile ranges, plotted for AL-TM, AL-L and AL-NL for the Norway and Scotland lake classes.	151
Figure 4.20	Box plots, with means and 25 percentiles ranges, plotted for TOC for the Norway and Scotland lake classes.	152
Figures 4.21, 4.22	Box plots, with means and 25 percentile plotted, for annual precipitation and ice-cover duration for the Norway and Scotland lake classes.	153
Figures 4.23, 4.24	Box plots, with means and 25 percentile ranges plotted, for average January and July air temperature for the Norway and Scotland lake classes.	153
Figure 4.25	PCA biplot of the environmental data for the 40 lake training set and 25 environmental variables.	157
Figure 4.26	Summary diatom diagram of 40 samples arranged in order of increasing pH from low (SC0339) to high (CN0019).	162
Figure 4.27	PCA biplot of the 40 surface sample diatom assemblages, only sites are shown.	164
Figure 4.28	RDA biplot of 152 diatom species, 25 environmental variables and 40 samples.	169
Figure 4.29	RDA biplot of 152 diatom species, 22 environmental variables and 40 samples.	172
Figure 4.30	RDA biplot with 17 environmental variables, 152 species and 40 sites.	174
Figure 4.31	RDA biplot of 152 diatom species.	176
Figure 4.32	A graphical representation of the types of species response identified by the HOF programme.	179
Figure 4.33	The relationship between species number and ice-cover duration (days), with a linear regression line plotted.	180
Figure 4.34	The relationship between species number and altitude (m), with a linear regression line plotted.	180
Figure 4.35	RDA plot showing the abundance of 'plankton species', displayed as proportional circles.	182
Figure 4.36	Summary diagram of 40 samples arranged according to increasing ice-cover.	186
Figure 4.37	HOF model responses for selected <i>Achnanthes</i> spp. within the 40 lake training set for altitude and ice-cover.	188
Figure 4.38	HOF model responses for selected <i>Aulacoseira</i> spp. within the 40 lake training set for altitude and ice-cover.	191
Figure 4.39	HOF model responses for selected <i>Brachysira</i> spp. within the 40 lake training set for altitude and ice-cover.	192

Figure 4.40	HOF model responses for selected <i>Cymbella spp.</i> within the 40 lake training set for altitude and ice-cover.	193
Figure 4.41	HOF model responses for selected <i>Fragilaria and Synedra spp.</i> within the 40 lake training set for altitude and ice-cover.	195
Figure 4.42	HOF model responses for selected <i>Peronia, Amphicampa and Eunotia spp.</i> within the 40 lake training set for altitude and ice-cover.	197
Figure 4.43	HOF model responses for selected <i>Navicula and Nitzschia spp.</i> within the 40 lake training set for altitude and ice-cover.	201
Figure 4.44	HOF model responses for selected <i>Tabellaria spp.</i> within the 40 lake training set for altitude and ice-cover.	202
Figure 4.45	HOF model responses for selected <i>Pinnularia spp.</i> within the 40 lake training set for altitude and ice-cover.	203
Figure 4.46	A histogram showing the bi-modal distribution of ice-cover duration along the gradient.	204
Figure 4.47	A comparison of ice-cover optimum and tolerances produced using Weighted Averaging (WA) and Maximum Likelihood (ML, GLR model) for the 59 species found to have a statistically significant relationship with ice-cover using the HOF model.	206
Figure 4.48	Measured ice-cover and WA predicted ice-cover data with loess smoother line plotted.	211
Figure 4.49	Measured ice-cover and WA(tol) predicted ice-cover data with loess smoother line plotted for the model with just the 59 significant ice-cover species used.	212
Figure 5.1	Box plots of lake depth, with means and 25 percentile ranges shown, for both the Norway and Scotland lake classes.	223
Figure 5.2	Box plots of lake area, with means and 25 percentile ranges shown, for both the Norway and Scotland lake classes.	223
Figure 5.3	Box plots of altitude, with means and 25 percentile ranges shown, for both the Norway and Scotland lake classes.	223
Figure 5.4	Box plots of pH, with means and 25 percentile ranges shown, for both the Norway and Scotland lake classes.	224
Figures 5.5, 5.6	Box plots of Ca^{2+} and Alk, with means and 25 percentile ranges shown, for both the Norway and Scotland lake classes.	225
Figure 5.7	Box plots of Conductivity, with means and 25 percentile ranges shown, for both the Norway and Scotland lake classes.	225
Figures 5.8-5.13	Box plots of Chloride, Sodium, Sulphate, Magnesium, Potassium and Nitrate, with means and 25 percentile ranges, shown for both the Norway and Scotland lake classes.	227
Figure 5.14	Box plots of Ammonium, with means and 25 percentile ranges shown, for both the Norway and Scotland lake classes.	228
Figures 5.15-5.17	Box plots of Aluminium (TM, Non- Labile and Labile), with means and 25 percentile ranges, shown for both the Norway and Scotland lake classes.	229

Figure 5.18	Box plots of TOC, with means and 25 percentile ranges shown, for both the Norway and Scotland lake classes.	230
Figures 5.19-5.21	Box plots of precipitation, January air temperature and July air temperature, with means and 25 percentile ranges shown for both the Norway and Scotland lake classes.	231
Figure 5.22	PCA biplot of the environmental variables for the 79 lake training set only samples are shown.	233
Figure 5.23	PCA biplot of the environmental data for the 79 lake training set and 22 environmental variables.	236
Figure 5.24	a) Summary diatom diagram of 79 samples, <i>Achnanthes</i> – <i>Aulacoseira</i> species. b) Summary diatom diagram of 79 samples, <i>Brachysira</i> - <i>Tabellaria</i> species.	239 240
Figure 5.25	DCA biplot of the 79 surface sample diatom assemblages, only sites are shown.	245
Figure 5.26	RDA biplot of 187 species, 79 samples and 22 environmental variables. Only the environmental variables and sites/ samples are displayed.	248
Figure 5.27	Attribute plots of the species associated, negatively and positively, with Axis 1 of the RDA.	251
Figure 5.28	Attribute plots of the species associated, negatively and positively, with Axis 2 of the RDA.	252
Figure 5.29	RDA biplot on axes 1 and 2, with 6 environmental variables, 187 species and 79 sites. Only sites/ samples and environmental variables are displayed.	254
Figure 5.30	A Venn diagram showing the results of the partial RDA's. The unique contribution of pH (P), TOC (T) and JanT (J) are displayed as well as the interaction between these variables.	259
Figure 5.31	Measured pH with WA(tol) predicted pH using; a) inverse de-shrinking b) classical de-shrinking coefficients	263
Figure 5.32	a) Plot of predicted – measured pH, against measured pH, using WA(tol) with inverse de-shrinking. b) Plot of predicted- measured pH, against measured pH, using WA(tol) with classical de-shrinking.	263 263
Figure 5.33	A comparison of pH optima and tolerances produced using Weighted Averaging (WA) and Maximum Likelihood (ML) for the 126 species found to have a statistically significant relationship with pH.	266
Figure 5.34	Plots of measured January Temperature (°F) using WA-PLS (3 components) against; a) predicted January temperature (°F) b) predicted January temperature- measured January temperature (the residuals).	272
Figure 5.35	January temperature optima and tolerances produced using Weighted Averaging (WA) for the 114 species found to have a statistically significant relationship with January temperature.	274

Figures 6.1 and 6.2	Core profile and %DW and %LOI for core 98-18 from Lake Hornsjøen.	279
Figure 6.3	Radiometric chronology of Hornsjøen.	281
Figure 6.4	Summary diatom diagram for Hornsjøen.	283
Figure 6.5	Biplot of diatom samples in the 110 samples for Lake Hornsjøen on PCA axis 1 and 2.	285
Figure 6.6	Biplot of 110 diatom samples (o) for Lake Hornsjøen and species (Δ, with selected taxa labelled) on PCA axis 1 and 2.	286
Figure 6.7	DCA biplot of the 79 surface sample diatom assemblages (circles) and the fossil diatom assemblages (squares).	287
Figure 6.8	Diatom inferred pH for Lake Hornsjøen using the AL:PE data set and the 79 lake data set.	289
Figure 6.9	Diatom inferred Total Phosphorous for Lake Hornsjøen using the EDDI data base and WA reconstruction method.	290
Figure 6.10	Diatom inferred January temperature, using the 79 lake data set, with (b) and without (a) a running mean, diatom inferred ice-cover duration (days) using the 40 lake data set and a model with all the species in the training set used (c) and reconstructed using a model with only the species that had a significant relationship with ice-cover used (d).	291
Figure 6.11	Summary diatom diagram with species arranged in order of ice-cover duration optima.	293
Figure 6.12	Summary diatom diagram for Hornsjøen with taxa <2% abundance deleted, arranged in order of WA January temperature optima presented in brackets. Species with no significant relationship with January temperature, or those which were not present in the training set are also presented (n/s in brackets).	294
Figure 6.13	Summary diagram of reconstructed environmental variables, lithostratigraphic data, ordination results and diatoms habitat ratios for Lake Hornsjøen.	297
Figure 6.14	Instrumental record of average May and June temperature (°C) for Lake Hornsjøen.	306
Figure 6.15	Diatom inferred January temperature and its comparison with the spring temperature instrumental record.	307
Figure 6.16	The diatom inferred January temperature reconstructions with the years of warmest and coldest winter temperature, derived from the instrumental record plotted.	308
Figure 6.17	Attribute plots of species against environmental variables using RDA on the 79 lake training set. Those species increasing significantly in abundance at 0-9cm within the core are plotted.	310
Figure 6.18	Attribute plots of species against environmental variables using RDA on the 79 lake training set. Those species increasing abundance at 16-19cm within the core are plotted.	315
Figure 7.1	Core photograph and %DW and %LOI for core 01-03 from Lake Gåvålivatnet.	321

Figure 7.2	Radiometric chronology of Lake Gåvålivatnet.	322
Figure 7.3	Summary diatom diagram for Lake Gåvålivatnet.	324
Figure 7.4	Biplot of diatom taxa in the 117 samples for Lake Gåvålivatnet on PCA axis 1 and 2.	326
Figure 7.5	Biplot of 117 diatom samples (o) for Lake Gåvålivatnet and species (Δ- with selected taxa labelled) on PCA axis 1 and 2.	327
Figure 7.6	DCA biplot of the 79 surface sample diatom assemblages (circles) and the fossil diatom assemblages (squares) as passive samples.	329
Figure 7.7	Diatom inferred pH for Lake Gåvålivatnet using the AL:PE data set and the 79 lake data set.	330
Figure 7.8	Diatom inferred TP for Lake Gåvålivatnet using the EDDI data base and WA reconstruction methods.	331
Figure 7.9	Diatom inferred January temperature, using the 79 lake data set, a) with and b) without a running mean and diatom inferred ice-cover using the 40 lake data set c) using the significant species model d) using the all species model.	332
Figure 7.10	Summary diatom diagram for Lake Gåvålivatnet with species arranged in order of ice-cover duration optima.	333
Figure 7.11	Summary diatom diagram for Lake Gåvålivatnet, with taxa <2% deleted and species arranged in order of January temperature optima (shown in brackets). Species with no significant relationship with January temperature, or those which were not present in the training set are also presented (n/s in brackets)	334
Figure 7.12	Summary diagram of reconstructed environmental variables, lithostratigraphic data, ordination results and diatom habitat ratios for Lake Gåvålivatnet.	337
Figure 7.13	Instrumental record of average annual temperature (°C) for Lake Gåvålivatnet.	346
Figure 7.14	Diatom inferred January temperature, using the 79 lake data set a) with and b) without a running mean, and January temperature from the instrumental record c) with and d) without a running mean.	347
Figure 7.15	Scatter plot of diatom inferred reconstructed January temperature against the January temperature from the instrumental record.	348
Figure 7.16	Predicted January temperatures- measured January temperatures against core depth for the samples 0-9.75cm in the Gåvålivatnet core.	348
Figure 7.17	Diatom inferred January temperature (o) and January temperature from the instrumental record (♦) plotted against core sample.	348
Figure 7.18	Diatom inferred January temperatures (♦) and January temperatures from the instrumental record (o), both with linear regression lines plotted, against down core sample number.	349
Figure 7.19	Diatom inferred January temperature and PCA axis 2 scores plotted stratigraphically for Lake Gåvålivatnet.	353

Figure 8.1	Summary diagram of various lithostratigraphic parameters, diatom composition data, diatom inferred January temperature and the Central England Temperature series for Lake Hornsjøen.	364
Figure 8.2	Summary diagram of various lithostratigraphic parameters, diatom composition data, diatom inferred temperature reconstruction and the Central England Temperature series applied to Lake Gåvålivatnet.	365
Figure 8.3	Diatom inferred temperature reconstructions for Lake Hornsjøen and Gåvålivatnet (°F), Central England Temperature series (°F), Winter and annual NAO index reconstructions for the Northern Hemisphere. Each variable is constrained by the chronology for Lake Hornsjøen.	366

List of plates

Plate 3.1	Light micrographs of the different forms of <i>Cyclotella</i> sp. found within the 80 lake training set.	118
------------------	--	-----

List of Appendices

Appendix 3.1	Scatterplot of thermistor ice-cover duration (days) against altitude (m a.s.l) for 19 sites from the Scotland sub set of lakes with the R ² value displayed.	394
Appendix 3.2	Summary of environmental data for the AL:PE training set used for the pH reconstruction in chapters 6 and 7.	395
Appendix 3.3	Summary table of environmental data for the EDDI Swiss dataset used for the TP reconstruction in chapters 6 and 7.	396
Appendix 4.1	Table summarising the results of the water chemistry for the 40 lake data set.	397
Appendix 4.2	Histograms with normal distribution curves plotted for a) Alkalinity and b) Alkalinity log transformed.	399
Appendix 4.3	Species found within the 40 lake training set, species, codes and authorities are provided.	400
Appendix 4.4	GLR ice-cover (days) optima and tolerances for the 59 species which have a significant relationship with ice cover. Those species marked in bold indicate species which either have optima outside the ice cover range or where GLR failed to calculate optima measures.	407
Appendix 5.1	Table summarising the results of the water chemistry for the 80 lake data set.	408
Appendix 5.2	Species found within the 80 lake training set, species, codes and authorities are provided.	412
Appendix 6.1	Full list of species, authorities and species codes found within core 98-18	421
Appendix 6.2	Graphs showing the reliability of the pH and TP transfer functions for Lake Hornsjøen (Calibration set sum refers to WA methods and Min DC refers to MAT methods)	426
Appendix 7.1	Species names, codes and authorities for species found in Lake Gåvålivatnet	427
Appendix 7.2	Graphs showing the reliability of the pH and TP transfer functions for Lake Gåvålivatnet (Calibration set sum refers to WA methods and Min DC refers to MAT methods)	433

Chapter 1

Introduction- The use of palaeolimnology for climatic reconstruction and research rationale

Introduction

The chapter introduces the focus of the study through a discussion of the current literature concerning climate change and palaeolimnology, with specific reference to changes in ice-cover and how this may affect diatom assemblages. Both the qualitative and quantitative representation of climatic change, using lake sediment proxy techniques, is discussed. The research explores how known climatic events occurring over the last 500 years in central Norway are recorded by the palaeolimnological record. Therefore, an evaluation of climatic changes occurring over the late Quaternary within Europe, and in particular within central Norway, is presented within this chapter with specific reference to the climatic changes associated with the 'Little Ice Age' (LIA). The research rationale and the study objectives are also presented.

Analysis of the instrumental record indicates that 20th century climate has been dominated by an almost globally universal warming trend, with temperatures at the end of the century being significantly higher than those at the beginning (Jones *et al.*, 1999; Parker *et al.*, 1994). The instrumental record, however, provides only a limited temporal perspective and changes over longer time spans are not recorded. The true extent of this 'anthropogenic warming', in comparison to previous decades and centuries, when the climate varied due to 'natural forcing mechanisms', cannot therefore be analysed as the instrumental record is limited. An increased demand for 'evidence' of recent climate change, in relation to past climatic fluctuations occurring over the Holocene, has therefore arisen. The inherent variability of the climate, however, means that most climate studies should concern at least decadal, and preferably centennial, scale analysis.

Although recent climate warming has been global in nature there are marked regional differences, with some areas showing heightened responses to changes in climate. It has been shown that high altitude or high latitude sites may show the greatest evidence

of recent climate change (*c.f.* Douglas *et al.*, 1994; Smol *et al.*, 1991; Sorvari and Korhola 1998; Barber *et al.*, 1999). Yet the paucity of long term monitoring data is a common feature for these ecosystems, due to their remote locations and problems of accessibility, and accurate long-term climate data are not available for many of these areas.

In such cases proxy data become important to determine the scale and duration of climatic fluctuations. Lake sediments, which contain the preserved biological remains from the lake, can often be used as a climate proxy in these areas. By extracting and identifying the preserved remains of pollen, invertebrates or algae from the sediment, as well as assessing shifts in productivity, pH and sediment accumulation, extensive environmental and climatic histories of individual lakes can be produced (*c.f.* Lotter *et al.*, 1997; Walker *et al.*, 1997; Korhola *et al.*, 1998; Birks *et al.*, 2000). Therefore, palaeolimnological records can be viewed as natural archives containing both biological and lithostratigraphic proxies of climate- related lake responses. They represent a consistent and long term natural time series covering thousands of years of climatic history. Consequently, much work has focused on the potential of palaeolimnology for the reconstruction and inference of changes in past climate.

This chapter focuses specifically on how climatic changes are represented in the palaeolimnological record of remote, high altitude or high latitude freshwater lakes, which often form the focus of such climatic studies due to their relatively pristine catchments and lack of anthropogenic disturbance. The relationship between air temperature and lake water temperature, and the effect this has on the ice-cover regime of a lake is discussed. Changes to a lake's thermal and mixing regimes, due to changes in climate, and how these might manifest themselves in the palaeolimnological record of the lake, are also evaluated. Alterations to the rate and delivery of sediment to a lake, indicated by changes in the lake's lithostratigraphic record, are discussed and in turn how these can be used to make climatic inferences. Particular emphasis is placed on the interaction between climate, lake ice-cover and the diatom record of high altitude /latitude lakes. The potential value of diatoms as recorders of past climatic conditions is evaluated, in terms of both their qualitative and quantitative inference potential. Through the analysis of the current

palaeolimnological studies, 'gaps' in the current research agenda will become apparent. Some of these 'gaps' have directly moulded the research focus of this study (see section 1.6).

The next section discusses the relationship between air temperature, lake water temperature and lake ice-cover in a typical high altitude lake. The thermal, mixing and ice-cover regime of such a lake is discussed, in order to assess how this is driven by climate and to establish what effects changes in climate might have on the biological system of the lake.

1.1 The relationship between air temperature, lake temperature and ice-cover

Lakes at high altitudes/ latitudes may be ice-covered for a significant proportion of the year due to their high number of freezing degree days, when air temperatures drop below 0°C (Kettle *pers. com.*). Air temperatures have been shown to have a direct impact on lake water temperatures and, therefore, exert a significant control on the ice-cover regime of a lake (Livingstone 1997; Livingstone and Lotter 1998; Livingstone *et al.*, 1999; Livingstone 1999b). Consequently, changes in lake ice-cover are a useful proxy for climate changes because it has been shown that a small change in air temperature will often produce a large change in ice-cover on a lake (Robertson, *et al.*, 1992; Assel and Robertson 1995).

In this way ice duration, measured in freeze-up and break-up dates, and ice thickness can be used to represent changes in climate. Due to the fact that air temperatures are so closely linked to ice-cover they have been used to model/predict ice-cover regimes in mountain lake systems (Battarbee *et al.*, 2002b; Agusti- Panareda and Thompson 2002). These models use melting degree days (used to predict ice-off, by counting the number of days where air temperature >0°C) and freezing degree days (used to calculate ice-on days by counting the number of days <0°C) to calculate the duration of ice-cover (Kettle *pers. com.* see also section 3.2.2).

The records of freeze-up and ice break-up represent the integration of local weather conditions and particularly air temperature at a given site. However, the ice regime on a lake can also reflect larger changes in regional climatic processes (Anderson *et al.*,

1996; Livingstone 1997). For example, large scale events, such as the North Atlantic Oscillation (NAO, see section 1.3.3.1 for definition), which has a major influence on the climate in the Northern Hemisphere, are often reflected in lake ice-cover patterns (Livingstone 1999). These events are usually evident in shifts in ice break-up dates.

Livingstone (1997) also suggested that ice break-up dates, for high altitude lakes in the Swiss Alps, were determined largely by synoptic scale meteorological processes. He also stressed, however, that the effect of local weather, degree of sheltering and lake morphology should not be neglected when comparing the timing of ice break-up. The extent to which the lake ice-cover reflects the air temperature is, therefore, dictated by both lake morphology and location.

This is supported by extensive work on the lake ice-cover dynamic for Hagelseewli a remote mountain lake in the Swiss Alps (Goudsmit *et al.*, 2000). Shading was shown to significantly effect the radiation balance of the lake, due to the presence of the high cliff face on the southward lake end. As is often the case in high mountain lakes cliff shading will reduce the solar radiation on a daily basis, reduce the day length and increase ice-cover duration. Because of the local topography and the extensive ice-cover the relationship between water temperature and air temperature is reduced. In general though it is unusual for shading to exert such a large control over ice-cover and air temperature is usually the more dominant control.

Recent climate warming has also been reflected in recent changes in lake ice-cover regimes. Hanson *et al.*, (1992) demonstrated that over the past 35 years ice break-up dates have been progressively earlier within the North American Great Lakes region, a statistically significant trend which is directly correlated with increasing temperature readings for the area. Anderson *et al.*, (1996) also found, through the analysis of 20 lakes in Wisconsin, that ice break-up dates were becoming earlier, indicating a climate warming trend.

1.2 Stratification patterns, lake mixing and ice-cover in high altitude lakes

A lake's thermal stratification follows a pattern of a warm surface layer (the 'epilimnion'), with a layer beneath this, which has a strong thermal gradient (the

‘metalimnion’ or ‘thermocline’), and finally the deep bottom, cold water layer (the ‘hypolimnion’). The inherent relationship between water density and temperature dictates, therefore, the annual pattern of stratification and mixing within a lake.

The typical annual thermal regime of a high altitude lake which stratifies (referred to as dimictic, i.e. a lake which circulates freely twice a year in spring and autumn and is directly stratified in summer and inversely stratified in winter) and is ice-covered for a large proportion of the year is summarised in Table 1.1. It can be seen that the lake’s productivity is divided into two periods, a long period when the lake is ice-covered characterised by low productivity, light limitation and oxygen depletion and, a shorter more productive, ice free season when the lake stratifies, but mixes in late spring and autumn.

Therefore, the presence, absence and duration of ice-cover on a lake affect the relationship between the atmosphere and the lake, which will influence the length of the lake stratification period. In this way the open water period of the lake is affected by the length of the ice-cover period which is directly related to air temperatures within these high altitude lake systems (Livingstone 1997; Livingstone and Lotter 1998). Shifts in freeze-up or break-up dates will, therefore, change the seasonal patterns of lake circulation and stratification (Livingstone 1997) and have consequences for the lake biota (see section 1.3.2 and 1.3.3). The next section discusses how climate, both directly and indirectly, specifically effects diatom growth and composition.

Table 1.1: The main stages of annual ice formation and mixing in a typical European high altitude lake

Lake ice stages	Lake characteristics
Overturn/ lake mixing. Late Autumn	<ul style="list-style-type: none"> - Solar radiation decreases in the autumn and air temperatures lower. - A loss of heat exceeds inputs from solar radiation. Surface waters cool, become more dense than the underlying water - a deepening of the seasonal thermocline. - The mixing produces the transport of fine active surface sediments to the water column.
Clear ice formation	<ul style="list-style-type: none"> - As the temperature of the water reaches maximum density 4°C, surface ice can form. - Lake ice effectively seals it off from the effects of the wind - The longer the clear ice period the thicker the ice sheet and the lower the temperature within the lake for the rest of the year - Light can still penetrate to a significant depth, allowing primary production under the ice (Catalan and Camarero 1991).
Opaque ice cover	<ul style="list-style-type: none"> - when snow accumulation reduces penetration of photosynthetically active radiation to <1% of radiation outside the lake, there is no under ice production of phytoplankton and all non living suspended matter sinks. - Long durations of ice-cover, appears to leave ecosystems relatively unaffected by air temperature fluctuations during winter and early spring- unless the duration of ice-cover is affected.
Thaw, ice-cover breaks. Late spring	<ul style="list-style-type: none"> - Breakage often along the shoreline due to an increase in lake water volume and increases in lake water level due to thawing of snow in the catchment. - With ice-cover break-up spring mixing of the water column occurs - As the flow decreases and deep mixing occurs (through convection), this is often a time of lowered pH and high dilution and exposure to light extremes- (fluctuations between harmful radiation and light limited conditions)- phytoplankton communities may be stressed (Catalan 1992). - In extremely cold years the ice may not completely melt, creating a 'moat effect'- plankton growth is restricted, favouring the growth of periphyton communities (Smol and Douglas 1996; Douglas and Smol 1994) (See section 1.3.3.1 and 1.4.1.2).

1.3 The relationship between diatoms and climate

1.3.1 The diatoms

Diatoms (Bacillariophyceae) are unicellular or colonial algae which range in size from approximately 5µm to 500µm. They live in a wide range of habitats where there is moisture (Barber and Haworth 1981) and are highly diverse, inhabiting both freshwater and marine environments. These algae have a silica cell wall, the 'frustule', which is highly resistant and usually remains long after its death (Lewin 1962). The 'frustule' is composed of two components the 'hypovalve' and the 'epivalve' which

are linked together by 'girdle bands'.

Primarily diatoms reproduce by cell division and, therefore, for most species the average cell size decreases with each round of cell division. When the cells reach a minimal size, sexual reproduction may occur creating auxospores increasing the cell size and a new series of vegetative cell reproduction can occur (van den Hoek *et al.*, 1995). The taxonomy of the algae is based on the species-specific characteristics of their cell wall which are often very distinctive. Consequently, identification of species is precise and can be to a low taxonomic level (Battarbee 1986). Diatom taxa can often be separated into two major ecological groupings based on life strategies; those with optimal growth and completion of their life cycle within the open water (planktonic) and those attached in the littoral zone (periphyton).

Diatoms, due mainly to their short life cycles, tend to show a rapid response to changes in lake environmental conditions, allowing them to respond quickly to changes in seasonal weather patterns and, therefore, can be used to reflect climatic trends over longer term records (Smol *et al.*, 1991; MacDonald *et al.*, 1993; Douglas *et al.*, 1994, discussed further in section 1.3.2). This rapid response is advantageous, as other climate proxies may not be suitable. For example, analysis of periglacial features may involve a time lag response (MacDonald *et al.*, 1993; Smol 1988), or low pollen production levels in arctic systems and issues related to the transport of pollen, means their suitability for short term climate studies are often limited (Smol 1988).

Diatoms may respond to climate directly, to changes in water temperature, or indirectly driven by changes in the lake due to shifts in climate, such as changes in lake mixing, nutrient supply and/or ice-cover. In addition, successional patterns of diatom species are often related to seasonality, related to water temperature changes, nutrient supply and lake mixing, and these factors are also discussed in the following sections. Often, however, many of these driving variables are interconnected and involve several inter-connected feedback mechanisms affecting the diatom composition both directly and indirectly. Figure 1.1, therefore, helps to illustrate the various weather/climatic variables which may affect the diatom growth and is provided in order to help with the discussion that follows in sections 1.3.2 and 1.3.3.

1.3.2 The direct effects of climate on diatom growth

Water temperatures regulate many algal processes. Cold temperature is known to restrict algal growth via its effect on photosynthesis and synthesis of proteins, mobility, and other metabolic processes such as respiration (Raven and Geider 1988). Temperature controls the rate of these metabolic processes which in turn adjust the rate of algal growth. It has been shown that temperature has a direct influence on algal cell division and hence succession patterns (Raven and Geider 1988).

Some work has been conducted on the direct limiting effect of temperature on diatom populations (Rodhe 1948a; Ruttner 1952; Hutchinson 1975; Foy and Gibson 1993). The precise influence, however, of temperature on biological processes is often hard to separate from other factors such as light and oxygen, which follow similar seasonal cycles.

Rodhe (1948) investigated the limiting temperature optima for plankton species (cited in Hutchinson 1975). The species were grown in cultures at 5°C, 10°C and 20°C. It was suggested that those species with high limiting optima, for example *Asterionella formosa*, would hardly grow at all at high temperatures (Rodhe 1948a) or low light conditions (Lund 1955). Further work on the temperature preferences of diatom species was conducted by Findenegg (1943) and Ruttner (1952) using lakes in Austria. Several discrepancies in the species temperature optima were identified between the results of the two studies (e.g. *Cyclotella comensis* 12.5°C by Findenegg and 9.5°C by Ruttner), suggesting, therefore, that defining temperature optima for diatoms can be problematic.

Furthermore, Hutchinson (1975) states that it is probable for some species, such as *A. formosa* and *F. crotonensis*, that thermal ecotypes are adapted to different temperature regimes. Ruttner (1952) also highlighted that two races of *A. formosa* exist in the Austrian Alps, one with a temperature optima of 5.9°C and the other with an optima

of 12.2°C (var. *hypolimnetica* and var. *epilimnetic* respectively). If this is the case then regular behaviour from lake to lake cannot be expected and comparisons between lakes, in this manner, may, therefore, be unproductive.

The seasonal succession of diatoms may, however, be directly related to water temperature. Hutchinson (1975) proposes that the seasonal cycle in the phytoplankton may be formally explicable in terms of temperature. For example, a lake may see an early bloom in *Aulacoseira* species, implying that they can prosper in lower temperatures and lower light conditions (for e.g. *Aulacoseira subarctica* requires a dark period to optimise growth rate, Foy and Gibson 1993). Whereas, *F. crotonensis* and *A. formosa* may be species which appear in late spring or early autumn, implying that their temperature optima are higher (Hutchinson 1975).

Padisak *et al.*, (1998) studied the succession of the phytoplankton in Lake Stechlin, a deep, oligotrophic, glacial lake in Germany. They found that *Cyclotella* species (*C. tripartita*, *C. pseudocomensis* and a small *Cyclotella* sp.), rather than *Aulacoseira* sp., dominated the spring bloom and started to grow as early as February- March and continued to grow until the end of April (Padisak *et al.*, 1998). This implies that *Cyclotella* species may be able to tolerate and prosper under lower temperatures. It may not, however, be directly related to temperature but the fact that *Cyclotella* have lower nutrient requirements than *Aulacoseira*. In addition *C. comensis*, due to their smaller size, may be able to remain suspended in stratified waters for longer.

Pienitz *et al.*, (1995) in their work on surface sediment diatom assemblages showed that planktonic taxa generally had higher temperature optima and tolerances than benthic species. They stress, however, that the abundances of many of the taxa were low within their study and that the quantitative optima and tolerance estimates should be viewed as preliminary (this work is discussed further in section 1.4.1.3).

At present, however, there is limited knowledge of the specific thermal optima and tolerances of freshwater diatoms and especially those of high latitude areas (Fritz *et al.*, 1991; Fritz 1996; Smol *et al.*, 1991). Furthermore, many of the laboratory experiments, conducted under controlled conditions, cannot mirror conditions

occurring within the natural environment (also see section 1.3.3.3). The paucity of data, however, may be related to the complex effect that temperature has on the algal community, due principally to the fact that temperature can control many chemical and physical cycles indirectly (Pienitz *et al.*, 1995 Figure 1.1). These issues are discussed further in section 1.4.1.3 which explores the use of diatoms to quantify past air/water temperatures.

1.3.3 The indirect effects of climate on diatom growth

Although diatoms might respond to temperature changes directly, it has been shown that they respond to changes in climate through indirect mechanisms driven by the changes in climate. Many of these are discussed below. However, due the fact that the majority of these variables interact with one another the identification of section boundaries within the discussion is slightly arbitrary.

1.3.3.1 Changes in lake ice-cover and its relationship to diatom assemblages

This section evaluates the effect that ice-cover has on lake ecosystems and, consequently, diatom production and assemblage composition. Some of the expected impacts of climate change for high altitude lakes are changes in ice-cover, thermal conditions, light regimes, nutrient balance and pH (Rouse, *et al.*, 1997). Many of these processes are also indirectly linked to ice-cover changes. For example, ice-cover plays a key role in the stratification of a lake (See Table 1.1), which in turn will affect temperature gradients within the lake, mixing regimes, sedimentation patterns, the nutrient cycle, and ultimately the productivity of the lake system. Ice-cover also has a significant influence over light input to the lake and habitat availability within the lake (Smol 1988). Ice-cover, therefore, influences the biota of a lake both directly and indirectly and exerts a significant influence over numerous environmental variables.

Ice-cover, diatom productivity and diatom habitat shifts

Algae require light for photosynthesis and hence light is an important factor for determining primary productivity (Sze 1994). The influence that ice-cover has on a lakes radiation balance can be substantial. The growth of diatoms is generally seasonal, in response to changes in day length, the intensity of solar radiation and the supply of nutrients, starting in March/ April and declining in October/ November.

(Willen 1991). The duration and thickness of ice-cover will determine light penetration and growing season length, which will significantly affect both the productivity and the composition of the diatom community.

Fritsen and Priscu (1999) found that changes in the properties of the permanent ice-cover on a lake can have a profound effect on the primary productivity of the lake. Through their work on Lake Bonney, Antarctica, they showed that the timing and extent of 'ice whitening', caused by changes in the scattering properties within the upper ice layer, controlled both primary production and overall phytoplankton dynamics. On this permanently ice-covered lake the ice whitens when the ice temperature warms to 0°C and with this primary production in the water column decreases. It was shown that a delay in ice whitening with cold air temperatures in the spring might result in an increase in production and a more rapid depletion of nutrients. In contrast if ice whitening is early this should extend the time that nutrients are not limiting for phytoplankton growth.

The actual effect of limited light intensity due to ice-cover may, however, be over estimated. The extent of the light limitation is determined by the type of ice and the snow cover on the ice. Cole (1975) states that ice-cover will in effect close off the lake from the atmosphere and terminate circulation, but it does not stop light penetration. In fact clear ice can often transport light better than the water underneath it (Cole 1975).

Sauberer (1950) measured the transparency of ice covering Lunzer Untersee in comparison to that of distilled water and the lake water (Table 1.2). These calculations show that the transparency of the ice is much greater than the lake water from which it was frozen. Clear ice, therefore, seems to have little effect on the light penetration. However, if the ice is covered in snow or fallen debris, or the ice itself contains many bubbles the situation is otherwise. For example, 20cm of freshly fallen snow will reduce the light that penetrates the ice to 6.7%. For older compacted snow of the same depth the light transparency will be reduced to 1% before the water is reached (Ruttner 1952).

Table 1.2: Measurements for various wavelengths of the visible spectrum (given as percentile transmission per metre). Source Sauberer 1950.

Wave length, m μ	400	500	600	700	800
Ice (Lunzer Untersee)	96.0	92.0	81.5	55.0	17.0
Distilled water	98.5	99.2	81.0	55.0	11.1
Lake water	33	68	63	31	10

Felip *et al.*, (1999) suggested that the transparency of ice, on high mountain lakes, can be greatly effected by the slush layers forming above it. They suggest that when the lake freezes a sheet of clear ice, referred to as 'black ice', forms on the surface and consequently, the salt concentration in the water beneath increases. As snow accumulates on the ice layer the stress produced causes the lake water to rise and flood the snowpack until a hydrostatic equilibrium is reached. This results in slush layers forming on top of the ice. If these freeze 'white ice' is produced, decreasing the light penetration. Therefore, it is not only the duration of ice-cover which may effect diatom productivity but the composition of the ice itself and the amount and timing of precipitation.

Much recent work has focused on the effect that ice-cover has on the ratio of planktonic to periphyton diatom species (Lotter and Bigler 2000; Smol 1988; Smol and Douglas 1996; Douglas and Smol 1994; Goudsmit *et al.*, 2000). It was shown in Hagelseewli, mentioned earlier, that ice-free conditions resulted in nutrient inflow, water exchange and phytoplankton growth. The resulting short productivity pulse was indicated by the growth of planktonic diatoms collected by sediment traps within the lake (Goudsmit *et al.*, 2000). Littoral species of *Fragilaria* and other periphytic taxa dominate the sediment traps during the periods of partial and complete ice-cover. In the ice-free period high accumulations of the planktonic diatom *Cyclotella comensis* were observed. It was shown that littoral *Fragilaria* sp. were transported to the centre of the lake as a result of sediment focusing and lateral water movement.

The influence of ice-cover on diatom plankton, however, is more likely to be indirect through its effect on lake mixing and nutrient limitation as key nutrients are unable to build up (Moss 1988). Possible effects of climate warming would be an increased ice-free period, with earlier ice break-up in the spring and later freeze-up dates, resulting

in increases in the length of growing season (Rouse, *et al.*, 1997). Changes, therefore, in the relative abundance of planktonic diatoms preserved in the lake sediment should reflect changes in the ice-cover regime of the lake (Ohlendorf, *et al.*, 2000). This is discussed further in section 1.4.1.2.

Ice-cover, large scale meteorological processes and diatom growth

Recently much work has focused on the effect of large scale meteorological processes on ice-cover (Anderson *et al.*, 1996b; Livingstone 1999a; Livingstone 1999b; Weyhenmeyer *et al.*, 1999). Due to the fact that ice-cover affects the diatom assemblages within a lake these large scale climatic changes are reflected in the patterns of diatom growth.

Weyhenmeyer *et al.*, (1999) observed that in Lake Erken in south-eastern Sweden considerable changes in the timing, and large variations in the composition, of phytoplankton spring peaks have been observed during the past 45 years and suggested that the NAO was responsible for these phytoplankton shifts. The NAO refers to the meridional pressure gradient between the high pressure system that lies around the Azores and the low pressure system that covers a broad area of the Atlantic arctic centered around Iceland (Hurrell 1995). The NAO is often defined in terms of differences in sea level pressure (the barometric pressure adjusted to the mean sea level) measured at stations close to the centres of the Azores High and the Iceland Low (Hurrell 1995).

It is represented by the tendency of the wintertime mean North Atlantic atmospheric circulation to oscillate between a strong and a weak state. The switches in sea level pressure from one to another state have numerous impacts including changes in the temperature regime (Plaudt *et al.*, 1995), west wind stress (Rogers 1997), winter precipitation (van Loon and Rogers, 1978) and the timing of lake ice break-up (Livingstone 1999). The NAO, therefore, exerts a strong influence on many of the physical parameters that are known to be important for the production of phytoplankton spring blooms.

Lake Erken is ice-covered for most of the year and ice break-up dates are available for

most years since 1954. In the study (Weyhenmeyer *et al.*, 1999) the concentrations of Chl *a* were used to assess the variations in maximum phytoplankton spring blooms. The variations in total Chl *a* seemed to be *independent* of ice-cover i.e. a high biomass was observed both when spring peak occurred below the ice and when it occurred after ice break-up. So phytoplankton as a whole was not affected by ice-cover. The diatom abundance, however, when separated out from the total phytoplankton appeared to be strongly correlated to ice-cover. A very low relative abundance of diatoms was observed at the time of the phytoplankton peak when the spring peak occurred below the ice. Therefore, if the peak occurs at or after ice- cover diatoms are the dominant species during the peak. If spring peak occurs while the ice is still on diatoms, as a percentage of abundance, decreases.

Both snow cover and the timing of the ice break-up are physical parameters that are known to be important for the occurrence of phytoplankton spring blooms. In the study these two parameters were also significantly related to the NAO. With high NAO values an increasing relative abundance of diatoms, during the spring peak, was observed and the spring peak was earlier. When their relative abundance decreased, dinoflagellates, became important. Limited water mixing, caused by the high NAO values, meant that the diatoms were not able to resist sedimentation. As the ice retreats the diatoms increase again and in comparison to the dinoflagellates. Over the last 45 years the timing of the ice break-up has shifted to an earlier date and the snow cover has decreased. Consequently, the timing of the phytoplankton spring peak occurs about 1 month earlier than 45 years ago.

In addition, changes in precipitation due to the NAO may cause ice break-up to be delayed because when snow falls earlier in the season ice becomes thicker due to the conversion of snow to ice and snow compaction (Vavrus *et al.*, 1996). In some studies precipitation during the ice-cover period was actually used as a surrogate indicator of ice thickness and thus the duration of the ice-cover (Koinig *et al.*, 2002). This is discussed further in section 1.5.1 with particular reference to changes in climate and the NAO in Norway.

1.3.3.2 The relationship between climate, water column mixing and diatom growth

Water-column mixing processes and thermal stratification are dominant controls on algal community structure (Sommer 1983; Reynolds 1984). They affect the distribution of algae in the photic zone¹ and the delivery and concentration of nutrients in the water column. Water column mixing and stratification is strongly affected by the ice-cover of the lake. Hence ice-cover changes will affect diatom production. This may occur for three reasons;

- Extended periods of ice-cover reduce the turbulence of a water body due to decreases in wind mixing.
- Temperature effects the water column stratification. Ice-cover will, therefore, affect the thermal stratification of the lake which controls deep water mixing.
- The stratification and mixing regimes significantly influence the nutrient supply in the lake.

These processes will influence the suspension of planktonic diatoms in the water column and production rates due to nutrient availability. Ice-cover prevents wind induced mixing of the water column. The water column will, therefore, become thermally stratified and, consequently, more stable (Spaulding *et al.*, 1993). In the ice-free season water stability breaks down. Reynolds (1984) suggests that as the water column becomes less stable physical controls, rather than biological controls, on the phytoplankton become more important. Physical controls, therefore, such as changes in water mixing depth and temperature become more important when the water stability decreases i.e. as a consequence of ice break-up.

The abundance of some diatoms are limited in the absence of mixing due to their dense silica walls, e.g. *Aulacoseira* spp. Phytoplankton production in lakes is therefore often seasonal exhibiting a spring maximum. This maximum is often dominated by centric diatoms in the non stratified spring season (*c.f.* Padisak *et al.*, 1998). These often sink to the hypolimnion with stratification of the lake or with ice-cover. Although convection currents do occur under the ice these tend to be weak (Spaulding

¹ The photic zone- the zone of water that ranges from the surface layer to a depth of light penetration corresponding to 1% of surface sunlight where net photosynthesis is zero.

et al., 1993). With extended periods of ice-cover planktonic diatoms, which rely on water column mixing, may be limited.

Agbeti *et al.*, (1997) studied the effect of frequent water column mixing on phytoplankton succession and species composition. They compared two lakes of different mixing regimes, Lake Opinicon and Upper Rock Lake, Kingston, Canada. Although they found that seasonal patterns of phytoplankton abundance were similar in the two lakes differences in species composition were apparent. In the dimictic lake (Upper Rock) lightly- silicified diatoms, such as *Rhizosolenia* and solitary *Fragilaria*, were more abundant. Other centric diatoms, excluding *Aulacoseira* species, were also present in the stratified system. As would be expected heavily- silicified diatoms, such as *Aulacoseira* species, were more abundant in the frequently mixed lake (Lake Opinicon). The difference in abundance of *Aulacoseira* was statistically significant between the two lakes. The lakes had similar chemical status and hence the high turbulence was thought to be the main factor controlling this abundance (Agbeti *et al.*, 1997).

Previous studies have also shown that high turbulence is needed to inoculate the water column with viable populations of resting *Aulacoseira* cells (Reynolds *et al.*, 1986; Miyajima *et al.*, 1994). *Aulacoseira italica* var. *subarctica*, for example, can be described as a meroplanktonic diatom species and live cells can survive in the sediments in a dormant state (Lund 1954). Mixing is needed to re-suspend these sediments and their resting cells and the maintenance of high turbulence is necessary to prevent further sinking. The species is, therefore, positively correlated to turbulence in lake systems (Lund 1954).

1.3.3.3 Changes in lake nutrient dynamics due to climate and the effect this has on diatom growth

Nutrient input to a lake is determined by the lake size, bedrock type, catchment size, catchment vegetation cover and human activity (Bronmark and Hansson 1998). Less productive lakes, therefore, are often situated at high altitudes, small in area with deep basins, in rocky upland catchments. In such systems nutrient limitation may limit diatom plankton growth (Moss 1988). Key nutrient ions such as phosphate, nitrate,

ammonium and sometimes silicate are not conservative, often fluctuating greatly over the year. In addition the demand for them by the living organisms is high relative to their supply (Moss 1988).

Pearsall (1932, cited in Hutchinson 1975) investigated the *seasonal* cycle of diatoms and claimed that the patterns were primarily due to nutrient concentrations, not light/temperature as suggested by Hutchinson (1975). He claimed that the dominant spring bloom species are replaced by a second species due to waxing nutrient levels. For example, *A. formosa* will appear first as this has higher nutrient requirements than *Tabellaria fenestrata* which will be abundant later in the season. This enables a species with a lower nutrient requirement to expand, and by so doing will further decrease the nutrients, and may finally replace the original dominant. A third dominant will then arise as the nutrient levels reach the limit of effective nutrition for the second dominant. Hutchinson indicates that factors such as parasitism may also be significant in the succession of the diatoms (Hutchinson 1975).

The competition of plankton for nutrients has been studied extensively in relation to Resource Competition Theory. The competitive exclusion principle (Hardin 1960) and the resource competition theory (Tilman 1977) have been major research paradigms and attempt to explain the patterns of distribution and succession seen in vegetation systems. According to the competitive exclusion principle organisms that overlap completely in the utilisation of a limiting resource are unable to coexist. The species, therefore, which is the most efficient at acquiring a limiting resource should displace all the competing species.

The pelagic zone of a lake represents a relatively uniform environment. According to the Gaussian principle of competitive exclusion, where a number of species will compete for the same resources with only slight differences in requirements, it would be expected that the pelagic zone of a lake would be dominated by one species in equilibrium. This 'tendency towards a unispecific equilibrium' does not seem to occur in the lake environment (Wetzel 1983b pg. 297). Although one species may dominant a large number of species co-exist within a lake at any one time. Under such relatively uniform conditions, species diversity is much higher than would be expected from

theory and mathematical derivations (Wetzel 1983a). In a lake ecosystem 30 species of phytoplankton, which have similar resource requirements, can generally coexist together (Bronmark and Hansson 1998). This inconsistency between theory and reality has been referred to by Hutchinson as the 'paradox of the plankton' (Hutchinson 1961).

The suggested reasons for this discrepancy are numerous. Some of the main reasons are summarised below;

1) Patchiness of resources in both space and time

Competitive exclusion is a relatively slow process and the physical conditions must be uniform for a relatively long period. For competitive exclusion to occur a time period of at least 25 days is needed. If these patches last between 10-25 days, competitive exclusion will not occur and the coexistence of numerous species will result (Bronmark and Hansson 1998).

Richardson *et al.*, (1970) showed that the rate of mixing was slow in relation to the reproduction rate of the plankton. This resulted in the development of several niches supporting many different species existing simultaneously. At any one time, therefore, many patches can exist in which one species has a competitive advantage over another. This would result in the existence of numerous 'dominant' plankton species at one time. Dominance of one species does not occur as the patches are mixed frequently.

2) Factors other than competition control plankton abundance

A species that under laboratory conditions may have displaced all other species may not be able to do so under the transient and heterogeneous environment of a lake. It may be vulnerable to low pH, or temperature fluctuations and its competitive ability may be compromised (Bronmark and Hansson 1998). Differences in natural enemies tend to reduce the competition process and exclusion does not occur (Hutchinson 1975).

3) *Diversity is maintained by disturbance*

This theory is partly related to that of patchiness of the system. Floder and Sommer (1999) suggest that diversity is maintained due to the intermediate disturbance hypothesis (IDH). Maximum diversity will occur if disturbance is intermediate, in both frequency and intensity, allowing coexistence of successful competitors and existence of competitively inferior pioneer species. They state that the former are not destroyed by the disturbances and the latter can find repeated opportunities for recovery after disturbance (Floder and Sommer 1999).

4) Some species occurring within the open water of a lake have resting stages in their life cycles (Lund 1954). They are excluded, therefore, from the competitive exclusion process and rest in the littoral zone sediments. Later the species may re enter the pelagic zone and represent a large proportion of the plankton community. This 'opportunistic expansion' usually occurs in relatively shallow lakes where the littoral zone is more extensive (Wetzel 1983b).

5) Tilman (1976, cited in Moss 1988) showed that co- existence of two species, competing for the same nutrient, may occur if the first species is more adept at taking up one nutrient and the other a second one, using culture experiments on *Asterionella formosa* and *Cyclotella meneghiniana*. The species could co-exist when the growth of each diatom species was limited by a different nutrient (*A. formosa* by phosphorous and *C. meneghiniana* by silicate). There will come a point when each species is limited by a different nutrient but each has similar requirements in terms of nutrients. The species are then able to co-exist.

The paradox of the plankton, therefore, is controlled by complex interactions of nutrients within the lake and competition between species of varying intensity. Changes in climate resulting in changes in ice-cover and nutrient supply, may therefore alter competition between planktonic species further and affect species diversity.

In addition changes in ice-cover may have a significant control over planktonic diatom growth due to their relatively high nutrient requirements. Kilman *et al.*, (1986) found

that many planktonic species, e.g. *A. formosa* and *A. subarctica*, need high nutrient concentrations implying that they will dominate in spring time when nutrients, especially dissolved silica, are highest. Consequently, with extended ice-cover, a late mixing period and early stratification abundances of *Aulacoseira* species will decrease. With an earlier ice break-up date mixing would be brought forward and probably more prolonged. With extended mixing periods pools of nutrients from the hypolimnion will be delivered to the surface waters (see section 1.4.1.2 Lake Saanajärvi example).

Nutrient availability appears, therefore, to be a dominant control over diatom plankton assemblages. Ice fluctuations will affect the nutrient variability due to its influence over lake mixing patterns. The date of ice-out and the duration of the spring overturn have a significant influence over the delivery of nutrients in ice-covered lake systems. With climatic fluctuations the delivery of nutrients to the lake from the catchment will also change, altering the diatom growth.

Reynolds (1998) suggests, however, that a ‘package of factors’ including basin morphometry, mixing dynamics, water clarity, and alkalinity, in addition to the size and nature of the resource base, will be important for plankton growth. The control that climate has over the nutrient regime should be seen as only one of these factors within the lakes nutrient system.

1.4 The detection of climatic change using palaeolimnology

It has been shown above that diatoms, and in particular planktonic diatoms, respond to climate, due primarily to indirect factors such as changes in the physical properties of the lake, mixing/thermal regime, habitat availability and chemical status. It therefore, follows that in colder years with increased lake ice-cover, the diatom assemblage and the productivity of the lake will be affected which will be evident in the lake’s sediment record. This is due to lower water temperatures, light limitation and biological habitat scarcity for open water/planktonic species. These changes in climate manifest themselves in the sediment record as, changes in chemical status, lake sedimentation rates, sediment composition and changing proportions of in-lake habitat availability reflected in the assemblage changes in the preserved lake biota. Many of

these factors are discussed and evaluated below, with particular reference to the potential use of diatoms as climatic indicators and the analysis of changes in lake sedimentation processes ('lithostratigraphy') to infer changes in climate.

1.4.1 Using the fossil diatom record to detect climate change

The fossil diatom record, preserved in lake sediment, can be used in numerous ways to infer changes in past climate both in a qualitative sense and through the quantification of climate change. Evaluation of diatom assemblages within the sediment record can provide two types of climatic proxy: changes in diatom species composition in response to water temperature changes (direct effects) and; records of biotic change in response to climatically-induced changes in lake processes other than temperature (indirect effects). Indirect factors may include changes in mixing regime/ wind patterns (Reynolds 1984; Agbeti *et al.*, 1997; Dean *et al.*, 1984), changes in nutrient supply (Catalan *et al.*, 2002b; Nickus *et al.*, 1998), changes in DOC/ light levels (Vinebrooke and Leavitt 1996; Bothwell *et al.*, 1994) and fluctuations in the duration of ice-cover (Lotter and Bigler 2000; Catalan *et al.*, 2002a; Korhola and Weckstrom 2000). Many of these factors are explored and discussed further below.

Firstly, however, it is important to establish to what extent the diatom record adequately reflects the status of a lake and whether diatoms from all the available lake habitats are adequately represented in the sediment record.

1.4.1.1 Diatom frustule preservation and habitat representation within the sediment record

Many studies have shown that diatoms derived from many different areas of the lake (e.g. littoral, planktonic, epilithic) are adequately represented within the lake sediment record (Cameron 1995; Jones and Flower 1996; Haworth 1980) and that even short lived fluctuations in the diatom community are recorded in the sediment profile (Cameron 1995). However, taphonomic processes, i.e. the process of transformation of a life assemblage of biological organisms in to a fossil one, may effect the representation of diatoms within the sediment and is, to a certain extent, lake specific. Dissolution of diatom frustules for example are affected by sedimentation processes, ionic composition, turbidity and sediment mixing (Ryves 1994). However, in high

altitude freshwater lake systems with relatively low pH, dissolution of diatom frustules is normally limited and creates few problems for the palaeolimnologist.

Furthermore, lake morphology will effect the sediment deposition and the potential for re-suspension of sediment. The accurate dating of the sediment record, and the development of a chronology, can help to eliminate some aspects of sedimentation disturbance and is an essential tool in palaeolimnological studies in order to identify sediment accumulation rates and to track the timing of events. Dating of recent sediments is normally achieved by the analysis of ^{210}Pb (Appleby and Oldfield 1983; Appleby and Oldfield 1978; Appleby *et al.*, 1986, see also section 3.2.8). For older sediment radiocarbon (^{14}C) dating techniques (not used in this study) are used (Goh 1991). The next section explores how the diatom record can be used in a qualitative way to make inferences about changes in past climate.

1.4.1.2 Qualitative inferences

Diatom assemblage change related to changes in micro habitat

Many palaeolimnological studies have related shifts in the ratio of planktonic to non planktonic diatom species to changes in climate, both during the Quaternary and occurring due to recent climatic warming.

Hickman and Reasoner (1998) when studying changes in diatom flora in relation to climate in Crawfoot Lake, Alberta, showed that peaks in the planktonic species *Cyclotella radiosa* corresponded to the warmest Holocene interval. A similar peak was also seen in Lake O'Hara and Mary Lake sediments (Hickman, 1994). It has been suggested that planktonic diatoms may need a water temperature of 10°C or higher (Stoermer and Ladewski 1976, Pienitz, *et al.*, 1995) suggesting that changes in lake water temperature may be responsible for the increases in these species at this time. In addition Wetzel (1983) suggests that the diversity of plankton increases as the waters warm. However, Hickman and Reasoner (1994) suggested that the relationship of the planktonic species to climate may in fact be indirect due to changes in nutrient levels via vegetation changes during the Holocene and fluctuations in ice-cover duration.

According to Smol (1988) it is unlikely that the slight difference in water temperature between warm and cold years would cause a direct response in the diatom community. Diatoms, however, due to their life strategies, (e.g. planktonic, benthic, periphyton etc.) are specific indicators of microhabitat (Smol, *et al.*, 1991). Changes in ice-cover should produce changes in microhabitat and consequently changes in diatom assemblages (see also section 1.3.3.1).

Smol (1982, 1988) has worked extensively in the Canadian Arctic investigating the effect of ice-cover on microhabitat in small relatively shallow lake systems. He suggests that during warmer periods greater areas are available for benthic diatom production. As the lake warms the ice may disappear from the lake completely, enabling the growth of phytoplankton. With an extended length of ice-cover period only the littoral area is available for algal growth. The development of planktonic diatoms may, therefore, be precluded by extensions in the period of ice-cover which will be evident in the sediment record.

He proposes that a 'moat effect' will be produced as the lake ice thaws around its edges creating shifts in available habitats. Although the actual differences in water temperature between warm and cold years may be slight the marked changes in ice/snow cover on the lake will be reflected in the preserved diatom community (Table 1.3). The effect may be most visible in relatively shallow, small lakes which have a large littoral habitat. This moat effect, however, is also evident in deeper lake studies. For example, the diatom record from the 56cm core from Baird Inlet, Ellesmere Island, Arctic Canada a small, deep closed basin lake also reflected these fluctuations in ice-cover (Smol 1983).

In a similar palaeolimnology study on Amarok Lake, Baffin Island N.W.T. Canada, Wolfe (1994) related the succession of planktonic diatoms to the effect of ice-cover and habitat availability. In the cores the planktonic diatoms dominate in the sediment zone representing the Late Wisconsinan period. Although little is known about the nature of the Late Wisconsinan regional climate it is suggested that the increase in *Aulacoseira* species is connected to the increases in ice-free summers creating sufficient turbulence to support the species. These thickly silicified diatom species

require a considerable amount of wind induced turbulence to maintain their position in the photic zone and, therefore, require a relatively long fetch of open ice free water.

This suggests that the late Wisconsin was a period of increased run-off hastening ice break-up and increasing supplies of silica resulting in increased *Aulacoseira* abundance.

Table 1.3: Climatic changes and the corresponding response in the diatom community (Source, Smol 1988)

Climate	Lake Conditions	Diatom response
Cold	Extended ice/ snow cover, very small moat	-aerophilic diatoms and taxa characteristic of very shallow water; low diatom production
Moderate	Moderate sized moat	Diatoms characteristic of deeper waters; moderate production
Warm	Pelagic region of lake is ice free	Progressively more deep water and planktonic taxa; relatively high production as larger area available for photosynthetic growth

Lami *et al.*, (1998) analysed the lake sediments from two remote high mountain lakes in Nepal. Both lakes were located above the permanent treeline and lay between 4800 and 5200m a.s.l., were relatively small and typically ice-covered for *ca.* 9-10 months of the year. Hence any changes in ice-cover were thought to be significant for these lake systems and that this would be reflected in the diatom composition. Inferences about the past climate were made using the diatom record including:

- *ca.* 2900 to 2200- 2000yrs BP- high abundance of *Aulacoseira valida* and *Cyclotella lacunarum*, indicating relatively warm fluctuating conditions. This was also mirrored by the pigment record and;
- 2200 and 750 yrs BP -increases in *Navicula schmassmannii* and small *Fragilaria* spp. (especially at *ca.* 1800-1000 yrs BP), indicating a colder period with fluctuations

The diatom and pigment records were compared with fluctuations in glacier extension in the area. It highlighted that some of the diatom inferred warmer periods did in fact coincide with the retreat of glaciers in the area, but there were some discrepancies.

In addition further work conducted on Hagelseewli lake in Switzerland has linked diatom production to climate through changes in habitat availability, (Ohlendorf, *et*

al., 2000; Lotter and Bigler 2000). The lake ice thaws from the North end of the basin due to the high shading at the southern end from the cliff face. The diatom assemblages in the surface sediments reflect the morphological zonation of the lake with periphytic *Fragilaria pinnata* assemblages dominating in the shallow areas, whereas the deeper parts are dominated by planktonic *Cyclotella comensis*. This suggests that growth of planktonic deeper water *Cyclotella* species would be limited in extended ice-cover periods.

Diatom analysis of the sediment cores from the lake and extensive surface sediment samples, show several changes between assemblages dominated by planktonic diatoms and those dominated by periphytic species. In conjunction with the sediment trap data, the authors suggest that these changes in the ratio of planktonic to periphytic diatoms down core may indicate periods of changing ice-cover length for Hagelseewli (Ohlendorf *et al.*, 2000; Lotter and Bigler 2000).

Furthermore, Wathne *et al.*, (1993) hypothesise that the absence of planktonic diatoms in the sediment cores of several high mountain lakes (Ovre Neådalsvatn in Norway, Lochnagar in Scotland, Etang d' Aube and Lago Paione Superiore) may be related to a combination of processes linked to ice-cover. These included extended periods of ice-cover and the low nutrient concentration and circulation.

Sporka *et al.*, (2002) found that in a high mountain lake in the High Tatras, Slovakia (Lake Nizne Terianske-Pleso), that diatom assemblages changes down core were reflecting possible changes in climate. The lower portion of the core was dominated by *Asterionella formosa*, *Fragilaria construens*, *Fragilaria pinnata* var. *pinnata*, and *F. tenera* which have been associated with deep, cold lakes in high latitudes (Juris & Kovacik, 1987, cited in Sporka *et al.*, 2002). In the upper layers of the sediment, species such as *Achnanthes marginulata*, *Achnanthes subatomoides*, *Navicula schmassmannii* and *Neidium bisulcatum* dominate. These species are often associated with shallow lakes in lower latitudes with higher mean annual temperatures, suggesting that the lake has undergone warming in recent years.

Finally, many palaeolimnological studies have related the increases in planktonic

diatom species over recent decades to climatic warming (Korhola and Weckstrom 2000; Korhola *et al.*, 1998; Sorvari and Korhola 1998; Rautio *et al.*, 2000; Catalan *et al.*, 2002a; Lotter and Bigler 2000). Many of these have indicated that the significant increases in the small *Cyclotella* sp. are correlated with recent climatic warming and a subsequent reduction in lake ice-cover (e.g. *C. comensis* Lotter and Bigler 2000 and Rautio *et al.*, 2000, Sorvari and Korhola 1998, *C. pseudostelligera* Catalan *et al.*, 2002a).

Diatom species richness

Anderson *et al.*, (1996) suggested that there was a positive relationship between diatom species *richness* and summer temperature evident in the palaeolimnological record. The response of lake biota to changes in temperature was analysed in the varved lake sediments of a northern Swedish lake (Kassjön, Våsterbotten). The results showed that catchment disturbance processes controlled diatom *productivity*, but that diatom species *richness* was related to shifts in temperature.

A clear decrease in diatom richness occurred when summer temperatures, inferred from tree ring analyses, were at a minimum (AD 1610-1620). Using Redundancy Analysis (RDA, see section 3.3.2.3) of diatom species richness, 23.1% of the variance was explained by summer temperature. This relationship between summer temperature and species richness was also observed by Simola *et al.*, (1990, cited in Anderson *et al.*, 1996) in a varved Finnish lake with a decline in richness also in AD 1601 suggesting that the response may be regional. A time lag, however, of twenty years was observed for this relationship. This may be related to the catchment- soil biogeochemical interactions such as changes in nutrient cycling.

Diatom productivity has been related to the extent of summer lake ice and snow cover (Smol and Douglas 1996; Smol 1983; Smith 2002; Anderson *et al.*, 1996a). High absolute diatom abundance has been correlated with 'warm' summers and low abundance with 'cold' summers especially in areas of low diatom productivity (Smith 2002). In addition, as noted earlier Wetzel (1983) suggested that the diversity of the plankton increases with increases in water temperature which would also be reflected in the sediment record.

Diatom assemblage change related to water column mixing and changes in nutrient regime

Dean *et al.*, (1984) suggested that the peaks of *Aulacoseira* sp. in the sediment core of Elk Lake, Minnesota suggest periods of increased duration and intensity of spring circulation and summer turbulence. They suggested that changes in *Aulacoseira* may reflect short term changes in the limnology of the lake driven by changes in climate.

Bradbury and Dieterich-Rurup (1993) continued this work and used the relationship between the lake circulation patterns, nutrient delivery and diatom assemblages, in Elk Lake, Minnesota, to reconstruct climate change using the diatom record. They suggested vertical mixing of the water column brings nutrients from the deep water to the surface. An extensive palaeolimnological study highlighted how the shifts in planktonic species indicated shifts in limnological conditions and subtle changes in nutrient supply governed by climatic conditions (summarised in Table 1.4).

Bradbury and Dieterich-Rurup (1993) suggested that an extended spring mixing would result in long periods of high phosphorous values in relation to silica values. This would result from phosphorous regeneration from the hypolimnion. By looking at the changes in species with differing Si:P ratios a palaeolimnological proxy for the duration of spring mixing could be found. As Kilham *et al.*, (1996) noted, however, this method should only be used where there is an extensive knowledge of the specific lake system, its mixing regime, nutrient and climate interactions.

Table 1.4: Shifts in the main planktonic diatoms species in Elk Lake and the suggested climatic reasons for the changes in abundance throughout the core (Source, Bradbury and Dieterich-Rurup 1993)

Species increases	Species characteristics	Implied climatic conditions
<i>Stephanodiscus minutulus</i>	Blooms in early spring due to extended and deep circulation providing abundant phosphorous	-cold dry climate in late spring and early summer
<i>Fragilaria crotonensis</i>	Typically a summer and early fall diatom, prosper when silica is high in comparison to phosphorous, i.e. in shortened spring circulation.	-hot summers with frontal storm activity - high moisture and warmer climates
<i>Aulacoseira ambigua</i>	Prosper in turbulent conditions and high nutrient conditions, especially silica	- high summer turbulence probably associated with increased winds and storms

Korhola *et al.*, (1998) who analysed the response of Lake Saanajarvi, in Finnish Lapland, to climate change also suggested that the thermal stratification of the lake has intensified due to climate warming and that this could be detected using the diatom record. The lake is above treeline, nutrient poor and isolated from human disturbance. They suggested that during the Little Ice Age the lake was only weakly thermally stratified during summer. In recent years with the increase in air temperature, and the consequent rise in the temperature of the epilimnion, a steep summer stratification has developed in the lake. This steeper thermocline would have produced increased thermal stability and consequently more turbulent conditions in the upper waters and in addition changes in nutrient availability.

The changes produced more favourable conditions for phytoplankton growth, causing a replacement of benthic species with planktonic. The change is clearly shown in the diatom record with a large increase in planktonic centric diatoms at *ca.*1900. The strong summer stratification of the lake is unusual for the area with most tree line lakes staying unstratified throughout the summer.

1.4.1.3 Quantitative inferences

Using diatoms to directly infer past climatic conditions

Recently much work has been conducted to explore the potential use of diatoms to directly reflect changes in air/ water temperatures and to quantify changes in past climate. The accuracy of these diatom derived reconstructions, developed using the 'transfer function' approach, is discussed below.

As discussed above climate can effect the diatom assemblage of a lake significantly and climate changes will be reflected in the diatoms preserved in the lake sediments. Increasingly attempts to *quantify* these changes in climate have been made using diatom derived temperature 'transfer functions'. It has been shown that the response of diatoms to changes in climate may be indirect or direct. The quantification of their response may, therefore, be a reflection of either indirect or direct processes.

The most responsive areas to climate change are those with steep climatic gradients often near major ecotones or treelines (Weckstrom *et al.*, 1997). Major climate shifts

in these areas are expected to generate large changes in biota. Climatic transects can be used to evaluate the differing effect of temperature on diatom distribution. The following studies have attempted to quantify the changes in climate by the development of temperature transfer functions derived from the diatom fossil record taken from lakes covering a climatic gradient.

A transfer function is a 'set of equations formalising the relationship between species abundance and one or more environmental variables' (Charles *et al.*, 1994). The process contains two steps: the creation of a modern training set and the calculation of the transfer function and; the application of the transfer function to the fossil assemblage in the core. The transfer function approach uses weighted averaging regression equations (WA) and calibration techniques to reconstruct or infer an environmental variable from diatom data (ter Braak 1987; Birks 1995, see also section 3.3.3 for further transfer function discussions). The approach can potentially enable *quantification* of biotic responses to climate change and recent studies using this approach are discussed below.

Pieinitz *et al.*, (1995) studied the surface sediment diatom assemblage from 59 lakes located in the Yukon and Northwest Territories, Canada. Using statistical techniques (CCA, see section 3.3.2.4) they showed that maximum depth and July surface water temperature accounted for most of the variance in the diatom data. They used this information further to develop a statistical model, based on weighted averaging regression and calibration techniques, to predict surface water temperature from diatom assemblages.

The model's prediction for lake temperatures correlated well with actual measured water temperatures for the lakes, with a Root Mean Squared Error (RMSE) of 1.84-2.0°C. They stressed, however, that an expansion of the data set is needed to decrease the error and that the study is area specific to the Canadian Arctic.

Korhola and Weckstrom (2000) evaluated the relationship between environmental variables and surficial sediments from 38 lakes in the Northern Scandinavian subarctic. The lakes were in general oligotrophic, clear water, non-stratified drainage

lakes. The analysis showed that mean July air temperature accounted for a statistically significant proportion of the variance in the diatom data. Mean July air temperature was reconstructed using WA-PLS with a temperature reconstruction error (RMSEP-Root mean squared error of prediction) of 0.9- 1.1°C.

In a similar way Rosen *et al.*, (2000) used a surface sediment training set from 50 lakes in Northern Sweden to reconstruct mean July temperature. The resulting WA-PLS model resulted in an reconstruction error (RMSEP) of only 0.86°C. Bigler and Hall (2002) also used diatoms to reconstruct mean July air temperature by modelling the relationship between climate and diatoms in the surface sediment of 100 lakes in Swedish Lapland and created an inference model with a reconstruction error of 0.96°C.

Lotter *et al.*, (1997) explored the potential of several different aquatic organisms for the quantification of climate change in the Central Alps. The 68 study sites spanned an altitudinal range in the Swiss Alps. They discovered that a strong relationship existed between air temperatures and diatom inferred temperature with a RMSEP of 1.62°C. The authors concluded that the training set compared favourably with the RMSE of similar inference models for diatoms and surface water temperature and that the potential of diatoms as palaeoclimatic indicators was considerable.

The quantification of the response of diatoms to changing climate may be due to direct or indirect processes acting to change assemblages. The timing and intensity of thermal stratification, the length of ice-cover period, turbidity and light penetration are all factors that are often climatically driven and changes in them may affect diatom composition. It is assumed, therefore, that climatic change can be reconstructed via analysis of the diatom assemblage changes down core.

These transfer functions have been shown to have relatively low error reconstruction values, but it should be remembered that an error value of even 0.5°C represents a significant shift in terms of temperature and, in relation to interglacial periods and recent climate change the scales of climate change are not dissimilar to the error of the transfer function prediction (Battarbee 2000). In addition these climatic

reconstructions will most probably only work in areas where climate may be the dominate control over biotic processes and/ or conducted over strong climatic gradients. In some areas other environmental processes may control diatom assemblages more, such as pH, which would mask the influence of climate on the diatom record (Anderson, 2000). It might, therefore, be more appropriate to use these diatom inferred temperature transfer functions in conjunction with other climate proxy methods and by using *a priori* knowledge of diatom ecological preferences as discussed above (section 1.3.3).

Using diatoms to infer changes in other chemical parameters occurring due to climate change

Diatom inferred reconstructions of other chemical parameters can also be used to help make inferences about past climate. Dissolved organic carbon (DOC) and Total organic carbon (TOC) are both factors which change with climate fluctuations, due to changes in soil development, catchment vegetation and erosion rates. DOC and TOC are measurements of the amount of organic carbon in the water column and are often directly related to the light availability within the lake (see section 4.6.2 also). This relative turbidity will affect light penetration due to changes in the filtering of light and the type and density of suspended material (Patrick 1977). This has implications for both planktonic and periphytic diatom growth (Korsman and Birks 1995; Vinebrooke and Leavitt 1996; Williamson *et al.*, 1996; Leavitt *et al.*, 1999).

In addition, with increasing DOC levels the amount of organic acids delivered to the lake will increase, due to increased organic decomposition, lowering the water pH. The reconstruction of DOC using transfer functions can assist in past climatic interpretation because it enables a distinction to be made between changes in acidity due to catchment/natural changes or to anthropogenic pollution (see Leavitt *et al.*, 1999; Philibert and Prairie 2002; Enache and Prairie 2002; Ruhland and Smol 2002; Pienitz and Smol 1993).

The effect of changes in pH on diatom communities has been extensively studied and the diatom record has been used to infer past pH conditions with great success, resulting in small error estimates for the reconstructed pH (Birks *et al.*, 1990;

Cameron *et al.*, 1999; Renberg and Hultberg 1992; Stevenson *et al.*, 1991; Jones *et al.*, 1989; Rosen *et al.*, 2000b; Weckstrom *et al.*, 1997). In addition, many studies have directly related shifts in pH to climatic fluctuations in high altitude soft water lakes systems (Psenner and Schmidt 1992; Leira and Santos 2002, Sommaruga-Wogarth *et al.*, 1997; Schmidt *et al.*, 2002; Wolfe 2002), with warm and dry years correlated to high pH and cold years with long periods of ice-cover, correlating with decreases in lake water pH.

Wolfe (2002) showed that lake pH declined in accordance with Neoglacial cooling through the analysis of the diatom record on dated lake sediments from two lakes situated in the Arctic. In a similar study Schmidt *et al.*, (2002) related warm and dry periods between 7000 and 5000 cal BP to rises in the lake pH of a high altitude Austrian lake. Lower pH levels were correlated with cool and wet periods between 5000 and 1400 cal. BP associated with extended periods of snow cover in the area. Leira and Santos (2002) also correlated long ice-cover durations and cold conditions in an Iberian lake with a period of low water pH during the Holocene.

The link between changing air temperature and lake pH have also been evaluated for more recent time periods through the analysis of surface samples in 57 remote alpine mountain lakes (Sommaruga-Wogarth *et al.*, 1997). It was concluded that changes in pH were driven by temperature effects, rather than acid deposition in such remote locations, through its control over weathering rates and changes in biological activity.

Psenner and Schmidt (1992) demonstrated that the acidity of two soft water, high altitude lakes in the central Alps was correlated with regional temperature during the entire nineteenth century. Colder years were correlated with lower pH and vice versa. The process was controlled by the temperature dependency of the in-lake processes governing alkalinity generation within these soft water systems. One suggested mechanism for this is the longer ice free season with increased light availability and water temperatures, coupled with reduced precipitation and, therefore, an increase in water retention times, resulting in an increase in biological activity and the potential for in-lake alkalinity generation and a subsequent increase in pH (Sommaruga-Wogarth *et al.*, 1997). The climate/ pH relationship breaks down towards the end of

the twentieth century as anthropogenically derived acid deposition caused a rapid decrease in pH which could not be linked to climate. The study demonstrates, however, that high mountain lakes, which have limited anthropogenic catchment disturbance, and are situated in areas of relatively low acid deposition provide perfect palaeoclimate pH archives. The reconstruction and use of pH in order to make climatic inferences is discussed further in Chapter 5.

1.4.2 The use of lithostratigraphic analyses to detect changes in climate

The previous two sections have demonstrated how diatoms can be used to make inferences about climatic change. Changes in the lithostratigraphic record of a lake can also be interpreted in a similar way. Within lake productivity changes may be due to nutrient enrichment, possibly from a direct input from an anthropogenic source or changes in erosion, and/ or lake temperature changes linked to higher biomass production at higher temperatures and a longer open water season. In high altitude lake systems direct anthropogenic input of nutrients is minimal as the catchments are not used for agriculture, or densely inhabited.

Catchment productivity can often be related to climate change through vegetation assemblage shifts and changes in erosion, resulting from variation in the extent of bedrock weathering, and alterations in catchment thaw governing overland in-wash. Productivity within the catchment can also be related to anthropogenic interference (afforestation etc.), or catchment disturbances resulting in changes in erosion rate and the delivery of nutrients to the lake system.

Patterns in %LOI, used as a measure of organic matter, of sediment sequences have often been used as direct proxies of palaeoclimate variability (Levesque *et al.*, 1993; Willemse and Tornqvist 1999; Schindler 1990; Battarbee *et al.*, 2001; Battarbee *et al.*, 2002a) and %LOI profiles have also been used to track past glacial activity in glaciolacustrine sediment cores (Matthews *et al.*, 2000b; Nesje *et al.*, 1995a; Nesje *et al.*, 2001b; Nesje *et al.*, 1991; Nesje *et al.*, 1994; Nesje and Dahl 2001; Sletten *et al.*, 2002).

These studies assume a strong link either, between in-lake productivity and

temperature, or between climatic oscillations and changes in the lake's catchment, recognised through changes in the mineralogy of the lacustrine sediment sequence. Interpretation of the %LOI sequence is, however, complex due to the various inputs of inorganic matter (e.g. silts, biogenic silica, carbonates) which may change with climatic alterations. Furthermore, production and input of organic matter due to changes in lake productivity and allochthonous inputs will also be altered due to changes in climate and differences in the preservation of organic matter.

For remote mountain lakes, however, whose catchments are sparsely vegetated with thin soils, small and insignificant inflow streams and limited macrophyte production, the %LOI signal may be easier to interpret. In addition, in many of these high mountain lakes the organic matter preservation may be better than in lower altitude systems due to the reduced hypolimnetic oxygen concentration, due to long periods of ice-cover and summer stratification in deep lakes. Warmer climate should result in increased primary production both within the lake, due to recycling processes (Catalan *et al.*, 2002b), and within the catchment, and, therefore, result in higher %LOI.

The discussion above has highlighted how preserved diatoms and lake productivity shifts can be used to infer past climate conditions. In order to establish to what extent the palaeolimnological record can actually be used to represent shifts in climate it can be useful to analyse a sediment core from a lake which has been known to experience fluctuations in recent climate. Over the last 800 years in Europe two significant climatic trends have been detected/ recorded;

- 1) Recent climatic warming- indicated by the instrumental record (see sections 1.5.1 and 6.3.1 and 7.3.1)
- 2) Climatic cooling/ weather alteration associated with the 'Little Ice Age' (LIA)
- indicated by documentary evidence and independent climatic proxies (see section 1.5.1).

The next section describes the extent and magnitude of these climatic events, with particular reference to central Norway, an area known to have been significantly affected by the LIA.

1.5 Climatic changes in Europe over the last 800 years

Throughout most of Europe the conventional view of climatic change over the past 800 years followed the pattern of a 'Medieval warm period' (MWP), which was superseded by a cool 'Little Ice Age' (LIA) and then warming since the later part of the 18th century until the present (Lamb 1979; Lamb 1966). Generally the MWP was thought to be a period of high temperatures during the 11th -13th century (Lamb 1979; Grove 1988a). The evidence for a long lasting globally uniform, warm period is, however, often contested (Hughes and Diaz 1994; Crowley *et al.*, 2000; Hughes and Graumlich 1996). In terms of the scale of the change recent evidence, based on Greenland borehole temperatures, estimate temperatures to have been 0.5- 1°C above 1970 mean temperatures during the MWP (Dahl-Jenson *et al.*, 1998). In addition high latitude tree ring data show temperatures in the MWP well above, at least in the summer months, the 20th century mean (Briffa 2000). Leaving the debate about MWP *temperature* changes aside it would seem that there were changes in precipitation during MWP, with many areas experiencing protracted drought episodes (Stine 1998).

Like the MWP the severity and extent of the LIA, that followed it, is also debated. It was thought to not be uniformly global, and its initiation and termination dates differ substantially due to regional differences (Grove 2001; Williams and Wigley 1983b; Williams and Wigley 1983). Commonly dates for the LIA are quoted as ~A.D. 1550-1850 (Bradley and Jones 1992). This is discussed further in the following section, with particular reference to the timing, extent and duration of the LIA in Scandinavia.

In the period after the LIA, temperatures in Europe have risen and unprecedented warming has occurred over the latter part of the 20th century and, it would appear, that this has been almost universal. Nicholls *et al.*, (1996) observed that the global mean temperature has increased by 0.3 to 0.6°C over the late 20th century to 1995, and by 0.2 to 0.3°C during the period 1940 -1995.

It has also become apparent that inter-annual and decadal variations in North Atlantic climate are closely linked to the North Atlantic Oscillation (NAO, see section 1.3.3.1 for definition). The regional moisture balance and the tendency for severe winter storms in Europe are governed by the state of the NAO due to its control over the

westerly air flows. The late 20th century has experienced a very variable NAO, including an unprecedented period of high NAO index winters between 1998-1995 (Cullen *et al.*, 2001). This has led to unusual warmth and storminess across Europe in recent decades.

Norway represents a useful location for palaeoclimate study due to its high abundance of relatively undisturbed lake systems and its relatively long and accurate climate instrumental records. In addition, it is an area which has well documented evidence for the occurrence of the LIA. The next two sections discuss the climatic history of Norway over the past 800 years.

1.5.1 Climatic changes in Norway over the last 800 years

20th century climate change in Norway

Typically instrumental records for central Norway extend back approximately 150 years providing a useful mechanism for the validation of palaeoclimate reconstructions. It was noted above that temperatures have increased globally over the latter part of the 20th century, and this is also the case within Norway. During the period 1876- 1997 there was a positive mean annual increase in temperature trend everywhere in Norway (Hanssen-Bauer *et al.*, 1996). In most regions this temperature increase lies between 0.4 and 1.2°C, with significant increases in the periods from 1876 to the 1930s, and the 1960s and/or the 1970s in particular. The maximum annual temperatures are found around 1935 and/or 1990 (Hanssen-Bauer *et al.*, 1996).

Recent changes in precipitation within Norway have also been linked to the changes in the NAO index over the last few decades. In the 1990s there was a period of high winter precipitation (strongly positive NAO index) resulting in the large glacial advances for the outlet glaciers from Jostedalsgreen (see Figure 1.2 for glacier location) despite the increases in annual temperature (Hurrell 1995; Nesje and Dahl 2002).

Evidence of climatic change associated with the ‘Little Ice Age’ in Norway

Traditionally the dates given to the LIA period in Europe are 1550 -1850 (Nordli 2001; Jones and Bradley 1992). Reconstructions of glacier variations show that most

Scandinavian glaciers reached their LIA maximum approximately 1750 (Nesje *et al.*, 1991; Nesje *et al.*, 1995b; Matthews 1991; Matthews *et al.*, 2000a; Winkler 2003), (see Figure 1.2), based on glaciolaustrine evidence, lichenometry and glacier mass balance studies. Glacier advance in this period was significant and estimated to be approximately 100m annually for Nigardsbreen, an outlet glacier from Jostedalbreen, in Western Norway (Nesje *et al.*, 1991; Matthews *et al.*, 2000a; Nordli *pers.com*, Nordli *et al.*, 2003 in press See Figure 1.2).

The cause of the great Norwegian glacial advances in the mid 18th century were thought to be lower annual temperature and, therefore, lower glacier ablation rates (*c.f.* Matthews and Karlen 1992). Recently, however, evidence from proglacial lakes has shown that the rapid glacier advance in Southern Norway was mainly due to increased winter precipitation and not only lower summer temperatures (Nesje and Dahl 2002, Nordli *et al.*, 2003 in press). These mild wet winters have been associated with the prevailing positive NAO weather mode for the period covering 1690-1750 (Luterbacher *et al.*, 1999; Luterbacher *et al.*, 2000, see Figure 1.2).

The link with the NAO index accounts for the asynchronous LIA in Scandinavia and the Alps. In the Alps the glaciers reached their Little Ice Age maxima in the *ca.* 1850's (Grove 1988b). This is attributed to multi-decadal trends in the north- south dipole NAO pattern. Positive NAO index winters are related to above normal precipitation over Britain, Iceland and Scandinavia, and below normal precipitation over central and southern Europe and the Mediterranean region (van Loon and Rogers 1978), resulting in glacier advances being asynchronous between the Alps and Scandinavia. The NAO index variations are reflected in the mass balance records and estimates of Scandinavian and Alpine glaciers (Six *et al.*, 2001; Nesje *et al.*, 2000; Nesje *et al.*, 2000, Nordli *et al.*, 2003 in press).

In addition, tree ring reconstructions for eastern and Northern Norway (Kalela-Brundin 1999; Briffa 2000) indicate that summers in the early 18th century were not cold enough to explain the huge glacial advance in Western Norway (Nesje and Dahl 2002). The summer temperatures were estimated to be about 0.5 to 1.0°C lower than today (Matthews *et al.*, 2000a).

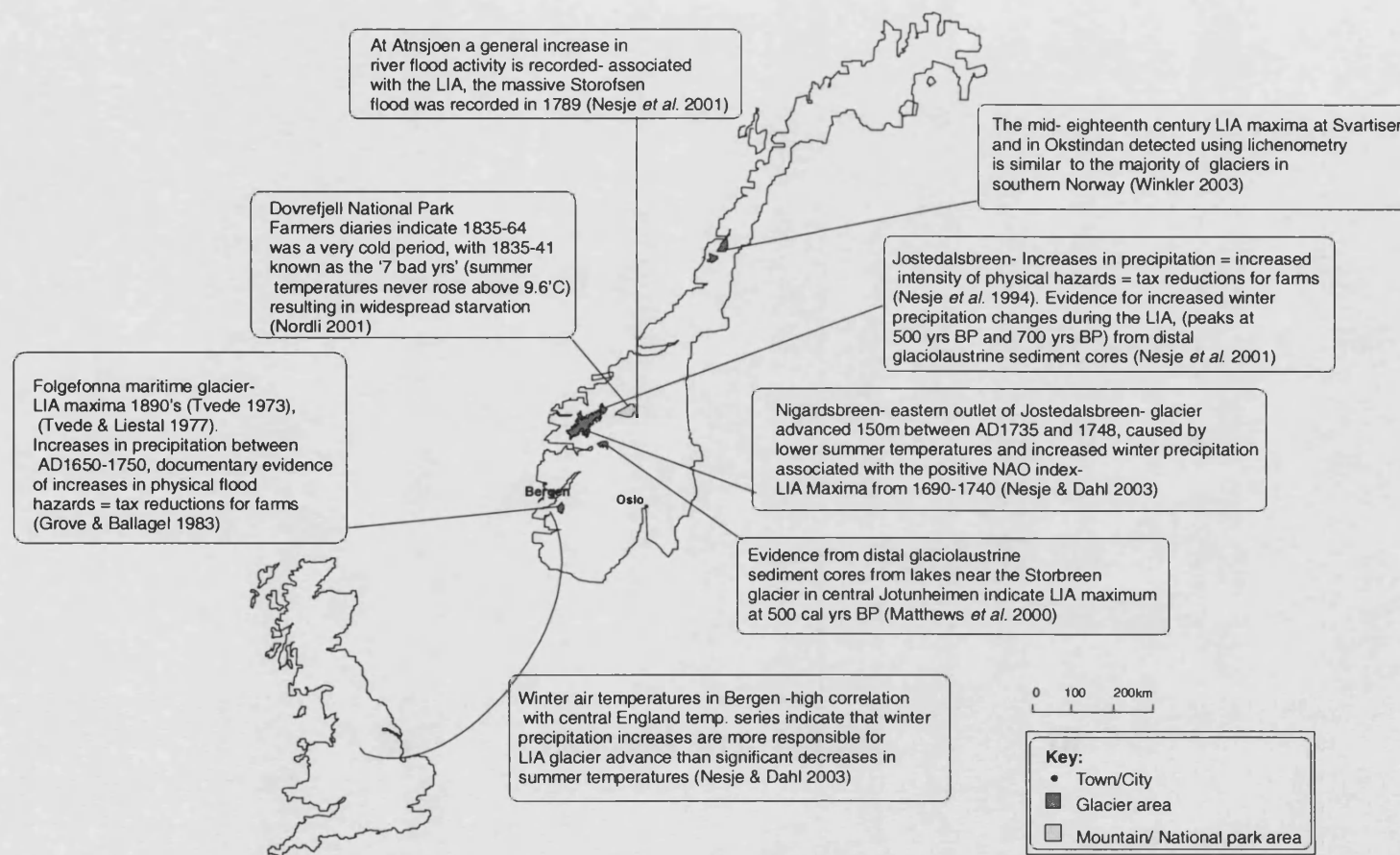


Figure 1.2: Summary diagram illustrating evidence of climate changes during the LIA in Norway (Adapted from various sources including: Nordli 2001; Nordli *et al.*, 2003 in press, Nesje *et al.*, 2001b; Nesje and Dahl 2003; Nesje *et al.*, 1991; Matthews *et al.*, 2000b; Nesje *et al.*, 2001a; Winkler 2003; Nesje *et al.*, 1994; Grove and Battagel 1983; Tvede 1973; Tvede and Liestol 1977).

Furthermore, the Central England winter temperature record (Parker *et al.*, 1992; Manley 1974), indicates a significant *rise* in winter temperature in NW Europe in the first half of the 18th century resulting in mild and wet winters (*c.f.* Ingram *et al.*, 1978; Glueck and Stockton 2001).

Further evidence of an unstable climate during the LIA is recorded in the flood records for the central Norwegian area. As Norway recovered from the LIA the amount of water released from snow pack thawing and glacier retreat caused many major flooding events in the region. One such event in 1789, the ‘Storofsen’ flood event, is recorded in a sediment core from Atnsjoen in eastern Norway (see Figure 1.2 for location). These flood events caused major changes to erosion patterns and sediment supply to lakes and rivers in the area (Nesje *et al.*, 2001a).

Documentary evidence of the latter part of the LIA exists in the form of Norwegian farmers’ diaries dating back to 1800 (Figure 1.2). Direct weather descriptions, dates of the commencement of spring work, first day of haymaking, the first day of grain harvest and fluctuations in farming taxes have been used to infer 19th century summer temperatures (Nordli 2001, Nordli *et al.*, 2003, in press). These have shown that a climate deterioration took place in the middle of the 19th century with the coldest period recorded for 1835-64 for the Kjøremsgrendi reconstruction, in the Døvre mountains (See Figure 1.2 for location) causing glacial re-advance and extensive starvation. The date of the termination of the LIA in Norway is debated but temperatures in Scandinavia were thought to rise again at approximately *ca.*1800-1850 (Nesje *et al.*, 1991; Korhola and Weckstrom 2000).

Evidence suggests, therefore, that central Norway experienced a combination of colder summers and more snow fall (i.e. rises in precipitation), but not overly cold winters during the LIA. These changes would have impacted significantly on the thermal/ice-cover regime of lakes in central Norway. Precipitation has been shown to be a major factor influencing the thickness and duration of lake ice and snow cover and, consequently, the length of the growing season for a lake (Koinig *et al.*, 2000; Koinig *et al.*, 2002). The timing and type of precipitation, i.e. whether as rain or snowfall may determine the length of ice-cover on a lake with high winter

precipitation often increasing the ice thickness (Varvus *et al.*, 1996), and consequently have huge implications for the lakes light regime.

Increased precipitation during the LIA would result in a longer opaque lake ice-cover period with a more persistent snow cover, having consequences for diatom growth within the lakes due to changes in productivity, habitat availability, alterations to the lakes thermal and light regimes and its mixing and nutrient recycling/supply (Section 1.4.1.2). Furthermore, changes in the catchment snow pack and increased thawing will influence the lake through changes in catchment erosion and weathering. These changes should, therefore, be evident in the palaeolimnological record of lakes within the central Norwegian area. The following section outlines the main aims and objectives of the study, and addresses how changes in the diatom assemblage and lithostratigraphy of lake sediment cores may be used to investigate changes in Norwegian climate.

1.6 Research rationale, study aims and thesis structure

It has been demonstrated (in sections 1.2 and 1.4 inclusive) that at the individual lake level diatoms, and especially planktonic diatoms, respond to changes in lake ice-cover/ air temperature. Several studies have quantified this response in the form of diatom inferred air temperature reconstructions using transfer functions (see section 1.4.1.3). Several studies at individual sites have also investigated the link between ice-cover and diatom assemblages and have shown that the relationship is significant (see section 1.4.1.2). Few studies to date have investigated whether a link can be made between diatom assemblages and lake ice-cover when the focus of the research is up-scaled to include many lakes. This research, therefore, up-scales the focus of the previous studies to establish whether the relationship between diatom assemblages and lake ice-cover, is significantly correlated when a number of high mountain lakes are studied in the form of a surface sediment training set. The training set is then used to develop climatic diatom transfer functions to explore changes in the palaeoclimatic record of two high altitude lakes in central Norway (i.e. lakes within an area known to have experienced significant changes in climate, see section 1.5).

The specific aims of the study. are listed below;

- To assess the relative influence of lake ice-cover as a driving mechanism for diatom composition, and in particular planktonic diatom abundance and composition, using surface sediment samples and contemporary environmental data for sites in North West Europe.
- To evaluate if this relationship is strong enough to produce a robust statistical model to reconstruct lake ice-cover/ climate based on the training set samples, and if so to apply such a model to two dated sediment cores from central Norway.
- To assess the linkages between other indirect effects of climate, such as pH change and nutrient fluctuations, within the sediment records of the two Norwegian high altitude lakes.
- To evaluate whether known climatic events occurring within Norway over the last 500 years are recorded by the palaeolimnological record of lakes within central Norway.

The following chapter (Chapter 2) explores the location of the training set sites and the two sites in central Norway cored and used for detailed palaeolimnological research. Chapter 3 explains the methods used in the collection and analysis of the training set and the sediment core samples. It also details the numerical analyses used for both the exploration of the biological/ environmental data and the techniques involved in development of the diatom transfer functions. Chapters 4 and 5 explore the training set samples in conjunction with the available environmental/ climatic variables. Chapters 6 and 7 present the palaeolimnological analyses of the two central Norwegian lakes and assess how faithfully the palaeolimnological record documents changes in climate over the last 500 years. Chapter 8 summarises the main findings of the research.

Chapter 2

Site selection and description

2.1 Introduction

This chapter describes the rationale behind the selection of the 80 lake training set, used to satisfy some of the aims outlined in section 1.6. The 80 lake training set consists of three sub sets, 'Norway 1', 'Norway 2' and 'Scotland'. From each of the lakes a sediment surface sample, contemporary water chemistry measurements, and selected lake and catchment characteristics/ environmental parameters were collected and recorded (see section 3.1.1 and 3.2 for methods of collection and analysis).

In addition to the training set, six sites were chosen to be cored with the intention that the most suitable of these would be chosen for detailed palaeolimnological analyses and the application of various diatom transfer functions. The chosen six sites are all located at high altitudes, in undisturbed catchments and in an area of Central Norway known to be affected by the LIA (see Figures 1.2 and 2.9). The selection of the six sites is discussed further in section 2.3. Two sites were eventually chosen for more detailed analysis. The selection procedure, and selection rationale, for these sites are discussed within this chapter (section 2.3.8).

2.2 Training set site selection rationale

All the sites within the 80 lake training set are located above the theoretical tree-line, with the Norwegian sites at or above 728m a.s.l (one was located at 466m a.s.l, but this site is later excluded, see section 5.1.1 and 5.1.2) and the Scottish sites at or above 520m a.s.l. Sites above the tree line were selected in order to minimise the impact of direct anthropogenic disturbance to both the catchments and the lakes, in terms of agricultural land-use and habitation. Although the influence of air-borne anthropogenic pollutants (see Figure 1.1) cannot be dismissed entirely, none of the sites within the training set, in either Norway or Scotland, are in areas of intense industrial development. In addition many of the lakes have relatively high alkalinity values (see sections 4.1.1 and 5.1.1) suggesting that they are able to buffer the limited acidic atmospheric pollution input. Therefore, any relationship between the environment, climatic variables and the lake biota is not adversely affected and any climatic response signal within the biological system is maximised.

It is assumed that altitude differences can be linked to a climatic gradient for the lakes within a region, with higher altitude lakes having lower air/ water temperatures (Section 1.1). Therefore, the sites were selected along a wide and evenly distributed altitudinal gradient (see later section 2.2.4 and Figure 2.8). In this way the lake ice-cover gradient would also be maximised. However, the training set was derived from two different countries and the altitudinal gradient, therefore, had to be maximised in each (See section 2.2.4).

2.2.1 Scotland ('EMERGE' sites)

The sites sampled within the Scottish data set are presented in Figure 2.1 and listed in Table 2.1. The sites selected for Scotland form part of a wider EU project entitled 'European Mountain Lake Ecosystems: Regionalisation, Diagnostics & Socio-economic Evaluation' (EMERGE see <http://www.mountain-lakes.org/>). These sites were selected based on tree-line limits for Scotland, geological sensitivity class and lake area, based on guidelines within the EU project. All the lakes selected were greater than 5 hectares in area and above the theoretical treeline for Scotland, and located in the Scottish Highlands, north of the Central Lowlands (Figure 2.1).

In Scotland the theoretical tree line varies with latitude and longitude. It was possible, from the literature, to identify regions within the Scottish mountain sampling area to which altitude thresholds could be allocated as follows;

- i) Western Grampian - 716m (Donner 1962)
- ii) Eastern Grampian - 700m (Huntley 1981)
- iii) Cairngorms 793m (Pears 1968)
- iv) North-west Highlands 500m (H.J.B. Birks & H.H. Birks (unpublished))

399 lochs above the altitude thresholds were identified and from these 30 sites were chosen to be sampled for surface sediments, selected according to geological sensitivity classes (See <http://www.mountain-lakes.org/>) and along an altitudinal gradient. Two lochs could not be sampled, due to the fact that one proved inaccessible due to the rocky terrain and the other had very little sediment, and consequently the Scotland data set consisted of 28 lochs.

A geology map of Scotland is displayed in Figure 2.2. It can be seen that most of the lochs are situated on metamorphic/ igneous base-poor geologies. Photographs of some of the Scottish lochs sampled are presented in Figure 2.3. The majority of the lochs are within barren, sparsely vegetated, and often in catchments with thin soils (e.g. Figures 2 a and f). Most of the lakes have few macrophytes which is typical of such upland 'oligotrophic' lake systems. Some of the lakes do, however, drain more peaty catchments resulting in slightly higher TOC levels (Figures 2 c and e). Many of the sites are located near the west coast of Scotland and so are subjected to significant inputs of sea-salts (Figure 2.1).

Figure 2.1: Map of sites in the Scotland data set.

1= SC0349, 2-3= SC0197, SC0211, 4-6= SC0204, SC0165, SC0190, 7-8=SC0180, SC0189, 9= SC0153, 10= SC0124, 11= SC0191, 12= SC0335, 13=SC0140, 14= SC0108, 15= SC0029, 16= SC0068, 17= SC0101, 18-20= SC0076, SC0067, SC0084, 21= SC0002, 22= SC0010, 23=SC0172, 24=SC0271, 25=SC0330, 26=SC0366, 27=SC0399, 28=SC0386, 29=SC0379, 30=SC0382 (SC0140 and SC0379 no core was retrieved).

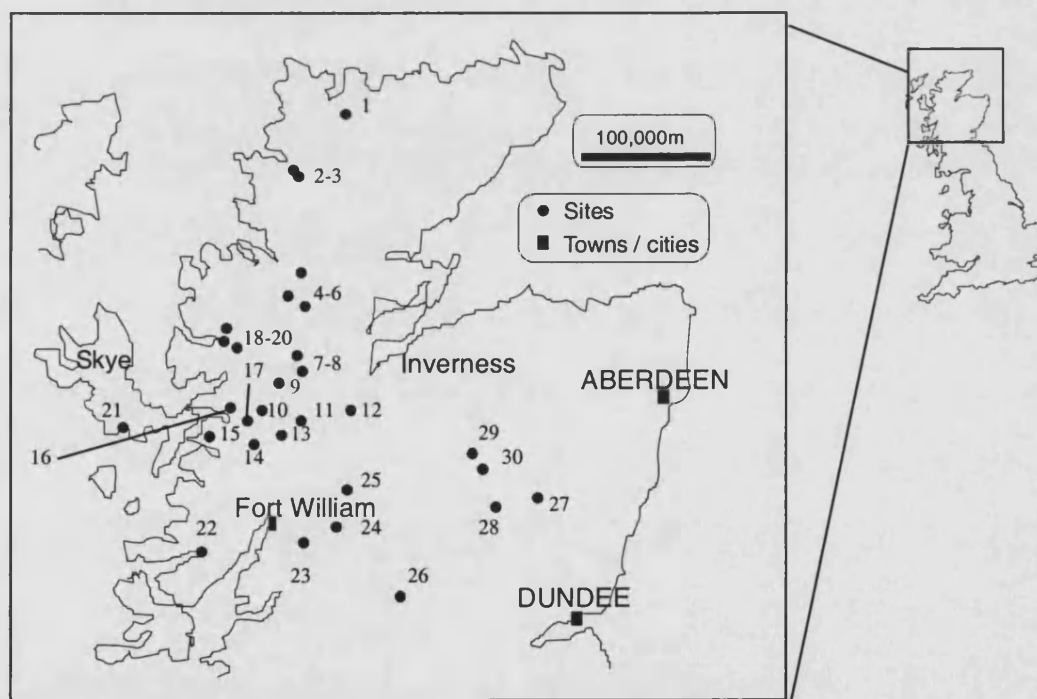


Figure 2.2: Geology map of Scotland
 (Source, http://www.scottishgeology.com/regional_geology/map_regions.html)

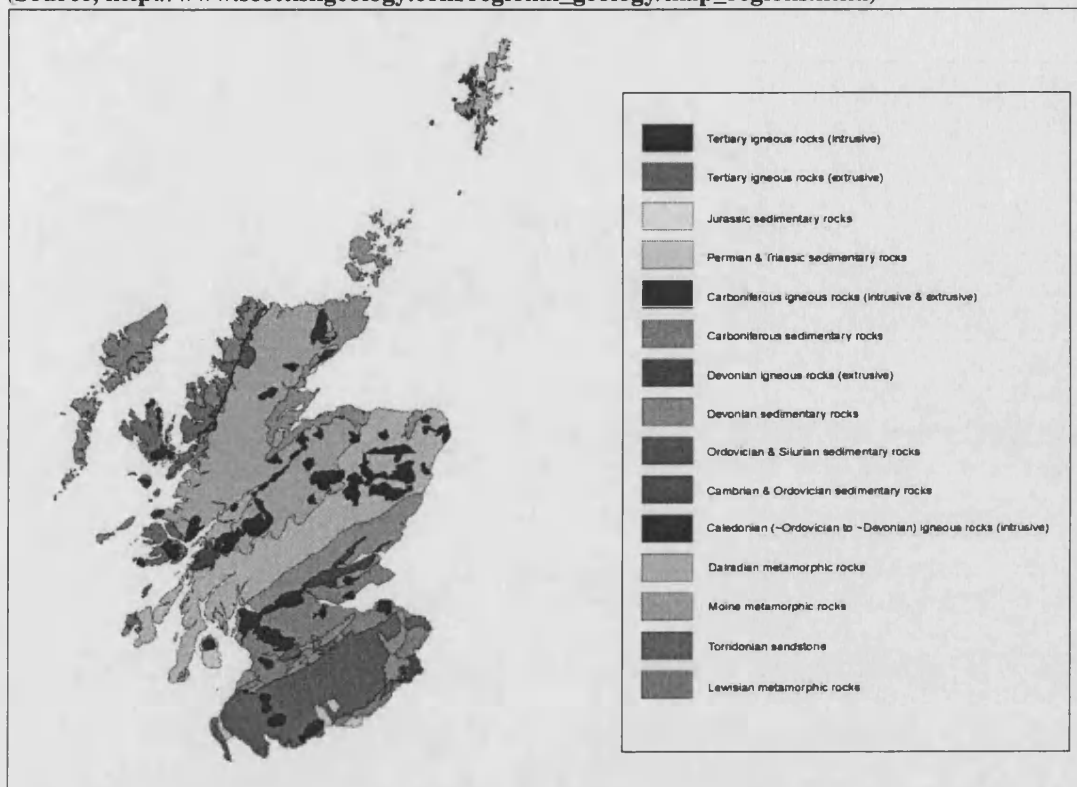


Figure 2.3: A selection of sites within the Scotland data set

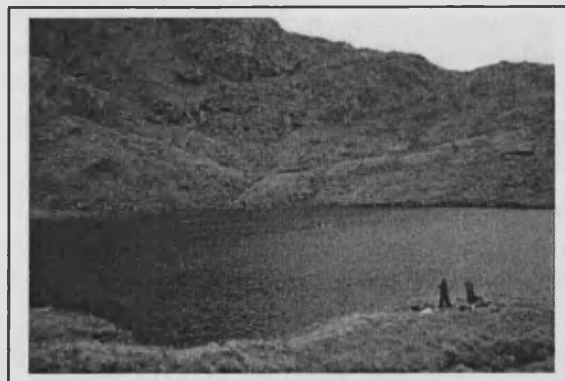
a) Lochnagar (Code SC0399)

Alt. 790m, Depth 24m, pH 5.42 TOC 1.6mg/l



b) Unnamed (Code SC0108)

Alt. 720m, Depth 8.1m, pH 5.92 TOC 2mg/l



c) Loch Bealach na h-Uidhe (Code SC0211)

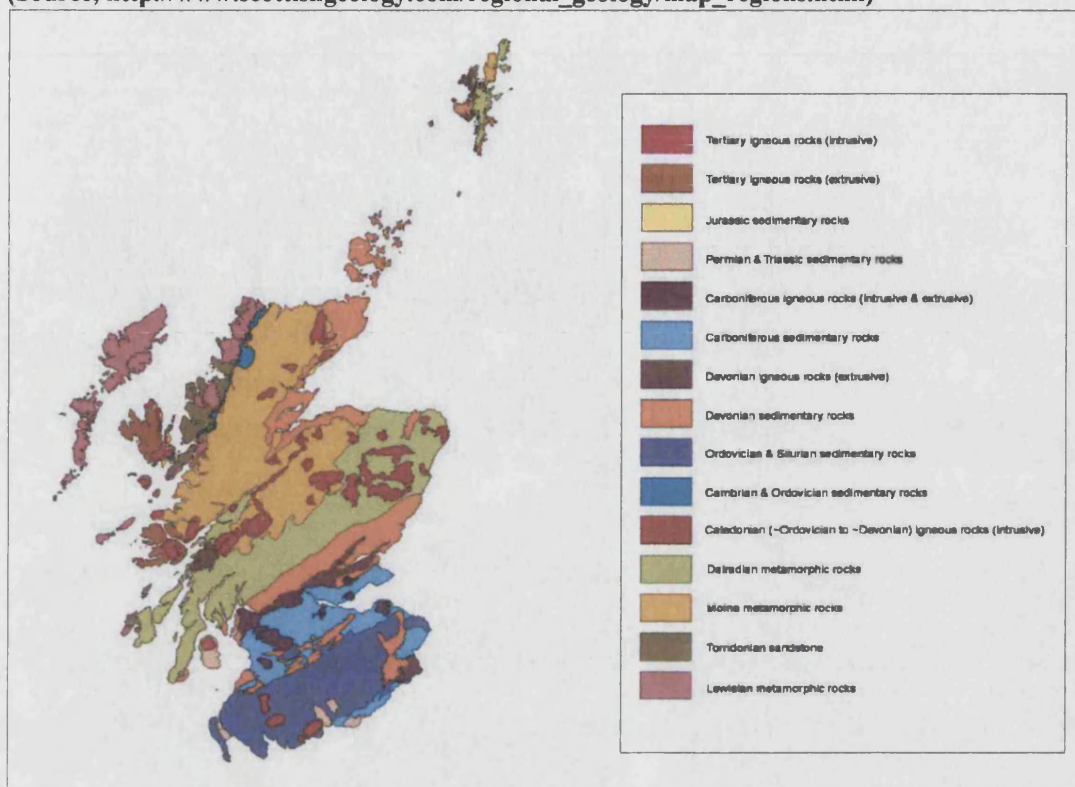
Alt. 530m, Depth 3.5m, pH 6.17 TOC 3.5mg/l



d) Loch an Fhuar-thuill Mhoir (Code SC0189)

Alt. 770m, Depth 15m, pH 6.15 TOC 0.7mg/l

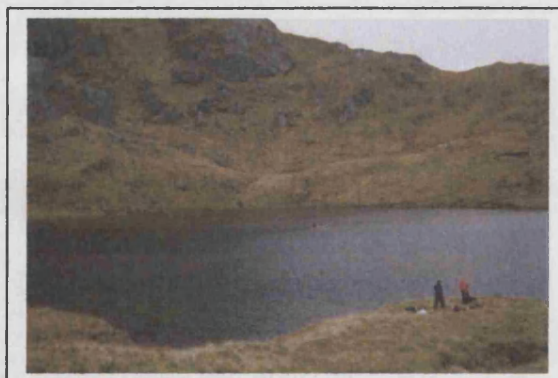


Figure 2.2: Geology map of Scotland(Source, http://www.scottishgeology.com/regional_geology/map_regions.html)**Figure 2.3: A selection of sites within the Scotland data set****a) Lochnagar (Code SC0399)**

Alt. 790m, Depth 24m, pH 5.42 TOC 1.6mg/l

**b) Unnamed (Code SC0108)**

Alt. 720m, Depth 8.1m, pH 5.92 TOC 2mg/l

**c) Loch Bealach na h-Uidhe (Code SC0211)**

Alt. 530m, Depth 3.5m, pH 6.17 TOC 3.5mg/l

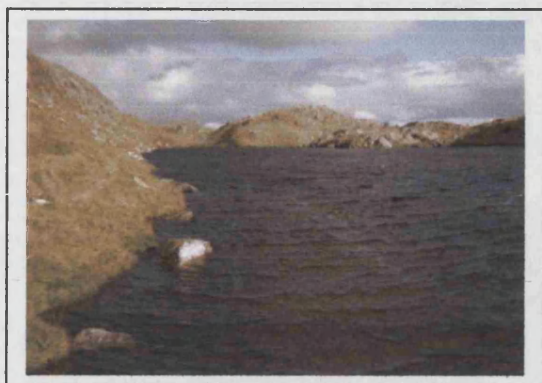
**d) Loch an Fhuar-thuill Mhoir (Code SC0189)**

Alt. 770m, Depth 15m, pH 6.15 TOC 0.7mg/l



Figure 2.3 cont:**e) Lochan Bac an Lochain (Code SC0010)**

Alt. 590m, Depth 4.3m, pH 6.32 TOC 2.4mg/l

**f) Loch Coire na Caimhe (Code SC0067)**

Alt. 530m, Depth 5.1m, pH 5.95 TOC 1mg/l

**2.2.2 Norway 1**

The sites selected within the Norway 1 data set are listed in Table 2.1 (Prefix 96, 98, 99) and their locations are illustrated in Figure 2.4. During 1996–1998 *ca.* 165 surface sediment samples were collected from various lakes across Central Norway and Southern Norway as part of a larger project led by Professor Birks (University of Bergen). At the time of sediment sampling, samples for water chemistry were also taken for each lake. These sediments and the water chemistry data were inspected to assess their suitability for inclusion in this study. From these 165 sites, 29 were chosen to be included as part of the overall training set.

The specific reasons for selecting these 29 sites were as follows;

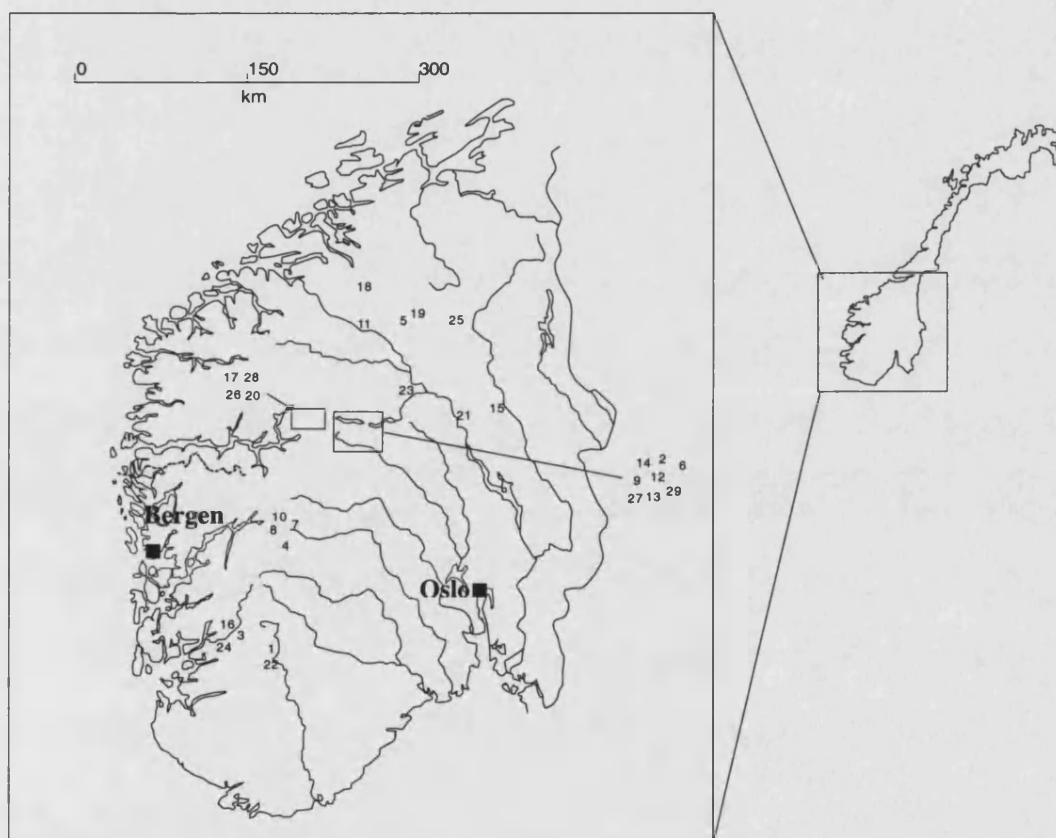
- The 165 lake data set spanned an altitudinal range of 1- 1594m a.s.l. In order to maximise the climatic signal all sites above 1000m were selected for further analysis. Any climatic signal in these areas is less likely to be affected by any anthropogenic influence because the lakes will be remote and the catchments will be relatively undisturbed.
- Sites above 1,000m are likely to be ice-covered for a large proportion of the year. Thus high altitude sites were selected covering an altitudinal range of *ca.* 1000m to 1,600m thereby maximising the variation in ice-cover regimes for the area.
- These sites had a large range of % diatom plankton abundance (scanned prior to selection). In order to investigate further the links between plankton and climate (discussed in section 1.4.1.2) lakes with a significant proportion of

plankton should be sampled and, therefore, it was important that the sites selected covered a wide range of plankton abundance.

- The 29 sites selected were chosen to be of a similar limnological type (in terms of pH ranges, nutrient status, altitude ranges and size/ depth) to those selected for the Norway 2 and Scotland data sets, discussed below, which are also all above the tree-line.

Figure 2.4: Sampled sites map for lakes in the 'Norway 1' data set.

1= 96-54, 2= 98-23, 3=96-36, 4=98-5, 5=98-15, 6=98-22, 7=98-2, 8=98-1, 9=98-21, 10=98-3, 11=98-13, 12=98-7, 13=98-20, 14=98-6, 15=99-43, 16=96-71, 17=98-10, 18=98-14, 19=98-16, 20=98-8, 21=99-44, 22=96-78, 23=98-17, 24= 96-37, 25= 99-50, 26= 98-9, 27=96-10, 28=96-9, 29= 96-12.

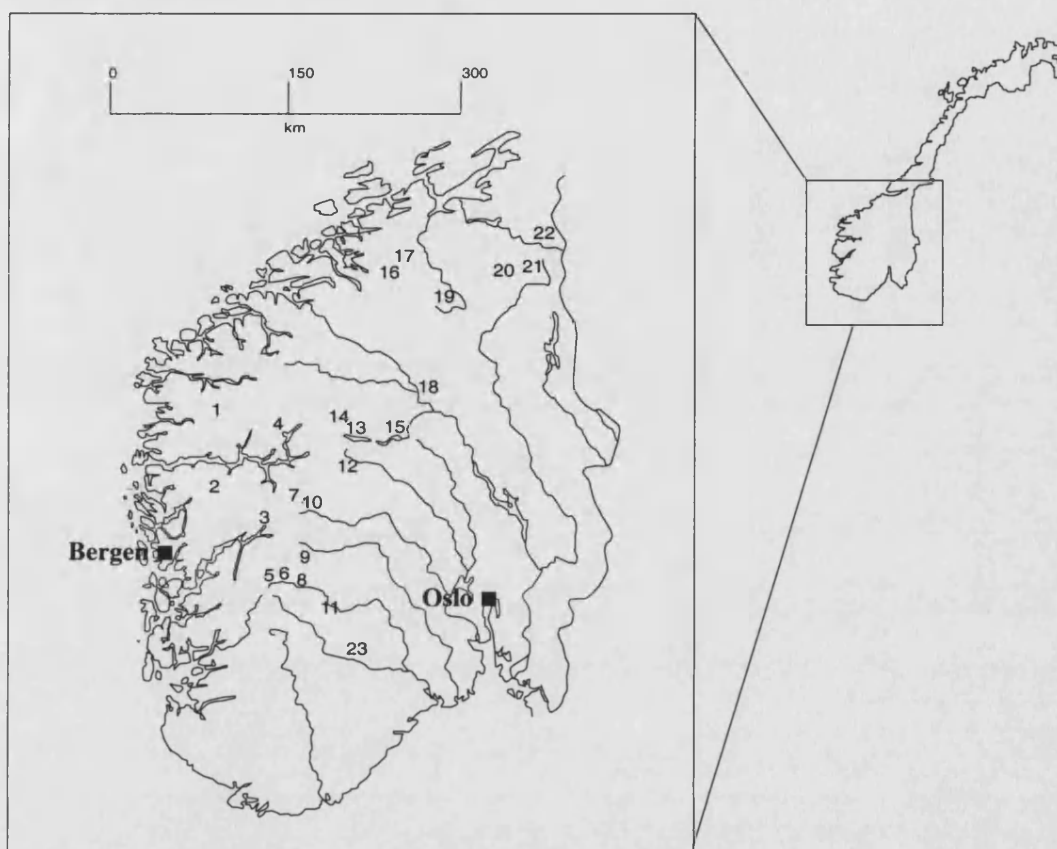


2.2.3 Norway 2 ('EMERGE' sites)

The 23 sites selected within the Norway 2 data set are listed in Table 2.1 (Prefix CN, SN) and their locations are illustrated in Figure 2.5. The Norway 2 sites were also part of the EMERGE project and their site selection followed the same principles as the Scotland data set, with selection based on tree-line limits, geological class and lake size. 23 sites were selected. It was thought suitable to use these sites in this study because they were derived from similar areas within Norway as the Norway 1 sites with similar geology (see below) and were all located above the tree-line, again minimising any anthropogenic disturbance.

Figure 2.5: Sampled sites map for lakes in the 'Norway 2' data set.

1=CN0001, 2=CN0002, 3=CN0003, 4=CN0004, 5=CN0005, 6=CN0006, 7=CN0007, 8=CN0008, 9=CN0009, 10=CN0010, 11=CN0011, 12=CN0012, 13=CN0013, 14=CN0014, 15=CN0015, 16=CN0016, 17=CN0017, 18=CN0018, 19=CN0019, 20=CN0020, 21=CN0021, 22=CN0022, 23=SN0023.



A geology map of Norway is presented in Figure 2.6. Most of the sites in the western part of Norway, for both the Norway 1 and Norway 2 data sets, are located on slow weathering Gneiss, granites and mica schist bedrock. Some of the more central and northern Norwegian sites are located on bedrock associated with the Cambro-Silurian era and are in areas of strongly weathered rocks, with a high proportion of sedimentary rock, which has a higher mineral nutrient content (Moen 1999).

A selection of sampled sites located within Norway is presented in Figure 2.7. It can be seen that many of the lakes are again in sparsely vegetated catchments. Often the sites are surrounded by extensive lichen growth (98-15, Figure 2.7 a) and dwarf birch/scrub vegetation (99-43, Figure 2.7 b). Many of the lake catchments are rocky with only a thin covering of soil, and several of the sampled sites were still ice-covered (96-78, Figure 2.7 c) at the time of sampling in late summer. Most of the higher altitude Norwegian lakes are clear water with low TOC values (e.g. 96-10 and 98-8, Figure 2.7 d and e).

Figure 2.6: Geology map of Norway. The rock groups are arranged according to age, the oldest being placed lowermost in the key (Source, National Atlas of Norway, Moen 1999)

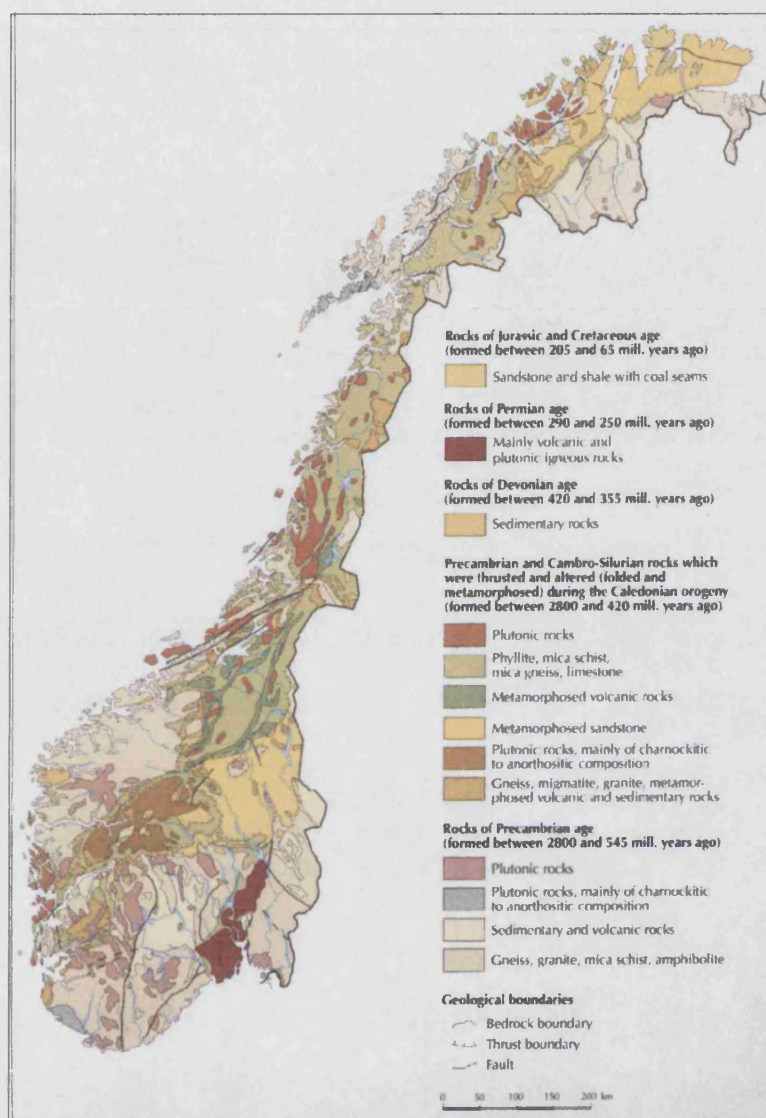


Figure 2.7: A selection of training set sites located within Norway
 a) Råtassjøen (Code 98-15), Alt. 1169m, Depth 6m, pH 7.17, TOC 1.5mg/l

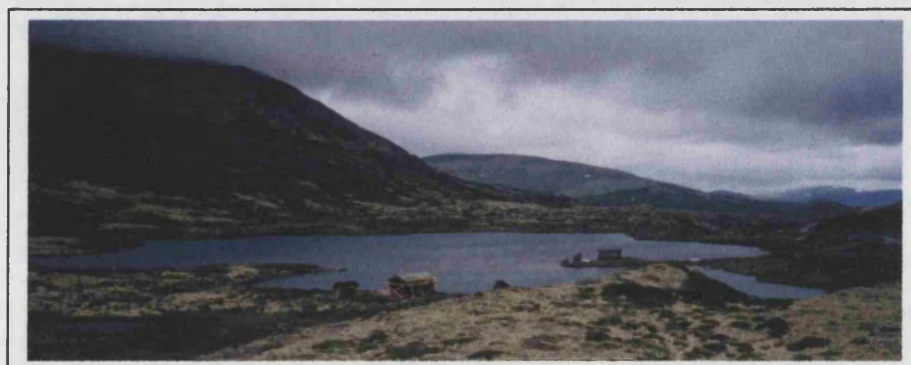


Figure 2.7 cont:

b) Langrumpa (Code 99-43), Alt. 1013m, Depth 1.6m, pH 5.99, TOC 6.5mg/l



c) Reinstjønn (Code 96-78), Alt. 1318m, Depth 15.5m, pH 5.42, TOC 1mg/l



d) Nøglavatnet (Code 96-10), Alt. 1440m, Depth 3.5m, pH 5.82, TOC 0.8mg/l



e) Gryta (Code 98-8), Alt. 1371m, Depth 11m, pH 5.79, TOC 0.8mg/l



Table 2.1: Lake code, Lake name, Longitude, Latitude, Altitude and lake area measurements for each of the 80 lakes within the training set. Lakes with the prefix CN, SN refer to the ‘Norway 2’ lakes. Lakes with prefix 96, 98 or 99 refer to ‘Norway 1’ data set lakes and those with the prefix SC refer to the ‘Scottish’ lochs.

Lake Code	Lake Name	Latitude °N	Longitude °E	Altitude (m a.s.l)	Lake area (ha)
CN0001	Vonavatn	61.61314	6.00545	466	165
CN0002	Vestre Kvammavatn	60.90039	6.15556	990	30
CN0003	Slondalsvatn	60.6921	6.94891	751	60
CN0004	Halsavatnet	61.27935	7.06557	820	27
CN0005	Litlosvatn	60.07385	7.17075	1172	153
CN0006	Valgardsvatn	60.10275	7.31845	1324	180
CN0007	Hornsvatnet	60.95012	7.36255	1289	30
CN0008	Dargesjøen	60.08436	7.58903	1209	55
CN0009	Skiftesjøen	60.38419	7.57971	1239	95
CN0010	Holmavatnet	60.84198	7.65144	1525	80
CN0011	Urdevatn	59.97336	7.712	1329	150
CN0012	Grønevatnet	61.20113	8.07898	1184	130
CN0013	Kvitevatnet	61.39568	8.17811	1396	140
CN0014	Leirvatnet	61.54781	8.24935	1401	100
CN0015	Øvre Heimdalsvatnet	61.41877	8.89696	1088	77.5
CN0016	Øvre Neådalvatn	62.77778	8.98237	728	50
CN0017	Fallbekktjøna	62.74996	9.03719	1043	27
CN0018	Høvringsvatn	61.88982	9.56498	1121	18
CN0019	Lille Innsjøen	62.55216	10.26587	938	40
CN0020	Haltdalstjønna	62.77426	11.06703	1058	8
CN0021	Gjeltsjøen	62.716	11.60089	799	55
CN0022	Øvlingen	62.90288	11.7848	844	20
SN0023	Stavsvatn	59.635	8.11	1053	40
SC0002S	Loch Coir' a' Ghrunnda	57.20192	-6.22107	750	2.9
SC0067S	Loch Coire na Caime	57.56594	-5.47594	530	3.2
SC0101S	Loch a' Chleirich	57.2507	-5.30537	750	1.4
SC0172S	Un named	56.74677	-4.90413	740	9.3
SC0180S	Loch Toll Lochan	57.49554	-4.95487	520	7.5
SC0197S	Loch a' Choire Dhaig	58.19929	-4.97635	530	4.2
SC0330S	Lochan Coire Choille- rais	56.94521	-4.57701	810	7.4
SC0349S	Un named	58.41689	-4.59531	530	3.8
SC0366S	Lochan nan Cat	56.55618	-4.2063	720	12.4
SC0382S	Lochan Uaine	57.06306	-3.64865	910	3.8
SC0386S	Loch nan Eun	56.88503	-3.53822	790	14.5
SC0399S	Lochnagar	56.95914	-3.23128	790	9.9
SC0335S	Un named	57.26925	-4.58286	540	1.9
SC0165S	Loch a' Mhadaidh	57.71257	-5.02443	570	31.1
SC0271S	Lochan Coire an Lochain	56.83151	-4.68428	740	5.1
SC0211S	Loch Bealach na h-Uidhe	58.185	-4.95355	530	2.9
SC0204S	Lochan a' Chapaich	57.80984	-4.93559	690	5.6
SC0191S	Loch Carn a' Chaochain	57.22027	-4.91542	660	2.3
SC0190S	Loch Gorm	57.68133	-4.95438	540	21.6
SC0189S	Loch an Fhuar-thuill Mhoir	57.45238	-4.93654	770	5.4
SC0124S	Loch an Fhraoich-choire	57.2746	-5.22603	660	4.4
SC0108S	Un named	57.14285	-5.28714	720	1.9
SC0084S	Un named	57.5168	-5.39224	670	9.6
SC0076S	Loch Coire Mhic Fhearchair	57.59115	-5.44503	600	10

Table 2.1 continued

Lake Code	Lake Name	Latitude °N	Longitude °E	Altitude (m a.s.l.)	Lake area (ha)
SC0068S	Loch Bhuic Moir	57.2785	-5.44811	540	3.6
SC0010S	Lochan Bac an Lochain	56.72325	-5.65692	590	1.8
SC0029S	Un named	57.17348	-5.59274	720	2.5
SC0153S	Loch Beag	57.372	-5.08451	660	2.5
96-10	Noglavatnet	61.54	8.25	1440	unknown
96-12	Luckes (unofficial)	61.7016	8.8616	1294	7.5
96-36	Hender (unofficial)	59.8483	6.9393	1020	5
96-37	Elversvatn	59.8416	6.73	1052	18.3
96-54	Hermoholtjørni	59.8083	7.2533	1107	8.1
96-71	Holebudalen	59.8433	6.9933	1144	4.4
96-78	Reinstjønn	59.8566	7.0216	1318	8.8
96-9	Goodwin (unofficial)	61.548	7.9066	1376	10
98-1	Mendel (unofficial)	60.925	7.315	1290	2.5
98-10	Bobbin (unofficial)	61.5383	7.8483	1301	5
98-13	Sjutjørnin	62.0266	8.9633	1194	3.2
98-14	Vesleguttj	62.0666	8.9433	1080	<2.5
98-15	Tåtasjøen	62.2683	9.8366	1169	10
98-16	Langsjoflysi	62.3216	9.87	1075	6.3
98-17	Grønbakddtj	61.1	9.4483	1114	12.5
98-2	Hornsvatn	60.965	7.3633	1289	38.1
98-20	Rasletjern	61.39	8.7633	1461	12.5
98-21	Fisketjerni	61.3933	8.795	1377	22.5
98-22	Fisketjerni	61.3766	8.8416	1329	45
98-23	Stavtjern	61.3183	8.82	1055	30.6
98-3	Chillon (unofficial)	60.9266	7.3283	1240	<2.5
98-5	Vargebovatn	60.7416	7.5333	1400	30.7
98-6	Leirvatn	61.5466	8.2583	1401	103.1
98-7	Storbreen (unofficial)	61.59	7.9483	1221	9.4
98-8	Gryta	61.5783	7.9483	1371	10.6
98-9	Davialec (unofficial)	61.55	7.9483	1391	26.3
99-43	Langrumpa	61.6983	10.155	1013	6.9
99-44	Gututjorn	61.7283	10.1766	1056	unknown
99-50	Midttjørna	62.3833	10.0216	1000	unknown

2.2.4 The 80 lake set

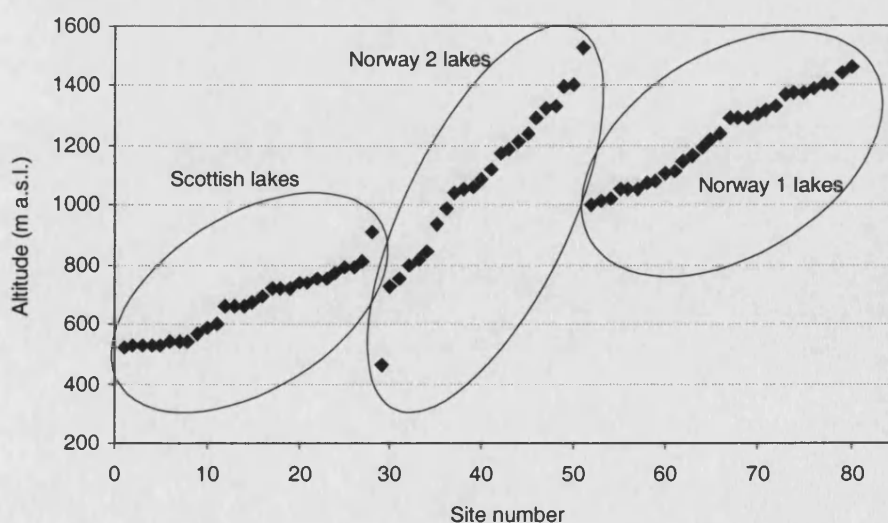
The combined training set consisted of 80 lakes, 28 from Scotland and 52 from Norway. Although the training set is made up of sites from different countries it was thought appropriate to combine them because they are all of a comparatively similar limnological character in terms of nutrient status, and all are located above the theoretical tree-line and, therefore, at similar altitudes. In addition all the lakes were within sparsely vegetated and relatively undisturbed catchments.

It was realised, however, that some of the Norwegian sites might be more 'base rich' than the Scottish sites, due to their location on mineral rich sedimentary bedrocks in

the more Northern sampling areas of Norway (See Figures 2.4, 2.5 and 2.6). In addition, due to the proximity of some of the Scottish sites to the coast there may be a separation according to conductivity (Na^+ , Cl^- , K^+ , and Mg^{2+}). Many of the Norwegian sites are also located close to the coast (e.g. CN0001, CN0016, CN0017, Figure 2.5) and a chemical separation, according to location, between the inland and coastal sites may be evident within the whole data set. The selection of a relatively large data set was, however, essential in order to maximise the altitudinal/ climatic gradient (see below) and, therefore, it is inevitable that some of the chemical variables cannot remain constant when the whole data set is considered. This separation according to chemical status is discussed further in Chapters 4 and 5.

In order to maximise the climatic signal within the data set the sites chosen had to span a long and evenly distributed altitudinal gradient. The gradient spans 466 - 1,525m a.s.l and this is illustrated in Figure 2.8. It can be seen that there is a large degree of over lap between the three data sets in terms of the lakes altitudes. The Norway 2 set has the widest altitudinal range (466- 1525m a.s.l.). It can also be seen that there are no real gaps in the altitudinal gradient due to the overlapping nature of the three sets. In this way the ice-cover gradient within the data set is maximised. The training set sites, and their chemical and environmental parameters, are explored in more detail in Chapters 4 and 5.

Figure 2.8: The altitudinal gradient for the 80 lake training set.



2.3 Lakes selected for sediment coring

Six high altitude lakes in Norway were selected for coring. These were to be used for detailed palaeolimnological analyses (see Chapters 6 and 7) and the application of the transfer functions developed in Chapters 4 and 5. The sites chosen were all selected because they are located in relatively undisturbed lake catchments and in areas thought to be significantly impacted by the Little Ice Age in Norway (Birks *pers com.* and see Figure 1.2). In this way the lakes are regarded as highly suitable for palaeoclimatological analysis and any potential relationship between the climatic changes, occurring during the LIA, and diatom assemblages might be maximised in this central Norwegian location.

Initially, six cores were collected (Figure 2.9) and preliminary diatom and lithostratigraphic analyses were performed on each (see section 3.1 and 3.2), the results of which are presented in this chapter. In order to assess the diatom assemblages of each of the cores in a short space of time all six cores were initially scanned for diatoms with typically six diatom samples counted per core. The diatom slides were prepared using methods described by Renberg (1990) (See section 3.2.4) and counted at regular intervals down the core, resulting in a 'skeleton' diatom profile.

Cores that were considered to be suitable for further high resolution palaeolimnological analyses had to fulfill three main criteria:

1. The cores should be taken from undisturbed lake systems in order to maximise the climatic signal evident within the palaeolimnological record;
2. Distinct changes in %LOI should be evident within the core profile which could possibly be related to changes occurring within the lake during the LIA shown to be evident in other study lakes in the area (Matthews *et al.*, 2000; Nesje *et al.*, 1995; Nesje *et al.*, 2001; Nesje *et al.*, 1994, also see section 1.5.1) and;
3. The cores should have a high, and varying, abundance of planktonic diatoms in order to explore further the hypothesised link between planktonic diatom composition and climatic change.

2.3.1 The six cored lakes

This section presents the six cored lakes and describes their chemical and catchment characteristics. The results of the scanned diatom samples, and the %Dry Weight (%DW) and %Loss on Ignition (%LOI) analyses are also presented. The coring procedures, extrusion process, laboratory lithostratigraphy methods, diatom preparation, counting and taxonomic remarks are all described in Chapter 3.

In 2000 four sites were selected in Norway for coring (lake codes 98-20, 98-6, 98-9 and 98-2 (Table 2.2). All these sites are situated above 1,000m a.s.l. In 2001 two further high altitude sites in Norway were selected and cored (core codes 01-03, 98-18). One of these sites (Gåvålivatnet, 01-03) is situated below 1000m at 939 m (Table 2.2). The site, however, is still considered to be relatively undisturbed (see section 2.3.6 for further site details). In addition all the sites are located within a particularly 'clean' area of Norway, in terms of air borne industrial pollutants (Birks *pers. com.*).

The locations of the cored sites are shown in Figure 2.9. All six short sediment cores, measuring *ca.*30cm long, were extruded at 2.5mm intervals in the field and changes in colour and texture were recorded. The sites are hereafter referred to in this chapter by lake name.

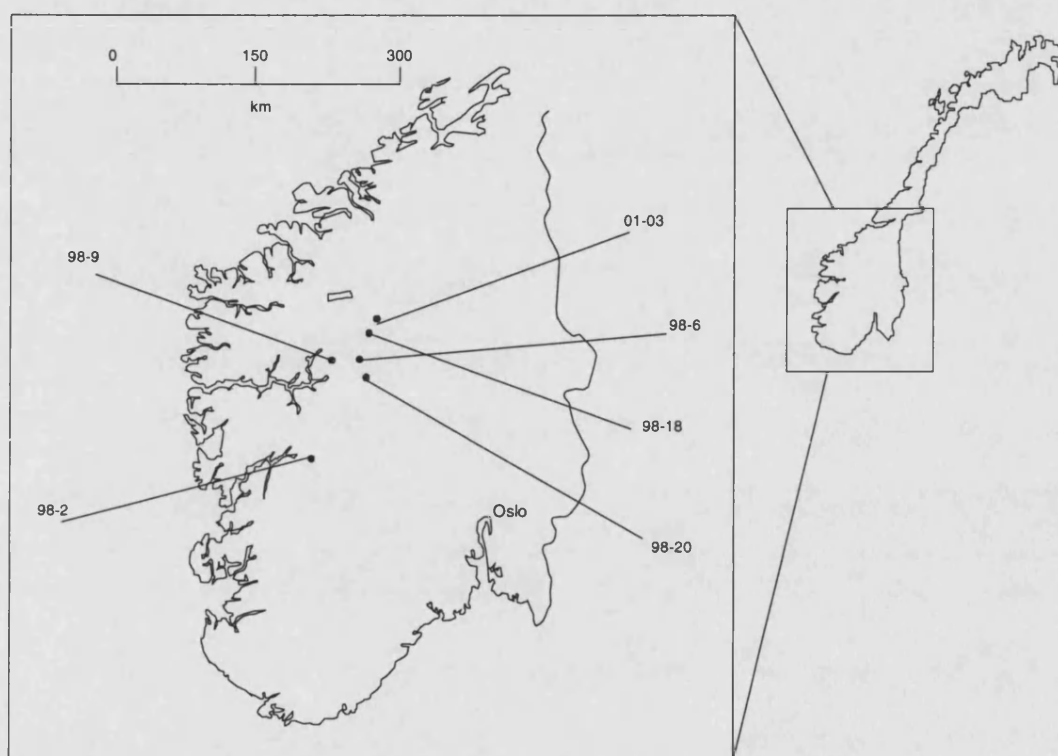
Table 2.2: Summary table of the six lakes cored

Lake Code	Lake Name	Lake depth (m) max	Coring depth (m)	Lake Altitude (m)	Lake area (ha)
98-20	Rasletjernet	4.5	4.3	1461	12.5
98-6	Leirvatn	15	11.5	1401	103
98-9	Davialec	17	17	1391	26.3
98-2	Hornsvatn	13.5	13.5	1289	38.1
01-03	Gåvålivatnet	16.5	14.5	939	80 approx
98-18	Hornsjøen	12.5	12.5	1261	17 approx

A photograph of each cored lake is presented (Figures 2.10a, 2.12a, 2.14a, 2.16a, 2.18a and 2.20a), a topographic map for each is provided (Figures 2.10 b, 2.12 b, 2.14 b, 2.16 b, 2.18 b and 2.20 b, Source; Statens Kartverk Norge 1:50000 Topografisk Hovedkartseries) together with a brief description of each site. Often due to their remote nature little is known of the lakes' histories. The sampling region has relatively dry and cold winters (average January to February temperatures -10°C) and

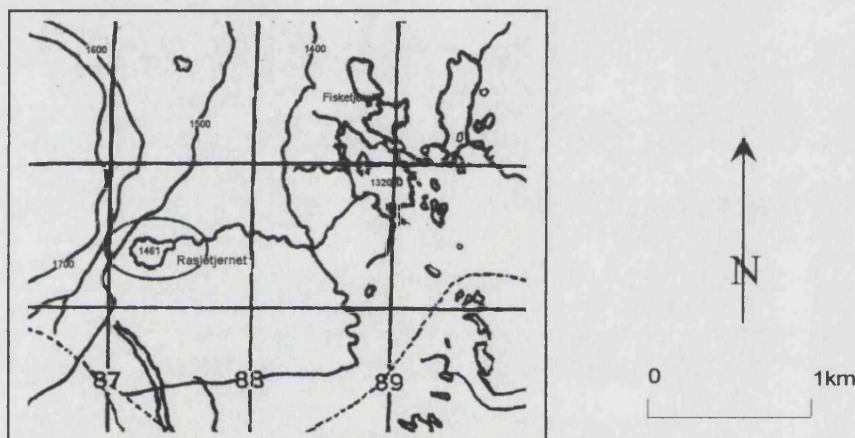
wet and warm summers (average June to August temperatures of 10°C), therefore, the climate is considered to be continental. The results of the diatom counts, the %Loss on Ignition and %Dry Weight are also presented in Figures 2.11, 2.13, 2.15, 2.17, 2.19 and 2.21.

Figure 2.9: The location of the six cored lakes within Norway. 98-20 (Rasletjernet), 98-6 (Leirvatn), 98-9 (Davialec), 98-2 (Hornsvatn), 01-03 (Gåvålivatnet), 98-18 (Hornsjøen).



2.3.2 Rasletjernet, Code 98-20

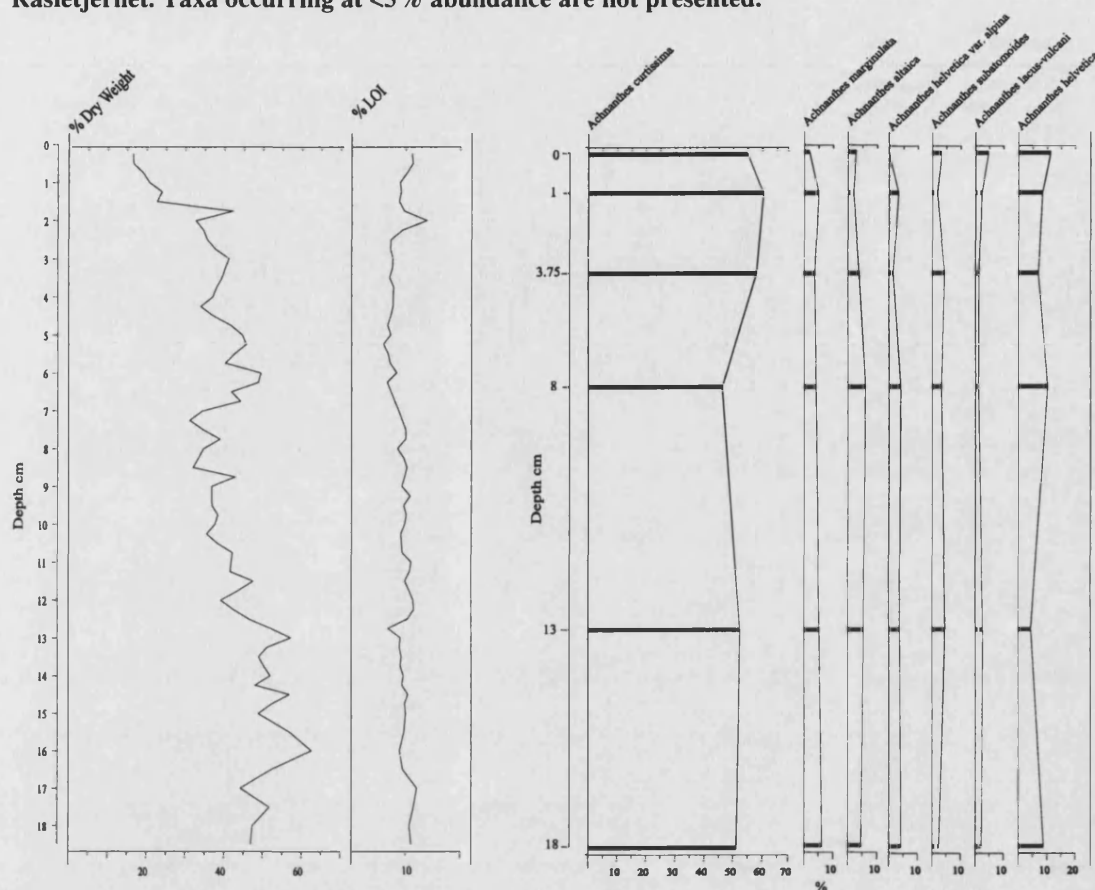
This lake is very remote and located in an undisturbed catchment. The surrounding area is barren in terms of vegetation and no huts are built in the lake vicinity (Figure 2.10 a and b). The site has a steep back wall and the lake water is exceptionally clear (TOC = 0.7mg/l). The lake is relatively small and shallow in comparison to the other lakes cored, but has a similar pH (6.15 units). Of the six lakes this lake is located at the highest altitude.

Figure 2.10 a) Rasletjernet, Code 98-20Altitude 1461m a.s.l., Area 12.5m², Depth 4.5m, pH 6.15, TOC 0.7mg/l**b) Topographic map of Rasletjernet (circled), Code 98-20** (Source Statens Kartverk Norge 1:50000 Topografisk Hovedkartseries)

The 19cm long core was taken at 4.3m depth and showed few significant changes in colour or texture throughout. At 12-13cm and 15-16cm slightly grey/ green grittier layers were evident. The percentage dry weight (%DW) for Rasletjernet is relatively low for the top of the core (*ca.*25%) and generally increases down core to an unusually high 63% maximum at *ca.*16cm (Figure 2.11). The percentage loss on ignition (%LOI) is low throughout (*ca.*10%) the core with few changes in its profile.

The diatom profile of Rasletjernet is dominated by *Achnanthes curtissima* with 55% maximum abundance occurring in the top 5cm (Figure 2.11). *Achnanthes curtissima* is correlated with changes in *Achnanthes helvetica*, which decreases as the former increases and vice versa. Various other *Achnanthes* spp. occur throughout the rest of the core but their abundances never exceed 10% maximum abundance. The assemblage is dominated by benthic diatom species with no planktonic diatoms occurring at more than 5% abundance throughout the core profile.

Figure 2.11: Percentage dry weight, percentage loss on ignition graphs and diatom profile for Rasletjernet. Taxa occurring at <5% abundance are not presented.



2.3.3 Leirvatn, Code 98-6

This site is located in a popular area for walking within Norway but it is still relatively undisturbed and the lake is away from the main tourist area. This is a very large lake in comparison to the most of the other lakes cored (Figure 2.12 a and b) and only Gåvålivatnet is of a similar size. The lake is also relatively deep and located at a similar altitude to Rasletjernet (Table 2.2). Its pH is relatively low at 6.01 pH units and the TOC is also relatively low (0.8mg/l). The 25cm core was taken at 11.5m depth, from 1-5cm the sediment was loose and organic and from 5-20cm the sediment became darker. From 20-25cm the sediment became slightly lighter in colour and consisted of denser/ finer particles.

The %DW for Leirvatn is fairly constant throughout the profile and fluctuates around 15-20% (Figure 2.13). This is low in comparison to Rasletjernet and the same increases %DW towards the bottom of the core, seen in the previous site, are not

evident in this core. The %LOI curve also shows few major changes in its profile and fluctuates between 10-20%.

The diatom profile for this site is dominated by benthic *Achnanthes* spp. and *Aulacoseira* spp. (Figure 2.13). Significant diatom changes within the core are hard to detect due to the fact that many species occur at similar abundances throughout the profile. There does appear to be an interplay between *Achnanthes marginulata* and *Fragilaria exigua* to some extent, with the former decreasing as the latter increases. *Fragilaria exigua* reaches a maximum abundance of ca. 20% in the 20cm sample. In addition *Achnanthes altaica* has a negative correlation with *Aulacoseira distans* var. *nivalis*. No planktonic diatom species occur at significant abundances within the core.

Figure 2.12 a) Leirvatn, Code 98-6

Altitude 1401m a.s.l., Area 103m², Depth 15m, pH 6.01, TOC 0.8mg/l



b) Topographic map of Leirvatn (circled), Code 98-6 (Source Statens Kartverk Norge 1:50000 Topografisk Hovedkartseries)

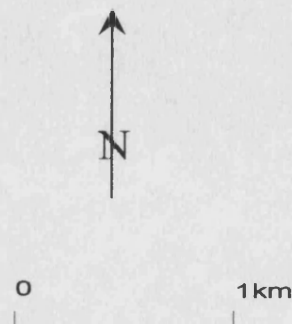
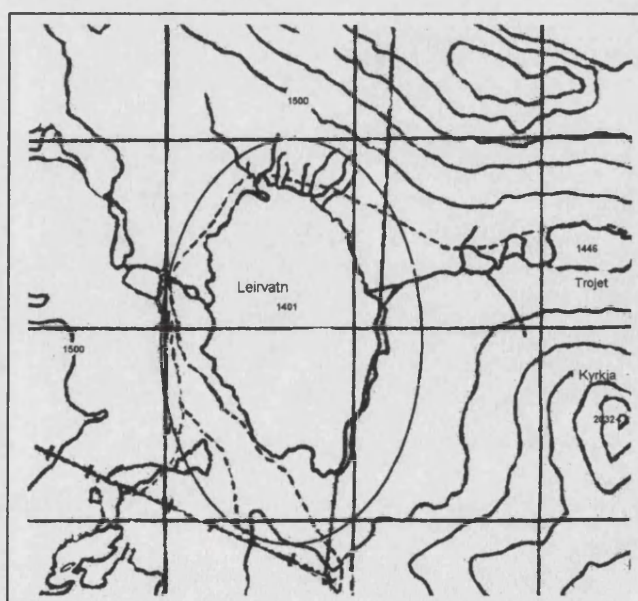
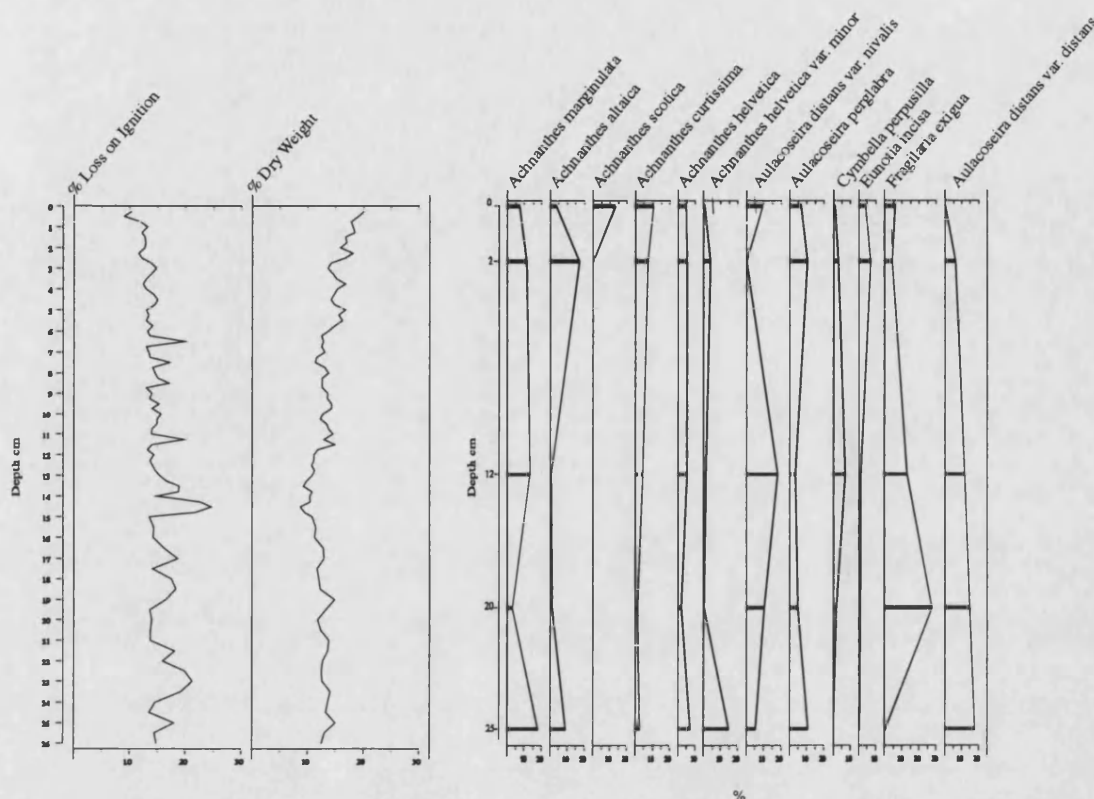


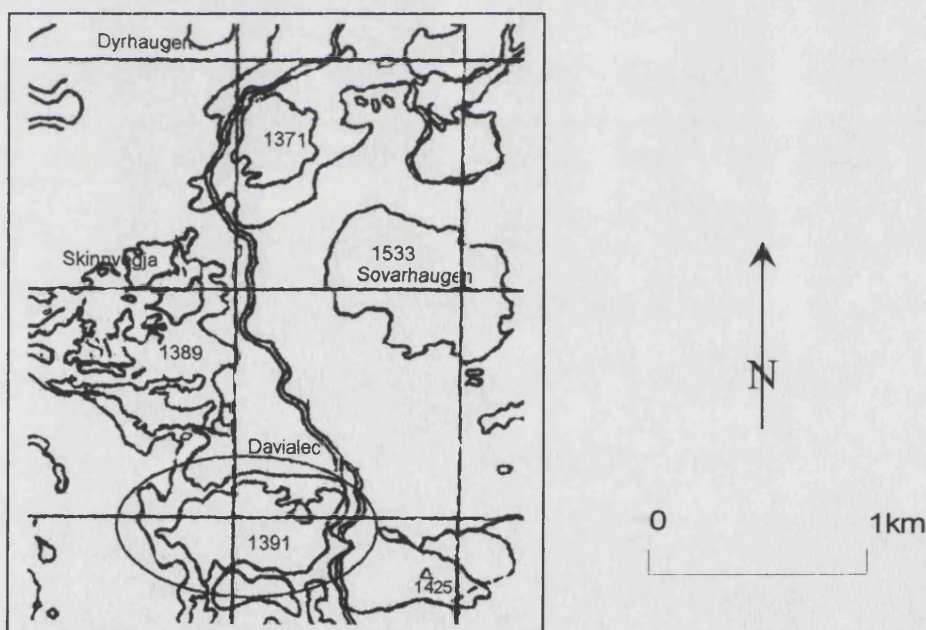
Figure 2.13: Percentage dry weight, percentage loss on ignition graphs and diatom profile for Leirvatn. Taxa occurring at <5% abundance are not presented



2.3.4 Davialec, Code 98-9

This lake is located within a relatively undisturbed catchment (Figure 2.14 a and b) with a high density of lakes in the surrounding area. The catchment has a large proportion of bare rock within it with only thin soils, with no shrub vegetation. The lake is quite deep but relatively small and its pH (5.69 units) is the lowest of the six lakes cored.

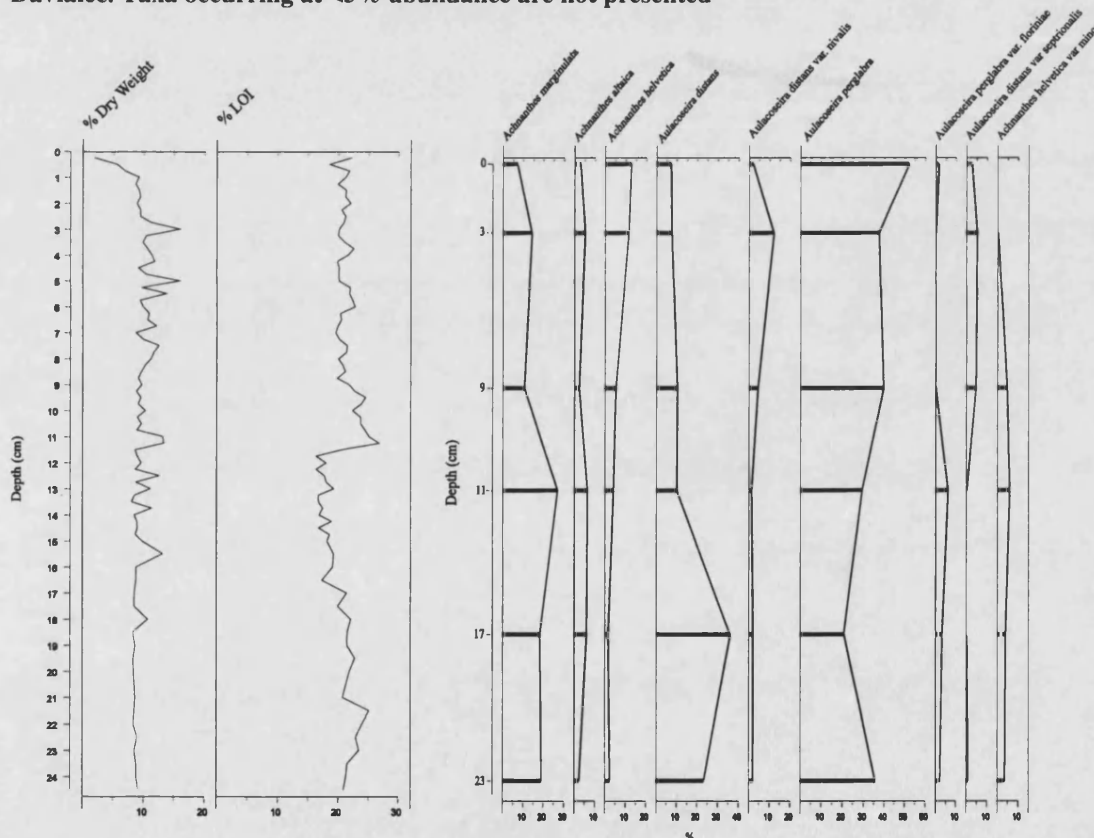
The 29cm core was taken at 17m depth. The surficial layers were orange and floccy but from 1-11cm dark organic sediments persisted throughout. After 11cm the sediment became slightly lighter to the bottom. The %DW for Davialec is relatively low but there are several peaks within the profile (Figure 2.15). These peaks may have been caused by storage of samples after extrusion resulting in water losses from some samples, as they are not reflected in the %LOI profile. The %LOI is higher than the previous two sites suggesting that it is a more organic sediment. The %LOI gradually decreases from the bottom of the core until *ca.*11cm, when a sharp increase occurs from 16% to 26%. Above this the %LOI remains consistently high through to the surface sediments.

Figure 2.14 a) Davialec (unofficial name), Code 98-9Altitude 1391m a.s.l., Area 26.3 m², Depth 17m, pH 5.69, TOC 1.8mg/l**b) Topographic map of Davialec (circled), Code 98-9** (Source Statens Kartverk Norge 1:50000 Topografisk Hovedkartseries)

The diatom profile (Figure 2.15) shows that this site is predominately composed of benthic taxa of *Aulacoseira* spp. and *Achnanthes* spp., dominated by *Achnanthes marginulata* (ca.22% maximum abundance), *Aulacoseira distans* var. *distans* (ca.30% max. abundance) and *Aulacoseira perglabra* var. *perglabra* (ca.45% max. abundance) (Figure 2.15). *Aulacoseira distans* var. *distans* is negatively correlated with *Achnanthes marginulata* and *Aulacoseira perglabra* var. *perglabra*. The decrease in %LOI at ca.11cm corresponds with changes in the diatom profile. From 11-23cm the

profile is dominated by *Aulacoseira distans* var. *distans* and *Achnanthes marginulata*. Above 11cm these two species decline as *Aulacoseira perglabra* var. *perglabra* becomes dominant. *Aulacoseira distans* var. *septentrionalis* also appears at this 11cm level and increases in conjunction with *Achnanthes helvetica* and *Aulacoseira distans* var. *nivalis* in the top 10cm of the profile. The variations within the diatom profile seem to mirror the changes in the lithostratigraphy. It should be noted, however, that the low resolution of analysis may mask other more subtle changes in the diatom assemblages within the core. These *Aulacoseira* species are not thought of as being planktonic (see section 3.2.5) and, therefore, again planktonic diatom abundance within this core is minimal.

Figure 2.15: Percentage dry weight, percentage loss on ignition graphs and diatom profile for Davialec. Taxa occurring at <5% abundance are not presented



2.3.5 Hornsvatnet , Code 98-2

Like Davialec this is a remote site in a relatively undisturbed catchment. There is a road nearby but again this is unlikely to affect the lake to any major degree (Figure 2.16 a and b). The lake was about a quarter ice-covered when the core was taken in late summer. As with the other lakes the catchment is barren and rocky. The core was

taken from 13.5m depth and measured 26cm. There were few changes in sediment type or colour throughout the core.

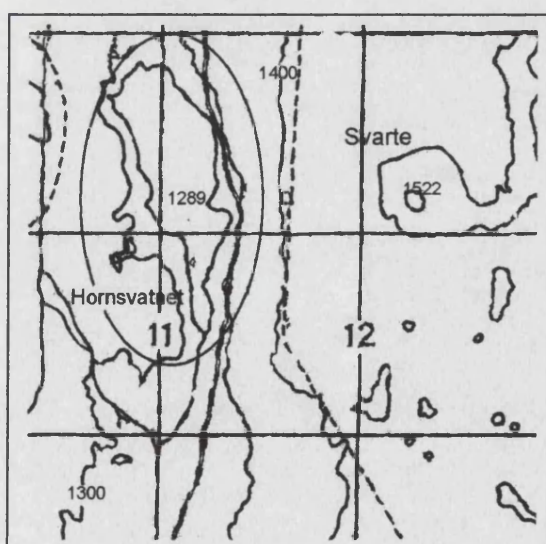
The %DW profile for Hornsvatnet has several peaks in the top section of the core, as in Davialec, these are attributed to water losses whilst the sediment was in storage as no similar changes are evident in the %LOI (Figure 2.17). Excluding these peaks the %DW is fairly constant throughout the core with slightly higher values in the bottom section. At ca.21-20cm the values decrease and then increase and generally fluctuate around 10%DW, excluding the aforementioned peaks, to the surface.

Figure 2.16 a) Hornsvatnet, Code 98-2

Altitude 1289m a.s.l., Area 38m², Depth 12.5m, pH 6.15, TOC 0.9mg/l



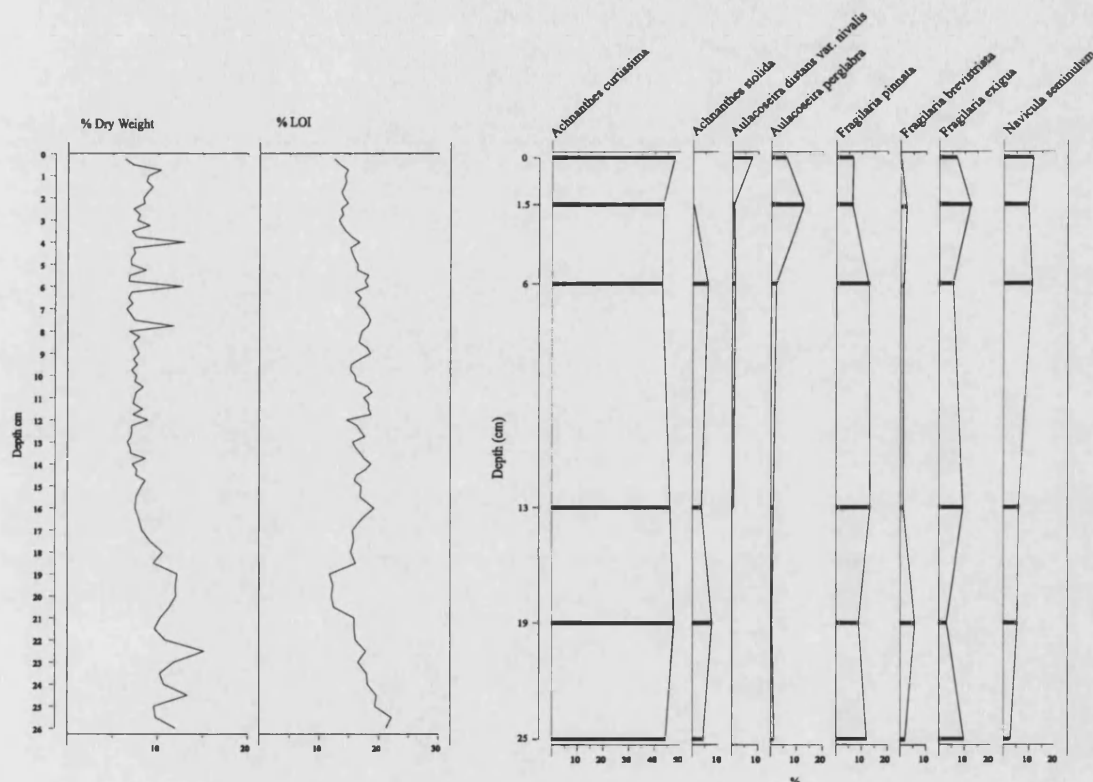
b) Topographic map of Hornsvatnet (circled), Code 98-2 (Source Statens Kartverk Norge 1:50000 Topografisk Hovedkartseries)



The diatom assemblage is dominated by *Achnanthes curtissima*, reaching 45% maximum abundance, but varying little throughout the profile (Figure 2.17). The rest of the core shows varying proportions of *Aulacoseira* spp., *Fragilaria* spp. and

Navicula seminulum. The main change in the assemblage occurs in the top 6cm of the core, with increases in *Aulacoseira perglabra* and *Fragilaria exigua*, and corresponding decreases in the abundance of *Fragilaria pinnata* and *Achnanthes stolidus*. Again there are no planktonic species present in significant numbers in the core.

Figure 2.17: Percentage dry weight, percentage loss on ignition graphs and diatom profile for Hornsvatnet. Taxa occurring at <5% abundance are not presented



2.3.6 Gåvålivatnet, Code 01-03

Gåvålivatnet is the only lake out of the six cored sites that is not located above the tree line (939m a.s.l). However, it is at a similar altitude to the other cored lakes. The site is located within the Døvreffell National Park, near the Snøhetta mountain range, in an area of especially rich/ diverse flora due, primarily, to its calcareous base rock (Birks *pers. com*) and this is probably reflected in the high lake water pH (7.52 pH units). The lake is also slightly higher than the other five in terms of the lakes TOC (3.99mg/l). This is a two basin lake, each basin being 15.5m deep, divided by a stretch of lake 5.5m deep in between. The basin farthest away from the outflow and near the steeper back wall was used for coring (Figure 2.18b).

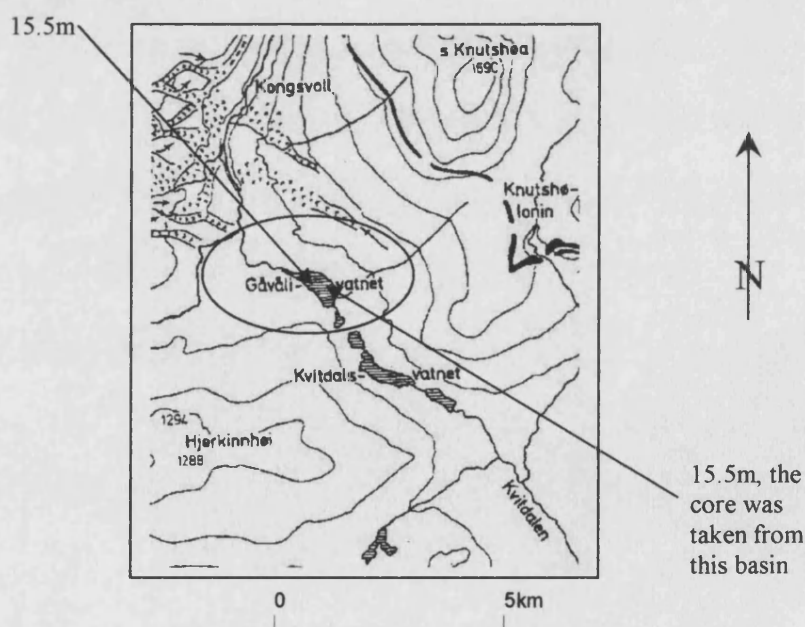
A small boat house was built in the catchment *ca.*1900. There is some pine forest growth on the eastern flank of the lake (Figure 2.18a). The area was also used for grazing horses, but no evidence of this remains. These activities may have adversely affected the lake sediment record, but it is unlikely to have caused any major disruption, as the lake is relatively large with a large proportion of the catchment remaining undisturbed.

Figure 2.18 a) Gåvålivatnet, Code 01-03

Altitude 939m a.s.l., Area 80ha. approx., Depth 15.5m, pH 7.52, TOC 3.9mg/l



b) Topographic map of Gåvålivatnet (circled), Code 01-03 (Source Statens Kartverk Norge 1:50000 Topografisk Hovedkartseries)



The core was taken at 14.5m and measured 27cm. The surficial layers were highly organic, flocculent, orange stained, iron rich deposits which at *ca.*2.5cm graded in to browner sediments. At 10cm the sediments began to change to a lighter grey colour.

At ca.14cm there was a distinct light grey, very compact, clay like layer which stopped at ca.18cm when the sediment became brown and fibrous. At about ca.26cm there was a very distinct and discrete dark horizon. Below this the sediment was brown in colour but more fibrous in comparison to the layer above. This could have been a layer with higher proportions of macrofossil deposits within the core.

The lithostratigraphy for Gåvålivatnet is significantly different from the previous four cores (Figure 2.19). The %DW profile is jagged but shows a general increase from the bottom of the core until 17cm where there is a sharp increase in %DW from ca.30% to ca.67% representing sediment with a very high water content. This decreases again dramatically at 16cm to ca.35% increasing just as quickly in the next centimetre. After this final increase at ca.14cm the %DW declines steadily towards the upper section of the profile.

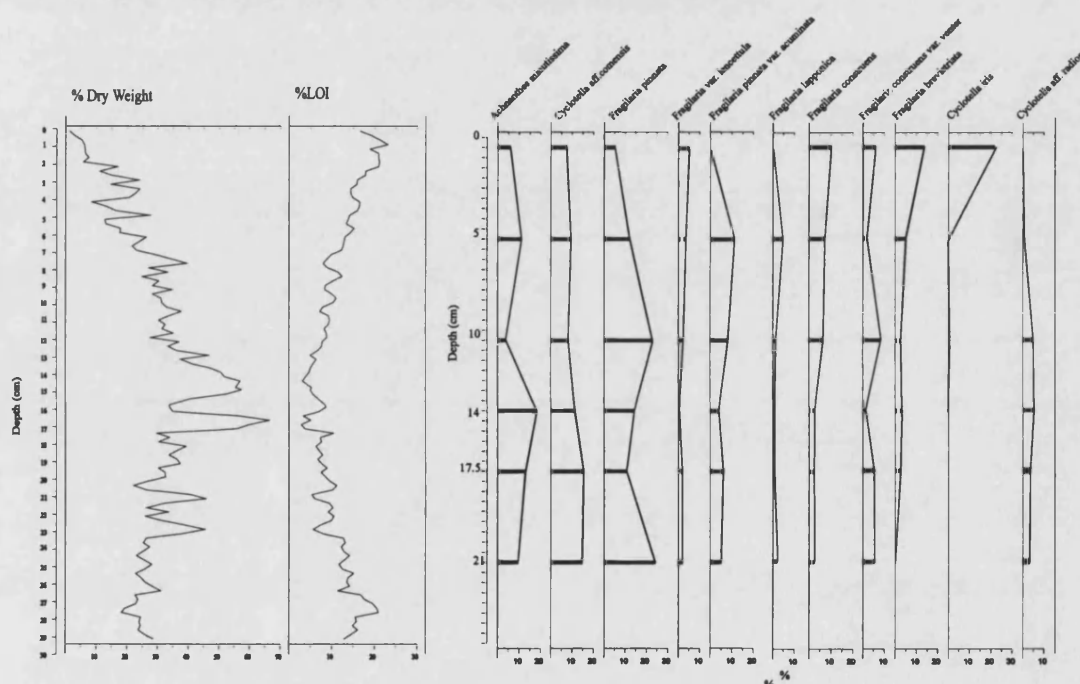
There is an obvious inverse relationship between %DW and %LOI in this core and the %LOI shows a correspondingly sharp increase and decrease around 15-16cm. The maximum %LOI for the core is 24% which occurs in the upper levels, with a low minimum %LOI value of <5% at ca.17cm. The dramatic colour changes in the profile correspond to changes in sediment type/ lithostratigraphy within the core.

The diatom profile of Gåvålivatnet is dominated by *Achnanthes minutissima*, *Cyclotella* aff. *comensis*, *Fragilaria pinnata* and *Fragilaria pinnata* var. *acuminata* (Figure 2.19). *Achnanthes minutissima* is negatively correlated with both *Fragilaria pinnata* and *Fragilaria construens* var. *venter* throughout the profile. The abundance of *Cyclotella* aff. *comensis* is fairly constant throughout the core.

In the upper section of the core (1-5cm) there is a dramatic rise in *Cyclotella iris* which is absent in the lower section of the profile. The increase in this species corresponds with a decrease in *Fragilaria pinnata*, *Fragilaria pinnata* var. *acuminata* and *Cyclotella* aff. *radiosa*. In addition *Cyclotella* aff. *radiosa* appears to be negatively correlated with the two other *Cyclotella* species, its abundance, however, is relatively low throughout the core.

The changes in lithostratigraphy are reflected in the diatom profile which shows an increase of *Achnanthes minutissima* var. *minutissima* and *Cyclotella radiosa* at ca. 14-17cm and a corresponding decrease of *Fragilaria pinnata*, *Fragilaria pinnata* var. *acuminata*, *Fragilaria construens* var. *venter* and *Fragilaria pinnata* var. *lancettula* at this level. *Cyclotella* taxa are planktonic (see section 3.2.5) and therefore the diatom scan shows that this core has a relatively large proportion of planktonic diatoms present within it.

Figure 2.19: Percentage dry weight, percentage loss on ignition graphs and diatom profile for Gåvålivatnet. Taxa occurring at <5% abundance are not presented.



2.3.7 Hornsjøen, Code 98-18

This site is remote and undisturbed and also located within the Døvre fell National Park but on a more base-poor bedrock geology in comparison to Gåvålivatnet. The lake pH measurement, however, (6.89 pH units) is still quite high. One small hut has been built in the catchment (Figure 2.20 a and b) but this is obviously too small to have any impact on the lake system.

The 27.5cm core was taken at 12.5m depth and it had a loose orange top from 1-2cm, and a brown organic layer, changing little in colour or texture, from 2-19cm followed with a blacker layer from 19-21cm. Below 21cm the sediment becomes lighter, finer

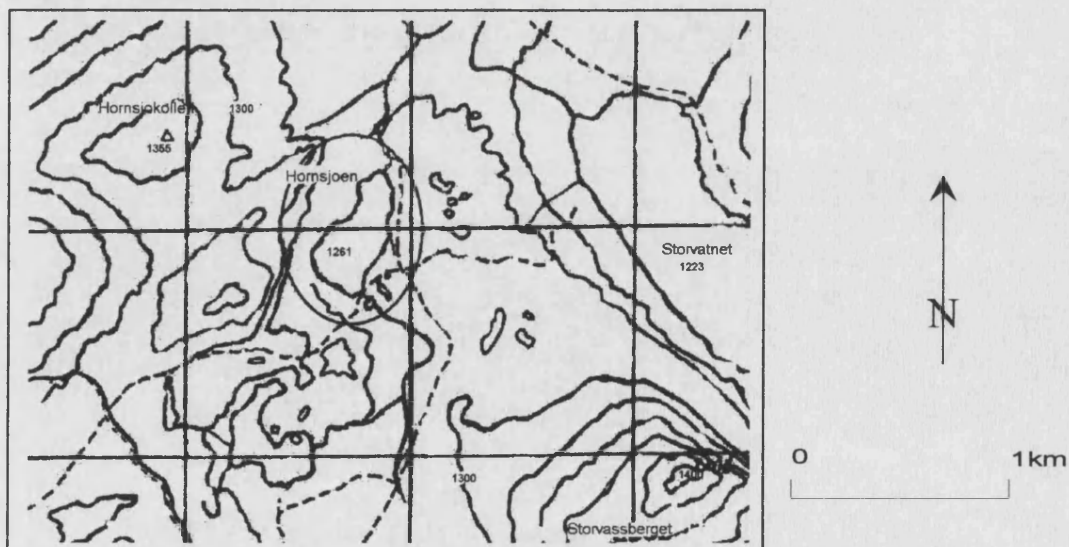
and more clay like. The %DW profile for Hornsjøen shows a marked increase in %DW at 18cm which decreases gradually above this level (Figure 2.21). This change can also be seen inversely in the %LOI curve which shows a increase from 16% at 20cm to 27% at 18cm. The changes in the colour and texture of the core, noted above, seem to correspond to the changes in the %LOI profile also.

Figure 2.20 a) Hornsjøen, Code 98-18

Altitude 1261m.a.s.l., Area 17ha. approx., Depth 12.5m, pH 6.89, TOC 1.6mg/l



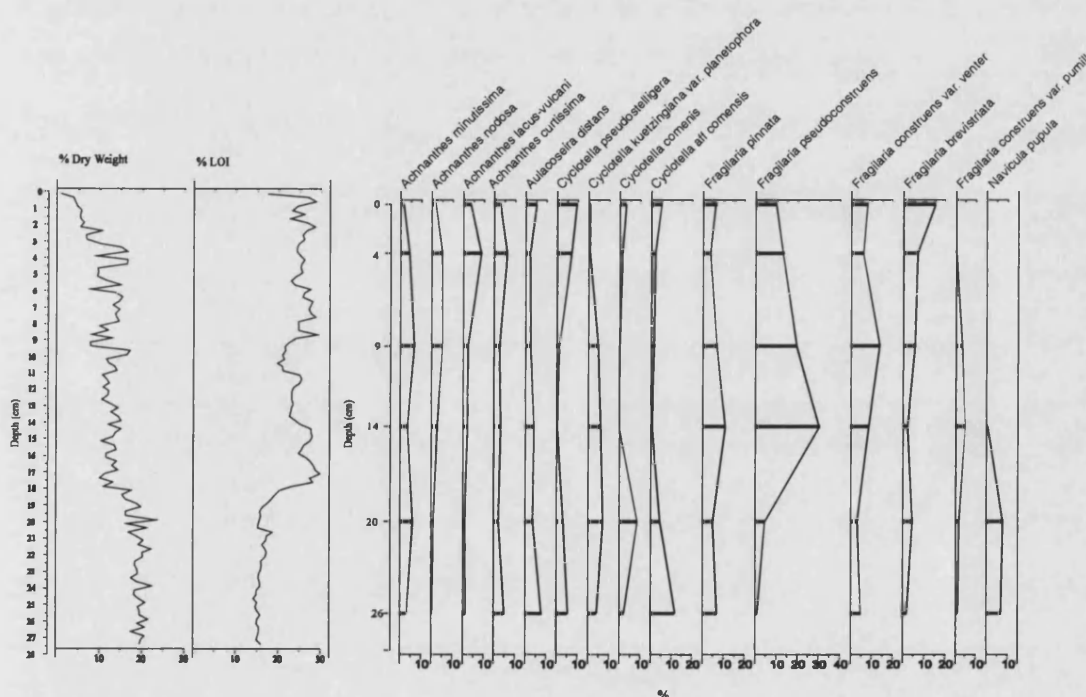
b) Topographic map of Hornsjøen (circled), Code 98-18 (Source Statens Kartverk Norge 1:50000 Topografisk Hovedkartseries)



The diatom profile corresponds to the changes in the %LOI and %DW. At 14cm there is a sharp increase in *Fragilaria pseudoconstruens*, from <5% at 20cm to 30% at

14cm, with further minor increases in *Fragilaria construens* var. *venter* and *Fragilaria pinnata* at this level. In addition *Navicula pupula* is not found above 14cm. Throughout the core *Cyclotella pseudostelligera* and *Fragilaria brevistriata* are negatively correlated with *Fragilaria pseudoconstruens*. Few of the *Cyclotella* species ever exceed 10% maximum abundance in the profile but in combination they form a substantial proportion of the diatom composition. As with Gåvålivatnet, therefore, this core also has a large proportion of planktonic taxa (*Cyclotella* sp. combined) within it.

Figure 2.21: Percentage dry weight, percentage loss on ignition graphs and diatom profile for Hornsjøen. Taxa occurring at <5% abundance are not presented.



2.3.8 The selection of cores for further palaeolimnological analyses

It would appear that only two sites fitted the criteria outlined in Section 2.3. Both Hornsjøen and Gåvålivatnet proved to have more potential for climatic reconstruction, due to the presence of planktonic diatoms within the cores and the fact that both sites exhibited distinct changes in their %LOI profiles which might potentially signify changes in production of the lake or catchment associated with the LIA.

High altitude lakes within Europe, due to their relatively low nutrient concentration and long ice-cover periods tend to have characteristically low plankton abundances in comparison to many lowland systems. Hornsjøen and Gåvålivatnet, had planktonic

diatom abundances exceeding 10% in total and were, therefore, considered to be the most suitable for further high resolution diatom analysis, the reconstruction of the environmental/ climatic variables (discussed in Chapters 4 and 5) and to further investigate the linkages between planktonic diatoms and climate change to satisfy the aims outlined in section 1.6.

2.4 Conclusion

This chapter has presented the site locations for the 80 lake training set sampling sites. Photographs of some of the sites located within both Norway and Scotland illustrate some of the characteristics of the lake systems represented in the training set. These, and their descriptions show how the systems are similar, in terms of altitude, catchment type and nutrient status, regardless of country, and therefore suitable for amalgamation in to a single training set.

The chapter also presented the site locations and brief descriptions of each of the six cored lakes. The diatom scans, %DW and %LOI profiles for six short sediment cores collected in Norway were illustrated and discussed. Although several sites were cored and analysed eventually two of these sites (Hornsjøen discussed in Chapter 6 and Gåvålivatnet discussed in Chapter 7) were selected for further palaeolimnological analyses due to the fact that they were more suitable for a detailed palaeoclimatic study. The next chapter describes the methods involved in the collection of the samples from both the training set sites and the coring sites, and the laboratory and numerical techniques used in their analyses.

Chapter 3

Methods

Introduction

The last chapter presented the site selection criteria and catchment characteristics for both the training set sites and the six sites from which sediment cores were retrieved. It also summarised the selection of the two cored sites used for detailed palaeolimnological analyses (Chapters 6 and 7). In this chapter the methods used for the collection of the training set sediment samples and the short sediment cores are presented. Eventually two training sets were developed, a 40 lake 'ice-cover' training set (discussed and analysed in Chapter 4), made from a subset of the 80 lakes, and the full 80 lake training set (discussed and analysed in Chapter 5). The selection of these two training sets, and the environmental and chemical variables available for each, is presented. Laboratory methods and numerical techniques used in the analyses of both the training sets (Chapters 4 and 5) and the core analyses (Chapters 7 and 8) are discussed.

3.1 Field methods

3.1.1 Surface sediment retrieval, sediment core sampling and water sample collection

For each of the lakes within the training set, the maximum lake depth was measured using an echo sounder and, where possible, a surface sediment sample was taken from the deepest area of the lake. In a few cases it was not possible to retrieve a sample at maximum lake depth, and the sample was taken from an area close to the maximum. For the Norway 1 data set (section 2.2.2) the samples were taken with a Renberg gravity corer (Renberg 1991) during the late Autumn between 1996-1999. For the Norway 2 (section 2.2.3) and Scottish sites (section 2.2.1) the samples were taken using a Glew gravity corer (Glew 1988), in September and early October 2000. These surface samples are thought to represent an integrated sample of the taxa that have accumulated in the recent past and to be derived from a variety of lake habitats (Cameron 1995; Jones and Flower 1986, see section 1.4.1.1).

At the same time water samples were also taken from the centre of each lake, 1m below the surface, for water chemistry analysis. For all the water samples collected

the 2x 250ml sample bottles were either acid washed or new to minimise problems of contamination. Sample bottles were also washed in the field with lake water.

The six short sediment cores were collected using a Renberg gravity corer (Renberg 1991), four during 2000 (98-20, 98-6, 98-9 and 98-2), and two in 2001 (01-03 and 98-18), and these were extruded in the field at 2.5mm resolution (Section 2.3.1). As with the training set, water samples were also taken at the time of sampling for these lakes. The changes in sediment colour and texture were noted down as the cores were extruded in the field (sections 2.3.1- 2.3.7).

3.1.2 Ice-cover measurements- surface water thermistor installation

Surface water temperature mini- thermistors (Vemco 8-TR Miniloggs) were installed in some of the Norway 2 and Scotland training set sites. These were anchored near the outflow of the lake to ensure a continual flow of epilimnetic water past them, thus minimising local littoral effects. The sensors were attached to a rope and positioned between 5 and 10cm below the surface anchored by a heavy stone. These thermistors measured surface water temperature, at 1 or 2hr intervals, every day for a year from October 2000 to October 2001.

From these measurements approximate ice-cover duration, in days per year, could be calculated from ice break-up and freeze-up dates. The ice freeze-up and break-up dates were calculated by Kamenik and Livingstone at EAWAG (Swiss Federal Institute for Environmental Science and Technology) as part of the EMERGE project. The freeze and break-up dates were based solely on the thermistor data i.e. without reference to any Automatic Weather Station data which may have been available. This avoided the creation of a circular argument when ice-cover duration was modelled using air temperatures for the same lakes (see section 3.2.2).

It should be noted, however, that the thermistor ice-cover duration measures represent 'best estimates' only of ice-cover extent. In some cases two ice-cover break-up or freeze-up dates were given when the thermistor results were not conclusive. In such cases an average date between the two was used to calculate total ice duration days. The ice-cover duration measures derived from the thermistor data are, therefore, often

not absolute values but are useful measures to compare ice-cover duration for the sites.

Originally, through the EMERGE project, thermistors were to be installed in all the Norway 2 and Scottish training set sites (51 sites). Unfortunately only five thermistors were installed in the Norway 2 lakes and one of these could not be retrieved. Although all 28 were installed within the Scotland region some were lost due to ice melting, ice drag, breaking of the attached rope and flushing from the lake, and only 19 thermistors, recorded both ice freeze-up and break-up dates. This reduced the total number of sites with ice-cover data derived from the thermistors to 23 (see section 3.2.3 for further discussion).

3.2 Laboratory methods

The following section presents the environmental variables for the 80 lake training set and the methods involved in their measurement. Measurement problems associated with some of the variables are discussed and the final design of the two training sets is presented. In many cases variables are missing for the 3 subsets (either Norway 1, Norway 2 or Scotland) and the implications of this for the design of the training sets are discussed.

3.2.1 Environmental data and water sample analyses

For the Scotland and Norway 2 sites the water samples were analysed for 22 chemical determinands at the Fisheries Research Services freshwater laboratory (FRS) and the Norwegian Water Research Institute (NIVA) respectively. The samples were analysed for pH, conductivity (Cond), alkalinity (Alk), ammonium (NH_4^+), potassium (K^+), calcium (Ca^{2+}), magnesium (Mg^{2+}), sodium (Na^+), nitrate (NO_3^-), sulphate (SO_4^{2-}), chloride (Cl^-), dissolved silica (DS), soluble reactive phosphorous (SRP or $\text{PO}_4\text{-P}$), total phosphorous (TP), total nitrogen (TN), aluminum (Total monomeric- Al-TM, non labile- Al-NL, aluminum labile- Al-L), absorption (Abs 250, not available for the Norway 2 sites), total organic carbon (TOC). altitude (Alt), lake area (LArea), July and January air temperatures and annual precipitation measures (ppt) are also available for these sites.

The Norway 1 samples were originally analysed for all of the above excluding TP, SRP, TN, DS and chl *a*. Again the water chemistry analyses were conducted at the FRS laboratory. For some sites lake area was calculated using a planometer directly from maps, however, lakes >2.5ha were too small to register (Table 2.1).

It was thought necessary, however, to obtain nutrient and silica data (TP, SRP, DS and Chl *a*) for these Norway 1 sites. In 2000, therefore, the 29 sites were revisited and new water samples for nutrient analysis were taken. These samples were analysed for DS, SRP, TP and Chl *a* at the Centre for Ecology and Hydrology, NERC, Edinburgh (CEH). The main variables, their unit measure, the abbreviations used hereafter, and a brief description of each are presented below.

- *Altitude (Alt), metres above sea level (m a.s.l)*

Measured on site using a GPS.

- *Lake Depth (Dmax), metres (m)*

Measured from the boat using an echo sounder.

- *Lake area (Area), hectares (ha)*

Measured directly from the lake map.

- *Secchi depth (Secchi), metres (m)*

Measured from the boat using a Secchi depth disc. The disc was suspended in the lake and the depth at which it was no longer visible was recorded. This was often the lake's maximum depth due to the low colour of the lakes in the training set. Secchi depth is not available for the Norway 1 and Norway 2 data sets (Table 3.1).

- *January and July Air temperature (JanT, JulyT), degrees centigrade (°C)*

This was taken from the nearest automatic weather station and alterations for differing altitude were made using environmental lapse rate equations. This was conducted at Edinburgh University, by Professor Roy Thompson, and Bergen University, by Professor John Birks.

- *Annual Precipitation (ppt), millimetres per year (mm)*

These were calculated by Professor Roy Thompson at Edinburgh University as part of the EMERGE project using Automatic Weather Station data and at Bergen University by Professor John Birks.

- *pH*

pH measurements for Norway 1 were conducted in the field, on unfiltered samples using a Jenway pH meter with a BDH Gelplas general purpose combination electrode. The electrode was allowed to stand in the solution for several minutes before the pH value was recorded. Values were recorded to the nearest 0.1 pH unit. The pH meter was calibrated using pH buffer 7 and 4 solutions prior to measurement. Test measurements were made on distilled water samples before each run. For the Norway 2 and Scotland sites pH analyses were conducted in the FRS and NIVA laboratories, within 48 hours of collection, using the methods outlined above.

- *Conductivity (Cond), Micro– Siemens cm^{-1} ($\mu\text{S}/\text{cm}^{-1}$)*

Conductivity represents the ability of a body of water to conduct electricity. It is a measure of the concentration of ions in solution. In bicarbonate dominated systems conductivity is a useful measure as it has been shown to be directly proportional to the concentration of the major cations (Ca^{2+} , Mg^{2+} , Na^{+} and K^{+}) in solution (Wetzel and Likens 1991). Conductivity measures were produced at the FRS and NIVA laboratories.

- *Alkalinity (Alk1), ($\mu\text{eq}/\text{l}$)*

Alkalinity of waters refers to the quantity and kinds of compounds present which collectively shift pH to the alkaline side of neutrality (Wetzel 1983b). It is usually only carbonate, and in particular bicarbonate alkalinity, that is important in freshwaters, but in theory alkalinity can be caused by any weak acid anion (Wetzel and Likens 1991). The unit measure refers to the amount of hydrogen ions that can be potentially neutralised. In essence a water body's alkalinity refers to its 'buffering capacity' and the measure is the equivalent of the commonly used 'acid neutralizing capacity' (ANC). In order to measure alkalinity at very low levels the use of an

automatic titrator and Gran's titration was required (Gran 1950; Gran 1952). Alkalinity was measured at the FRS and NIVA laboratories.

-Ionic composition

The concentrations of four major cations, calcium (Ca^{2+}), magnesium (Mg^{2+}), sodium (Na^{+}), potassium (K^{+}) were measured for the training set, and three major anions, nitrate (NO_3^{-}), sulphate (SO_4^{2-}) and chloride (Cl^{-}).

Analytical quality control was conducted by the calculation of ionic balances for each sample (ref. Heathcote and Lloyd 1984). The basic assumption for this method of control is that pH, ammonium, calcium, magnesium, sodium, potassium, bicarbonate, sulphate, nitrate and chloride account, almost completely, for the ions present in solutions. The anion and cation sums should balance because all potable waters are electrically neutral. The total number of negative and positive charges must be equal. This equality was checked for each sample at the FRS and NIVA laboratories.

Cations: calcium (Ca^{2+}) $\mu\text{eq/l}$, magnesium (Mg^{2+}) $\mu\text{eq/l}$, sodium (Na^{+}) $\mu\text{eq/l}$, and potassium (K^{+}), $\mu\text{eq/l}$

The sample for cation analyses was acidified with approximately 1% by volume of concentrated nitric acid. This enabled the metal ions to be kept in solution. The solutions were then analysed at the FRS and NIVA laboratories using a spectrophotometer.

Anions: sulphate (SO_4^{2-}) $\mu\text{eq/l}$, chloride (Cl^{-}) $\mu\text{eq/l}$, nitrate (NO_3^{-}) $\mu\text{eq/l}$

The anions were analysed at the FRS and NIVA laboratories.

-Total nitrogen (TN), nitrate (NO_3^{-}), ammonium (NH_4^{+}), $\mu\text{eq/l}$

Nitrogen exists in four major forms in freshwaters: nitrite (NO_2^{-}), ammonium (NH_4^{+}), nitrate (NO_3^{-}) and organic nitrogen. TN is not available for the Norway 1 data set (Table 3.1). Ammonium and nitrate were determined spectrophotometrically. As before all these variables were measured at the NIVA and FRS laboratories.

- Dissolved silica, (DS)

In solution silica exists as either silicate (SiO_3^{2-}) or silicate acid (H_4SiO_4). Water samples for silica were collected in the field. 12mls of filtered water was collected and

refrigerated. An acidic ammonium molybdate solution was added to the filtered sample, which forms a yellow coloured silico-molybdate complex. This was reduced with ascorbic acid to a more stable molybdenum blue complex. The addition of oxalic acid eliminated the interference from any phosphate-molybdate complex formation. The absorbencies of the samples were compared with that of known standard solutions (corrected for the distilled water blank) at 810nm using a spectrophotometer fitted with a 10mm flow cell. Standard samples and distilled water blanks were also run to check for accuracy and contamination. Silica measurements were conducted at the FRS laboratory for the Scottish lochs and at CEH for the Norway 1 lakes. Dissolved silica is not available for the Norway 2 lakes.

- Total Organic Carbon (TOC), mg/l

TOC was measured at the FRS and NIVA laboratories using a TOCSIN TOC analyser- method. This assesses the total amount of organically bound carbon which is subsequently broken down in to single carbon units. These units can subsequently be measured quantitatively.

- Total Phosphorus (TP) $\mu\text{g/l}$, Soluble Reactive Phosphorus (SRP) $\mu\text{g/l}$

Total phosphorus includes all inorganic and organic forms both dissolved and in solid particulate phase. The total phosphorous contained within the water can be divided into dissolved phosphorous and particulate phosphorous by filtration, using the methods outlined for chl *a* below. SRP refers to the measurement of the filterable, inorganic fraction. SRP is often referred to as filterable reactive phosphorus (FRP) or ortho-phosphate.

TP is measured by taking an unfiltered, (frozen in the field for later analysis) sample and converting all forms of P to orthophosphate using a sulphuric acid- potassium persulphate digestion. The resulting molybdenum blue solution was then measured by the intensity of the blue colour of the sample against a set of digested standards of known concentration.

The determination of lake SRP is important because it provides an estimate of the amount of phosphorus that exists in a form that can be readily utilized by the algae. SRP was measured spectrophotometrically in a similar way to TP but on a filtered water

sample (frozen in the field). The absorbance of the samples was then measured by spectrophotometry. The blue colour formed was proportional to the amount of SRP present and measured against a set of standards. SRP is not available for the Norway 2 data set (Table 3.1).

- *Chlorophyll a (Chl a), $\mu\text{g/l}$*

For Chl *a* ≥ 3 litres of lake water were filtered through a GF/C Whatman® filter using a simple hand pump and filter apparatus. The paper filter, through which a known and recorded volume of water had been filtered, was frozen and kept in the dark until analysis in the laboratory.

The filters were ground to a paste in a solution of *ca.*90% acetone. 1ml of MgCO_3 suspension (5%) was added to this. The samples were centrifuged and left to settle. The absorbencies of the supernatant were determined by spectrophotometry in comparison to an acetone blank at the FRS and CEH laboratories. Chl *a* is not available for the Norway 2 data set (Table 3.1). There is often a close link between chl *a* and nutrient status in freshwater lake systems (Jones and Juggins 1995; Dillon and Rigler 1974). Chl *a*, therefore, can be used as a rough guide of lake productivity and trophic status.

- *Aluminium (Al- TM, Al-NL and AL-LM), $\mu\text{g/l}$*

The subtraction of Al-NL from Al-TM results in Al-LM and it is this form which is toxic to organisms (Ormerod *et al.*, 1987b; Ormerod *et al.*, 1987a). Aluminium was analysed at the NIVA and FRS laboratories.

The last section has briefly discussed the collection and analyses of many of the training set variables. Because several variables were not collected/ analysed for some of the training set sites Table 3.1 is presented later to summarise which environmental variables are available for each of the lake sets. The following section evaluates the accuracy of some of the environmental parameters available for the training set sites.

3.2.1.1 Problems with nutrient analyses: detection limits and inter-comparisons

The Scotland nutrient analyses (TP, SRP, TN and Chl *a*) were conducted at the FRS laboratory. The Norway 2 nutrient analyses were undertaken at NIVA. CEH

conducted the nutrient analyses for the Norway 1 data set. Typically high altitude lake systems are low in nutrients and have relatively low primary productivity, resulting in low TP and correspondingly low chl *a* levels.

The TP detection limit, defined here as the smallest amount that can be detected above the noise in a procedure and within a stated confidence limit, of the FRS laboratory is $2.5\mu\text{g/l}$ and at CEH it is $2\mu\text{g/l}$. The total phosphorus measurements for the Scottish sites were, in the majority of cases, below the detection limits. Only three sites had measurements above this value with a maximum of $6\mu\text{g/l}$ (Figure 3.1a). For the Scottish sites, therefore, there is no detectable TP gradient.

The NIVA laboratory were able to detect TP to $1\mu\text{g/l}$. The reliability of such a low detection limit is, however, questionable using the methods outlined above (Kirika *pers. com.*, Harriman *pers. com.*). Many of the TP values for the Norway 2 sites were below $2.5\mu\text{g/l}$, with only six sites above this level (Figure 3.1b) The TP gradient is not large, therefore, for the combined Scotland and Norway 2 data set (Figure 3.1c).

Figure 3.1a: The 'TP gradient' for the Scotland data set. The sites are arranged in order of increasing TP

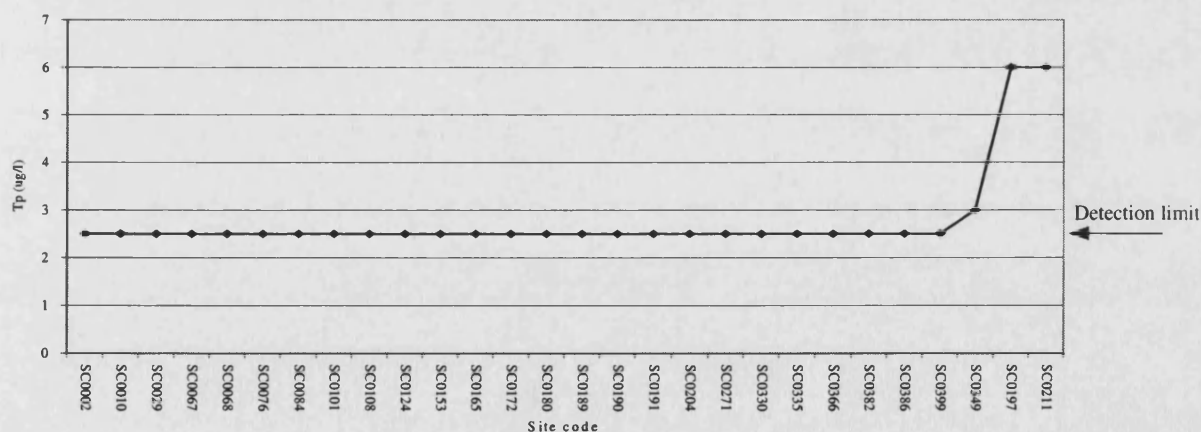


Figure 3.1b: The 'TP gradient' for the Norway 2 sites, four sites have TP data missing. The sites are arranged in order of increasing TP values.

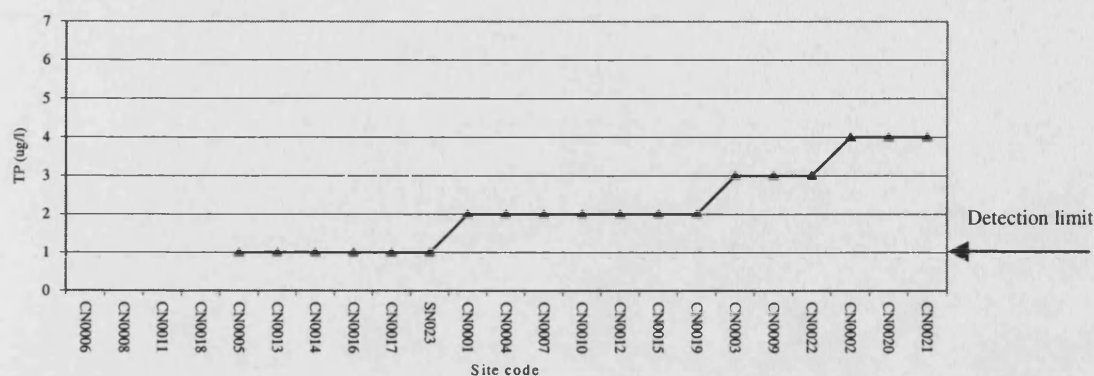
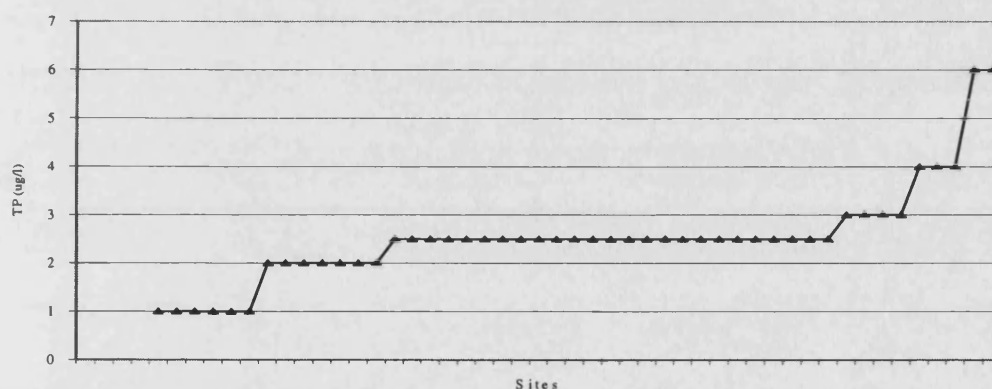


Figure 3.1c: The 'TP gradient' for the Scotland and Norway 2 data set (51 sites, 4 Norwegian sites missing TP data). The sites (not labelled) are arranged in order of increasing TP.



The SRP re-analysis (Figure 3.4) showed generally slightly higher SRP values for the re-analysis samples at the lower end of the SRP gradient, with significantly lower values on re-analysis at the higher end of the gradient (For e.g. 98-23 and 98-6, Figure 3.4). Many of the samples on re-analysis, however, retained inexplicably high TP or SRP levels for such oligotrophic lakes, when the chl *a* values are all near detection limits. The results also highlight the possible methodological inconsistency in the analysis and the danger of using 'individual spot' samples for nutrient analyses.

Explanations for such results could be contamination in the field or within the laboratory, sample misidentification or the presence of a 'random' source of organic matter within the sample such as a large zooplankton, or plant debris. Sample misidentification and contamination within the field seems unlikely because all the tubes used were new, screw-capped, polypropylene tubes, which were labeled and checked independently in the field. In addition the presence of random large fragments of organic matter seems unlikely in so many samples. The discrepancies between the SRP and TP amounts, resulting in values which are theoretically impossible, may suggest methodological problems.

It was decided, therefore, that more samples should be collected for further analyses and comparison. Five of the Norway 1 sites were sampled again in 2001. These were selected to cover a wide range of TP values, dictated by the original analysis results: two sites had relatively high TP values (98-18: TP 26.5µg/l and 98-6: TP 34.2µg/l initial analyses), one with medium TP (98-2: 18.9µg/l) and two with relatively low TP values (98-15: TP 9.6µg/l and site 98-23: TP 5.3µg/l, which is also the site with inexplicably high SRP values, see above). The sites with extremely high TP results in the original analysis could not be re-sampled, unfortunately, due to logistical problems of access.

The samples were again analysed at CEH. Sub samples were also sent to a marine laboratory, CEFAS (Centre for Environment, Fisheries and Aquaculture Science, Plymouth), which specialises in low nutrient analyses and have lower detection limits than most freshwater chemistry laboratories. They were, however, only able to produce PO₄ (SRP) results for comparison.

Figure 3.2: Graph comparing TP and chl *a* (log scale for ease of comparison) for Norway 1 data set (TP ($\mu\text{g/l}$)-filled squares and chl *a* ($\mu\text{g/l}$)-open diamonds). The sites are arranged in order of increasing TP.

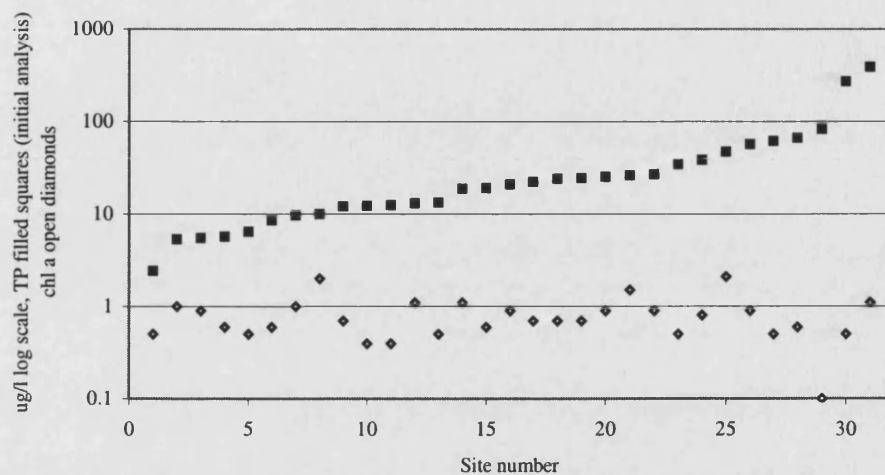


Figure 3.3: TP results for Norway 1 data set (open diamonds- initial analysis, filled squares- re-analysis on the same sample) arranged in order of increasing TP (initial analysis results).

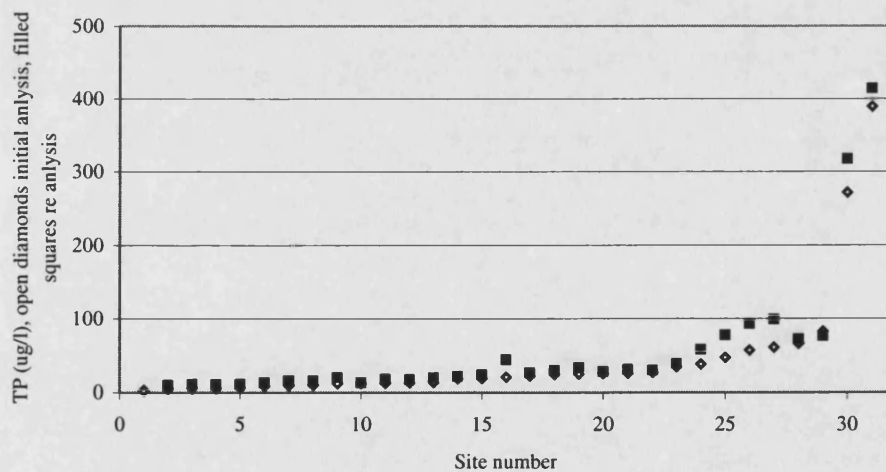


Figure 3.4: SRP results for Norway 1 data set (open diamonds- initial analysis, filled squares- re-analysis on the same sample) arranged in order of increasing SRP (initial analysis results).

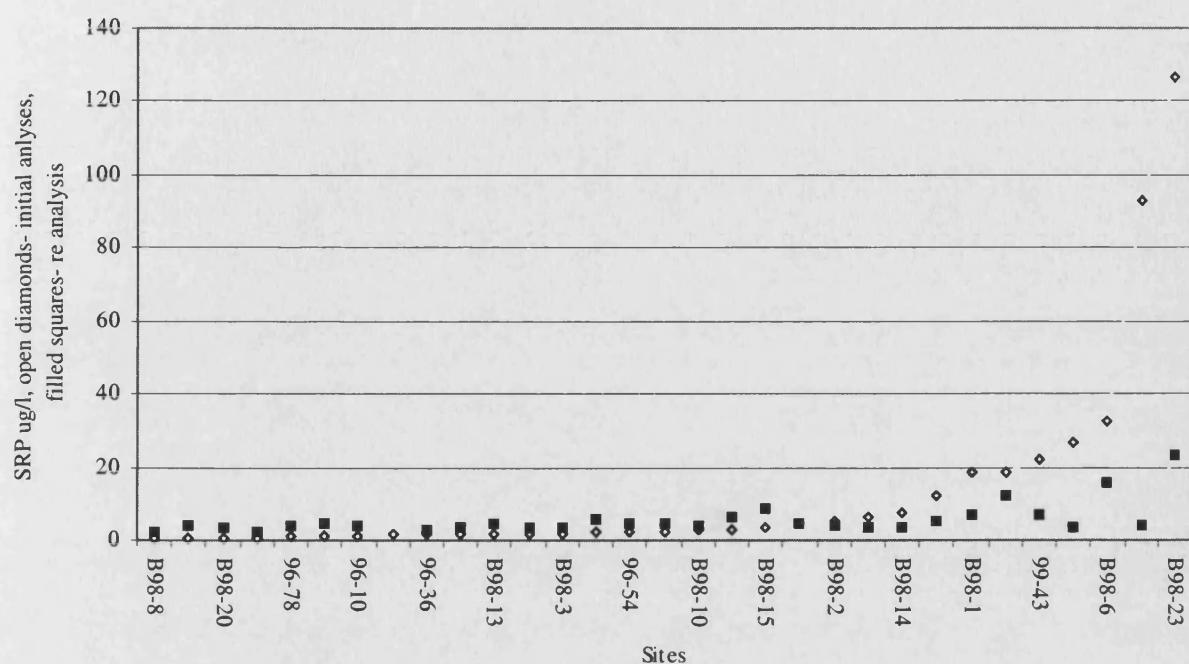


Figure 3.5: Comparison of TP ($\mu\text{g/l}$) for five Norway 1 sites. TP 'initial' and TP 're-done' collected in 2000, TP 'new sample' collected in 2001 all samples were analysed at CEH

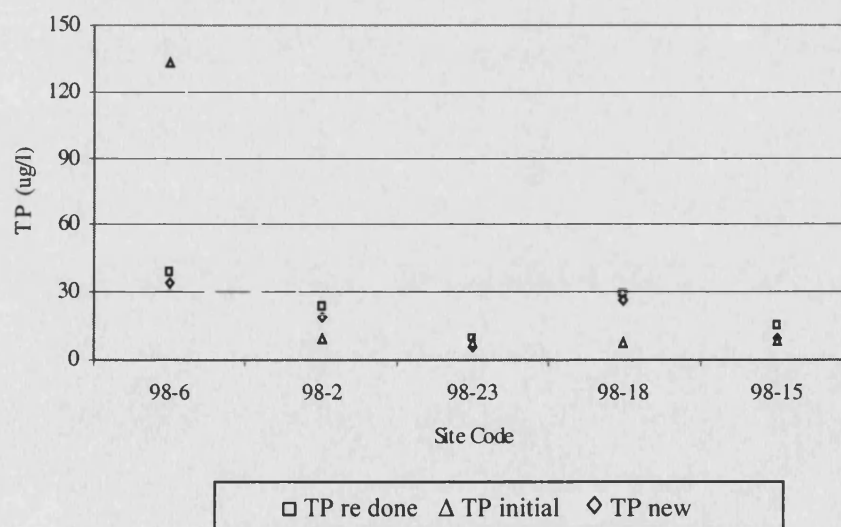


Figure 3.6: Comparison of SRP ($\mu\text{g/l}$) values (log scale, for ease of comparison) for five Norway 1 sites. SRP 'initial' and SRP 're-analysis' collected in 2000 and both analysed at CEH. 'SRP new' collected in 2001, one sample was analysed at CEH (SRP new (CEH)) and one analysed at CEFAS (SRP new (Marine)).

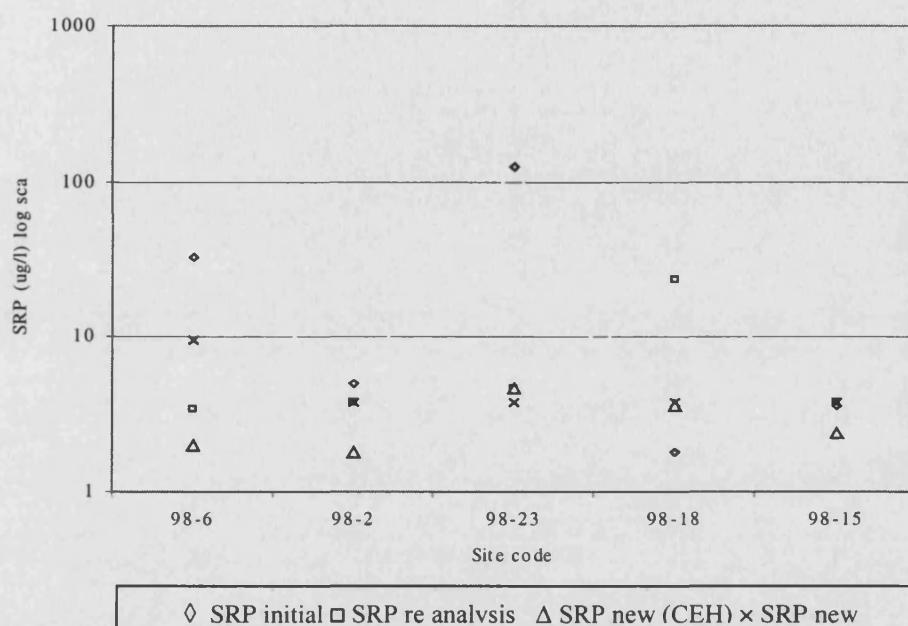


Figure 3.5 show the TP results of the initial analysis, the re-analysis and the results of the 2001 sample analysis all produced by the CEH laboratory. For four of the sites the new sample has lower TP values than the previous years sample, suggesting consistent over estimation in the initial analyses for some unknown reason. With 98-6 the TP value is much higher for the new sample with a TP of $133\mu\text{g/l}$ (replicates $133\mu\text{g/l}$ and $133\mu\text{g/l}$), initial TP was $34.2\mu\text{g/l}$. For a remote high altitude lake to change its nutrient status so dramatically within one year seems unlikely. This result again highlights the need for constant lake monitoring of the lake systems under study and the collection of multiple samples if realistic nutrient values are to be determined.

Figure 3.6 shows the comparison of SRP values for the initial analyses, the re-analyses (both conducted at CEH) and the 2 results for the 2001 sample (CEH and CEFAS). As with TP, the SRP results for the new sample are consistently lower than the initial analysis for four sites out of the five. In some cases, for e.g. 98-6 and 98-23, the results are *significantly* lower for the new sample, suggesting that the inexplicable high SRP value for 98-23 for the initial analysis may have been due to methodological measurement error. The results from CEFAS ('SRP new Marine) are all consistently

low (max 9.49 $\mu\text{g/l}$) and correspond with the expected SRP values for such high altitude sites. The wide variability between the four analyses for all five sites, bearing in mind that these are supposedly low nutrient lakes with undisturbed catchments, is obvious and illustrates the problems of nutrient analysis in typically low nutrient systems. In such systems a difference of 10 $\mu\text{g/l}$ SRP would have a profound effect on the biota of the system and should, in theory, be reflected in the chl *a* results.

Overall the low, or near detection limits, TP measurements for the Norway 2 and Scotland data sets and the inconclusive results for the Norway 1 sites has resulted in a TP gradient for the training set sites which is difficult to amalgamate. In the future the use of marine laboratories such as CEFAS, with lower detection limits and possibly more reliable methods of analysis, may represent a solution to this problem. The cost of such analyses, however, would create further logistical problems for a large training set such as this. The collection of multiple samples throughout the year would also be preferable. The increased laboratory costs involved and problems with fieldwork logistics of such an undertaking also made this option unfeasible.

The option of using Chl *a* as a substitute for TP is possible for the Norway 1 and Scotland sites. Unfortunately, however, although Chl *a* measures should have been taken for the Norway 2 lakes through the EMERGE project the samples were not collected by NIVA in the field (Table 3.1). It remains that the TP results for the Scotland and Norway 2 sites are within the ranges expected for such oligotrophic lakes and, therefore, one option is to exclude Norway 1 sites from the design of the final training sets. TN is also available for both the Scotland and Norway 2 sites (but not for Norway 1, Table 3.1). The exclusion of Norway 1 from the training set is discussed further in section 3.2.3.

3.2.2 Ice-cover modelling

The methods involved in the modelling of lake ice-cover are presented in this section. The availability and accuracy of the modelled ice-cover data are evaluated. The subsequent rationalisation of the 80 lake training set, to a 40 lake subset, due to the missing ice-cover variables is discussed. The environmental/ chemical variables available for both the 40 lake 'ice-cover' training set and the 80 lake training set are presented.

Ice-cover duration for the training set sites was calculated in three ways:

- a) Direct estimates using the mini- thermistor data (see section 3.1.2)
- b) Modelled ice-cover data
- c) Ice-cover estimates based on altitude measures

Points b and c are discussed in this section.

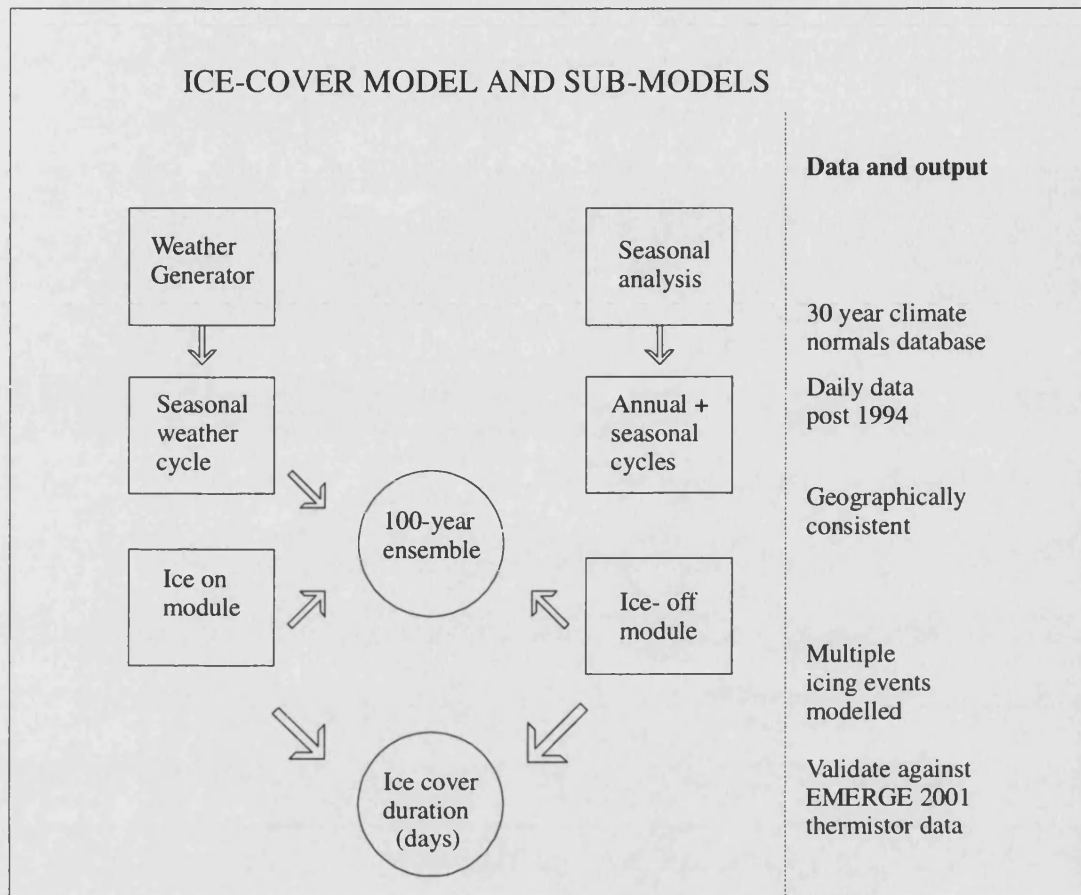
- Modelled ice-cover data

Ice-cover data was modelled for 31 sites out of the total 80 sites, by R. Thompson and D. Price at Edinburgh University, based on an empirical ice cover model developed for the MOLAR project (MOLAR 2002; Battarbee *et al.*, 2002). Originally it was anticipated that ice-cover estimates were to be provided for all 80 of the training set sites. This was not possible, however, due to time constraints at the Edinburgh Institute and complications with the ice-cover models' performance in maritime climates such as Scotland (Thompson, *pers. com.*). As a consequence only 10 Scottish sites and 21 Norwegian sites had modelled ice-cover data, with none modelled for the sites in the Norway 1 data set (Table 3.1).

The ice-cover model is based on air temperature, retrieved from AWS data, and the assumption that lake water temperatures are closely related to air temperature (*c.f.* Livingstone 1997; Livingstone 1999; Anderson *et al.*, 1996). The Edinburgh thermal degree-day model, that was developed and employed in the EC MOLAR project (Battarbee *et al.*, 2002) in order to reconstruct ice- cover duration during the last 217 years, (Agusti- Panareda and Thompson 2002; Agusti- Panareda *et al.*, 2002), was extended to incorporate a weather generator element (Figure 3.7) as part of the EMERGE project.

The weather generator element essentially tries to generate the weather at the sites using annual and 6 month cycles from climate normal data. Daily air temperature data were then incorporated to take into account the daily variations in air temperature by analysis of trends since 1994. This daily variation was then added to the low resolution climate data.

Figure 3.7: The components of the empirical ice-cover model (Source; Roy Thompson, Edinburgh University)



The model was validated using data from the EMERGE project generated from the installation of mini- thermistors in Scotland, the Southern Alps and the Pyrenees (Thompson *pers. com.*). The model parameters were identical to those derived in the MOLAR project (Thompson *pers. com.*).

- Estimates of ice-cover data using altitude

The ice-cover durations of the remaining sites in the Scotland and Norway 2 data set, which did not have either modelled or thermistor ice-cover data, were estimated based solely on altitude measures with an adjustment for latitude at Edinburgh University by Professor Thompson. This is a very crude way to estimate ice-cover (see Appendix 3.1) due to the complex interactions which determine lake ice-cover extent. It was decided, therefore, that this ice-cover data would not be used in this project due to its potential inaccuracies.

3.2.2.1 The accuracy of the ice-cover estimates from the empirical model

The accuracy of the modelled ice-cover data derived from the empirical model described above can be assessed by comparing the modelled data with the mini thermistor ice-cover estimates. Due to the lack of thermistor ice-cover data for the Norway 2 sites (section 3.1.2) and the lack of modelled data for the Scotland sites (section 3.2.2) comparisons within this data set are limited. Only 7 sites have both modelled ice-cover data and ice-cover data derived from the thermistors (Figure 3.8). The R^2 for the relationship between the modelled ice-cover data and the thermistor data is high, suggesting that there is good agreement between the two methods of estimation for these sites. The overlap of only 7 sites, however, limits the significance of this R^2 value.

For this reason other data were sought, beyond the sites in this study, to validate the ice-cover model. Within the EMERGE project mini thermistors were installed in several other European countries and calculations of ice duration were made from these (following the methods outlined in section 3.1.2). Many of these sites also had modelled ice-cover durations derived from the empirical ice-cover model discussed above. Within the EMERGE project a total of 58 sites had both thermistor ice-cover duration data and modelled ice-cover data. These data provided a more statistically significant way to test the accuracy of the modelled ice-cover data. The relationship between these estimates is illustrated in Figure 3.9 and Figure 3.10.

Figure 3.8: A comparison of the thermistor ice-cover duration (days) with the modelled ice-cover duration (days) with linear/ regression line plotted and R^2 values presented for 7 sites within the 80 lake training set

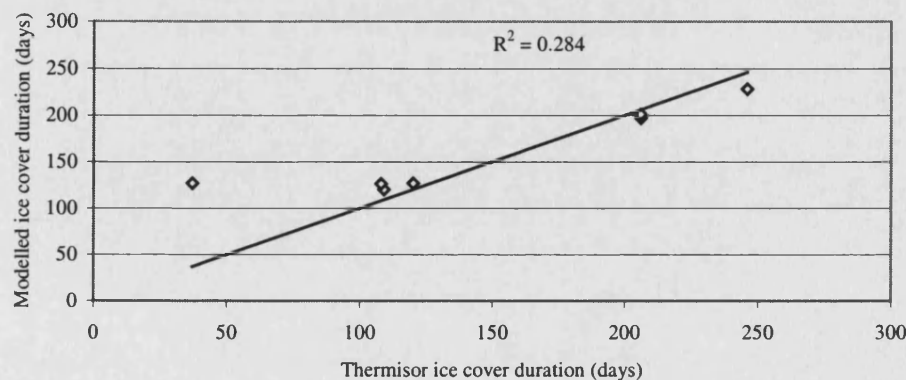
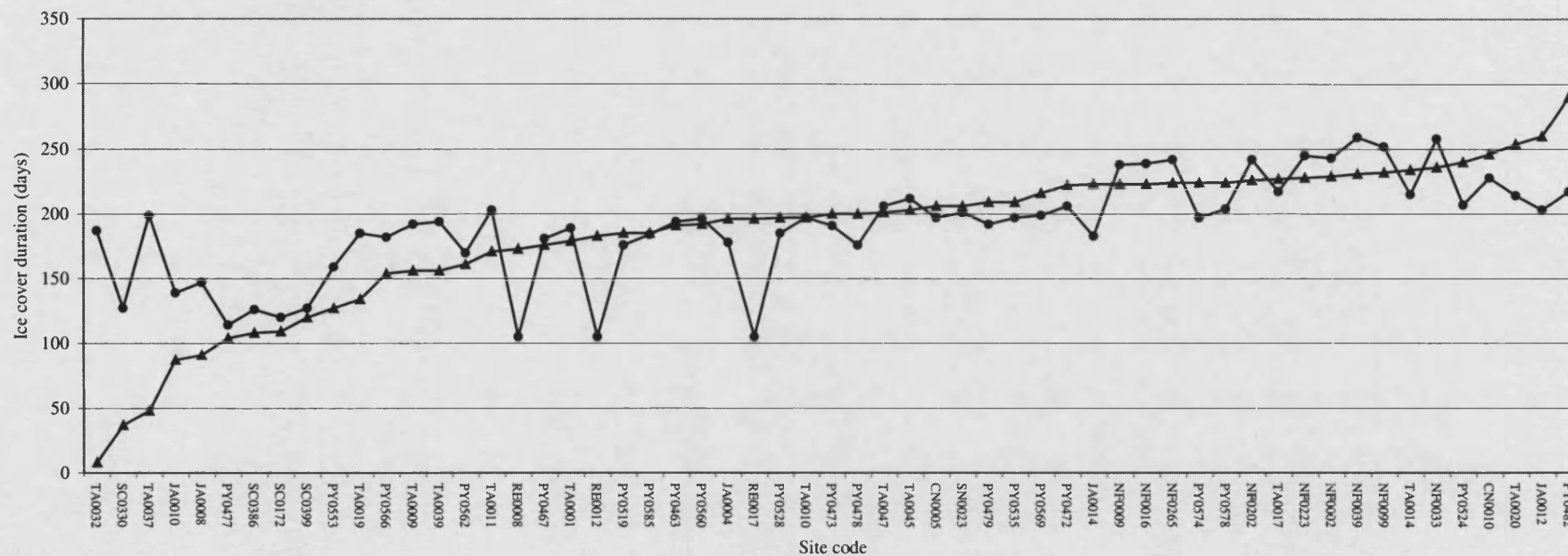
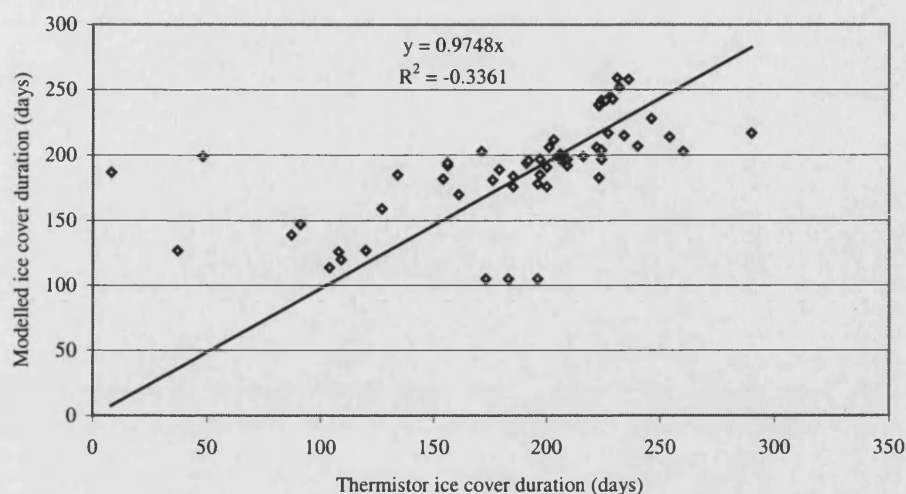


Figure 3.9; A comparison between thermistor ice- cover duration (filled triangles) and modelled ice- cover duration (filled circles) for 58 EMERGE sites across Europe, arranged in order of thermistor ice cover duration



Key to sample prefixes: TA= Tatra mountains, PY= Pyrenees, RE= Retezat, JA= Julian Alps, CN= Norway, NF= Northern Finland, SC= Scotland

Figure 3.10: A comparison of the thermistor ice-cover duration (days) and the modelled ice-cover duration (days) for 58 EMERGE sites. Linear regression line plotted and R^2 value presented.



It can be seen from Figure 3.9 that the modelled ice-cover estimates become more accurate, assuming that the thermistor results reflect the true ice-cover duration, as ice-cover duration increases. When the ice-cover duration is above *ca.*150 days the empirical ice-cover predictions are more accurate (the durations at a limited number of the coldest sites are still, however, under estimated). It seems that when the ice-cover duration is reduced the model does not predict ice-cover particularly well, resulting in the poor R^2 value (Figure 3.10). Several sites in particular at the lower end of the *thermistor* ice-cover gradient (e.g. RE0008, RE0012, RE0017, all Retezet mountain lakes) have a poor relationship with the modelled ice-cover results. This suggests that the model does not work well for sites with ice-cover duration of <150 days, but can be used with confidence for sites which have relatively long annual ice-cover durations.

The apparent problems with the inaccuracies of the modelled ice-cover data may not, however, affect the training set ice-cover estimates in this study adversely. It has been demonstrated that the ice-cover model works well for sites with long ice-cover duration. Because the Norwegian sites are at a higher altitude and latitude than the Scottish sites the model will perform better for these sites as their annual ice duration is likely to be over 150 days. Therefore, the modelled ice-cover data for the 22 Norwegian sites can be assumed to be accurate. Following on from this the sites with lower ice-cover duration, i.e. the Scottish sites, are problematic to model due to the on/ off nature of the ice-cover and the maritime climate. These are, however, the sites

in the training set with the most thermistor data, which are assumed to be accurate (19 Scottish sites with thermistor ice-cover data). It can be concluded, therefore, that a sub set of 40 lakes can be made consisting of 21 sites with accurate *modelled* ice-cover duration (the Norwegian sites) and 19 sites with accurate *thermistor* data (the Scottish lakes, Table 3.1). It should be noted, however, that no ice-cover variables, either thermistor based or modelled, are available for the 29 Norway 1 sites. In addition, 11 sites remain within the Scotland and Norway 2 data sets which do not have *reliable* ice-cover estimates.

3.2.3 Selection of the transfer function training sets

One of the main aims of the thesis is to investigate the relationship between ice-cover and diatom assemblages in high altitude lakes. Due to the limited availability and varying accuracy of the ice-cover data it seemed sensible to reduce the number of sites in the whole 80 lake training set to form an 'ice-cover' training set. This was done to minimise the problem of missing ice-cover variables and to ensure that any modelled data used could be done so with confidence.

Table 3.1: Environmental and chemical variables available for each data set (N/A= not available)

Determinand	Norway 1	Norway 2	Scotland
Lake Depth	Yes	Yes	Yes
Altitude	Yes	Yes	Yes
Lake Area	Yes	Yes	Yes
pH	Yes	Yes	Yes
Alk	Yes	Yes	Yes
Cond	Yes	Yes	Yes
Na ⁺	Yes	Yes	Yes
K ⁺	Yes	Yes	Yes
Mg ²⁺	Yes	Yes	Yes
Ca ²⁺	Yes	Yes	Yes
Cl ⁻	Yes	Yes	Yes
NO ₃ ⁻	Yes	Yes	Yes
SO ₄ ²⁻	Yes	Yes	Yes
Abs 250	Yes	N/A	Yes
TN	N/A	Yes	Yes
TP	Yes but not reliable	Yes	Yes
Chl <i>a</i>	Yes	N/A	Yes
SRP	Yes but not reliable	N/A	Yes
NH ₄ ⁺	Yes	Yes	Yes
DS	Yes	N/A	Yes
Al-TM	Yes	Yes	Yes
Al-L	Yes	Yes	Yes
Al-NL	Yes	Yes	Yes
TOC	Yes	Yes	Yes
ppt	Yes	Yes	Yes
Accurate ice duration measures (either modelled or thermistor)	N/A	21(modelled or thermistor)	19 (thermistor)
January Temp	Yes	Yes	Yes
July Temp	Yes	Yes	Yes
Secchi depth	N/A	N/A	Yes

Eventually the training set was reduced from 80 to 40 sites forming an 'ice-cover training' set (Table 4.1) which is discussed further in Chapter 4. Any Scottish sites with just modelled ice-cover data were not included, because these data were regarded as inaccurate and the set contained no sites from the Norway 1 data set. The 27 environmental/ chemical variables available for these 40 sites were: pH, Alk, Conductivity, Na^+ , NH_4^+ , K^+ , Mg^{2+} , Ca^{2+} , Cl^- , NO_3^- , SO_4^{2-} , TP, TN, Al-TM, Al-NL, Al-L, TOC, JanT, JulyT, ppt annual, lake depth, lake area, Altitude, Longitude, Latitude and ice-cover duration (a variable consisting of data from 19 thermistors and 21 modelled durations).

Despite the fact that ice-cover data were not available for all the 80 sites (Table 3.1) it was thought that the full data set should be analysed to aid the interpretation of any patterns evident within the 40 lake training set and for the reconstruction of variables which might prove to be indirectly linked to climate (pH, nutrients etc. see section 1.6). The 80 lake training set is discussed in Chapter 5. The environmental/chemical variables available for all the 80 lakes are: lake depth, altitude, longitude, latitude, lake area, pH, Alk, Cond, Na^+ , K^+ , Mg^{2+} , Ca^{2+} , Cl^- , NO_3^- , SO_4^{2-} , NH_4^+ , AL-TM, Al-L, Al-NL, TOC, ppt annual, JanT and JulyT (Table 3.1). It should be noted that no nutrient or silica data are available for the 80 lake data set due to problems discussed earlier (section 3.2.1.1).

3.2.4 Diatom preparation and counting

Diatom slides were prepared for each core sample and each surface sample. Diatom samples were prepared using methods described by Renberg (1990) using a water bath and hydrogen peroxide procedure. The samples were then washed and cleaned with distilled water, centrifuged, and the supernatant was discarded. The samples were sub sampled and diluted to a suitable concentration with distilled water and plated out on to a cover slip using a pipette. These were left over night to dry. The coverslips were then inverted and mounted on to microscope slides using Naphrax, a toluene-based diatom mountant, which was heated to ensure the cover slips were secure.

For the training set slides ≥ 500 diatom valves were counted for each sample. For the diatom scans of the six short sediment cores (section 2.3) only 300 valves were

counted to provide a general overview of species assemblage. For the high resolution diatom analysis of the cores 01-03 and 98-18 the number of valves counted depended on the species diversity of each core (see section 3.2.6). The counting strategy followed the procedure suggested by Battarbee (1986). A Zeiss light microscope was used with x1000 phase objective. Total chrysophyte cyst numbers were also recorded for each of the diatom slides counted but were not identified.

- Qualitative diatom slides

For the training set surface samples the diatom preparations were qualitative (as opposed to quantitative, see below) because diatom concentration measures were not necessary for the surface samples. When the six short sediment cores were scanned for diatom species these slides were also qualitative.

- Quantitative diatom slides

For the diatom analyses on cores 01-03 and 98-18 quantitative diatom slides were prepared. This was achieved by the addition of external markers in this case microspheres, which are commercially supplied in a suspension of a known concentration. A known number of microspheres can, therefore, be added to the diatom suspension, enabling the determination of relative diatom numbers, and the calculation of diatom concentration down core (Battarbee and Keen 1982). The amount of microsphere solution added should ideally result in a diatom valve:microsphere ratio of 1:1. In reality this is often hard to achieve so samples were only re-made if the ratio dropped below 1:3. An equation is then used to calculate the number of diatom valves per unit area (or cells per g dry weight) (Battarbee 1986).

$\text{Total valves in sample} = \frac{\text{Microspheres introduced} \times \text{Diatoms valves counted}}{\text{Microspheres counted}}$

The raw diatom counts for the cores and the surface samples were entered into the ECRC diatom database, AMPHORA (Beare 1995). These data were downloaded and transformed using the TRAN program (Juggins 1997b).

3.2.5 Diatom taxonomy and classification/nomenclature

Diatom taxonomy mainly followed the guidelines of the Surface Waters Acidification Project (SWAP) (Stevenson *et al.*, 1991) and the main floras used for identification were Camburn *et al.*, (1984- 1986), Krammer and Lange Bertalot (1986-1991) and

Camburn and Charles (2000). Nomenclature also followed the SWAP and AL:PE projects by retaining the old genera names (e.g. *Cymbella sinuata* was used instead of *Reimeiria sinuata*, and *Achnanthes clevei* was used instead of *Karayevia clevei* etc. ref. Round *et al.*, 1990 for other ‘new’ genera names).

In the current research several splits were made in the *Cyclotella* complexes and the *Tabellaria flocculosa* species as follows:

***Cyclotella stelligera* complex**

(*Cyclotella pseudostelligera* Hustedt 1939, *Cyclotella stelligera* (Hustedt) Haworth and Hurley 1986 (Haworth and Hurley 1984), *Cyclotella glomerata* (Bachmann) Haworth and Hurley 1986, *Cyclotella gordonensis*)

The form of *Cyclotella pseudostelligera* referred to in this thesis have bifurcate interstriae, well developed marginal processes and an almost stellate pattern in its central area (Plate 3.1 a-f). In *Cyclotella stelligera* this stellate pattern was much more distinct. *Cyclotella glomerata* tended to be smaller in size with distinct striae around its outer rim and a less regular or pronounced pattern in its central area (Plate 3.1 i-j).

Much discussion has taken place as to the benefit of splitting this complex with Haworth and Hurley (1984) suggesting that *Cyclotella pseudostelligera*, *Cyclotella stelligera*, *Cyclotella glomerata*, *Cyclotella stelligeroides* and *Cyclotella woltereckii* are all part of the same *Cyclotella* continuum at different growth/ reproductive stages and should be referred to as *Cyclotella stelligera*. It was noted by the authors, however, that morphotypes of this species have been known to favor different environmental conditions and so it was thought best to split them in this study. Few different very small *Cyclotella* species of this type were in fact found, in either the training set or the core samples, and so the complex was just split into *Cyclotella pseudostelligera*, *Cyclotella stelligera* and *Cyclotella glomerata*. Very small, faint *Cyclotella* species were also present within the training set samples and were referred to as *Cyclotella cf gordonensis* (Plate 3.1 g-h)

***Cyclotella ocellata/ Cyclotella krammeri/ Cyclotella comensis* complex**

(*Cyclotella ocellata* Pantocsek 1901, *Cyclotella krammeri* Håkansson 1990, *Cyclotella comensis* Grunow in Van Heurck 1882, *Cyclotella* aff. *comensis* following Rioual 2000).

Teuber (1995) suggested that the complex *Cyclotella ocellata*/ *Cyclotella krammeri*/ *Cyclotella comensis* was in fact a continuum of the same polymorphic species and that the different 'types' represented different stages of the life cycle of that species. However, he also suggested that these different morphotypes may have formed due to different environmental conditions. Therefore, the complex was split as much as was feasibly possible using a Light Microscope (LM).

Few *Cyclotella ocellata*, with distinctive ocelli (Håkansson and Carter 1990; Håkansson 1990), were found within the cores or the training set (Plate 3.11 is similar to *C. ocellata* but the ocelli are not present). A large number of similar *Cyclotella* species were found within the training set samples thought to belong within this *Cyclotella krammeri*/ *ocellata* complex (Plate 3.1 k-t). They were referred to in this study as *Cyclotella kuetzingiana* and *Cyclotella kuetzingiana* var. *planetophora* (see Håkansson 1990). *Cyclotella kuetzingiana* complex was renamed in 1990 by Håkansson as *Cyclotella krammeri* after its misidentification by Thwaites (Håkansson 1990). The original name was, however, used in this study with *C. krammeri* reserved for different *Cyclotella* types which tended to be larger, with more irregular length striae extending in to the central area (Plate 3.1 s-t, for similar illustrations see Håkansson (1990)- Figures 7, 8 for *Cyclotella krammeri* and Figure 10 for *Cyclotella kuetzingiana* var. *planetophora* type). The central area for *Cyclotella krammeri* types also tended to be smaller in size, in proportion to the marginal striae.

Often intermediate forms were found between *Cyclotella kuetzingiana* var. *planetophora* and *Cyclotella krammeri*, which had long irregular striae and four or five irregular punctae (Plate 3.1 q-r). These were split as consistently as possible using only a LM, based mainly on the extension of the striae into the central area and their irregularity, but *Cyclotella* aff. *krammeri* was also used when a distinction could not be made (for similar discussions see Wunsam *et al.*, 1995). It should be noted, however, that Teuber (1995) considered that the length of the striae, when splitting *C. ocellata* from *C. krammeri*, had no taxonomic value.

Cyclotella aff. *comensis* (Plate 3.1 u-w) was distinguished from *Cyclotella comensis* (Plate 3.1 x-z) based primarily on the regularity of its central area depressions.

Cyclotella comensis tended to have 5/4 valve depressions in a radial pattern. *Cyclotella* aff. *comensis* had a more disorganised (colliculate) central area.

***Tabellaria flocculosa* (Roth) Kutz 1844**

This species was split primarily according to its length and the shape of its central inflation in comparison to those at the apices and following the SWAP taxonomic guide (Stevenson *et al.*, 1991). *Tabellaria flocculosa* [long] refers to longer forms over $\geq 39 \mu\text{m}$. *Tabellaria flocculosa* [short] applies to forms $\leq 39 \mu\text{m}$ with a central inflation wider than that at its apices.

The classification of planktonic species

In order to distinguish between plankton and non plankton species it was important to classify the diatoms' habitat preferences. This was based primarily on the information collated by Denys (1991) who compiled a list of diatom species, their ecological and habitat preferences, derived from a review of the current literature (Denys 1991). Planktonic species, identified within the training set and the cores, and their classification according to Denys (1991) are listed below:

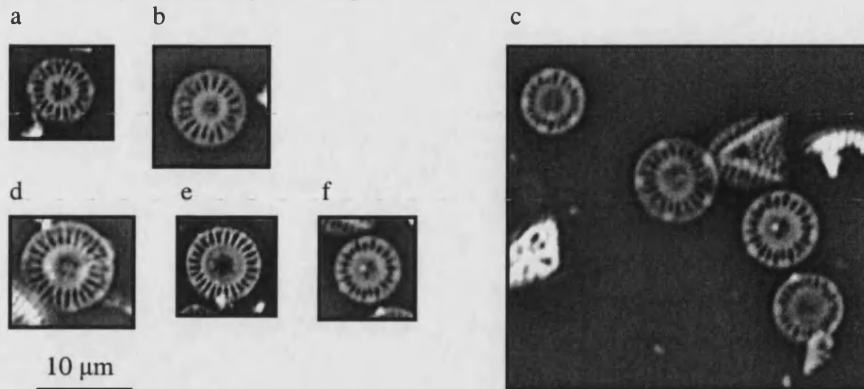
Asterionella formosa (euplanktonic)
Aulacoseira subarctica (tychoplanktonic)
Aulacoseira ambigua (euplanktonic)
Cyclotella comensis/ *Cyclotella* aff. *comensis* (tychoplanktonic)
Cyclotella gordonensis (tychoplanktonic, benthic origin)
Cyclotella iris (tychoplanktonic, benthic origin)
Cyclotella kuetzingiana/ *C. krammeri* (tychoplanktonic, benthic origin)
Cyclotella kuetzingiana var. *planetophora* (tychoplanktonic, benthic origin)
Cyclotella kuetzingiana var. *radiosa* (tychoplanktonic, benthic origin)
Cyclotella ocellata (tychoplanktonic, benthic origin)
Cyclotella radiosa/ *Cyclotella* aff. *radiosa* (euplanktonic)
Cyclotella stelligera (tychoplanktonic, benthic origin)
Cyclotella pseudostelligera (tychoplanktonic, benthic origin)

The classification of tycho planktonic refers to species that readily occur in the plankton but are derived primarily from other habitats. Often they may metabolize and reproduce in the plankton just as well as in their original situation.

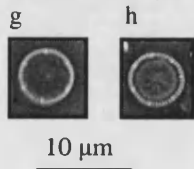
Plate 3.1: Light micrographs of the different forms of *Cyclotella* sp. found within the 80 lake training set

***Cyclotella stelligera* complex**

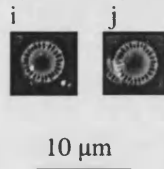
- *Cyclotella pseudostelligera* complex



- *Cyclotella* cf. *gordonensis*

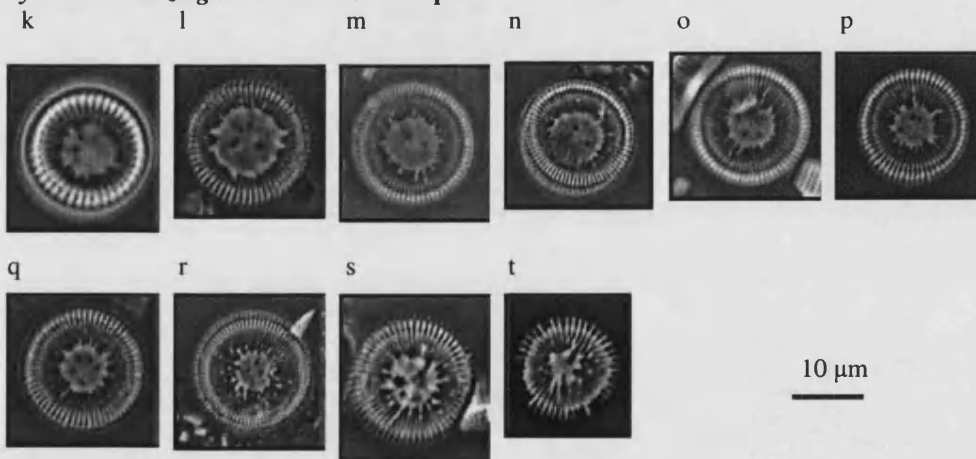


- *Cyclotella glomerata*

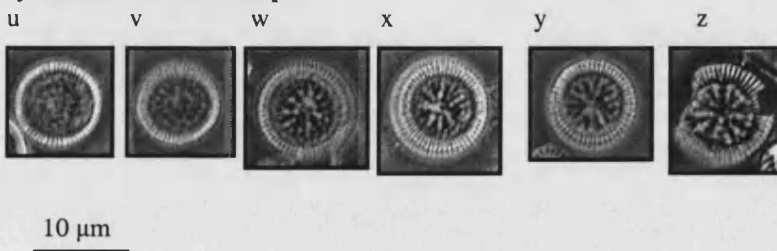


***Cyclotella ocellata*/ *Cyclotella krammeri*/ *Cyclotella comensis* complex**

- *Cyclotella kuetzingiana*/ *krammeri* complex



- *Cyclotella comensis* complex



3.2.6 Down core diatom analysis

For the two lakes selected for further analysis (see section 2.3) diatom slides were prepared for every 2.5mm sample. These slides had microspheres added to enable the quantification of diatom valve concentration in each sample (ref section 3.2.4). To enable the full diatom species diversity of the sample to be captured it was necessary to calculate how many diatom valves should be counted per slide. Therefore, a species number to valve count was performed. It has been shown that the number of new diatom species will diminish as the diatom valve count increases, eventually reaching an equilibrium represented graphically by a horizontal line (Battarbee 1986).

For one slide in each core the valve count and species number were recorded at regular intervals and plotted. The number of diatom valves to count for each core was calculated as the point at which the species to valve count reached a constant (i.e. a relative levelling off on the graph) as fewer new species were recorded in relation to the increasing valve count.

For Hornsjøen (code 98-18) the number of new species in relation to valves counted tended to level off slightly earlier than in the Gåvålivatnet (code 01-03) sample (Figure 3.11 and 3.12 respectively). It was decided that 400 valves per 2.5mm sample would be counted for the core from Hornsjøen. For Gåvålivatnet it was decided that 450 valves for each 2.5mm level would adequately capture the diatom species diversity in the core.

Figure 3.11: The relationship between species number and valve count for Hornsjøen

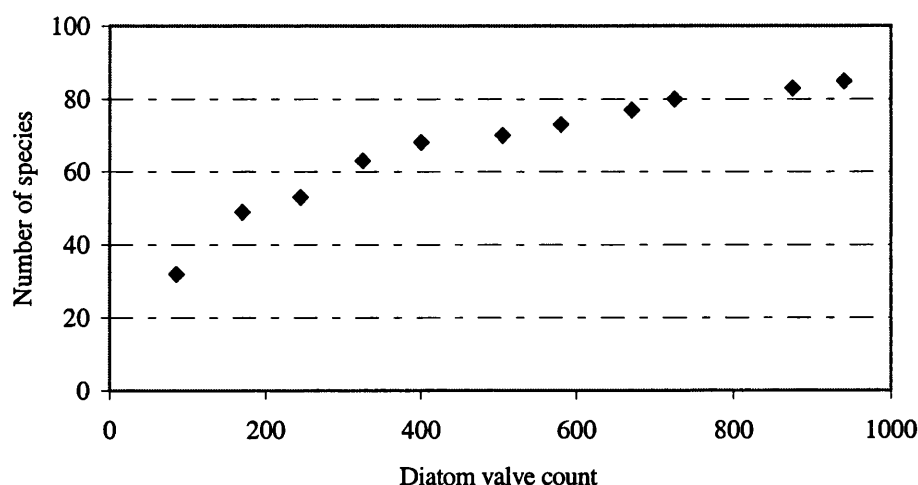
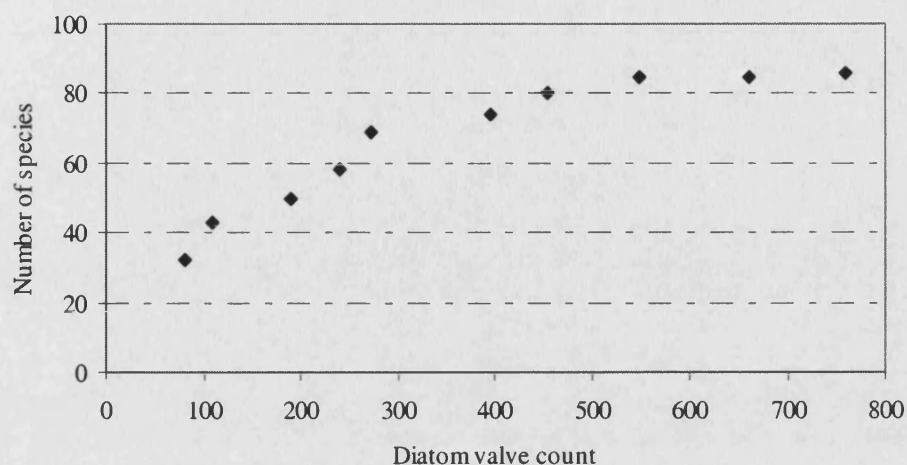


Figure 3.12: The relationship between species number and valve count for Gåvålivatnet

3.2.7 % Loss on Ignition and % Dry Weight analyses

Percentage dry weight (%DW) and percentage loss on ignition (%LOI) analyses were performed on each of the six cores (results described in section 2.3) providing an estimate of the organic content of the sediment. For each 2.5mm slice *ca.* 1g of sediment was dried in an oven at 105°C overnight and then reweighed to calculate the 'percentage Dry Weight' (%DW). The same sediment was placed in a furnace for 4-6 hours and burnt at 550°C and after cooling was re-weighed and calculations of the 'percentage loss on ignition' (%LOI) were made.

3.2.8 Core chronologies

The cores (from Gåvålivatnet and Hornsjøen) were analysed for ^{210}Pb , ^{226}Ra and ^{137}Cs by direct gamma assay (Appleby *et al.*, 1986). The method is based on the disintegration of an intermediate isotope, Radium-226 (^{226}Ra), which decays to Radon 222 which consequently escapes to the atmosphere, where it decays to ^{210}Pb . This ^{210}Pb enters the lake by precipitation and eventually is stored in the lake sediments. This input of ^{210}Pb is referred to as the 'unsupported' ^{210}Pb because it was not created by decay of radium within the lake sediments themselves which is termed the 'supported' ^{210}Pb (Oldfield and Appleby 1984). The 'supported' ^{210}Pb represents the background levels of ^{210}Pb in the sediments and the 'unsupported' represents the 'excess' ^{210}Pb (Oldfield and Appleby 1984). By subtracting the background levels, 'supported' ^{210}Pb , from the total ^{210}Pb a measurement of the 'unsupported' ^{210}Pb can be determined.

The concentration of ‘unsupported’ ^{210}Pb will decrease with depth in the sediments due to radioactive decay (radioactive half- life of 22.26 yrs) (*c.f.* Oldfield and Appleby 1984 for the assumptions of this model). Therefore, the age of the sediment at a particular point in the core can be calculated from its activity of ‘unsupported’ ^{210}Pb relative to that at the surface because the radioactive half- life is constant.

Detection of ^{137}Cs and ^{241}Am within the sediments can be used as validation for ^{210}Pb dating. ^{137}Cs and ^{241}Am have been present in the atmosphere since 1954 due to the testing of atomic bombs. It is assumed that the two elements fallout with rain and become attached to particles and that these particles are transported to the lake sediment relatively quickly and within <1yr (Ritchie *et al.*, 1973).

^{210}Pb , ^{226}Ra , ^{137}Cs and ^{241}Am measurement were conducted down each of the two cores. These were analysed by direct gamma assay using Ortec HPGe GWL series, well type, low background intrinsic germanium detectors (Appleby *et al.*, 1986). Two models were used to calculate the sediment dates, the CRS model (constant rate of supply) and the CIC model (constant initial concentration). These models allow for variations in dry mass, sedimentation rate and the effects of slumping or sediment mixing (Appleby and Oldfield 1978; Appleby and Oldfield 1983). Mean sedimentation rates were calculated in cm/yr. Chronologies were then calculated following standard procedures (Appleby 2001; Appleby and Oldfield 1978; Appleby and Oldfield 1983) The sediment accumulation rate was used to extrapolate down core to provide an estimate of sediment age reaching beyond the ^{210}Pb record to the basal sediments.

3.3 Numerical methods

Many statistical techniques are used within this thesis primarily to explore the variation within the biological data and its relationship to the various environmental parameters available. The techniques used, and their theoretical basis, are described briefly below.

3.3.1 Transformation of data prior to analyses

In order to use regression/ ordination models in the statistical analyses, described below, some of the environmental data were transformed to achieve frequency distributions which were normal. Many of the parameters displayed a right skewed distribution with numerous small values and a few very high values (e.g. Ca^{2+} , displayed a right skewed distribution for both the 40 and 80 lake training sets). In these cases the parameters were log transformed (or $\log(x+1)$ transformed for those parameters with many values less than detection limits). These transformations prevented the few high values influencing the regression analysis unduly. Transformations such as these are discussed further in Chapters 4 and 5.

In addition diatom assemblage data from the surface samples and the core samples, were also square root transformed to reduce the effect of dominant species within the data and to stabilize the variance within the data (Birks *pers. com.*). Rare diatom species were also down-weighted in the ordination analyses in direct proportion to their abundance.

3.3.2 Gradient analysis- Ordination and constrained ordination

Gradient analysis/ ordination analysis is based on the theory of regression analysis and enables investigation of the possible causes of variation within data sets (ter Braak and Prentice 1988). There are two main types of gradient analysis: direct and indirect. Direct gradient analysis is where the response variables are explored without reference to any explanatory variables (ter Braak and Prentice 1988). Any variation within the data is due to its inherent configuration (ter Braak 1988). For example, variation within several diatom samples (the 'response variable') might be explored independently of any environmental data, such as pH or salinity (the 'explanatory variables').

Direct gradient analysis is when the response variables and explanatory variables are analysed at the same time (ter Braak 1988). The patterns evident within the response variable are explained, albeit partially, by the explanatory variables. This is referred to as 'constrained ordination' because the response variables are being constrained by the use of the explanatory variables. Any patterns within the biological data are now interpreted in relation to the explanatory variables. For example, the diatom data are

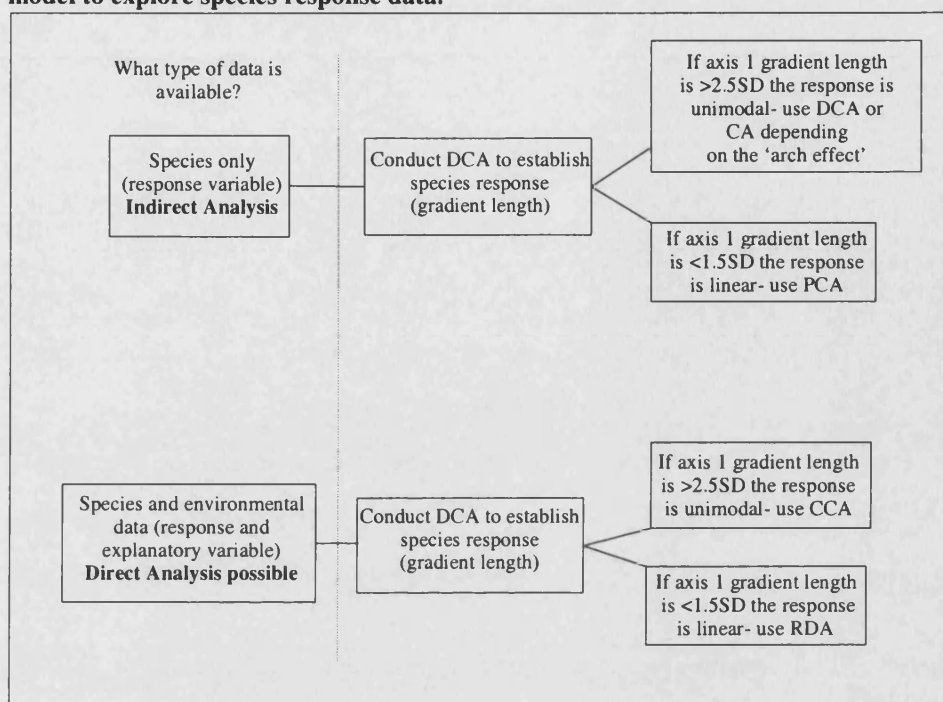
now analysed in conjunction with environmental data and the species response is linked to, and partially explained by, the environmental gradients within the data set.

There are two basic ordination methods available for both direct and indirect gradient analyses. The first is based on a linear response within the data under study and the second on a unimodal response. In order to select the most appropriate ordination technique to use the amount of variation within the response variable, the 'gradient length', should be calculated thereby determining whether the response is linear or unimodal. This response can be modelled using a mathematically defined Gaussian curve. The variation within the data is measured in Standard Deviations (SD). If a data set is highly variable its gradient length will be large ($>2.5SD$) and unimodal ordination methods are appropriate. If the gradient length is relatively small ($<1.5SD$), the variation within the data is smaller (i.e. the samples within the set are similar in composition) and the response is said to be linear (ter Braak 1987; Birks 1995). A total turnover of species would occur within $4SD$ (Jongman *et al.*, 1987). A gradient length between 1.5 and $2.5SD$ represent a 'grey' area and either linear or unimodal techniques may be appropriate.

Therefore, the choice of technique is firstly dictated by whether the analysis is to be indirect ('response variable only') or direct ('response and explanatory variable simultaneously'), and secondly the amount of variation within the response variable (small variation- linear methods, large variation- unimodal methods).

In order to assess the variation within the response variable the ordination technique of Detrended Correspondence Analysis (DCA) (ter Braak 1988) should firstly be conducted on the ecological data, regardless of whether indirect or direct gradient analysis is to be conducted. This directly determines the gradient length of the data in relation to the underlying environmental gradients, expressed as SD for each axes, and helps determine which ordination model is the most appropriate (Figure 3.13). Each ordination technique is described in the following section.

Figure 3.13: Diagram explaining the various steps involved in the selection of an ordination model to explore species response data.



3.3.2.1 PCA- Principal components analysis

PCA was conducted using CANOCO version 3.10, a FORTRAN programme for canonical community ordination (ter Braak 1988; ter Braak 1990). PCA is a method of indirect gradient analysis based on a linear response within the data. It is the most appropriate method to use when the chemical or biological data have low variance (ter Braak 1988). The distribution of the samples within the ordination is dictated by their similarity and linked to the ordination axes which represent unknown explanatory variables. Interpretation of the principle explanatory variables, responsible for the inherent variation within the data, can be achieved by analysis of the known ecological preferences of the species/ response variables.

For example, if sites dominated by taxa with low pH optima occur at one end of axis 1 and sites dominated by taxa with high pH optima occur at the other end of axis 1, axis 1 could represent a pH gradient. Ordinations such as these within this study are represented graphically as biplots using the CALIBRATE programme (Juggins and ter Braak 1993).

For PCA methods, therefore, the variance within the data is summarised by the axes of ordination, the first axis being responsible for the most explained variation, the second the second most explained etc. The amount of explained variance by each subsequent axis will decrease. Usually much of the variance within the data set is captured by the first few ordination axes. The relative contribution of each component to the total variation is measured in eigenvalues (λ) with axis 1 having a higher eigenvalue than axis 2 etc. The eigenvalues are multiplied by 100 to represent the percentage variance explained by each axis.

PCA can also be used for analysis of chemical data to determine the variance within, and similarity between, each chemical parameter. These ordinations can also be plotted using CALIBRATE and each variable is typically depicted by a biplot arrow. The direction of the arrow represents an increasing value for that variable. The length of the arrow indicates the variance within the chemical variable i.e. longer arrow-more variance representing a longer chemical gradient. The position of the biplot arrow in relation to the other biplot arrows determines the relationship between chemical parameters. For example variables with high positive correlation (e.g. pH and Ca^{2+}) would have small angles between their biplot arrows.

3.3.2.2 Correspondence Analysis (CA), Detrended Correspondence Analysis (DCA)

CA and DCA are indirect (response variable only) gradient analysis techniques. The underlying theory behind the analyses is described by Kent and Coker (1992). Indirect gradient analysis is the appropriate technique to use if the variation within the data is relatively high representing a unimodal response. CA and DCA can be useful tools for detecting possible extreme values or outliers within data sets (ter Braak 1987), in this case atypical diatom assemblages within the surface samples or down core analyses. The choice between whether to use DCA or CA is dictated by whether the data under study displays an 'arch effect' (curvature in the data at both extremities of the gradient) when CA is conducted, if so a DCA is the more appropriate method. DCA methods remove the arch effect by flattening out variation within the data, this is achieved by the option to detrend by segments or polynomials (hence the name detrended).

CA and DCA were again conducted using the CANOCO programme (ter Braak 1988, Birks *et al.*, 1990). CA/DCA biplots were constructed in the CALIBRATE programme (Juggins and ter Braak 1993). These position data in accordance with their species assemblages, i.e. samples close together on the biplot are more similar, floristically, than those at a further distance. As with PCA the relative importance of each axes, for explaining the amount of variance within the data, is expressed as eigenvalues and the total variance as the total inertia.

3.3.2.3 RDA –Redundancy analysis

The recommended direct ordination technique to model species environment relationships where the variation within the response variable is linear is RDA (ter Braak 1988; van den Wollenberg 1977). This is a constrained (direct) form of ordination, i.e. where the variations within the species response are expressed in relation to the explanatory variables, and the equivalent of a constrained PCA. The method assumes that there is a relationship between the response variable and the explanatory variables that increase linearly, either positively or negatively, across the environmental gradient.

The method is based on ordination (models the response variable as a function of the ordination axes) and multiple regression (which models the ordination axes as a function of the environmental variables, i.e. links the environmental variable to the ordination axes), in one technique. RDA selects the linear combination of explanatory variables, based on least squares regression, which minimise the total residual variation (Smallest total residual sum of squares) (ter Braak and Prentice 1988). RDA is a useful technique because it enables the identification of several explanatory variables which best explain the variation within the response data (ter Braak and Prentice 1988). RDA can be performed using CANOCO and plotted in the CALIBRATE programme as before.

3.3.2.4 CCA- Canonical Correspondence analysis

CCA is a direct gradient analysis technique, which identifies the main explanatory environmental variables responsible for the variance within the response data. Thereby response variables and explanatory variables are explored simultaneously (ter Braak 1988). With CCA the response variable should be unimodal. CCA is based on

the theories of correlation and regression between the response data and the environmental factors. CCA is a constrained technique where multiple regression is used to identify the combination of environmental variables that best explain the variation within the response variable.

Each ordination axes is independent, in that for the first axis species scores and sample scores are chosen to maximise the correlation between them. For the second axis the sample scores and species scores are again chosen to maximise the correlation between them but are uncorrelated to the previous axes. And likewise each subsequent axis is unrelated to any of the axes previously identified. Weighted averaging is used to maximise the covariance between the response and explanatory variables (ter Braak 1986).

As with the previous ordination techniques CCA was conducted using the CANOCO programme and biplots were created using CALIBRATE. These positioned samples/species in the ordination space according to the explanatory variables associated with them. The explanatory variables were displayed as vectors. The angle between these vectors and their relative length again denoted their similarity to other environmental variables and their importance for explaining the variance within the data set. Environmental variables with relatively long axes are more strongly correlated with the ordination axes and are more closely related to the inherent patterns of variation within the response variable (ter Braak 1987).

For example, a sample dominated by species with low pH optima might be positioned near the vector associated with low pH, if pH was the primary factor driving the variance within that sample. If, however, low TP also influenced the variation within the sample equally as much as low pH the site might be positioned between the low TP and low pH vectors.

Within the ordination some environmental parameters included in the analyses and displayed on the biplot may not be responsible for explaining any statistically significant proportion of the variance. These variables can be identified using the option of 'forward selection' within CANOCO. This in essence selects the most important explanatory variables and helps identify the simplest response–explanatory

model relating the biological data to the environmental data. The option adds environmental variables to the analysis one by one, in a step wise regression procedure, until no other variables significantly explain the remaining variation. With each environmental variable that is added CANOCO orders the variables in accordance with how much variance is explained by each environmental parameter.

A further extension of the ordination techniques described above is partial constrained ordination which can be used to quantify the amount of variance explained by each explanatory variable independently, by eliminating the effects of co-variables (Korsman and Birks 1990)

3.3.2.5 Species response models

The response of individual species to a specific environmental variable was evaluated using the HOF programme (Huisman *et al.*, 1993). This programme attempts to fit the simplest significant response model to the species data. Five hierarchical models are available within the programme: a skewed asymmetric unimodal response model (model V), a symmetric Gaussian response model (model IV), a monotonically increasing or decreasing response model (model Iii and IId) and the null/ no response model (model I see Figure 4.32). The models decrease in complexity (i.e. have fewer parameters) from the skewed asymmetric unimodal model through to the no relationship model, the last model. The programme works through these models systematically, with the most complex first, testing the significance of each model in terms of the response data. As each response model is fitted to the data, HOF drops a parameter until it cannot make the model any simpler without losing statistical significance. With fewer parameters, i.e. the simpler models, there are fewer degrees of freedom. HOF is applied in the current study in Chapters 4 and 5.

The specific preference and tolerance of an individual species to an environmental variable (i.e. the species niche) can be ascertained using weighted-averaging (WA) (ter Braak 1987) or Gaussian logit regression (GLR) (Juggins 1997a). GLR and WA are used in this way in Chapters 4 and 5 and a detailed description of GLR and WA techniques can be found in Odland *et al.*, (1995) and Birks *et al.*, (1990).

3.3.3 Inference models

Several techniques are available to quantify the relationship between species and environmental data in order to create a transfer function to be applied to a sediment core. Linear methods include partial least squares regression (PLS) (Geladi and Kowalski 1986). Weighted Averaging (WA) (ter Braak 1987) and Weighted Average Partial least squares regression (WA-PLS) (ter Braak *et al.*, 1993) are all unimodal methods.

These techniques can be used to develop a model or 'transfer function' to quantify and reconstruct an environmental variable. The theory behind transfer functions is that the preserved biological record, in this case diatom data, acts as a proxy and is used to infer past environmental conditions when such values are unknown. The generation of a transfer function is a two step process:

1. Regression step, where the relationship between modern diatom samples in a 'training set' and contemporary water chemistry conditions are quantified, where it is assumed that the biological data are a function of the environmental conditions (Birks 1995). This is conducted through the analysis of modern surface diatom assemblages and contemporary water samples/ environmental data for several sites, referred to as the 'training set' sites.
2. Calibration step (often referred to as inverse regression) involves the reconstruction of past environments from the fossil diatom assemblages using the regression function generated in the first step i.e. the environmental variable is inferred from the fossil diatom assemblages within the core based on their floristic composition.

There are various assumptions underpinning the transfer function technique and these are discussed in Birks (1995). Whether to use linear or unimodal techniques, for the generation of a transfer function, is generally dictated by the length of the gradient of species variation within the fossil biological data, measured in standard deviations (SD). A gradient length of 4SD deviation represents high variability within the biological data set and the species present at one end of the gradient will not be present at the other end, representing a total 'turnover' of species. As with the ordination

techniques with a short gradient, typically $<2SD$, linear methods are more appropriate to use (PLS). With longer gradient lengths $>1.5SD$ unimodal methods are more suitable (WA, WA-PLS) (ter Braak and Prentice 1988; Birks 1995). Often though a comparison of many calibration methods is recommended (Birks 1995).

PLS (Partial Least Squares) is related to PCA and represents an extension of inverse regression in that it considers multiple species. The technique aims to maximise the correlation between the variance within the response data (biological data) and the environmental variables. PLS is considered most appropriate for data with relatively small amounts of variation within it, i.e. a linear response within the diatom data, and for 'noisy' data. Such noise in diatom data may present itself as data with high sample dissimilarities, a large number of rare species present within the data set, and data with many zero values.

For PLS the computer programme CALIBRATE was used (Juggins and ter Braak 1993). The model produced consists of a two step regression and calibration components/ stages (see Chapters 4 and 5), with each stage, or component of the model, an R^2 value is generated along with its associated error (or Root Mean Squared Error, RMSE).

WA (Weighted Averaging) can be used to produce a model which estimates each diatom species response to an environmental variable across its gradient in the training set. The evaluation of this response generates an optimum or indicator variable for the species. A simple estimate of the species optima for an environmental variable is generated using an average of all the values for the sites in which that species occurs (the regression step). The calibration step involves the calculation of the environmental variable using weighted averaged species scores. The species are weighted according to their abundance, and species with a higher abundance are more influential within the model development. An estimate of the environmental variable can, therefore, be made based on the diatom species assemblage data.

For example, in a lake with a certain pH range diatoms with their optima close to the lakes pH will flourish and become abundant within the assemblage. The pH optima of the species can be estimated by taking the mean of the pH values of all the lakes in

which that species occurs. The pH value, however, is weighted according to the abundance of the species within each lake. The WA species optima for each species can be used to infer past lake conditions (the calibration step). An estimate of a lake's pH is derived from the pH optima and the relative abundance of all the species present within that sample.

WA is the most appropriate method to use if the data set is particularly species rich, 'noisy' data, if the environmental gradient lengths are long and the variance within the biological data is relatively high (unimodal) (ter Braak 1987). This makes it a useful analysis tool for diatom data which are characteristically species rich.

WA can also be conducted where a species tolerance to a particular environmental variable is also taken into account, called weighted-averaging-tolerance-downweighted (WA_{tol}) and species are weighted according to their tolerance. Both WA and WA_{tol} can be implemented using the CALIBRATE programme (Juggins and ter Braak 1993).

Weighted Average- Partial Least squares (WA-PLS) is a technique which is generally used with species rich data with long environmental gradient lengths. The technique can on occasions, however, perform well with short gradients (ter Braak *et al.*, 1993). WA-PLS combines the technique of WA with the model's residual correlations in species data information to help improve the species optima estimates (ter Braak *et al.*, 1993). This is conducted through a series of regressions and component extractions from the model. Again, as with HOF and PLS, the WA-PLS error decreases as each component is extracted and the simpler model (i.e. one with fewer components) the lower the error produced.

The predictive power of these inference models, or transfer function, can be assessed through the R^2 value which evaluates the strength of the relationship between the observed and inferred values. The higher the R^2 the more efficient the model predictions are. The amount of unexplained variance is represented by the Root Mean Squared Error (RMSE). This measure indicates the amount of unknown variance remaining after the structured variance associated with the predictor variable is subtracted. The RMSE evaluates whether the inferred reconstructed values are reliable

and is routinely measured to assess the predictive ability of the inference model (Prairie 1996). With the construction of any inference model error generation is to be expected as it is unrealistic to extract a single environmental variable from species assemblages (ter Braak and Prentice 1988). Inference models such as these are developed and discussed in Chapters 4 and 5.

Validation of inference models can be achieved using a leave- one-out jack- knifing process, which estimates the error in the prediction of the environmental variable under study. This cross validation process results in the Jack-knifed Root Mean Square Error of Prediction (RMSEP_{jack}) (Kowalski and Seasholtz 1991), which is an approximation of the predication error and is usually expressed as a \pm error value for the reconstructed environmental variable.

3.3.4 Down core reconstruction of environmental variables

For both Hornsjøen and Gåvålivatnet (see section 2.3 for site selection) environmental reconstructions, inferred from the down core diatom assemblages, were performed to assess changes in Total Phosphorous (TP), pH, ice-cover and January temperature (see Chapters 6 and 7). The pH, ice-cover and January temperature transfer functions are developed and discussed in Chapters 4 and 5, using the PLS, WA, WA_(tol), and WA-PLS methods as outlined above. Their application is discussed further in Chapters 6 and 7. Before the reconstructions of pH, January temperature and ice-cover the diatom counts were converted to percentages and taxa occurring at $\leq 1\%$ were deleted to minimise the noise within the core data (see later discussions within this chapter for EDDI taxa deletion).

It was thought, however, that the reconstruction of TP might also provide insights in to the trophic status of the lakes which could be related to productivity changes. Therefore, further reconstructions of both pH, using a different data set, for comparison purposes, and TP were conducted using the EDDI project (See <http://craticula.ncl.ac.uk:8000/Eddi/jsp/index.jsp> European Diatom Database system and Battarbee *et al.*, 2001). This is a web-based system which enables users to reconstruct various environmental parameters for sediment cores using harmonised data from a combination of smaller diatom surface sample data sets, originating

primarily from studies within Europe. The EDDI project contains several training sets available for reconstruction purposes.

The original down core data were uploaded to the server and verified against an existing EDDI training set. At this stage some re-naming of taxa and merging of species was necessary so that the core data were comparable, in terms of taxonomy, with the training set data, thereby maximising the reliability of the reconstruction results. The merging of the taxa to higher taxonomic units in this way, however, is not thought to degrade the performance of the transfer functions to any significant extent (Battarbee *et al.*, 2001).

Within EDDI the user chooses a training set which matches, most closely, the range of past environmental conditions likely to be represented by the core sediment sequence. A reconstruction is then performed online and the results downloaded.

For the pH reconstruction for both Gåvålivatnet and Hornsjøen the AL:PE diatom pH calibration data set (Wathne *et al.*, 1993, Cameron *et al.*, 1999) was chosen as the most suitable for the two Norwegian cores because its mean pH was closest to the present day pH of the lake sites. This training set, of 118 surface samples, is an amalgamation of surface sediment diatom samples from high altitude or high latitude lakes in the Alps, Norway, Svalbard, Kola Peninsula, UK, Slovenia, Slovakia, Poland, Portugal, and Spain, representing remote lake systems with relatively undisturbed catchments. More information about the training set can be found at <http://craticula.ncl.ac.uk:8000/Eddi/jsp/index.jsp> and a summary of the main environmental data for the training set is presented in Appendix 3.2.

Currently through EDDI the only reconstruction methods available using the AL:PE training set are Weighted Averaging (WA) and Modern Analogue Technique (MAT) (see section 3.3.5 for further discussion of the MAT technique). The MAT analysis provided a further method of diatom inferred pH reconstruction for comparison purposes with the WA method. This method links floristically the core diatom assemblage sample with its five closest analogues in the training set, given as squared chi-squared distances (SCSD), essentially representing a dissimilarity measure. For the EDDI reconstruction as a general rule if any squared chi-squared distance

measures are over 100 this represents a 'no close modern analogue' situation and the resulting reconstruction should be treated with caution (Battarbee *et al.*, 2001 and ref. to Jones and Juggins 1995; Flower *et al.*, 1997 for similar discussions). In such cases none of the samples in the training set represent 'good' matches floristically with the core samples. This measure can be used to indicate where the reconstructions may be less reliable. The output lists the reconstructed environmental pH value for the sample based on the mean pH of the five closest analogue sites. It also lists how similar the sites are using a minimum dissimilarity measure (minDC).

Rare taxa (typically <1%) are not deleted from the EDDI training sets and, therefore, the reconstructions were performed using all the diatom taxa present in the cores. This minimises the dissimilarity which would occur if rare taxa present in the training set had been deleted from the core, increasing the resulting SCSD measure. However, such SCSD cut off values are arbitrary and the critical limits can depend on the range and size of the training set data (Juggins *pers. com*).

Total Phosphorous (TP) reconstruction

Diatom inferred TP reconstructions were calculated for Gåvålivatnet and Hornsjøen using the fossil diatom data generated for the cores. The EDDI training set most suitable for the Norwegian cores is the Swiss high altitude data set (Lotter *et al.*, 1997; Lotter *et al.*, 1998) because the mean TP was relatively low (41.9 µg/l, see also appendix 3.3) in comparison to the other TP data sets available through the EDDI project, and therefore the training set lakes reflect the environmental conditions likely to be represented by the core. This training set consists of 68 small lakes situated in the Swiss mountains, the Jura mountains, the foreland of the Southern Alps and the Alps.

For the Swiss data set only WA and MAT reconstruction methods were available through the EDDI programme. For the WA reconstruction inverse deshrinking was used as the reconstructed values would be closer to the mean than to the extremes of the TP training set gradient.

3.3.5 Analogue matching techniques

The computer programme MAT (Juggins 1994) essentially evaluates the floristic similarity between samples. It was devised to analyse modern diatom assemblages (Flower *et al.*, 1997) but can also be used with fossil diatom samples. The technique assesses the similarity between samples by calculating the Chi-squared distance in which diatom proportions are weighted to emphasise their dissimilarity. Applications of the technique are numerous but in this study MAT was used for two purposes:

1. for diatom inferred reconstructions of pH and TP using the EDDI programme. As discussed above (Battarbee *et al.*, 2001) (see Chapters 6 and 7 for the reconstructions) the programme consists of many surface diatom samples and the MAT finds the closest modern analogue site for the samples submitted for analysis.
2. MAT was used to compare the similarity between the modern training set samples and the samples from two Norwegian short sediment cores (Chapter 6 and 7). In this way inferences about past lake conditions can be made using the closest analogues from the modern training set lakes which have measured environmental values.

3.3.6 Down core ordination and zonation

Ordination techniques described in section 3.3.2 and used in Chapters 4 and 5 were also used for the fossil diatom assemblages of Hornsjøen and Gåvålivatnet. A PCA was performed on each core on to which a time track was applied, which joins the samples stratigraphically from the core top to the core bottom on the biplot, to enable the rate and direction of diatom assemblage change to be assessed. In addition the Axis 1 and Axis 2 sample scores, derived from the diatom assemblages, for the PCA analysis were extracted and plotted stratigraphically, in essence, providing a 'down core PCA' record of diatom composition change, which can then be related to the environmental reconstructions. If samples are very different floristically, their sample scores will reflect this difference. A sudden shift in diatom sample score down the core profile helps to identify major diatom compositional changes within the core sequence.

In addition, for the diatom data from the cores taken from Gåvålivatnet and Hornsjøen cluster analysis was performed using the ZONE programme version 1.2 (Juggins 1991). The programme performs a constrained classification or zonation of stratigraphically ordered data in order to classify diatom data down core into zones of similar diatom assemblages.

Several zonation analysis tools are available in this programme. These are: CONSLINK, CONISS, SPLITLSQ, SPLITINF (*c.f.* Gordon and Birks 1985; Grim 1987), which were run simultaneously and the zonations were then compared. If the results of the zonation techniques did not agree a subjective judgment of which technique to choose was made. The methods are essentially based on dissimilarity measures. The within sample variance is minimised, thereby maximising the between sample variance.

3.3.7 Summary of numerical methods

The last section has shown that several methods can be used to quantify species responses to environmental gradients. In summary indirect gradient analysis can be seen as regression analysis but where the environmental variables are not known ('latent variables'). Direct gradient analysis links the response variable to the explanatory variable. These explanatory variables explain, to varying degrees, the variance within the response data. In general unimodal statistical methods are more appropriate than linear methods for complex, heterogeneous data sets (Gauch 1982).

3.4 The use of older surface sediment in data set Norway 1

The Norway 1 set of surface samples were collected in the years 1996, 1998 and 1999. In order to demonstrate that it is appropriate to combine the samples taken in different years in the Norway 1 data set, with the Norway 2 and Scotland data set, ordination analyses were used to demonstrate that diatom assemblages do not usually change significantly over the course of several years. Surface samples were retrieved from four lakes in 1998 (lake codes 98-6, 98-9, 98-20 and 98-2) and were counted for diatoms. The lakes were re-visited and cored in 2000 and the surface samples were counted. The two surface samples were then compared using ordination techniques (PCA, due to the short gradient length Table 3.2) to assess if their assemblages were similar (Table 3.3 and Figure 3.14). The PCA arranges the samples in the ordination

space according to their floristic assemblage, samples that are positioned close to each other indicate that they have similar assemblages. It can be seen that despite the fact that samples were taken over the space of 2 years (i.e. one in 1998 and one in 2000) the assemblages have not changed substantially. In this way, therefore, it is appropriate to combine samples that have been taken between the years 1996- 2000 and be sure that the lake assemblages can be compared.

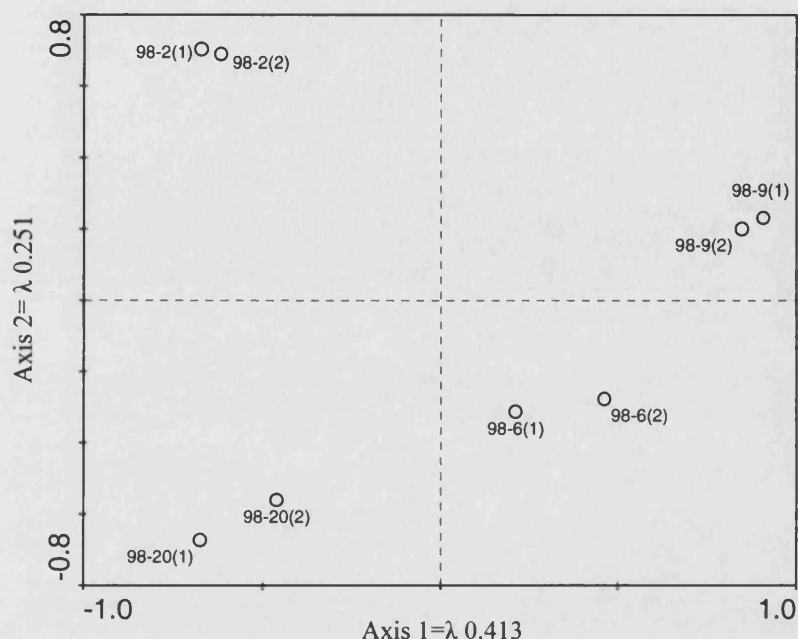
Table 3.2: Summary of DCA ordination, eigenvalues and cumulative % variance, of the 8 surface samples taken from 4 lakes.

DCA axes	1	2	3	4
Eigenvalues (λ)	0.486	0.096	0.007	0.001
Lengths of gradient	2.49	1.92	0.93	1.33
Cumulative percentage variance of the species data	28.3	33.9	34.3	34.4
Sum of all eigenvalues	1.717			

Table 3.3: Summary of PCA ordination, eigenvalues and cumulative % variance, of the 8 surface samples taken from 4 lakes.

PCA axes	1	2	3	4
Eigenvalues (λ)	0.413	0.251	0.151	0.096
Cumulative percentage variance in the species data	41.3	66.3	81.5	91
Total inertia	1			
Sum of all eigenvalues	1			

Figure 3.14: PCA biplot on axis 1 and 2, of 8 surface samples taken from four lakes. 98-2(1), 98-20(1), 98-6(1), 98-9(1) taken in 2000 and 98-2(2), 98-20(2), 98-6(2) and 98-9(2) taken in 1998.



3.5 Instrumental records of climate for Gåvålivatnet and Hornsjøen

For the lakes Gåvålivatnet (01-03) and Hornsjøen (98-18) instrumental records of climate are available dating back to 1864. For Gåvålivatnet monthly air temperature and annual precipitation data are available dating back to 1864, for air temperature, and to 1957, for precipitation. Gåvålivatnet is situated near the weather station Fokstua which is at the same altitude as the lake and no apparent differences in local climate have been detected between the lake and the weather station (Nordli *pers. com.*) and so the data from the weather station were used directly for Gåvålivatnet. Fokstua started in 1923 and therefore, in order to generate climatic data before this the weather station at Kjoremsgrenden was used, adjusted for Fokstua/ Gåvålivatnet. These adjustments are based on the rather long overlapping period for Fokstua and Kjoremsgrenden and therefore providing accurate data back to 1864 (Nordli *pers. com.*).

The close proximity of the lakes Gåvålivatnet and Hornsjøen (Figure 2.9) means that the temperature record from Fokstua/ Kjoremsgrenden can simply be adjusted to accommodate for the difference in altitude between the two lakes. A constant adjustment term of -2°C (Hornsjøen is slightly higher in altitude than Gåvålivatnet

and, therefore, higher than the weather station) was applied for the season April-October. Direct linear adjustments are not so appropriate for the winter months (Nordli *pers. com.*). Therefore, monthly air temperature data dating back to 1864 are only available for April to October for Hornsjøen. The instrumental climate record is used in Chapters 6 and 7 to evaluate the accuracy of the diatom inferred climate reconstructions.

3.6 Conclusion

This chapter has briefly explained the methods involved in this study. The laboratory methods for the water chemistry analysis and problems with these are presented. The issue of missing environmental parameters is considered and the rationalisation of the training set, as a consequence of this, is discussed. Methods for the numerical analyses of both the cores and the surface samples were also presented. The following chapter presents the 40 lake ‘ice-cover’ training set and identifies which environmental variables are driving the diatom variance evident within the 40 surface sample assemblages.

Chapter 4

Analysis of the 40 lake training set

Introduction

The last chapter described the methods involved in the collection of the modern surface sediment training set and the short core sampling procedures. The numerical methods used for the analysis of the biological and environmental data were discussed. The chapter described the design of the two training sets; the first containing 40 surface sediment samples (the 'ice-cover' training set) and the second 80 samples. The first is a sub-set of the 80 lake training set and is separated from the 80 because these 40 lakes had ice-cover duration measurements. The 80 lake training set is explored and discussed in Chapter 5.

The 40 lake training set is presented and discussed within this chapter. The chapter identifies which environmental variables may determine the diatom variance within the 40 samples. One of the main aims of the thesis is to determine the amount of diatom variance explained by ice-cover duration, independent of other environmental variables, within high mountain lakes. This aim is addressed in this chapter. The suitability of using diatoms to reconstruct ice-cover duration, through the development of an ice-cover transfer function, is also evaluated.

The results section is separated into five parts:

- Exploration of the environmental data for the 40 lakes
- Exploration of the diatom surface sample data for the lakes
- Analysis of the environmental and biological data in conjunction with each other
- The specific relationship between lake ice-cover duration and diatom assemblages
- The feasibility of creating an ice-cover transfer function

The discussion section evaluates which environmental gradients are important for explaining the diatom variance within the data set and the relative influence of ice-cover as a driving variable. The suitability of the data set to derive a diatom based transfer function for the reconstruction of past climate is evaluated.

4.1 Results

The sites within the 40 lake training set are presented in Table 4.1. The site locations and catchment characteristics have been discussed in Chapter 2. The lake numbers in column 2 of the Table 4.1 relate to the figures produced by the ordination analyses which are presented later in this chapter.

4.1.1 Environmental data

The environmental variables, including the catchment and water chemistry parameters, are presented and summarised in this section. The data set was designed in order to maximise the climatic gradient. This was achieved through the selection of sites which spanned a long altitudinal gradient and consequently a long ice-cover duration gradient. It was necessary to design the training set so that lakes were well represented along this gradient (see section 2.2.4 and Figure 2.8). Therefore as far as possible each ice-cover class and altitudinal denomination should be well represented within the data set. This was, however, compromised by the reduction of the 80 lake training set to 40 (the implications of this are discussed in sections 4.4.4 and 4.4.5).

In addition, the numerical techniques of direct and indirect gradient analysis require that the environmental data within the training set should display 'normal' distributions. For example if one environmental variable has many sites with low values, and only a few sites with high values the distribution of that variable will be skewed. In such cases data transformations, such as \log , $\log^x + 1$, or square root transformation of the variable may be necessary (see section 3.3.1). For each variable histograms, to assess the 'normality' of the variable's distribution, were produced. The histograms are not presented here but from analysis of these, decisions about data transformation could be made (Section 4.1.1.2). Box plots are presented for each environmental variable in order to identify outliers and compare variable differences between the two countries. The section assesses how well represented the sites are along each environmental gradient, identifies any gaps, in terms of representation within the data set and identifies any possible outliers samples, in terms of environmental variables, within the 40 samples.

4.1.1.1 Summary environmental statistics

The 40 lake data set has a total of 23 environmental variables included within it (see section 3.2.3). Table 4.2 summarises the environmental parameters for the set. The full water chemistry and site characteristics are listed in Appendix 4.1. Box plots of the environmental variables are displayed in Figures 4.1 to 4.24. It should be noted that the medians displayed in the box plots do not take in to account the outliers (presented as circles) in the calculation of the medians and hence the means in Table 4.2 and the box plots medians are not be the comparable.

Table 4.1: Lake code, Longitude, Latitude, Altitude and lake area measurements for each of the 40 lakes within the training set. Lakes with the prefix CN or SN refer to Norwegian lakes and those with the prefix SC refer to the Scottish lochs.

Lake Code	Lake number for ordinations	Longitude °E	Latitude ° N	Altitude (m a.s.l)	Lake Area (ha)
CN0003	1	6.9489	60.6921	751	60.0
CN0004	2	7.0656	61.2793	820	27.0
CN0005	3	7.1708	60.0738	1172	153.0
CN0006	4	7.3184	60.1028	1324	180.0
CN0007	5	7.3625	60.9501	1289	30.0
CN0008	6	7.5890	60.0844	1209	55.0
CN0009	7	7.5797	60.3842	1239	95.0
CN0010	8	7.6514	60.8420	1525	80.0
CN0011	9	7.7120	59.9734	1329	150.0
CN0012	10	8.0790	61.2011	1184	130.0
CN0013	11	8.1781	61.3957	1396	140.0
CN0014	12	8.2493	61.5478	1401	100.0
CN0015	13	8.8970	61.4188	1088	77.5
CN0016	14	8.9824	62.7778	728	50.0
CN0017	15	9.0372	62.7500	1043	27.0
CN0018	16	9.5650	61.8898	1121	18.0
CN0019	17	10.2659	62.5522	938	40.0
CN0020	18	11.0670	62.7743	1058	8.0
CN0021	19	11.6009	62.7160	799	55.0
CN0022	20	11.7848	62.9029	844	20.0
SN0023	21	8.1100	59.6350	1053	40.0
SC0002S	22	-6.22107	57.20192	750	2.9
SC0010S	23	-5.65692	56.72325	590	1.8
SC0029S	24	-5.59274	57.17348	720	2.5
SC0067S	25	-5.47594	57.56594	530	3.2
SC0068S	26	-5.44811	57.27850	540	3.6
SC0076S	27	-5.44503	57.59115	600	10.0
SC0108S	28	-5.28714	57.14285	720	1.9
SC0165S	29	-5.02443	57.71257	570	31.1
SC0172S	30	-4.90413	56.74677	740	9.3
SC0180S	31	-4.95487	57.49554	520	7.5
SC0191S	32	-4.91542	57.22027	660	2.3
SC0197S	33	-4.97635	58.19929	530	4.2

Table 4.1 Continued

Lake Code	Lake number for ordinations	Longitude °E	Latitude ° N	Altitude (m.a.s.l)	Lake Area (ha)
SC0204S	34	-4.93559	57.80984	690	5.6
SC0211S	35	-4.95355	58.18500	530	2.9
SC0330S	36	-4.57701	56.94521	810	7.4
SC0335S	37	-4.58286	57.26925	540	1.9
SC0349S	38	-4.59531	58.41689	530	3.8
SC0386S	39	-3.53822	56.88503	790	14.5
SC0399S	40	-3.23128	56.95914	790	9.9

Table 4.2: Selected descriptive statistics for the environmental parameters in the 'ice-cover' training set (untransformed data)

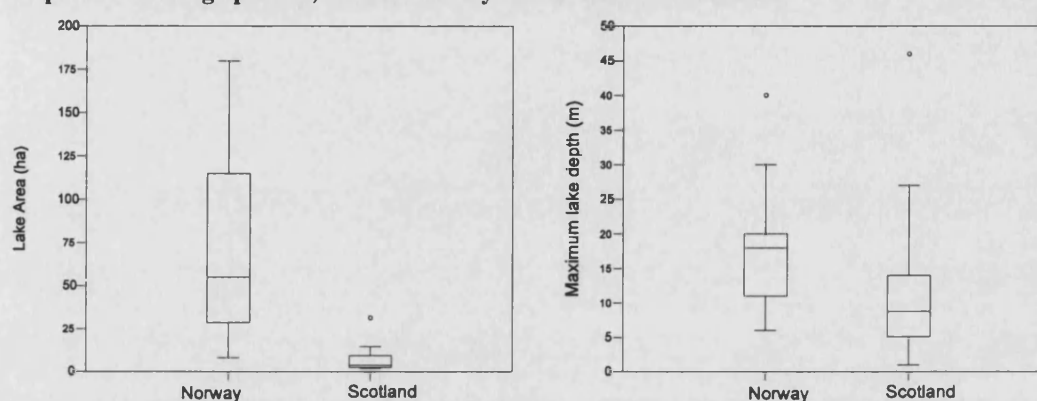
Determinand	Units	Min	Max	Mean	St. Dev.	Norway mean	Scotland mean
Lake Depth	m	1	46	15	9.8	18	10.5
Altitude	m a.s.l	520	1525	886	298	1110	601
Area	ha	1.8	180	41.5	49.9	52	5.74
pH	Units	5.42	7.65	6.4	0.45	6.48	6.12
Alk	µeq/l	6	467	61.19	96.2	76.5	34.7
Cond	µS/cm	4.14	48.3	20.12	13	12.4	24.13
Na ⁺	µeq/l	0	250	81.62	79.3	15.5	132.86
K ⁺	µeq/l	1.02	27.11	5.89	4.94	5.67	5.04
Mg ²⁺	µeq/l	5.3	119.2	32.4	24.98	18.06	40.9
Ca ²⁺	µeq/l	14	445	72	84.8	84.1	48.5
Cl ⁻	µeq/l	2.8	274	83.6	85.1	14.2	137.8
NO ₃ ⁻	µeq/l	0	13	1.86	2.86	1.0	2.34
SO ₄ ²⁻	µeq/l	10.41	83.2	29.48	14.4	25.5	28.0
TN	µg/l	40	331	144	83.6	88.0	175
TP	µg/l	0	6	2.25	1.31	1.59	2.5
NH ₄ ⁺	µeq/l	0	2	0.57	0.59	0.95	0.09
Al-TM	µg/l	0	65	12.75	13.2	9.54	13.6
Al-L	µg/l	0	31	2.61	5.69	3.11	1.63
Al-NL	µg/l	0	41	10.18	10.7	6.5	12
TOC	mg/l	0.1	9.2	2.14	2.13	1.0	3.4
ppt	mm annual	583	2699	1418	560	1021	1858
Ice duration	Days	0	228	131	84.1	192	47
January Temp	°F	18.9	35.2	27.4	0.8	22.4	32.8
July Temp	°F	37.3	51.2	44.6	0.6	40.6	49.1

Lake depth and lake area

The range of lake depth is relatively large (1-46m) and the deeper lakes are located in Norway, which has a much higher lake mean depth value (Table 4.2, Figure 4.2). Two lakes appear as outliers, having depths over 40m, one occurring in each of the Norway and Scotland sets (CN0013 and SC0165, Figure 4.2 not labelled). The higher number of shallower lakes within the data set resulted in a slightly left skewed distribution curve.

As with lake depth most of the larger lakes occur within the Norwegian part of the training set and both regions have very different mean lake areas (Table 4.2, Figure 4.1). In fact 13 of the 21 Norwegian lakes are over 50ha whereas the largest Scottish loch (SC0165) is only 31ha. The range of lake area is also higher for the Norwegian lakes (Figure 4.1) spanning 8 to 180ha. The distribution pattern for lake area is also not normal and is influenced by the larger number of smaller lakes within the training set.

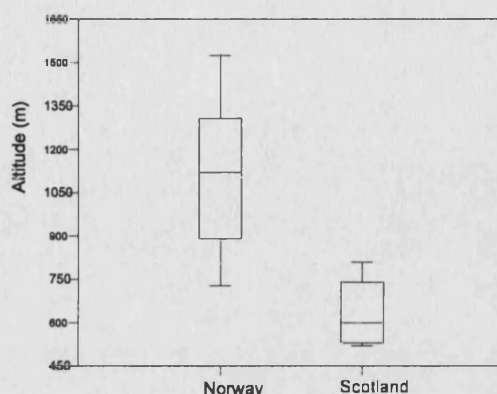
Figure 4.1 and 4.2: Box plot of maximum lake area and maximum lake depth, with median and 25 percentile range plotted, for the Norway and Scotland lake classes.



Altitude

As with lake depth and area, a distinction can be made by country in terms of altitude (Figure 4.3). The Norwegian lakes occur at much higher altitudes than the Scottish lochs. This is probably due to the fact that Norway has higher mountains than Scotland resulting in more lakes at a higher altitude available for selection. The lower altitude lakes are located in Scotland with the site SC0330 being the highest of the Scottish sites at just 810m a.s.l. All the lakes above 1000m, therefore, are Norwegian lakes. The range 900-1,000m lakes are particularly poorly represented within the training set and the altitudinal distribution of the lakes is slightly skewed but near normal.

Figure 4.3: Box plots of altitude, with medians and 25 percentile ranges plotted, for both the Norway and Scotland lake classes.



pH, Calcium and Alkalinity

For pH, Ca^{2+} and Alk the Norwegian sites on average have higher values (Table 4.2, Figure 4.4, 4.5 and 4.6). The difference between the mean pH for the Norway and Scotland sites is only 0.36 pH unit (Table 4.2). The pH values will, however, vary seasonally and these values, derived from samples retrieved in late summer, may represent the highest annual pH measures for the lakes. Typically, lower pH values may be recorded in the winter and spring time.

The median Ca^{2+} and Alk are also much higher for the Norwegian lakes (Figure 4.5 and 4.6). The differences between the countries may be related to the different bedrock types for the two areas with more of the Norwegian lakes located on strongly weathered sedimentary rock types (see section 2.2.2 and 2.2.3). The Ca^{2+} and Alk gradient is large for the data set, ranging from 14- 445 $\mu\text{eq/l}$ for Ca^{2+} and 6-467 $\mu\text{eq/l}$ (Table 4.2) for Alk. The relatively high mean Alk (61.19 $\mu\text{eq/l}$, Table 4.2) suggests that most of these systems have a high capacity to buffer pH change. In terms of outliers for Ca^{2+} and Alk there appear to be three outliers for the Norwegian set of lakes and one for the Scottish, all with very high Ca^{2+} and Alk (Figure 4.5, and 4.6 not labelled). These outliers are the same lakes for each variable and are CN0019, CN0022, CN0021 and SC0335 (listed in order from high Alk and Ca^{2+} to lower).

The distribution of pH is near normal. The distributions for both Alk and Ca^{2+} are strongly skewed. Many more sites have lower values and only a few sites with very

large values for both Alk and Ca^{2+} . In order to use some ordination techniques many variables need to be transformed so that they exhibit normal distribution curves (see section 3.3.1). As an example the histograms prior to, and after transformation for Alkalinity are presented in Appendix 4.2 which shows how the distribution pattern is altered when Alkalinity is log transformed. After transformation the distribution pattern achieved is much more normal. The transformation of similar skewed variables within this training set is discussed later (see section 4.1.1.2).

Conductivity

The Scottish lochs on average have higher conductivity than the Norwegian lakes, due primarily to their relative proximity to the coast (Table 4.2, mean Norway $12.4\mu\text{S}/\text{cm}$ and Scotland $22.13\mu\text{S}/\text{cm}$ and Figure 4.7). The lakes overall have relatively low conductivity values, which may be due to the late summer sampling period when ionic input from sea salts may be reduced due to less precipitation and calmer weather.

Figure 4.4 and 4.5: Box plots of pH and Ca^{2+} , with median and 25 percentile ranges shown, for both the Norway and Scotland lake classes.

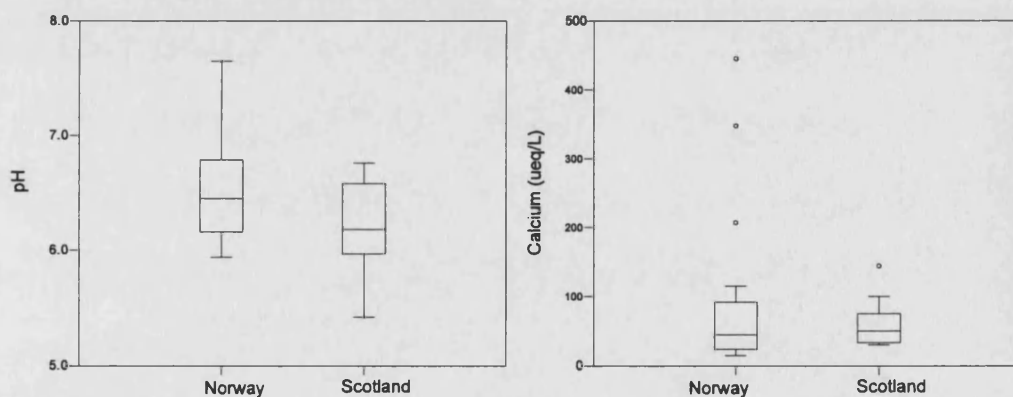


Figure 4.6: Box plot of Alkalinity for the Scotland and Norway lakes with medians and 25 percentile ranges displayed.

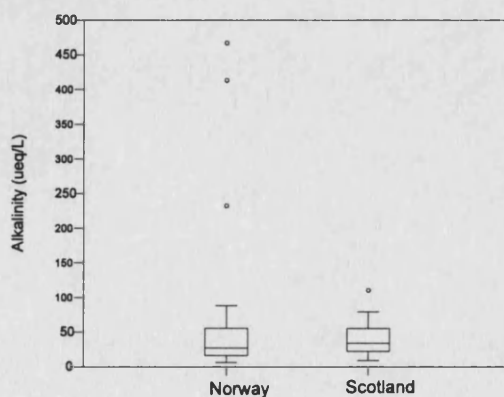
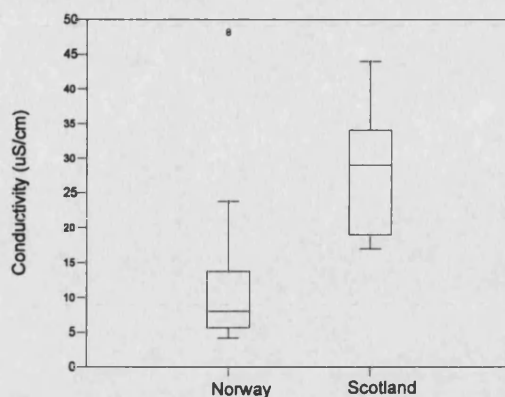


Figure 4.7: Conductivity box plots for the Norway and Scotland lakes, with medians and 25 percentile ranges plotted



Major ions (excluding Ca^{2+}), Cl^- , NO_3^- , SO_4^{2-} , Mg^{2+} , Na^+ and K^+

Of the major ions, Mg^{2+} , Na^+ and K^+ are considered 'conservative' ions in the sense that they undergo relatively minor changes due to biotic utilization and usually supply far out strips demand. Cl^- is also relatively conservative. This is opposed to the 'dynamic' ions, such as NO_3^- and SO_4^{2-} , whose concentrations can be influenced strongly by biotic metabolism (Wetzel 1983).

Most of the lakes have low ionic values, and only a few have larger values creating skewed distributions. Cl^- , NO_3^- and Na^+ have especially strongly skewed distributions. There are also gaps present within the gradients for many of the ions (e.g. Mg^{2+} , K^+ , SO_4^{2-}) suggesting possible under representation along the gradient.

There is little difference in the means between the two countries for K^+ , SO_4^{2-} and NO_3^- (Figure 4.11, 4.9 and 4.10). Mg^{2+} , Na^+ , and Cl^- show greater differences between the means for Norway and Scotland with the Scottish lochs, on average, having much higher values for these three parameters, resulting in a higher mean (Figures 4.12, 4.8 and 4.13). This is most probably due to the maritime influence and the sea salt precipitation of these ions for the Scottish lochs.

The length of the gradients Cl^- and Na^+ are particularly large, probably reflecting the differences between the countries and the proximity of many of the sites to the coast. The higher input of the sea salts in the Scottish lochs may be reflected in the lower pH mean for these sites as sea salts will contribute to the lowering of pH and an increase

in aluminium concentration (*c.f.* Anderson and Seip 1999; Evans *et al.*, 2001). This influence may, however, only be temporary and reflect sea salt induced acid events of limited duration (*c.f.* Wright *et al.*, 1988).

The large gradient for Mg^{2+} and also Ca^{2+} (See Figure 4.5 for Ca^{2+} and 4.12 for Mg^{2+}) may be due to the differences in catchment rock type for the lake regions (See Figure 2.2 and 2.6). Many of the Scottish lochs are located on more base poor geology than the Norwegian lakes accounting for the lower mean Ca^{2+} and Mg^{2+} for Scotland. These ions are directly derived from weathering of the base rock and soil within the catchment and also, to a lesser extent, marine input which may again explain their slightly different concentration in the Scottish lochs. The influence of sea salt input is discussed further in section 4.7.3.

The outliers mentioned above for Ca^{2+} and Alk are the same for Mg^{2+} (lake CN0022, 119 $\mu\text{eq/l}$, Figure 4.12 not labelled) and K^+ (CN0019, 22 $\mu\text{eq/l}$ and CN0022, 27 $\mu\text{eq/l}$ Figure 4.11 not labelled). Outliers for SO_4^{2-} are CN0006 with 83 $\mu\text{eq/l}$ and CN0022 with 56 $\mu\text{eq/l}$ (Figure 4.8 not labelled). It is not surprising, therefore, that CN0019 and CN0022 are also outliers for conductivity (Figure 4.7 not labelled).

Nutrients: TN, TP and NH_4^+ (excluding NO_3^-)

TN and NH_4^+ both display skewed distribution patterns for the data set (not presented) and are dominated by lakes with relatively small values of these variables. The difference in mean TN for the two regions is distinct with the Norwegian mean value being considerable higher than the Scotland mean TN (88 $\mu\text{g/l}$ and 17 $\mu\text{g/l}$ respectively, Table 4.2). The TP gradient is not as large as the TN gradient and many measures for TP are near detection limits (2 $\mu\text{g/l}$, see section 3.2.1.1) for both regions and the differences in their means are minimal (Figure 4.15). From their TP measures all the lakes within this training set would be confirmed as ‘oligotrophic systems’ (OECD 1982). Scotland has one outlier, in terms of TP, which is SC0211 but it is not an outlier in any other respect.

The gradient length for NH_4^+ is only 0-2 $\mu\text{g/l}$, but Scotland has a much lower mean NH_4^+ value of 0.09 $\mu\text{g/l}$ compared to the Norwegian average of 0.95 $\mu\text{g/l}$ (Table 4.2). These means are deceptive, however, as the Scotland set contains many NH_4^+

measures below detection limit within it (resulting in the unusual box plot distribution, Figure 4.14).

Figure 4.8- 4.13: Box plots, with medians and 25 percentiles plotted, for the major ions (excluding Ca^{2+} , Mg^{2+} , K^+ , Na^+ , SO_4^{2-} , NO_3^- , Cl^-).

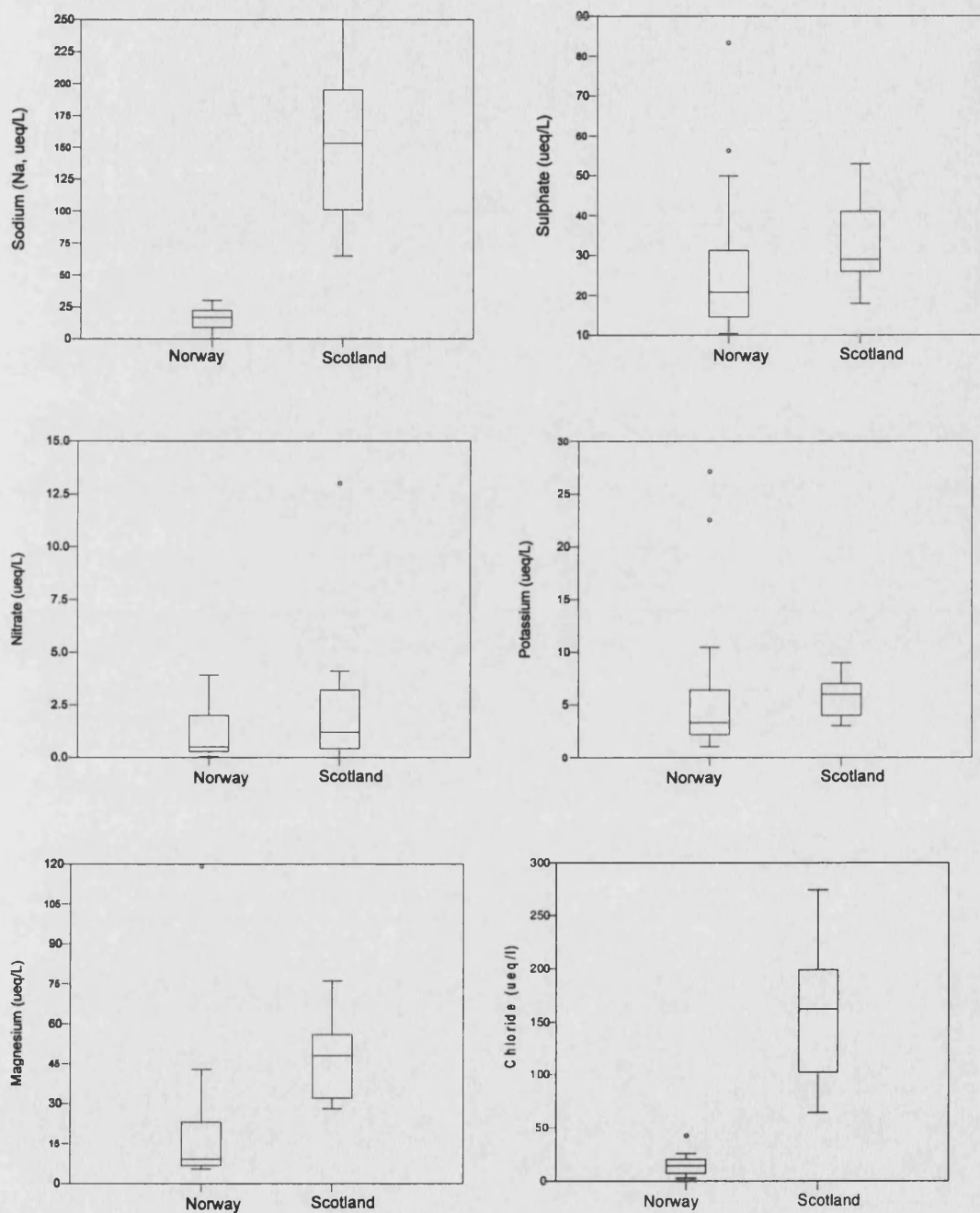


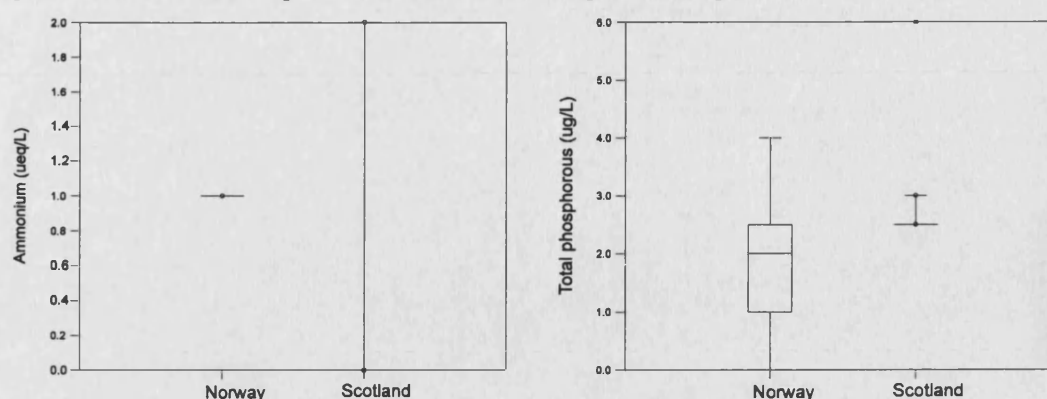
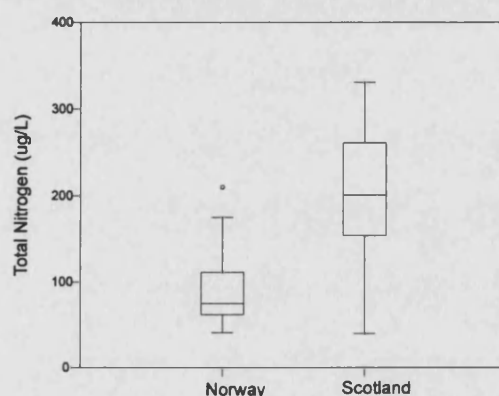
Figure 4.14 and 4.15: Box plots, with medians and 25 percentiles plotted, for NH_4^+ and TP

Figure 4.16: Box plots, with medians and 25 percentiles plotted, for TN



Aluminium: Al- L, Al- NL and Al- TM

The levels of Al-TM within the forty lake training set ranged from 0-65µg/l with a mean of 12.75µg/l, suggesting that most values lie at the lower end of the gradient (Table 4.2). There is little difference in the means of the two countries for Al-TM with Scotland having a slightly higher mean of 13.6µg/l compared to Norway's mean of 9.54µg/l (Table 4.2).

Labile aluminium can become toxic for organisms at high levels >40µg/l. The toxicity of aluminium is also positively related to acidity levels (Ormerod *et al.*, 1987). The relatively low levels of Al-L in this training set, however, should not adversely affect the biota of the systems (Figure 4.18). Most aluminium is present as non-labile aluminium (Figure 4.19) and is bound to organic matter. All three aluminium distributions are skewed with large numbers of low values and a few high values which adversely influence the distribution curves (not presented).

Total Organic Carbon

TOC nearly wholly consists of dissolved organic carbon (DOC) and dead particulate carbon (POC) (Wetzel 1983). The majority of the TOC values for the training set are low and between 0-5mg/l (Figure 4.20). The maximum TOC is 9.2mg/l. Scotland has, on average, higher TOC levels (mean 3.4mg/l) than Norway with a mean of 1.0mg/l (Table 4.2). This may be related to the fact that the Scottish lakes are at lower altitudes and may have more vegetation coverage and peat deposits within their catchment area. However, none of the lakes could be considered particularly 'humic' (i.e. over >10mg/l, Kramer *et al.*, 1990). TOC levels are often related to the brown colouration of lake waters, with studies showing a linear relationship between colour units and DOC (Juday and Birge 1933). Often colour increases with depth in strongly stratified waters as DOC and ferric compounds increase in concentration near the sediments.

Figure 4.17- 4.19: Box plots, with medians and 25 percentile ranges plotted, for Al-TM, AL-L and AL-NL.

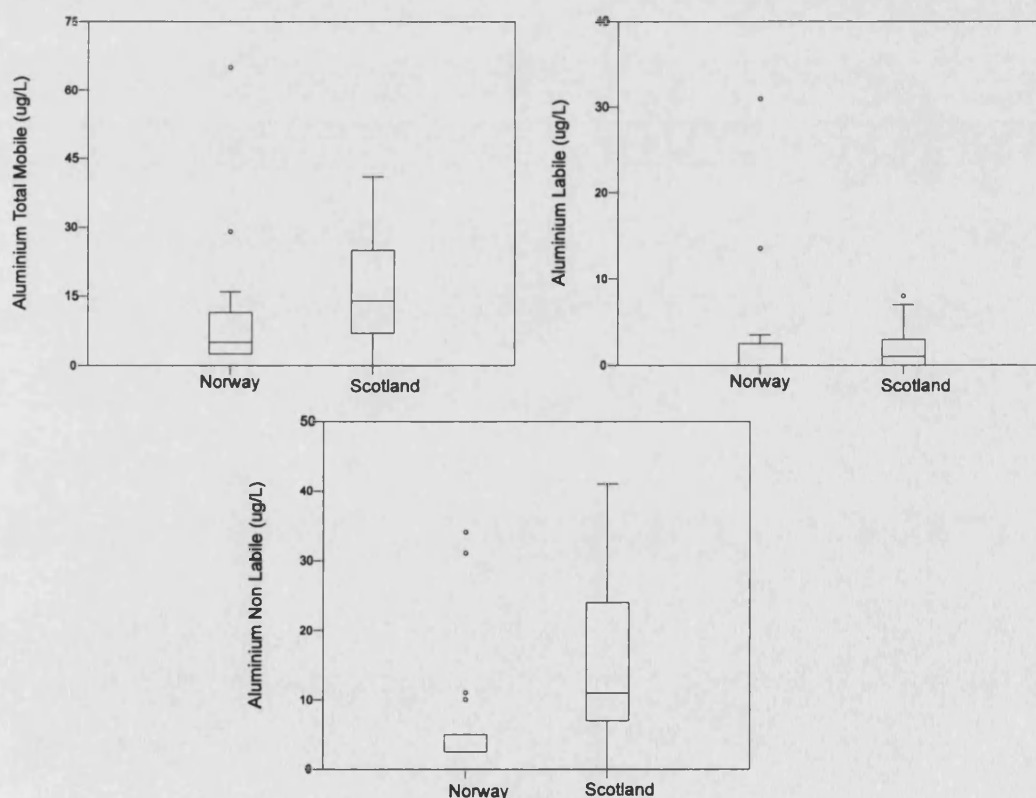
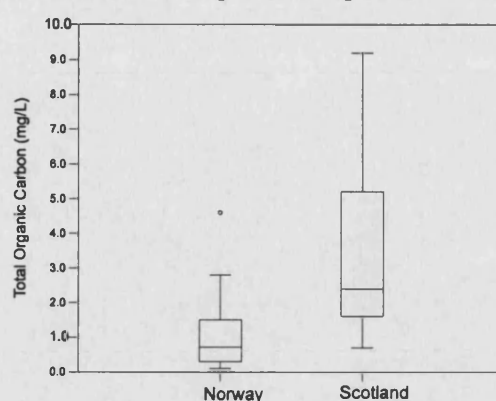


Figure 4.20: Box plots with medians and 25 percentiles plotted for TOC.



Precipitation and lake ice-cover duration

The minimum annual rainfall for the data set is 583mm and the maximum is 2699mm, representing a large precipitation gradient (Table 4.2). On average the Scottish lochs receive more precipitation (mean 1858mm) than the Norwegian lakes (mean 1021mm, Table 4.2).

The ice-cover duration gradient covers values from 0-228 days duration (Table 4.2). There are no lakes with permanent ice-cover within the data set, but seven with no ice-cover, all occurring in Scotland. The mean ice duration for the Scottish lakes is 47 days which is much lower than the 192 day mean for the Norwegian region (Figure 4.22). There is a large proportion of lakes with no ice-cover, occurring mainly in Scotland, and a large proportion with over 200 days lake ice duration, occurring mainly in Norway (Figure 4.22, 4.47), causing the over representation of lakes at the extremes of the gradient. Lakes with ice-covers of between 20-60 days duration are not well represented within the training set.

January and July air temperature

The January and July air temperatures were converted to °F so that negative numbers were not used in the ordinations presented in the next section. Scotland has a much higher mean air temperature for both January and July (Table 4.2). The range of January temperature is much higher for the Norwegian sites with Scotland having a much smaller 25 percentile range. There are no obvious outliers for January or July temperature. It can be seen, however, that the middle of the gradient is not well

represented for both the January and July variables, resulting in a bi-modal distribution of the sites along the relatively long gradients (Figures 4.23 and 4.24).

Figure 4.21 and 4.22: Box plots, with medians and 25 percentiles plotted, for annual precipitation and ice- cover duration.

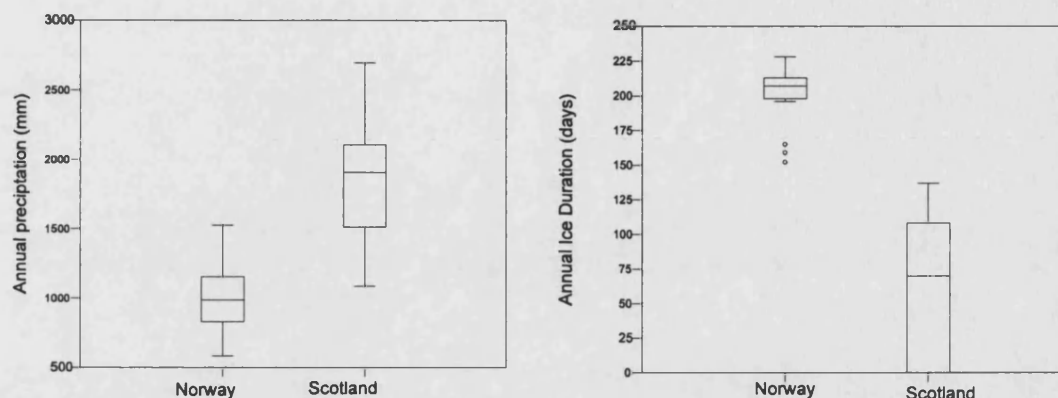
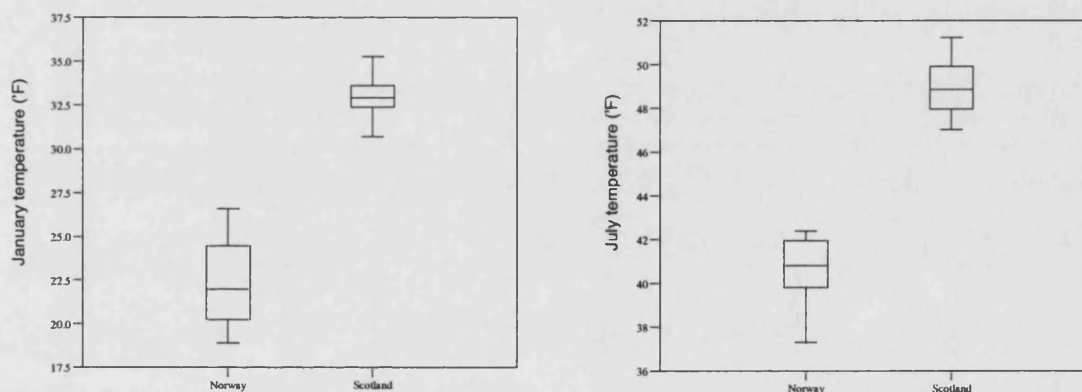


Figure 4.23 and 4.24: Box plots, with medians and 25 percentiles plotted, for average January and July air temperature.



4.1.1.2 Relationships between environmental variables

The environmental variables have been presented and discussed above. This section analyses the relationship between the environmental variables for the training set sites. It was established in section 4.1.1.1, and through the plotting of distribution histograms, that many of the variables were not normally distributed. Therefore, prior to further statistical analyses some variables were transformed: area, alkalinity, conductivity, Na^+ , Mg^{2+} , Ca^{2+} , Al-NL, Cl^- , SO_4^{2-} , TN were all log transformed, K^+ , NO_3 , NH_4^+ , Al-TM, Al-L, and TOC were all \log^{x+1} transformed and precipitation, ice duration, altitude, maximum depth, pH, latitude, TP, JanT and JulyT were not transformed (either these variables displayed near normal distributions or their distributions were not improved with transformation, e.g. ice-cover, or it was not appropriate to transform them e.g. pH). These transformations were performed to

achieve near normal distributions for each environmental variable (see Appendix 4.2 for an example).

In order to evaluate the relationships between environmental variables a Pearson product moment correlation analysis was performed (Table 4.3). The matrix demonstrates that many of the variables have linear relationships with each other. Significant relationships, (significance at $P < 0.001$) either negatively or positively are marked with bold type.

Altitude is strongly negatively related to TP, TOC and TN, indicating that higher lakes have lower nutrient concentrations and are less coloured. As would be expected altitude is also positively related to ice-cover and negatively related to January and July air temperatures, indicating longer ice-cover periods and cooler air temperatures at the higher altitude lakes. Altitude is also positively related to area suggesting that the higher altitude lakes are bigger. This is probably only due to the fact that the Norwegian lakes are larger on average than the Scottish lakes (mean 69ha Norway, 5ha Scotland) and occur at higher altitudes than the Scottish lakes. This is not a meaningful relationship, therefore, and only reflects a function of the sampling. Altitude is also positively correlated with conductivity, Na^+ , K^+ , Mg^{2+} and Cl^- .

Conductivity is strongly positively correlated with Mg^{2+} and is also positively correlated with all the anions and cations. This link is unsurprising because in bicarbonate dominated systems conductivity is often directly proportional to the concentration of the major cations in solution. Area is also negatively correlated with conductivity, with the larger, higher altitude lakes possibly having lower concentration of cations. Conductivity is also negatively correlated to ice duration.

Maximum depth is not correlated with many other variables, the highest is TOC (-0.49) with deeper lakes tending to have lower TOC levels. pH is negatively related to Alk and Ca^{2+} , indicating that lakes with lower pH have lower Ca^{2+} and Alk concentrations.

Overall the data matrix demonstrates that at higher altitudes there tends to be less precipitation and longer lake ice-cover durations. The high altitude lakes also tend to be larger with less TOC and lower nutrients than systems at lower altitudes. Many of

these links, however, may be due to the major difference in altitude and lake type between the two sets of lakes, with the Norwegian lakes occurring at higher altitude and being generally much larger and deeper than the Scotland sites.

To gain a better overview of the relationships between the environmental variables a PCA ordination was conducted and the results are displayed in Table 4.4 and Figure 4.25. Ordination of the environmental variables enables the internal variability in the data set to be explored. A large proportion of the total variance is captured by axes 1 and 2 (62.7%) with axes 3 and 4 only explaining 15.9% of the variance (Table 4.4). Axis 1 appears to represent several linked variables of Alt, Area, NH_4^+ , Ice, Cond, Cl^- and, to a lesser extent, a nutrient gradient (Figure 4.25). Sites 16, 13, and 7 (CN0018, CN0015, CN009) are all above 1050m and have Cl^- measures all below $15\mu\text{eq/l}$. In contrast sites 35, 31, and 24 (SC0211, SC0180 and SC029) are sites which all occur below 500m and all have Cl^- measures in excess of $190\mu\text{eq/l}$.

Axis 2 appears to be associated with a pH, Alk and Ca^{2+} gradient. For example, sites 20 and 17 (CN0022, CN0019) both have pH measures of 7.65 units and calcium measures of $445\mu\text{eq/l}$ and $347\mu\text{eq/l}$ respectively. These two sites often appeared as outliers, in terms of their environmental characteristics, in section 4.1.1 above. In comparison, Site 40 (SC0399) appearing at the opposite end of the pH gradient has a pH of just 5.42 and an Alk of $9\mu\text{eq/l}$ and Ca^{2+} of $32\mu\text{eq/l}$. The small acute angles between many of the determinands vectors (for e.g. Ca^{2+} and Alk) represent the high correlations between some of these environmental variables.

Table 4.3: Pearson product moment correlation matrix between 26 chemical determinands for 40 sites.

	Lat	Alt	Area	Dmax	ppt	pH	Alk	Cond	Na	K	Mg	CA	Cl	NO3	SO4	TN	TP	NH4	Al-TM	Al-L	Al NL	Toc	JanT	JulyT
Alt	0.6	1																						
Area	0.69	0.79	1																					
Dmax	0.2	0.35	0.55	1																				
ppt	-0.77	-0.57	-0.64	-0.19	1																			
pH	0.41	0.09	0.18	-0.22	-0.31	1																		
Alk	0.18	-0.17	-0.08	-0.32	-0.13	0.93	1																	
Cond	-0.5	-0.77	-0.67	-0.43	0.45	0.31	0.57	1																
Na	-0.83	-0.68	-0.63	-0.19	0.68	-0.47	-0.27	0.44	1															
K	0.37	-0.48	-0.38	-0.26	-0.02	0.52	0.65	0.67	-0.08	1														
Mg	-0.52	-0.79	-0.74	-0.43	0.45	0.24	0.51	0.94	0.46	0.68	1													
CA	0.09	-0.15	-0.05	-0.30	-0.13	0.86	0.94	0.62	-0.23	0.59	0.49	1												
Cl	-0.77	-0.89	-0.83	-0.33	0.74	-0.22	0.05	0.79	0.76	0.35	0.77	0.10	1											
NO3	-0.27	-0.13	-0.08	0.18	0.12	-0.46	-0.36	0.06	0.27	-0.14	0.07	-0.26	0.21	1										
SO4	-0.37	-0.20	-0.21	-0.19	0.25	0.18	0.32	0.62	0.18	0.26	0.51	0.49	0.37	0.34	1									
TN	-0.56	-0.62	-0.58	-0.32	0.30	-0.09	0.20	0.61	0.44	0.32	0.63	0.25	0.63	0.26	0.20	1								
TP	-0.27	-0.59	-0.53	-0.33	0.22	0.09	0.26	0.56	0.29	0.49	0.63	0.18	0.55	0.11	0.20	0.48	1							
Nh4	0.79	0.74	0.8	0.23	-0.76	0.37	0.11	-0.62	-0.78	-0.16	-0.64	0.08	-0.85	-0.18	-0.27	-0.55	-0.44	1						
Al-TM	-0.13	-0.36	-0.3	-0.34	0.00	0.02	0.18	0.31	0.08	0.25	0.29	0.19	0.30	-0.12	0.01	0.42	0.22	-0.16	1					
Al-L	-0.03	-0.17	-0.20	-0.37	-0.05	0.20	0.28	0.26	-0.12	0.29	0.21	0.30	0.10	-0.03	0.18	0.18	-0.02	-0.01	0.55	1				
Al NL	-0.2	-0.35	-0.32	-0.25	0.05	-0.18	-0.03	0.18	0.23	0.05	0.18	-0.01	0.32	-0.09	-0.11	0.41	0.23	-0.21	0.92	0.24	1			
Toc	0.49	-0.68	-0.71	-0.49	0.29	0.12	0.37	0.65	0.39	0.46	0.67	0.38	0.64	-0.22	0.12	0.73	0.46	-0.49	0.67	0.25	0.66	1		
Ice	0.78	0.86	0.81	0.35	-0.69	0.30	0.03	-0.68	-0.80	-0.25	-0.70	0.03	-0.89	0.16	-0.27	-0.60	-0.49	0.82	-0.29	-0.05	-0.34	-0.64	1	
JanT	0.91	-0.83	-0.79	-0.27	0.8	-0.4	-0.16	0.61	0.88	0.11	0.61	-0.11	0.9	0.26	0.28	0.55	0.37	-0.86	0.22	0.07	0.28	0.54	-0.91	
July T	0.84	-0.89	-0.84	-0.28	0.7	-0.22	-0.07	0.74	0.8	0.31	0.77	0.07	0.91	0.17	0.29	0.63	0.51	-0.86	0.29	0.09	0.32	0.69	-0.9	1

Figure 4.25: PCA biplot of the environmental data for the 40 lake training set and 25 environmental variables. Norwegian sites appear as triangles and the Scotland sites as circles (refer to Table 4.1 for lake codes/ numbers).

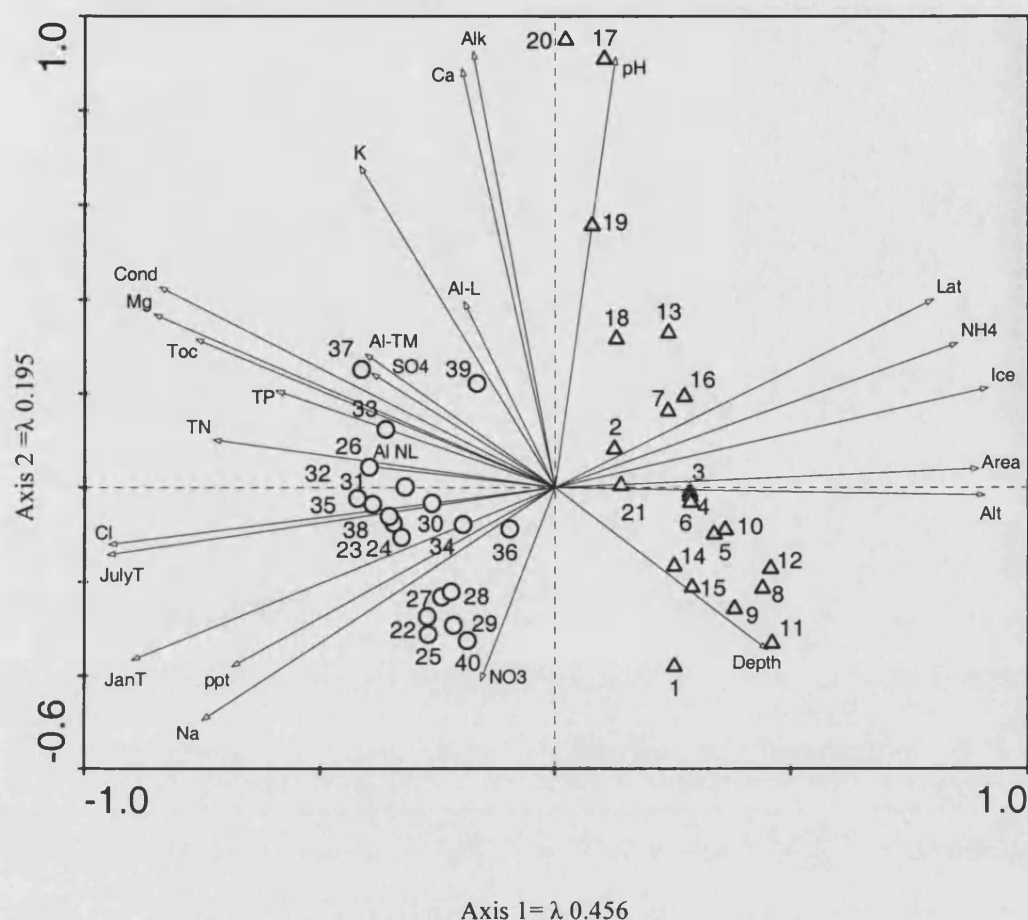


Table 4.4: Summary of PCA ordination, eigenvalues and cumulative % variance, of the 25 environmental variables and 40 sites, with centering and standardisation by species.

PCA axes	1	2	3	4
Eigenvalues (λ)	0.456	0.195	0.094	0.053
Cumulative percentage variance in the species data	45.6	65.1	74.5	79.8
Total inertia 1				
Sum of all eigenvalues 1				

The links between ordination axes and the environmental variables can be explored further through the PCA scores for each environmental variable, which appear as the length of the vectors in Figure 4.25 (summarised in Table 4.5). These show clear links between Axis 1 and Alt, Area, Cond, Cl^- , Ice duration, January and July air temperatures. Axis 2 has high scores for pH, Alk and Ca^{2+} . Axis 3 and 4 can be linked with Aluminium and Nitrate respectively.

Table 4.5: PCA scores for the 23 environmental variables on the first four axes (bold denotes all values >0.7 or >-0.7 for ease of comparison)

Variable	Axis 1	Axis 2	Axis 3	Axis 4
Latitude	0.800	0.4008	0.1064	-0.082
Altitude	0.909	-0.015	0.0175	0.108
Area	0.895	0.040	0.0663	0.101
Depth Max	0.451	-0.345	0.201	0.059
ppt	-0.687	-0.380	0.232	-0.168
pH	0.128	0.914	0.213	-0.164
Alk	-0.175	0.925	0.186	-0.09
Cond	-0.842	0.426	0.245	0.083
Na ⁺	-0.750	-0.496	0.078	-0.079
K ⁺	-0.416	0.683	0.124	-0.067
Mg ²⁺	-0.853	0.368	0.213	0.006
Ca ²⁺	-0.198	0.889	0.217	0.086
Cl ⁻	-0.949	-0.121	0.078	-0.021
NO ₃ ⁻	-0.158	-0.411	0.266	0.716
SO ₄ ²⁻	-0.391	0.243	0.501	0.548
TN	-0.728	0.101	-0.168	0.187
TP	-0.594	0.206	0.053	-0.109
NH ₄ ⁺	0.852	0.307	-0.115	0.093
Al-TM	-0.405	0.285	-0.794	0.240
Al-L	-0.195	0.396	-0.342	0.467
Al-NL	-0.394	-0.044	-0.831	0.102
Toc	-0.765	0.316	-0.414	-0.142
Ice	0.915	0.212	0.002	0.093
JanT	-0.899	-0.366	0.049	-0.064
JulyT	-0.952	-0.143	0.047	-0.077

Figure 4.25 shows the clear geographical clustering of the two sets of sites. With the Norwegian sites located in the right two quartiles and the Scottish sites located in the left hand section of the graph. This is probably primarily driven by altitude with the Norwegian sites being located at substantially higher altitudes than the Scottish sites. The Norwegian sites also, on average, have longer ice-cover durations, lower January and July air temperatures, higher pH, lower Ca²⁺ and considerably lower Cl⁻ (Table 4.2). The different sea salt inputs for the Norwegian and Scottish lakes are also apparent within the diagram and these are also positively correlated with precipitation.

The ammonium gradient is surprisingly long within this data set. This may be due to the bi-modal distribution of the variable within the Scottish lochs (between 0 and 2 µeq/l with many zero measurements, see box plot Figure 4.14) creating a distinct separation of sites between the Norwegian and Scottish sites. It is also surprising that NO₃⁻ is positioned within a different area on the biplot to the other nutrient variables, TN and TP. The reason for this is as yet unknown.

No particular outlier samples, in terms of their environmental variables, appear to be evident within the data set. Sites 20 and 17 are orientated separately from the rest of the samples but this is probably due to their unusually high Ca^{2+} values (see 4.1.1.1 above). The biplot displays a good dispersion of sites indicating that there are clear and long chemical/environmental gradients within the data set.

4.2 Biological data analysis

This section explores the diatom surface sample assemblages for the 40 lake training set. Initially the analysis is conducted independently of any explanatory variables. Ordination techniques are used to explore the variation between the diatom data in Norway and Scotland and to assess if there are any outliers within the data set. 331 species were identified in the forty lake set and a full list of diatom species and their codes, which are used subsequently in many illustrations, appear in Appendix 4.3. All counts were transformed to percentages (see also section 3.2.5 for taxonomic remarks)

4.2.1 Exploration of the dominant and most abundant taxa

The 25 most abundant (i.e. the sum of their counts in all 40 samples) are listed in Table 4.6. *Fragilaria exigua* is the most abundant species and occurs in 37 of the 40 samples. It can be seen that many *Aulacoseira* species and *Achnanthes* species are present suggesting that they are both common and abundant within the training set. Many species with high abundances also have a high number of occurrences within the training set (e.g. AC022A). Some species, however, have relatively high overall abundances and high maximum abundances but do not occur in many sites within the training set (e.g. CY006B, AU005E, AU022A). This indicates that when these species do occur they tend to dominate the lake assemblages, accounting for their high overall abundance sums, regardless of their low number of occurrences. Interestingly these species are all mainly centric diatom species (see section 1.3.3.3 for plankton growth dynamics). The N2 value is a measure of the effective occurrences of an individual species and is closely related to species occurrence and abundance (i.e. the number of samples the species occurs in and its percentage abundance).

Table 4.6: A list of the most abundant species (in terms of % sum abundance from all 40 samples), minimum and maximum abundance for the species, and the number of samples that the species occurs in. The species N2 value refers to the effective number of occurrences of that species calculated by CALIBRATE.

Taxon	N2	Number of samples the species occurs in (maximum 40)	Max abundance (%)	Sum of abundance of the species in all 40 samples (%)
FR064A <i>Fragilaria exigua</i>	20	37	33	377
AC022A <i>Achnanthes marginulata</i>	15	37	29	341
AC060A <i>Achnanthes curtissima</i>	14	36	30	274
AC013A <i>Achnanthes minutissima</i>	14	38	32	268
AC134A <i>Achnanthes helvetica</i>	12	39	27	193
BR010A <i>Brachysira neoexilis</i>	15	36	19	182
FU002A <i>Frustrulia rhomboides</i>	15	35	19	180
CY006B <i>Cyclotella kuetzingiana</i> var. <i>planetophora</i>	7	17	22	130
AC048A <i>Achnanthes scotica</i>	20	23	9.5	124
TA9997 <i>Tabellaria flocculosa</i> (short)	19	33	6.6	124
AC136A <i>Achnanthes subatomoides</i>	11	33	12	104
EU047A <i>Eunotia incisa</i>	14	33	33	104
AU005E <i>Aulacoseira distans</i> var. <i>nivalis</i>	9	19	14	102
AC046A <i>Achnanthes altaica</i>	22	35	4.9	99
ZZZ986 <i>Aulacoseira distans</i> var. <i>septentrionalis</i>	3	10	25	94
AU022A <i>Aulacoseira subborealis</i>	3	6	25	88
PE002A <i>Peronia fibula</i>	13	29	9	87
CM018A <i>Cymbella gracilis</i>	22	35	4.5	87
BR006A <i>Brachysira brebissonii</i>	16	32	6.4	85
FU002B <i>Frustrulia rhomboides</i> var. <i>saxonica</i>	16	33	5	79
CM010A <i>Cymbella perpusilla</i>	16	33	5.4	75
AC134B <i>Achnanthes helvetica</i> var. <i>alpina</i>	2	21	18	73
CM020A <i>Cymbella gaeumannii</i>	18	33	3.3	71
AU005A <i>Aulacoseira distans</i>	11	21	8	70
EU009A <i>Eunotia exigua</i>	11	27	6.2	69

Figure 4.26 shows a summary diagram of the most abundant species in the training set. The set is dominated by *Achnanthes*, *Aulacoseira* and *Fragilaria* species and some planktonic *Cyclotella* species are also present. Typically 'oligotrophic' upland lakes assemblages are often dominated by the genera *Achnanthes* and *Fragilaria* (Anderson 2000; Battarbee *et al.*, 2002; Flower and Jones 1989b).

The sites in Figure 4.26 have been arranged in order of increasing pH (ranging from 5.42 pH for SC0399 to 7.65pH for CN0019). It can be seen that the three *Cyclotella* species, *Achnanthes nodosa* and *Achnanthes minutissima* tend to prefer higher pH conditions. The planktonic species mainly occur in the Scottish lochs with the exception of CN0018 which has a high percentage of *Cyclotella kuetzingiana* var. *radiosa* and *Cyclotella kuetzingiana* var. *planetophora*. Other centrics such as *Aulacoseira distans* and *A. distans* var. *nivalis* tend to be more abundant in the lower pH sites. The *Aulacoseira* species also tend to occur in the Norwegian lakes and this may be due to their greater depth as these species usually occur in deeper lakes (Pienitz and Smol 1993).

Fragilaria exigua appears in the assemblages of nearly all the 40 sites as does *Frustulia rhomboides*, *Achnanthes marginulata*, *Achnanthes curtissima*, *Achnanthes helvetica*, *Tabellaria flocculosa* and *Brachysira neoexilis* suggesting that they have less specific pH requirements. The N2 value is the number of effective occurrences and all these species have relatively high N2 values (≥ 14).

The acidophilous species *Eunotia incisa* is slightly more abundant at the lower pH sites and has a high N2 value of 14, but it is present in low abundances at most sites. In contrast the acidophilous species *Frustrulia rhomboides* does not increase in the lower pH sites but is present in most of the lakes. *Achnanthes marginulata* also seems to be more dominant in the lower pH lakes

In addition some species seem to be country specific and only occur in either the Scottish or the Norwegian lakes. Many of the *Achnanthes* and *Aulacoseira* only occur

in the Norwegian lakes (e.g. *Achnanthes lucus-vulcani*, *Achnanthes curtissima* and *Aulacoseira distans* var. *septrionalis*, *Aulacoseira distans* var. *nivaloides*, *Aulacoseira perglabra* var. *florinae*). Also *Fragilaria pinnata* only occurs in the Norway sites. These distribution patterns are unlikely to be a biogeographical feature as many of these species have also been found in Scottish lochs (Jones *pers. com.*). The only species that tends to prefer the Scottish lochs rather than the Norwegian lakes is *Peronia fibula* which reaches 9% maximum abundance and occurs in 29 of the 40 lakes but in fewer numbers in the Norwegian samples. This species is also known to favour higher DOC waters which may account for its prevalence in the Scottish lochs (Stevenson *et al.*, 1991). *Brachysira neoexilis*, *Eunotia exigua* and *Eunotia incisa* also occur in higher abundances in the Scottish lochs compared to the Norwegian lakes, possibly reflecting the more acidic nature of the Scottish sites.

4.2.2 Indirect ordination analysis of the surface sediment diatom assemblages

To limit the 'noise' within the training set all taxa occurring at <1% abundance and occurring in <2 samples were deleted. This left a data set consisting of 152 species. Ordination of the diatom data was conducted to explore the variability of the diatom assemblages and any outliers within the data set. DCA was conducted to establish the gradient length. Rare species were down weighted. Different transformation options were conducted within the DCA to see how these affected the ordination results (Table 4.7). Square root and log transformed data resulted in shorter gradient lengths than when using untransformed data. However, the variance explained by axis 1 (λ_1) and axis 1 and 2 (λ_2) in combination is similar for all three methods. Log (x^{+1}) and untransformed data had the highest inertia. The best transformation option, therefore, appeared to be the square root transformed data and this choice is often suggested for use with ecological data (Birks, *pers. com.*).

The DCA results showed relatively low gradient lengths for axis 1 (2.42 SD) which is within the 'grey' area between unimodal and linear response (see section 3.3.2), with some species responding in a unimodal fashion and some linearly. More assumptions, however, are involved in DCA ordination techniques (Birks, *pers. com.*) and, therefore, it was decided that linear PCA methods would be used, the results of which are summarised in Table 4.8.

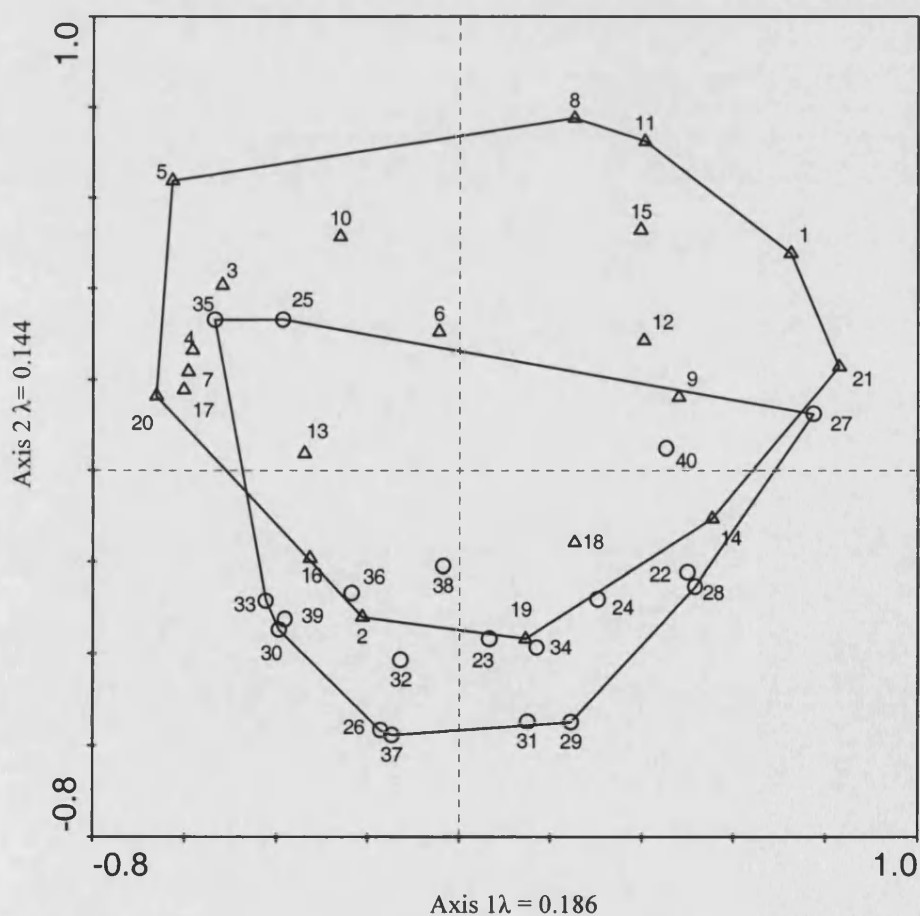
Table 4.7: Results of DCA analysis with different transformation options for the species data. In all options rare species are down weighted

Type of data transformation	Gradient length (Axis 1, SD units)	Axis 1 Eigenvalue λ_1	\sum inertia $\sum \lambda$	% variance explained λ_1	% variance explained $\lambda_1 + \lambda_2$
Square root	2.42	0.28	1.964	14.2	23.3
Log (x+1)	2.60	0.32	2.212	14.5	23.5
Untransformed	3.82	0.43	3.346	13	21.3

Table 4.8: Summary of PCA ordination results of 152 species in 40 samples, eigenvalues and cumulative % variance are displayed. The data were square root transformed.

PCA axes	1	2	3	4
Eigenvalues (λ)	0.186	0.144	0.067	0.057
Cumulative percentage variance in the species data	18.6	33	39.8	45.5
Sum of all eigenvalues 1				

Figure 4.27: PCA biplot of the 40 surface sample diatom assemblages, only sites are shown. Norwegian sites appear as triangles and Scottish sites as circles (refer to Table 4.1 for lake number/codes)



A large proportion of the variance within the diatom data is captured by axis 1 (18.6%) and axis 2 (14%) (Table 4.8). Relatively little variance is explained by axes 3 and 4 (combined 12.5%). The ordination was plotted on the biplot in Figure 4.27. Envelopes have been drawn round the Norway sites (triangles) and the Scottish sites (circles).

The variation within the diatom data is larger for the Norwegian sites than the Scottish samples which are more tightly clustered. It should be noted that the separation between the countries is not as distinct for the diatom data, in comparison to the environmental data ordination biplot (Figure 4.25), and there is considerable overlap in the ordination diagram, suggesting that there is a high degree of floristic similarity despite the separation of samples according to the chemical variables.

The high calcium, high pH lakes, 20 and 17 are located on the left of the biplot and sites 27 and 21, with lower pH and calcium ($\text{pH} < 6.2$ and $\text{Ca} \leq 38 \mu\text{eq/l}$), are located to the right suggesting that axis 1 might represent a pH/ calcium gradient. Axis 2 is slightly more complex but seems to represent an altitude/ ice-cover/ area/ TOC gradient. Sites 8 and 11 appearing at one extreme of this gradient occur at 1526m and 1396m respectively and both have areas $\geq 80\text{ha}$ and ice-cover durations of ≥ 224 days. These sites also have low TOC values of $\leq 0.5\text{mg/l}$. In contrast sites 26, 37 and 31 all have ≤ 10 days ice-cover, occur at $< 600\text{m}$ altitude and are relatively small lakes (all $\leq 7.5\text{ha}$). They also have considerably higher TOC levels ranging from 7.5mg/l to 9.2mg/l .

More information about which environmental variables the two axes might represent can be derived from the known ecological preferences of the diatoms associated with each axis of the ordination (Table 4.9). The table lists the species with the highest ordination scores, both positively and negatively, associated with each ordination axis. The species ordination score reflects their importance on the ordination axis. *Eunotia incisa*, *Peronia fibula* and *Achnanthes marginulata* are all positively associated with axis 1 and are all species which tend to prefer lower pH conditions (Figure 4.26) and typically have low pH optima (SWAP optima ≤ 5.3 pH units, Stevenson *et al.*, 1991, Battarbee *et al.*, 2001). Weighted Averaging analysis, using

this data set, was conducted to calculate the pH optima and tolerance for these species (calculated using CALIBRATE, see sections 3.3.3 for methods and 4.4.2 and 4.4.3 for similar examples). The species positively associated with axis 1 all have pH optima of 6.1. The pH optima for *Achnanthes didyma*, *Navicula seminulum* and *Fragilaria brevistriata*, which are negatively associated with axis 1, all have much higher optima at 6.7, 6.5 and 7.1 pH units respectively.

Table 4.9: Species ranking, based on their PCA ordination scores, for ordination axes 1-4

Axis 1 = 17.5 % of variance	
(+) Achnanthes marginulata Peronia fibula Eunotia incisa Aulacoseira distans var. tenella Achnanthes marginulata f.major	(-) Fragilaria brevistriata Achnanthes stolidia Achnanthes didyma Navicula seminulum Achnanthes minutissima var inconspicua
Axis 2 = 13.7% of variance	
(+) Achnanthes scotica Navicula leptostriata Navicula cryptocephala Aulacoseira distans var. nivalis Aulacoseira distans var septentrionalis	(-) Brachysira vitrea Cymbella gracilis Tabellaria flocculosa Eunotia rhyncephala Achnanthes pseudoswazi
Axis 3 = 6.5 % of variance	
(+) Navicula sp Naviculadicta circumborealis Cymbella amphicephala Achnanthes suchlandtii Cyclotella pseudostelligera	(-) Achnanthes curtissima Cymbella gaeumannii Fragilaria exigua Frustulia rhomboides Stauroneis anceps
Axis 4 = 5.5% variance	
(+) Fragilaria exigua Fragilaria construens Fragilaria pinnata var. lancettula Eunotia faba Eunotia serra	(-) Achnanthes helvetica Cyclotella kuetzingiana var. planetophora Cyclotella kuetzingiana var. radiosa Achnanthes holstii Navicula bremensis

The species positively associated with axis 2 should, if the interpretation above is correct, occur in sites of high altitude and relatively low TOC. The altitude WA optima using CALIBRATE (Juggins and ter Braak 1993) for *A. scotica*, *N. leptostriata*, *A. distans* var. *nivalis* and *A. distans* var. *septrionalis* are 973m, 706m, 903m and 1200m respectively. Their TOC optima are 3.31mg/l, 4.6mg/l, 1.89mg/l, 1.3mg/l. In comparison the altitude WA optima range for the five species negatively associated with axis 2 was between 597-744m, substantially lower than those positively associated with axis 2. Their TOC optima are 3.8mg/l (*B. vitrea*), 3.5mg/l (*C. gracilis*), 3.3mg/l (*T. flocculosa*) and 4.9mg/l (*A. pseudoswazi*). The TOC optima

on average are higher than those positively associated with axis 2 (See section 4.6.2 for further DOC and diatom discussion).

The relationship, however, between the diatoms and altitude is unlikely to be a direct cause and effect mechanism and more likely to be related to other variables linked to altitude such as lake area, lake ice-cover and nutrients (see Figure 4.25).

4.3 The relationship between the environmental and species data

In order to explore the relationship between diatom species and environmental variables further, direct gradient analysis was conducted on the 40 samples. The samples were constrained by the environmental data and the relationships between the response variables (the diatoms) and the explanatory variables, (the environmental data) were evaluated. In addition the response of individual species to various environmental variables was conducted using the HOF program (Oksanen 2001, Oksanen and Minchin 2002). These analyses will be used to establish which environmental variables are driving the variation within the diatom data. The results are also used to evaluate the specific influence of ice-cover duration on the diatom assemblages.

4.3.1: Indirect gradient analysis

A DCCA was conducted initially to establish if linear or unimodal methods were more appropriate (Table 4.10). The short gradient length indicated that linear Redundancy Analysis (RDA) was a more appropriate method to use (ter Braak 1987). The results of the RDA are shown in Table 4.11 and the biplot of the first two ordination axes in Figure 4.28.

Table 4.10: Summary results from the DCCA of 25 environmental variables, 40 sites and 152 species, with square root transformation of species data.

DCCA axes	1	2	3	4
Eigenvalues (λ)	0.220	0.178	0.064	0.047
Lengths of gradient	2.16	2.07	1.409	1.112
Species environment correlations	0.909	0.96	0.945	0.954
Cumulative percentage variance of the species data	11.2	20.3	23.6	25.9
of species- environment relation	15.6	29.3	0	0
Sum of all eigenvalues 1.964				
Sum of all canonical eigenvalues 1.379				

Table 4.11: Summary results of the RDA conducted on 40 samples, 152 species and 25 environmental variables, with square root transformation of species data.

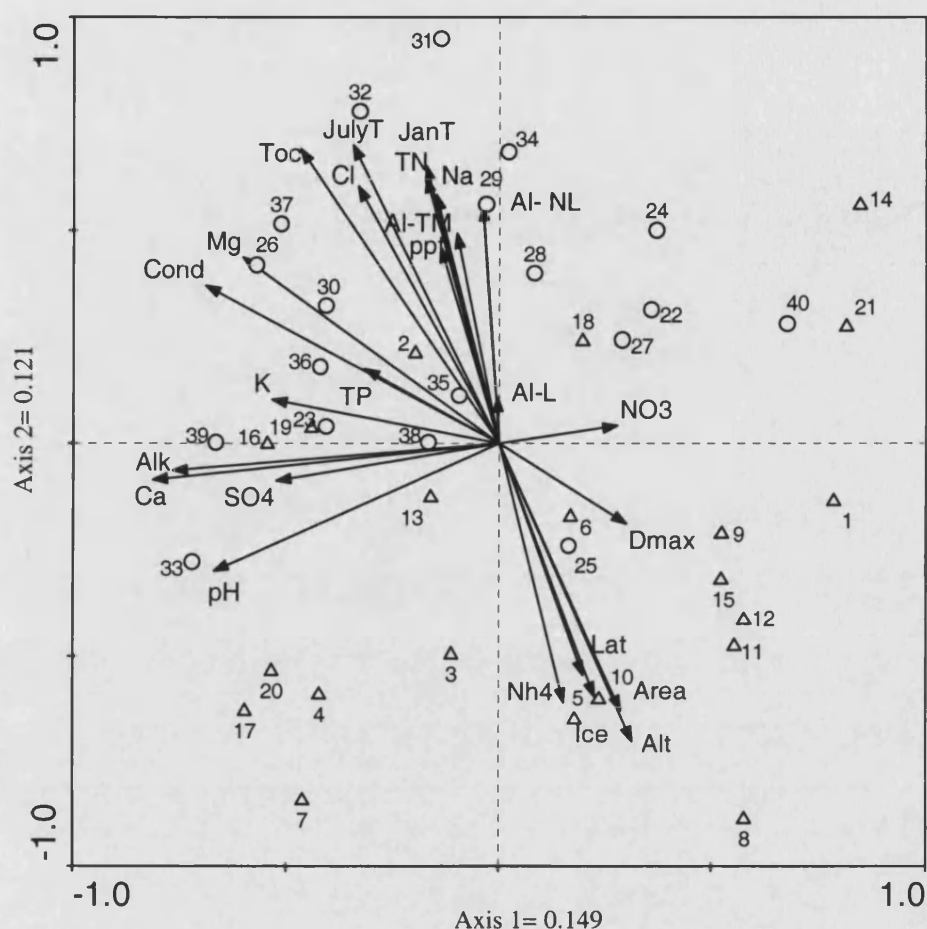
RDA axes	1	2	3	4
Eigenvalues (λ)	0.149	0.121	0.054	0.050
Species environment correlations	0.932	0.903	0.916	0.952
Cumulative percentage variance of the species data	14.9	27.1	32.4	37.4
of species- environment relation	20.6	37.4	44.8	51.8
Sum of all eigenvalues 1				
Sum of all canonical eigenvalues 0.723				

Axis 1 and 2 capture 27.1% of the variance within the diatom data (Table 4.11). Axes 3 and 4 have low eigenvalues and are relatively unimportant for explaining further floristic variation. In Figure 4.28 the length of the biplot vectors illustrates the importance of that variable for explaining variation within the diatom data. It can be seen that TOC, pH, Cond, Mg^{2+} , Ca^{2+} , Alk, Alt, Ice, Area and NH_4^+ are all important variables.

Axis 1 appears to be a pH / Ca^{2+} / Alk axis, with sites with high pH and Calcium appearing in the negative area of the biplot and sites with lower pH/ Ca^{2+} situated in the positive pH/ Ca^{2+} area. There is a clear spatial separation between the Norwegian and Scottish sites which is primarily driven by altitude and associated with axis 2.

The small acute angles between some of the vectors, however, suggest a high degree of co-linearity between variables. In essence these environmental variables can be substituted for each other (e.g. pH, Ca^{2+} and Alk, or Alt and Area) and excluded from further consideration. The variance inflation factor (VIF) for each environmental variable, an output of the RDA analysis, is listed in Table 4.12. Variables with high VIF's indicate co-linearity with other variables (ter Braak 1987). Generally VIFs above 20 illustrate high co linearity and removal of some environmental variables is desirable and by doing so the explanatory power, and significance of the model is increased (Kent and Coker 1992). 15 of the 25 variables have VIFs over 20. The VIF values indicate the degree of co-linearity within the data set and do not indicate which variables can be excluded. The next section evaluates, using further ordinations, which environmental variables could be eliminated.

Figure 4.28: RDA biplot of 152 diatom species, 25 environmental variables and 40 samples. Only the samples/sites are shown. Triangles represent Norwegian sites and circles represent Scottish sites. See Table 4.1 for lake codes/ numbers



4.3.2 Identification of the most important environmental variables

In order to ascertain which variables should be removed constrained ordinations were conducted with each of the explanatory variables and the results are displayed in Table 4.13. The amount of variance explained by each variable is listed and those which have a significant response are starred. It can be seen that calcium explains the highest amount of diatom variation within the data set, followed by conductivity and TOC. It should be noted here that ice-cover duration explained 6.8 % of the diatom data and was significant using Monte Carlo permutation test techniques, indicating that there is an ice signal within the diatom data. The 6.8% variance explained may not, however, be solely due to ice-cover but ice-cover and other variables which have co-linearity with ice-cover (e.g. Ice and Area together may explain a proportion of the 6.8%). The variables DMax, Al-L and TP did not significantly explain any species

response and these were, therefore, excluded from further ordination analyses leaving 22 significant variables.

Table 4.12: VIF values for the RDA with 25 environmental variables (variables with VIF's above 20 are in bold type)

Variable	Weighted Average	Standard deviation	Inflation factor	Variable	Weighted Average	Standard deviation	Inflation factor
Latitude	59.46	2.135	89.1	Cl ⁻	1.9	0.59	26.5
Altitude	886	294	51.8	NO ₃ ⁻	0.34	0.28	4.8
Area	1.23	0.63	23.0	SO ₄ ²⁻	1.42	0.19	9.1
Dmax	15.01	9.63	4.05	TN	2.08	0.25	11.5
ppt	1418	553	8.15	TP	2.25	1.29	3.6
pH	6.40	0.44	74.5	NH ₄ ⁺	0.17	0.15	14.1
Alk	1.54	0.40	117.7	Al-TM	0.95	0.42	150.3
Cond	1.19	0.31	148	Al-L	0.31	0.39	14.0
Na ⁺	1.58	0.647	12.1	Al-NL	0.86	0.41	126.7
K ⁺	0.76	0.22	7.5	TOC	0.41	0.25	33.7
Mg ²⁺	1.36	0.38	34.5	Ice	131.8	83.11	14.0
Ca ²⁺	1.71	0.33	87.0	JanT	27.4	5.49	176.0
				JulyT	44.6	4.3	59.5

Table 4.13: Results of the RDA of diatom data constrained against each environmental variable independently. The significant variables are highlighted by * (p value ≤0.05) and ordered in terms of the variance explained by each.

Variable	λ1	Species-environment correlation	%Variance explained	Significance achieved
Ca ²⁺	0.109	0.824	10.9	0.001*
Conductivity	0.102	0.854	10.2	0.001*
TOC	0.102	0.877	10.2	0.001*
Alkalinity	0.099	0.794	9.9	0.001*
Mg ²⁺	0.092	0.829	9.2	0.001*
pH	0.090	0.759	9	0.001*
JulyT	0.09	0.848	9	0.001*
Altitude	0.088	0.83	8.8	0.001*
Cl ⁻	0.078	0.817	7.8	0.003*
Area	0.076	0.805	7.6	0.001*
JanT	0.07	0.78	7.2	0.001*
Ice	0.068	0.781	6.8	0.003*
NH ₄ ⁺	0.066	0.773	6.6	0.002*
TN	0.066	0.744	6.6	0.002*
K ⁺	0.065	0.718	6.5	0.002*
Na ⁺	0.063	0.766	6.3	0.003*
SO ₄ ²⁻	0.060	0.671	6.0	0.007*
Latitude	0.058	0.732	5.8	0.005*
Al-NL	0.055	0.710	5.5	0.009*
Al-TM	0.053	0.727	5.3	0.011*
ppt	0.046	0.687	4.6	0.027*
NO ₃ ⁻	0.044	0.714	4.4	0.029*
TP	0.041	0.662	4.1	0.05
Dmax	0.041	0.657	4.1	0.049
Al-L	0.032	0.752	3.2	0.205

The RDA was re-run with these 22 variables and the results and RDA biplot are displayed in Table 4.14 and Figure 4.29. The co-linearity of the remaining variables was again examined visually and using the VIF values (Table 4.15). Many of the VIF values remain high and the positions of the biplot vectors show that there is still great co-linearity between the remaining environmental variables (Figure 4.2.9). The exclusion of further variables, therefore, was desirable. This was done visually by assessing which variables share similar biplot positions and which of the co-linear variables had the lower biplot scores. The reasons for inclusion or exclusion of variables from the RDA model are summarised in Table 4.16 and described below.

Variables which shared similar positions on the biplot were Alk and Ca^{2+} . Ca^{2+} was retained due to the fact that it explained greater diatom variance. Secondly, Alt and Area are co-linear. Altitude was retained due to the fact that it explained greater variance than Area. Thirdly, latitude and ice-cover share similar positions on the biplot and, latitude was deleted due to its smaller biplot score. A further cluster of vectors sharing similar biplot positions are, TN, JanT, JulyT, Na^+ , ppt, Al-TM, Al-NL. Precipitation was excluded due to its low biplot score. The others were retained. A further RDA was, therefore, performed with only 17 variables the results of which are displayed in Figure 4.30 and Table 4.18

Table 4.14: RDA of 40 sites, 152 species, and 22 environmental variables with square root transformation of species data.

RDA axes	1	2	3	4
Eigenvalues (λ)	0.146	0.114	0.051	0.045
Species environment correlations	0.925	0.877	0.910	0.936
Cumulative percentage variance of the species data	14.6	26.1	31.1	35.6
of species- environment relation	22.2	39.5	47.2	53.9
Sum of all eigenvalues 1				
Sum of all canonical eigenvalues 0.66				

The VIF's of this RDA with the reduced environmental data set are greatly reduced and 12 of the 17 now fall below 20 (Table 4.17).

Axis 1 and 2 account for 25.1% of the total diatom variation (Table 4.18). The biplot scores associated with each axis (Table 4.17) indicate that axis 1 (14.4% variance) represents a Ca^{2+} /Cond gradient and to a lesser extent pH and Mg^{2+} , and axis 2

(10.7% variance) an Altitude, July temperature and TOC gradient. The cluster of Norwegian high altitude sites is evident again in the upper left quartile, with the lower altitude, higher TOC sites located in the bottom left quartile (Figure 4.30).

Figure 4.29: RDA biplot of 152 diatom species, 22 environmental variables and 40 samples. Only the samples/sites are shown. Triangles represent Norwegian sites and circles represent Scottish sites. See Table 4.1 for lake codes/ numbers

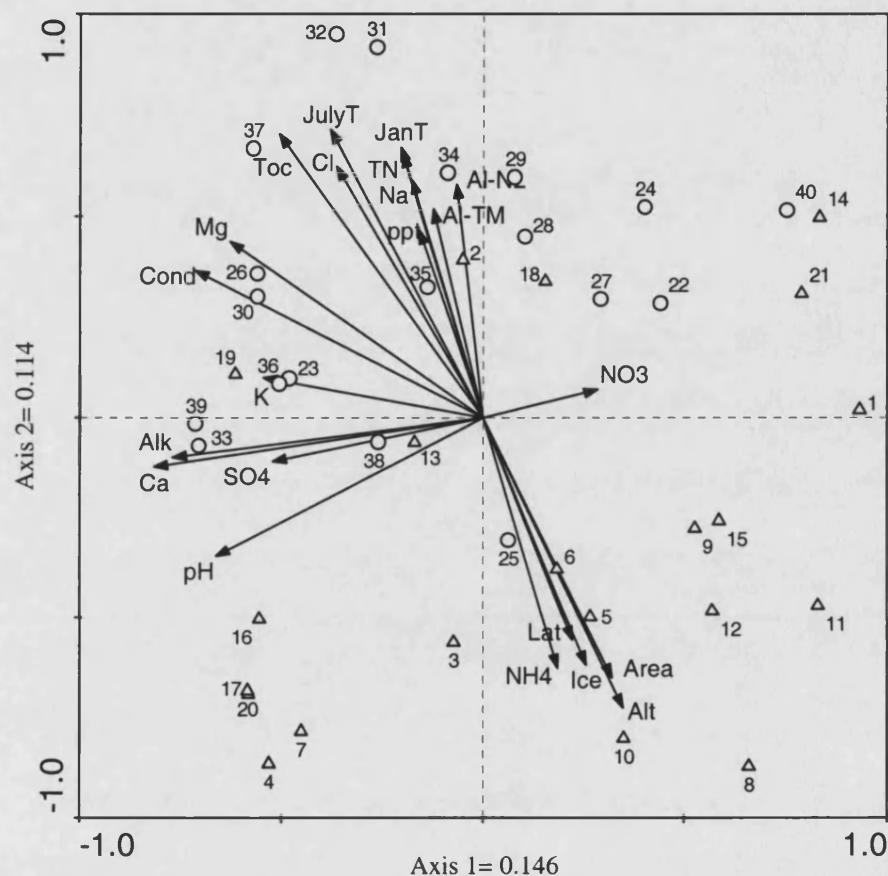


Table 4.15: VIF values generated by the RDA analysis of 18 environmental variables. VIF values over 20 are marked by bold type.

Variable	VIF value	Variable	VIF value
Latitude	65.6	Cl ⁻	22.4
Altitude	40.9	NO ₃ ⁻	4.6
Area	12.0	SO ₄ ²⁻	8.1
ppt	6.6	TN	10.4
pH	54.4	NH ₄ ⁺	11.4
Alk	96	Al-TM	19.9
Cond	116	Al-NL	25.6
Na ⁺	10.4	TOC	32.7
K ⁺	5.6	Ice	13.8
Mg ²⁺	31.8	JanT	134.3
Ca ²⁺	69.7	JulyT	54

Table 4.16: Reasons for inclusion or deletion of environmental variables within the ordination analyses

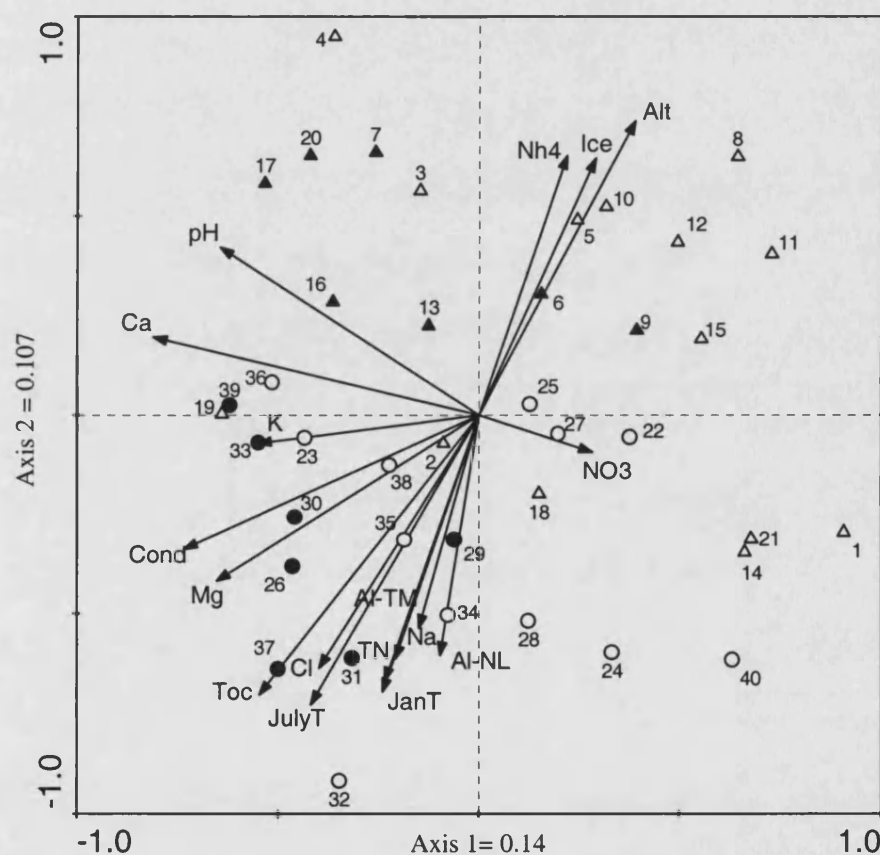
Variable	Inclusion or deletion	Co-linearity with other variables	Reason for deletion/ inclusion
Ca ²⁺	Retain	Alk	Greater variance explained than Alk
Conductivity	Retain	TP	Greater variance explained than TP
TOC	Retain	None closely	N/A
Alkalinity	Delete	Ca ²⁺	Less variance explained than Ca ²⁺
Mg ²⁺	Retain	None closely	N/A
pH	Retain	None	N/A
JulyT	Retain	None closely	N/A
Altitude	Retain	Area	Less variance explained than area
Cl ⁻	Retain	None closely	N/A
Area	Delete	Alt	Less variance explained than Alt
JanT	Retain	TN, ppt and Na	Has co- linearity but variables not related to each other, not appropriate to delete
Ice	Retain	Lat	Greater variance explained than Lat
NH ₄ ⁺	Retain	None closely	N/A
TN	Retain	JanT, ppt and Na	Has co- linearity but variables not related to each other, not appropriate to delete
K ⁺	Retain	None closely	N/A
Na ⁺	Retain	TN, JanT, and ppt	Has co- linearity but variables not related to each other, not appropriate to delete
SO ₄ ²⁻	Delete	Ca ²⁺ and Alk	Less variance explained than Ca ²⁺ and Alk
Latitude	Delete	Ice	Less variance explained than ice
Al-NL	Retain	None closely	N/A
Al-TM	Retain	None closely	N/A
ppt	Delete	JanT, Na and TN	Limited variance explained
NO ₃ ⁻	Retain	None closely	N/A
TP	Delete	Cond	Did not explain a significant proportion of the diatom variance
Dmax	Delete	None	Did not explain a significant proportion of the diatom variance
Al-L	Delete	Al-NL	Did not explain a significant proportion of the diatom variance

Table 4.17: VIF values (those >20 in bold) and RDA biplot scores for axes 1-4 (those > 0.7 positively or negatively in bold for ease of comparison) for the RDA of 17 environmental variables and 152 species.

Variable	Inflation factor	Axis 1	Axis 2	Axis 3	Axis 4
Altitude	9.8	0.3889	0.739	-0.265	0.006
pH	14.6	-0.646	0.421	0.153	0.214
Cond	72	-0.736	-0.33	0.35	0.19
Na ⁺	8.8	-.0209	-0.614	-0.124	-0.371
K ⁺	5.0	0.552	-0.0717	0.395	0.233
Mg ²⁺	20	-0.654	-0.418	0.367	0.103
Ca ²⁺	36.8	0.812	0.195	0.277	0.291
Cl ⁻	18.8	-0.399	-0.637	0.174	0.030
NO ₃ ⁻	3.4	0.282	-0.094	0.553	-0.469
TN	4.6	-0.236	-0.669	0.34	0.108
NH ₄ ⁺	7.5	0.218	0.65	0.05	0.07
Al-TM	17.5	-0.15	-0.537	0.04	0.49
Al-NL	20	-0.097	-0.605	-0.17	0.29
TOC	17.2	-0.54	-0.703	-0.015	0.268
Ice	12.6	0.29	0.645	-0.113	0.01
JanT	28.7	-0.241	-0.696	0.121	-0.163
JulyT	22.9	-0.418	-0.727	0.176	-0.137

Table 4.18: RDA of 40 samples, 17 environmental variables and 152 species with square root transformation.

RDA axes	1	2	3	4
Eigenvalues (λ)	0.144	0.107	0.048	0.044
Species environment correlations	0.924	0.856	0.896	0.939
Cumulative percentage variance of the species data	14.4	25.1	29.9	34.3
of species- environment relation	25.5	44.4	53	60.7
Sum of all eigenvalues 1				
Sum of all canonical eigenvalues 0.565				

Figure 4.30: RDA biplot on axes 1 and 2 with 17 environmental variables, 152 species and 40 sites. Norwegian sites are displayed as triangles and Scottish sites as circles. Filled symbols indicate site with $\geq 5\%$ plankton.

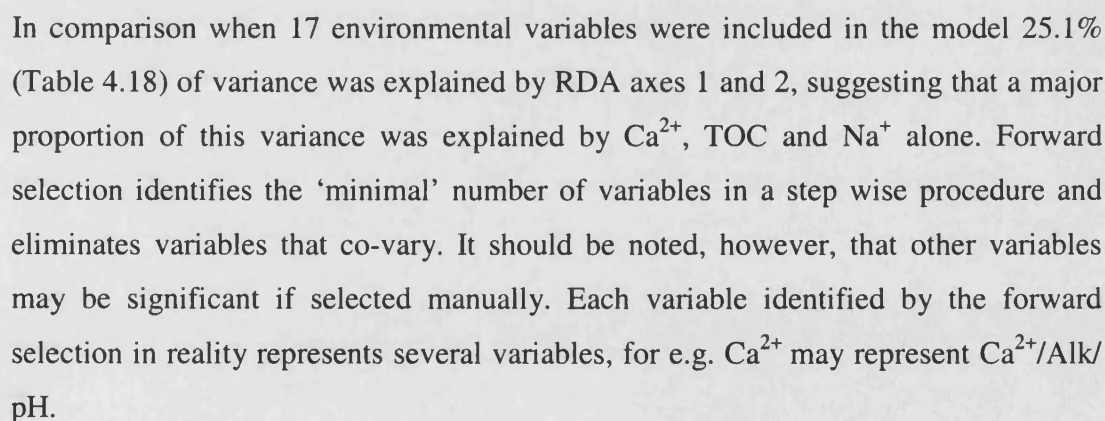
One of the aims outlined in Section 1.6 was to evaluate which environmental factors govern plankton abundance in high altitude lakes and in particular if ice-cover has an influence on the growth of planktonic diatoms. This is discussed further in section 4.4.2 but Figure 4.30 highlights the ordination distribution of sites with planktonic diatoms present (filled symbols). There is a tendency for the planktonic diatoms to be present in higher than average pH and Ca^{2+} sites with higher than average TOC. Most

of the sites with plankton present are located in the Scottish samples which are from lower altitude lakes with less ice-cover. However, it should be noted that $\geq 5\%$ plankton abundance does not represent a large proportion of the diatoms present within each sample and any trends in the ordination may not be significant. The clustering of planktonic diatom sites is not discrete and it is possible that several factors are responsible for the occurrence of the planktonic diatoms within the data set. This is discussed further in section 4.4.2.

Figure 4.31 illustrates which species are associated with the ordination axes 1 and 2. A grouping of *Aulacoseira* species (code prefix AU) is evident at the high altitude sites. Many *Fragilaria* species (prefix FR) seem to occur in the higher pH sites as do the planktonic *Cyclotella* species (prefix CY). Many species in the *Eunotia* genera (code prefix EU) seem to be more associated with high TOC and TN levels and occur at the lower altitude sites.

A further way to evaluate which environmental variables are the most important for describing the variation within the diatom data is the use of the 'forward selection' option within the ordination program CANOCO. This option identifies the minimum number of variables that significantly explains the diatom variance (Table 4.19). When using this technique a Bonferroni correction to the p-value, which determines the significance of the environmental variable, has to be made because multiple tests are being performed simultaneously. The p-value is adjusted by taking $\alpha=0.05$ and dividing by the number of tests being run resulting in an adjusted p-value (Table 4.19). Only three variables were identified as significant with the forward selection procedure and these were calcium, total organic carbon and sodium. Nitrate was the fourth variable tested but proved not to be significant.

This forward selection procedure in essence identifies a 'minimal set' of environmental variables which account for significant independent diatom species variation (ter Braak 1987). The RDA results for just these three explanatory variables and shows that 21.3% of diatom variance is explained by the first two RDA axes (Table 4.20).



176

Table 4.19: Forward selection of environmental variables using RDA of 25 environmental variables. Significance of each variable was assessed using Bonferonic required significance values.

Forward selection variable	Variance explained %	F ratio	Bonferonic required significance	Significance (p-value)	
Ca ²⁺	0.11	4.67	0.05/1 = 0.05	0.001	Significant
TOC	0.09	4.19	0.05/2 = 0.025	0.001	Significant
Na ⁺	0.04	1.95	0.05/3 = 0.0166	0.007	Significant
NO3 ⁻	0.04	1.82	0.05/4 = 0.0125	0.014	Not significant
Al-L	0.03	1.41	0.05/5 = 0.01	0.083	Not significant
Variance explained by all variables 0.69					

Table 4.20: RDA of 40 samples, 3 environmental variables and 152 species, with square root transformation of species data

RDA axes	1	2	3	4
Eigenvalues (λ)	0.127	0.086	0.028	0.126
Species environment correlations	0.904	0.787	0.859	0
Cumulative percentage variance of the species data	12.7	21.3	24.1	36.7
of species- environment relation	52.7	88.3	100	0
Sum of all eigenvalues 1				
Sum of all canonical eigenvalues 0.241				

4.4 The relationship between diatoms and ice-cover duration

Although ice-cover duration was not identified by the forward selection technique it still appeared to be significant in terms of diatom variance (See Table 4.13). The specific influence of ice-cover duration on the diatom assemblages is evaluated in the next section in order to satisfy one of the aims of the thesis (section 1.6). It was shown above that ice-cover explained 6.8% of variance and was significant suggesting that ice-cover does influence diatom assemblages but it should be remembered that this may not be a direct relationship. The relationship between ice-cover and diatom species is assessed in the next section through the use of WA and Gaussian Logit Regression methods. Specific species responses to ice-cover duration are also assessed using the HOF model (see section 3.3.2.5). These results are compared with the responses of the diatoms to other environmental variables available for the 40 lakes.

4.4.1 Individual species responses to ice-cover duration in relation to other environmental variables

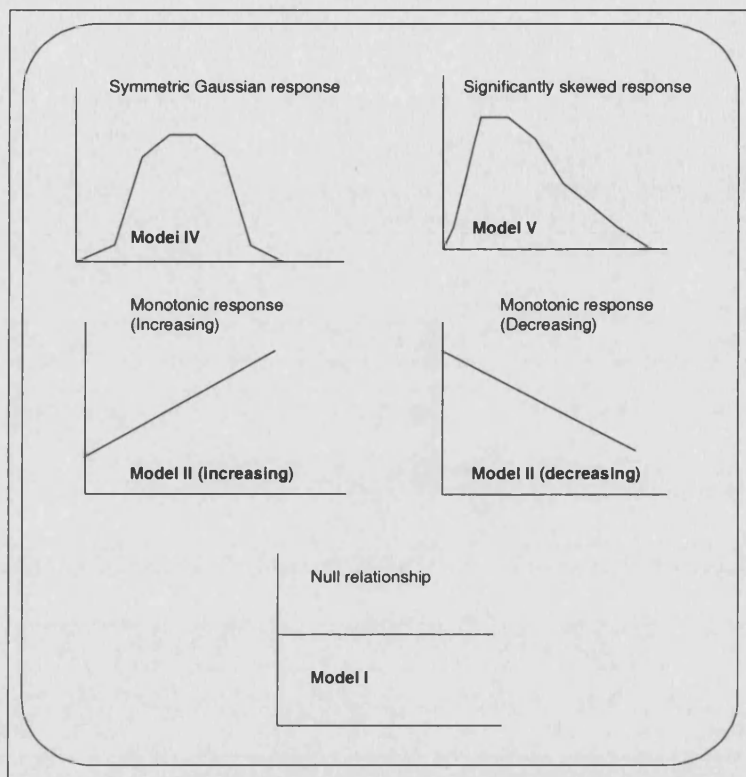
It has been shown above that several variables have a significant influence on the diatom variation within the 40 lake training set. The actual response of individual taxa to various environmental variables can be calculated using maximum likelihood with Poisson error methods using the HOF program (Oksanen 2001). The program tests statistically whether a response is significantly skewed [Model V], a symmetric Gaussian response [Model IV], a monotonic response [Model II increasing or decreasing], or has a null response [Model I] (indicating no significant relationship between the diatom and the predictor variable) (See Figure 4.32). The simplest significant response model is generated for each taxon. The HOF program was used to test the species responses to pH, Ca^{2+} , Alt, Ice, TOC, Na^+ , TN, and NO_3^- . The results are displayed in Table 4.21. Only taxa with >1% abundance and occurring in ≥ 5 sites were tested, a total of 128 species.

It can be seen that 46% of all the taxa tested respond to ice-cover duration in a significant way. Ca^{2+} , Alt and pH had the most number of species responding significantly to them. However, it is unlikely that some of these responses are direct responses to the environmental variable. For example, it is unlikely that diatoms respond to altitude specifically but to variables that are co-linear with altitude in this data set, such as lake area or lake depth or nutrient availability.

Table 4.21: Results using the HOF program for 128 species in the data set (only species over 1 % abundance with 5 occurrences or more are included in the analyses).

Taxon response model type	Ca^{2+}	Alt	pH	TOC	Na^+	TN	Ice	NO_3^-
Null model (I)	38	50	52	57	59	66	69	84
Sigmoidal increasing Model (IIi)	24	12	18	23	22	26	15	10
Sigmoidal decreasing Model (IIi)	16	28	14	13	12	8	12	15
Symmetric unimodal Model (IV)	41	33	28	26	21	20	30	11
Skewed unimodal Model (V)	9	5	16	9	14	8	2	8
Number of species showing a significant response	90	78	76	71	69	62	59	44
% of species showing a significant response to the variable $[(\text{IIi}+\text{IIi}+\text{III}+\text{IV}+\text{V})/128]\times 100$	70%	60%	59%	55%	53%	48%	46%	34%

Figure 4.32: A graphical representation of the types of species response identified by the HOF programme



Anderson *et al.*, (1996) have shown that there was a positive relationship between diatom species richness and summer temperature (Anderson *et al.*, 1996). Diatom species diversity, in terms of species number (adjusted for the number of cells counted), does not, however, seem to be affected by ice-cover in this data set (Figure 4.33). Diatom species numbers, however, do seem to generally decrease with increasing altitude (Figure 4.34) which may be linked to decreasing air and water temperature.

Figure 4.33: The relationship between species number and ice-cover duration (days), with a linear regression line plotted.

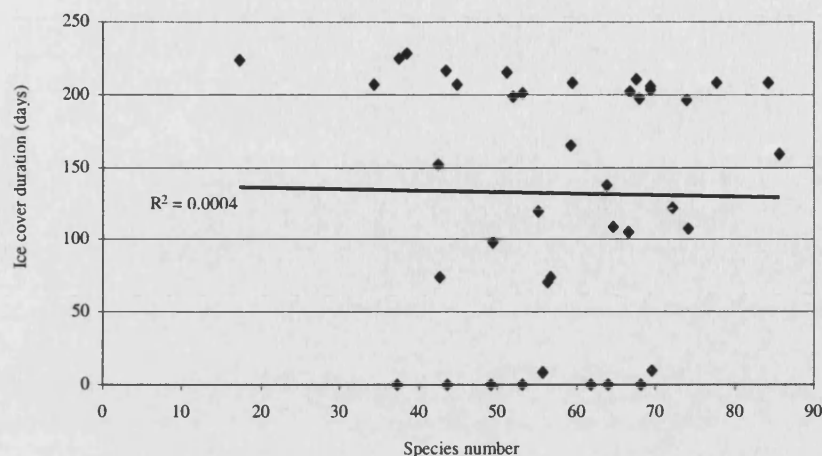
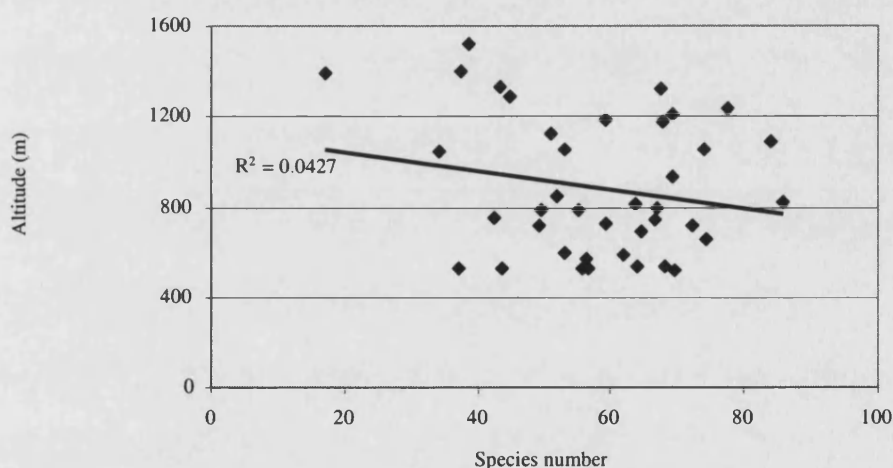


Figure 4.34: The relationship between species number and altitude (m), with a linear regression line plotted.



4.4.2 The relationship between planktonic diatoms and ice-cover duration

The HOF program was used to identify significant taxon responses to ice-cover. This section looks at the HOF models generated for the planktonic diatom species (Table 4.23). In order to satisfy the aims listed in section 1.6 the specific response of planktonic diatoms to ice-cover duration, in relation to other environmental variables, was explored using Weighted Averaging (see methods 3.3.2.5 and 3.3.3 and Table 4.24) calculated in the CALIBRATE program (Juggins and ter Braak 1993). The planktonic diatoms found within the 40 samples and their maximum % abundances are listed in Table 4.22. It should be noted that some of these species have low abundances and low N2 values and, therefore, interpretation of some relationships should be treated with caution.

Table 4.22: The planktonic diatoms found with the 40 lake training set, their N2 values and their maximum abundances are listed.

Code	Name	N2	Max % abundance
AU002A	<i>Aulacoseira ambigua</i>	7	5.1
AU020A	<i>Aulacoseira subarctica</i>	4.9	2.8
CY006A	<i>Cyclotella kuetzingiana/ Cyclotella krammeri</i>	2.1	4.1
CY006B	<i>Cyclotella kuetzingiana</i> var. <i>planetophera</i>	7.4	22
CY006C	<i>Cyclotella kuetzingiana</i> var. <i>radiosa</i>	3.3	13.2
CY010A	<i>Cyclotella comensis</i>	3	1.1
CY9987	<i>Cyclotella aff. comensis</i>	4.9	12.9
CY9984	<i>Cyclotella aff. krammeri</i>	2.9	3.5

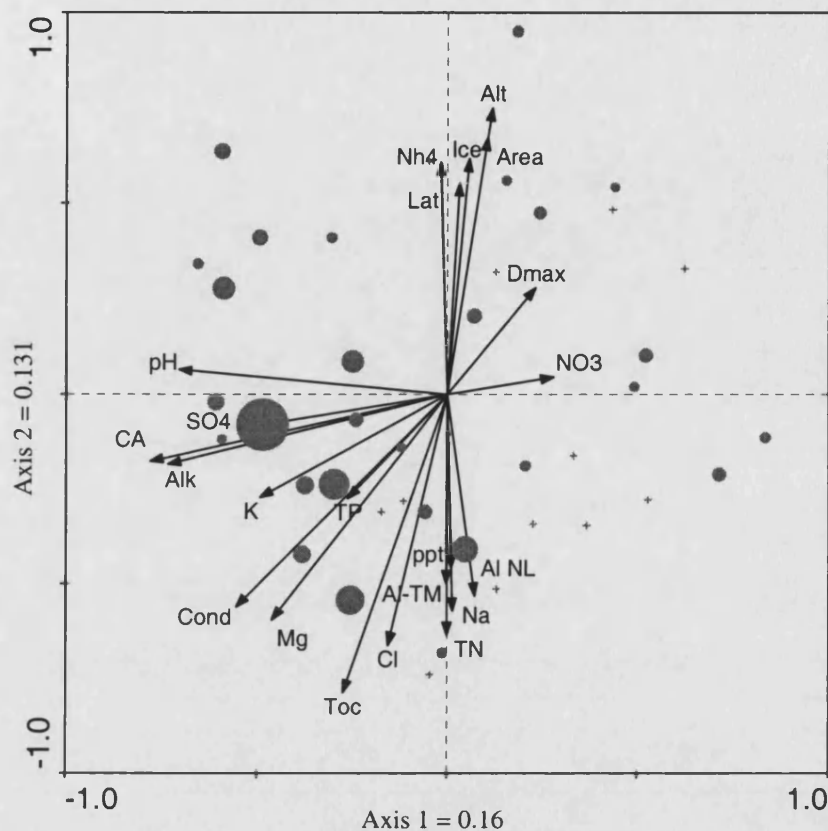
Table 4.23: WA optima and tolerances for ice-cover and altitude for the planktonic species occurring within the 40 samples. The HOF model associated with each taxa and each environmental variable are also listed, significant relationships are starred.

Variable	Ice (days)			Alt (m)		
Species	Opt	Tol	Model	Opt	Tol	Model
<i>A. ambigua</i>	139	100	I	928	360	I
<i>A. subarctica</i>	199	36	IIi*	1066	239	IV*
<i>C. kuetzingiana/ C. krammeri</i>	103	67	V*	704	286	I
<i>C. kuetzingiana</i> var. <i>planetophera</i>	141	81	I	897	284	I
<i>C. kuetzingiana</i> var. <i>radiosa</i>	134	117	I	908	341	I
<i>C. comensis</i>	142	89	I	920	447	I
<i>C. aff. comensis</i>	127	88	I	752	224	I
<i>C. aff. krammeri</i>	212	4.6	IV*	1162	85	V*

It can be seen that only three planktonic species have a significant relationship with ice-cover duration (Table 4.23, *A. subarctica*, *C. kuetzingiana*, and *C. aff. krammeri*) and these only occur in very low abundances within the data set (maximum abundance of 4.1%, Table 4.22). The ice-cover optima for these 'significant' species ranges from 103 to 212 days which is relatively high. Their ice-cover tolerances ranged from 36 days (*A. subarctica*) to 117 days (*C. kuetzingiana* var. *radiosa*). *C. aff. krammeri* and *A. subarctica* both have narrow ice-cover tolerances.

The planktonic species which do not have a significant relationship with ice-cover all tend to display a wide spread of abundance along the environmental gradient resulting in large tolerances (Table 4.23). Even fewer planktonic species had a significant response to altitude measures. Only *A. subarctica* and *C. aff. krammeri* responded significantly to altitude and, as with ice-cover, they both had high altitude optima and small tolerance ranges.

Figure 4.35: RDA plot showing the abundance of 'plankton species', displayed as proportional circles (+ indicates no planktonic species are present within that sample)



In order to gain an overview of the ecological preferences of the planktonic diatom species within this data set an RDA attribute plot is presented (Figure 4.35). The 8 planktonic species present in the data set (Table 4.22) have been 'combined' to form a plankton abundance measure. The circles on the plot represent the samples, but their size is proportional to the amount of plankton within the sample. It can be seen that the planktonic species do have a negative relationship with ice-cover as the sites with high abundances of plankton are located in the shorter ice-cover duration quartile of the graph. This pattern, however, could also reflect a pH/ Ca^{2+} response within the planktonic diatoms with higher abundances of plankton at the high pH/ Ca^{2+} sites.

The HOF program was re-run using other variables to assess which environmental variables the planktonic species might be associated with or responding to (Table 4.24). It can be seen that both pH and Ca^{2+} significantly affect planktonic diatom growth and many of the species have a significant relationship with these two variables (see also Figure 4.35, the plankton rich samples seem to be associated with

higher pH and Ca^{2+} values). Neither of the *Aulacoseira* species have a significant relationship with either pH or Ca^{2+} . It should be noted that *C. aff. comensis* appears to have a high pH and Ca^{2+} optima and displays an increasing model II response for both variables, which may account for its high abundance in site CN0022 despite its high ice-cover duration of 199 days (7.65 pH, Ca^{2+} 347 $\mu\text{eq/l}$, see Figure 4.25- site number 20).

Although it has been shown that only three of the planktonic species had a statistically significant relationship with ice-cover, the HOF program identified 56 (59 minus the three 'significant' planktonic species) non planktonic species which responded significantly to ice-cover duration. The HOF program calculates whether the species response is significantly related to the environmental variable but it is unable to produce specific optima and tolerances for any individual species and an environmental variable. WA and GLR was, therefore, again used to calculate ice-cover optima and tolerances for the non planktonic diatom species the results of which are presented in the next section.

Table 4.24: WA optima and tolerances for pH, Ca^{2+} , TOC, Na^+ and TN for the planktonic species occurring within the 40 samples. The HOF model associated with each taxa and each environmental variable are also listed, significant relationships are starred.

Species/ Variable	pH			Ca^{2+} ($\mu\text{eq l}^{-1}$)			TOC (mg l^{-1})		
	Opt	Tol	Model	Opt	Tol	Model	Opt	Tol	Model
<i>A. ambigua</i>	6.29	0.37	I	37	1.9	I	2.6	1.6	I
<i>A. subarctica</i>	6.59	0.37	I	45	2.1	I	1.7	1.2	IV
<i>C. kuetzingiana</i>	6.54	0.33	I	41	1.5	IV*	2.5	1.3	V*
<i>C. kuetzingiana</i> var. <i>planetophera</i>	6.63	0.21	IV*	64	1.5	IV*	2.8	1.6	I
<i>C. kuetzingiana</i> var. <i>radiosa</i>	6.63	0.21	IV*	72	1.2	IV*	3.1	1.9	I
<i>C. comensis</i>	6.66	0.37	IV*	100	1.6	IV*	2	1.7	I
<i>C. aff. comensis</i>	7.05	0.55	III*	146	2.3	III*	3.1	1.8	I
<i>C. aff. krammeri</i>	6.69	0.28	IV*	62	1.5	IV*	1.6	1.1	V*

Species/ Variable	Na^+ ($\mu\text{eq l}^{-1}$)			TN ($\mu\text{g l}^{-1}$)		
	Opt	Tol	Model	Opt	Tol	Model
<i>A. ambigua</i>	30	5.6	I	112	1.7	I
<i>A. subarctica</i>	23	1.6	I	68	1.2	IV
<i>C. kuetzingiana</i>	113	2.6	III*	124	1.5	IV*
<i>C. kuetzingiana</i> var. <i>planetophera</i>	51	2.8	I	105	1.6	I
<i>C. kuetzingiana</i> var. <i>radiosa</i>	49	3.6	I	103	1.9	I
<i>C. comensis</i>	53	6.7	I	107	1.6	IV*
<i>C. aff. comensis</i>	18	15.5	I	133	1.6	I
<i>C. aff. krammeri</i>	20	1.1	V*	68	1.2	IV*

4.4.3 The relationship between ice-cover duration and non planktonic diatom species

Before the specific responses of the benthic species to ice-cover duration are explored an overview of the diatom response to ice-cover within the training set is presented. A diagram was plotted (only species $\geq 6\%$ are presented, so some planktonic species mentioned above are not presented) in order to compare the response of the planktonic diatom species to ice-cover duration with the non- planktonic species (Figure 4.36). All species are plotted regardless of whether they were shown to have a statistically significant relationship with ice-cover. The sites are ordered according to increasing ice-cover duration (Figure 4.36, SC0067S has no ice-cover and CN0010 has the longest ice-cover at 228 days).

It can be seen that *C. kuetzingiana* var. *planetophora* and *C. kuetzingiana* var. *radiosa* are distributed widely between the sites and do not tend to favour either higher or lower ice-cover durations. *A. subarctica* does seem to prefer lakes with higher ice-cover durations reflecting its high ice-cover optima above. *A. subarctica* has often been found to be restricted to cold waters (Stoermer and Ladewski 1976) and the species is also a good competitor in low light conditions (Kilham *et al.*, 1996) which might occur with long ice-cover durations as snow is compacted on the ice reducing the light penetration.

Cyclotella aff. *comensis* also tends to favour the lower ice-cover duration sites which is consistent with the current literature which cites this species increasing due to climate warming and the subsequent reduction in lake ice-cover (Sorvari and Korhola 1998; Korhola and Weckstrom 2000; Catalan *et al.*, 2002). However, it does occur at ca. 14% abundance in CN0022 which has a relatively high ice-cover duration of 199 days. This site, however, also has particularly high pH and Ca^{2+} values (see Figure 4.25, site number 20 is CN0022).

The specific ice-cover optima and tolerances for the 57 species, identified as significant by the HOF program, (i.e. the non plankton species with a significant relationship with ice-cover) have been plotted below in Figures 4.37 to 4.45. They have been loosely arranged in genera and the results are discussed in this format.

For each species the HOF model response has been plotted with the WA optima plotted for ice-cover and altitude as a black tick marks (for ice-cover the GLR optima for model IV responses have also been plotted, as a grey tick mark, for comparison purposes which are discussed further in section 4.4.4). It would be expected that if a species had a high ice-cover optimum it would also have a high altitude optimum because the two environmental variables are positively related to each other (see Table 4.3 and Figure 4.25).

***Achnanthes* species**

Seven of the eleven *Achnanthes* species had ice-cover optima of >150 days duration with *A. carissima*, *A. pusilla*, and *A. kriegeri* having particularly distinct distributions (Figure 4.37). Species with lower ice-cover optima include *A. levanderi*, *A. nodosa*, *A. flexella* and *A. pseudoswazi*, the latter two, however, only occur at very low abundances. Of the species which have high abundances *A. scotica* has a high ice-cover optima but its distribution spread is wide, suggesting it has a wide tolerance value (see Figure 4.36 the species occurs in most sites regardless of its ice-cover optima). The tendency of *A. minutissima* to prefer low ice-cover durations is shown in Figure 4.36 in which it occurs primarily in the Scottish lochs, but it does not have a significant relationship with ice-cover according to the HOF analyses (hence not plotted in Figure 4.37)

A. curtisima, however, occurs mainly in the Norwegian lakes with the higher ice-cover durations (but again is shown not to have a significant relationship with ice-cover using HOF). The fact that the majority of the *Achnanthes* spp. have high ice-cover optima is not surprising as these species are often common in upland acid oligotrophic lakes (Flower and Jones 1989a). In addition Rosen *et al* (2000) found that the relative number of *Achnanthes* species increased with decreasing summer temperatures.

***Aulacoseira* species (non-planktonic, see section 3.2.5)**

Four *Aulacoseira* species had a significant response to ice-cover duration and all had high ice-cover duration optima (≥ 183 days, Figure 4.38). All species responded according to the Model II monotonically increasing model suggesting that their abundances increase with higher ice-cover durations. The species also tend to have discrete abundance distributions shown by their small ice-cover ranges. Many of the *Aulacoseira* spp. are abundant within the training set but they tend to occur in the assemblages of only a few lakes, suggesting that when they occur they are dominant or co-dominant with other species. Their abundances are more discrete for ice-cover than for altitude, which show a wider spread of abundance along the altitudinal gradient.

The tendency for the *Aulacoseira* spp. to occur in the lakes with longer ice duration is shown in Figure 4.36 where they tend to dominate in the Norwegian lakes. This tendency may not, however, be a direct ice-cover signal but due to the fact that the Norwegian lakes are deeper (Table 4.2) and *Aulacoseira* spp. often tend to occur in deeper lakes due to their need to stay suspended in the photic zone, with deeper lakes having different mixing regimes (see section 1.3.3.2). In addition many *Aulacoseira* species are characterised as early bloomers, linked to the amount of turbulence and the lake's circulation regime, and in addition have been shown to tolerate relatively low water temperatures and low light intensities (Hutchinson 1975; Round *et al.*, 1990; Rautio *et al.*, 2000)

***Brachysira* species**

The *Brachysira* species all tended to prefer lakes with lower ice-cover optima of ≤ 91 days (Figure 4.39). Their abundance distribution spread along the ice-cover gradient is quite wide indicating that they have relatively large ice-cover tolerances. Their altitude optima are also low. *B. neoexilis* occurs at a relatively high abundance within the data set and tends to prefer the Scottish lochs (Figure 4.36). *B. brebissonii* did not have a significant relationship with ice-cover and occurs in equal abundance in both the Norwegian and Scottish lakes (Figure 4.36). *Brachysira* species have often been associated with waters of higher humic content (Pienitz and Smol 1993) which may account for their prevalence in the Scottish lochs which on average have higher TOC values (Figure 4.20).

Figure 4.37: HOF model responses for selected *Achnanthes* spp. within the 40 lake training set for altitude and ice-cover. The WA optima is also plotted (black tick marks) for ice-cover and altitude and a GLR optima for model IV species responses only is also plotted (grey tick marks).

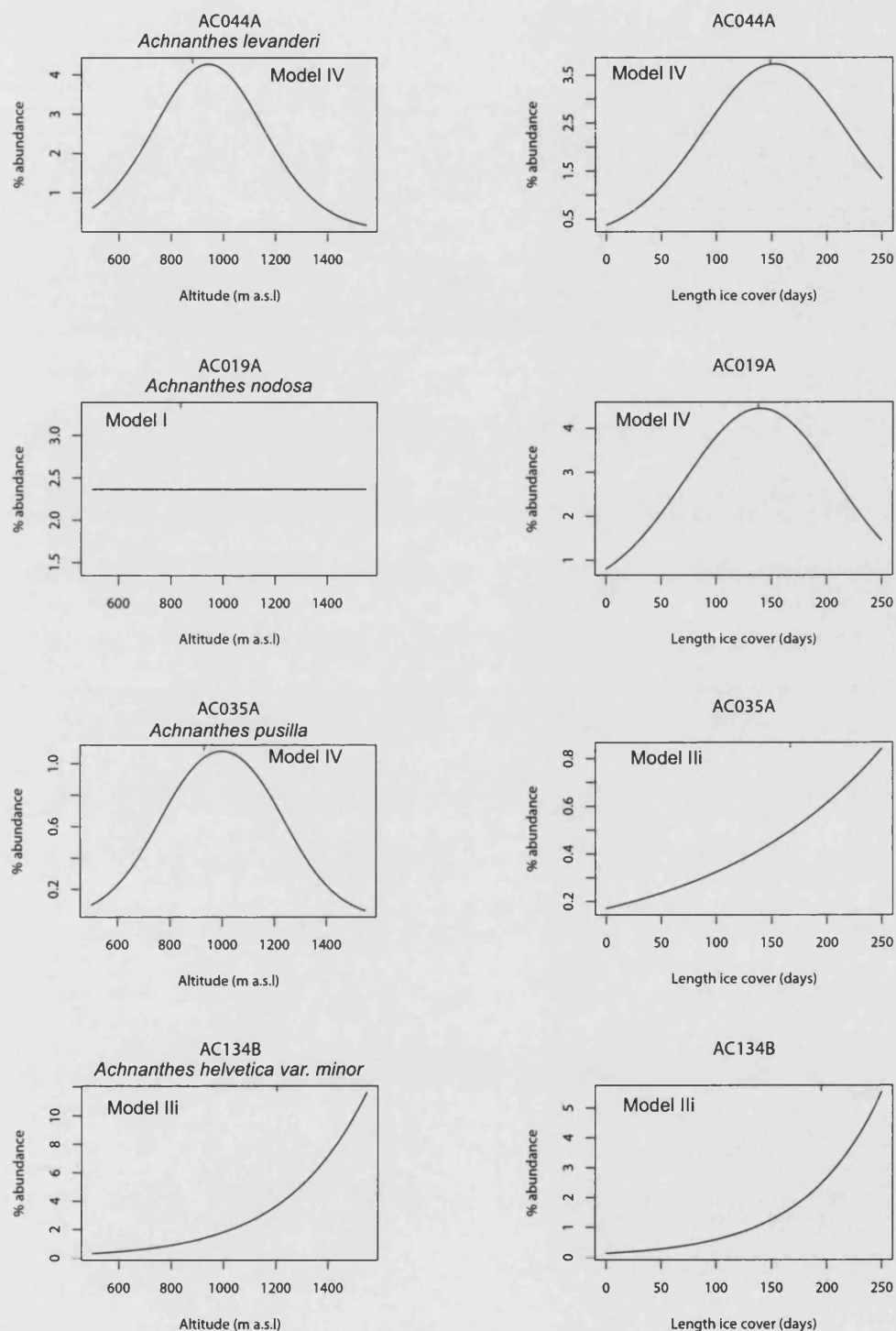


Figure 4.37 continued

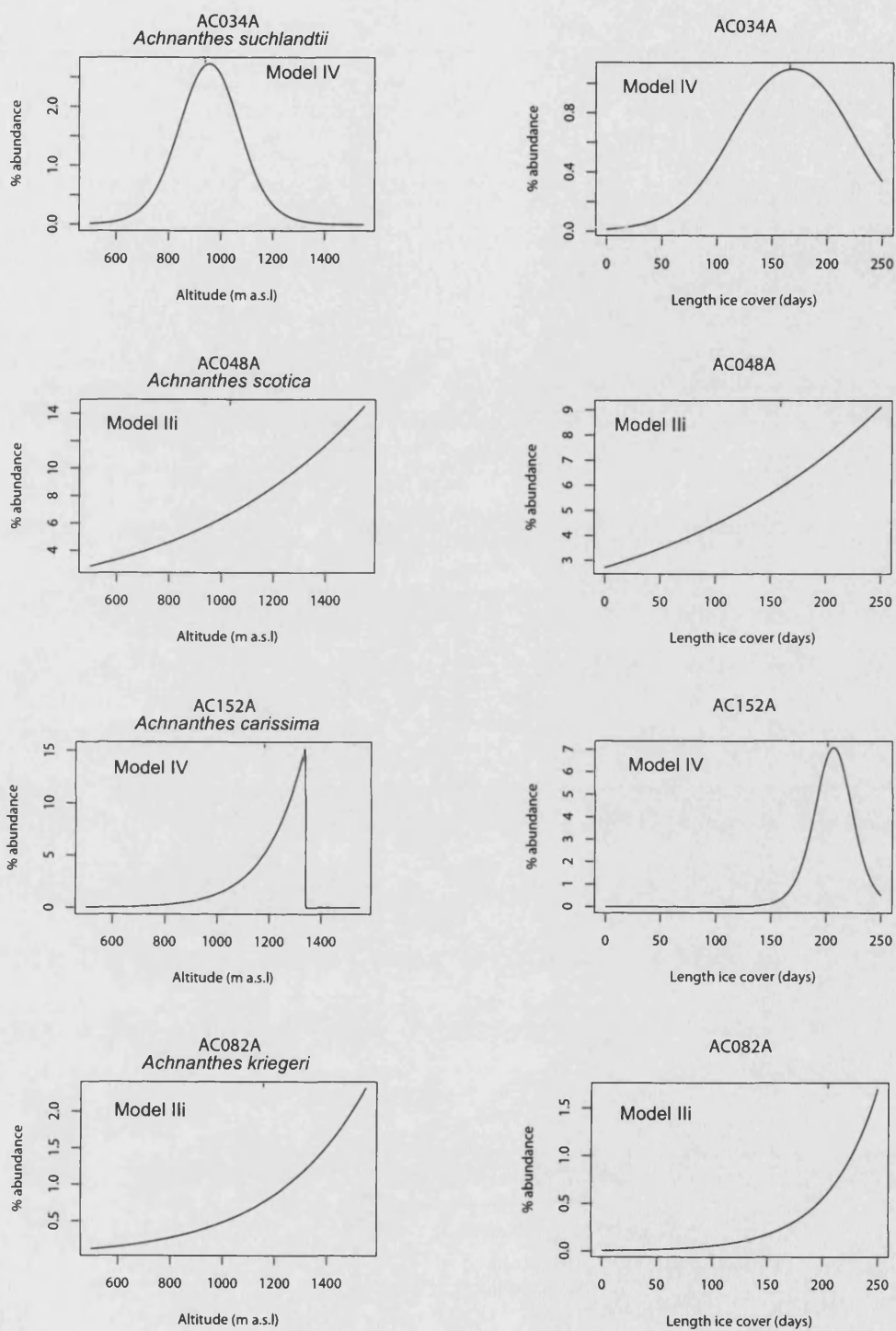


Figure 4.37 continued:

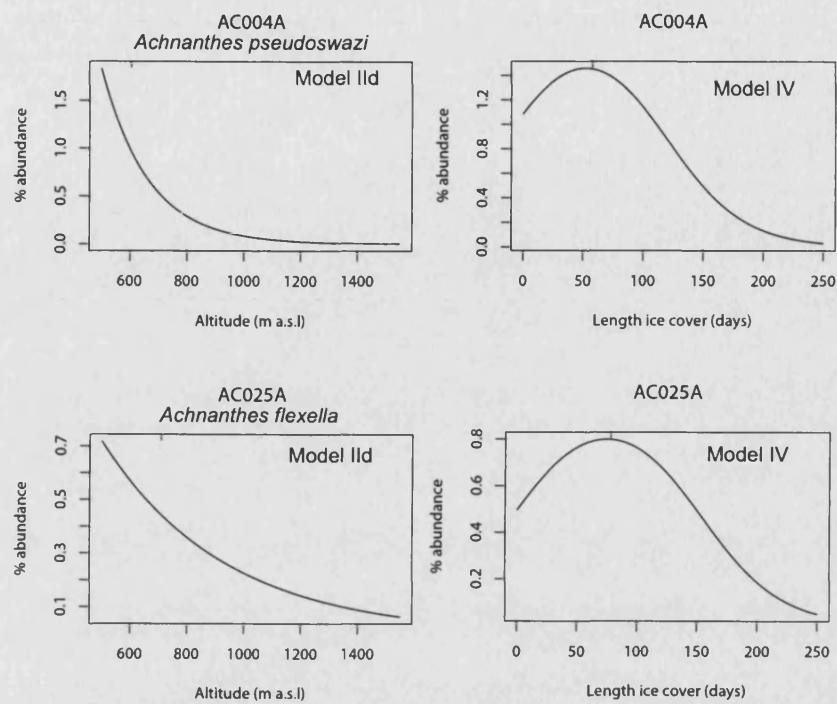


Figure 4.38: HOF model responses for selected *Aulacoseira* spp. within the 40 lake training set for altitude and ice-cover. The WA optima is also plotted (black tick marks) for ice-cover and altitude and a GLR optima for model IV species responses only is also plotted for ice-cover (grey tick marks).

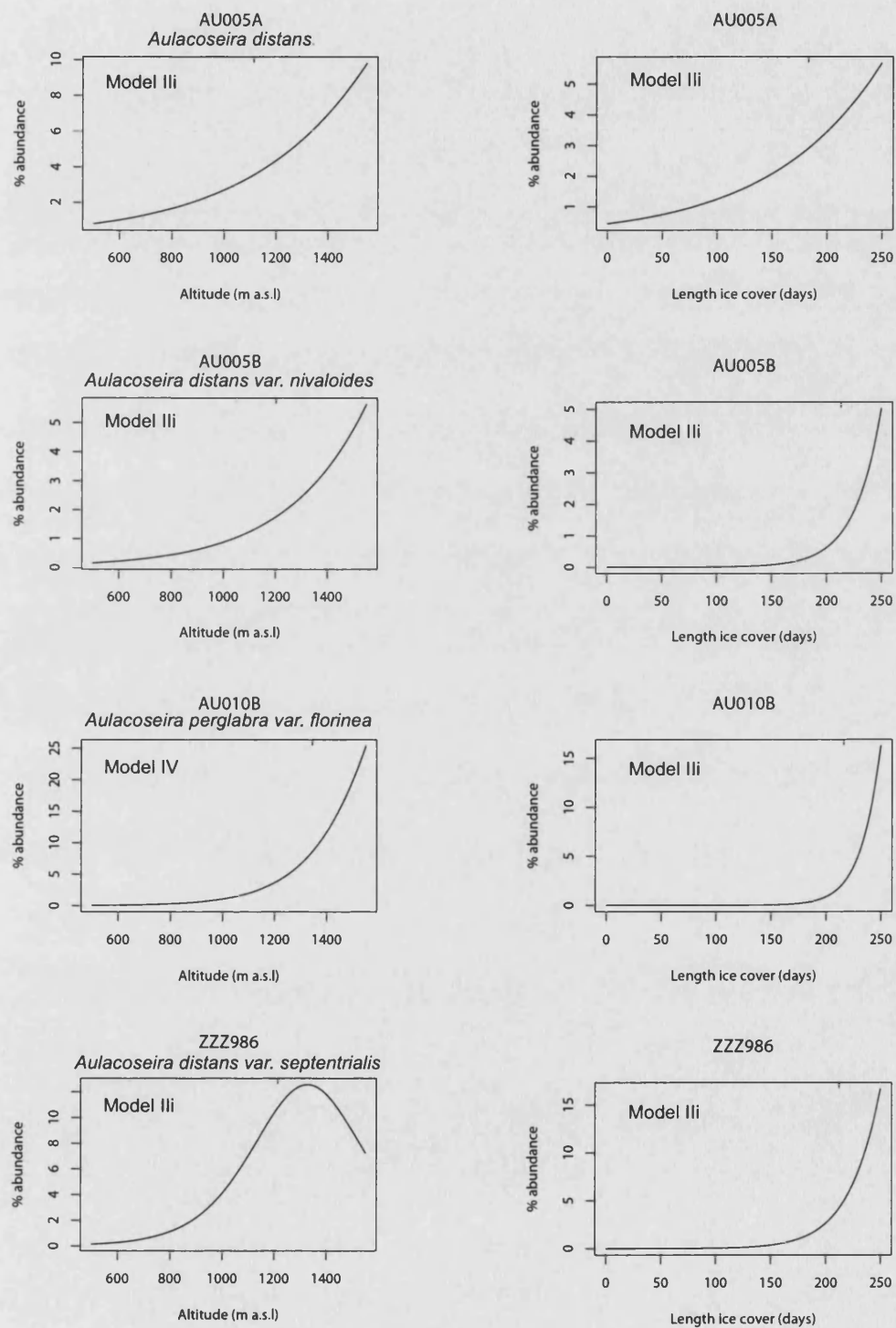
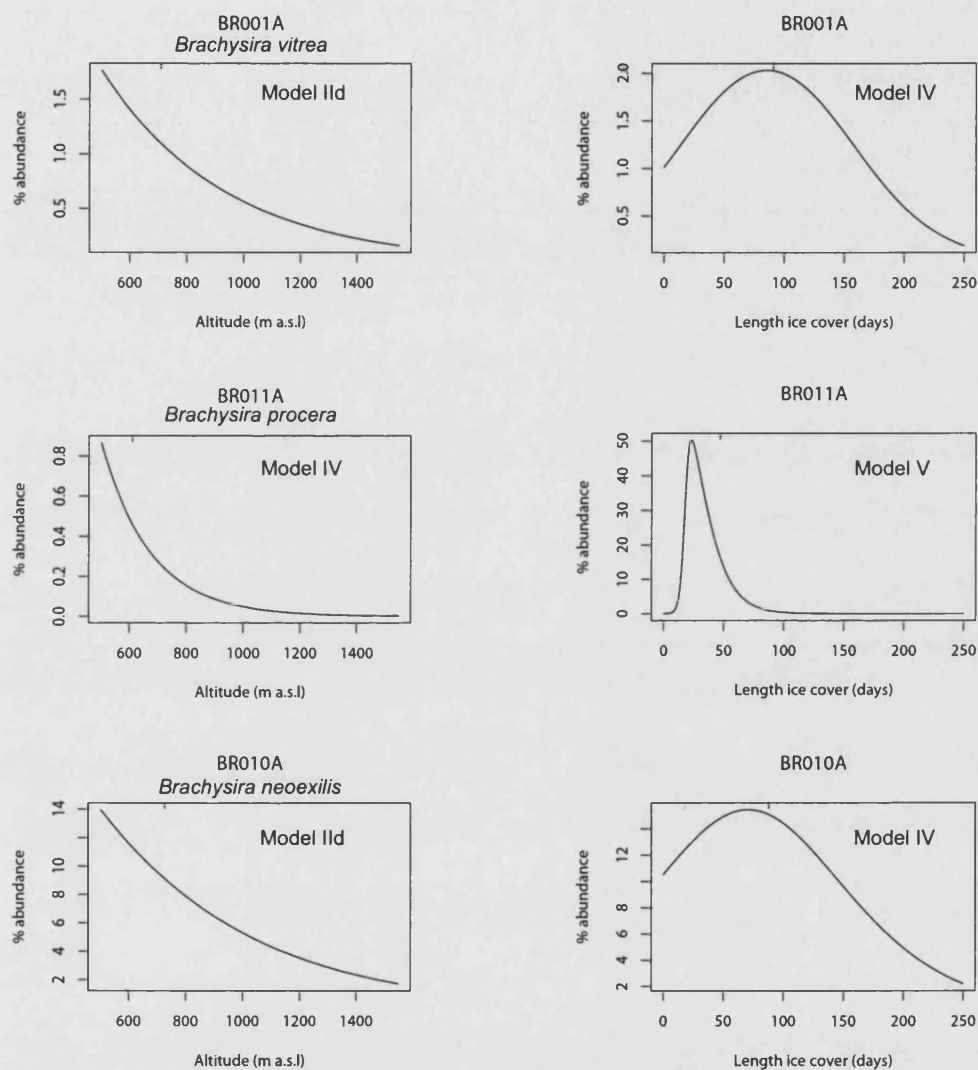


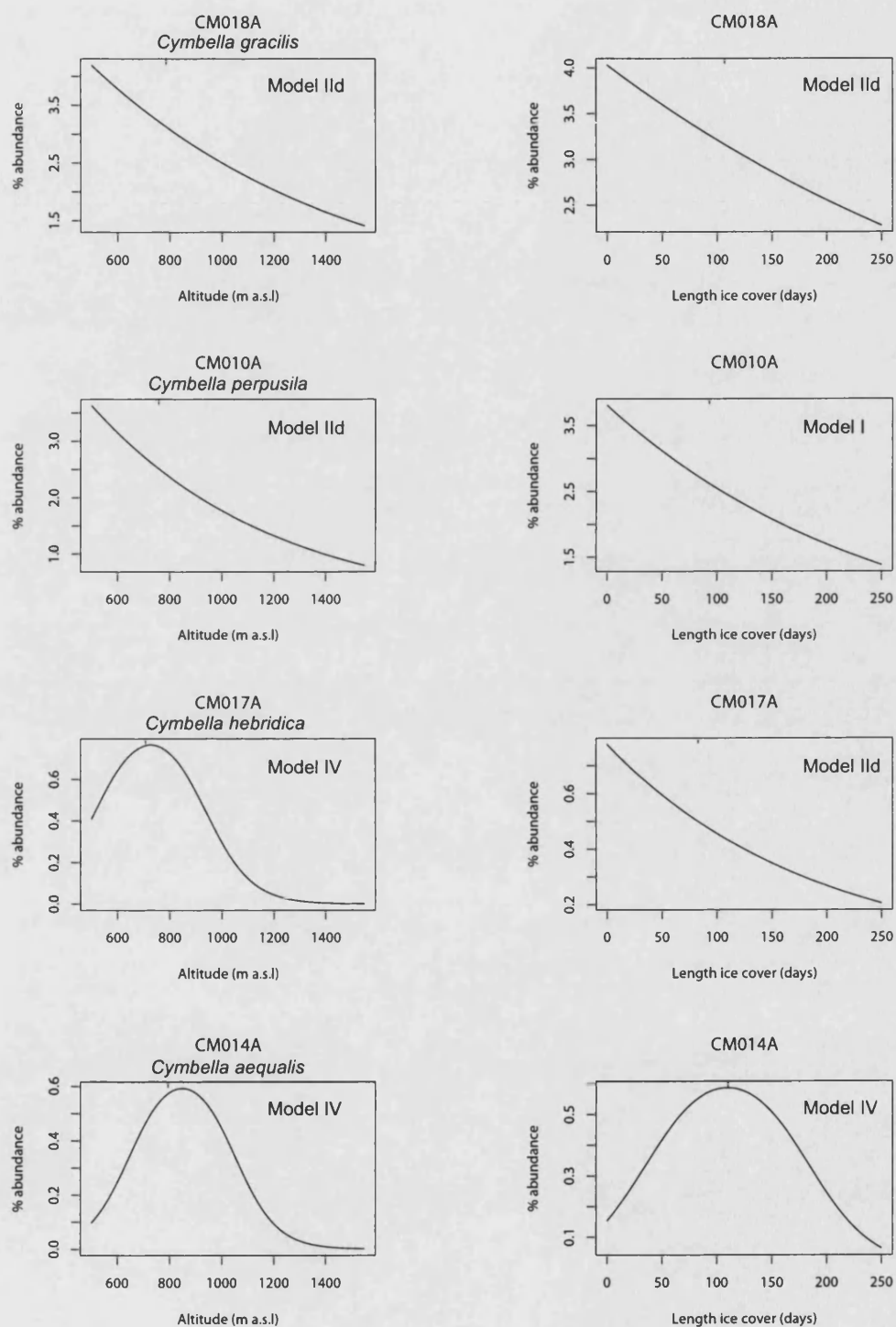
Figure 4.39: HOF model responses for selected *Brachysira* spp. within the 40 lake training set for altitude and ice-cover. The WA optima is also plotted (black tick marks) for ice-cover and altitude and a GLR optima for model IV species responses only is also plotted for ice-cover (grey tick marks).



Cymbella species

The *Cymbella* species do not occur in high abundances within the data set but when they do occur tend to prefer lakes with ice-covers of about 90 days (optima range of 82- 109 days) but they have large ice-cover tolerances and occur along the length of the gradient (Figure 4.40).

Figure 4.40: HOF model responses for selected *Cymbella* spp. within the 40 lake training set for altitude and ice-cover. The WA optima is also plotted (black tick marks) for ice-cover and altitude and a GLR optima for model IV species responses only is also plotted for ice-cover (grey tick marks).



Fragilaria and Synedra species

Many of the *Fragilaria* species have high ice-cover optima and discrete distributions (Figure 4.41). *F. pinnata*, *F. pinnata* var. *accuminatum*, *F. microstriata* and *F. brevistriata* all have optima over 190 days, suggesting that they are able to prosper in extreme environments. This preference for high ice durations is shown in Figure 4.36 which shows that many of the *Fragilaria* species occur in the Norwegian lakes. *F. construens* var. *venter* also tends to favour lakes with long ice-cover periods (Figure 4.36) but it does not have a significant response to ice-cover duration.

F. exigua, which is the most abundant taxa in the training set, has an ice-cover optima of 100 days but tends to prosper along the length of the gradient and has a large ice-cover tolerance (Figure 4.41). This species has also been found to have wide pH tolerances (Stevenson *et al.*, 1991) which may also account for its prevalence in many of the samples.

Peronia, Eunotia and Amphicampa species

Amphicampa hemicyclus has the lowest ice-cover optima of all the 59 species showing a significant response (Figure 4.36). It occurs in low abundance throughout the samples but reaches 9% in one of the Scottish lochs (SC0029). *Peronia fibula* also has a relatively low ice-cover optima (Figure 4.42) and occurs mainly in the Scottish lochs (Figure 4.36).

The ice-cover optima for the *Eunotia* species ranges from 55 to 107 days and most are relatively low (Figure 4.42). They also tend to occur primarily in the Scottish lochs (Figure 4.36) reflecting their low altitude optimum. *Eunotia incisa* is the most abundant *Eunotia* species in the data set, has an ice-cover optima of 95 days, and is most abundant within the Scottish lakes. This distribution may, however, be a pH/DOC signal rather than an ice-cover response as the species is considered as an indicator of low pH and relatively high DOC conditions (Stevenson *et al.*, 1991; Jones *et al.*, 1989) and the Scottish lochs have a lower mean pH value and higher TOC measurements.

Figure 4.41: HOF model responses for selected *Fragilaria* and *Synedra* spp. within the 40 lake training set for altitude and ice-cover. The WA optima is also plotted (black tick marks) for ice-cover and altitude and a GLR optima for model IV species responses only is also plotted for ice-cover (grey tick marks).

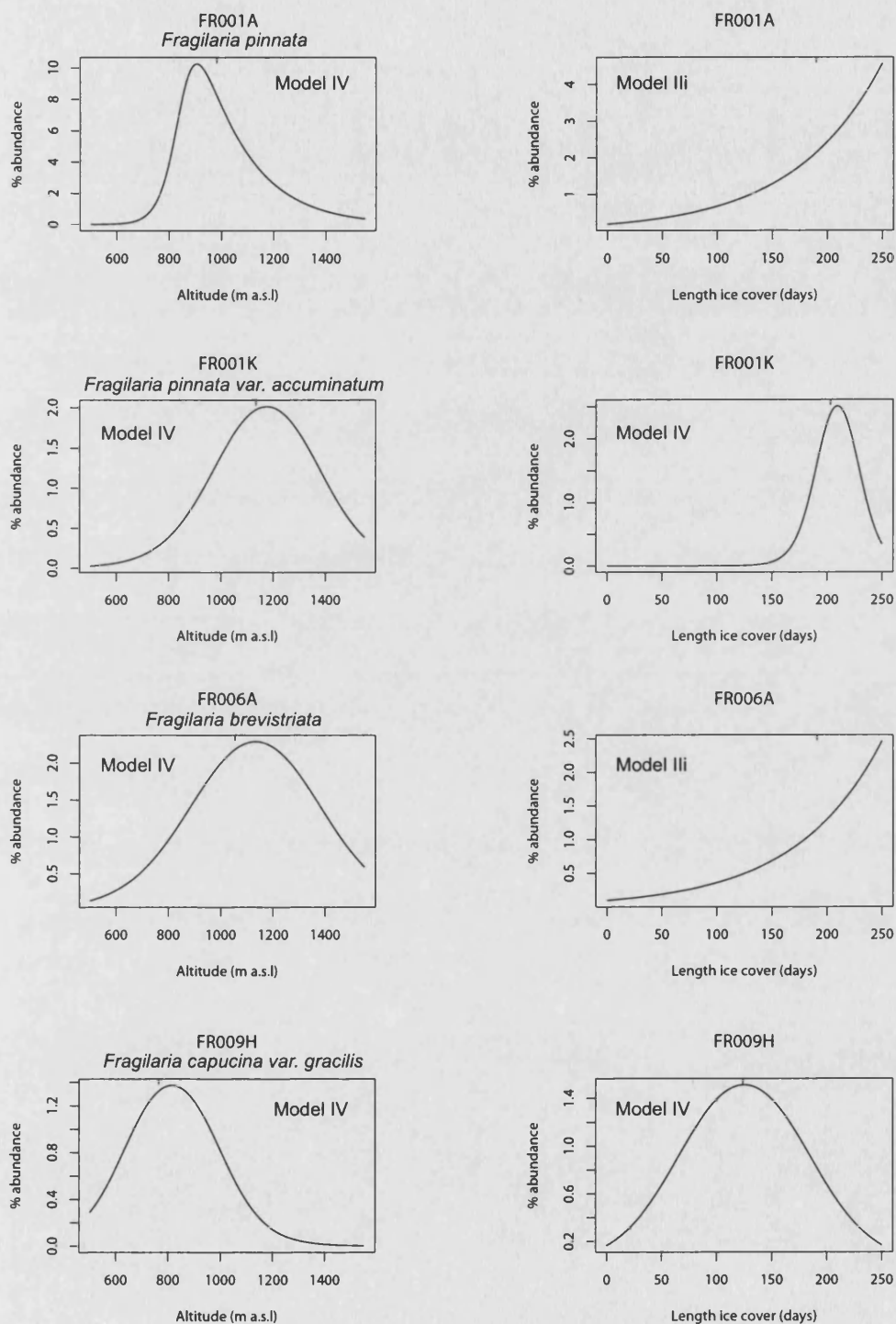


Figure 4.41 continued:

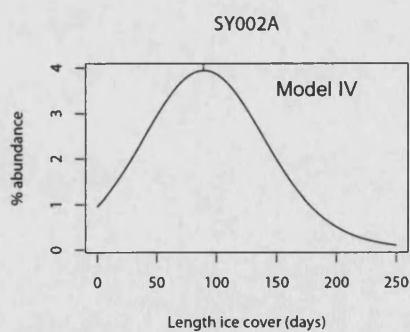
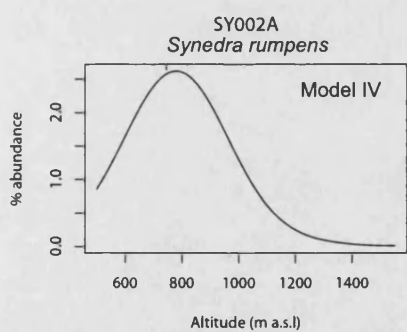
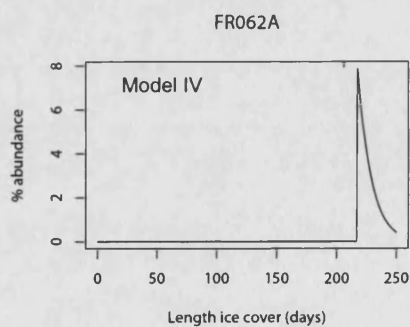
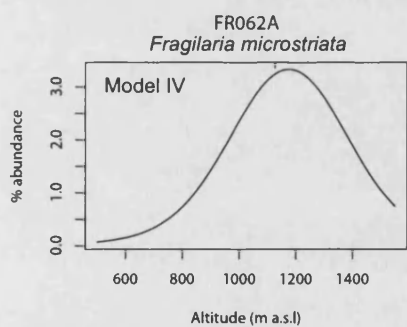
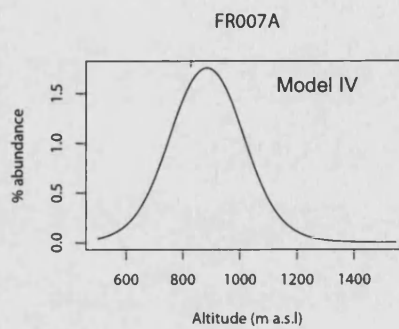
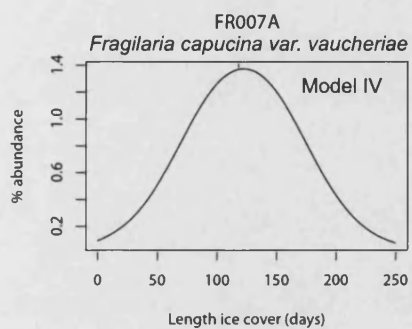
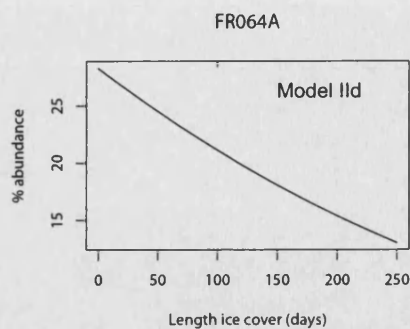
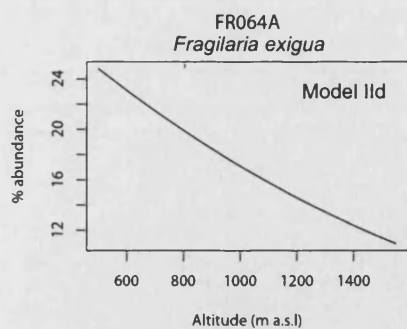


Figure 4.42: HOF model responses for selected *Peronia*, *Amphicampa* and *Eunotia* spp. within the 40 lake training set for altitude and ice-cover. The WA optima is also plotted (black tick marks) for ice-cover and altitude and a GLR optima for model IV species responses only is also plotted for ice-cover (grey tick marks).

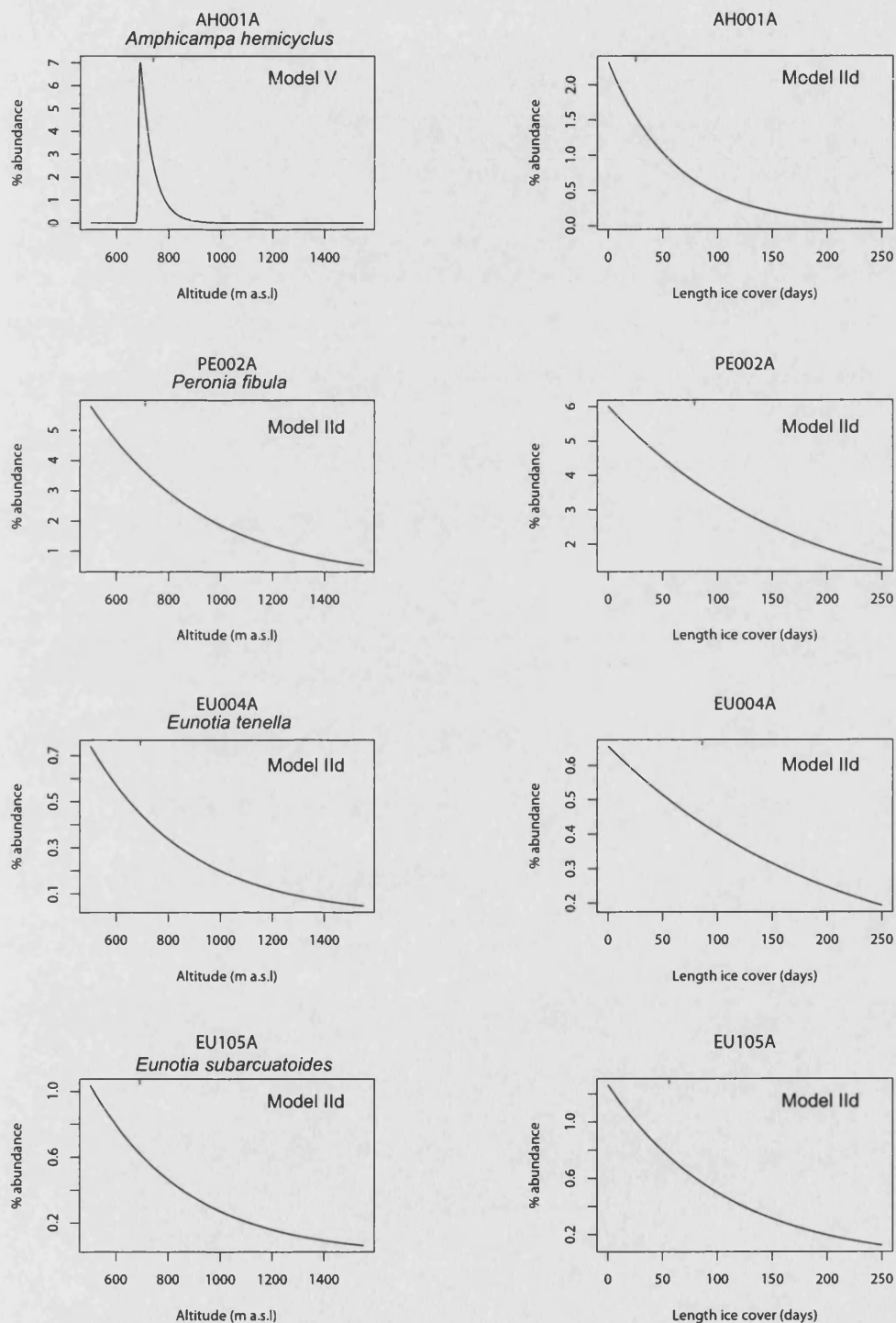


Figure 4.42 continued:

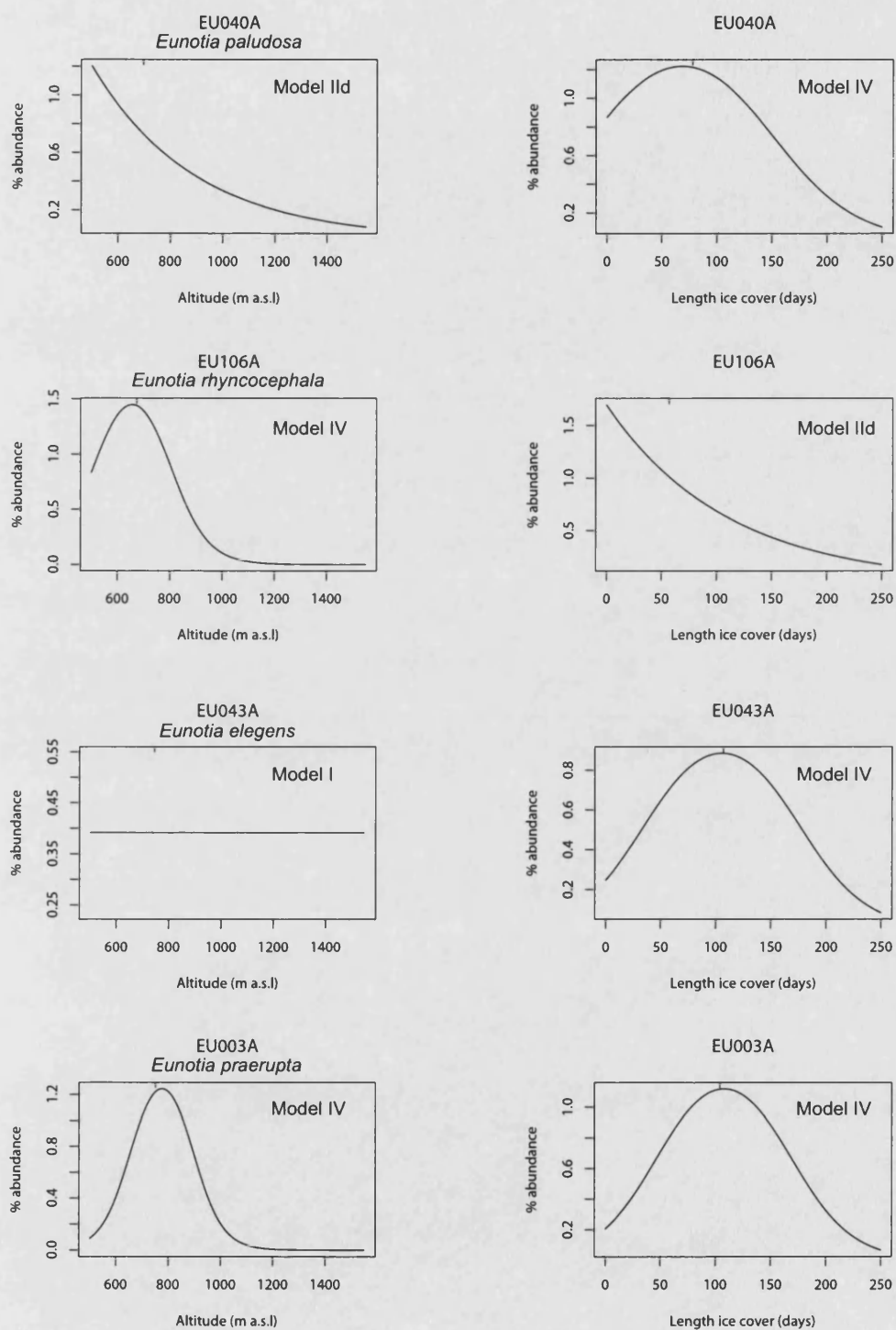
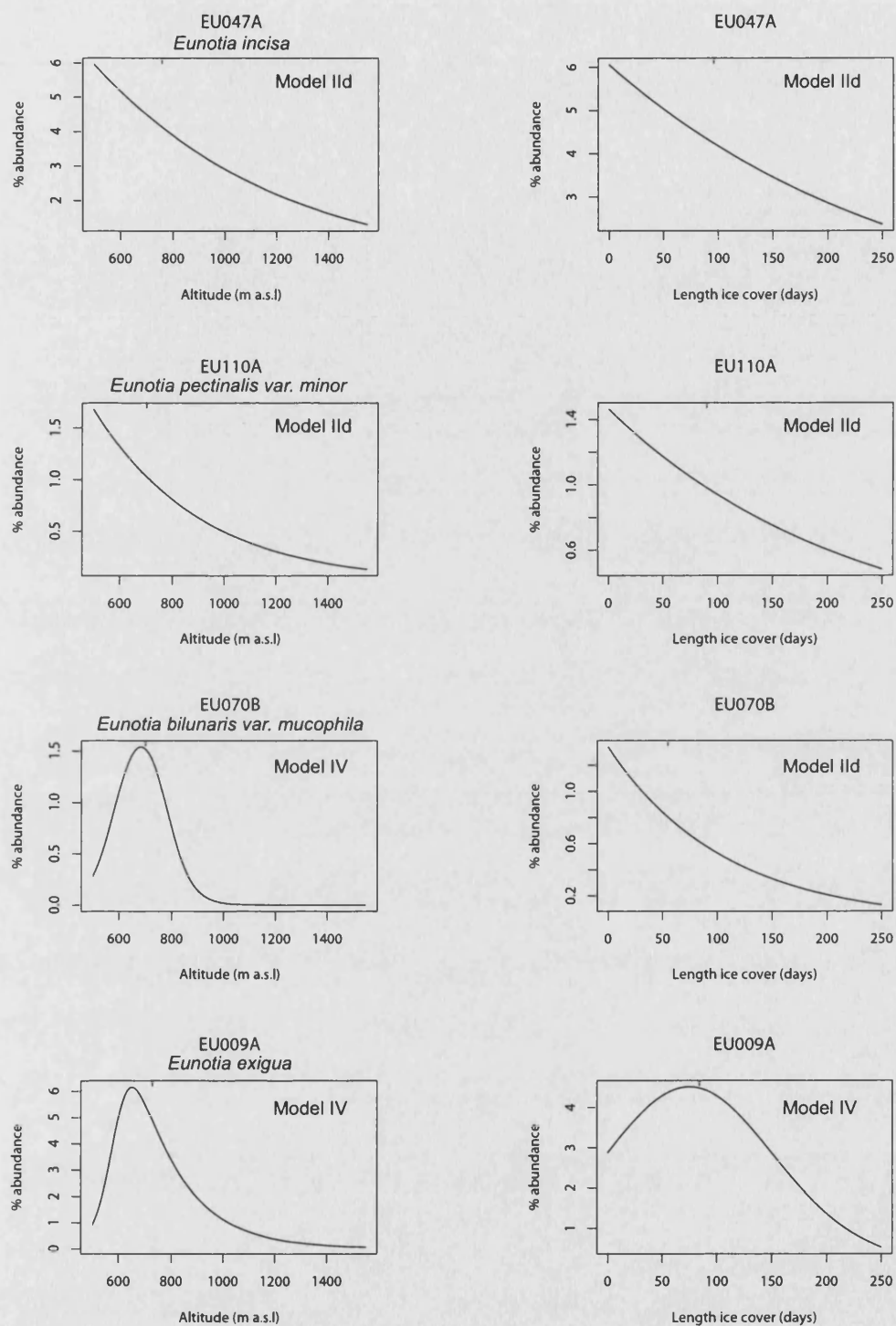


Figure 4.42 continued:

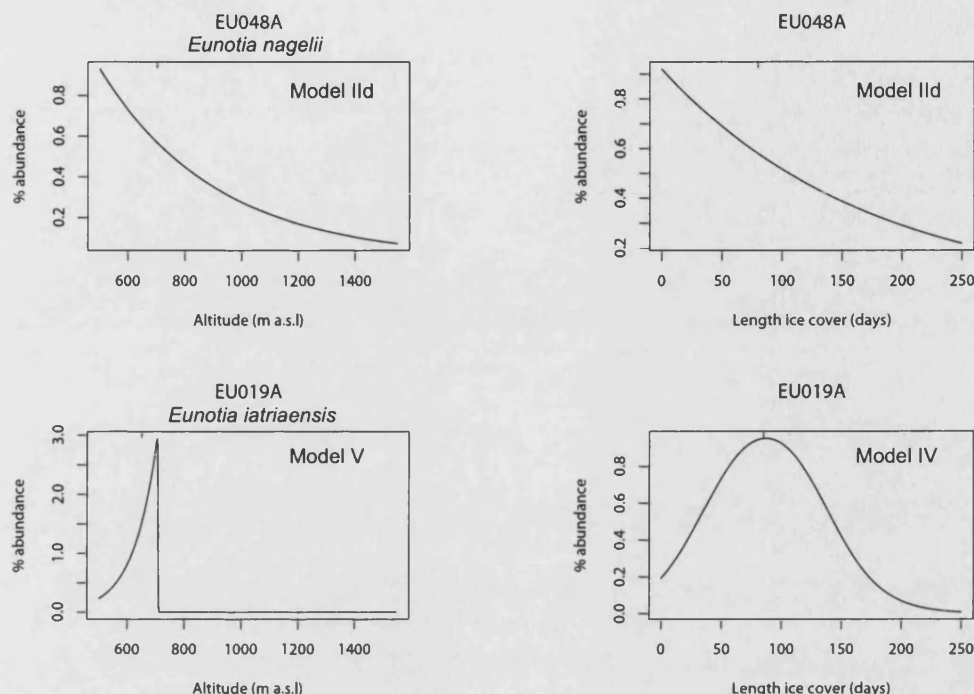


Navicula and *Nitzschia* species

Three *Navicula* species had high WA ice-cover optima, *N. pupula*, *N. digitulus* and *N. krasskei* (Figure 4.43). The other *Navicula* species had optima of *ca.* 100 days duration and exhibited a wide abundance distribution along the ice-cover gradient. The two *Nitzschia* species responding in a significant way to ice-cover also had optima which

fell in the middle of the gradient and displayed wide tolerances to ice-cover (Figure 4.43).

Figure 4.42 continued



Pinnularia and *Tabellaria* species

Two *Tabellaria* species were identified within the training set but *T. flocculosa* was split into two depending primarily on its length (see section 3.2.5). Only the short variety of *T. flocculosa* had a significant relationship with ice-cover, but displayed a wide ice-cover tolerance and a medium ice-cover duration optima (Figure 4.44). The short variety occurs in nearly all of the Scottish lochs (Figure 4.36). This variety was documented as having a low pH optimum in the SWAP data set of 5.4 units (Stevenson *et al.*, 1991) and possibly many of the Norwegian lakes have too high a pH for this species to prosper.

T. quadrisepata has a low ice-cover optima of just 35 days but does not occur in high abundances within the training set. This species is often representative of strongly acid conditions (SWAP pH optima of 4.9 units, Stevenson *et al.*, 1991) and is usually not found in waters of <6.0 pH (Stevenson *et al.*, 1991; Flower and Battarbee 1985). In this data set, however, it reaches its maximum abundance of 1.8% in SC0068 which has a pH of 6.47 units.

Pinnularia interrupta had a high ice-cover optima of 173 days with increasing abundance at higher ice-cover durations (model III, Figure 4.45). The other two *Pinnularia* species occurred across a wide spectrum of different ice-cover durations.

Figure 4.43: HOF model responses for selected *Navicula* and *Nitzschia* spp. within the 40 lake training set for altitude and ice-cover. The WA optima is also plotted (black tick marks) for ice-cover and altitude and a GLR optima for model IV species responses only is also plotted for ice-cover (grey tick marks).

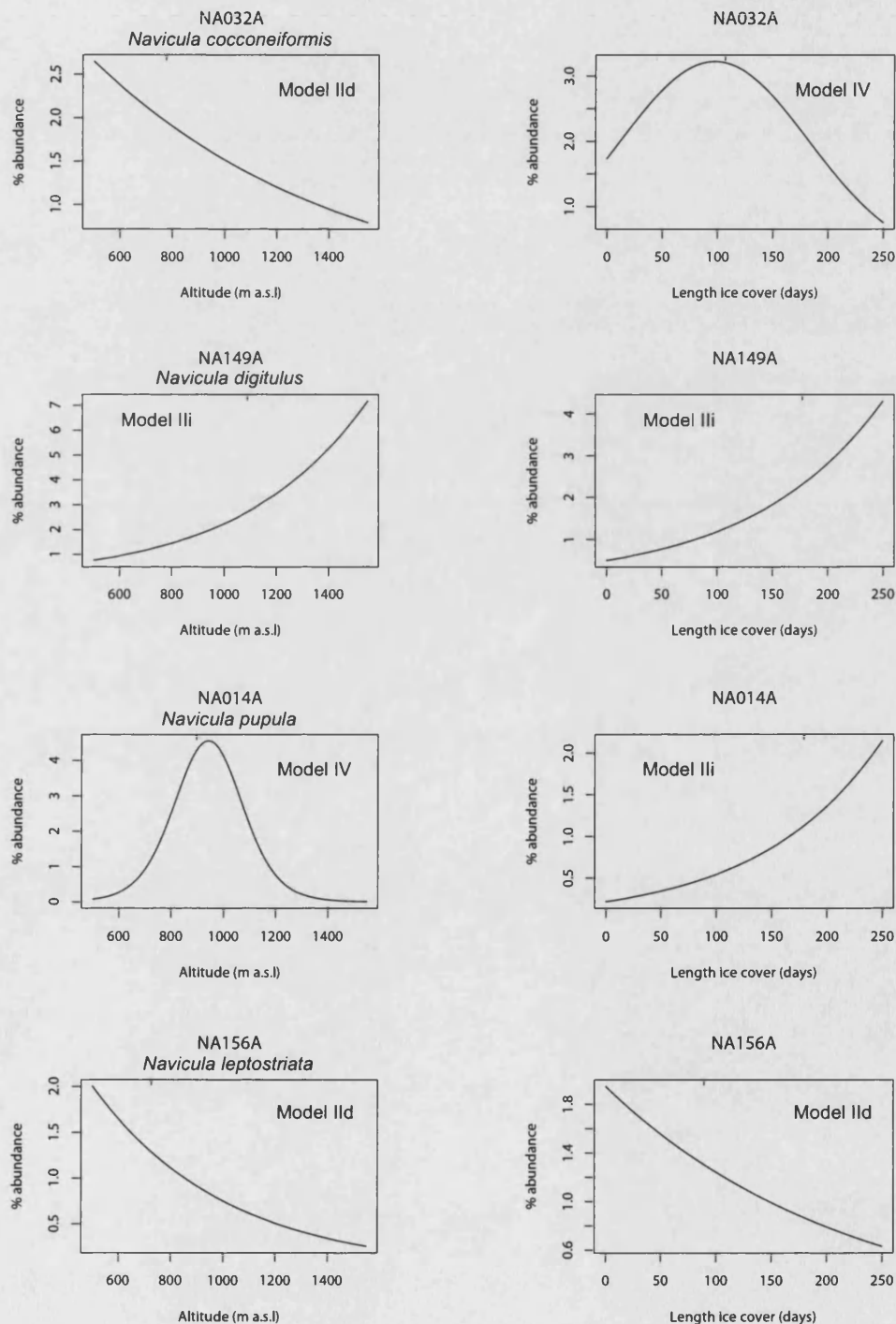


Figure 4.43 continued:

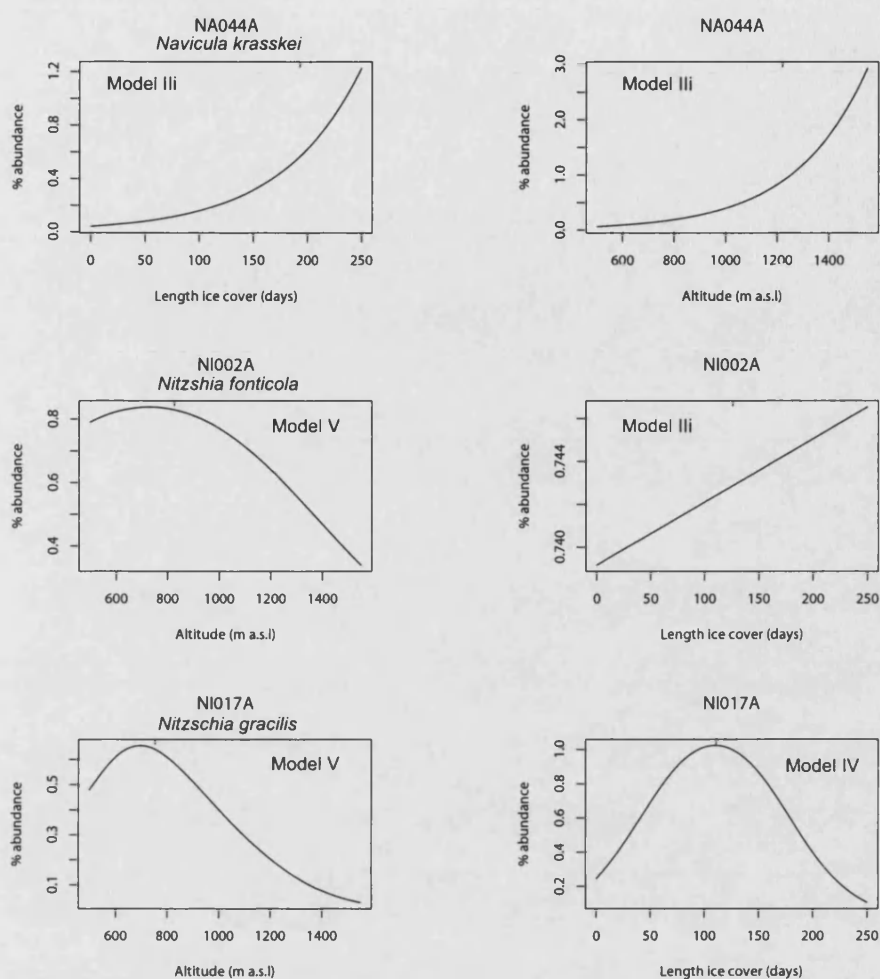


Figure 4.44: HOF model responses for selected *Tabellaria* spp. within the 40 lake training set for altitude and ice-cover. The WA optima is also plotted (black tick marks) for ice-cover and altitude and a GLR optima for model IV species responses only is also plotted for ice-cover (grey tick marks).

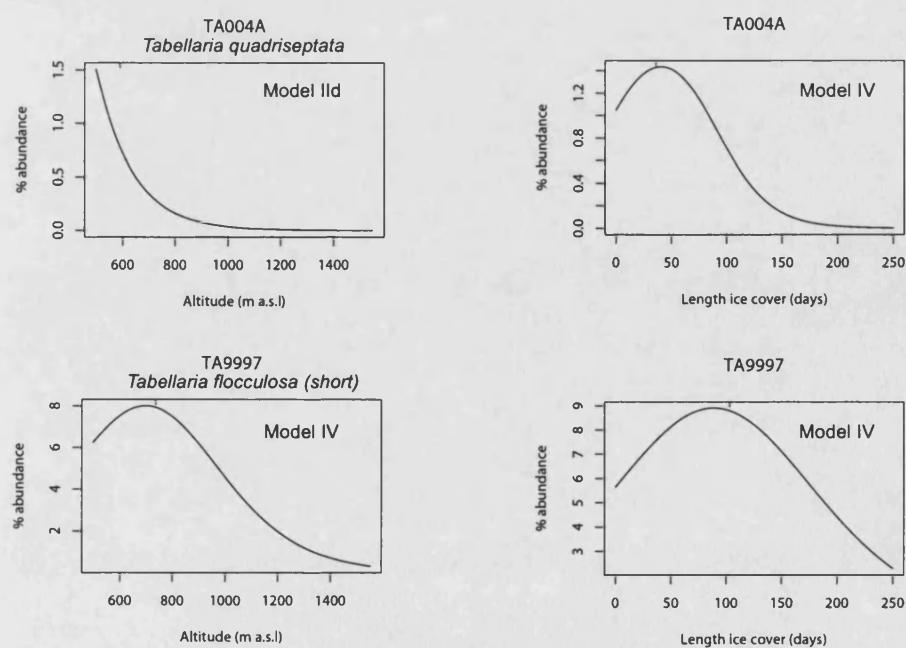
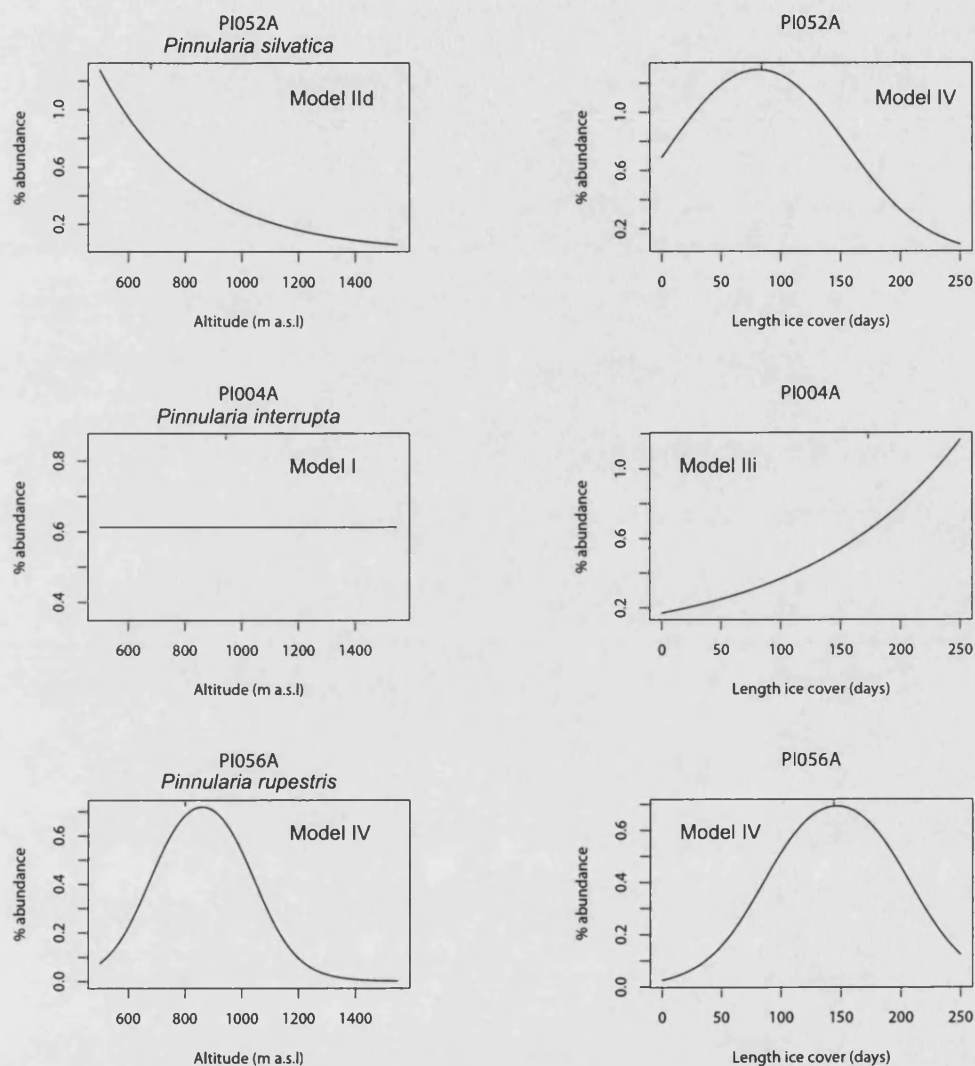


Figure 4.45: HOF model responses for selected *Pinnularia* spp. within the 40 lake training set for altitude and ice-cover. The WA optima is also plotted (black tick marks) for ice-cover and altitude and a GLR optima for model IV species responses only is also plotted for ice-cover (grey tick marks).



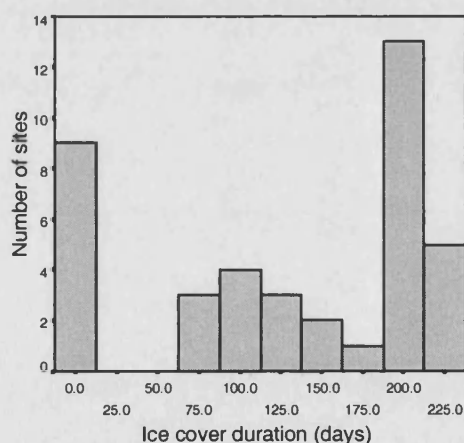
4.4.4 The identification of ice-cover indicator species

In order to identify indicator species for ice-cover duration (used in Chapters 6 and 7) several species with significant responses to ice-cover having optima that span the length of the ice-cover gradient need to be identified. The species selected should also have relatively low tolerance measures, i.e. specific and distinct ice-cover niches. The GLR programme (Juggins 1997) was used in order to compare ice-cover optima and tolerances for the species with those generated by the WA method and a comparison of the results are shown in Figure 4.47. GLR uses Maximum Likelihood regression

(ML) and failed to generate optima for many of the species and on occasions generated optima outside the ice-cover range (e.g. for *Aulacoseira subarctica* (AU020A) the GLR optima was calculated as 6507 days (See Appendix 4.4). These species are plotted as zero values on the graph.

Although HOF identified significant species responses for all of these 59 species GLR could only derive optima for 28 of these 59 species. Failure to generate optima is possibly associated with the low number of sites within the training set and the uneven distribution of the ice-cover gradient (Birks *pers. com.*) with large numbers of sites with no ice-cover, and many sites with ice-covers of >200 days duration (see Figure 4.22 and 4.46). In addition there is an under-representation of sites with ice-cover between 25 and 50 days, creating an almost bi-modal ice-cover gradient (Figure 4.46). Unfortunately, as mentioned earlier transformation of the ice-cover gradient did not increase the normality of the distribution.

Figure 4.46: A histogram showing the bi-modal distribution of ice-cover duration along the gradient.



In addition the GLR method is limited in terms of this sort of data response analysis, however, because it assumes that the data follow a Gaussian response model (i.e. model IV in HOF). The method may fail to calculate optima if most of the maximum range of the environmental variable is not covered by the distribution of the species or if the nature of the response curve is very acute (Birks *pers. com.*). Failure to generate so many optima is, however, unusual. For example in the SWAP data set GLR only

failed to generate optima for one species out of all the 167 sites (Birks, 1990; Stevenson *et al.*, 1991). SWAP, however, had many more sites and was concerned with the generation of pH optima, a variable which usually exhibits a near normal distribution curve.

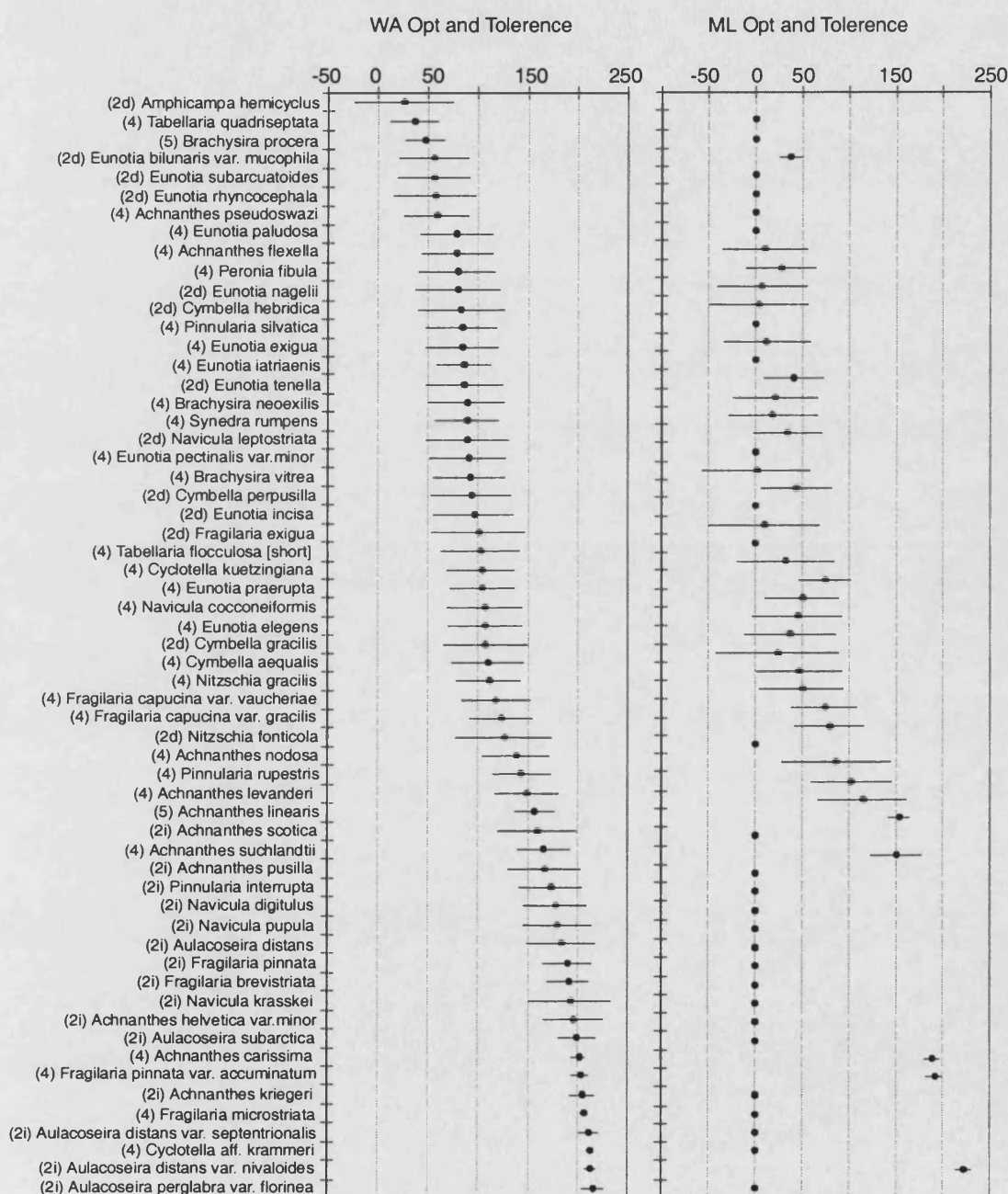
In order to assess whether the GLR method can be used for species without Gaussian responses, i.e. unimodal or monotonic etc. response, the HOF response model associated with each species is presented in brackets on Figure 4.47. For the 28 species that the GLR method failed to converge for, 14 of these had model monotonic increasing responses (model 2i), 6 had monotonic decreasing response (model 2d) 1 had a skewed response (model 5) and 7 had symmetric Gaussian responses (model 4). The over representation of the model 2 responses within the 28 species that failed to converge using GLR may be significant considering the most common type of species response for the 59 species was model 4 (see Table 4.21). Species, however, with Model 2 responses are often harder to fit because they are often poorly defined (Birks *pers. com.*).

In summary it has been shown that the GLR method works most efficiently for species with symmetrical responses rather than for those with monotonic increasing or decreasing responses, due primarily to the fact that the programme is based on a Gaussian logistic regression and, therefore, if the taxa have monotonic responses the application of this model may not be appropriate for those species. In addition if the responses are monotonic increasing or decreasing the actual idea of defining specific species optima is in a sense meaningless. In such cases the optimal conditions for the species are not adequately covered by the environmental gradient. Therefore, the highest or lowest observed value is often used to define the optima for species with increasing or decreasing sigmoidal curves (*c.f.* Birks *et al.*, 1990).

This does, however, highlight the problems/ suitability of generating species optima for species with different response patterns and illustrates the complexity of modelling species responses to uneven environmental gradients. Despite these problems the optima generated from the WA method were used for the generation of ice-cover indicator species (Chapters 6 and 7). For those with monotonic increasing or

decreasing responses the highest and lowest observed value was taken as the optima (following Birks *et al.*, 1990).

Figure 4.47: A comparison of ice-cover optimum and tolerances produced using Weighted Averaging (WA) and Maximum Likelihood (ML, GLR model) for the 59 species found to have a statistically significant relationship with ice-cover using the HOF model (Figure 4.32, and Table 4.21). The HOF model related to each species is presented in brackets (2i= model II increasing, 2d= model II decreasing). For the species where ML failed to generate optima, or the optima generated were outside the ice-cover range, the optima are plotted as zeros.



Both methods, however, show that the species tolerances at the higher end of the ice-cover gradient are small suggesting that these might be appropriate 'cold' species

indicators. GLR calculates similar optima for *A. carrisima*, *A. distans* var. *nivaloides* and *F. pinnata*. Although GLR failed to generate optima for many of these ‘cold’ indicator species it remains that *F. microstriata*, *F. pinnata* var. *accuminatum*, *Cyclotella* aff. *krammeri* and many of the *Aulacoseira* species may be good indicators of long periods of ice-cover using the results from the WA.

There appear to be less appropriate indicators for shorter ice-cover durations because their tolerances are not as narrow. Species which might be suitable are *T. quadrisepata*, *B. procera*, *A. pseudoswazi*, *E. iatriaenis*, *E. tenella* and *S. rumpens*. These ‘cold’ and ‘warm’ indicator species are used cautiously in chapters 6 and 7, due to the problems associated with their optima generation, when inferences about past ice-cover durations are discussed.

4.4.5 The feasibility of creating an ice-cover transfer function for down core climate reconstruction

Although ice-cover duration was not selected by the forward selection technique the relationship between diatom variance and ice-cover was shown to be significant (Table 4.13). Two of the primary aims of this study were to evaluate the strength of the relationship between diatoms and ice-cover and to assess the viability of using diatoms for climate reconstructions through the development of an ice-cover model (section 1.6). The next section discusses the second of these aims and the suitability of applying an ice-cover model to short sediment cores from lakes in Central Norway in order to make inferences about past climate change (see chapters 6 and 7).

It was shown above that 46% of all species in the training set had a statistically significant relationship with ice-cover duration and that it explained 6.8% of the diatom variance. Therefore, it can be regarded as a key variable accounting for a significant proportion of the biological variance and can be considered robust in terms of the creation of a diatom inference model (Pienitz and Smol 1993). The performance of this model, however, needs to be evaluated before it can be applied to a down core diatom sequence.

The suitability of creating a diatom ice-cover model can be further assessed statistically by calculating the ratio of the variance explained by ice-cover

individually, divided by the variance of the whole data set (ter Braak 1987; Hall and Smol 1992). This is achieved by dividing the eigenvalue of axis 1 (λ_1) by the eigenvalues of axis 2 (λ_2) when ice-cover is constrained on the first ordination axis. If the ratio is high (>1.0) the variable is considered as being suitable for developing a diatom predictive model (ter Braak and Prentice 1988). The ratio of λ_1/λ_2 and the results of the RDA constrained by ice-cover duration on axis 1 are shown in Table 4.25. The λ_1/λ_2 ratio is only 0.365 which suggests that ice-cover may not be a suitable variable for development of a diatom inference model. It should be noted, however, that some previous studies have reconstructed variables which have lower λ_1/λ_2 ratios than this value (e.g. Dixit *et al.*, (1993) performed a DOC reconstruction with a ratio of 0.21 and Fritz *et al.*, (1993) produced a Secchi depth transfer function with a ratio of 0.28).

Table 4.25: RDA of ice-cover duration with 152 species. Species data are square root transformed.

RDA axes	1	2	3	4
Eigenvalues (λ)	0.068	0.186	0.110	0.067
Cumulative percentage variance Of the species data	6.8	25.4	36.4	43.1
Sum of all canonical eigenvalues	0.068			
Ratio of λ_1/λ_2 (0.068/0.186)	0.365			

Inference models have been made when the ratio is low, but usually result in large errors of prediction (Hall and Smol 1992) and interpretations of such models should be treated with caution (ter Braak 1987). It was decided, therefore, to produce several inference models (using PLS, WA, WA-PLS and WA_{tol}) in order to calculate the predictive ability of the diatoms for ice-cover and to determine if an ice-cover model was in fact suitable for down core ice-cover reconstruction. Both linear (PLS) and unimodal (WA, WA_{tol}) and WA-PLS) methods were used because the diatom data were seen to be on the cusp of the 3SD cut off measure which dictates which method to use (see Figure 3.13 and section 4.2.2). The results are presented in Table 4.26 and Table 4.27. The outputs are all generated by the programme CALIBRATE (Juggins and ter Braak 1993).

The appropriateness of creating an ice-cover transfer function can be evaluated by comparing the R^2 values, the errors associated with the developed model (RMSE), the R^2 value when jackknifing is used (R^2_{jack}) and the errors associated when jackknifing is

used (RMSEP_{jack}) (see methods section 3.3.3). To date there are few published ice-cover transfer functions using diatoms so comparison of R^2 , R^2_{jack} and RMSE is not possible.

Table 4.26: A comparison of WA and WA(tol) calibration and prediction techniques for ice-cover duration for the 40 lakes training set. Analyses were conducted on square root transformed species data and untransformed ice-cover duration data. Deshrinking using the inverse approach was used.

Prediction	RMSE	R^2
WA	49.4	0.64
WA tol	46.4	0.68
Calibration	RMSEP	R^2_{jack}
Cross Val WA	66.4	0.36
Cross Val WA tol	69.2	0.38

Table 4.27: The results of the PLS and WA-PLS calibration and prediction techniques for ice-cover duration for the 40 lakes training set. Analyses were conducted on square root transformed species data and untransformed ice-cover duration data.

PLS			WA-PLS		
No of components	Apparent errors of estimation		No. of components	Apparent errors of estimation	
	RMSE	R^2		RMSE	R^2
1	51.5	0.61	1	49.5	0.64
2	32.5	0.84	2	36.7	0.80
3	22.1	0.92	3	22.9	0.92
4	12.4	0.97	4	14.3	0.97
5	7.3	0.99	5	9.2	0.98
6	3.9	0.99	6	8.6	0.98
Prediction errors			Prediction errors		
No. of components	RMSEP _{jack}	R^2_{jack}	No. of components	RMSEP _{jack}	R^2_{jack}
1	69.6	0.32	1	66.5	0.36
2	70.3	0.33	2	74.2	0.28
3	73.1	0.29	3	83.3	0.18
4	79.6	0.23	4	91.8	0.12
5	81.6	0.22	5	94.76	0.12
6	82.3	0.21	6	96.4	0.11

Although the R^2 values are high for both WA and WA(tol) the errors associated with both models are also high and increase with cross validation to between 66- 69 days (Table 4.26). Obviously the maximum length of the gradient is 365 days, representing permanent ice-cover, and so this error estimate represents approximately a fifth of this gradient. With cross validation the R^2 values drops dramatically to 0.36 (WA) and 0.38 (WA(tol)). The reason for this might be the small number of sites in the training set, the number of lakes with no ice-cover, the under representation of ice-cover durations of between 25-50 days, and the fact that each lake is quite different so that

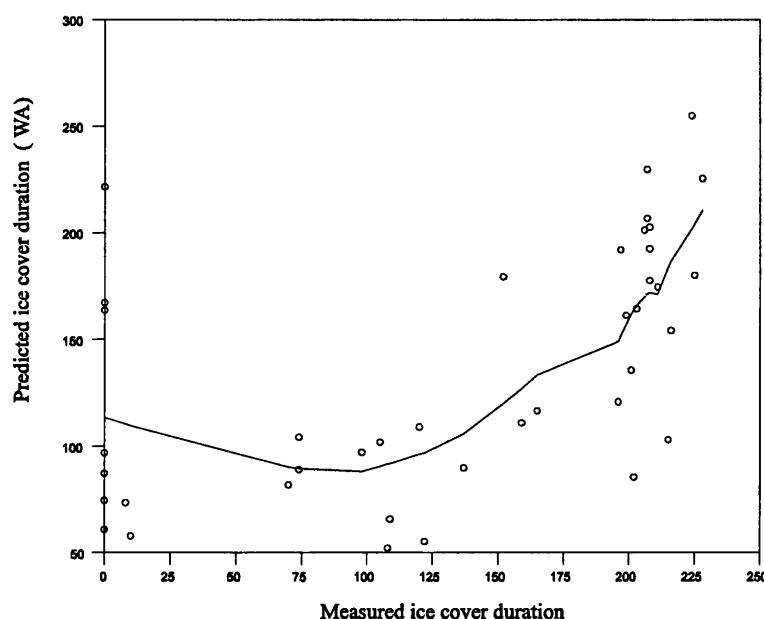
when it is taken out and the model re-run in its absence this might make a marked difference (Birks *pers. com.*).

The output for the PLS and WA-PLS methods both show that the errors decrease with each component of the model. A model with 6 components only has errors of 3.9 days (PLS) and 8.6 days (WA-PLS) and very good R^2 values. These error values are not, however, realistic because only the training set data are used to produce the estimates and no cross validation is conducted. It is more appropriate to assess the errors produced when cross validation is conducted, i.e. the RMSEP_{jack} in Table 4.27. A one component model appears to produce the lowest errors and the highest R^2 values for both PLS and WA-PLS. Again as with WA and WA(tol) these errors are between 66-69 days.

It is apparent that regardless of which method is used the error estimates associated with each model are still high. The predicted ice-cover has been plotted against the modelled ice-cover to try and evaluate if the model performs better at different points along the ice-cover gradient and to see why the error estimates are so high (Figure 4.48). Only the results for WA have been plotted as all methods incur similar errors. Ideally the lowess smoother line should be at a 45° angle and represent a straight line, in which case the predicted diatom ice-cover would be the same as the measured ice-cover. It can be seen that the model grossly over estimates ice-cover at lakes with no measured ice-cover. Seven of the lakes within the training set had no ice-cover and yet the model predicted that these lakes had between *ca.* 60- 220 days of ice-cover. As the ice-cover increases the predictive power of the model improves.

In order to try and decrease the prediction errors of the model a new model was constructed using only the 59 species that were shown to have a significant relationship with ice-cover (see Table 4.21 and Figure 4.47). This would give the model 'the best chance' possible at predicting ice-cover.

Figure 4.48: Measured ice-cover and WA predicted ice-cover data with lowess smoother line plotted



WA, WA(tol) and WA-PLS, with associated jack-knifed errors, were calculated for the 40 lake training set using only the 'significant ice-cover species' and the results are presented in Table 4.28 and Table 4.29. The WA-PLS model which performs the best, i.e. has the lowest RMSE and highest R^2 after jack-knifing, is the one component model. It can be seen that the R^2_{jack} measures have increased for all the reconstruction techniques, suggesting the 'reduced species' model is performing better than the full 'all species' model (Table 4.26 and 4.27, full model R^2_{jack} WA- 0.368, WA(tol)- 0.386 and WA-PLS, one component- 0.369). The errors for the 'reduced species model' vary between 47-55 days ice-cover which represent a reduction in the errors associated with the 'full species model'. The lowest error of 47 days is less than the lowest errors of the 'full species model' (66 days) but still represents ice-cover errors of over one month and is indicative of a 1/7th of the total gradient error when the whole ice-cover gradient is considered (47/365).

The errors of prediction for the lower end of the gradient seem to have been significantly lowered using this new model (Figure 4.49). Even so it remains that the model still predicts ice-cover durations of 110 days for sites with no measured ice-covers. This is, however, a great improvement on the first model and possibly accounts for the 'reduced model's' higher R^2_{jack} value but the model is still relatively inaccurate.

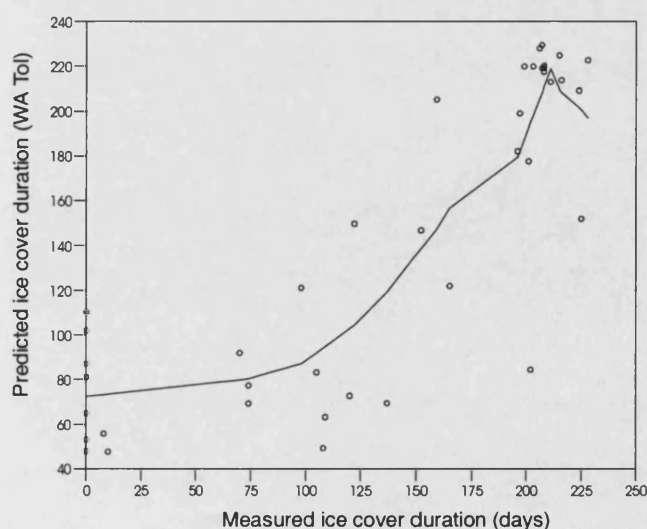
Table 4.28: A comparison of WA and WA(tol) calibration and prediction techniques for ice-cover duration for the 40 lakes training set using only the 59 species that had a significant relationship with ice-cover. Analyses were conducted on square root transformed species data and untransformed ice-cover duration data. Deshrinking using the inverse approach was used.

Prediction	RMSE	R ²
WA	46.6	0.68
WA tol	36.9	0.80
Calibration	RMSEP	R ² _{jack}
Cross Val WA	55.1	0.56
Cross Val WA tol	47.6	0.68

Table 4.29: Results of the WA-PLS calibration and prediction techniques for ice-cover duration for the 40 lakes training set using only the 59 species that had a significant relationship with ice-cover. Analyses were conducted on square root transformed species data and untransformed ice-cover duration data.

WA- PLS	Apparent errors of estimation	
No of components	RMSE	R ²
1	46.6	0.68
2	33.4	0.83
3	27.3	0.89
4	23.3	0.92
5	20.5	0.93
6	18.2	0.95
Prediction errors		
No. of components	RMSEP _{jack}	R ² _{jack}
1	55.1	0.56
2	57.8	0.55
3	61.7	0.51
4	68.8	0.44
5	72.2	0.40
6	75.7	0.38

Figure 4.49: Measured ice-cover and WA(tol) predicted ice-cover data with lowess smoother line plotted for the model with just the 59 significant ice-cover species used



It has been shown in the last section that when diatoms are used as a predictive tool for determining ice-cover duration large errors are incurred and the relationship between diatoms and ice-cover breaks down when cross validation is used. Therefore, the usefulness of applying a diatom inferred ice-cover model down core to quantify changes in lake ice-cover seems limited. It is applied down core in Chapters 6 and 7 to see if it might be appropriate to use it as a qualitative tool only to predict when conditions were either 'warmer' or 'colder' in the past and to take the analysis to its logical conclusion. Likewise it may be suitable to use some of the ice-cover indicator species, identified in section 4.4.3, to make qualitative inferences about past climates. These approaches are adopted and discussed further in Chapters 6 and 7.

4.5 Discussion

The following section discusses briefly how the environmental variables, identified as explaining the majority of the diatom variance above, are influencing the diatom assemblages of the 40 lakes. Due to the poor performance of the ice-cover transfer function the feasibility of creating a pH transfer function is suggested (developed in Chapter 5) which may be used to indirectly infer changes in past climate.

4.6 The main environmental variables determining the diatom variance within the data set

Several variables were identified as being significant for explaining diatom variance within the 40 lake data set (Table 4.13). The variables identified as the most important, in terms of the explanation of the diatom variance, by the forward selection technique are discussed below.

4.6.1 The Ca^{2+} / pH/ Alkalinity gradient

Ca^{2+} explained 10.9% of the diatom variance, and was selected by the forward selection technique with 70% of species having a significant relationship with Ca^{2+} . The Ca^{2+} gradient is especially long in this data set (Figure 4.5) and the selection of Ca^{2+} over the other co-variables of pH and alkalinity is probably a function of this gradient length. All three variables are highly co-dependent and each could technically be substituted for the other.

In previous similar studies pH has been identified as the dominant variable in explaining diatom variation in upland lake training sets (Stevenson *et al.*, 1991; Battarbee *et al.*, 1985; Fritz *et al.*, 1990). Many species tend to show narrow ecological preferences for pH and respond directly to lake pH changes demonstrated in the various palaeolimnological acidification studies (Flower and Battarbee 1983; Jones *et al.*, 1989; Allott *et al.*, 1995; Stevenson *et al.*, 1991).

The pH/ Ca^{2+} / Alk gradient also exerts some control over the occurrence of the planktonic *Cyclotella* species within the data set, with the majority of the *Cyclotella* species occurring at the higher pH sites (Figure 4.30). The strength of the pH and diatom relationship is discussed further in chapter 5 when the feasibility of creating a pH transfer function is evaluated using the 80 lake data set.

4.6.2 The TOC gradient

Total organic carbon was documented as explaining 10.2% of the diatom variance within the 40 surface samples, and identified as significant by the forward selection technique with 55% of species having a significant relationship with TOC. The sources and composition of organic matter, in lake waters are, however, diverse and poorly understood (Wetzel 1983). The direct influence of TOC/DOC on diatoms is complex, and possibly primarily of an indirect nature resulting from inter-linking factors such as changes in lake water acidity (*c.f.* Kullberg *et al.*, 1993) and changes in light penetration due to colouration, which has implications for the habitats of both planktonic and periphytic organisms (Leavitt *et al.*, 1999; Korsman and Birks 1995).

The relationship has been proved to be so strong, however, that transfer functions have been developed to reconstruct past DOC from fossil diatoms (Philibert and Prairie 2002; Enache and Prairie 2002; Pienitz and Smol 1993; Ruhland and Smol 2002). The apparent importance of TOC as a driving variable for the diatom variance in this data set is, therefore, unsurprising. The length of the TOC gradient is large reflecting the differences in mean TOC between the two countries (see Figure 4.20 and 4.25). The TOC range for Scotland is wide and its mean TOC is considerably higher than the mean for the Norwegian lakes, probably reflecting the peaty soil types draining the Scottish sites.

Within the training set several species were shown to be associated with high TOC conditions (Figure 4.31). Some of these species have been identified as having high DOC optimum derived from the aforementioned transfer function studies. These include *Navicula leptostriata* (NA156A) (Optima 14.21mg/l Philibert and Praire, 15mg/l Ruhland and Smol, and 15.48mg/l Enache and Praire), *Eunotia rhyncephala* (EU106A) (11.4mg/l, Philibert and Praire, and 11.4mg/l Enache and Praire). Many of the *Eunotia* species associated with higher TOC (EU048A, EU110A) have relatively low documented DOC optima indicting that their position on the ordination may be more driven by the lower pH conditions often associated with higher levels of TOC, and the subsequent increase in organic acidity.

It should be noted, however, that the response of the diatoms to the TOC gradient may not be direct and may reflect other factors which co-vary with TOC. For example water depth and lake area, are both negatively correlated with TOC (Table 4.3) and this depth/area ratio may also be an important factor affecting diatom growth. In addition both TN and TP are positively correlated with TOC and, therefore, this may also represent a nutrient signal.

The apparent importance of TOC within the training set may be a combination of the indirect affects of TOC on the diatom species and the influence of lake type between each area, with Scotland having shallower, smaller, more acidic lakes at lower altitudes, compared to Norway having larger deeper, clearer lakes draining less peaty catchments. All these elements might be reflected within the TOC gradient.

4.6.3 The Na⁺ gradient

Section 4.1.1.1 demonstrated that there were large differences between the means for conductivity, Na⁺, Cl⁻ and Mg²⁺ for the Norwegian and Scottish lakes (See Table 4.2 and Figure 4.25). All of these ions, to some extent, are due to the input of dissolved salts from atmospheric precipitation derived from the ocean. The amount of sea salt deposited decreases the farther away from the coast. The PCA diagram illustrates this separation of sites, in terms of their environmental characteristics, which is driven primarily by altitudinal/ latitudinal factors and but is also separated by Cl⁻ and Na⁺ (Figure 4.25). The sea salt gradient within this training set is, therefore, distinct and long. Separation of sites occurs due to the majority of the atmospheric salinity being

precipitated close to the coast, i.e. primarily to the Scottish sites and selected Norwegian sites (see Figure 2.1, 2.4 and 2.5). Those sites inland would receive less atmospheric sea salt input and have lower concentrations of Cl^- and Na^+ .

The degree and duration of the sea salt input episodes, however, will affect the chemical composition of a lake to varying degrees. Sea salt rich precipitation on to acid soils can cause acidification of runoff and the lowering of lake water pH, accompanied by a decrease in alkalinity and an increase in labile monomeric aluminium (*c.f.* Wright *et al.*, 1988; Harriman and Wells 1985; Skartveit 1981; Anderson and Seip 1999). This effect results from the cation exchange processes within the soils where a small amount of the incoming Na^+ and Mg^{2+} is exchanged for other cations in the soils. In acidic soils much of the exchanged cations will be the acid cations of Al^{3+} and H^+ . The duration of the pH lowering may be short lived and is often affected by the retention time of the lake. The effect is particularly pronounced in small catchments with acidic soils (Wright *et al.*, 1988), which may account for the lower pH values for the Scottish lakes. However, the intensity of acidity effect is not a simple relationship and is linked to the regional geology and soil type within the catchment (Evans *et al.*, 2001).

Due to this effect and the fact that sea salt inputs occur over long timescales their acidifying effect may be hard to separate from acid deposition from anthropogenic sources. Some work, however, has demonstrated the link between sea salt concentration and the North Atlantic Oscillation which both follow a similar cyclical pattern (Evans *et al.*, 2001).

The relationship between diatoms and salinity has been demonstrated in many studies (Fritz *et al.*, 1991; Cumming and Smol 1993; Gasse *et al.*, 1995; Roberts and McMinn 1999). These studies tend to have been conducted over very long gradients from freshwaters to brackish/marine waters or concerning estuary diatom samples. The salinity gradient within this study is relatively small in comparison and it may therefore be unlikely that the diatoms are responding directly to the Na^+ gradient. It was shown (Figure 4.25) that Na^+ shows a high degree of co-linearity with JanT and a strong negative relationship with ice duration and altitude suggesting that this might be a climate signal within the diatom assemblages. Na^+ also has a smaller biplot arrow

than the co-linear JanT, suggesting that it has a lesser influence on diatom variation than JanT. The relationship between diatoms and January temperature is explored further in Chapter 5.

4.7 Conclusion

This chapter has presented the key environmental variables responsible for the diatom variance within the 40 samples. The main variables responsible for the variance in diatom data were identified as Ca^{2+}/pH and secondly TOC and to a lesser extent Na^+ . The links between Ca^{2+}/pH and TOC were discussed briefly. It was concluded that the Na^+ gradient may not be exerting a direct ecological effect on the diatoms. The gradient may have been drawn out because it reflected differences in sea salt inputs between the two countries, creating a long environmental gradient exhibiting a bi-modal distribution pattern.

The specific influence of ice-cover duration on the diatom assemblages was evaluated using the 40 lake training set. Ice-cover duration was not extracted by the forward selection process but it was shown to be an important variable for explaining a significant proportion of the diatom variance. It would, however, be hard and possibly unproductive to identify how much of the diatom variance is explained by ice-cover alone using further variance partitioning analyses because it is probable that the ice-cover is affecting the diatoms indirectly through its influence on other interconnected variables (see Figure 1.1). For example, ice-cover influences the mixing of the lake water, thereby influencing the nutrient supply (Catalan *et al.*, 2002b), by using variance partitioning and identifying how much diatom variance is uniquely explained by the lake nutrients one may also be eliminating some of the variance which is actually connected to the lakes ice-cover regime. This illustrates the complexity of trying to identify, and quantify, the influence of a specific driving variable which is in fact just one member of a suite of influential variables, all of which may be interconnected.

The relationship of individual diatom species to ice-cover duration was presented in detail using WA techniques to identify potential ice-cover indicator species for use in chapters 6 and 7. It was concluded that the development of an ice-cover transfer function incurred large errors of reconstruction.

Due to this result the possibility of using pH reconstructions to make inferences about past climates are discussed and developed in the following chapter. It is clear from the discussion above that pH is one of the main explanatory variables for diatom variation within this 40 lake data set. Due to the demonstrated links between pH and climate (see section 1.4.3.1) and the strong relationship between diatom variance and pH measures within this training set, it was thought that the 80 lake training set could be explored in order to generate a pH inference model. In addition the lakes chosen for the climatic reconstructions have undisturbed catchments (See Section 2.3) and are not subject to high levels of acid deposition (Birks *pers. com.*) suggesting that they might be suitable for a pH/ climate analysis. The pH model is developed and discussed in the next chapter and applied in chapters 6 and 7.

Chapter 5

Analysis of the 80 lake modern sample training set

Introduction

The last chapter assessed the relative importance of lake ice-cover duration for explaining the diatom variance within the 40 lake training set. It was concluded that although there was a significant relationship between ice-cover duration and the diatom assemblages this did not prove to be robust enough to create an accurate ice-cover transfer function. For this reason and the proven link between pH and climate and the strong relationship between pH and the diatom assemblages in the 40 lake training set, the feasibility of creating a pH transfer function using the larger 80 lake training set is discussed within this chapter. Although many pH transfer functions have been generated previously (see section 1.4.1.3) it was thought that if a model was generated with this training set and applied down core any problems of taxonomic harmonisation, between the training set and the fossil diatom record, would be eliminated.

Firstly, summary environmental statistics are presented for the sites in the 80 lake training set in order to identify any outliers and assess the difference in geochemistry for the lakes. The diatom assemblage data for the 80 surface samples in the training set are presented and any outliers are identified. The main environmental variables driving the diatom variance are identified. The relative importance of pH for determining the diatom variance within the 80 lake training set is calculated. Finally the feasibility of creating, and the accuracy of, the 80 lake pH transfer function is evaluated. Due to the importance of the January temperature variable for explaining diatom variance (section 5.4.1.1) the value, viability of creating, and accuracy of a January temperature diatom transfer function is also discussed.

5.1 Environmental data

The environmental data for the sites includes both the catchment and water chemistry data for each lake. The lakes included in the 80 lake training set are listed in Table 5.1. There are less complete sets of environmental variables available for the 80 lake training set than those available for the 40 lake set, with the notable absence of any

nutrient data and an ice-cover duration variable (Table 5.2 and see section 3.2.3 and Table 3.1).

Table 5.1: Lake code, Longitude, Latitude, Altitude and lake area measurements for each of the 80 lakes within the training set. Lakes with the prefix CN, SN, 96, 98 and 99 refer to Norwegian lakes and those with the prefix SC refer to the Scottish lochs (see Chapter 2).

Lake Code	Numbers used in ordination plots	Numbers used in ordination plots after deletion of outliers	Longitude °E	Latitude ° N	Altitude (m.a.s.l)	Lake Area (ha)
96-10	1	1	8.25	61.54	1140	Unknown
96-12	2	2	8.8616	61.7016	1294	7.5
96-36	3	3	6.939	59.8483	1020	5
96-37	4	4	6.73	59.8416	1052	18.3
96-54	5	5	7.2533	59.8083	1107	8.1
96-71	6	6	6.9933	59.8433	1144	4.4
96-78	7	7	7.0216	59.8566	1318	8.8
96-9	8	8	7.9066	61.548	1376	10
98-1	9	9	7.315	60.925	1290	2.5
98-10	10	10	7.8483	61.5383	1301	5
98-13	11	11	8.9633	62.0266	1194	3.2
98-14	12	12	8.9433	62.0666	1080	2.5
98-15	13	13	9.8366	62.2683	1169	10
98-16	14	14	9.87	62.3216	1075	6.3
98-17	15	15	9.4483	61.1	1114	12.5
98-2	16	16	7.3633	60.965	1289	38.1
98-20	17	17	8.7633	61.39	1461	12.5
98-21	18	18	8.795	61.3933	1377	22.5
98-22	19	19	8.8416	61.3766	1329	45
98-23	20	20	8.82	61.3183	1055	30.6
98-3	21	21	7.3283	60.9266	1240	2.5
98-5	22	22	7.5333	60.7416	1400	30.7
98-6	23	23	8.2583	61.5466	1401	103.1
98-7	24	24	7.9483	61.59	1221	9.4
98-8	25	25	7.9483	61.5783	1371	10.6
98-9	26	26	7.9483	61.55	1391	26.3
99-43	27	27	10.155	61.6983	1013	6.9
99-44	28	28	10.1766	61.7283	1056	Unknown
99-50	29	29	10.0216	62.3833	1000	Unknown
CN0001	30	*	6.00545	61.6131	466	165
CN0002	31	30	6.15556	60.9003	990	30
CN0003	32	31	6.9489	60.6921	751	60.0
CN0004	33	32	7.0656	61.2793	820	27.0
CN0005	34	33	7.1708	60.0738	1172	153.0
CN0006	35	34	7.3184	60.1028	1324	180.0
CN0007	36	35	7.3625	60.9501	1289	30.0
CN0008	37	36	7.5890	60.0844	1209	55.0
CN0009	38	37	7.5797	60.3842	1239	95.0
CN0010	39	38	7.6514	60.8420	1525	80.0
CN0011	40	39	7.7120	59.9734	1329	150.0
CN0012	41	40	8.0790	61.2011	1184	130.0
CN0013	42	41	8.1781	61.3957	1396	140.0
CN0014	43	42	8.2493	61.5478	1401	100.0
CN0015	44	43	8.8970	61.4188	1088	77.5

Table 5.1: Continued.

Lake Code	Numbers used in ordination plots	Numbers used in ordination plots after deletion of outliers	Longitude °E	Latitude ° N	Altitude (m.a.s.l)	Lake Area (ha)
CN0016	45	44	8.9824	62.7778	728	50.0
CN0017	46	45	9.0372	62.7500	1043	27.0
CN0018	47	46	9.5650	61.8898	1121	18.0
CN0019	48	47	10.2659	62.5522	938	40.0
CN0020	49	48	11.0670	62.7743	1058	8.0
CN0021	50	49	11.6009	62.7160	799	55.0
CN0022	51	50	11.7848	62.9029	844	20.0
SN0023	52	51	8.1100	59.6350	1053	40.0
SC0002S	53	52	-6.22107	57.2019	750	2.9
SC0010S	54	53	-5.65692	56.7232	590	1.8
SC0029S	55	54	-5.59274	57.1734	720	2.5
SC0067S	56	55	-5.47594	57.5659	530	3.2
SC0068S	57	56	-5.44811	57.2785	540	3.6
SC0076S	58	57	-5.44503	57.5911	600	10.0
SC0084S	59	58	-5.39224	57.5168	670	9.6
SC0101S	60	59	-5.30537	57.2507	750	1.4
SC0108S	61	60	-5.28714	57.1428	720	1.9
SC0124S	62	61	-5.22603	57.2746	660	4.4
SC0153S	63	62	-5.08451	57.372	660	2.5
SC0165S	64	63	-5.02443	57.7125	570	31.1
SC0172S	65	64	-4.90413	56.7467	740	9.3
SC0180S	66	65	-4.95487	57.4955	520	7.5
SC0189S	67	66	-4.93654	57.4523	770	5.4
SC0190S	68	67	-4.95438	57.6813	540	21.6
SC0191S	69	68	-4.91542	57.2202	660	2.3
SC0197S	70	69	-4.97635	58.1992	530	4.2
SC0204S	71	70	-4.93559	57.8098	690	5.6
SC0211S	72	71	-4.95355	58.1850	530	2.9
SC0271S	73	72	-4.68428	58.8315	740	5.1
SC0330S	74	73	-4.57701	56.9452	810	7.4
SC0335S	75	74	-4.58286	57.26925	540	1.9
SC0349S	76	75	-4.59531	58.41689	530	3.8
SC0366S	77	76	-4.2063	56.5561	720	12.4
SC0382S	78	77	-3.64865	57.0630	910	3.8
SC0386S	79	78	-3.53822	56.88503	790	14.5
SC0399S	80	79	-3.23128	56.95914	790	9.9

5.1.1 Summary environmental statistics

Table 5.2 summaries the environmental parameters for the set. The full water chemistry and site characteristics are listed in Appendix 5.1. As in Chapter 4 a box plot is presented for each environmental variable to identify any potential outliers, in terms of the environmental variables, within the 80 lake sites and to summarise the differences in environmental variables between Norway and Scotland. These are

presented and discussed below. For the box plots the outliers (displayed as small circles) are not taken in to account when the median for the box plot is calculated hence the means in Table 5.2 will not correlate with the box plot medians.

Table 5.2: Selected descriptive statistics of the environmental parameters for the 80 lake training set (untransformed data)

Determinand	Units	Min	Max	Mean	St. Dev.	Norway mean	Scotland mean
Lake Depth	m	1	47	12.7	10.2	12.1	13.7
Altitude	m a.s.l	466	1525	986	301.4	1160	663
Area	ha	≥2.5	180	29.57	42.7	41.7	6.88
pH	Units	5.42	7.65	6.3	0.45	6.39	6.31
Alk	µeq/l	6	1498	105	210.5	133	51.7
Cond	µS/cm	4.14	173	23	25.3	20	27.5
Na ⁺	µeq/l	0	250	63	67.8	20	144
K ⁺	µeq/l	0	82	7.7	11.8	8.7	5.89
Mg ²⁺	µeq/l	5	197	34.2	33.15	28	45.8
Ca ²⁺	µeq/l	15	1585	127.5	234.6	161	65.2
Cl ⁻	µeq/l	2	274	60.4	75.37	12	148
NO ₃ ⁻	µeq/l	0	13	1.56	2.48	1.0	2.45
SO ₄ ²⁻	µeq/l	9	376	42.9	59.8	48.9	32
NH ₄ ⁺	µeq/l	0	4	0.56	0.84	0.77	0.18
Al-TM	µg/l	0	65	9.58	10.6	7.8	12.8
Al-L	µg/l	0	31	2.03	4.88	2.2	1.61
Al-NL	µg/l	0	41	7.57	8.45	5.5	11.2
TOC	mg/l	0.1	9.2	2.02	1.75	1.5	2.9
ppt	mm annual	400	2699	1233	603	886	1876
Jan Temp	°F	7.1	35.26	23.2	9.4	18	32
July Temp	°F	37.3	51.5	45.7	4.6	44	49

Lake Depth, Area and Altitude

The range of lake depth for the 80 lakes is between 1–47m but lake depth varies little between the Scottish and Norwegian lakes each having similar means (Table 5.2). There are two apparent outliers for the Scottish lochs (SC0165 at 46m and SC0190 at 47m Figure 5.1 not labelled) and two for the Norwegian set of lakes (CN0002 and CN0013 both at 40m depth overlapping in Figure 5.1, not labelled).

The gradient of lake area for the 80 lake set is large (2.5–180ha, Table 5.2). There is a large difference between the two means for the countries (Scotland 6.88ha and Norway 41.7ha). It can be seen from Figure 5.2 that several outliers are contributing to the difference in means between Scotland and Norway. Norway has six outliers ranging between 180 and 130ha and Scotland has two outliers of 31.1ha (SC0165) and 21.6ha (SC0190). The majority of the Scottish lochs, therefore, are much smaller than the Norwegian lakes.

Figure 5.1: Box plots of lake depth, with medians and 25 percentile ranges, shown for both the Norway and Scotland lake classes, outliers are marked with a circle.

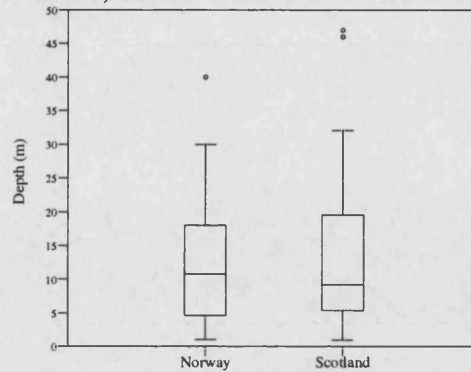
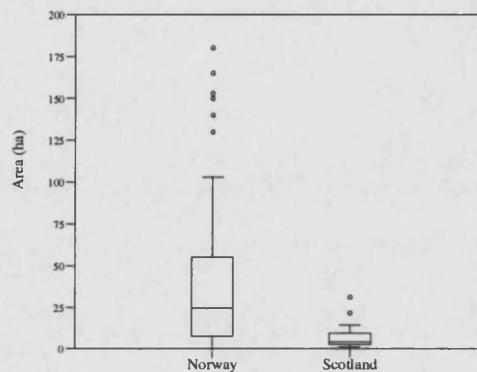
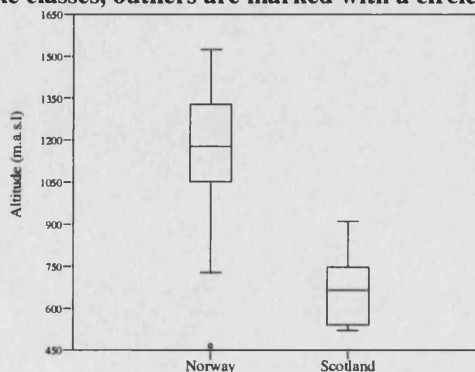


Figure 5.2: Box plots of lake area, with medians and 25 percentile ranges shown, for both the Norway and Scotland lake classes, outliers are marked with a circle.



As with mean area there is a large difference in means between the Scottish and Norwegian sites for Altitude (Table 5.2 and Figure 5.3). On average most of the Norwegian lakes lie above 1000m, there are 8 exceptions to this, out of a total of 52 Norwegian lakes. CN0001 only has an altitude of 466m a.s.l. This lake is below the tree line in Norway and so should be discarded from the training set in order to meet the selection criteria outlined in section 2.2 (see section 5.1.2. and 5.2 for deletion of outliers).

Figure 5.3: Box plots of lake altitude, with medians and 25 percentile ranges, shown for both the Norway and Scotland lake classes, outliers are marked with a circle.



pH, Calcium and Alkalinity

The pH range is large, covering values from 5.42-7.65 units (Table 5.2) but the medians for both Norway and Scotland are similar (Figure 5.4). The calcium gradient is also long spanning 15-1585 μ eq/l (Table 5.2). The difference between the calcium mean for Norway and Scotland is large (Norway 161 μ eq/l and Scotland 65.2 μ eq/l, Figure 5.5). This is driven primarily by the existence of several outliers in the Norwegian data set. For example, 99-50 has a calcium measure of 1582 μ eq/l and 98-13 has a measure of 977 μ eq/l (Figure 5.5 not labelled). Only three sites in the Scotland set of lakes have calcium values over 100 μ eq/l resulting in a lower calcium mean (Table 5.2).

As might be expected 99-50 is also an outlier in terms of alkalinity with a measure of 1498 μ eq/l (Figure 5.6 not labelled). The pH for 99-50 is, however, 6.78 and not the highest within the Norwegian set of lakes. Norway has the higher alkalinity mean of 133 μ eq/l, due to the presence of several sites with unusually high alkalinity values, compared with Scotland's mean of 51.7 μ eq/l (Table 5.2). The relatively high alkalinity measures indicate that these systems have a high capacity to buffer pH change.

Figure 5.4: Box plots of pH, with medians and 25 percentile ranges, shown for both the Norway and Scotland lake classes, outliers are marked with a circle.

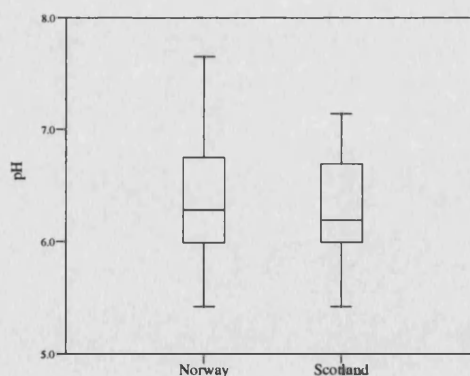
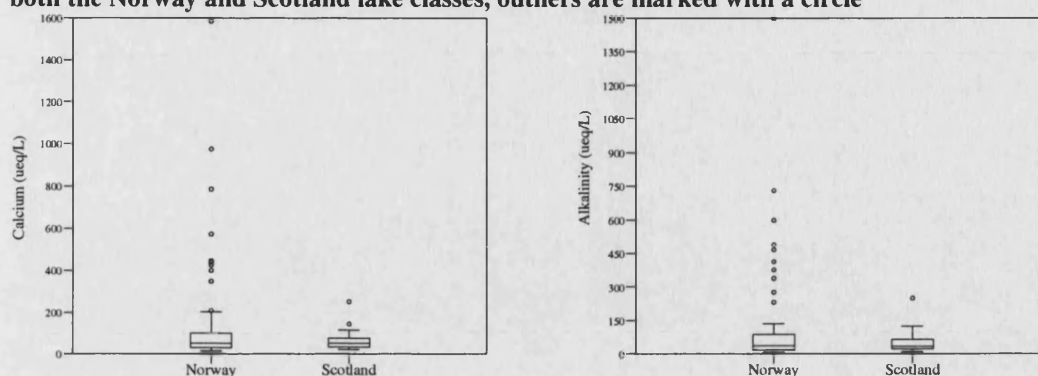


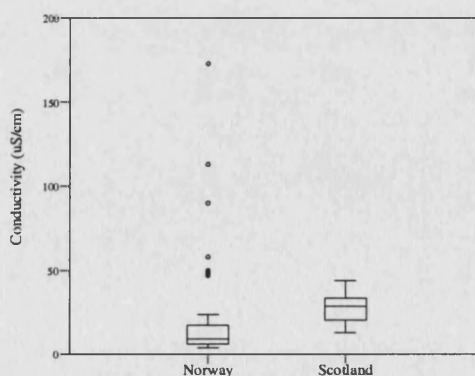
Figure 5.5 and 5.6: Box plots of Ca^{2+} and Alk, with medians and 25 percentile ranges, shown for both the Norway and Scotland lake classes, outliers are marked with a circle



Conductivity

The difference in conductivity medians for the two countries is not as large as the differences in the 40 lake training set (Table 4.2 and Table 5.2). Many of the Norway 1 sites are closer to the coast than the Norway 2 sites and their inclusion within this data set has narrowed the difference between the means of the two countries (see Figures 2.4 and 2.5). The mean for Scotland still remains higher, however, due to the sites' proximity to the coast. There are several outliers in terms of conductivity for the Norwegian lakes (Figure 5.7) for example 99-50 has a conductivity of $173\mu\text{S}/\text{cm}$, 98-13 has $113\mu\text{S}/\text{cm}$ and 98-16 has $90\mu\text{S}/\text{cm}$. This cannot be explained by a sea salt input because none of these sites are close to the coast (see Figure 2.4, site 11= 98-13, 25= 99-50, and 19=98-16), they are however, in a similar location indicating that the high values might have resulted from a different bedrock type in the region.

Figure 5.7: Box plots of conductivity, with medians and 25 percentile ranges, shown for both the Norway and Scotland lake classes, outliers are marked with a circle



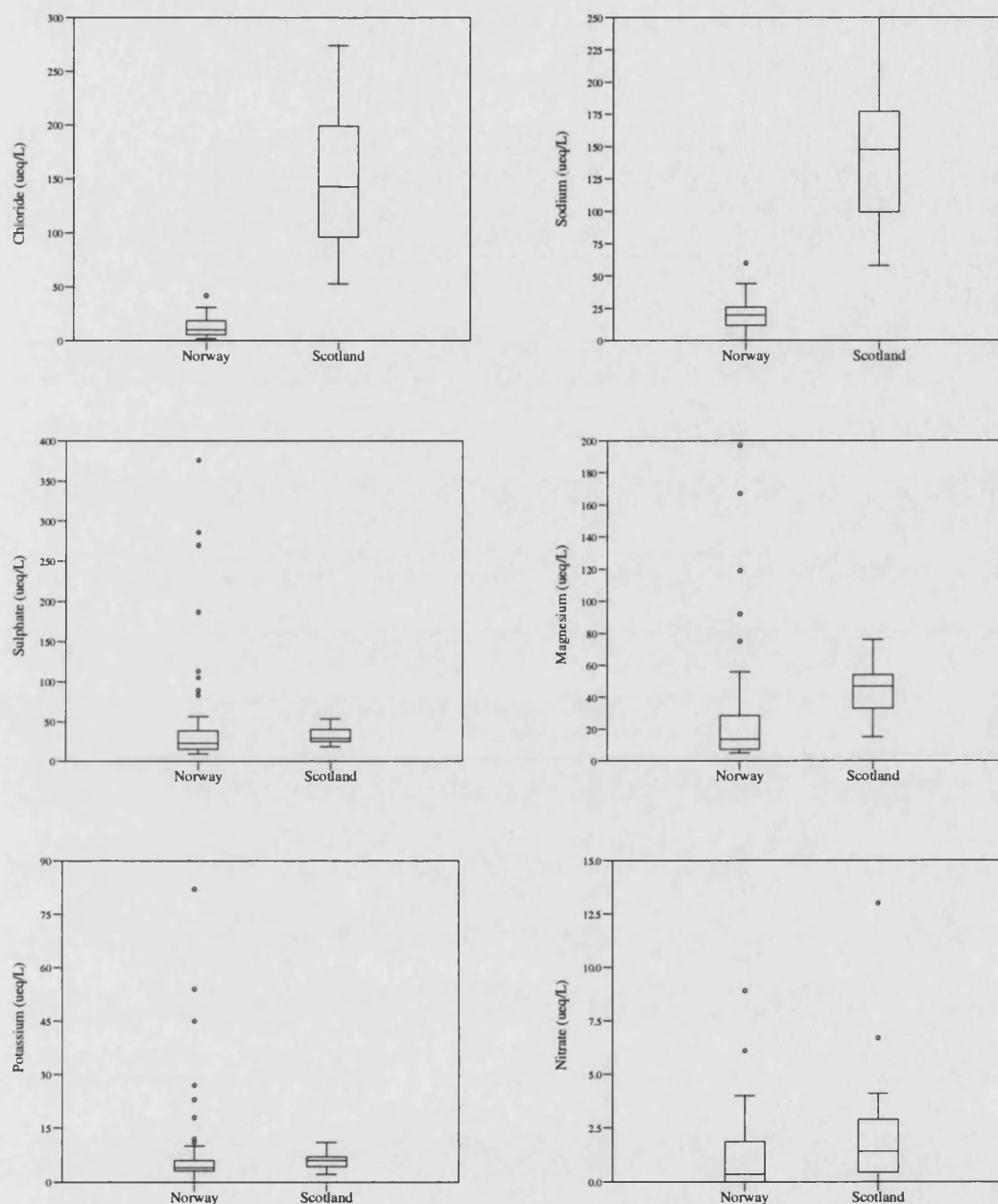
Major ions (excluding Ca^{2+}), Cl^- , NO_3^- , SO_4^{2-} , Mg^{2+} , Na^+ and K^+

There are major differences in the means of the two countries for Cl^- and Na^+ (Table 5.2 and Figures 5.8 and 5.9). This is again probably a reflection of the sea salt input gradient evident within the conductivity means discussed above. SC0349 has the highest chloride ($268\mu\text{eq/l}$) and sodium measurements ($250\mu\text{eq/l}$). This site is the farthest North of all the Scottish sites and is very close to the coast (Figure 2.1 site number 1).

There is also quite a large Mg^{2+} gradient and a substantial difference in the medians for each country probably due to the differences in bedrock for each area and the influence of sea salt deposition (Table 5.2, Figure 5.11 and Section 4.7.3). It can be seen that Norway has several outliers for sulphate, magnesium and potassium (Figure 5.10, 5.11 and 5.12). Many of these are common outliers (98-13, 99-50 and 98-16) and affect the means generated in Table 5.2 which show Norway to have higher overall potassium and sulphate.

There are many less than detection limit measurements in the nitrate gradient for both Norway and Scotland and overall nitrate levels are low within the training set. The majority of the nitrate levels for the lakes fall between 0- $3\mu\text{eq/l}$ (Figure 5.13). Two of the Scottish sites have high nitrate values (SC0399, $13\mu\text{eq/l}$ and SC0002, $13\mu\text{eq/l}$) and two of the Norwegian sites have high nitrate values (96-37, $8.9\mu\text{eq/l}$ and 96-78, $6.1\mu\text{eq/l}$).

Figure 5.8, 5.9, 5.10, 5.11, 5.12 and 5.13: Box plots of Chloride, Sodium, Sulphate, Magnesium, Potassium and Nitrate, with medians and 25 percentile ranges shown, for both the Norway and Scotland lake classes, outliers are marked with a circle

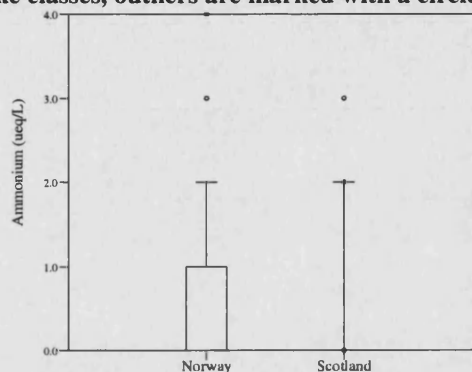


The NH_4^+ gradient and the absence of the TP and TN variables

The NH_4^+ gradient is small and ranges between 0-4 µeq/l (Table 5.2). The Scottish sites have a lower mean ammonia value than the Norwegian sites (Norway 0.77 µeq/l and Scotland 0.18 µeq/l). There are many values below the detection limit for NH_4^+ within the training set (47 sites out of the total 80 have values below the detection limit for NH_4^+ , Scotland only has 2 sites with NH_4^+ of above detection limit, 22 of the Norway 2 sites have NH_4^+ values of 1, one has an NH_4^+ measurement of below

detection limit) resulting in a strange box plot distribution (Figure 5.14). This may be a reflection of the detection limits for NH_4^+ and may not represent values which are truly zero.

Figure 5.14: Box plots of ammonium, with medians and 25 percentile ranges, shown for both the Norway and Scotland lake classes, outliers are marked with a circle



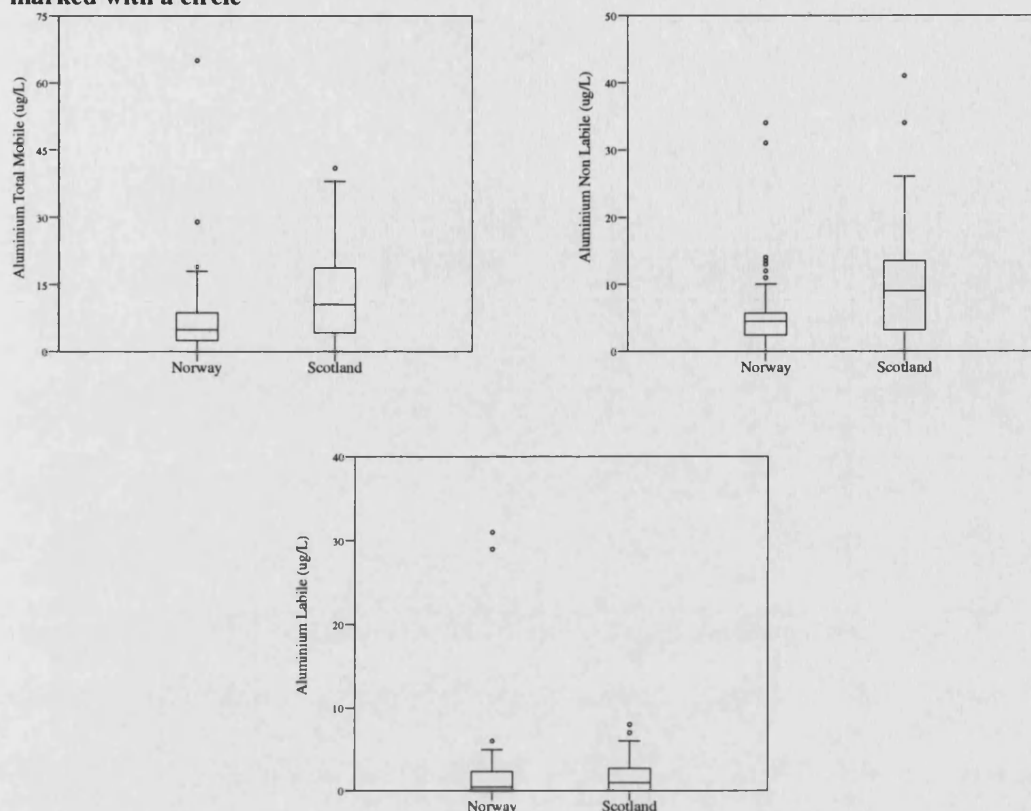
There are no total phosphorous (TP) and total nitrogen (TP) measurements available for all the lakes within this training set (Table 3.1). However, TP and TN were not identified as particularly important explanatory variables for diatom variance within Chapter 4 (see section 4.3) and, therefore, the absence of these variables in this data set is unfortunate but may not be significant.

Aluminium: Al-L, Al-NL and Al-TM

The levels of Al-TM range between 0-65µg/l with a mean of 9.58µg/l (Table 5.2) suggesting that most of the sites have low Al-TM measures and that there are outliers within this variable. SN0023 has a Al-TM of 65µg/l and SC0180 has a value of 41µg/l (Figure 5.15, not labelled).

SN0023 is also an outlier for Al-NL and Al-L (Figure 5.16 and 5.17). Other outliers for Al-NL are CN0020 (31µg/l) and SC0180 (41µg/l) and SC0029 (34µg/l). Outliers for Al-L are 98-1 (29µg/l) and SN0023 (31µg/l) but the means for the two countries are similar. Overall Scotland has higher Al-TM, Al-NL and Al-L when the outliers are disregarded (Figures 5.15, 5.16 and 5.17).

Figure 5.15, 5.16 and 5.17: Box plots of Aluminium (TM, Non-Labile and Labile), with medians and 25 percentile ranges, shown for both the Norway and Scotland lake classes, outliers are marked with a circle

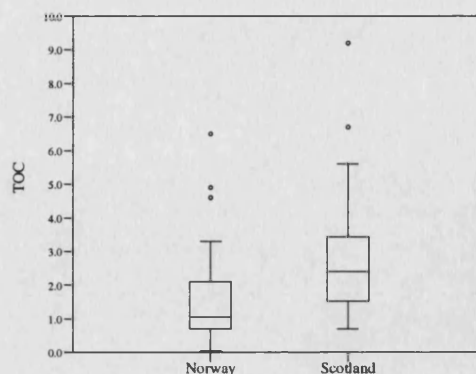


Total Organic Carbon

The TOC range is between 0- 9.2mg/l for the 80 lake set which is the same as the 40 lake set. Scotland has three outliers of 6.7mg/l, 6.7mg/l and 9.2mg/l (SC0180, SC0191 and SC0335, Figure 5.18). For Norway, 99-43, CN0020 and 99-50 are outliers (with 6.5mg/l, 4.6mg/l and 4.9mg/l respectively). The Scottish lochs have on average higher TOC measures than the Norwegian lakes (Norway mean 1.5mg/l and the Scotland mean is 2.9mg/l, Table 5.2). The difference between the means has, however, been reduced compared to the 40 lake training set. The inclusion of the Norway 1 lakes has in effect filled a gap within the TOC gradient which existed in the 40 lake training set.

During sampling, many of the Norway 1 lakes were noted as being brown in colour (e.g., 99-43, 98-23) and TOC is usually linearly related to colour units within lakes (Juday and Birge 1933). When the mean TOC is compared for the two Norwegian lake sets, Norway 1 has 1.9mg/l and Norway 2 has an average TOC of 0.9mg/l. Norway 1's mean TOC is closer to the mean for the Scottish lochs.

Figure 5.18: Box plots of TOC, with medians and 25 percentile ranges, shown for both the Norway and Scotland lake classes, outliers are marked with a circle

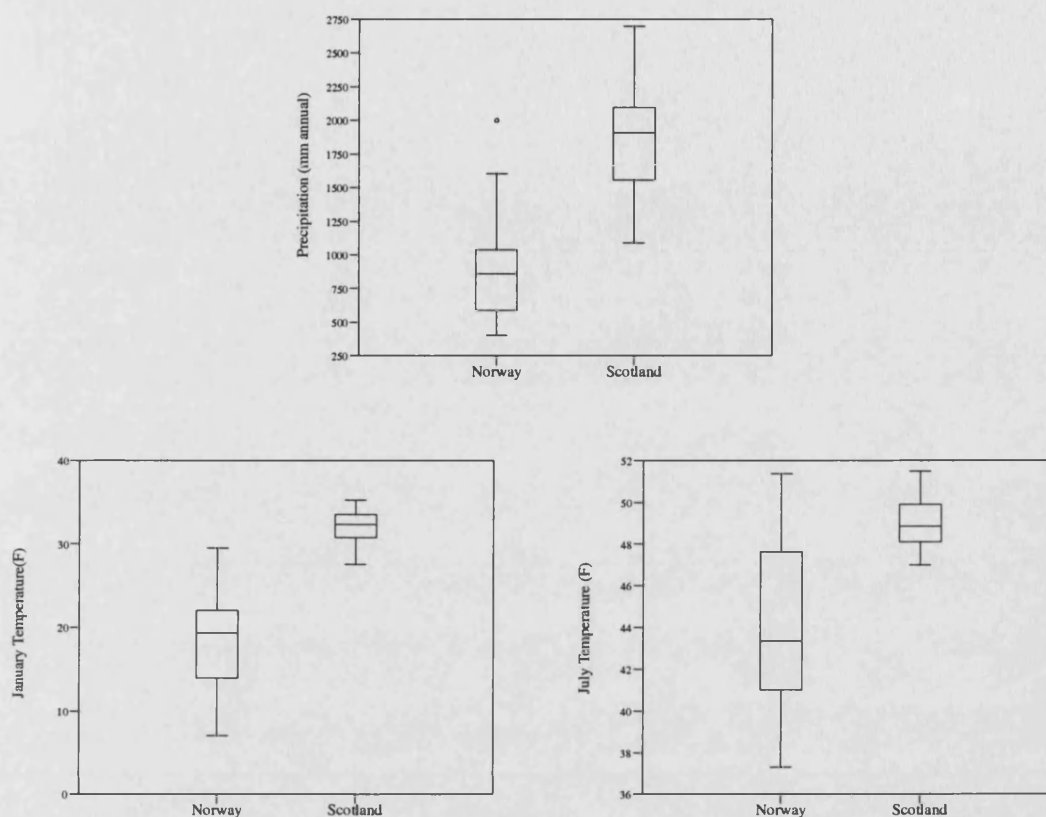


January and July air temperature and precipitation

There is a large difference between the mean precipitation measures for the Scottish and Norwegian lakes, with the Scottish lakes having a mean just under 1000mm higher (Table 5.2). There is one outlier, in terms of precipitation, 96-17 which has 2000mm of rain per year (Figure 5.19).

The January and July air temperatures were converted to °F so that negative numbers were not used in the ordinations presented in the next section. Not surprisingly the Norwegian lakes have lower January and July air temperatures than the Scottish lochs due primarily to their higher latitude and altitude (Table 5.1 and 5.2). For both the January and July air temperatures, Norway has the larger range in temperature, due mainly to the larger geographical spread of sites resulting in more variations in climate than the Scottish set, and the higher number of sites within the Norwegian set. The range of January temperature is particularly small for the Scottish set. There is also a larger difference in median temperature between Scotland and Norway for the January temperatures rather than for the July (Figure 5.20 and 5.21). There are no ice-cover duration measures for the 80 lake training set.

Figure 5.19, 5.20 and 5.21: Box plots of precipitation, January air temperature and July air temperature, with medians and 25 percentile ranges shown, for both the Norway and Scotland lake classes, outliers are marked with a circle



5.1.2 Identification of outliers and the transformation of environmental variables

The discussion above has identified some potential outliers, in terms of environmental variables, within the 80 lake training set. Lake CN0001 is an outlier within this set in terms of altitude (466m a.s.l). All the sites within the EMERGE project should technically be above the theoretical tree line to avoid any anthropogenic disturbance within the catchment. This lake, therefore, does not fit the specified criteria and should be deleted from this set.

The identification of other potential outliers can be explored further by the use of direct ordination techniques. A PCA of environmental variables was conducted on the 79 lakes (Figure 5.22, Table 5.3). Prior to the ordination several variables were transformed to increase their normality: Lat, Alt, Depth, Area, JanT, JulyT, ppt, Na^+ and pH were not transformed, Alk, Cond, Mg^{2+} , Ca^{2+} , Cl^- , SO_4^{2-} , were log transformed and NH_4^+ , K^+ , NO_3^- , Al-TM, Al-NI, Al-L and TOC were log (x+1) transformed.

Other potential outliers are sites 11, 14 and 29 (Figure 5.22, 98-13, 98-16 and 99-50 respectively) which are positioned away from the rest of the sites suggesting that they might be outliers in terms of their environmental variables (Figure 5.22).

Table 5.3: Summary of PCA ordination, eigenvalues and cumulative % variance, of the 22 environmental variables and 79 sites, with centering and standardisation by species.

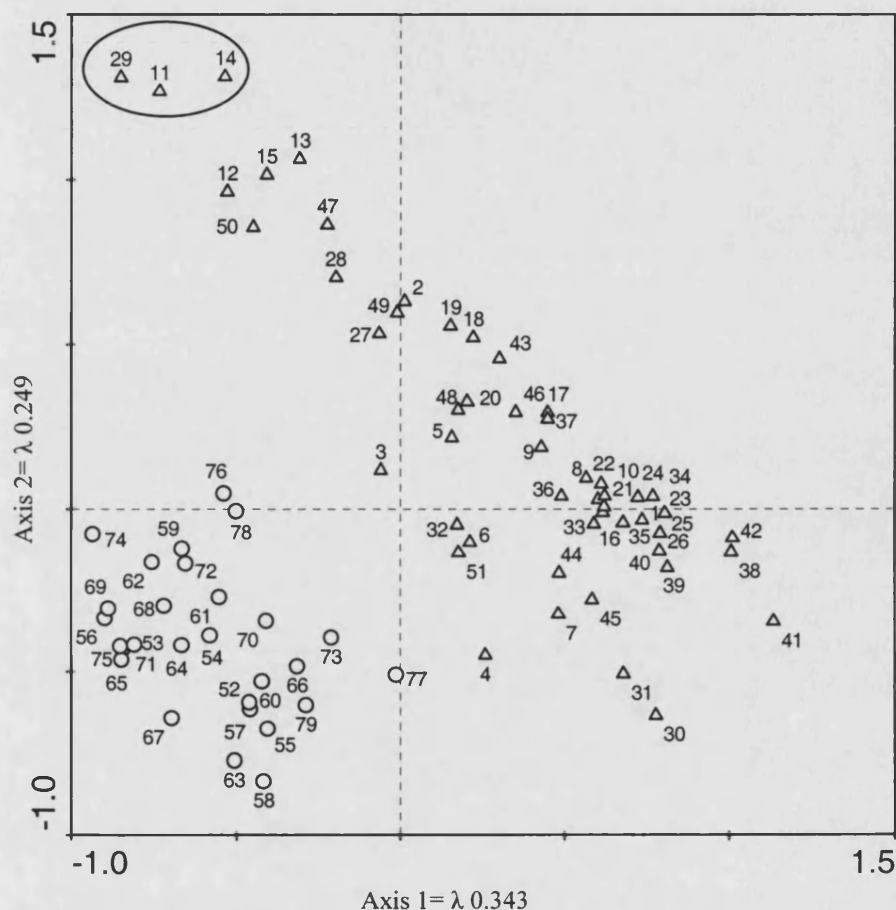
PCA axes	1	2	3	4
Eigenvalues (λ)	0.343	0.249	0.090	0.081
Cumulative percentage variance in the species data	34.3	59.2	68.2	76.3
Total inertia 1				
Sum of all eigenvalues 1				

Site 99-50 was identified in section 5.1.1 as having especially high Ca^{2+} (977 $\mu\text{eq/l}$) and Alk (1498 $\mu\text{eq/l}$). The reason for this cannot really be explained at present. The vegetation in the lake area does not indicate base rich conditions and there is no history of liming in the catchment (Birks *pers. com.*). The lake is particularly shallow (2.1m) but this should not affect the calcium measures significantly. 98-13 and 98-16 also have very high Ca^{2+} , 977 $\mu\text{eq/l}$ and 786 $\mu\text{eq/l}$ respectively, and Alk, 731 $\mu\text{eq/l}$ and 598 $\mu\text{eq/l}$ respectively. These sites are located near 99-50 suggesting that the bedrock may be the driving factor for these high values, unless any liming initiatives were widespread in nature. These three sites have the highest calcium and alkalinity measures out of all the 80 lakes, and in comparison to the mean Ca^{2+} of 127 $\mu\text{eq/l}$ and the mean Alk of 105 $\mu\text{eq/l}$, they represent outliers in terms of these two variables. In addition all three sites have the highest values for K^+ within the training set, with 98-13 at 45 $\mu\text{eq/l}$, 98-16 at 54 $\mu\text{eq/l}$ and 99-50 at 82 $\mu\text{eq/l}$ and SO_4^{2-} , with 98-13 at 376 $\mu\text{eq/l}$, 98-16 at 270 $\mu\text{eq/l}$ and 99-50 at 289 $\mu\text{eq/l}$. In terms of the whole training set they also represent outliers for these two variables (mean K^+ for all 80 lakes is 7.7 $\mu\text{eq/l}$ and mean SO_4^{2-} is 42.9 $\mu\text{eq/l}$).

The sites' positions on the biplot is distinct (Figure 5.22 circled) but they do seem to fit in with the overall spread of sites within the Norwegian samples. Their distance from the main cluster of sites is also not extremely large. The sites were not deleted at this stage but their potential inclusion within the data set is revisited within section 5.2 to assess whether they are outliers in terms of biological data. With the deletion of

CN0001 the training set consisted of 79 sites and the subsequent analyses uses these sites only.

Figure 5.22: PCA biplot of the environmental variables for the 79 lake training set (only samples are presented here in order to identify possible outliers). Norwegian sites appear as triangles and Scottish sites are represented by circles (refer to table 5.1 For lake codes used in the ordination, column after the deletion of outliers)



5.1.3 Relationship between environmental variables

This section evaluates the relationships between the environmental variables presented above. A Pearson product moment correlation analysis was performed (Table 5.4). It can be seen that many of the variables are directly related to each other either negatively or positively.

Altitude is negatively related to conductivity and also to many of the major cations and anions. This is probably driven by the Scottish sites which have higher conductivity than the Norwegian sites and occur at a lower altitude. This would also explain the negative relationship between TOC and altitude evident within Table 5.4.

As would be expected altitude is also negatively correlated with January and July air temperature, with increasing temperatures occurring with decreasing altitude.

Lake area is also negatively related to many of the anions and cations and again this is probably a reflection of the differences in sea salt input between the two sets of the lakes and the fact that the Norwegian lakes are larger on average than the Scottish lochs (N.B. Latitude is also positively related to lake area) rather than reflecting any direct causative relationship.

pH is most strongly positively related to calcium and alkalinity reflecting the obvious co-linearity between these variables. The three aluminium measures are positively related to each other. Al-TM and Al-NL are also positively related to TOC. TOC is also weakly positively correlated with Cl^- and Na^+ which is in agreement with other studies which show a weak positive relationship between TOC and these marine ions (Stevenson *et al.*, 1991; Anderson *et al.*, 1986; Pienitz and Smol 1993)

Finally, precipitation is negatively associated with altitude and latitude reflecting the higher precipitation measures for Scotland. It is also strongly positively associated with Cl^- and Na^+ suggesting that the sea salt concentration is a precipitation driven variable.

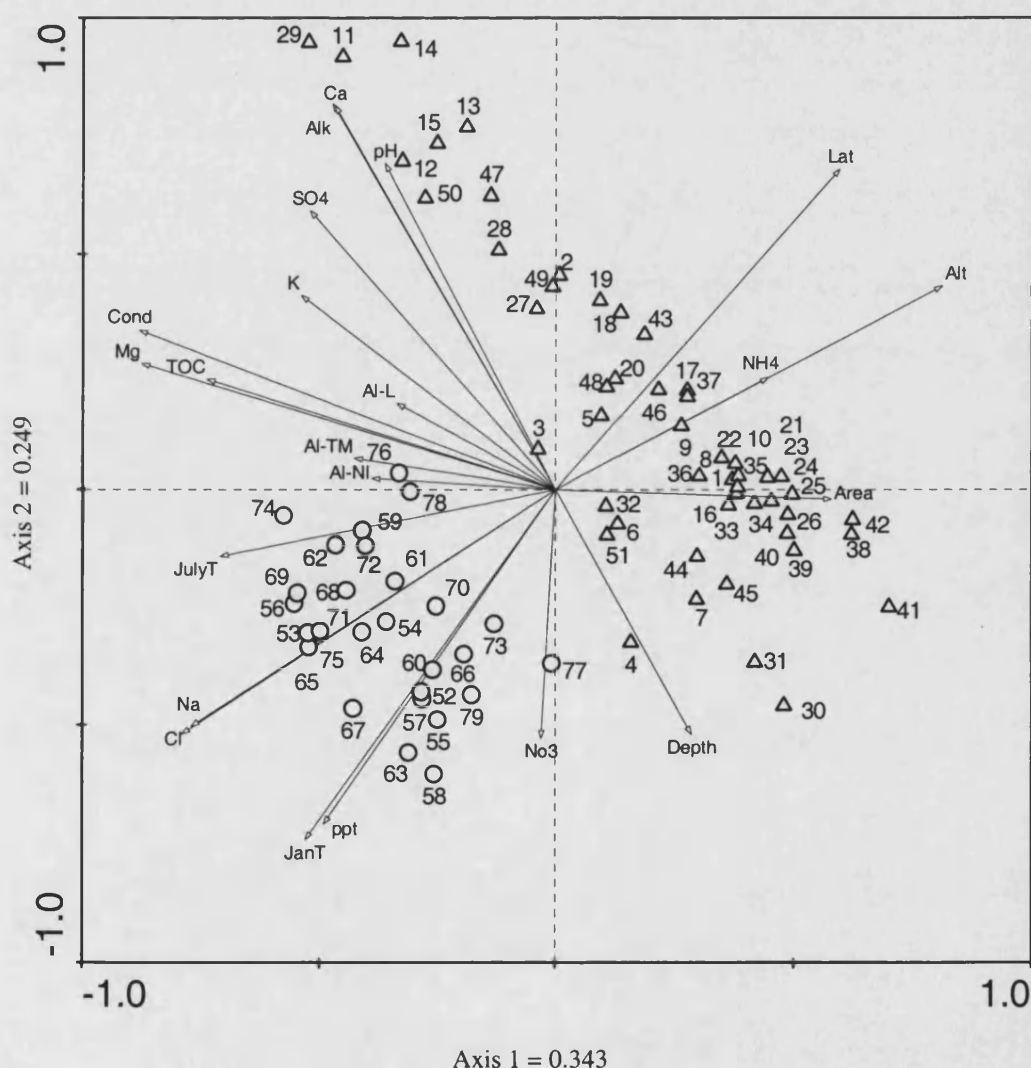
Ordination techniques were used to summarise the relationships between the environmental variables, the results of which are displayed in Figure 5.23 and Table 5.3. It can be seen that there are high correlations between many of the variables reflected in the small acute angles between some of the vectors (e.g. Ca^{2+} and Alk, JanT and ppt, Na^+ and Cl^-).

Table 5.4: Pearson product moment correlation matrix between 22 environmental variables (after transformation) for the 79 sites. Significance levels, at $\alpha= 0.01$ (99% confidence limit), for the correlations were estimated and are indicated by bold type.

	Lat	Alt	Area	Depth	pH	Alk	Cond.	Na ⁺	NH ₄ ⁺	K ⁺	Mg ²⁺	Ca ²⁺	Cl ⁻	NO ₃ ⁻	SO ₄ ²⁻	Al-TM	Al-NL	Al-L	TOC	ppt	JanT
Lat	1																				
Alt	0.71	1																			
Area	0.31	0.42	1																		
Depth	-0.07	-0.06	0.39	1																	
pH	0.14	-0.12	0.07	-0.28	1																
Alk	0.15	-0.10	-0.17	-0.46	0.87	1															
Cond.	-0.46	-0.70	-0.40	-0.23	0.52	0.63	1														
Na ⁺	-0.77	-0.84	-0.38	0.05	-0.06	-0.04	0.64	1													
NH ₄ ⁺	0.42	0.31	0.38	0.13	0.23	0.05	-0.28	-0.48	1												
K ⁺	0.15	-0.21	-0.24	-0.15	0.59	0.60	0.58	0.10	-0.01	1											
Mg ²⁺	-0.48	-0.66	-0.49	-0.28	0.47	0.57	0.88	0.66	-0.33	0.55	1										
Ca ²⁺	0.12	-0.08	-0.15	-0.42	0.79	0.95	0.67	-0.05	0.03	0.59	0.52	1									
Cl ⁻	-0.83	-0.92	-0.37	0.11	0.00	-0.04	0.65	0.90	-0.34	0.13	0.62	-0.04	1								
NO ₃ ⁻	-0.34	-0.19	0.04	0.35	-0.37	-0.36	0.04	0.23	-0.09	-0.18	0.02	-0.26	0.29	1							
SO ₄ ²⁻	0.06	-0.05	-0.08	-0.24	0.43	0.57	0.57	0.05	-0.11	0.51	0.39	0.67	0.00	-0.03	1						
Al-TM	-0.17	-0.41	-0.23	-0.19	0.15	0.19	0.39	0.32	-0.15	0.24	0.32	0.19	0.33	-0.10	0.08	1					
Al-NL	-0.18	-0.45	-0.16	-0.10	0.17	0.17	0.38	0.36	-0.17	0.27	0.30	0.16	0.38	-0.10	0.03	0.89	1				
Al-L	-0.01	0.01	-0.11	-0.18	-0.02	0.02	0.00	-0.06	-0.06	-0.07	0.00	0.05	-0.05	0.03	0.05	0.47	0.12	1			
TOC	-0.38	-0.54	-0.54	-0.43	0.25	0.47	0.61	0.44	-0.26	0.27	0.60	0.47	0.45	-0.24	0.17	0.57	0.57	0.09	1		
ppt	-0.82	-0.71	-0.23	0.16	-0.08	-0.18	0.40	0.69	-0.31	-0.08	0.38	-0.19	0.81	0.27	-0.12	0.11	0.16	-0.11	0.20	1	
JanT	-0.84	-0.86	-0.17	0.23	-0.07	-0.21	0.44	0.79	-0.24	-0.10	0.40	-0.21	0.90	0.31	-0.18	0.29	0.32	0.02	0.29	0.84	1
JulyT	-0.62	-0.56	-0.63	-0.24	0.02	0.20	0.57	0.63	-0.49	0.19	0.70	0.21	0.54	0.09	0.18	0.18	0.14	0.00	0.56	0.43	0.33

There is a clear geographical separation between the two sets of sites indicating that the Norwegian lakes have different environmental values to the Scottish lochs. This seems to be primarily driven by the variables of altitude and latitude, which also have a direct effect on the air temperatures, precipitation, and the marine ion variables. Some of the Norwegian sites also exhibit higher pH and Ca^{2+} values than many of the Scottish lochs but the Norwegian lakes do seem to have a wide pH and Ca^{2+} gradient.

Figure 5.23: PCA biplot of the environmental data for the 79 lake training set and 22 environmental variables. Norwegian sites are plotted as triangles and the Scottish sites as circles (refer to Table 5.2 for lake codes/numbers)



The correlation between ordination axes and the environmental variables is demonstrated further when the PCA scores for the environmental variables are analysed (Table 5.5). It can be seen that axis 1 is linked to altitude and latitude on the positive side and Cond, Na^+ , Mg^{2+} , Cl^- , TOC and JulyT on the negative side. Axis 2 reflects the Ca^{2+} , pH and Alk gradient. The biplot demonstrates that there is a good

distribution of sites in relation to the environmental variables indicating that there are long chemical and environmental gradients within the 79 lake data set.

Table 5.5: PCA scores for the 22 environmental variables on the first four axes (bold denotes all values > 0.7 or < -0.7 for ease of comparison)

Variable	Axis 1	Axis 2	Axis 3	Axis 4
Latitude	0.7266	0.5288	0.1143	-0.0778
Altitude	0.8838	0.2663	0.0384	0.1824
Area	0.5511	-0.0556	-0.2942	-0.4768
Depth Max	0.1962	-0.556	-0.1984	-0.4768
pH	-0.2770	0.7531	-0.2361	-0.3499
Alk	-0.3590	0.8724	-0.2113	-0.0844
Cond	-0.8776	0.3404	-0.2113	-0.0844
Na ⁺	-0.8408	-0.3799	-0.0722	-0.0018
K ⁺	-0.3796	0.6219	-0.1814	-0.1696
Mg ²⁺	-0.8606	0.2768	-0.1828	0.0887
Ca ²⁺	-0.3558	0.8554	-0.1726	-0.0386
Cl ⁻	-0.8610	-0.4146	-0.1056	-0.1591
NO ₃ ⁻	-0.0968	-0.5027	-0.2700	-0.0511
SO ₄ ²⁻	-0.2728	0.5661	-0.3031	0.0394
NH ₄ ⁺	0.4498	0.1960	-0.1116	-0.4860
Al-TM	-0.5049	0.1458	0.7348	-0.3427
Al-L	-0.0487	0.0748	0.5635	0.0156
Al-NL	-0.5093	0.1003	0.6081	-0.4317
TOC	-0.7196	0.2788	0.3654	0.1274
JanT	-0.6970	-0.5789	-0.0510	-0.2967
JulyT	-0.7318	-0.0458	-0.0644	0.4982
ppt	-0.6432	-0.5479	-0.2085	-0.0954

5.2 Biological data analysis

This section presents the diatom data for the 79 lakes. The most common, in terms of their presence in each sample, and most abundant species, in terms of their total % sum within the whole data set, are listed (Table 5.6). Ordination analyses, independent of any environmental variables, are presented to assess if there are any outliers, in terms of diatom assemblage, within the 79 lakes and to look at patterns of variation across the Norwegian and Scottish sites. 408 taxa were identified in the 79 lake training set (Full species list and the codes used in many of the graphics are presented in Appendix 5.2). All counts were transformed to percentages before analyses.

5.2.1 Exploration of the common and most abundant taxa

The 25 most abundant species, in terms of the sum of their counts in all 79 samples, are listed in Table 5.6. The data set is dominated by mainly *Achnanthes*, *Aulacoseira* and *Fragilaria* species, with some *Brachysira*, *Cymbella*, *Cyclotella*, *Eunotia*, *Frustrulia* and *Navicula* species also listed. *Achnanthes marginulata* occurs in 71 out of the 79 sites and has a 29% maximum abundance. This species was second most

abundant in the 40 lake training set. In fact the top five species are the same in both the training sets, albeit in a different order. Some species however do occur in this list which do not occur in the list of most abundant species for the 40 lake training set. These include many of the *Fragilaria* species (*F. construens* var. *venter*, *F. pinnata*, *F. construens*) and *Achnanthes levanderi* and *Aulacoseira perglabra*.

Table 5.6: A list of the most abundant species (in terms of % sum abundance from all 79 samples), maximum abundance for the species, the number of samples that the species occurs in (how common the species is), and the species N2 value (the effective number of occurrences of that species calculated by CALIBRATE)

Taxon	Number of samples the species occurs in (max 76)	Maximum abundance (%)	N2	Sum of abundance of the species in all 79 samples
AC022A <i>Achnanthes marginulata</i>	71	29	30	503
AC060A <i>Achnanthes curtissima</i>	63	49	21	427
FR064A <i>Fragilaria exigua</i>	63	33	30	408
AC013A <i>Achnanthes minutissima</i>	68	39	25	381
AC134A <i>Achnanthes helvetica</i>	70	28	26	277
FU002A <i>Frustrulia rhomboides</i>	61	19	27	202
BR010A <i>Brachysira neoexilis</i>	62	19	26	202
AU005E <i>Aulacoseira distans</i> var. <i>nivalis</i>	41	15	21	171
AC046A <i>Achnanthes altaica</i>	69	25	22	162
TA9997 <i>Tabellaria flocculosa</i> (short)	64	13	30	140
FR002C <i>Fragilaria construens</i> var. <i>venter</i>	36	28	10	137
AC048A <i>Achnanthes scotica</i>	50	10	32	136
AU005A <i>Aulacoseira distans</i>	33	43	7	124
AU010A <i>Aulacoseira perglabra</i>	29	43	6	120
AC136A <i>Achnanthes subatomoides</i>	62	13	25	118
CY006B <i>Cyclotella kuetzingiana</i> var. <i>planetophora</i>	21	22	10	110
FR002A <i>Fragilaria construens</i>	27	38	6	107
AC044A <i>Achnanthes levanderi</i>	45	17	14	101
BR006A <i>Brachysira brebissonii</i>	56	30	10	99
EU047A <i>Eunotia incisa</i>	54	11	25	98
FU002B <i>Frustrulia rhomboides</i> var. <i>saxonica</i>	60	9	29	94
PE002A <i>Peronia fibula</i>	47	9	21	90
ZZZ986 <i>Aulacoseira distans</i> var. <i>septentrionalis</i>	17	25	6	80
FR001A <i>Fragilaria pinnata</i>	36	11	13	80
CM018A <i>Cymbella gracilis</i>	66	5	38	78



Figure 5.24a: Summary diatom diagram of 79 samples (*Achnanthes* – *Aulacoseira* species displayed). The separation between the Scottish and Norwegian sites is plotted. Species <6% have been deleted

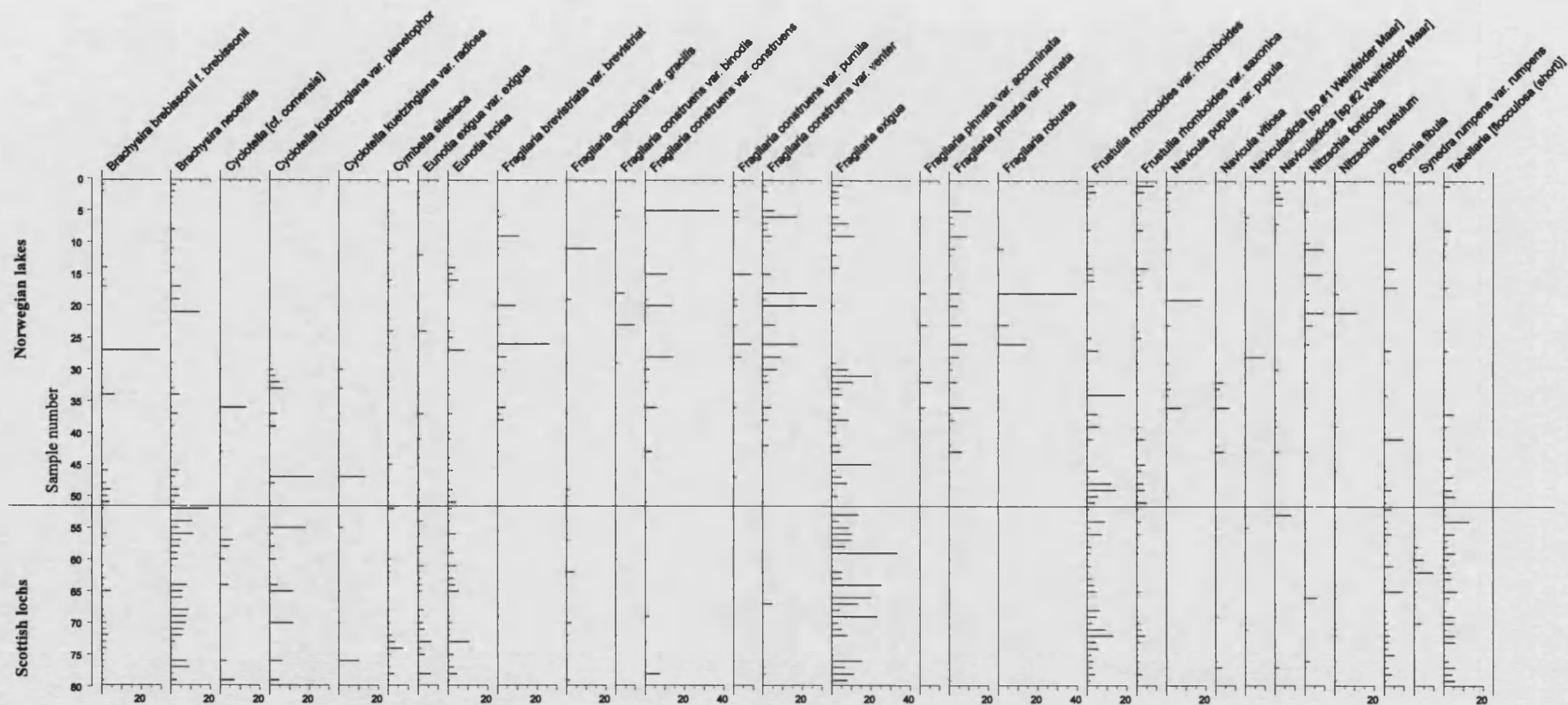


Figure 5.24b: Summary diatom diagram of 79 samples (*Brachysira-Tabellaria* species displayed). The separation between the Scottish and Norwegian sites is plotted. Species <6% have been deleted

The summary diagram of these species and the other high abundance species within the data set is presented (Figure 5.24a and b). It can be seen that *Achnanthes levanderi* and *Aulacoseira perglabra* (Figure 5.24a) occur mainly in the Norwegian sites and hence their presence in Table 5.6 (and not in Table 4.6) as more Norwegian sites are included in the 80 lake set. As seen in the 40 lake set many of the *Aulacoseira* species occur in higher abundances within the Norwegian lakes. Likewise many of the *Fragilaria* species tend to occur in higher abundance in the Norwegian sites, including *F. construens* var. *venter*, *F. construens*, *F. brevistriata*, and *F. robusta* (Figure 5.24b).

Tabellaria flocculosa, *Synedra rumpens*, *Achnanthes minutissima* and *Brachysira neoexilis* tend to reach higher abundances within the Scottish sites as do many of the planktonic *Cyclotella* species. It is more than likely that this is not a biogeographical feature because they are found within the Norwegian lakes also.

5.2.2 Indirect ordination analysis of the surface sediment diatom assemblages

As with the environmental data, ordination techniques were used to assess whether there are any outliers, in terms of biological assemblages, within the 79 lake data set. A DCA was conducted to calculate the gradient length and decide whether linear or unimodal ordination techniques were more appropriate for the biological data (Table 5.7).

The 79 lake data set consisted of 408 species but to limit the 'noise' within the data set species occurring at <1% abundance and occurring in <2 samples were deleted. The data set then consisted of 187 species. As with the 40 lake training set various transformation options for the diatom data were applied to see how this affected the ordinations (Table 5.7). Square root and log (x+1) transformed data resulted in shorter gradient lengths than the untransformed option. These two options also had much lower inertia and higher variance explained by both, axis 1 (λ_1), and axis 1 and 2 ($\lambda_1 + \lambda_2$). There is slightly more variance explained by the square root option and this also has a slightly lower total inertia than the log (x+1) transformation option. As with the 40 lake training set the best transformation option is to square root the species

data, which is often found to be the most appropriate option when dealing with biological data (Birks *pers. com.*).

Table 5.7: Results of the DCA analyses with different transformation options for the species data in the 79 samples, with 187 species. In all options rare species are down weighted

Type of data transformation	Gradient length (Axis 1, SD units)	Axis 1 Eigenvalue Δ_1	\sum inertia $\sum \lambda$	% variance explained λ_1	% variance explained $\lambda_1 + \lambda_2$
Square root	3.14	0.32	2.58	12.7	19.9
Log (x+1)	3.41	0.36	2.93	12.5	19.7
Untransformed	4.12	0.52	5.07	10.3	16.8

The gradient length for the square root option is 3.14 SD and this is just over the 3SD cut off level which indicates that unimodal techniques are more appropriate for the 79 lake set. The biplot of the square root DCA is presented in Figure 5.25 with envelopes displayed to show the differentiation between each country and the full summary details of DCA are displayed in Table 5.8.

The outliers, in terms of environmental variables, identified in section 5.1.2 (11, 14 and 29 sites 98-13, 98-16 and 99-50) do seem to be located away from the main cluster of the samples in Figure 5.25. However, other samples are also located away from the rest of sites. In addition the distance between these samples and the main clusters of samples is not large. In this sense it was felt it would not be appropriate to delete sites 11, 14 and 29

Table 5.8: Summary of DCA ordination, eigenvalues and cumulative % variance, of the 22 environmental variables and 79 sites, with square root transformation and down weighting of rare species.

DCA axes	1	2	3	4
Eigenvalues (λ)	0.327	0.187	0.082	0.073
Length of gradient	3.144	2.216	2.42	1.47
Cumulative percentage variance in the species data	12.7	19.9	23.1	25.9
Sum of all eigenvalues 2.586				

Axes 1 and 2 capture 19.9 % of the total diatom variance. This is less than the variance captured by axes 1 and 2 for the 40 lake training set (33%). This may be due to the fact that these data are slightly more ‘noisy’ with more sites and more species, and that unimodal methods are used instead of linear. Relatively little variance is explained by axes 3 and 4 (6%).

The diatom variance is larger for the Norwegian sites which show more dispersion across the graph than the Scottish samples (Figure 5.25). This may be related to the fact that there are simply more sites within the Norwegian set and that these sites cover a larger geographical area, possibly resulting in less homogenous environmental conditions. There is a large degree of overlap between the diatom samples for the two countries suggesting that many of the species are prevalent in both sets. It is interesting to note that discrete clusters of Norwegian and Scottish samples were evident in the environmental data (Figure 5.23), driven primarily by differences in altitude and sea salts for each country, and yet with the diatom data there is a much greater degree of overlap. This suggests that it is appropriate to merge the data sets from the two countries as they are similar floristically (see also section 2.2.4).

Sites at the positive extreme of axis 1 are 58, 41 and 30 (SC0084, CN0002 and CN0013) which all have low pH measurements (≤ 5.99 units) and relatively low calcium values ($\leq 23 \mu\text{eq/l}$). Sites 29, 12 and 13 (99-50, 98-14 and 98-15) located at the opposite end of axis 1 have pH measures of 6.78, 7.22 and 7.17 respectively and calcium measures of $1585 \mu\text{eq/l}$, $425 \mu\text{eq/l}$ and $399 \mu\text{eq/l}$ respectively. This suggests that the diatom variance associated with axis 1 is primarily driven by the variables of pH/ calcium.

Axis 2 has 76, 59 and 28 (SC0366, SC0101 and 99-44) located at the positive end of the axis and 17, 35 and 38 (98-20, CN0007 and CN0010) at the negative end. This axis seems to distinguish between sites according to altitude and JanT, which has a strong negative relationship with altitude, with 76, 59 and 28 all occurring below 1075m and having an average January temperatures above 26°F . Sites 17, 35 and 38 occur at 1461m, 1289m and 1525m representing some of the highest lakes within the training set and all have an average January temperature of 17.9°F .

In addition the sites can also be separated according to their TOC and Cl^- measures, with sites 76, 59, 64 and 28 having $\text{TOC} \geq 3.1 \text{mg/l}$ and an average Cl^- measurement of $73 \mu\text{eq/l}$. Whereas sites 17, 35 and 38 have TOC values of $\leq 0.7 \text{mg/l}$ and all have Cl^- measures of $\leq 8 \mu\text{eq/l}$. Axis 2, therefore, seems to reflect an altitudinal/ climate signal and secondly a TOC and Cl^- gradient.

In order to investigate further which variables are driving the diatom variance for the 79 lake data set the ecological preferences of the species associated with axis 1 and 2 can be investigated. The species associated with the two axes are listed in Table 5.9. The SWAP pH optimum for the species positively associated with axis 1 are between 5.1 – 5.4 pH units (Stevenson *et al.*, 1991). In contrast the *Fragilaria* species, *Navicula pseudoscutiformis* and *Achnanthes didyma*, which are negatively associated with axis 1, have SWAP pH optima of 6.3 (*F.pinnata*), 6.5 (*F.brevistriata*), 6.2 (*F.construens* var. *venter*) 6.1 and 6.3 which on average is about 1 pH unit more than the optima for the species positively associated with axis 1.

The known ecological preferences of many diatom species to climate (i.e. in terms of JanT and Altitude which are associated with axis 2) are limited at present and so interpretation of the species associated with axis 2 is more complex. Hall and Bigler (2002) have conducted some work on the responses of diatoms to lake water temperature, which is directly linked to air temperature. Their results suggest that both *Aulacoseira distans* var. *nivalis* and *Achnanthes curtissima* (species both negatively associated with axis 2) are cold water indicator species with optima of <7.0°C. In contrast they suggest that *Eunotia minor* and *Cymbella gracilis* (= *Cymbella lunata*) have water temperature optima of 9.6 and 11.1 °C respectively. This confirms the suggestion that axis 2 might partly be related to temperature. The general relationship between diatoms to climate is discussed further in section 5.3.2

DOC optima are available for some of the species from the SWAP data set, which may provide indications to the TOC preferences of the species. If the interpretation above is correct species positively associated with axis 2 should have higher DOC optima than those negatively associated with axis 2. *Tabellaria flocculosa*, *Eunotia minor* (= *Eunotia pectinalis* var. *minor* in SWAP), *Cymbella gracilis* (= *C. lunata* in SWAP) *Achnanthes pseudoswazi* have DOC optima between 5.6 and 2.9mg/l. *Aulacoseira distans* var. *nivalis*, *Navicula digitulus* and *Achnanthes helvetica* (= *Achnanthes austriaca* var. *helvetica* in SWAP) have DOC optima of 2, 1.6 and 1.5mg/l respectively. Only *Fragilaria brevistriata* does not support this trend of lower DOC optima, associated negatively with axis 2 with a SWAP optimum of 4.4mg/l.

Figure 5.25: DCA biplot of the 79 surface sample diatom assemblages, only sites are shown. Norwegian sites appear as triangles and Scottish sites as circles, envelopes are drawn around each countries samples (refer to Table 5.1 for lake number/codes)

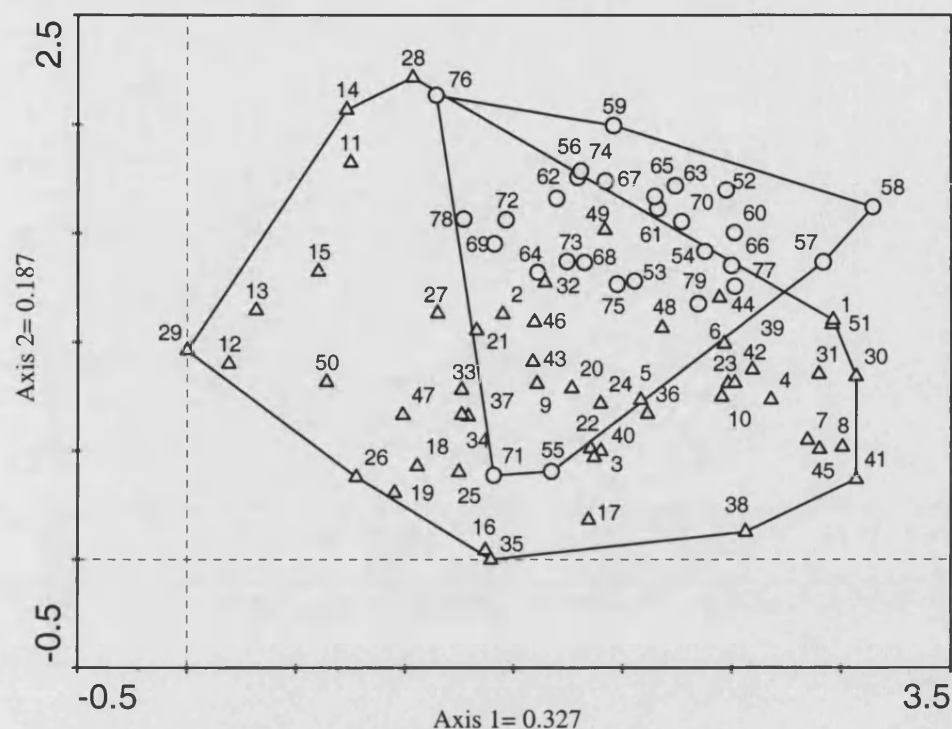


Table 5.9: Species ranking, based on their DCA ordination scores, for ordination axes 1-4

Axis 1 = 12.7 % of variance	
(+)	(-)
AC022A <i>Achnanthes marginalata</i>	FR001A <i>Fragilaria pinnata</i>
AU005E <i>Aulacoseira distans</i> var. <i>nivalis</i>	FR006A <i>Fragilaria brevistriata</i>
EU047A <i>Eunotia incisa</i>	NA013A <i>Navicula pseudoscutiformis</i>
PE002A <i>Peronia fibula</i>	FR002C <i>Fragilaria construens</i> var. <i>venter</i>
FU002B <i>Frustulia rhomboides</i> var. <i>saxonica</i>	AC039A <i>Achnanthes didyma</i>
Axis 2 = 7.2 % of variance	
(+)	(-)
BR010A <i>Brachysira neoexilis</i>	AU005E <i>Aulacoseira distans</i> var. <i>nivalis</i>
TA9997 <i>Tabellaria flocculosa</i> (short)	AC060A <i>Achnanthes curtissima</i>
EU110A <i>Eunotia minor</i>	NA149A <i>Navicula digitulus</i>
AC004A <i>Achnanthes pseudoswazi</i>	FR006A <i>Fragilaria brevistriata</i>
CM018A <i>Cymbella gracilis</i>	AC134A <i>Achnanthes helvetica</i>
Axis 3 = 3.2% of variance	
(+)	(-)
FR002B <i>Fragilaria construens</i> var. <i>binodis</i>	AC060A <i>Achnanthes curtissima</i>
NI043A <i>Nitzschia inconspicua</i>	FR064A <i>Fragilaria exigua</i>
FR001A <i>Fragilaria pinnata</i>	ND9997 <i>Naviculadicta</i> spp. 2
AC035A <i>Achnanthes pusilla</i>	NA005A <i>Navicula seminulum</i>
FR002A <i>Fragilaria construens</i>	SA001A <i>Stauroneis anceps</i>
Axis 4 = 2.8 % of variance	
(+)	(-)
AC134A <i>Achnanthes helvetica</i>	CM010A <i>Cymbella perpusilla</i>
AC013A <i>Achnanthes minutissima</i>	NA045A <i>Navicula bryophila</i>
DE001A <i>Denticula tenuis</i>	FR002C <i>Fragilaria construens</i> var. <i>venter</i>
AC134B <i>Achnanthes helvetica</i> var. <i>alpina</i>	FR002A <i>Fragilaria construens</i>
SY002A <i>Synedra rumpens</i>	NA156A <i>Navicula leptostriata</i>

It can be concluded therefore, that pH/Ca²⁺ seem to be the main driving variables, in terms of diatom variance, for the 79 lake data set with altitude, January temperature, TOC and Cl⁻ of secondary importance. The larger degree of overlap in ordination space for the biological data (Figure 5.25), as opposed to the chemical data (Figure 5.23), may be due to the fact that pH is driving the diatom variance and there is little difference between the mean pH measures for the Scottish and Norwegian lakes (pH 6.39 Norway, pH 6.31 Scotland, Figure 5.4) resulting in less spatial separation of the samples.

5.3 The relationship between the environmental and species data

Direct gradient analyses, where the samples were constrained by the environmental variables, were conducted for the 79 lake training set. The response of many of the most abundant individual taxa to a number of environmental variables was evaluated. Species responses to specific environmental variables were calculated using the HOF program as in Chapter 4. This helped identify which variables were driving the diatom variance within the data set. The techniques of forward selection and variance partitioning were applied to identify the most important environmental variables for explaining the variance within the response data.

5.3.1 Indirect gradient analysis

A DCCA was conducted initially to establish if linear or unimodal methods were more appropriate (see section 3.3.2) and the results are displayed in Table 5.10. The length of the gradient for the first axis was 3.0 which is just on the border where linear direct ordination methods are still appropriate (ter Braak 1987). An RDA was, therefore, conducted as with this method less assumptions are involved than with unimodal methods, and the results are shown in Table 5.11 and the RDA biplot is displayed in Figure 5.26.

Table 5.10: Summary results from the DCCA of 22 environmental variables, 79 sites and 187 species, with square root transformation of species data.

DCCA axes	1	2	3	4
Eigenvalues (λ)	0.261	0.157	0.060	0.041
Lengths of gradient	3.0	1.487	1.159	1.043
Species environment correlations	0.912	0.883	0.921	0.805
Cumulative percentage variance of the species data	10.1	16.2	18.5	20
of species- environment relation	23.9	38.8	0	0
Sum of all eigenvalues 2.586				
Sum of all canonical eigenvalues 1.072				

Table 5.11: Summary of RDA ordination results of 187 species in 79 samples, eigenvalues and cumulative % variance are displayed. The data were square root transformed.

RDA axes	1	2	3	4
Eigenvalues (λ)	0.132	0.086	0.052	0.027
Species- environment correlations	0.911	0.873	0.772	0.811
Cumulative percentage variance of the species data	13.2	21.8	27.1	29.8
of species- environment relation	28.2	46.7	57.9	63.7
Sum of all eigenvalues 1				
Sum of all canonical eigenvalues 0.468				

It can be seen that axes 1 and 2 explain a large proportion of the diatom variance (21.8%) and axes 3 & 4 explain relatively little variance (8%). Axis 1 independently explains 13.2% and axis 2 independently explains 8.6% indicating that the environmental variables associated with these 2 axes explain much of the diatom variance.

The variables associated with each axis are displayed in Figure 5.26. Axis 1 appears to represent a pH/ Ca^{2+} / Alk gradient and the associated co-linearity of these variables is also evident. Axis 2 is slightly more complex with several vectors, of substantial length, associated with this axis. Altitude and latitude are co-linear due mainly to the fact that the Norwegian lakes are at a higher latitude and altitude than the Scottish (hence the strong separation of samples along this gradient). JanT and ppt are also associated with axis 2 and this is due primarily to its negative relationship with altitude, the higher sites having a lower January temperature on average. In addition Cl^- , Na^+ , TOC and Mg^{2+} / Cond are also important variables for explaining the diatom variance along this gradient.

It can be seen that there is a large degree of co-linearity between certain variables with several vectors overlapping (e.g. JanT/ ppt and Cond/ Mg^{2+}) or having small acute

angles between them (pH/ Alk/ Ca^{2+}). The exclusion of some environmental variables, therefore, may be advantageous and this is discussed later.

Figure 5.26: RDA biplot of 187 species, 79 samples and 22 environmental variables. Only the environmental variables and sites/ samples are displayed. Triangles represent Norwegian sites and circles represent Scottish sites (See Table 5.1 for lake codes).

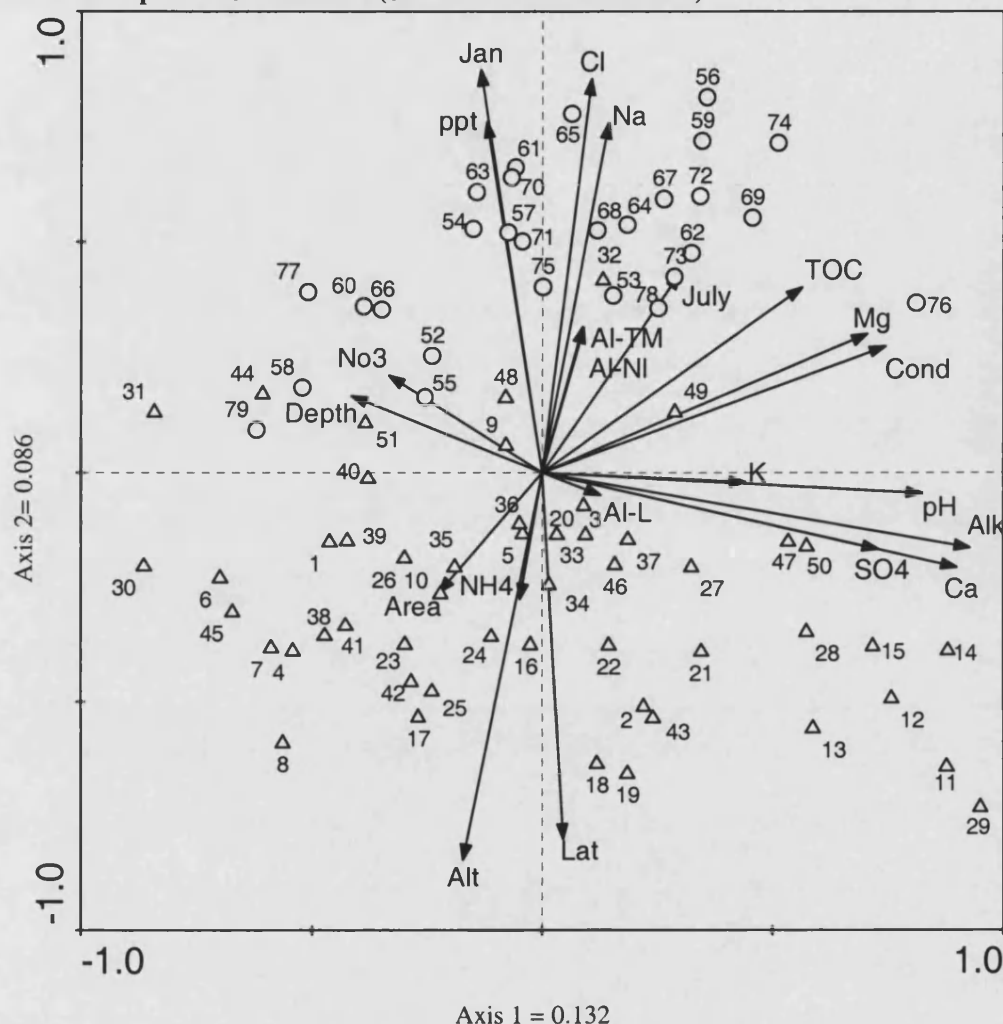


Table 5.12: Species with the highest species scores associated with axes 1 and 2 of the RDA of 79 samples and 22 environmental variables

Axis 1 = 13.2 % of variance	
(+)	(-)
AC013A Achnanthes minutissima	AC022A Achnanthes marginulata
AC003A Achnanthes microcephala	AU005E Aulacoseira distans var. nivalis
NI002A Nitzschia fonticola	AC134A Achnanthes helvetica
AC019 Achnanthes nodosa	AC134C Achnanthes helvetica var. minor
NI008A Nitzschia frustulum	AU005A Aulacoseira distans
Axis 2 = 8.6 % of variance	
(+)	(-)
FR001A Fragilaria pinnata	EU009A Eunotia exigua
FR006A Fragilaria brevistriata	TA9997 Tabellaria flocculosa (short)
FR002C Fragilaria construens var. venter	EU040A Eunotia paludosa
FR002B Fragilaria construens var. binodis	PE002A Peronia fibula
AC044A Achnanthes levanderi	EU110A Eunotia minor
	EU047A Eunotia incisa

Table 5.12 lists which species are associated with axes 1 and 2 and Figure 5.27 and 5.28 are attribute plots of these species with the environmental variables also plotted. These plots help to determine which environmental variable, or variables, the species are controlled by and to identify some of the most important environmental variables for the abundant diatom species.

Figure 5.27 shows that the species negatively associated with axis 1 show a strong tendency to be more abundant (indicated by the size of their circles) at lower pH and lower Ca^{2+} . *Achnanthes marginulata* in particular shows a strong tendency to be more abundant at lower pH/ Ca^{2+} . The signal within the species positively associated with axis 1 (*A. minutissima*, *A. microcephala* and *N. fonticola*) is less obvious because their abundances are lower but they do tend to be more common at higher pH and Ca^{2+} . *Achnanthes minutissima*, however, also seems to be responsive to higher TOC/ Cond and higher temperature levels.

Three *Fragilaria* species are associated positively with axis 2 (Table 5.12 and Figure 5.28). *F. pinnata* seems to be positively associated with altitude and, consequently more abundant at lower temperatures, but it also seems to be responsive to higher pH/ Ca^{2+} and shallower waters. Likewise *F. construens* may be responding to higher altitude and higher pH/ Ca^{2+} . There is a clear trend for *F. brevistriata* to prefer higher altitude lakes. These three species were also shown to be much more abundant within the Norwegian lakes than the Scottish lakes in Figure 5.24. Within the species negatively associated with axis 2, *Eunotia paludosa* and *Tabellaria flocculosa* [short] show a strong negative relationship with Altitude and positive relationship with JanT and TOC and Cl^- , Na^+ . The variable driving *Eunotia exigua* might be more of a lake depth/ area signal but is also associated with higher temperatures and lower altitudes. Axis 2 may also reflect a light gradient within the lakes, which is probably also associated with the TOC gradient due to the coloration of the water, unfortunately Secchi depth data are not available for the training set which could be used to investigate this further. The plots distinguish between *Fragilaria* spp., which tend to prefer clearer and relatively alkaline waters, with *Tabellaria flocculosa* and two *Eunotia* spp., which are all species that tend to favour lakes of lower pH and lower light intensities and higher DOC levels (Stevenson *et al.*, 1991; Round and Brook 1959; Enache and Prairie 2002b). *Fragilaria construens* var. *venter*, positively

associated with axis 2, is considered to be a benthic, alkaliphilous species occurring in shallow dilute lakes (Hall and Smol 1992).

5.3.2 The identification of the most important environmental variables

In order to ascertain which variables were the most important for explaining the diatom variance as a whole, constrained ordinations were performed with each environmental variable taken in turn, and the results are displayed in Table 5.13. Those with a significant response are marked with a star. It can be seen that all the environmental variables are significant in terms of explaining the diatom variance excluding Al-L. Alk/ Ca²⁺/ pH are the main variables explaining the largest amount of diatom variance with conductivity as the next most important, explaining 8.9% of the variance. The high degree of co-linearity, however, between the top three explanatory variables is illustrated in Figure 5.26.

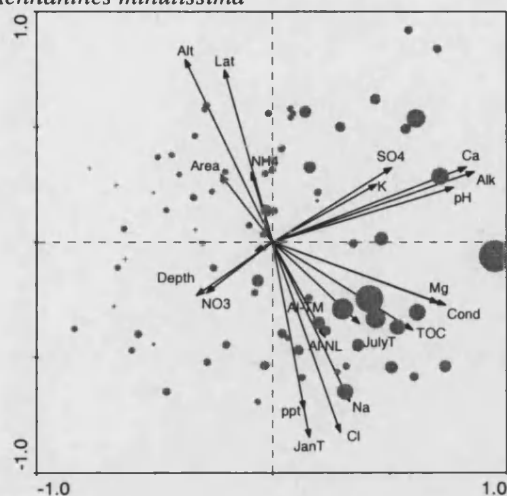
In order to try and eliminate some of the co-linear variables, and to simplify the species response signals, the Variance Inflation Factors were examined (Table 5.14). These confirmed that there is a high degree of co-linearity for many of the variables (indicated in bold type). In order to assess which variables might be substituted for one another and excluded, forward selection was performed in CANOCO (ter Braak 1988; ter Braak 1990). In essence this identifies the minimum number of variables which significantly explain the diatom variance. The results of the forward selection are displayed in Table 5.15.

Six variables were found to be significant using the forward selection technique, Mg²⁺ was the seventh variable tested and proved to be insignificant. The RDA for just these six environmental variables resulted in a variance of 19.9% explained by axes 1 and 2 (Table 5.16). In comparison when all 22 variables were included in the ordination 21.8% of the diatom variance was explained by axes 1 and 2 (Table 5.11), suggesting that a large proportion of this variance was explained by Alk, JanT, TOC, pH, Al-NL and Na⁺ alone. The RDA biplot of just these six variables is shown in Figure 5.29. There is a very clear separation by country for the diatom surface samples using only these variables.

Figure 5.27: Attribute plots of the species associated, negatively and positively, with Axis 1 of the RDA. The species' abundance in each sample are presented as proportional circles (+ indicates the species is absent within that sample)

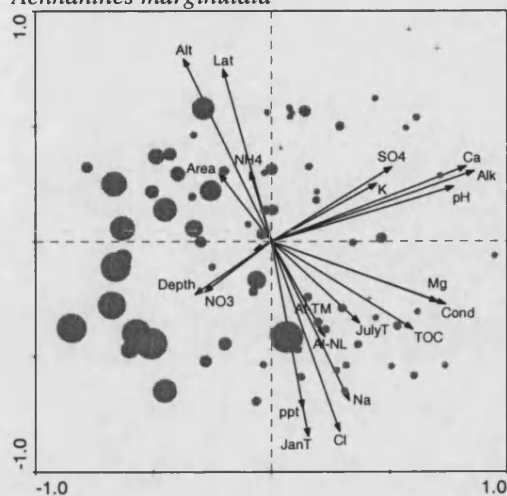
POSITIVE

Achnanthes minutissima

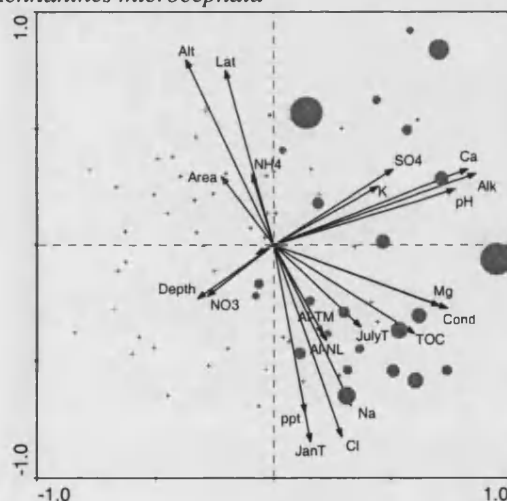


NEGATIVE

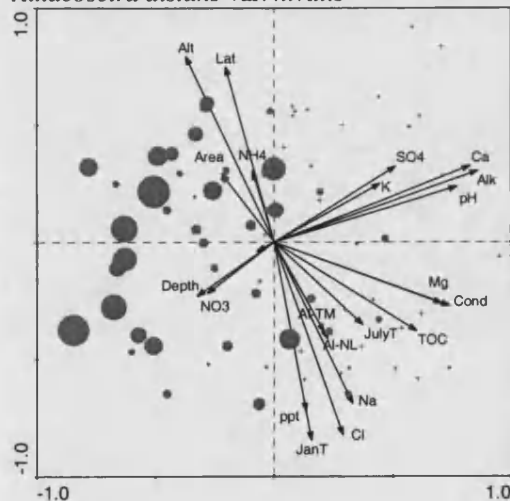
Achnanthes marginulata



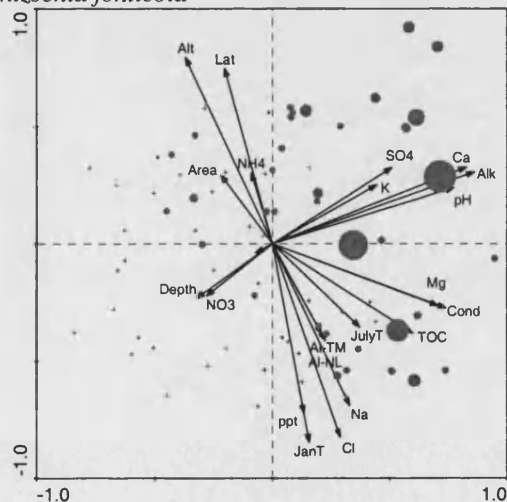
Achnanthes microcephala



Aulacoseira distans var. *nivalis*



Nitzschia fonticola



Achnanthes helvetica

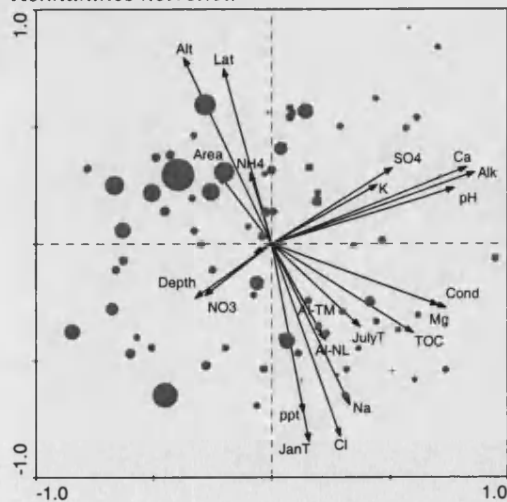
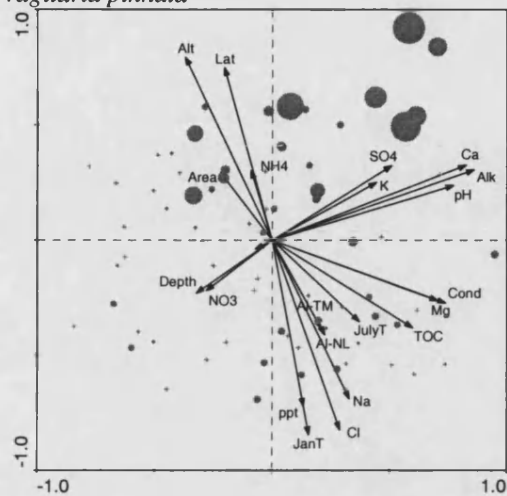


Figure 5.28 Attribute plots of the species associated, negatively and positively, with Axis 2 of the RDA. The species' abundance in each sample are presented as proportional circles (+ indicates the species is absent within that sample)

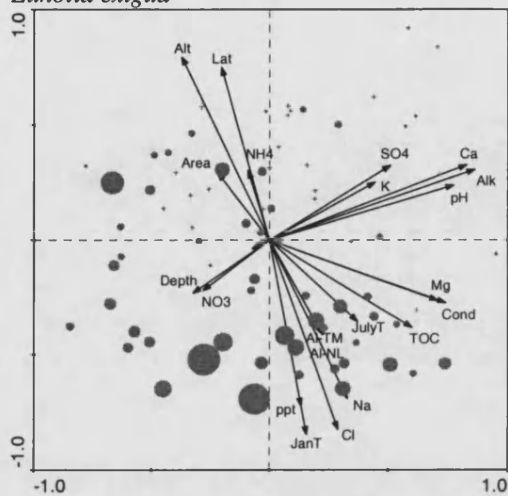
POSITIVE

Fragilaria pinnata

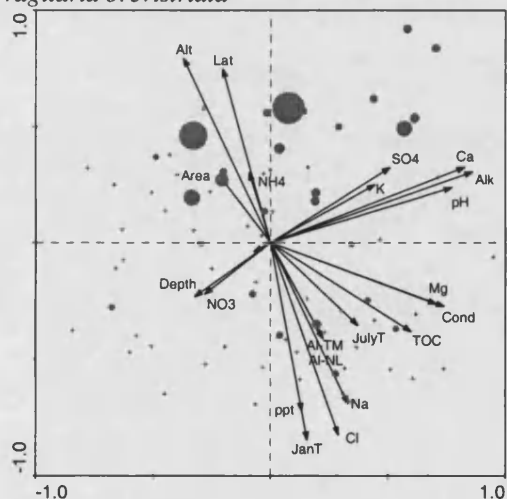


NEGATIVE

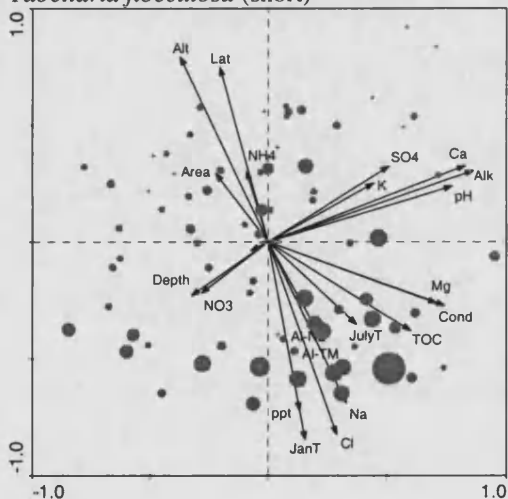
Eunotia exigua



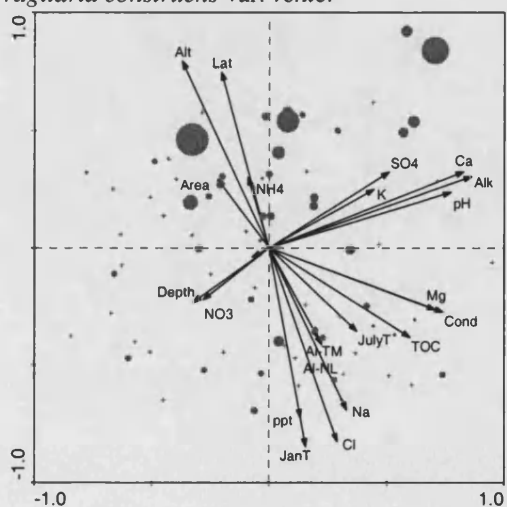
Fragilaria brevistriata



Tabellaria flocculosa (short)



Fragilaria construens var. *venter*



Eunotia paludosa

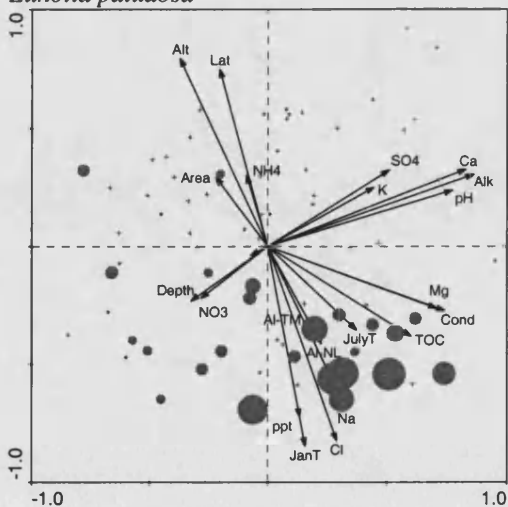


Table 5.13: Results of the RDA of diatom data for all the 79 samples constrained against each environmental variable independently. The significant variables are highlighted by * (p value ≤ 0.05) and ordered in terms of the variance explained by each.

Variable	λ_1	Species-environment correlation	% Variance explained	Significance achieved
Alkalinity	0.118	0.86	11.8	0.001*
Ca ²⁺	0.114	0.86	11.4	0.001*
pH	0.094	0.78	9.4	0.001*
Conductivity	0.089	0.81	8.9	0.001*
Mg ²⁺	0.082	0.77	8.2	0.001*
SO ₄ ²⁻	0.081	0.75	8.1	0.001*
JanT	0.071	0.80	7.1	0.001*
Altitude	0.070	0.80	7.0	0.001*
Cl ⁻	0.069	0.80	6.9	0.001*
TOC	0.068	0.75	6.8	0.001*
Lat	0.06	0.75	6	0.001*
Na ⁺	0.057	0.74	5.7	0.001*
ppt	0.056	0.72	5.6	0.001*
K ⁺	0.042	0.61	4.2	0.001*
JulyT	0.042	0.67	4.2	0.001*
Depth	0.038	0.57	3.8	0.001*
Area	0.033	0.63	3.3	0.003*
NO ₃ ⁻	0.033	0.56	3.3	0.003*
Al-NL	0.029	0.62	2.9	0.003*
Al-TM	0.027	0.57	2.7	0.003*
NH ₄ ⁺	0.021	0.61	2.1	0.04*
Al-L	0.001	0.48	1.5	0.20

Table 5.14: The Variance Inflation Factors for the RDA of 22 environmental variables (variables with VIFs above 20 are in bold type)

Variable	Weighted Average	Standard deviation	Inflation factor
Lat	59.8	2.03	16
Alt	993	295	20
Area	27.8	39.8	2.9
Depth	12.6	10.2	2.2
pH	6.3	0.51	10.6
Alkalinity	1.6	0.5	42
Conductivity	1.2	0.3	53
Na ⁺	64	67	10
NH ₄ ⁺	0.44	0.5	2.1
K ⁺	1.6	0.4	3.3
Mg ²⁺	1.3	0.3	12
Ca ²⁺	1.8	0.42	50
Cl ⁻	1.3	0.6	18
NO ₃ ⁻	0.7	0.6	1.9
SO ₄ ²⁻	1.4	0.3	7.2
Al-TM	1.6	0.59	9.9
Al-NL	1.5	0.64	8.9
Al-L	0.7	0.7	2.7
TOC	1.1	0.4	6.3
ppt	1228	602	6.1
JanT	23	7.8	39
JulyT	45	3.8	7.7

Table 5.15: Forward selection of environmental variables using RDA of 22 environmental variables. Significance of each variable was assessed using Bonferonic required significance values.

Forward selection variable	Variance explained %	F ratio	Bonferonic required significance	Significance (p-value)	
Alk	0.12	10.29	0.05/1 = 0.05	0.001	Significant
JanT	0.07	6.63	0.05/2 = 0.025	0.001	Significant
TOC	0.02	2.46	0.05/3 = 0.0166	0.002	Significant
pH	0.03	1.99	0.05/4 = 0.0125	0.002	Significant
Al-NL	0.02	2.12	0.05/5 = 0.01	0.002	Significant
Na ⁺	0.02	1.91	0.05/6 = 0.0083	0.006	Significant
Mg ²⁺	0.02	1.73	0.05/7 = 0.007	0.019	Not significant

Variance explained by all variables 0.468

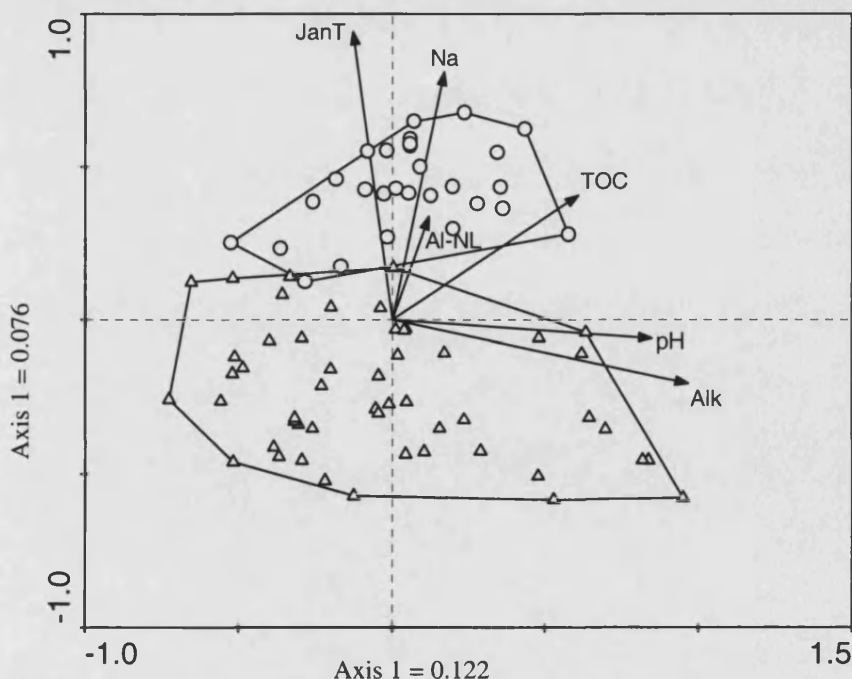
Table 5.16: RDA of 79 samples, 6 environmental variables and 187 species, with square root transformation of species data

RDA axes	1	2	3	4
Eigenvalues (λ)	0.122	0.076	0.026	0.019
Species environment correlations	0.889	0.841	0.635	0.701
Cumulative percentage variance				
Of the species data	12.2	19.9	22.5	24.3
Of species- environment relation	45.7	74.3	84	91

Sum of all eigenvalues 1

Sum of all canonical eigenvalues 0.26

Figure 5.29: RDA biplot on axes 1 and 2, with 6 environmental variables, 187 species and 79 sites. Only sites/ samples and environmental variables are displayed. Norwegian sites are represented by triangles and Scottish sites are displayed as circles, envelopes have been drawn around each.



The HOF program was used to assess further the relationship between the diatoms and these environmental variables. The results are displayed in Table 5.17. Over 70% of species have a statistically significant relationship with either Alk or pH. Few species appear to have a significant relationship with Al-NL and the variable also has a low biplot score (i.e. its vector is short in Figure 5.29). The selection of Al-NL by the forward selection technique is, therefore, surprising. There is very little difference between the number of species showing statistically significant relationships with TOC, Na⁺ and Mg²⁺ suggesting that the selection of TOC and Na⁺ as significant, rather than Mg²⁺, by the forward selection technique may be slightly arbitrary.

For Jan Temp relatively few species showed increasing sigmoidal responses (model Iii). It is interesting to note at this stage that many of the species which decreased with increasing January Temperature (i.e. potential 'cold' indicator species) were also identified as having high ice-cover optima in Chapter 4 (Figure 4.47). These included, *Aulacoseira perglabra*, *Fragilaria pinnata*, *Navicula pupula* and *Achnanthes pusilla*.

Table 5.17: Results using the HOF programme for 171 species in the data set (only species over 1% abundance with 5 occurrences or more are included in the analyses)

Taxon response model type	Alk	pH	JanT	TOC	Mg²⁺	Na⁺	Al-NL
Null model (I)	35	45	57	68	68	69	91
Sigmoidal increasing - Model (Iii)	37	31	46	7	11	17	31
Sigmoidal decreasing – Model (IId)	25	28	25	18	32	34	11
Symmetric unimodal - Model (IV)	60	52	31	38	40	36	34
Skewed unimodal - Model (V)	14	15	12	10	20	15	4
Number of species showing a significant response	136	126	114	103	103	102	80
% of species showing a significant response to the variable [(Iii+IId+III+IV+V)/171] x100	79	73	66	60	60	59	46

5.4 The development of an appropriate transfer function for climate interpretation

This section evaluates the feasibility of using the 80 lake training set to create a pH transfer function to investigate the possible relationship between climate and pH in the central Norwegian lakes (Chapters 6 and 7). The predictive strength of the model is evaluated in the next section in comparison to other pH transfer functions within the

current literature. This section also considers the feasibility of creating a January temperature reconstruction model and indicates why this might provide useful insights in to past climatic change in Norway. The actual creation of the January temperature transfer function is discussed further in section 5.4.3.

The relationship between pH changes and climate in undisturbed soft water lakes has been discussed previously (section 1.4.1.3). Due to the apparent importance of January temperature for the diatom variance (section 5.3.2 and Figure 5.29) it was thought that the feasibility of creating a January temperature transfer function should be evaluated further. Previously many studies have developed July/ mean summer air temperature transfer functions using diatom training sets (Korhola and Weckstrom 2000; Bigler and Hall 2002; Lotter *et al.*, 1997; Rosen *et al.*, 2000). Often the reason cited for reconstructing July/summer temperature is that it is highly correlated with the duration of the ice free season and epilimnetic water temperature (*c.f.* Livingstone and Lotter 1998).

The reconstruction of January air temperature and its relationship to water temperature in high altitude lakes is problematic due to the fact that the ice-cover closes the system off from the effect of air temperature oscillations. However, winter air temperature may affect the ice-cover of the lake, and therefore the lake's biology, due to its control over ice thickness, precipitation and the timing of ice break up. Livingstone (1999) demonstrated that ice break-up on Lake Baikal, during the latter part of this century, was related not only to the air temperature prevailing during thawing (April) but also to that occurring during the time of ice formation, when air temperatures are lowest (February) with lower air temperatures at this time resulting in later break up times. In addition he demonstrated that there was a significant correlation between the ice break-up dates for the lake and the North Atlantic Oscillation (NAO) index from January to March over the latter part of the last century.

In addition, Lotter *et al.*, (2002) suggested that the amount of snow accumulation on the ice has a strong influence on the length of the ice-cover on Lake Hagelseewli in the Swiss Alps. Therefore, an increase in winter precipitation, falling as snow, will increase the length of the ice-cover due to compaction. Although reconstructions of

January temperature will not provide insights in to the winter precipitation regimes it may be reflected in the biological record of a lake due to habitat changes and a change in the duration of the growing season. Winter precipitation was thought to increase in Norway during the Little Ice Age shown by the massive, and rapid, advance of glaciers recorded in both historical documents (unpublished farmers diary material, Nørdli, *pers. com.*; Grove 1988) and by the reconstruction of glacier movement through mass balance models directly relating precipitation changes to glacier advance (Six *et al.*, 2001; Nesje *et al.*, 2001; Nesje and Dahl 2003). With more winter precipitation during the LIA, a longer ice-cover period may result which might be reflected in the diatom record. In addition the milder winters occurring recently over the period of the instrumental record may result in decreases in lake ice-cover durations which again may be reflected in the diatom assemblage reconstructions (see Chapters 6 and 7).

The affect of mild winter temperatures on plankton dynamics has been studied in small lakes in Berlin (Adrian *et al.*, 1999; Adrian and Deneke 1996) and in addition these have also been linked to the NAO index in both marine environments (Reid *et al.*, 1998; Belgrano *et al.*, 1999) and lake systems (Straile and Adrian 2000). Therefore, the creation of a January air temperature transfer function may provide interesting and useful insights in to past climate variations which could also be linked to planktonic diatom abundance.

5.4.1 The feasibility of creating a pH transfer function

The feasibility of creating a pH transfer function using the 79 lake data set was assessed using variance partitioning and RDA analyses constrained by pH alone. The results of which are discussed below.

5.4.1.1 Variance partitioning of the main explanatory variables

In order to calculate the importance of pH in comparison to the other driving variables identified by the forward selection technique (section 5.3.2), variance partitioning was conducted. Variance partitioning assesses the unique contribution of each of the significant environmental variables independently of each other.

Although alkalinity was identified as an important explanatory variable for the diatom data its co-linearity with pH was highlighted earlier (Figure 5.26). In order to ascertain if pH could be substituted for Alkalinity within the variance partitioning process an RDA was run with just pH, TOC and JanT (Table 5.18). In effect this shows that pH can be substituted for Alk as the variance explained by axes 1 and 2 is 18.3% which is similar to that explained by axis 1 and 2 when all six significant variables are included ($\lambda_1 + \lambda_2 = 19.9\%$, Table 5.16). Variance partitioning was, therefore, conducted on just TOC, JanT and pH to assess the unique contribution of pH for explaining the diatom variance.

Table 5.18: RDA of 79 samples, 3 environmental variables and 187 species, with square root transformation of species data. No variance is explained by axis 4 because only three environmental variables were included in the analyses.

RDA axes	1	2	3	4
Eigenvalues (λ)	0.110	0.073	0.023	0.108
Species environment correlations	0.852	0.812	0.736	0
Cumulative percentage variance of the species data	11.0	18.3	20.5	31.3
of species- environment relation	53.5	89.0	100	0
Sum of all eigenvalues 1				
Sum of all canonical eigenvalues 0.205				

The concept of variance partitioning can be best explained by the use of a Venn diagram. The aim is to calculate the amount of variance explained for each section of diagram (Figure 5.30). So section “T” represents the variance explained uniquely by TOC. Portion “TP” is the amount of variance explained by both pH and TOC, independent of any affect of JanT, as these two circles overlap at this point in the figure. “TP”, however, is the variance explained by TOC and pH in combination excluding the variance uniquely explained by pH (Section “P”) or uniquely explained by TOC (Section “T”). The total variance for all of the three circles, i.e. when only TOC, pH and JanT are used as explanatory variables, is 20.5% (Table 5.18). The frame of the diagram represents the total variance and includes the variance explained by the other environmental factors and the unexplained variance (i.e. “U”= 100-20.5).

The RDA options involved and the results obtained in order to calculate the variance for each section are presented in Table 5.19. The calculations involved in determining the specific variance explained by each section are presented in Table 5.20. The results of the variance partitioning are summarised in Figure 5. 30.

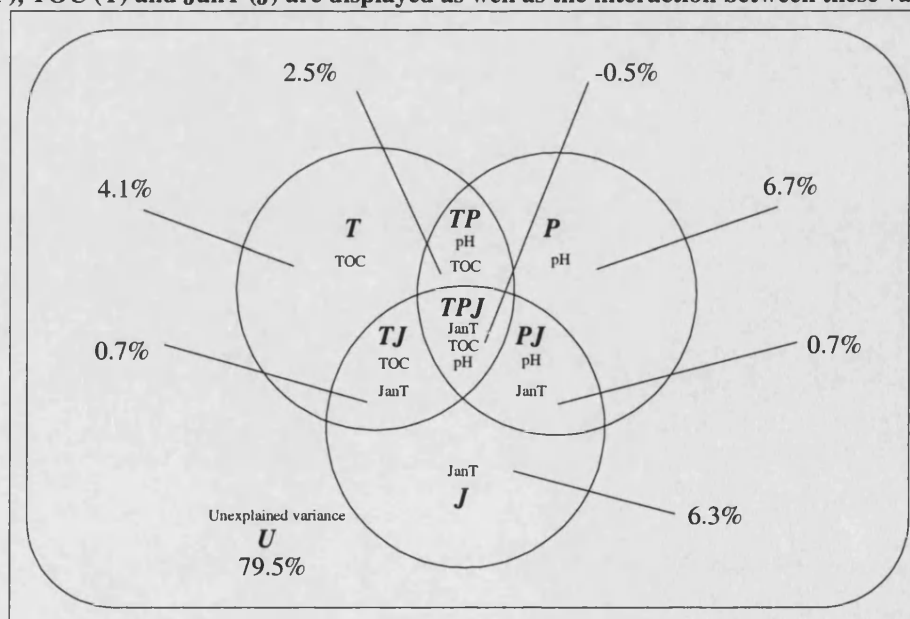
Table 5.19: The various CANOCO options involved in the calculation of the variance for each section using partial RDA (T=TOC, P=pH, J=JanT). The sum of the canonical eigenvalues and the % variance explained are listed for each option.

RDA options			Σ of all canonical eigenvalues	% variance explained
Area	Predictor variable	Co-variable		
P	P	TJ	0.067	6.7
T	T	PJ	0.041	4.1
J	J	PT	0.063	6.3
TP + P	P	J	0.092	9.2
PJ + J	J	T	0.07	7.0
TJ + T	T	P	0.048	4.8
P(total)= P+TP+PTJ+PJ	P	-	0.094	9.4

Table 5.20: The equations used for the calculation of the variance for each section displayed in Figure 5.30

Process	Results
P	0.067
T	0.041
J	0.063
TJ = (T+TJ)-T	0.048- 0.041= 0.007
PJ= (PJ+J)- J	0.07-0.063= 0.007
TP= (PT+P)-P	0.092- 0.067= 0.025
TJP= P(total)- (P+TP+PJ)	0.094-0.099= -0.005
Total explained variance= $\Sigma P+T+J+TJ+PJ+TP+TPJ$	0.067+0.041+0.063+0.007+0.007+0.025+-0.005= 0.205

Figure 5.30: A Venn diagram showing the results of the partial RDAs. The unique contribution of pH (P), TOC (T) and JanT (J) are displayed as well as the interaction between these variables.



The co-variance between TOC, pH and JanT is a negative number which indicates there is no co-variance between these variables but the sum of all the sections is still 20.5%. Negative interactions are theoretically possible (Birks *pers. com.*, *c.f.* Whittaker 1984). pH uniquely explains the most amount of the diatom variance of the three variables, with JanT as the second most important in terms of explanatory power.

5.4.1.2: Constrained RDA using only pH as the explanatory variable.

As with ice-cover, the suitability of creating a pH transfer function using the diatom response data can be assessed by looking at the ratio of λ_1/λ_2 when pH alone is constrained on the first ordination axis. The ratio between λ_1/λ_2 for the RDA with pH constrained on the first ordination axis for the 79 lake training set is shown in Table 5.21.

It can be seen that the ratio is 0.73, indicating that the 79 lake training set is appropriate for the development of a diatom pH transfer function. Although this ratio is not >1.0 many studies have reconstructed pH successfully with similar ratio values (e.g. Kingston *et al.*, 1992 with a ratio of 0.6 and Dixit *et al.*, 1991 with a ratio of 0.84, also see Hall and Smol 1992 and Bennion 1993 for reconstructions of TP with ratios of 0.4 and 0.5 respectively). The second unconstrained axis, however, is slightly higher than the first suggesting that there are also large secondary gradients in the diatom data, possibly reflecting the strong link between JanT and diatom variance shown in the variance partitioning.

Table 5.21: The results of the RDA of pH with 187 species and 79 samples. Species data are square root transformed.

RDA axes	1	2	3	4
Eigenvalues (λ)	0.094	0.128	0.092	0.077
Cumulative percentage variance of the species data	9.4	22.1	31.4	39.1
Sum of all eigenvalues 1				
Sum of all canonical eigenvalues 0.094				
Ratio of λ_1/λ_2 (0.094/0.128)	0.73			

5.4.2 The pH transfer function

The last sections have shown the relative importance of pH for describing the diatom variance within the 79 lake training set. One of the ecological assumptions of

quantitative environmental reconstruction using diatoms is that the variable to be reconstructed should be ecologically important to, or linearly related to an ecologically important variable controlling diatom composition. This has been established in the previous section for this data set and is also evident within the literature (Battarbee and Renberg 1990; Stevenson *et al.*, 1991; Charles 1985). Therefore, the creation of a pH transfer function is justified.

Various methods to quantify the relationship between the species and the environment can be used to generate a transfer function (see section 3.3.3). The methods of WA, WA_(tol), PLS and WA-PLS, using the CALIBRATE programme (Juggins and ter Braak 1993), were compared and the results are presented in Table 5.22 and 5.23. WA_(tol) resulted in the lowest RMSEP (0.328 pH units) and the highest R²_{jack} (see section 3.3.3). In WA_(tol) analysis two de-shrinking coefficient options are available, inverse and classical de-shrinking. Inverse de-shrinking tends to pull inferred values towards the mean of the pH gradient which can lead to an overestimation of pH at the low end of the gradient and an underestimation of values at the high end of the gradient. Inverse de-shrinking generally results in a lower RMSEP value but classical de-shrinking might be more appropriate if the sites to be used for the reconstruction are likely to have reconstructed values that occur at the extremes of the gradient (Birks *pers. com.*). For example, if pH was to be reconstructed with a training set that contained lakes with pH ranging from 5.4- 7.6 units and the sites for reconstruction had modern day pH of ≥ 7 , and were unlikely to have experienced much lower pH conditions in the past, classical de-shrinking might be more applicable.

Table 5.22: A comparison of WA and WAtol calibration and prediction techniques for pH for the 79 lake training set. Analyses were conducted on square root transformed species data and untransformed pH data. De-shrinking using the inverse approach was used

Prediction	RMSE	R ²
WA	0.2855	0.66
WA tol	0.28	0.67
Calibration	RMSEP	R ² _{jack}
Cross Val WA	0.353	0.48
Cross Val WA tol	0.328	0.55

WA and WA_(tol) were calculated using classical de-shrinking and the results are presented in Table 5.24. The RMSEP does increase slightly with the classical de-shrinking co-efficient but the R²_{jack} value also increases. For both de-shrinking co-

efficients the predictive power of the $WA_{(tol)}$ model is displayed in Figure 5.31 by plotting the predicted (jack-knifed) pH against the measured pH. Both methods show a strong correlation between the measured and the predicted pH.

Table 5.23: The results of the PLS and WA-PLS calibration and prediction techniques for pH for the 79 lake training set. Analyses were conducted on square root transformed species data and untransformed pH data.

PLS			WA-PLS		
Apparent errors of estimation			Apparent errors of estimation		
No of components	RMSE	R^2	No. of components	RMSE	R^2
1	0.27	0.69	1	0.28	0.66
2	0.17	0.87	2	0.19	0.83
3	0.11	0.94	3	0.14	0.91
4	0.08	0.97	4	0.11	0.94
5	0.05	0.98	5	0.09	0.96
6	0.03	0.99	6	0.07	0.97
Prediction errors			Prediction errors		
No. of components	RMSEP _{jack}	R^2_{jack}	No. of components	RMSEP _{jack}	R^2_{jack}
1	0.38	0.47	1	0.35	0.48
2	0.38	0.50	2	0.38	0.45
3	0.43	0.44	3	0.4	0.41
4	0.45	0.42	4	0.4	0.40
5	0.46	0.42	5	0.41	0.39
6	0.46	0.43	6	0.41	0.38

Figure 5.32a and b display the differences ('residuals') between the $WA_{(tol)}$ predicted pH and the measured pH, against measured pH for both the inverse and classical methods of reconstruction. There is a slight tendency, when using the inverse de-shrinking coefficient, for the predicted values to be slightly overestimated at low measured pH and underestimated at high measured pH (Figure 5.32a). With the classical de-shrinking coefficient this bias is eliminated as the de-shrinking coefficient no longer pulls inferred pH values towards the mean of the gradient which occurs with inverse de-shrinking. Clearly one sample is overestimated (98-14, Figure 5.32b) when that sample is left out of the data set cross validation (i.e. in the jack-knifing process which generates the predicted pH values). The reasons for this are probably due to the fact that the diatom assemblage for this site is dominated by two species, *Fragilaria construens* var. *venter* and *Fragilaria robusta* (39.8%). *F. robusta* does not occur in many of the other sites within the training set (Figure 5.24b) which may account for the high error associated with the reconstructed pH for this site. The model was remade excluding this site but its explanatory power did not improve significantly. The sites to be used for the reconstruction are discussed in chapters 6 and 7 and the suitability of using classical or inverse de-shrinking is evaluated further within these chapters.

Table 5.24: A comparison of WA and WA(tol) calibration and prediction techniques for pH for the 79 lake training set. Analyses were conducted on square root transformed species data and untransformed pH data. De-shrinking using the classical approach was used.

Prediction	RMSE	R ²
WA	0.351	0.66
WA tol	0.341	0.673
Calibration	RMSEP	R ² jack
Cross Val WA	0.402	0.49
Cross Val WA tol	0.341	0.56

Figure 5.31: Measured pH with WA(tol) predicted pH using a) inverse de-shrinking b) classical de-shrinking coefficients, with lowess smoother plotted.

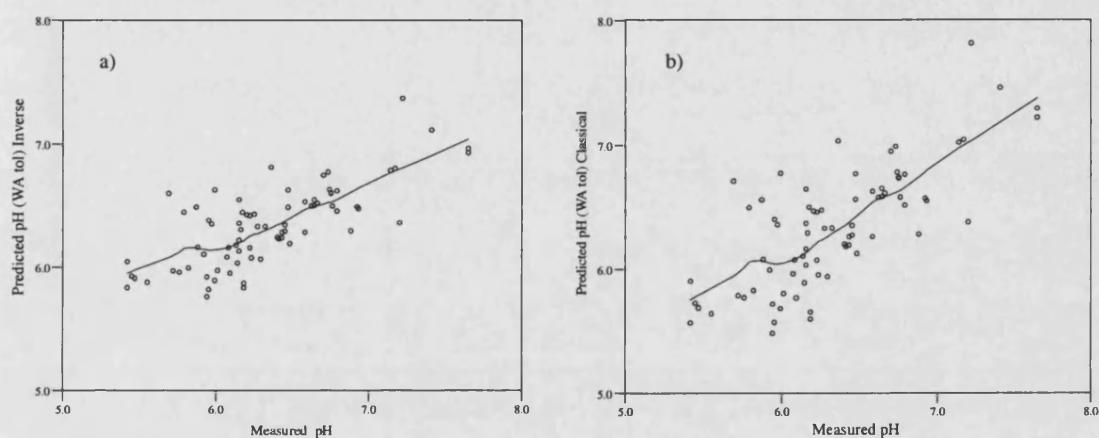
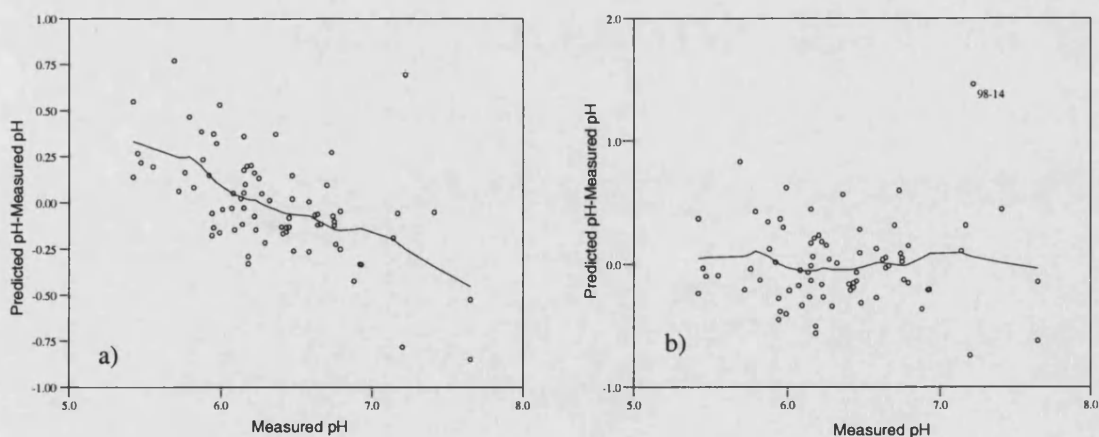


Figure 5.32: a) Plot of predicted – measured pH, against measured pH, using WA(tol) with inverse de-shrinking b) Plot of predicted- measured pH, against measured pH, using WA(tol) with classical de-shrinking, with lowess smoother plotted.



5.4.2.1. A comparison of pH inference models

Table 5.25 shows various results derived from other pH calibration transfer functions within the literature in comparison with the transfer function developed above. It can

be seen that the present study compares favourably in terms of RMSEP with other pH inference models. The R^2 is slightly less than many of the studies mentioned but this might be a function of the smaller size of the data set and the smaller pH gradient within this 79 lake data set in comparison with some of the other studies. It can be concluded, however, that the pH transfer function created from this data set is robust and has a good predictive ability.

Table 5.25: Summary of selected pH calibration transfer functions in comparison to the one generated from the 79 lake training set used in this study.

Training set	Number of sites	pH range	Best performing method if compared	R2	RMSEP
(Stevenson <i>et al.</i> , 1991) (Birks <i>et al.</i> , 1990)	167	4.3- 7.2	WA(tol)	0.941	0.278
(Cameron <i>et al.</i> , 1999a)	118	4.5-8	WA-PLS	0.82	0.33
(Cumming <i>et al.</i> , 1992)	71	4.4- 7.8	WA	0.91	0.35
(Enache and Prairie 2002b)	164	4.2- 8	WA-PLS	0.93	0.25
(Bigler and Hall 2002)	99	5.79- 8.07	WA-PLS	0.77	0.19
(Philibert and Prairie 2002;Enache and Prairie 2002a)	76	4.16-8	WA-PLS	0.91	0.42
(Weckstrom <i>et al.</i> , 1997)	37	5-7.7	WA(tol)	0.91	0.39
This study	79	5.4-7.65	WA (tol)	0.67	0.32

5.4.2.2 Individual species responses to pH

Figure 5.33 shows the optima and tolerances generated for all the species which were found to have a statistically significant relationship with pH using the HOF program, using both WA and ML methods for the generation of the optima and tolerances. There are several discrepancies between the results produced by the two methods. There is a higher degree of agreement for species with optima of between 6-7.0 pH, representing the mid-range area of the pH gradient. There is less agreement between the two methods for the extremes of the pH gradient.

Possible reasons for this might be that simple WA is sensitive to the distribution of the environmental variable in the training set (ter Braak *et al.*, 1993; ter Braak and Looman 1986). The pH optima generated by ML are in theory less sensitive to the

distribution of the environmental variable than in WA estimation (ter Braak and Looman 1986). However, ML also has weaknesses in that it is more influenced by distribution of zero values in the biological data (Cameron *et al.*, 1999b), these zeros are ignored by WA methods.

ML failed to generate pH optima for 29 species (plotted as blanks in Figure 5.33), of these two had a Model V response using HOF and 27 had either Model II increasing or Model II decreasing responses (see Figure 5.33, the model associated with each species is presented in brackets). This pattern of failure to converge for the monotonic response models occurred for the ice-cover optima also, again suggesting that ML works best when the species response is symmetrical Gaussian (Model IV) in distribution, due to the models underlying assumptions (i.e. based on Gaussian logistic regression). In addition for those species with very different ML optima and WA optima (such as *Cymbella minuta*, *Cymbella cesatii*, *Achnanthes ventralis*, *Cyclotella* aff. *comensis* and *Achnanthes helvetica*) many of these had monotonic Model II increasing or decreasing responses (see Section 4.4.4 for further discussion of the problems with defining optima for sigmoidal responses).

Comparisons of the optimum generated by the ML and WA methods were also explored by Cameron *et al.*, (1999) for the AL:PE data set. Large discrepancies between the two methods also occurred within this data set (e.g. pH optima *Achnanthes levanderi* ML-7.57, WA- 6.52, *Brachysira brebissonii* WA-6, ML-4.98, *Fragilaria pinnata* WA-7.13, ML- 8.25, *Eunotia naegelii* WA- 5.33, ML- 3.47).

When pH optima for individual species are compared *between* data sets, which have been derived from the WA method only, there are also large variations in results. Table 5.26 compares the optima generated for some of the most abundant species within this data set with their optima generated by previous pH diatom training sets using WA. There is a high degree of disagreement, in terms of the pH optima generated, between the studies. Many of the species listed have a pH optima variance of over 1 pH unit, for example *Achnanthes marginulata* (1.76), *Aulacoseira distans* var. *nivalis* (1.6) and *Frustulia rhomboides* var. *saxonica* (1.69).

Figure 5.33: A comparison of pH optima and tolerances produced using Weighted Averaging (WA) and Maximum Likelihood (ML) for the 126 species found to have a statistically significant relationship with pH (species with pH optima < 5.4 overleaf).

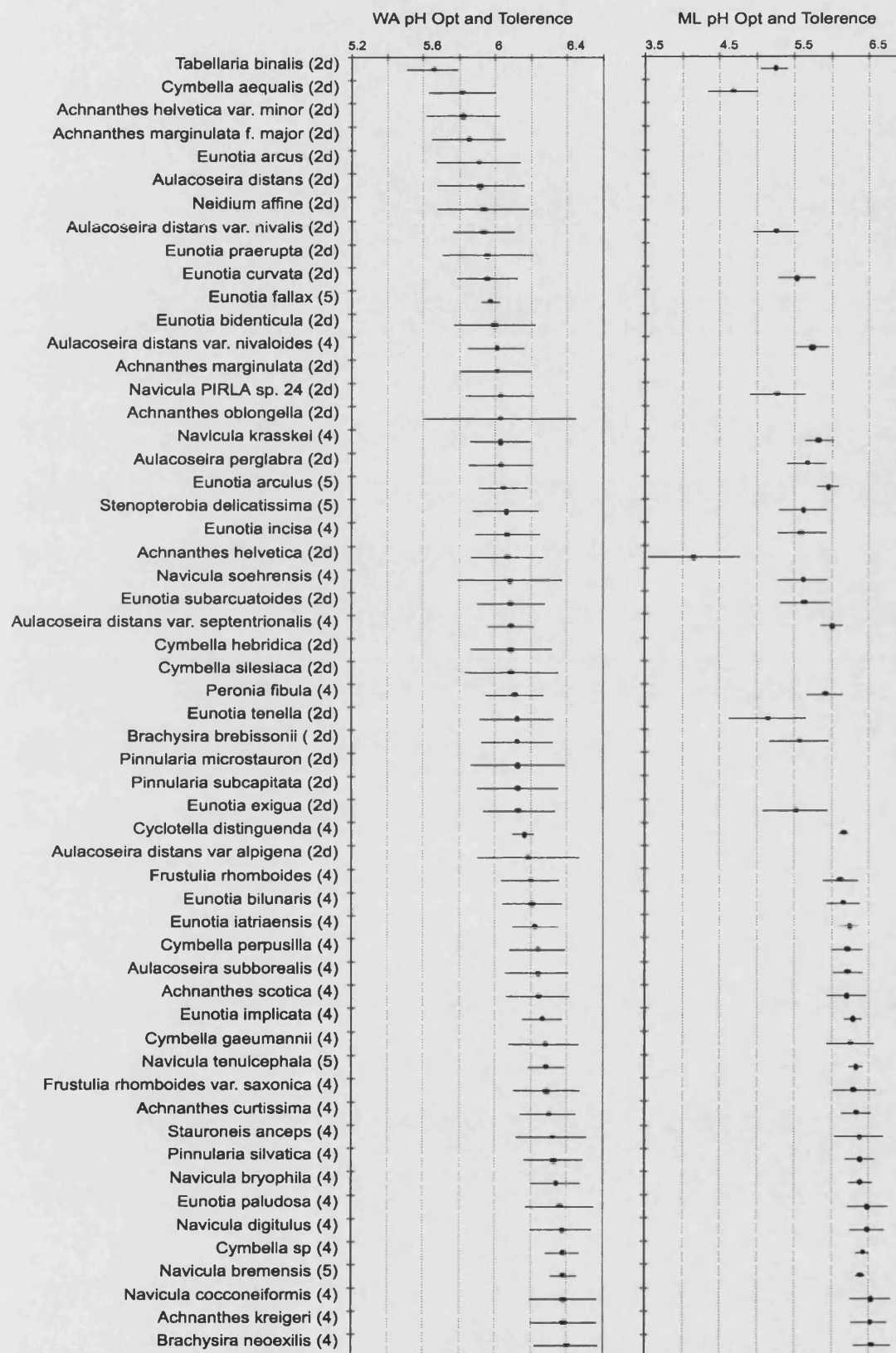
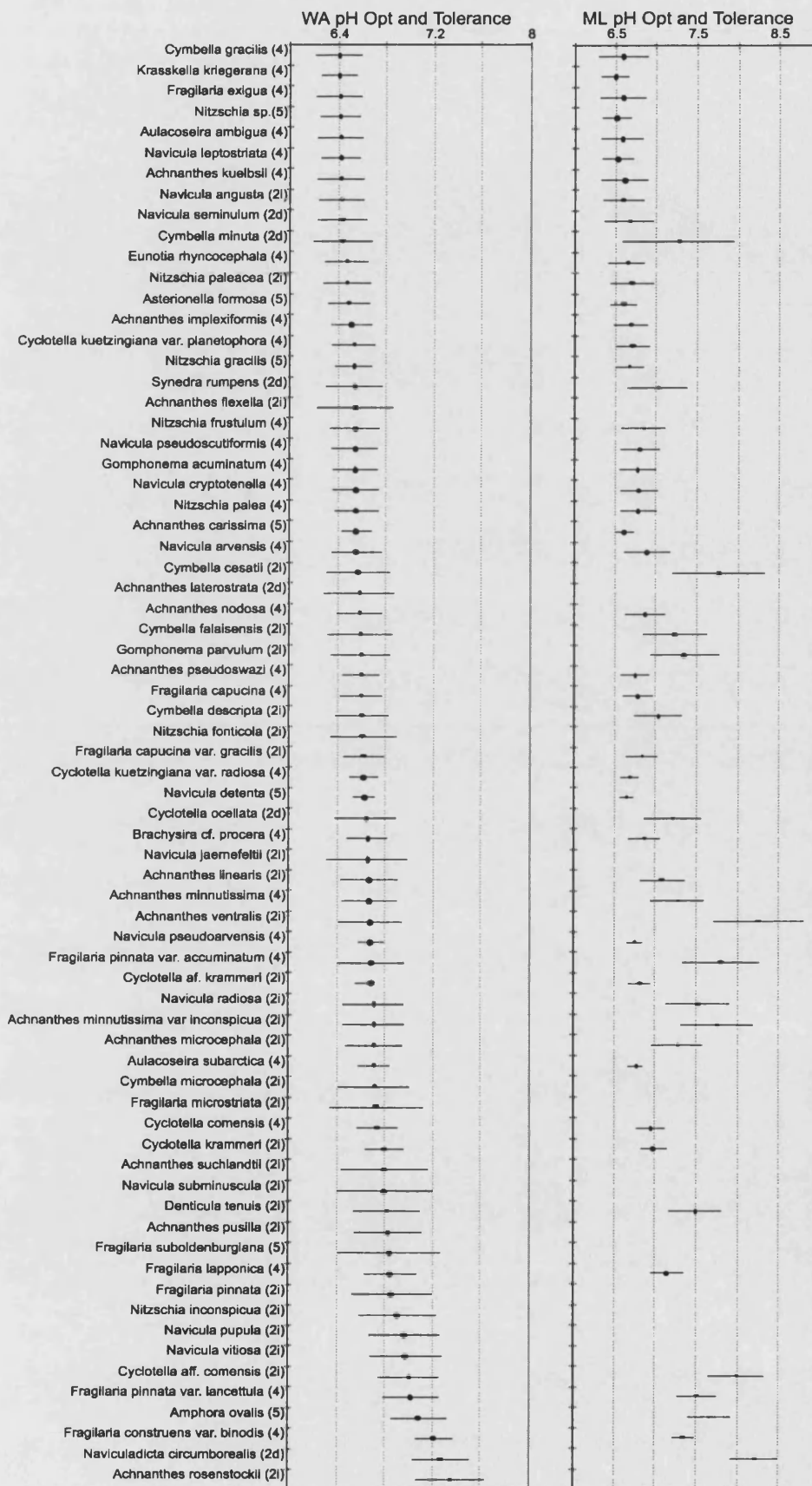


Figure 5.33 continued, species <5.4 displayed below



It is realised, however, that although the species are abundant within this data set they may not be as abundant within the data sets used for comparison which may affect the accuracy of the pH optima generated for these species (Kent and Coker 1992). Rarer species may have pH optima which have larger standard errors and associated confidence intervals, than the more abundant species within a given data set (ter Braak and Looman 1986). In addition many of the data sets have similar *ranks* of pH optima with, for example, *Fragilaria pinnata* and *Fragilaria construens* var. *venter* often having the two highest pH optima despite the fact that the actual values may be different. This suggests that when WA is used to reconstruct pH, the trends within the reconstructions should be similar albeit if the actual reconstructed values differ depending on which training set is used.

Similar discrepancies, however, were also found by Cameron *et al.*, (1999) when comparing species optima generated by the SWAP and AL:PE project using just the WA method. The reasons for these discrepancies were unclear, but the necessity of the development of different pH diatom training sets for lakes situated within the potential forest limit (SWAP) and for those located above the forest limit (AL:PE) was highlighted. The authors also suggested that there was a need for a critical approach to the generation of WA pH optima by using the ML method as a comparison. A high level of agreement, however, between the optima generated by ML and WA within this study was not achieved.

In conclusion, therefore, it would appear that there are discrepancies between the species pH optima generated when using the WA and ML methods (Figures 5.32). There are also large variations in the WA pH optima generated by different training sets (Table 5.26). The strong tendency for the WA optima to be over or under estimated might be related to the differing distributions of pH values within each data set and the variation in median pH for each set. The generation of pH species optima seems to be very dependent on the reconstruction methods used, the differences in the ranges of pH within the training set and the geographical location of the study. This highlights the advantages of developing a pH transfer function, which will be applied to sites within the same geographical area from which the training set is derived.

Table 5.26: Species pH optima generated for the 25 most abundant species within this data set using the 79 data set presented (current study) in comparison with similar studies within the current literature also using the WA technique (n/s- not significant using HOF programme, n/p- not present or presented within the data set/ paper, n/g- found but no optima generated/given). The maximum variance (i.e. the max optima – the min optima) within the data sets is presented in the last column.

Taxon	Current study	Various European SWAP (Stevenson <i>et al.</i> , 1991)	Quebec, Canada (Enache and Prairie 2002b)	Swedish Lapland (Bigler and Hall 2002)	Quebec (Philibert and Prairie 2002)	Subarctic Fennoscandia (Weckstrom <i>et al.</i> , 1997)	Various Europe (Cameron <i>et al.</i> , 1999a)	Variance within the pH optimum (max-min)
<i>Achnanthes marginulata</i>	6.0	5.2	n/p	n/g	n/p	6.96	5.71	1.76
<i>Achnanthes curtissima</i>	6.2	n/p	n/p	6.63	n/p	7.35	n/p	1.15
<i>Fragilaria exigua</i>	6.4	5.7	5.89	6.38	6.74	7.02	6.27	1.32
<i>Achnanthes minutissima</i>	6.6	6.3	6.7	>7.46	6.72	7.3	6.63	1.16
<i>Achnanthes helvetica</i>	6.0	5.4	n/p	n/g	n/p	6.92	5.9	1.52
<i>Frustrulia rhomboides</i>	6.19	5.1	4.5	6.01	n/p	6.17	5.75	1.69
<i>Brachysira neoexilis</i>	6.39	n/p	n/p	n/p	n/p	n/p	n/p	n/a
<i>Aulacoseira distans</i> var. <i>nivalis</i>	5.94	5.0	6.59	6.12	6.6	6.66	5.58	1.6
<i>Achnanthes altaica</i>	n/s	5.7	n/p	<5.79	n/p	6.97	n/p	1.27
<i>Tabellaria flocculosa</i> (short)	n/s	5.4	6.0	<5.79	5.9	6.63	5.69	1.23
<i>Fragilaria construens</i> var. <i>venter</i>	n/s	6.2	6.9	n/g	6.27	7.13	6.69	0.93
<i>Achnanthes scotica</i>	6.2	5.6	n/p	6.42	n/p	n/p	6.06	0.82
<i>Aulacoseira distans</i>	5.91	5.4	6.5	n/g	6.5	n/p	n/p	1.1
<i>Aulacoseira perglabra</i>	6.0	5.2	4.7	n/g	5.3	n/p	n/p	1.3
<i>Achnanthes subatomoides</i>	n/s	n/p	6.51	n/g	n/p	7.17	n/p	0.66
<i>Cyclotella kuetzingiana</i> var. <i>planetophora</i>	6.5	6.3 (sp.agg.)	n/p	n/p	n/p	n/p	n/p	0.2
<i>Fragilaria construens</i>	n/s	6.6	7.9	n/p	7.0	7.21	n/p	1.3
<i>Achnanthes levanderi</i>	n/s	5.6	n/p	n/g	n/p	7.27	6.52	1.67
<i>Brachysira brebissonii</i>	6.12	5.3	5.9	6.3	6.0	6.8	6	1.5
<i>Eunotia incisa</i>	6.06	5.1	5.8	n/g	6.14	6.36	5.48	1.26
<i>Frustrulia rhomboides</i> var. <i>saxonica</i>	6.28	5.2	5.4	5.82	4.59	6.2	5.74	1.69
<i>Peronia fibula</i>	6.11	5.3	n/p	n/p	n/p	n/p	5.34	0.81
<i>Aulacoseira distans</i> var. <i>septentrionalis</i>	6.09	n/p	n/p	n/p	n/p	n/p	n/p	n/a
<i>Fragilaria pinnata</i>	6.85	6.3	7.19	6.99	6.69	7.22	7.13	0.92
<i>Cymbella gracilis</i>	6.4	5.7	6.2	6.45	6.17	6.84	6.02	1.14

5.4.3 The feasibility of creating a January air temperature transfer function

The strong relationship between January air temperature and the diatom species was demonstrated in section 5.4.1 and through the variance partitioning analysis, where it was identified as explaining 6.3% of the diatom variance independently. An RDA analysis constrained by January temperature as the only explanatory variable was conducted (Table 5.2). The suitability of creating a January air temperature transfer function can again be assessed by looking at the ratio of λ_1/λ_2 when January temperature is constrained on the first ordination axis. This ratio is 0.43 which is significantly lower than that achieved when pH was constrained on the first ordination axes (0.73). In addition the eigenvalue for axis 2 is also substantially higher than that for axis 1, suggesting that there are other important explanatory variables for the diatom variance on the second axis, probably reflecting the strong pH gradient.

Other variables have been reconstructed with low ratios as discussed in 4.4.4 (e.g. TP $\lambda_1/\lambda_2 = 0.40$ - Hall and Smol 1992, DOC $\lambda_1/\lambda_2 = 0.21$ - Dixit *et al.*, 1993, Surface water temperature $\lambda_1/\lambda_2 = 0.5$ - Pienitz *et al.*, 1995) and the variable was selected by the forward selection technique as being important in describing a large proportion of the diatom variance. It was decided, therefore, that a January temperature transfer function would be produced to assess the errors incurred with the reconstruction and to provide qualitative inferences about climate change which could be used in conjunction with the pH transfer function (Chapters 6 and 7).

Table 5.27: The results of the RDA of January temperature with 187 species and 79 samples. Species data are square root transformed.

RDA axes	1	2	3	4
Eigenvalues (λ)	0.071	0.163	0.098	0.068
Cumulative percentage variance of the species data	7.1	23.4	33.2	40
Sum of all eigenvalues 1				
Sum of all canonical eigenvalues 0.071				
Ratio of λ_1/λ_2 (0.071/0.163)	0.43			

5.4.3.1 The January air temperature transfer function and comparison with other air temperature transfer functions

As with pH the methods of WA, WA_(tol), PLS and WA-PLS were used to model the relationship between January air temperature and the diatom species assemblages, and

the results are displayed in Table 5.28 and 5.29. The R^2 and R^2_{jack} for WA and WA_(tol) compare favourably with the pH transfer function developed in section 5.4.2 (pH WA_(tol) $R^2 = 0.67$ and $R^2_{\text{jack}} = 0.55$). However it is the WA-PLS three component model which results in the lowest prediction errors ($\text{RMSEP}_{\text{jack}} = 2.2^\circ\text{C}$) and the highest R^2_{jack} (0.71) and this performs significantly better than either the one or two component models. Therefore, it is this model which is selected for use within Chapters 6 and 7.

Table 5.28: A comparison of WA and WA (tol) calibration and prediction techniques for January air temperature for the 79 lake training set. Analyses were conducted on square root transformed species data and untransformed January air temperature data. De-shrinking using the inverse approach was used. RMSE are expressed as $^\circ\text{C}$.

Prediction	RMSE	R^2
WA	2.3	0.70
WA tol	2.2	0.72
Calibration	RMSEP	R^2_{jack}
Cross Val WA	3.0	0.52
Cross Val WA tol	2.9	0.54

Table 5.29: The results of the PLS and WA-PLS calibration and prediction techniques for January air temperature for the 79 lake training set. RMSE are expressed as $^\circ\text{C}$. Analyses were conducted on square root transformed species data and untransformed January air temperature data.

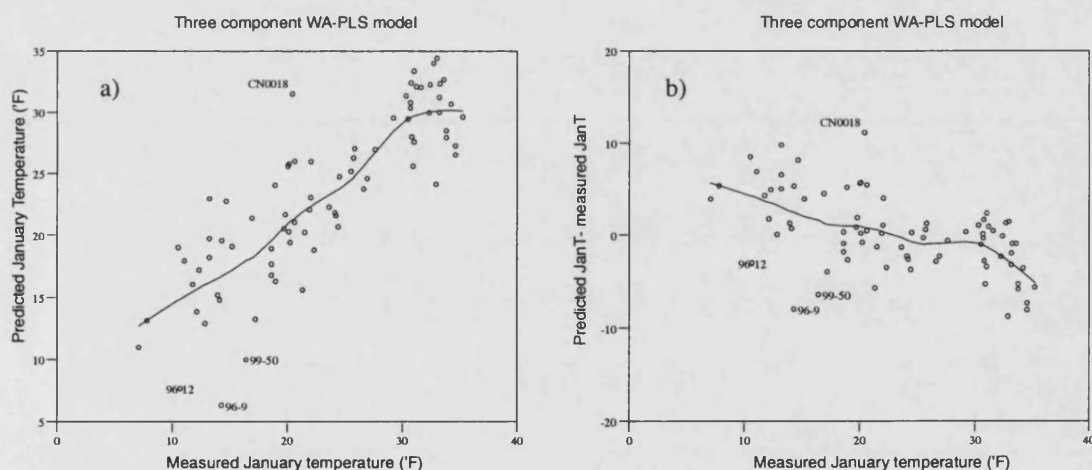
PLS			WA-PLS		
Apparent errors of estimation			Apparent errors of estimation		
No of components	RMSE	R^2	No. of components	RMSE	R^2
1	2.4	0.68	1	2.3	0.7
2	1.6	0.85	2	1.5	0.87
3	1.1	0.93	3	1.1	0.92
4	0.8	0.96	4	1.0	0.94
5	0.6	0.97	5	0.8	0.95
6	0.5	0.98	6	0.77	0.96
Prediction errors			Prediction errors		
No. of components	$\text{RMSEP}_{\text{jack}}$	R^2_{jack}	No. of components	$\text{RMSEP}_{\text{jack}}$	R^2_{jack}
1	3.2	0.48	1	3	0.52
2	3.1	0.55	2	2.5	0.66
3	3.3	0.55	3	2.2	0.71
4	3.4	0.55	4	2.3	0.7
5	3.5	0.52	5	2.4	0.7
6	3.8	0.48	6	2.5	0.68

The predictive power of the model is presented in Figure 5.34a in which the diatom predicted January temperatures are plotted against the measured January temperatures

and the model residuals are plotted (Predicted JanT – measured JanT) against the measured January temperatures in Figure 5.34b. It can be seen that the model overestimates January temperature for site CN0018 and underestimates January temperatures for sites 99-50, 96-9 and 96-12. The model, therefore, was re-made with these sites excluded but its predictive power did not increase significantly and subsequently the sites were retained.

It can be seen that the model slightly overestimates January temperature at the lower end of the gradient and slightly underestimates January temperature at the upper end of the gradient. This should not prove to be a problem if the sites to be reconstructed are not at the extremes of the January temperature gradient (see Chapters 6 and 7).

Figure 5.34: Plots of measured January Temperature (°F) using WA-PLS (3 components) against a) predicted January temperature (°F) and b) predicted January temperature- measured January temperature (the residuals).



As with pH the predictive power of the transfer function was compared with other available air temperature transfer functions (Table 5.30). The comparisons are limited, however, due to the small number of published diatom air temperature transfer functions. It can be seen that the current study compares favourably in terms of R^2_{jack} and λ_1/λ_2 ratio. However, the errors incurred are higher than many of the previous studies. It was decided that the transfer function would be applied down core in Chapters 6 and 7 in order to make qualitative inferences about past climate (i.e. indicating phases of warmer or colder climate) but any reconstructed temperature

values should be treated with caution. This technique was not considered robust enough for the absolute reconstruction of past temperatures.

Table 5.30: Summary of selected diatom air/ water temperature calibration transfer functions in comparison to the one generated from the 79 lake training set used in this study

Training set	No. of sites	Temperature Range	Best performing method if compared	λ_1 / λ_2	R^2_{jack}	RMSEP
Air temperature reconstruction						
(Lotter <i>et al.</i> , 1997)	68	7-20.6 °C Mean summer temp	WA-PLS (2)	1.4	0.79	1.6 °C
(Bigler and Hall 2002)	100	7-14.7 °C Mean July air temp	WA-PLS	0.39	0.75	0.96 °C
(Korhola and Weckstrom 2000)	38	7.9-14.9 °C Mean July air temp	WA-PLS (2)	0.86	0.78	0.9-1.1 °C
(Rosen <i>et al.</i> , 2000)	50	7.5- 15 °C Mean July air temp	WA-PLS	0.39	0.62	0.86 °C
This study	79	-13.8 to 1.7 °C Mean January air temperature	WA-PLS (3)	0.43	0.71	2.2 °C
Water temperature reconstruction						
(Pienitz <i>et al.</i> , 1995)	59	12-23.4 °C Lake surface water temp	WA	0.5	0.63	2.0 °C (Classical deshrinking) 1.84 °C (Inverse deshrinking)

5.4.3.2 The individual response of species to January air temperature

The individual species responses to January temperature are presented in Figure 5.35. Several species groupings are evident with many *Fragilaria* species having lower January temperature optima than the *Eunotia* and *Cyclotella* species which tend to have optima between >-2.5°C. The placement of planktonic species at the higher end of the temperature range was also found by Pienitz *et al.*, (1995) and may support the proposed relationship between plankton abundance (i.e. the *Cyclotella* species) and water temperature/ ice-cover evident within the literature (section 1.3). The prevalence of small benthic taxa, such as *Achnanthes levanderi*, *Fragilaria pseudoconstruens* and *Fragilaria brevistriata* at the lower end of the temperature gradient is also supported by other studies (Pienitz *et al.*, 1995).

Figure 5.35: January temperature optima and tolerances produced using Weighted Averaging (WA) for the 114 species found to have a statistically significant relationship with January temperature (species with JanT optima > 5.9°C overleaf).

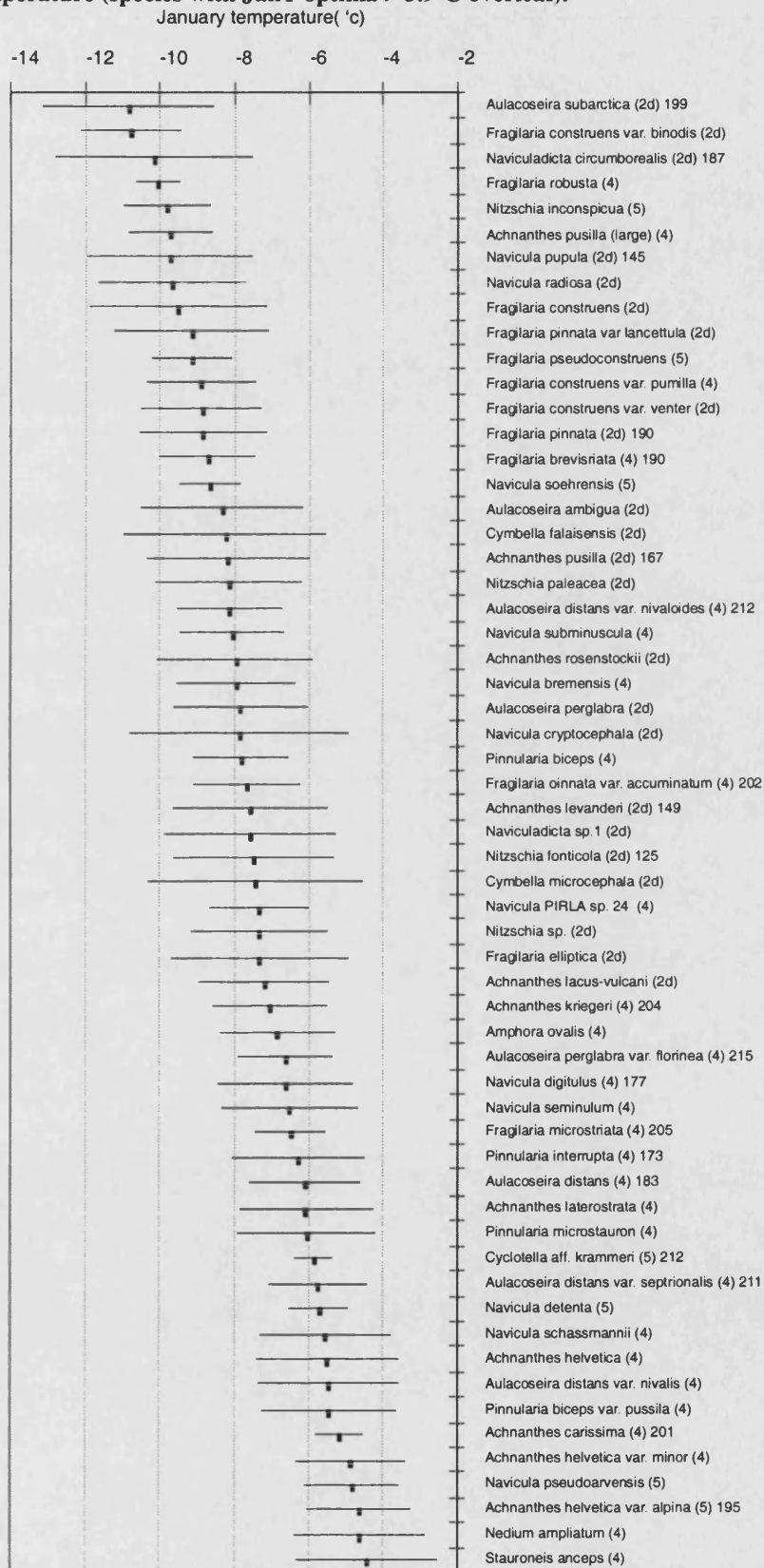
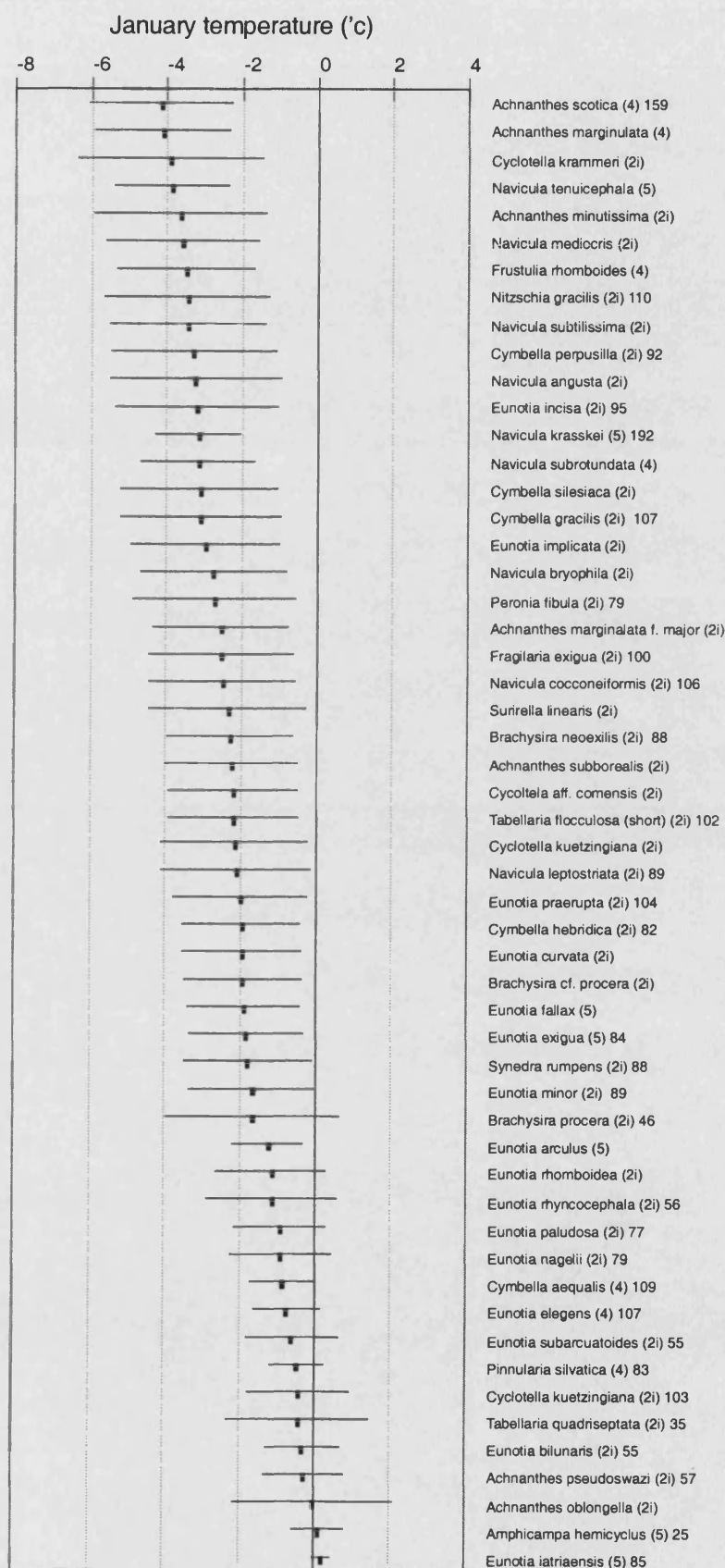


Figure 5.35: Continued



When available, the ice-cover duration optima of the species are presented in brackets on the graph. It would be expected that species with high January air temperature optima would have low ice-cover duration optima. This appears to be true in general but it should be noted that the relationship is not linear. For example, for the species with January air temperature optima of between -2.5 and 0.3°C, all ice-cover optima are between 25-110 days duration (e.g. *Brachysira neoexilis*, *Tabellaria quadrisepata*). Those with JanT optima of between -11 and -8°C have ice-cover optima of between 145-202 days (e.g. *Fragilaria brevistriata*, *Aulacoseira subarctica*). These species may be good warm or cold indicator species and are utilised in Chapters 6 and 7.

Because most other diatom climate transfer functions have focussed on July temperatures it is not appropriate to compare the temperature optima for each species. However, there is good agreement between the studies in terms of the ranking of species optima by temperature. For example, Rosen *et al.*, (2000) had lower temperature optima for *Aulacoseira perglabra* and *Fragilaria pinnata* (<7.5°C) and higher optima for *Eunotia nagelii* and *Tabellaria quadrisepata* (12.6 and 13.9°C respectively) which is also supported by this study.

5.5 Conclusion

This chapter has explored the environmental and biological data within the 80 lake training set. One outlier was identified and deleted leaving a training set of 79 sites. The main environmental variables controlling the diatom assemblages were identified as pH, January temperature and TOC, and the unique contribution of each variable, in terms of the amount of variance it explained, was calculated. The feasibility of creating a pH transfer function with the 79 sites was discussed and the data set proved to be suitable for the creation of such an inference model.

The predictive power of the model was assessed in comparison with other diatom pH transfer functions and it compared favourably. Species pH optima and tolerances, generated by the model, were presented and compared to the optimum generated by other published pH models. There was a large degree of discrepancy between the optima for each species generated by each data set. This was not regarded as a problem, in terms of the reconstruction of pH trends, due to the similar ranks of the

pH optima it did, however, highlight the importance of developing training sets and transfer functions from the area in which they will be applied.

January air temperature was shown to describe a large amount of the diatom variance within the data set. Due to this strong relationship the value and feasibility of creating a January air temperature transfer function was evaluated. The model, however, incurred large errors. It was decided, therefore, that the transfer function would be used as a climate predictor in a more qualitative sense to suggest periods of warmer or cooler years using the sediment cores in Chapters 6 and 7.

The following two chapters apply the pH and January air temperature transfer functions developed from this 79 lake training set to two sediment cores from high altitude lakes in central Norway. The application of the models provide insights into past pH conditions for the lakes and inferences of climate changes related to changes in the reconstructed pH and January air temperatures changes. These are evaluated in conjunction with diatom species assemblage shifts, to assess to what extent diatoms can be used to effectively detect past climatic change.

Chapter 6

Palaeolimnological analysis of Lake Hornsjøen (core 98-18)

Introduction

This chapter presents the high resolution diatom results, and the diatom inferred environmental reconstructions of pH, ice-cover duration, TP and January temperature for the core taken from Lake Hornsjøen. The ^{210}Pb dating results and core chronology are also presented. The discussion describes the changes occurring within the various palaeolimnological parameters in the core and links these to hypothesised changes in the lake system. Finally, the extent to which the changes in the lake biota, and the inferred variables within the core profile, can be related to known climatic changes occurring in Central Norway over the past 500 years is evaluated.

6.1 Results

6.1.1 Water chemistry and site details

The site details and catchment land use history have been presented in section 2.3.7. The full water chemistry results are presented in Table 6.1. The site has slightly higher pH than the mean pH for the Norwegian training set sites (6.39 units, see Table 5.2), but slightly lower Ca^{2+} and Alk (161 $\mu\text{eq/l}$ and 133 $\mu\text{eq/l}$ respectively, Table 5.2). The site has slightly lower precipitation than the mean for the training set sites (886mm, Table 5.2) it also has a lower January temperature (-7°C , Table 5.2) than the training set mean but a slightly higher July temperature mean (6.6°C , Table 5.2).

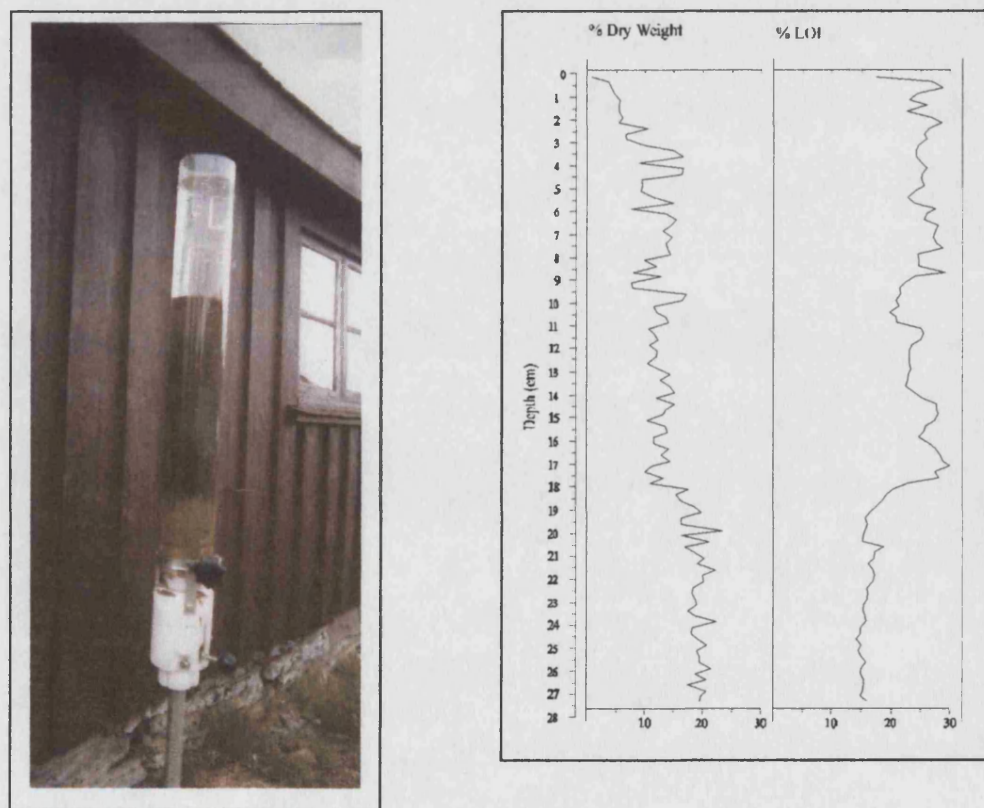
6.1.2 Lithostratigraphy

The core taken from Lake Hornsjøen was 27.5cm in length and had a distinct change in colour in the bottom section of the core profile (Figure 6.1). The colour and texture changes have been discussed previously in section 2.3.7. It should be noted that the distinct change from a more organic brown sediment to a more clay-rich lighter material occurred at *ca.*20cm which also corresponds to changes in the %DW and %LOI profiles (Figure 6.2).

Table 6.1: Summary of the environmental data for Hornsjøen

Variable	Units	
Lake altitude	m a.s.l	1261
Max Depth	m	12.5
pH	pH units	6.89
Alk	$\mu\text{eq/l}$	146
Cond	$\mu\text{S/cm}$	20
Na^+	$\mu\text{eq/l}$	24
NH_4^+	$\mu\text{eq/l}$	1
K^+	$\mu\text{eq/l}$	7
Mg^{2+}	$\mu\text{eq/l}$	35
Ca^{2+}	$\mu\text{eq/l}$	156
Cl^-	$\mu\text{eq/l}$	6
NO_3^-	$\mu\text{eq/l}$	0
SO_4^{2-}	$\mu\text{eq/l}$	41
Al-TM	$\mu\text{g/l}$	6
Al-NL	$\mu\text{g/l}$	6
Al-L	$\mu\text{g/l}$	0
Abs-250		0.032
TP	$\mu\text{g/l}$	5-30
Chl α	$\mu\text{g/l}$	0.9
SRP	$\mu\text{g/l}$	<10
Dissolved silica (DS)	mg/l	2.33
TOC	mg/l	1.6
Average July Temperature (TJuly)	$^{\circ}\text{C}$	8.5
Average January Temperature (TJan)	$^{\circ}\text{C}$	-11.8
Annual Precipitation	mm	500

Figure 6.1 and 6.2 Core profile and %DW and %LOI for core 98-18 from Lake Hornsjøen



6.1.3 Dating

Total ^{210}Pb activity for Lake Hornsjøen reaches equilibrium with the supporting ^{226}Ra at a depth of *ca.* 8 cm. ^{226}Ra activity is relatively uniform, with a mean value of 77 Bq kg^{-1} (Table 6.2). The unsupported ^{210}Pb activity versus depth profile is a little irregular. However, since the overall trend is one of exponential decline any disturbances appear to have been episodic, and relatively minor.

Table 6.2: Fallout radionuclide concentration in Hornsjøen core 98-18

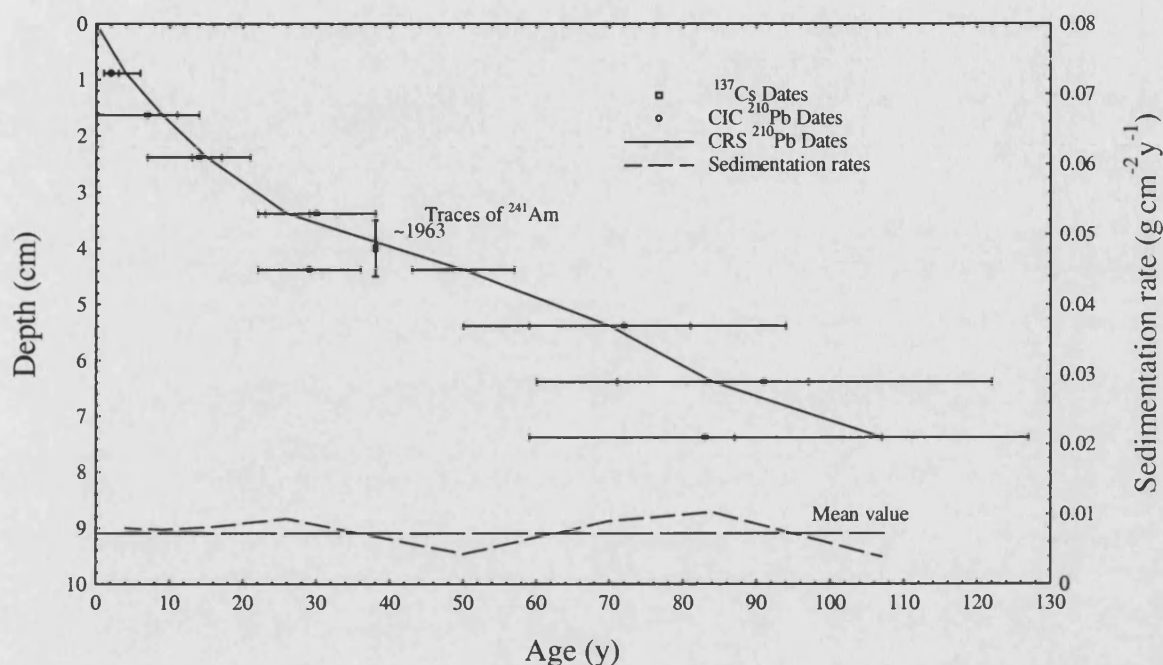
Depth		^{210}Pb						^{137}Cs		^{241}Am	
		Total		Unsupported		Supported		Bq kg^{-1}	\pm	Bq kg^{-1}	\pm
cm	g cm^{-2}	Bq kg^{-1}	\pm	Bq kg^{-1}	\pm	Bq kg^{-1}	\pm				
0.88	0.03	678.9	90.7	586.3	92.0	92.6	15.7	3174.8	37.2	0	0
1.63	0.07	587.2	60.7	508.0	61.6	79.2	10.7	2546.5	27.9	0	0
2.38	0.12	495.5	44.8	403.5	46.3	92.0	11.7	2501.4	31.6	0	0
3.38	0.22	326.2	40.5	247.6	42.0	78.7	11.1	1833.3	26.2	0	0
4.38	0.37	320.2	28.1	253.9	29.0	66.3	7.2	1109.5	14.6	3.5	2.4
5.38	0.49	151.0	41.5	66.6	44.1	84.4	14.8	656.7	20.6	0	0
6.38	0.62	101.3	34.2	37.7	34.9	63.7	6.9	353.2	9.8	0	0
7.38	0.77	106.5	33.6	47.7	34.1	58.8	5.9	246.2	8.2	0	0
8.38	0.91	60.5	22.0	-15.6	22.8	76.4	5.8	207.6	7.9	0	0

The record of fallout of the artificial radionuclides of ^{137}Cs appears to be dominated by the Chernobyl fallout. The absence of either a 1986 or 1963 peak is possibly due to post-depositional mobility (Appleby *pers. com.*). Traces of ^{241}Am in the 4.25-4.5 cm section do, however, suggest that sediments at this depth date from the period of high weapons test fallout in the 1960s (Appleby *et al.*, 1991).

Dates for the core were calculated using the CRS and CIC models, together with the 1963 depth indicated by the ^{241}Am record (Figure 6.3). There is little significant difference between the two ^{210}Pb dating models. Both suggest relatively uniform sediment accumulation rates during the past 100 years, with a mean value of $0.0072 \pm 0.0009 \text{ g cm}^{-2} \text{ y}^{-1}$ (0.07 cm y^{-1}), representing a slightly slower sediment accumulation rate than Lake Gåvålivatnet (Chapter 7, section 7.1.3). This places 1963 at a depth of 3.75 cm which correlates with the ^{241}Am trace. The ^{241}Am date, however, is not sufficiently well defined to validate the ^{210}Pb dates precisely; the dates, therefore, have been calculated using the mean accumulation rate. It should be noted, however, that the error bars associated with the chronology are particularly high towards the bottom of the record. The mean accumulation rate was used to estimate the dates

lower down the sediment sequence. It was calculated, therefore, that the basal sediments at 27.5cm represent *ca.* 1620.

Figure 6.3: Radiometric chronology of Hornsjøen, core 98-18 showing the CRS and CIC model dates and sedimentation rates, together with the approximate 1963 depth suggested by the ^{241}Am stratigraphy.



6.1.4 Diatom analysis

The diatoms present in the core are illustrated in Figure 6.4 and a description of the general changes throughout the core is presented in Table 6.3. A full list of diatom species and their codes are listed in Appendix 6.1. The zones used on the core diagram and in the table are calculated using ZONE (see section 3.3.6) and represent zones of diatom assemblage similarity, the zone boundaries indicate changes in species composition within the core profile. Overall the core is dominated by *Fragilaria*, *Achnanthes* and *Aulacoseira* species. There are three main diatom zones. Zone 3 is particularly distinct, with many species present in this zone which are not present in Zones 1 and 2 (e.g. *Cyclotella comensis*, *Cyclotella kuetzingiana* var. *radiosa* and *Sellaphora/Navicula verecundiae*)

A DCA was performed on the core diatom samples (Table 6.4). This showed that the length of the first gradient was <1.5 so a linear PCA method was deemed more suitable for this core (Table 6.5).

Table 6.3: The main changes in diatom species assemblage for Hornsjøen, core 98-18

Diatom zone	Depth and approx. date	Species assemblage summary
1	1-7cm 2001- 1902	<p>- <i>F. brevistriata</i> is constant throughout the core but rises in abundance in this zone to max 15% near the surface, <i>C. pseudostelligera</i> also has its maximum abundance in this zone c.15% at 1cm, <i>C. comensis</i> also increases in the surface sediments.</p> <p>- <i>F. pinnata</i> declines rapidly in this zone, and <i>F. pseudoconstruens</i> decreases slightly.</p>
2	7- 18.5cm 1902- 1741	<p>Dominated by <i>Achnanthes minutissima</i>, <i>F. pinnata</i> (max c. 25% at 17cm), <i>F. pseudoconstruens</i> (c.30% at 14.5cm), <i>F. construens</i> var. <i>venter</i> (constant around 5%), <i>F. construens</i> var. <i>pumilla</i>. <i>C. aff. krammeri</i> peaks in this zone at max abundance of c. 15% at 9.5cm), <i>C. krammeri</i> also appears in this zone and is absent in the rest of the profile.</p> <p>- Apart from the rise in <i>C. aff. krammeri</i> this zone shows a relative decrease in most of the <i>Cyclotella</i> species and an increase in the main <i>Fragilaria</i> taxa.</p>
3	18.5- 27.5cm 1741-1622	<p>-This zone is dominated by various <i>Achnanthes</i> species, <i>Aulacoseira distans</i> (max c. 10%), <i>Aulacoseira perglabra</i> var. <i>florinae</i> and <i>Aulacoseira subarctica</i>, <i>F. microstriata</i> (max c. 10%) Several <i>Cyclotella</i> sp. are present including <i>C. kuetzingiana</i> var. <i>planetophora</i>, <i>C. aff. comensis</i> (max c.20 at 23cm) and <i>C. kuetzingiana</i> var. <i>radiosa</i> (max c.10%).</p> <p>-Several species occur in this zone which do not appear in the rest of the core profile, namely <i>A. subarctica</i>, <i>F. microstriata</i>, <i>C. kuetzingiana</i> var. <i>radiosa</i>, <i>P. microstauron</i>, <i>P. nodosa</i> and <i>Sellaphora verecundiae</i></p>
Overall patterns throughout core		<p>- A cyclical pattern is evident in the core for species <i>C. pseudostelligera</i> and <i>C. kuetzingiana</i> var. <i>planetophora</i></p> <p>- There appears to be an interplay between the <i>Cyclotella</i> species, with <i>C. aff. krammeri</i> increasing as <i>C. pseudostelligera</i>, <i>C. kuetzingiana</i> var. <i>radiosa</i> and <i>C. kuetzingiana</i> var. <i>planetophora</i> sp. decreasing.</p> <p>- Overall, however, the percentage of <i>Fragilaria</i> is greatest in Zone 2</p>



Figure 6.4: Summary diatom diagram for Hornsjøen with taxa <2% abundance deleted (planktonic species=*Aulacoseira subarctica* and all the *Cyclotella* species)

Table 6.4: Summary statistics for the first four axes of the DCA of Lake Hornsjøen, core 98-18 with 236 diatom species and 110 samples with square root transformation of species data and downweighting of rare species

DCA Axes	1	2	3	4
Eigenvalues	0.217	0.043	0.019	0.016
Lengths of gradient	1.425	0.945	0.681	0.713
Cumulative % variance of species data	23.1	27.7	29.7	31.5
Sum of all unconstrained eigenvalues	0.939			

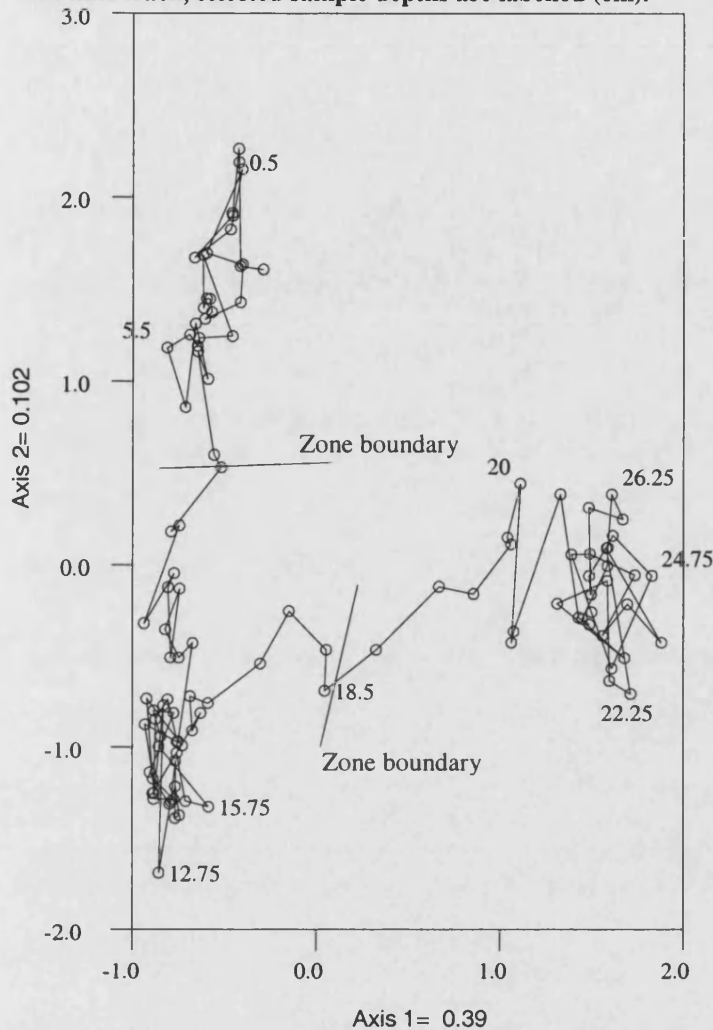
Table 6.5: Summary statistics for the first four axes of the PCA of Lake Hornsjøen, core 98-18 with 236 diatom species and 110 samples with square root transformation of species data and downweighting of rare species

PCA Axes	1	2	3	4
Eigenvalues	0.390	0.102	0.038	0.028
Cumulative % variance of species data	39.0	49.2	53.0	55.8
Sum of all unconstrained eigenvalues	1.0			

The PCA biplot (Figure 6.5) shows the diatom assemblage scores for the 110 diatom samples in the core. The various changes evident within the core profile are listed below:

- The surface samples are tightly clustered in the top left corner of the biplot, a second cluster exists in the lower left of the plot associated with samples *ca.* 12-15cm. The change from the surface clustering to the second down core cluster seems to be strongly associated with axis 2.
- Further changes, this time associated with axis 1, occur between the cluster at *ca.* 13cm to a cluster of samples representing levels 22-27cm in the core.
- The biplot show three distinct zones in terms of diatom assemblage, the surface sediments- 5cm, 12-15cm and 22-27cm, with periods of diatom species assemblage change between these clusterings.
- 49.2% of the total variance in the diatom species is captured by axes 1 and 2. This suggests that the environmental gradients represented by axes 1 and 2 are strongly correlated with the changes in diatom species within the core.

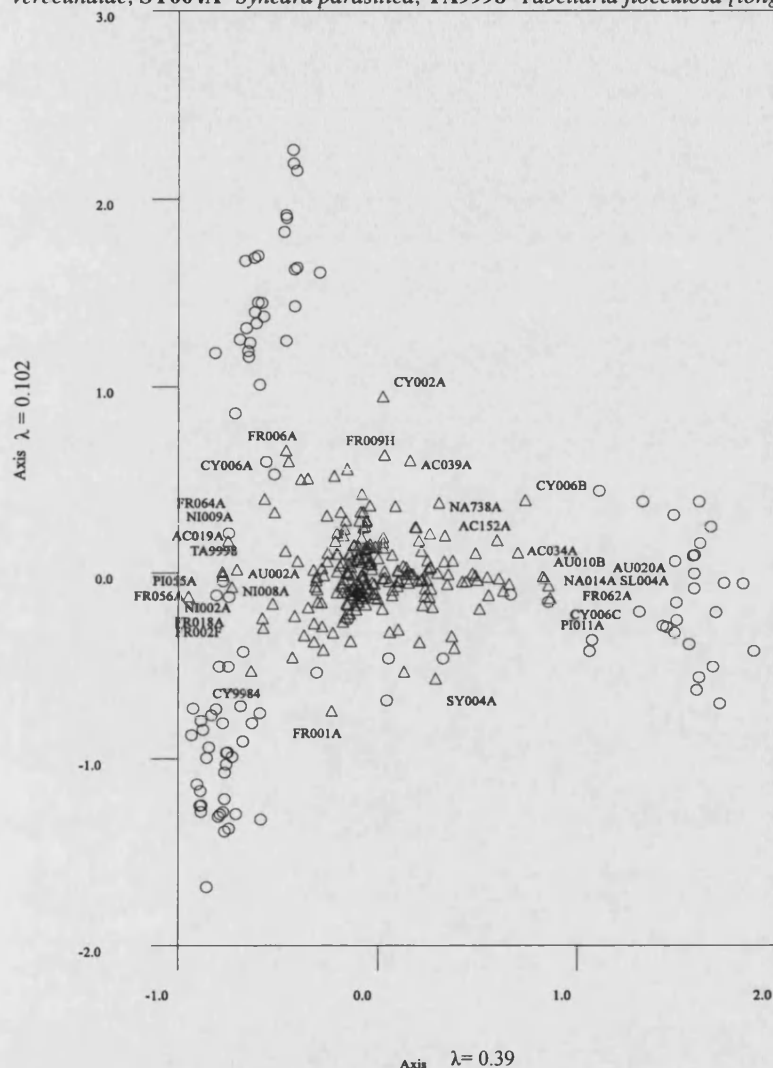
Figure 6.5: Biplot of diatom samples in the 110 samples for Lake Hornsjøen on PCA axis 1 and 2 with time track, selected sample depths are labelled (cm).



There are several individual species associated with these diatom assemblage clusters (Figure 6.6). *Cyclotella pseudostelligera*, *C. kuetzingiana* and *F. brevistriata* seem to be associated with the samples in the top 5cm clusterings. The clusterings around 12-15cm (Figure 6.5) are associated primarily with several *Fragilaria* species (*F. exigua*, *F. pinnata*, *F. construens* var. *pumilla*, and *F. elliptica*) and *Cyclotella* aff. *krammeri*. The species orientated around the lower section of the core are *Pinnularia microstauron*, *Sellaphora verecundiae* (formally *Navicula*), *Cyclotella kuetzingiana* var. *radiosa*, *F. microstriata* and two *Aulacoseira* species (*A. subarctica* and *A. perglabra*). These zones, and the species associated with them in the PCA (Figure 6.5), can be clearly seen in Figure 6.4. The ZONE programme creates boundaries within the areas of rapid diatom assemblage change indicated on the PCA (Figure 6.5) i.e. at ca.7cm and ca.18.5cm. The changes in diatom species are discussed further in section 6.2.

Figure 6.6: Biplot of 110 diatom samples (o) for Lake Hornsjøen and species (Δ , with selected taxa labelled) on PCA axis 1 and 2. Labelled taxa as follows;

AC152A- *Achnanthes carissima*, AC039A- *A. didyma*, AC019A- *A. nodosa*, AU002A- *Aulacoseira ambigua*, AU010B- *A. perglabra*, AU020A- *A. subarctica*, CY9984- *Cyclotella* aff. *krammeri*, CY006A- *C. kuetzingiana*, CY006B- *C. kuetzingiana* var. *planetophora*, CY006C- *C. kuetzingiana* var. *radiosa*, CY002A- *C. pseudostelligera*, FR006A- *Fragilaria brevistriata*, FR009H- *F. capucina* var. *gracilis*, FR002F- *F. construens* var. *pumila*, FR018A- *F. elliptica*, FR064A- *F. exigua*, FR062A- *F. microstriata*, FR001A- *F. pinnata*, FR056A- *F. pseudoconstruens*, NA738A- *Navicula vitiosa*, NI002A- *Nitzschia fonticola*, NI008A- *N. frustulum*, NI009A- *N. palea*, PI055A- *Pinnularia balfouriana*, PI011A- *P. microstrauron*, SL004A- *Sellaphora verecundiae*, SY004A- *Synedra parasitica*, TA9998- *Tabellaria flocculosa* [long]



6.1.5 The reconstruction of environmental variables

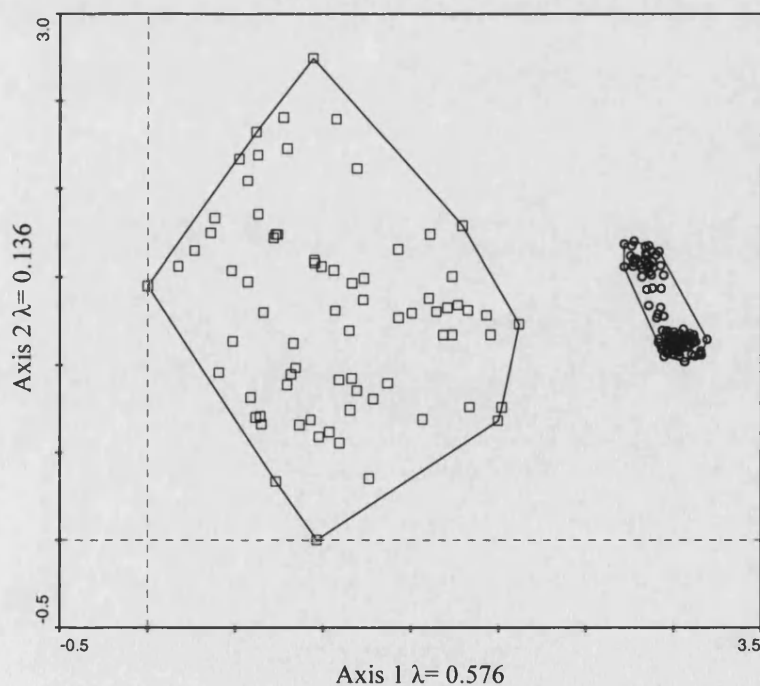
This section presents the reconstructions of pH, total phosphorous (TP), ice-cover duration, and January temperature for Lake Hornsjøen. The diatom inferred reconstruction of pH is performed using both the WA_(tol) transfer function for the 79 lake data set (Chapter 5) and the AL:PE training set derived from the EDDI programme using both WA and MAT (See section 3.3.4). TP was reconstructed using the Swiss training set through the EDDI programme using WA methods (see section 3.3.4). The diatom inferred reconstruction of ice-cover is achieved by using the 40

lake WA transfer function developed in Chapter 4. Finally January air temperature was reconstructed using the 79 lake training set using the WA-PLS 3 component model developed in Chapter 5. The diatom inferred reconstructions are presented in turn in the following sections (sections 6.5.1-6.5.3).

In order for the reconstruction of both pH and January temperature to be accurate a large proportion of the diatoms present within the 79 lake training set should also be present within the fossil diatom assemblages. To assess this, a DCA of both the training set species and the core species was conducted in conjunction (summary results of the 79 samples DCA are shown in Table 5.8).

It can be seen from the DCA biplot (Figure 6.7) that the species within the core are located slightly away from the diatom variance space of the training set (a distance of $<1SD$ on axis 1), suggesting that they have some species in common, resulting in more reliable environmental reconstructions. The two envelopes do not however overlap, suggesting that some species that occur in the core do not occur in the training set (discussed later). The reliability of the reconstructions using other training sets (i.e. pH with the AL:PE set and TP) are discussed later.

Figure 6.7: DCA biplot of the 79 surface sample diatom assemblages (circles) and the fossil diatom assemblages (squares). Envelopes are drawn around the training set sites and the core samples.



6.1.5.1 pH reconstruction

A pH transfer function was developed and discussed in Chapter 5. This was used to reconstruct pH for Lake Hornsjøen using $WA_{(tol)}$ (Figure 6.8). The results of the reconstructions using both Inverse and Classical regression were compared with the pH reconstructions conducted using the AL:PE training set, through the EDDI programme using both WA and MAT (See section 3.3.4).

The present day pH of the Lake Hornsjøen is 6.8 pH units. For the WA method of reconstruction it is recommended that when the mean values of the parameter to be reconstructed lie close to the mean of the training set values inverse de-shrinking should be used (Birks *et al.*, 1990). The mean pH for the AL:PE training set is 6.15 pH units, therefore, inverse de-shrinking is a more accurate method for the AL:PE WA reconstruction. For the reconstruction using the 79 lake data set both de-shrinking co-efficients were used as the mean pH of the training set was 6.3 pH units. The reconstruction using classical WA had the closest match with the present day pH (Figure 6.8).

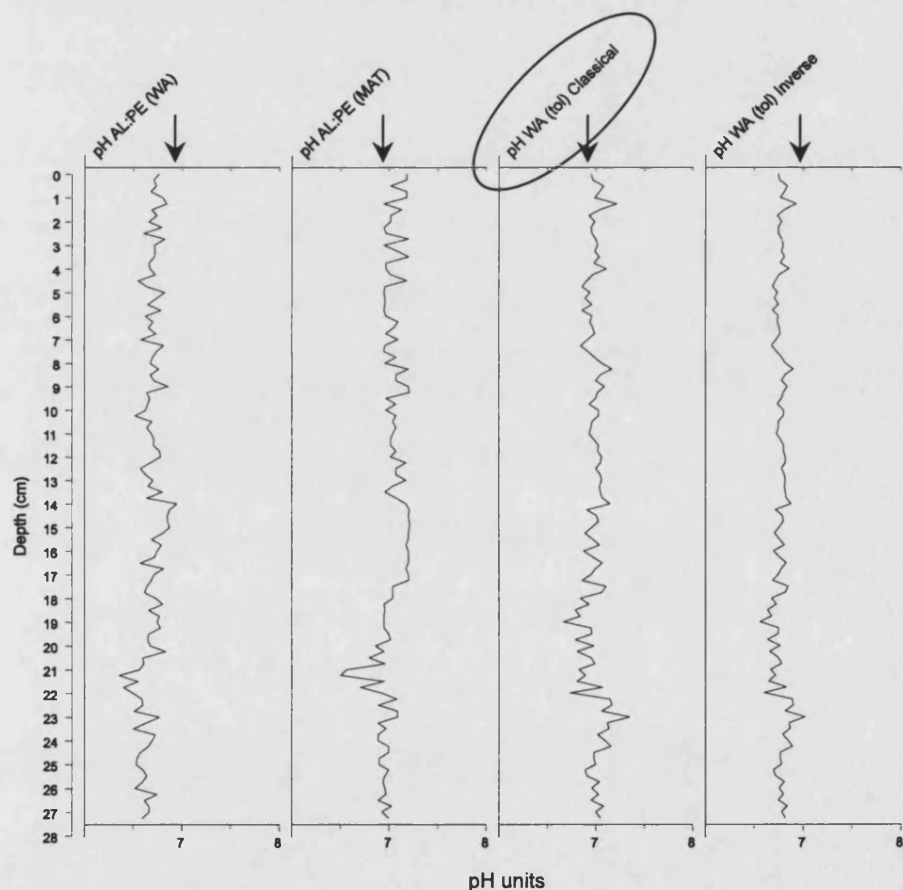
MAT techniques were also used with the AL:PE training sets to compare them to the results generated by the AL:PE WA analysis and the 79 lake training set $WA_{(tol)}$ methods (Figure 6.8, see sections 3.3.4).

Both the MAT and $WA_{(tol)}$ classical (79 lakes set) techniques give pH higher reconstructions than the WA AL:PE and $WA_{(tol)}$ inverse (79 lakes set) techniques. All the reconstructions methods, however, show that the pH fluctuates but overall varies little throughout the profile with only a slight lowering between 18 and 21cm. This suggests that the lake is not particularly sensitive to pH changes related to climate change as the pH does not vary.

The reliability of the reconstructions can be evaluated by looking at the percentage of species present in the training set which are also present within the core (the calibration set sum for WA or the Min DC for MAT). When the calibration percentage drops below 65% then the reconstructions are thought to be less accurate (Birks *pers. com.*). When the min DC is above 100 the MAT reconstructions are believed to be less reliable (Juggins *pers. com.*). The reliability of the reconstructions

using the AL:PE data set are good for the top section of the core but should be treated with more caution below 20cm (Appendix 6.2). The reliability of the reconstruction for the 79 lake set is good throughout the core and the calibration percentage never drops below 75%. The reconstruction using the classical $WA_{(tol)}$ of the surficial sediments is 6.95 units and is the closest to the measured pH (Figure 6.8). It is this pH reconstruction which is therefore used for this core and discussed further in later sections in conjunction with the other inferred environmental variables.

Figure 6.8: Diatom inferred pH for Lake Hornsjøen using the AL:PE data set (using both WA and MAT) and the 79 lake data set (using $WA_{(tol)}$ with both inverse and classical de-shrinking coefficients). The arrow indicates the current pH measurement of 6.89 pH units. The circled technique is the one adopted for further discussion.

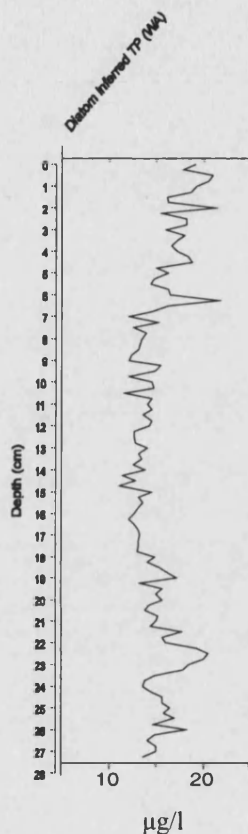


6.1.5.2 TP reconstruction

The diatom inferred TP fluctuates between 12 and 22 $\mu\text{g/l}$ throughout the profile (Figure 6.9). The present day TP was measured as between 5- 30 $\mu\text{g/l}$ (section 3.2.1.1 for problems associated with the TP measurement) suggesting that the diatom inferred TP is close to the measured value range. The diatom inferred TP profile exhibits several fluctuations and has lower values in the central section of the core. Again the

reconstruction is not as reliable in the lower section of the core (Appendix 6.2). The reconstruction will, therefore, be used only to indicate general trends in TP rather than absolute values.

Figure 6.9: Diatom inferred Total phosphorous for Lake Hornsjøen using the EDDI data base and WA reconstruction method. The current TP value is between 5-30 $\mu\text{g/l}$

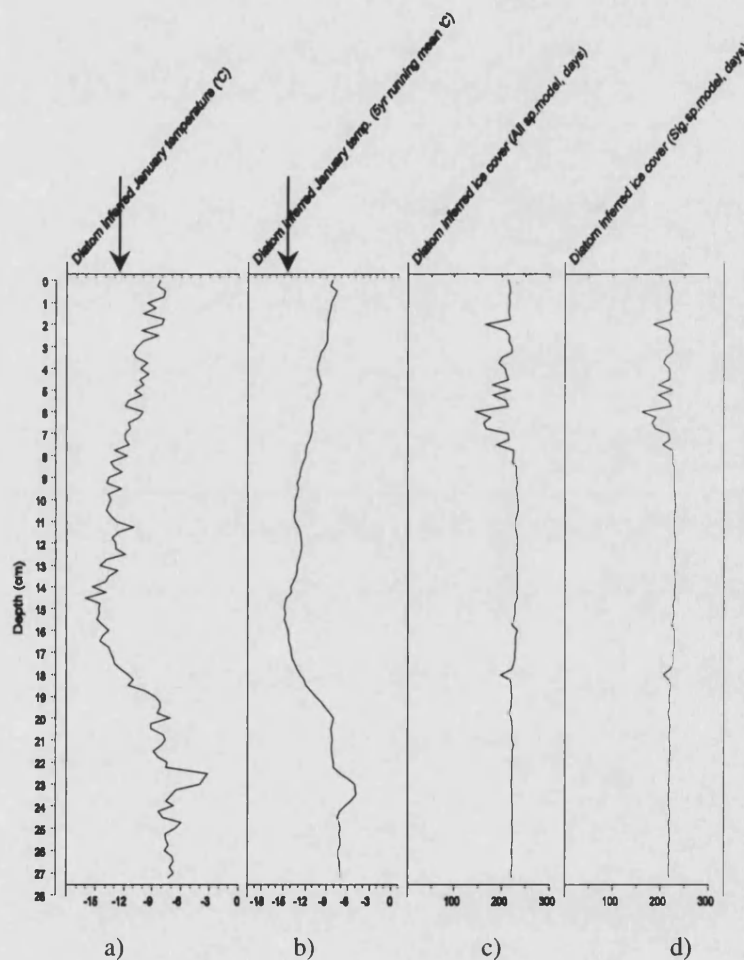


6.1.5.3 Diatom inferred ice-cover and diatom inferred January temperature reconstructions

Figure 6.10 illustrates the reconstructed ice-cover duration in days using the 40 lake training set (Chapter 4). One profile shows the reconstruction using all species present within the training set (Figure 6.10 c) the other uses only the species which have a significant relationship with ice-cover (Figure 6.10 d). Unfortunately ice-cover duration data or January temperature data are not available for the site (see Table 3.1, Norway 1 sites do not have ice-cover values). It is likely, however, that the lake would be ice-covered from late September to late June, which would represent over 200 days of ice-cover, i.e. similar to the reconstructed values.

It can be seen that the reconstructed ice-cover values vary little throughout the profile, this is probably due to the fact that relatively few species were shown to have a significant relationship with ice-cover (Section 4.4) and few of the ones that did, do not appear in large abundances within the core (Figure 6.11).

Figure 6.10: Diatom inferred January temperature, using the 79 lake data set, b) with and a) without a running mean, diatom inferred ice-cover duration (days) using the 40 lake data set and c) a model with all the species in the training set used and d) reconstructed using a model with only the species that had a significant relationship with ice-cover used (see section 4.4).



In Figure 6.11 the species have been ordered in terms of ice-cover optima to assess if any pattern is evident within the down-core diatom abundances. In terms of ice-cover indicator species, Figure 6.11 indicates that many species with lower ice-cover optima tend to occur, or be more abundant, in diatom zones 1 and 2 (e.g. *Fragilaria exigua*, *Fragilaria capucina* var. *gracilis* and *Achnanthes nodosa*). Species with higher ice-cover optima such as *Fragilaria microstriata*, *Aulacoseira subarctica*, *Aulacoseira perglabra* var. *florinae* tend to occur in the lower section of the core (see Figure 4.47

for optima). The pattern is confused however, by species such as *Cyclotella kuetzingiana* var. *radiosa* and *Cyclotella kuetzingiana* var. *planetophora* which have lower ice-cover optima but predominately occur in the zone 3, *Fragilaria brevistriata* which has a higher ice-cover optima but increases in zone 1 and species such as *Cyclotella* aff. *krammeri* that has a high ice-cover optima and is very clearly associated with zone 2.

The lack of an ordered pattern within the diatom assemblage, in terms of diatom zones, suggests that the generation of ice-cover optima may not be appropriate. For this reason and the fact that large errors were incurred with the ice-cover model, the diatom inferred ice-cover duration reconstructions are not discussed further. The main reason that the ice cover durations could not be quantified was probably that 'ice-cover' is not the main environmental variable determining the diatom response and in addition its relationship to the diatoms is of an indirect nature, complicating the climate signal. In addition it could also be argued that the diatoms are in fact responding to ice-cover but that 'ice-cover duration' as a measure does not encapsulate this response and it would be more appropriate to look at variables such as 'ice on' an 'ice off' data' in combination with temperature variables. Unfortunately, due to the missing thermistors this was not possible within this project.

The diatom inferred January temperature reconstruction (Figure 6.10a and b) shows greater variability down core than the ice-cover model. Larger numbers of species had a significant relationship with January air temperature compared to ice-cover (Figure 6.12) and the calibration sum was over 75% for the reconstruction. Much lower air temperatures are reconstructed in the middle section of the core which appear to be controlled by the fluctuations in *Fragilaria pinnata* (-8.8°C optima), which rises in abundance at 18cm and decreases in the *Cyclotella* aff. *comensis* and *C. kuetzingiana* types. The present day January temperature is -11.8°C and it can be seen that the reconstructed value of -7°C, is slightly overestimating the temperature. Air temperatures do, however, tend to vary greatly from year to year (see also section 6.3.1). In addition, the relatively large errors involved in the reconstruction technique (2.2°C) suggest that the reconstruction of absolute values rather than just trends should be treated with caution.

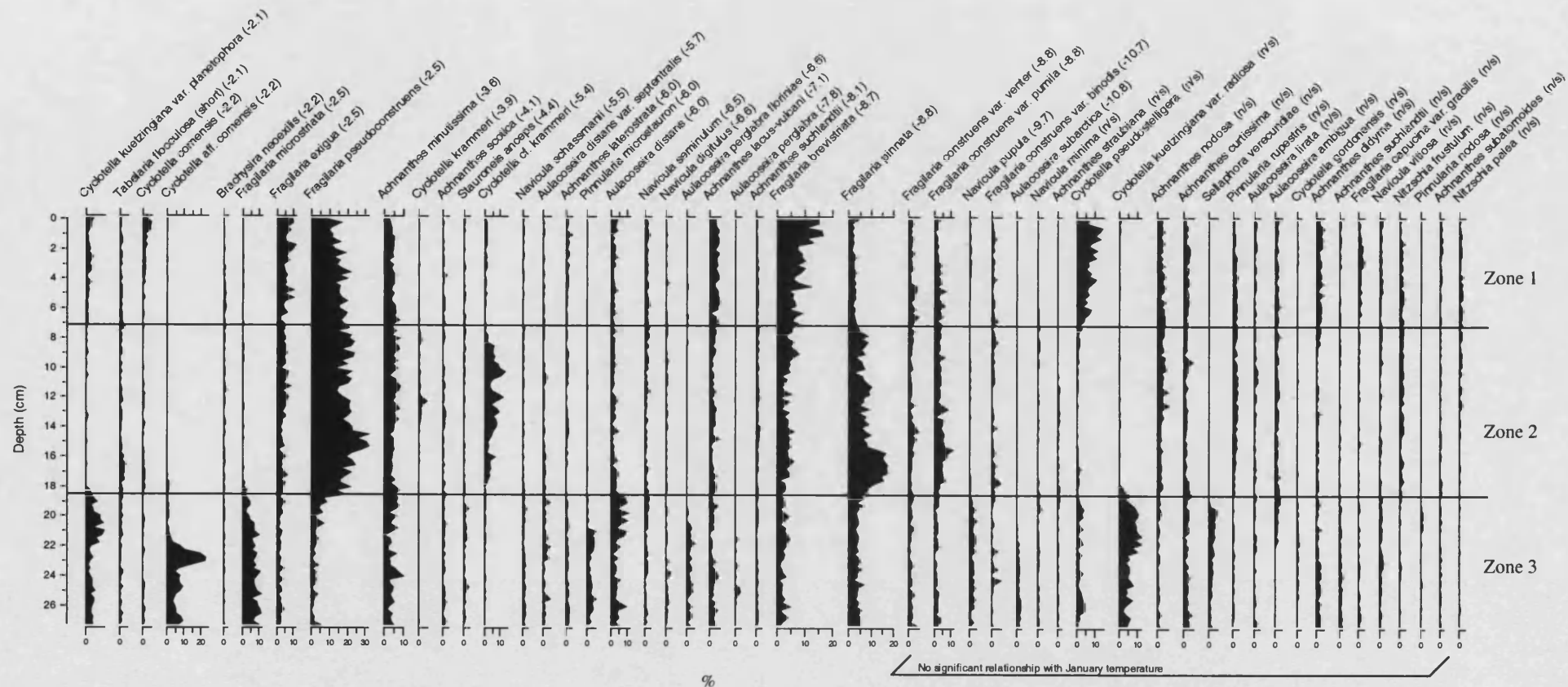


Figure 6.12: Summary diatom diagram for Hornsjøen with taxa <2% abundance deleted, arranged in order of WA January temperature optima presented in brackets. Species with no significant relationship with January temperature, or those which were not present in the training set are also presented (n/s in brackets)

6.2 Discussion

This section firstly combines and summarises some of the results above into a synthesis diagram (Figure 6.13). The diagram includes various diatom inferred reconstructions, lithostratigraphic parameters and calculations of the changes in the habitat availability for the lake biota throughout the core profile. The diagram is introduced and discussed briefly in the following section. The discussion then focuses on the diatom species changes and diatom inferred parameter fluctuations, occurring in the three diatom zones identified (Figure 6.4) and relates them to hypothesised changes in various environmental/climatic parameters within the lake.

The discussion section concludes with a detailed evaluation of whether the palaeolimnological changes seen in the core, taken from Lake Hornsjøen, can be related to changes in the Norwegian climate over the past 500 years, and in particular to the climatic changes known to have occurred within the region during the LIA (see section 1.5.1) and over the period of the instrumental record. Finally, the suitability of using diatoms and diatom inferred variables for climatic reconstructions at this site is evaluated and summarised.

6.2.1 Summary results and synthesis

The main findings from the results above are combined in Figure 6.13. The diagram presents the diatom inferred reconstructions (TP, pH, and January Temperature), the %DW, %LOI, diatom concentration and species number, ratios of diatom type (sum of all non planktonic species divided by sum of all planktonic species to create a ratio, high ratio= low plankton abundance) and diatom to chrysophyte cyst ratio (calculated by dividing 'diatom valves' by 'chrysophyte cysts number'), diatom species number, and PCA axis 1 and 2 scores. Many of these variables are included due to their previously documented control over diatom assemblages (e.g. diatom inferred pH and TP- see section 1.3.3.3, 1.4.1.2 and 1.4.1.3) and their links with climatic change (diatom inferred January temperature, plankton to non-plankton ratio, diatom to chrysophyte cyst ratio, species number and diatom concentration see section 1.3 and 1.4). It is suggested, however, that the reconstructions of both TP and January temperature should be used to evaluate *trends* in the variables and not taken as absolute value reconstructions (*c.f.* Laing *et al.*, 1999 for similar discussions).

Diatom species number and concentration have been linked to climate in previous studies (see section 1.4.1.2 and see Smith 2002; Anderson *et al.*, 1996) but these variables may also be related to changes in the nutrient supply to a lake and subsequent changes in the biological competition processes (see section 1.3.3.3 and 1.4.1.2). However, changes in the nutrient supply to a lake may also be caused by changes in climate (Figure 1.1), so species number and concentration are therefore useful variables to consider. Likewise the ratio of chrysophyte cysts to diatoms has been included because chrysophytes are planktonic and, therefore, also supposedly decrease with increased lake ice-cover duration and colder climate (Battarbee *et al.*, 2002; Koinig *et al.*, 2002). However, changes in the habitat availability in a lake may also be a reflection of changes in other parameters such as lake water level, mixing regime and light penetration due to siltation in lake littoral areas.

PCA axis 1 and 2 scores, derived from the diatom assemblages and plotted stratigraphically, are also included in Figure 6.12 in order that changes in the diatom composition can potentially be related to other diatom inferred values or lithostratigraphic parameters. Finally, variables that indicate changes in, within lake, and/or catchment productivity (%DW, %LOI, diatom inferred TP see section 1.3.3.3 and 1.4.2) are included in the summary diagram.

In this way the diagram and the discussion that follows provides an overview of changes occurring in the lake in terms of variations in physical, chemical and climatic parameters.

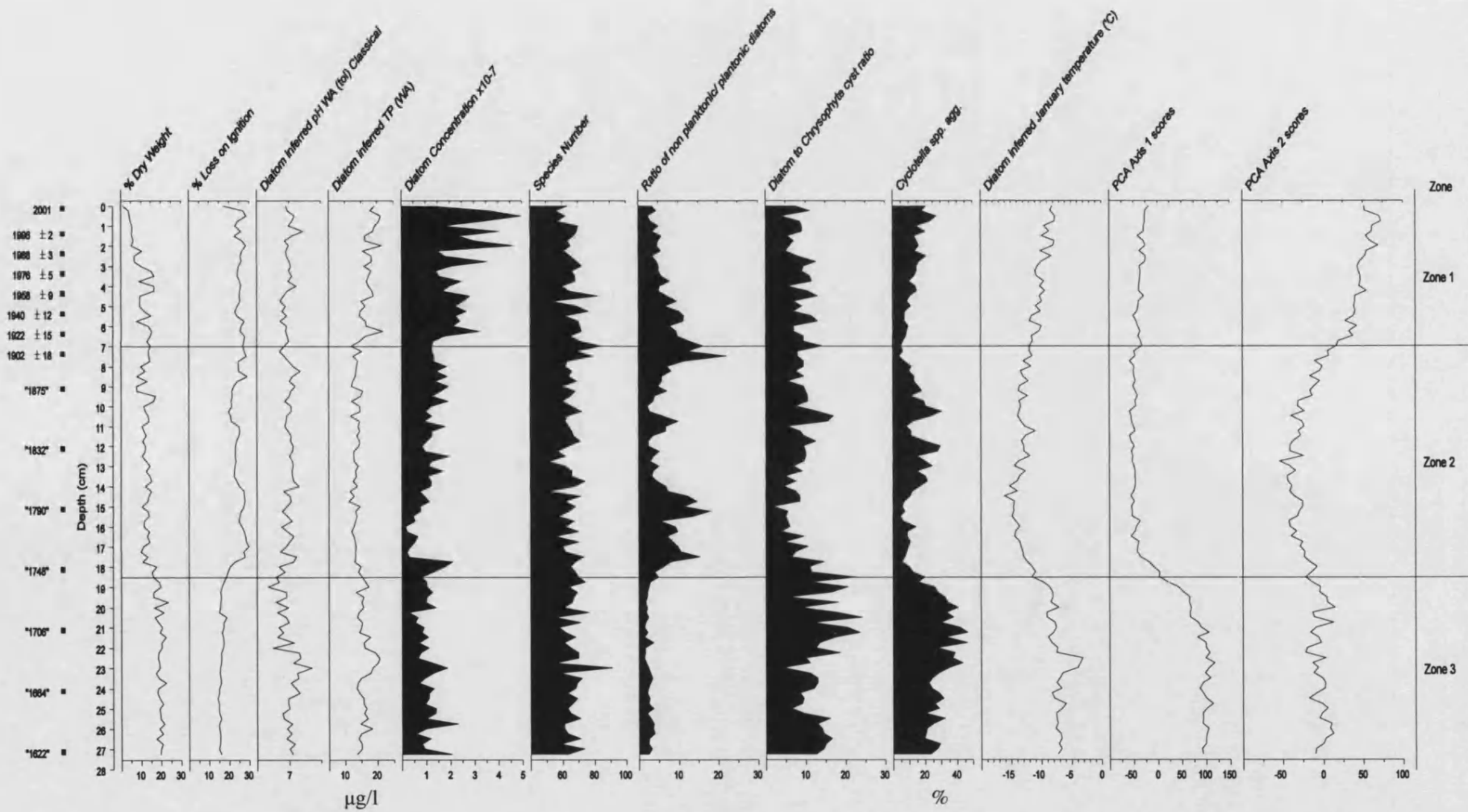


Figure 6.13: Summary diagram of reconstructed environmental variables, lithostratigraphic data, ordination results and diatom habitat ratios for Lake Hornsjøen

6.2.2 Diatom zone three, covering the period from *ca.*1740 (18.5 cm) to *ca.*1622 (27.5 cm)

- *Temperature changes and changes in the relative proportions of the lake habitats*

This zone is characterised by higher than average diatom inferred January temperatures. If this reconstruction trend is to be believed then this would indicate a reduced ice-cover period.

Lake Hornsjøen is dimictic (see section 1.2) and follows a pattern of ‘stratification’ when the lake is ice-free and predominately productive, and an ‘ice-covered period’ resulting in limited within-lake productivity, respiration and lack of aeration in the hypolimnion.

An increase in January temperature may result in an increase in the length of the ice-free period, which would have two possible outcomes for the mixing regime of the lake. Firstly, it might result in a longer stratification period, due to the decrease in ice duration, possibly resulting in an increase in planktonic diatom forms due to a prolonged ‘open water’ season. Secondly, the reduced ice-cover might result in increased ‘wind induced’ water column mixing, lengthening the period in which planktonic diatom forms can remain suspended in the lake’s photic zone. This would again result in an overall increase in the abundance of planktonic diatom species.

It can be seen that the diatom non plankton/ plankton ratio in this section of the core is indeed relatively low (indicating high plankton abundance), supporting the notion of a reduced ice-cover duration at this time. The apparent longer duration of the open water season is not substantiated, however, by the low relative abundance of chrysophyte cysts within this zone.

The lower section of the core has much higher abundances of many *Aulacoseira* species (*A. subarctica* and *A. perglabra* var. *floriniae*) and large *Cyclotella* species (*C. kuetzingiana* var. *radiosa*, *C. kuetzingiana* var. *planetophora*). The presence of the various *Aulacoseira* species and the larger *Cyclotella* species may indicate periods of higher turbulence (Lund 1954; Dean *et al.*, 1984; Agbeti and Dickman 1989; Reynolds *et al.*, 1986 see also section 1.2.3.2) at this time in the lakes history possibly associated with the longer ice free season. The high abundance of *Fragilaria*

microstriata within this zone may also indicate higher turbulence as it is a species which is known to tolerate physical disturbance.

The PCA axis 2 scores are also higher in this lower part of the core. The change in the PCA between this zone and zone 2 is driven by several species which occur in this lower section of the core but which disappear within zone 2. The presence of *Aulacoseira subarctica*, *Aulacoseira perglabra* var. *florinae*, *Cyclotella* cf. *comensis*, *Pinnularia microstauron*, *Sellaphora/ Navicula vercundiae* and *F. microstriata* in zone 3 are particularly pronounced.

Both *Aulacoseira subarctica* and *Fragilaria microstriata* were found to have low January air temperature optima of -10.8°C and -6.4°C, respectively, within this study (Figure 5.35) contradicting the notion that this is in fact a warmer period for the lake. Sporka *et al.*, (2002), however, related the growth of *Aulacoseira subarctica* in a mountain lake from the Tatras to higher mean annual temperatures and recent climate warming. In addition the temperature optima found in this study for *Navicula/ Sellaphora pupula*, which only really occurs in the bottom of the core, was -9.5°C (Figure 5.35). Again this is contradicted by previous research which indicates that *Navicula/ Sellaphora pupula* has a relatively high air temperature optimum of 11.4°C (Rosen *et al.*, 2001b). These comparisons illustrate the problems associated with the generation of, and comparison of specific temperature optima for diatoms (see section 5.3.2 and Anderson 2000).

The high abundance of *C. cf. comensis* in this zone and its disappearance in zones 1 and 2 is particularly clear. These small *Cyclotella* species are often cited as being indicative of recent climate warming and associated with decreases in ice-cover duration (Sorvari and Korhola 1998; Korhola and Weckstrom 2000; Bigler and Hall 2002 and section 1.4), suggesting that its presence here may be related to higher temperatures at this time.

C. comensis is, however, present throughout the core in low numbers and increases in the surficial sediments. This could be related to taxonomic difficulties and the splitting of these species associated with the *Cyclotella* continuum (see Plate 3.1).

This is unlikely, however, as all the samples in the training set and the core were counted by the same person, maximising the taxonomic control. It is more likely that these two *C. comensis* types do in fact have significantly different growth regimes accounting for their asynchronous abundances within the core. These patterns may not, however, be related to climate but to nutrient dynamics within the lake system (c.f. Scheffler *et al.*, 2000 for similar observations for two morphotypes of *C. pseudostelligera* cited in Lotter *et al.*, 2000).

- pH changes

The diatom inferred pH does not change significantly throughout the core profile and the pH in zone 3 fluctuates around 7 pH units. There is a slight decline in diatom inferred pH in the upper part of the zone (between 18.5 and 22.5cm) driven primarily by the decrease in *Cyclotella cf. comensis* at ca.18.5cm.

- Lake/ catchment productivity

The zone is characterised by a lower than average %LOI and variable, but slightly higher than average, diatom inferred TP values. These trends are somewhat contradictory as the increases in TP suggest that within lake productivity is higher at this time but the decreased %LOI values suggest the opposite.

The TP values are driven by changes in the small *Cyclotella* species (excluding *C. cf. krammeri*) with high abundances of these species in this zone and also zone 1 corresponding to higher TP inferred values.

The relatively low %LOI for this period does not correlate with the evidence discussed above which indicate that this zone represents a warmer period for the lake. This %LOI anomaly is discussed further in the following section. It is interesting to note, however, that two of the other cored sites, 98-9 and 98-2 show similar decreases in %LOI at 12cm and 18cm respectively (Figures 2.15 and 2.17, the decrease at lake 98-2 is, however, not as prolonged and does not extend to the basal sediments). All these lakes are located within a similar area of Norway (Figure 2.9) which may suggest that this is some sort of regional lithostratigraphic signal. The other two cores, however, have not been dated and, therefore, it is hard to draw definitive conclusions about regional lake conditions from these patterns.

In addition, however, the diatom concentrations remain relatively low throughout the zone suggested that within lake productivity may be low which might be reflected in the suppressed %LOI values. Species numbers tend to vary little throughout the core profile and are not discussed further.

6.2.3 Diatom zone two, covering the period from *ca.*1910 (7cm) to *ca.*1740 (18.5cm)

- Temperature changes and changes in the relative proportions of the lake habitats

Several distinct changes occur in the transition period between zones 3 and 2 in terms of species assemblage and abundance. Several species which were abundant at the top of zone 3 disappear in zone 2. These include *Fragilaria microstriata*, *Sellaphora/Navicula pupula*, *Cyclotella kuetzingiana* var. *planetophora*, *Cyclotella kuetzingiana* var. *radiosa*, *Cyclotella* c.f. *comensis*, *Pinnularia microstauron* and *Sellaphora/Navicula verecundiae* (Figure 6.4). These species are replaced by several *Fragilaria* species (*F. pinnata*, *F. construens* var. *pumila* and *F. pseudoconstruens*) which rise in abundance dramatically.

At the bottom of zone 2 the number of planktonic diatom species decreases dramatically (Figure 6.13), due to the relative increases in the abundance of *Fragilaria pinnata* and *Fragilaria pseudoconstruens* in this section of the core (Figure 6.14). The diatom inferred January temperatures also decrease in the lower portion of this zone. All these variables indicate that this is a period of increased ice-cover for the lake with a reduction in the length of the open water season. Furthermore, *Fragilaria pinnata* was shown to be a 'cold indicator' (as noted in Chapters 4 and 5) in terms of both its ice-cover and January temperature optima, and its dramatic increase in the lower section of zone 2 could be due to a colder climate. However, as pointed out by Anderson (2000) *Fragilaria* sp. are notoriously cosmopolitan and other factors, such as higher TOC/DOC causing lower light penetration, may be more influential for the growth of this species.

It should be noted that the PCA axis 2 scores also decrease between 18.5-14cm and overall the scores follow a similar pattern to the January air temperature

reconstructions throughout the core, both probably being driven by the relative abundance of *Fragilaria pinnata*.

Towards the upper section of zone 2 the inferred January temperature increases again as do the number of planktonic species, primarily driven by the clear rise in *Cyclotella* aff. *krammeri* and the decreases in *Fragilaria pinnata*. *Cyclotella* aff. *krammeri* is a large planktonic species and its abundance in this section may indicate higher turbulence in the lake at this time due to a reduced ice-cover and higher wind mixing (see section 1.3.3.2). In addition with the increase in lake mixing, nutrient recycling patterns would also be altered, possibly resulting in increased nutrient availability, which could also affect the growth of this *Cyclotella* species.

- pH changes

There is no significant pH change within this section of the core. In addition the apparent links between the diatom inferred temperatures and the pH shifts proposed in zone 3 are not present within this zone.

- Lake/ catchment productivity

The %LOI increases and levels off within this zone to a constant level which continues for the duration of the core. The PCA axis 1 scores inversely reflect the %LOI by decreasing significantly in this lower section of the zone and levelling off to a constant throughout the rest of the profile.

The %LOI is relatively high for this period in the lakes history, suggesting relatively high productivity within the lake or its catchment at this time. This contradicts the evidence presented above suggesting that the lake was more ice-covered at this time, particularly in the lower section of the zone.

Although %LOI is often directly related to changes in climate, with increased productivity in warmer years (Catalan *et al.*, 2002c), the productivity signal is often complex. %LOI varies in relation to climate fluctuations but it is not conclusively proven in which direction the productivity changes take place. For example, Battarbee *et al.*, (2001) negatively correlated %LOI to winter temperature due to changes in mixing regime and a lower retention of nutrients, due to a longer ice-cover period.

Furthermore, if temperatures were indeed colder, at this point in the lake history this might result in a more stable catchment reducing the influence of catchment erosion. In this way less inorganic catchment material might be deposited in the lake which might result in the more organic %LOI sequence (seen in zone 2) as it is just reflecting the *within* lake productivity.

On the other hand increases in precipitation for the lake at this time might also increase the %LOI as more material (both inorganic and organic) is washed in from the catchment. Furthermore, the texture and colouration within the core changed dramatically at *ca.*19cm to much darker, organic sediment from this point and above (Figure 6.1). This may indicate some sort of catchment disturbance in the area or a major change in the lake's stratification pattern affecting the production and deposition of sediment. The catchment of Lake Hornsjøen is, however, less impacted than Lake Gåvålivatnet and major anthropogenic catchment disturbance is unlikely (see section 2.3.7).

The proposed higher productivity, indicated by the %LOI, is not substantiated by either the inferred TP values, which are relatively low for this section of the core, or the concentration of diatoms which is particularly low in the lower section of the zone. The reconstructed TP values show minimum levels between 15 to 18cm which correspond with the minimum levels of *Cyclotella* sp. agg.

6.2.4 Diatom zone one, covering the period from *ca.*1910 (7cm) to 2001 (surface sediments)

- Temperature changes and changes in the relative proportions of the lake habitats

Several species assemblage changes can be seen in the top section of the core which could be related to changes in recent climate. There is a marked increase in the small *Cyclotella* species (*Cyclotella comensis*, and *C. pseudostelligera*) which have often been linked with positive temperature changes (see section 1.4.1.2). In addition many of these *Cyclotella* species show a cyclical distribution pattern (*Cyclotella pseudostelligera* and *C. kuetzingiana* var. *planetophora*) throughout the core which may be related to changes in climate within the profile. The increases in these small *Cyclotella* species have resulted in lower non plankton to plankton ratio reflecting the

higher abundances of planktonic diatoms at this time. These trends are discussed further in section 6.3.1

Fragilaria pinnata decreases dramatically in the upper 6cm possibly indicating increasing mean temperatures. However, *Fragilaria brevistriata* another species shown to have a low temperature and ice-cover optima in Chapters 4 and 5 increases in the upper section of the core. As noted earlier *Fragilaria* species are, however, known to be particularly cosmopolitan and may not directly reflect changes in climate

The reconstructed January temperatures in this section of the core continue to rise throughout the zone and the PCA axis 2 scores mirror this increase.

- pH changes

As with zone 2 there are no significant changes in pH in the surface sediments of the core, despite the changes in diatom species composition and abundance.

- Lake/ catchment productivity

Figure 6.13 shows that zone 1 is characterised by a relatively high %LOI and diatom concentration and slightly higher than average TP levels, all indicating high levels of productivity for this period.

The increases in the *Cyclotella* species in this zone could be related to nutrient levels as *C. comensis* has been shown to have a relatively high TP optima in other training sets also (25µg/l Stevenson *et al.*, 1991). In addition *Fragilaria virescens* var. *exigua* (= *F. exigua*), also increases in this zone which has a relatively high Chl *a* and a high nutrient status (Jones and Juggins 1995). Increased nutrient levels may also, however, be related to increasing temperatures due to changes in nutrient cycling, weathering in the catchment and the release of previously locked-up nutrients (esp. nitrogen) due to snowpack thawing (Nickus *et al.*, 1998). The %LOI, however, does not alter significantly throughout both zones 1 and 2.

6.3 How faithfully are known climatic changes occurring over the last 500 years recorded by the palaeolimnological record at Lake Hornsjøen

The last section has discussed the changes shown in the diatom species and the diatom reconstructed variables and related them to hypothesised changes in climate, lake productivity, habitat availability, nutrient supply and the lake's mixing regime.

The following sections (6.3.1- 6.4.3) assess the extent to which the specific, and well documented, climate changes occurring, either during the LIA or, during the past 140 years, are portrayed in the palaeolimnological record from Lake Hornsjøen. The following section discusses the detection of recent climate change using the sediment record and assesses which parameters are responding to the recorded climatic warming. In this way suitable climatic proxies (contained in Figure 6.13) for this lake can be identified.

6.3.1 The detection of recent climatic change using the palaeolimnological record at Lake Hornsjøen

Recent climatic records within Norway show that there is a positive trend in annual temperatures, during the period 1876-1997, and that this relationship is statistically significant (to the 5% level in at least in 5 out of the 6 regions studied, Hansenn-Bauer and Nordli 2000). Trends, however, are often hard to decipher due to the high noise to signal ratio within the climate data.

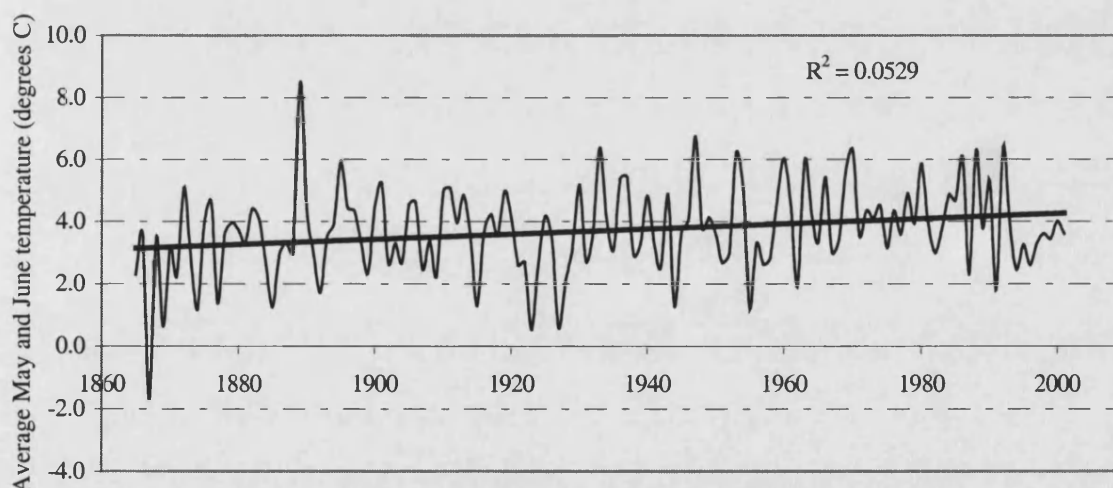
This high noise to signal ratio is illustrated in Figure 6.14 which shows the average spring (May- June) temperatures at Lake Hornsjøen (see 3.5 for climate station data and locations). Despite the high degree of variability over the last 150 years the record does show an increase in spring temperature of *ca.*1.5°C over the time of the instrumental record (*ca.*140yrs) (Figure 6.14). Only spring/ summer temperatures are available for Lake Hornsjøen and the extent to which the winter temperatures might reduce or increase this warming trend, therefore, cannot be calculated.

Recently, however, instrumental records from adjacent areas of Norway from the early 1990s have shown large increases in winter precipitation and milder winters, in conjunction with the rises in spring/ summer temperatures (Hansenn-Bauer and Nordli

2000) causing the advance of many Norwegian glaciers despite the occurrence of slightly higher annual temperatures (Nesje *et al.*, 2001b).

These temperature changes will have affected the ice-cover regime at Lake Hornsjøen in recent years. It is not only the change in temperature, however, that will affect the ice-cover of the lake but also the temporal variation of the precipitation (i.e. whether it falls as snow or rain) and the total amount of precipitation (Smith 2002). More precipitation in the late Autumn, which will most likely fall as snow, will shorten the period of clear ice formation and, therefore, the overall thickness of the ice will be less and more susceptible to increases in temperature in early summer, causing earlier ice break-up. The recent wet winters in Norway may, therefore, result in a shorter clear-ice formation period. Furthermore, the higher annual temperatures over the instrumental record, causing increased spring melt, will cause earlier ice-break as the lake volume increases and the ice breaks from the lake edge. The next four sections evaluate whether these changes are reflected within the sediment record of the lake and the diatom inferred parameters.

Figure 6.14: Instrumental record of average May and June temperature (°C) for Lake Hornsjøen



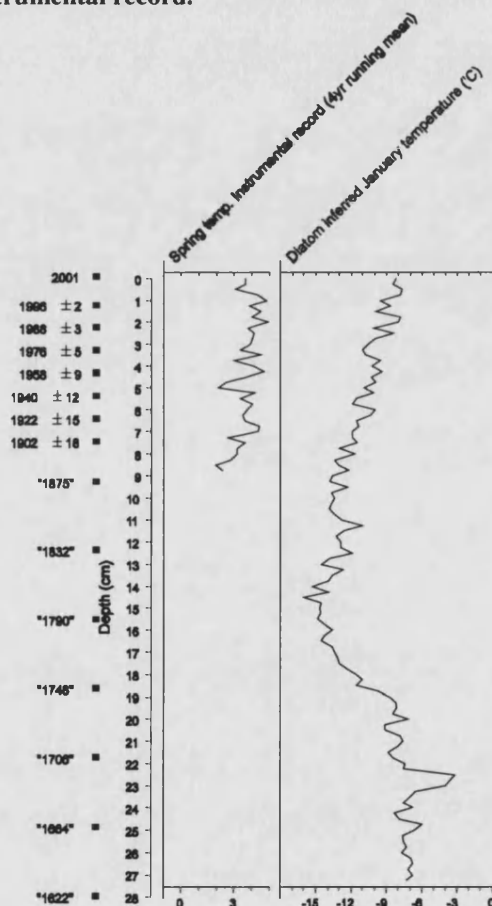
6.3.1.1 Does the January temperature transfer function reflect the increase in temperature occurring over the period of the instrumental record?

Unfortunately recorded January temperatures are not available for the site (section 3.5), therefore the accuracy of the reconstructed January temperature cannot be compared statistically. The instrumental record, spanning the last *ca.* 140 yrs, does

have measurements for spring temperature and these have been plotted, constrained against the ^{210}Pb chronology, for the core (Figure 6.15). These indicate a general warming from 8.5cm (*ca.*1865) to the surface which corresponds with the general trend shown within the reconstructed January temperature profile.

The diatom inferred reconstructed January temperatures (Figure 6.15) show an increase of *ca.* 3°C over the same time period, suggesting a degree of exaggeration in the reconstruction trends. The direction of trend, however, is correct and this suggests that the reconstructed values can be used in a qualitative sense to infer colder or warmer periods within the core.

Figure 6.15: Diatom inferred January temperature and its comparison with the spring temperature instrumental record.

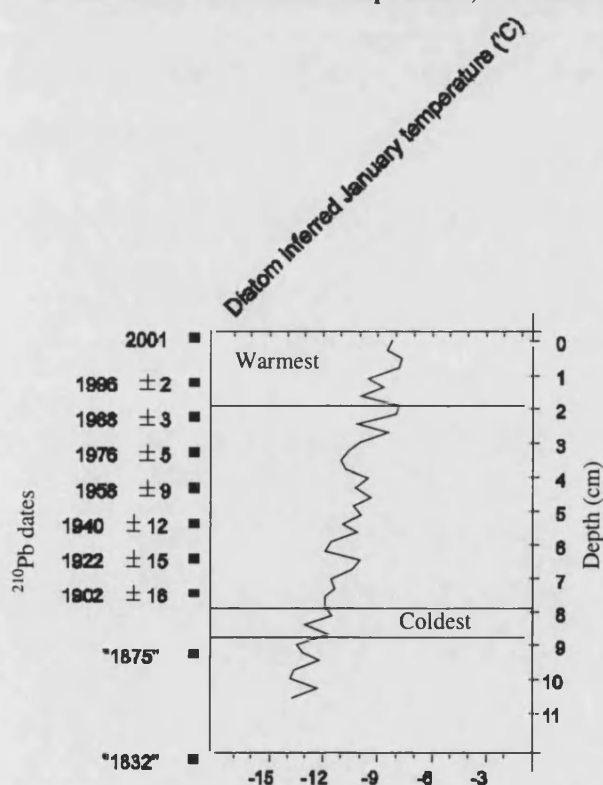


It is possible, however, to use more regional climate data to investigate the accuracy of the January temperature transfer function in more detail. It has been reported that over the last 120 years of the instrumental record for central Southern Norway the

lowest winter minima are found in the 1880s (1881, 1888 found to be the coldest) (Hansenn-Bauer and Nordli 2000). The 1990s and late 1980s have as mentioned above, been a decade of particularly warm winters (1989, 1990, 1992 as the warmest in rank order) for central southern Norway (Hansenn-Bauer and Nordli 2000).

This information is shown graphically (Figure 6.16) against the diatom inferred temperature record, which is again constrained by the ^{210}Pb dates. The general trends, documented in the winter instrumental records, seem to fit in well with the reconstructed temperatures, it should be noted however that this could simply be coincidental as there is no way of independently verifying the ^{210}Pb dates and the errors associated with the techniques increase with increasing depth (see also section 6.3.3). In addition the errors associated with the January temperature transfer function are high and this should not be forgotten. It is tentatively suggested however that the diatom inferred reconstructions can be used, in a qualitative sense, to infer changes in climate for this site.

Figure 6.16: The diatom inferred January temperature reconstructions with the years of warmest and coldest winter temperature, derived from the instrumental record plotted.



6.3.1.2 Do changes in species abundance reflect recent climate warming?

By plotting the abundant species in zones 1, the period associated with recent climatic warming as shown from the instrumental record, against the environmental variables within the training set insights in to the response of these diatoms to climate can be made (Figure 6.17). In this way the ecological preferences of the species in the contemporary training set can be evaluated to see if they respond positively or negatively to the climate variables within the training set, such as January or July temperature and altitude (used here as a surrogate for climate).

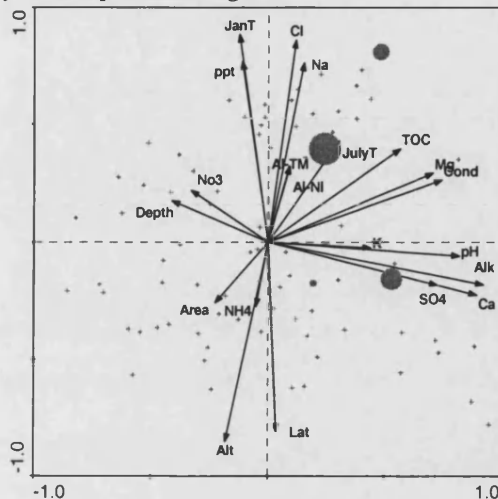
In order to explore the ecological preferences of these species, RDA attribute plots of species rising in abundance in zone 1 (*Cyclotella pseudostelligera*, *Cyclotella comensis* and *Cyclotella kuetzingiana* var. *planetophora*) were plotted and are presented in Figure 6.17.

It can be seen that *Cyclotella pseudostelligera* and *Cyclotella comensis* both tend to favour the higher temperature lakes, but the pattern may also be related to a pH/conductivity signal. This is also the case for *Cyclotella kuetzingiana* var. *planetophora* with the exception of one site (CN0018, in the bottom right quartile). But again this could equally be a reflection of a sea salt gradient preference rather than a temperature one. In general though, it could be concluded that the abundances of these species might reflect the recent increases in temperature within Norway.

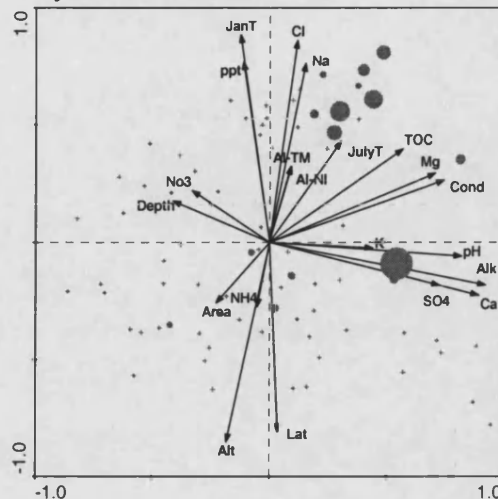
The contemporary data set was also used to analogue match the samples down the core. Diatom assemblages from the 79 lake data set are matched using dissimilarity coefficients to similar assemblages within the core. In this way environmental conditions can be inferred from the contemporary environmental information collected for the site. It was intended that this would be used to show changes in climate if samples from different altitudes (altitude being used in this instance as a climate proxy) were matched with samples in the core; matches of lower altitude sites would imply warmer conditions and should occur at the top of the core. Unfortunately, the matches did not alter significantly in terms of altitude and the results are not presented here. The EDDI training set was also used in a similar way but the samples proved to be too dissimilar in terms of diatom assemblages (i.e. representing a no good modern analogue situation) to infer climatic conditions.

Figure 6.17: Attribute plots of species against environmental variables using RDA on the 79 lake training set. Species abundance in each sample are presented as proportional circles (+ indicates the species is absent within that sample). Those species increasing significantly in abundance at 0-9cm within the core are plotted.

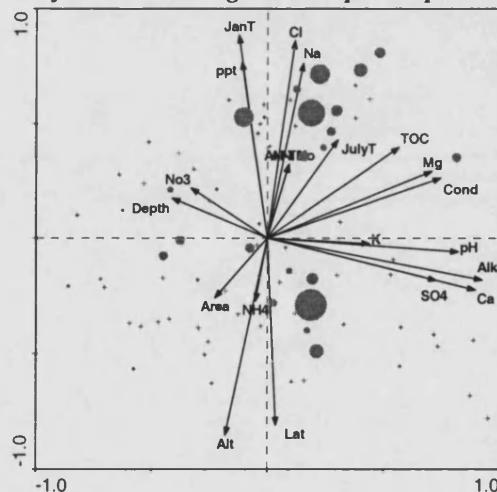
Cyclotella pseudostelligera



Cyclotella comensis



Cyclotella kuetzingiana var. *planetophora*



6.3.1.3 Do changes in habitat availability reflect recent climatic change?

Following on from the evidence presented above the ratio of non planktonic to planktonic species is lower in the upper sediments of the core, reflecting the increased growing season and reduced ice-cover which would favour the growth of planktonic species (see section 1.3 and 1.4).

As noted earlier many palaeoclimatic records from high mountain lakes across Europe have focused on the increases in planktonic diatom species as indicators of climatic warming, related to ice-cover changes, and other linked indirect mechanisms (Bigler and Hall 2002; Rosen *et al.*, 2001a; Sorvari and Korhola 1998; Catalan *et al.*, 2002b;

Koinig *et al.*, 2000). These have often related changes in the abundance of planktonic diatoms to the instrumental record which demonstrated that their relative abundance followed roughly the mean annual air temperature. During warm periods more planktonic diatoms were observed than during cold ones (Koinig *et al.*, 2002).

These studies showed, however, that the impact of changes in *winter* and *spring* temperature was stronger than that of *summer* temperature, suggesting that the duration of ice-cover is more important than absolute temperature values during the open water period. It was also shown that warm winters tended to cause an earlier ice-break and consequently a longer growing period for *Cyclotella* even if summer temperatures were low (Koinig *et al.*, 2002).

Temperatures in Norway over the last 20 years show a positive linear trend (Figure 6.14) with increases in winter temperature as well as spring (Nesje *et al.*, 2001b, section 6.3.1), suggesting that recent milder winters for the lake area could be responsible for the increased *Cyclotella* sp. growth evident in the top of this core. In addition the clear increase in *Cyclotella pseudostelligera* at the top of the core might be related to a delay in the formation of the lake ice-cover in autumn, associated with the increased annual temperatures, as this species has been shown to bloom in the late autumn possibly associated with a temperature threshold and the lakes overturn period (Catalan *et al.*, 2002a).

It has also been shown previously that chrysophytes can be related to the ice duration and in particular ice-out timing (i.e. Spring) in lakes due to the onset of the stratification period (Pla 1999). Ice-out would be earlier over recent decades at Lake Hornsjøen due to the mild winters, suggesting that chrysophyte cysts should increase in the upper sections of this core. The chrysophyte cyst relative numbers, however, do not increase significantly in the upper sediment of zone 1. Therefore, it would appear that the chrysophyte cyst to diatom ratio does not represent a good climate proxy measure for this particular site.

6.3.1.4. Do changes in lake productivity indicate recent climate warming?

The %LOI pattern in Lake Hornsjøen does not show any increases in the surface samples, suggesting few changes in productivity due to increased air temperature in

the latter part of the present century. The TP reconstructions do appear to be higher in the upper 9cm of the core which could be associated with higher in lake productivity due to the positive temperature changes over the last 100 years.

6.3.1.5 Summary of evidence reflecting recent climate warming

It has been suggested above that the ratio of non planktonic to planktonic diatoms indicate recent climatic change. In addition the shifts in diatom species, evident within the upper section of the core, were also shown to be correlated to climate warming. The January temperature transfer function also shows increases in temperature in accordance with the instrumental temperature record. The reconstructions are, however, grossly overestimated and the errors associated with the model should be noted. It would appear, however, that the chrysophyte cyst to diatom valve ratio, the diatom species number, %LOI and %DW, and the diatom inferred TP and pH reconstructions do not reflect changes in recent climate for this core.

Following on from this it is suggested that the climatic proxies, shown to respond to the known climatic changes occurring over the instrumental record identified above, can therefore be used to detect changes in climate associated with the LIA. This is discussed in the following section.

6.3.2 The detection of climatic changes associated with the LIA at Lake Hornsjøen

There is strong evidence for major climatic shifts occurred during the LIA in the area surrounding Lake Hornsjøen (see section 1.5.1). This section assesses the limnological changes that might have occurred within Lake Hornsjøen at the time of the LIA, and how these are represented by the sediment/ palaeolimnological record.

According to the literature the LIA occurred within the central Norwegian area from approximately 1650 to 1800 reaching its maxima in 1750 for this part of Norway (section 1.5.1 and Figure 1.2). Assuming that the core chronology for Hornsjøen is correct the LIA maxima should be represented within the sediment between *ca.*24cm to 13cm within this core, with the LIA maxima occurring at the transition between diatom zones 2 and 3 (Figure 6.4).

The changes in climate occurring during the LIA are likely not only to have reduced the average annual temperatures by about 1-1.5°C for the region but also to have resulted in increased winter precipitation and lower than average summer temperatures (Nesje and Dahl 2002; Nesje and Dahl 2003 see also section 1.5.1). In addition there may have been increases in the storminess in the area during the recovery from the LIA, documented by the detection of storm debris deposits in the region around 1789 (Nesje *et al.*, 2001a, Figure 1.2). It should be noted, however, that due to its long duration many climatic fluctuations may have occurred throughout the time of the LIA.

Using the proxies identified as responding to changing climate in the top of the core, the next section evaluates how the LIA is represented in the sediment at 13-24cm, and the LIA maxima occurring at 15-19cm

6.3.2.1 Does the January temperature transfer function record LIA cooling?

It would appear that, based on the chronology alone, the January temperature transfer function does indicate periods of cooler climate during 1740- 1830 (18.5cm- 12cm). The transfer function detected the recent climatic warming successfully, albeit at a different magnitude, suggesting that it is appropriate to use it to look at temperature shifts in this way but only in a qualitative sense.

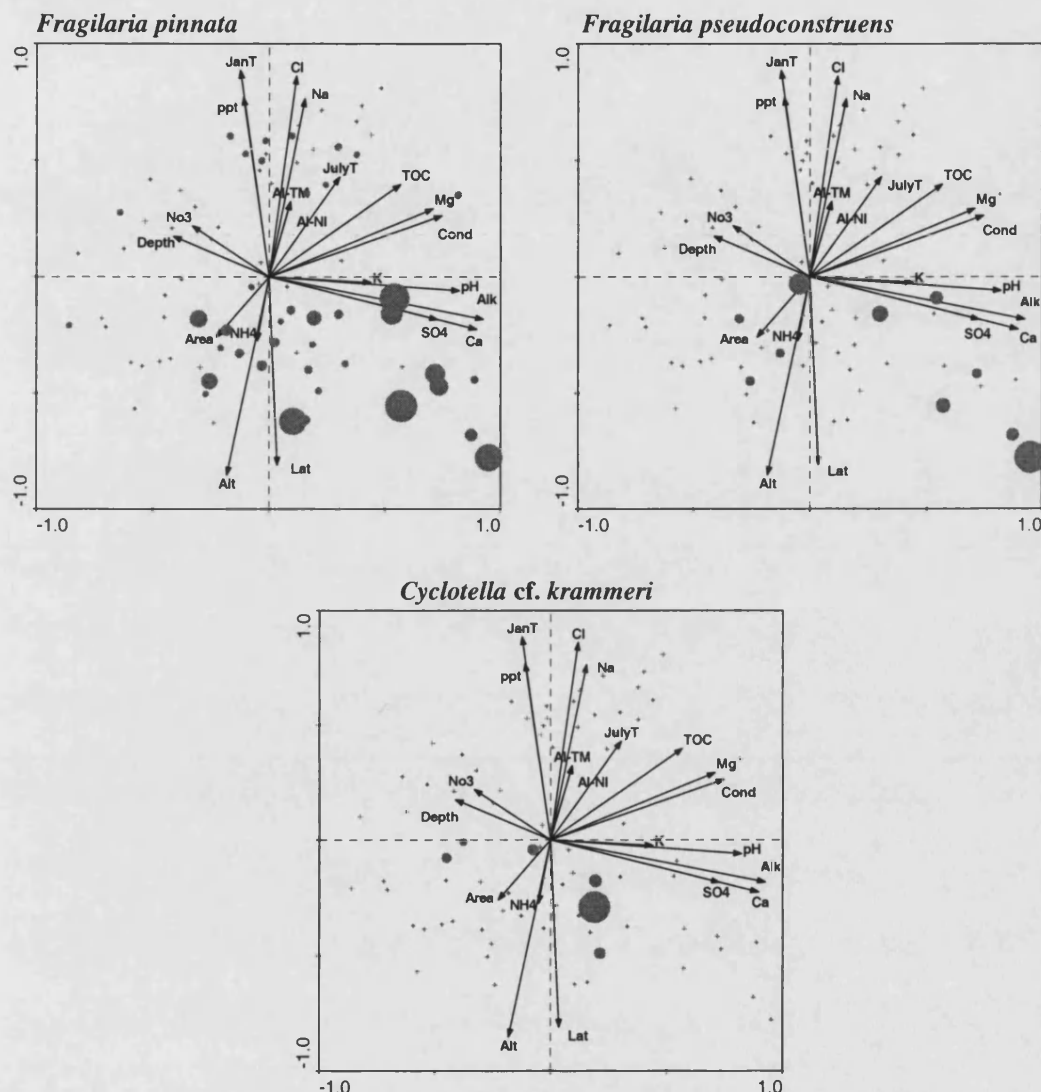
6.3.2.2 Changes in diatom species related to the LIA

It was suggested above that strictly according the chronology, that the LIA maxima might be recorded within the transition zone between zones 2 and 3 and with the lower part of zone 2 representing the maxima (i.e. 16-19cm). Several distinct changes in the species assemblages occur in the transition period between zones 2 and 3 as discussed in section 6.2.3 (Figure 6.4). Again the information from the training set was used to evaluate the ecological preferences of the dominate species in this section of the core. RDA plots of species occurring in high abundances in zone 2 (*Fragilaria pinnata*, *Fragilaria pseudoconstruens* and *Cyclotella cf. krammeri*) were plotted from the 79 lake training set in conjunction with the environmental variables available (Figure 6.18).

Fragilaria pinnata, *Fragilaria pseudoconstruens* and *Cyclotella* cf. *krammeri* (Figure 6.18) all show distinct preferences for lower January and July temperatures within the training set sites. Their increase in abundance, therefore, at a time within the core when temperatures would have been relatively colder is significant. It is realised, however, that these patterns might be due to a combination of environmental factors related to the type of lakes within the training set with lower January temperatures. For example, the lakes with lower temperatures tend to be the clearer and larger, and predominately in Norway, and therefore the patterns could be a reflection of a light or TOC based gradient, as the Norwegian lakes tend to have lower TOC measurements (See chapter 2). In addition *Cyclotella* cf. *krammeri* is only really abundant within one sample in the training set and so any conclusions drawn from this should be treated with caution.

Although the link between diatom species and temperature is probably due to indirect factors *F. pinnata* is characteristically known as a ‘cold indicator’ species (Seppa and Birks 2001; Rosen *et al.*, 2001b) with estimated July air temperature optima of <7.5°C (Rosen *et al.*, 2001b). Rosen’s study also linked the abundance of *Fragilaria pinnata* to the LIA period (Rosen *et al.*, 2001b) when it re-appeared in a sediment sequence at a time corresponding to the LIA, after it had been absent for several centuries. Likewise in the Lake Hornsjøen core *Fragilaria pinnata* decreases after the time associated with the LIA maxima at 14cm and has limited abundance in zone 1. These trends, however, are more likely to be a response to indirect climatic changes occurring during the LIA, such as habitat availability, mixing regimes, increased snow cover etc. rather than absolute air/ lake temperature changes.

Figure 6.18: Attribute plots of species against environmental variables using RDA on the 79 lake training set. Species abundance in each sample are presented as proportional circles (+ indicates the species is absent within that sample). Those species increasing in abundance at 16-19cm within the core are plotted.



6.3.2.3 The detection of the LIA using lake habitat availability shifts

The reduced temperatures occurring during the LIA would result in a shorter open water period causing a decrease in planktonic diatom growth. The core from Hornsjøen shows that there is a large decrease in planktonic diatoms in the lower section of zone 2 which could be related to the LIA maxima. There is a general increase in planktonic forms again above 13cm (*ca.*1820) which could be associated with the lakes recovery after the LIA.

The pattern, however, is complicated by the increase in non planktonic diatoms between 4-9cm mainly driven by the relatively high abundances of the *Fragilaria* spp. and the decline in *Cyclotella* cf. *krammeri*. It is possible that this increase might be related to the cold winters associated with the 1880's as shown in the instrumental record but the link is tenuous and unlikely to result in such a large increase in non planktonic species. As noted earlier, some *Fragilaria* species are considered to be opportunistic and compete well under numerous different growing conditions and it is therefore highly probable that their abundance here is not directly related to climate.

6.3.2.4 Detecting the LIA using patterns of lake/ catchment productivity

Although it was concluded above %LOI had not responded to the recent climatic warming, the dramatic shift in %LOI and sediment colour at the transition between zones 2 and 3 may be significant in terms of LIA cooling. The shift at the bottom of zone 2 to higher %LOI could be co-incidental but it could equally in some way be related to the onset of the LIA. However, the %LOI does not decrease again in the upper section of zone 2 representing the termination of the LIA.

The diatom inferred TP reconstructions do not seem to show any conclusive links with changes that might have occurred during the LIA and remain relatively constant throughout zone 2 (see also section 6.2.3 for further %LOI and climate discussion).

6.3.3 Dating caveat

Although the ^{210}Pb dates are thought to be reasonably accurate for this core it should always be remembered in palaeolimnological studies, that the standard errors for the dating technique increase dramatically with increasing core depth (see Figure 6.3). Although the sediment accumulation rate was thought to be constant, the large standard errors recorded at the bottom of the ^{210}Pb record may influence the extension of the dating using the sediment accumulation rate. For example, if the date at the bottom of the ^{210}Pb record is in fact 40 years either earlier or later then the dates calculated hereafter using the bottom ^{210}Pb date would also be inaccurate.

It is fortunate, however, that the duration of the LIA is relatively long (Section 1.5.1), in terms of the time it represents within the whole core profile. The shifts in the palaeolimnological record should, therefore, reflect the gradual trends regardless of

the dating inaccuracies. The dates just help to confirm that the changes seen in the core can hypothetically be linked with climatic changes through *a priori* knowledge of species ecological preferences etc. and by using climatic proxies shown to have responded to recent climate warming.

6.4 Summary and conclusions

In summary it is tentatively suggested that the upper section of Zone 1 shows changes in various palaeolimnological indicators that can be associated with the recent temperature increases recorded by the instrumental record. These include dramatic changes in species assemblages in the upper 9cm of the core in particular related to the rise in small *Cyclotella* species. In addition changes in the non planktonic to planktonic diatom ratio, suggesting a longer ice-free season related to the elevated temperatures.

Several parameters which it was thought would react to the positive warming trend occurring over recent decades appeared not to do so. No definitive trends were evident in the %LOI, the diatom species number, the relative production of chrysophyte cysts or the pH within the upper part of the core.

The parameters shown to respond to the changes in recent climate warming were then used to detect changes occurring due to the LIA in Lake Hornsjøen's sediment record. The marked decrease in the diatom concentration, species diatom shifts and an increase in the proportion of non planktonic to planktonic species, all indicated a reduced ice-free period and lower in lake productivity for the lake in the LIA period. These trends, however, are not conclusive due to an increase in non planktonic diatoms in a period not associated with dramatic climate cooling (1900-1930's, at 5-7cm) and the fact that the diatom species could be responding to other environmental factors.

Several parameters showed no clear trends associated with the LIA period. These included the diatom inferred pH and the diatom species number. In addition although %LOI changed significantly in the lower section of zone 2 its constancy throughout the rest of zones 1 and 2 could not be related to changes in climate and, therefore, its initial shift at 18.5cm might in fact be co-incidental.

Finally, despite the large errors associated with the January temperature transfer function the diatom inferred temperatures appear to fit in well, both in terms of the timing and direction of temperature change, with the changes in temperature occurring during both the LIA and over recent decades.

This chapter has presented the results of the high resolution diatom and lithostratigraphic work for Lake Hornsjøen. Climatic and environmental parameters inferred from the diatom record were presented. It was investigated whether the changes evident in the palaeolimnological record could be linked to known climatic changes occurring during both the LIA and the period covering the instrumental record. It was concluded that although some parameters could be related to climate the signal from the palaeolimnological record was in no way conclusive.

The next chapter presents the results of the palaeolimnological analyses for Lake Gåvålivatnet. It assesses whether the changes in climate during the LIA and over recent decades, evident within the palaeolimnology of Lake Hornsjøen, are in fact evident within other lake sediment records from the region.

Chapter 7

Palaeolimnological analysis of Lake Gåvålivatnet (core 01-03)

Introduction

This chapter is similar in structure to Chapter 6. The water chemistry, lithostratigraphy, core chronology and diatom analysis results are presented for Lake Gåvålivatnet. Distinct down core changes in diatom assemblage are identified. The reconstruction of TP, pH, ice-cover duration and January temperature are illustrated and discussed. The changes in the various diatom inferred parameters, lithostratigraphy and diatom habitat changes down the core are discussed, and related to hypothesised changes in the lake system.

Finally, changes in the profile of Gåvålivatnet are evaluated in relation to the climatic events of the LIA and over the period of the instrumental record. The accuracy of the January temperature model is evaluated through a comparison with the historical temperature series for the lake. Similarities and differences in lake response between Lake Hornsjøen and Gåvålivatnet are also explored.

7.1 Results

7.1.1 Water chemistry and site details

It can be seen from Table 7.1 that Lake Gåvålivatnet has significantly higher Ca^{2+} , alkalinity and pH values in comparison to Lake Hornsjøen. These variables are highly correlated and are probably due to the differing underlying bedrock of the lakes (Section 2.3.6). The two sites have similar levels of precipitation, Lake Gåvålivatnet is slightly milder in terms of both summer and winter temperatures but this is probably due to its lower altitude. Lake Gåvålivatnet is also larger in area than Hornsjøen (Section 2.3.6 and Figure 2.18b), but has a similar lake depth. The lake differs in bathymetry from Hornsjøen in that it has two lake basins (Figure 2.18b).

Table 7.1: Summary of the environmental data for Gåvålivatnet

Variable	Units	
Lake altitude	m a.s.l	939
Max Depth	m	16.5
pH	pH units	7.52
Alk	µeq/l	806
Cond	µS/cm	82
Na ⁺	µeq/l	44
NH ₄ ⁺	µeq/l	0
K ⁺	µeq/l	33
Mg ²⁺	µeq/l	91
Ca ²⁺	µeq/l	725
Cl ⁻	µeq/l	13
NO ₃ ⁻	µeq/l	0
SO ₄ ²⁻	µeq/l	31
Al-TM	µg/l	11
Al-NL	µg/l	4
Al-L	µg/l	7
Abs-250		N/a
TOC	mg/l	3.9
Average July Temperature	°C	10
Average January Temperature	°C	-14.3
Annual Precipitation	mm	450
TP	µg/l	5-30
Chl <i>a</i>	µg/l	n/a
SRP	µg/l	<10
DS (Dissolved silica)	mg/l	7.1

7.1.2 Lithostratigraphy

Changes in the colour and texture of the core were noted when the core was extruded (see section 2.3.6) and it can be seen that these correspond to the changes evident within the %LOI profile (Figure 7.1) with the compact grey area having a very low %LOI and the orange/brown layers being much more organic in content.

7.1.3 Dating

Equilibrium between total ²¹⁰Pb activity and the supporting ²²⁶Ra is reached at a depth of about 11cm. It is suggested that the higher ²²⁶Ra activity in the top 4cm may indicate some changes in the mineralogy of the sediments although this is uncertain (Appleby *pers. com.*). Unsupported ²¹⁰Pb activity declines more or less exponentially with depth, suggesting uniform sediment accumulation during the past 130 years of the ²¹⁰Pb record (Figure 7.2, Table 7.2).

High ^{137}Cs concentrations in the surficial sediments suggest that the ^{137}Cs record is dominated by fallout from the 1986 Chernobyl accident. The ^{137}Cs inventory (10300 Bq m^{-2}) is at least 3-4 times higher than the inventory typical of weapons test fallout in central Norway. Downward diffusion of Chernobyl ^{137}Cs appears to have obscured the weapons ^{137}Cs record, and there is no indication of the location of the 1963 fallout maximum. The alternative indicator, ^{241}Am , was also not detected.

Figure 7.1: Core photograph and %DW and %LOI for core 01-03 (ca.29cm long) from Lake Gåvålivatnet

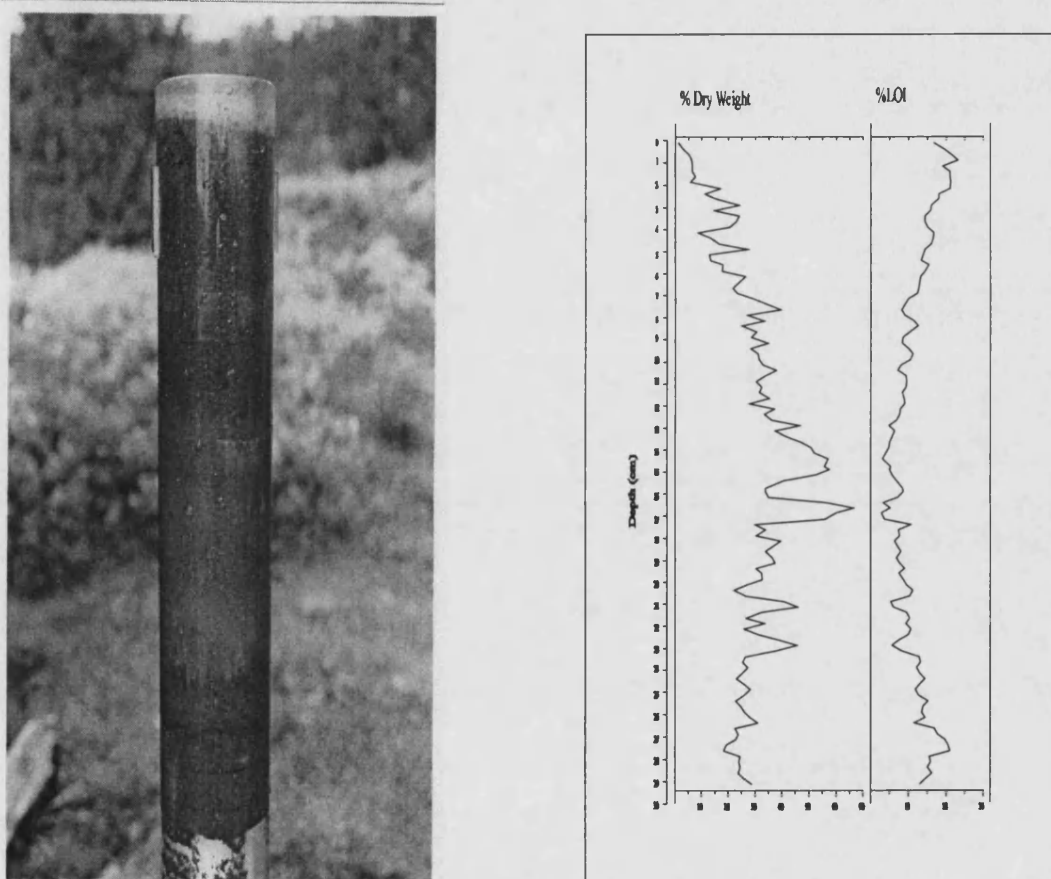


Table 7.2: Fallout radionuclide concentration in Gåvålivatnet, core 01-03

Depth		²¹⁰ Pb						¹³⁷ Cs	
		Total		Unsupported		Supported			
		cm	g cm ⁻²	Bq kg ⁻¹	±	Bq kg ⁻¹	±	Bq kg ⁻¹	±
0.63	0.02	683.1	71.8	570.4	73.0	112.7	13.2	2617.9	30.9
2.38	0.18	380.2	35.5	280.1	36.7	100.1	9.4	1961.5	23.0
3.38	0.38	271.8	21.2	193.6	21.9	78.2	5.4	752.6	10.2
4.63	0.61	223.0	18.1	163.7	18.7	59.3	4.7	399.0	7.2
6.38	1.00	94.4	12.5	51.0	12.9	43.4	3.2	165.1	4.2
8.13	1.63	68.2	7.6	25.9	7.9	42.3	2.1	65.1	2.8
10.13	2.39	61.3	7.1	13.9	7.4	47.4	2.1	42.9	1.7
12.13	3.22	27.9	6.6	-17.5	6.9	45.4	2.0	31.3	1.7

High ^{137}Cs concentrations in the surficial sediments suggest that the ^{137}Cs record is dominated by fallout from the 1986 Chernobyl accident. The ^{137}Cs inventory (10300 Bq m^{-2}) is at least 3-4 times higher than the inventory typical of weapons test fallout in central Norway. Downward diffusion of Chernobyl ^{137}Cs appears to have obscured the weapons ^{137}Cs record, and there is no indication of the location of the 1963 fallout maximum. The alternative indicator, ^{241}Am , was also not detected.

Figure 7.1: Core photograph and %DW and %LOI for core 01-03 (ca.29cm long) from Lake Gåvålivatnet

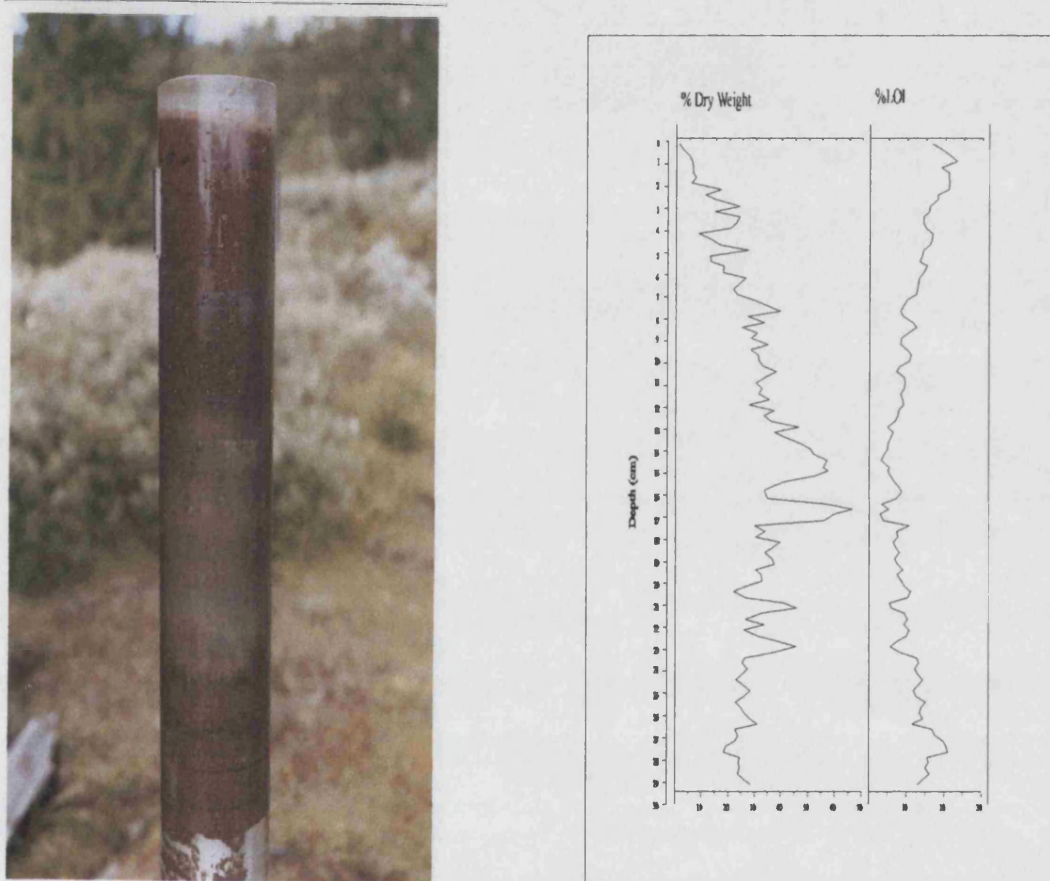
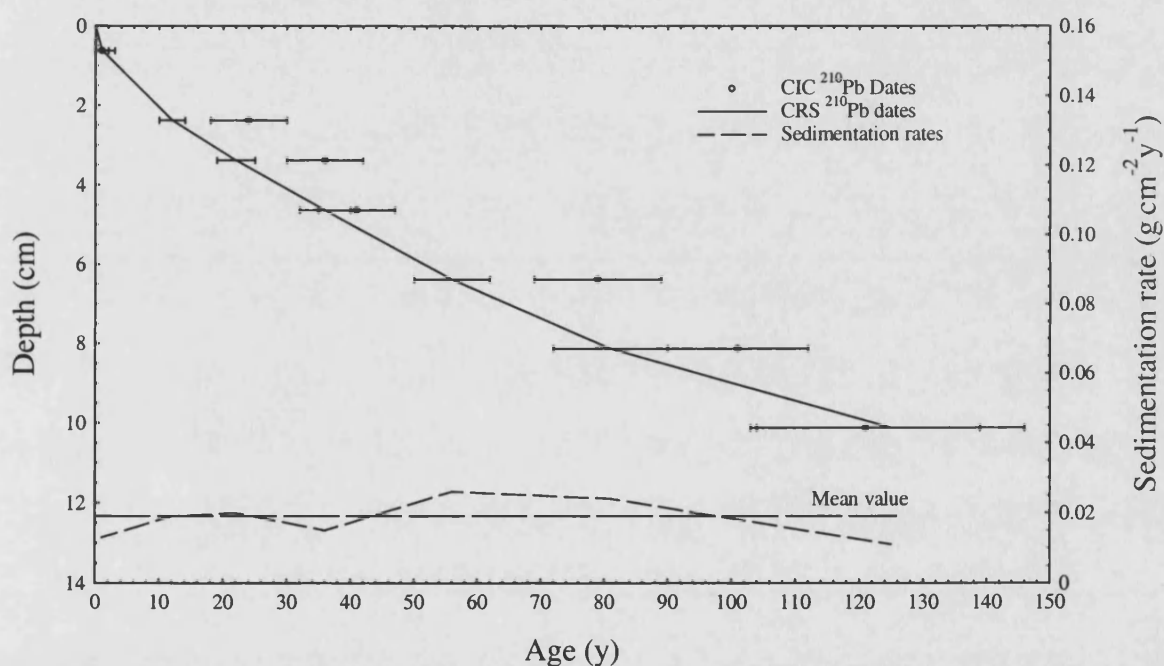


Table 7.2: Fallout radionuclide concentration in Gåvålivatnet, core 01-03

Depth		²¹⁰ Pb						¹³⁷ Cs	
		Total		Unsupported		Supported			
		cm	g cm ⁻²	Bq kg ⁻¹	±	Bq kg ⁻¹	±	Bq kg ⁻¹	±
0.63	0.02	683.1	71.8	570.4	73.0	112.7	13.2	2617.9	30.9
2.38	0.18	380.2	35.5	280.1	36.7	100.1	9.4	1961.5	23.0
3.38	0.38	271.8	21.2	193.6	21.9	78.2	5.4	752.6	10.2
4.63	0.61	223.0	18.1	163.7	18.7	59.3	4.7	399.0	7.2
6.38	1.00	94.4	12.5	51.0	12.9	43.4	3.2	165.1	4.2
8.13	1.63	68.2	7.6	25.9	7.9	42.3	2.1	65.1	2.8
10.13	2.39	61.3	7.1	13.9	7.4	47.4	2.1	42.9	1.7
12.13	3.22	27.9	6.6	-17.5	6.9	45.4	2.0	31.3	1.7

A core chronology was developed (Figure 7.2) and shows that there is little significant difference between ^{210}Pb dates calculated using both the CRS and CIC dating models (Appleby and Oldfield 1978). There is slight disagreement between the two methods between 2cm and 6cm. Both, however, suggest relatively uniform sediment accumulation rates during the past 120 years, with a mean value of $0.019 \pm 0.003 \text{ g cm}^{-2} \text{ y}^{-1}$ (0.08 cm y^{-1}). Since there is no ^{137}Cs date to validate the ^{210}Pb dates precisely the dates have been calculated using the mean sedimentation rate. The mean sedimentation rate was then used to estimate the dates of the sediments below the ^{210}Pb record. The bottom of the core, therefore, is dated at *ca.* 1650, which is slightly younger than the bottom sediments in the Lake Hornsjøen core (*ca.* 1620).

Figure 7.2: Radiometric chronology of Lake Gåvålivatnet, core 01-03, showing the CRS and CIC model ^{210}Pb dates and sedimentation rates.



7.1.4 Diatom analysis

The diatoms present within the core of Lake Gåvålivatnet are shown in Figure 7.3 and described in Table 7.3. It can be seen that the core is dominated by *Fragilaria*, *Cyclotella* and *Achnanthes* species. There are particularly large abundances of *Fragilaria pinnata*, *Fragilaria brevistriata*, *Fragilaria construens* var. *venter*, *Cyclotella* cf. *comensis* and *Achnanthes minutissima* throughout. The diagram can be divided into 4 zones according to the diatom composition. A list of the diatom species found in the core is presented in Appendix 7.1.

Table 7.3: The main changes in diatom assemblage in the core from Lake Gåvålivatnet

Diatom Zone	Depth and approx. dates	Species assemblage summary
1	0-1.5cm 2001-1996	<ul style="list-style-type: none"> - Dominated by <i>C. aff. comensis</i>, <i>A. minutissima</i>, <i>C. iris</i>, <i>F. pinnata</i> and <i>F. brevistriata</i>. - <i>C. iris</i> enters the profile in this zone and increases to over 20% abundance at 0-1cm. - <i>C. pseudostelligera</i> also increases in the surficial sediments.
2	1.5- 12cm 1994-1853	<ul style="list-style-type: none"> - <i>F. construens</i> var. <i>venter</i> reaches its maximum abundance in this section at c.25% at 8cm. - <i>C. comensis</i> declines between 4.5- 8cm but rises again above 4cm. - <i>A. minutissima</i> slightly reduced abundance in this zone - <i>F. microstriata</i> which has been present throughout the core decreases in this upper zone.
3	12-14cm 1853-1828	<ul style="list-style-type: none"> -Significant and discrete rise in both <i>C. aff. comensis</i> (c.30% max abundance at 13.5cm), and <i>C. comensis</i> (c.12% at 13.5cm). - There are corresponding decreases in various <i>Fragilaria</i> species and <i>Achnanthes</i> sp., including <i>F. pinnata</i>, <i>F. pseudoconstruens</i>, <i>F. construens</i> var. <i>venter</i> and <i>Achnanthes minutissima</i>
4	14-29 cm 1828-1640	<ul style="list-style-type: none"> -Dominated by <i>C. aff. comensis</i>, <i>A. minutissima</i> (max. abundance c.20% at 15cm), <i>F. pinnata</i> (c.20% at c. 20.5cm and <i>F. brevistriata</i> (max abundance 20% at 27cm) -<i>C. aff. comensis</i> fluctuates greatly throughout this section of the core, the peaks and troughs are similar to the changes in the <i>C. comensis</i> profile. - <i>F. construens</i> var. <i>binodis</i>- reaches its max. abundance in this section of the core at 5%, but it is present throughout the profile. - In samples 14-15cm there appears to be a change in the profile with a sharp decline and increase in <i>C. aff. comensis</i>, several species enter the profile or increase in abundance at this level, as a sort of short lived 'pulse', including <i>T. flocculosa</i>, <i>Hannaea arcus</i>, <i>Pinnularia subcapitata</i>, <i>P. borealis</i>. There are corresponding decreases in <i>C. radiosa</i> and <i>F. construens</i> var. <i>venter</i> at this level.

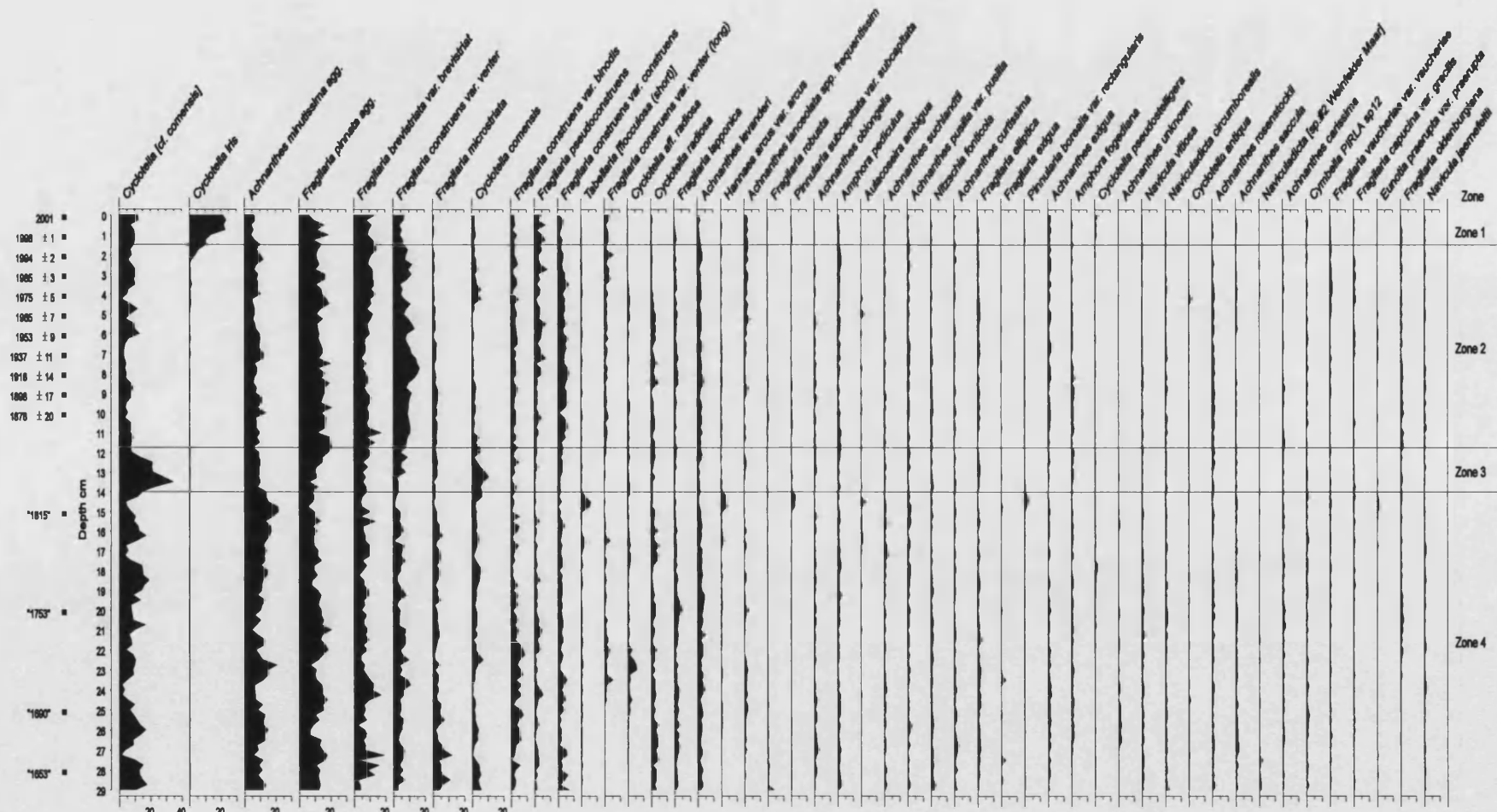


Figure 7.3: Summary diatom diagram for Lake Gåvålivatnet <2% taxa deleted

A DCA was performed on the 117 diatom samples from Lake Gåvålivatnet (Table 7.4). The gradient length for axis 1 is 1.2 standard deviation units (SD). The relatively small axis 1 gradient length (i.e. <1.5SD) implies that the diatom assemblage does not change significantly throughout the core and that linear PCA methods are more appropriate (see section 3.3.2).

Table 7.4: Summary statistics for the first four axes of the DCA for Lake Gåvålivatnet with 234 diatom species, 117 samples with square root transformation of species data and downweighting of rare species

DCA Axes	1	2	3	4
Eigenvalues	0.078	0.046	0.024	0.022
Lengths of gradient	1.200	1.310	0.999	0.631
Cumulative % variance of species data	7.6	12.0	14.3	16.5
Sum of all unconstrained eigenvalues	1.032			

A PCA was, therefore, performed (Table 7.5). The biplot (Figure 7.4) shows the diatom assemblage PCA scores for the 117 samples in Lake Gåvålivatnet. Various patterns are evident in this plot and these are listed below:

- The surface samples show a relatively high rate of change primarily associated with axis 2
- There is a cluster of similar assemblages at *ca.* 8cm- the change from the surface clustering to these sites seem to be orientated to axis 2
- A third zone seems to be associated with the samples at 13-14cm in the core.
- The lower section of the core is tightly clustered, suggesting relatively minor changes in diatom species assemblages in this section.
- Throughout the core the rate of diatom species change is not as great as those seen at Lake Hornsjøen (Figure 6.5), indicating fluctuations in diatom species abundance rather than many different species entering and leaving the core sequence.
- Relatively little variance is captured by axis 1 and 2 (20.3%), indicating that there is not a strong relationship between the diatom assemblages and the environmental gradients represented by axes 1 and 2. In comparison axis 1 and 2 captured 49.2% of the diatom variance at Lake Hornsjøen.

Table 7.5: Summary statistics for the first four axes of the PCA for Lake Gåvålivatnet with 234 diatoms species and 117 samples, with square root transformation of species data and downweighting of rare species

PCA Axes	1	2	3	4
Eigenvalues	0.126	0.077	0.064	0.039
Cumulative % variance of species data	12.6	20.3	26.7	30.6
Sum of all unconstrained eigenvalues	1.000			

Figure 7.4: Biplot of diatom taxa in the 117 samples for Lake Gåvålivatnet on PCA axis 1 and 2 with time track added, selected core depths are labelled (cm).

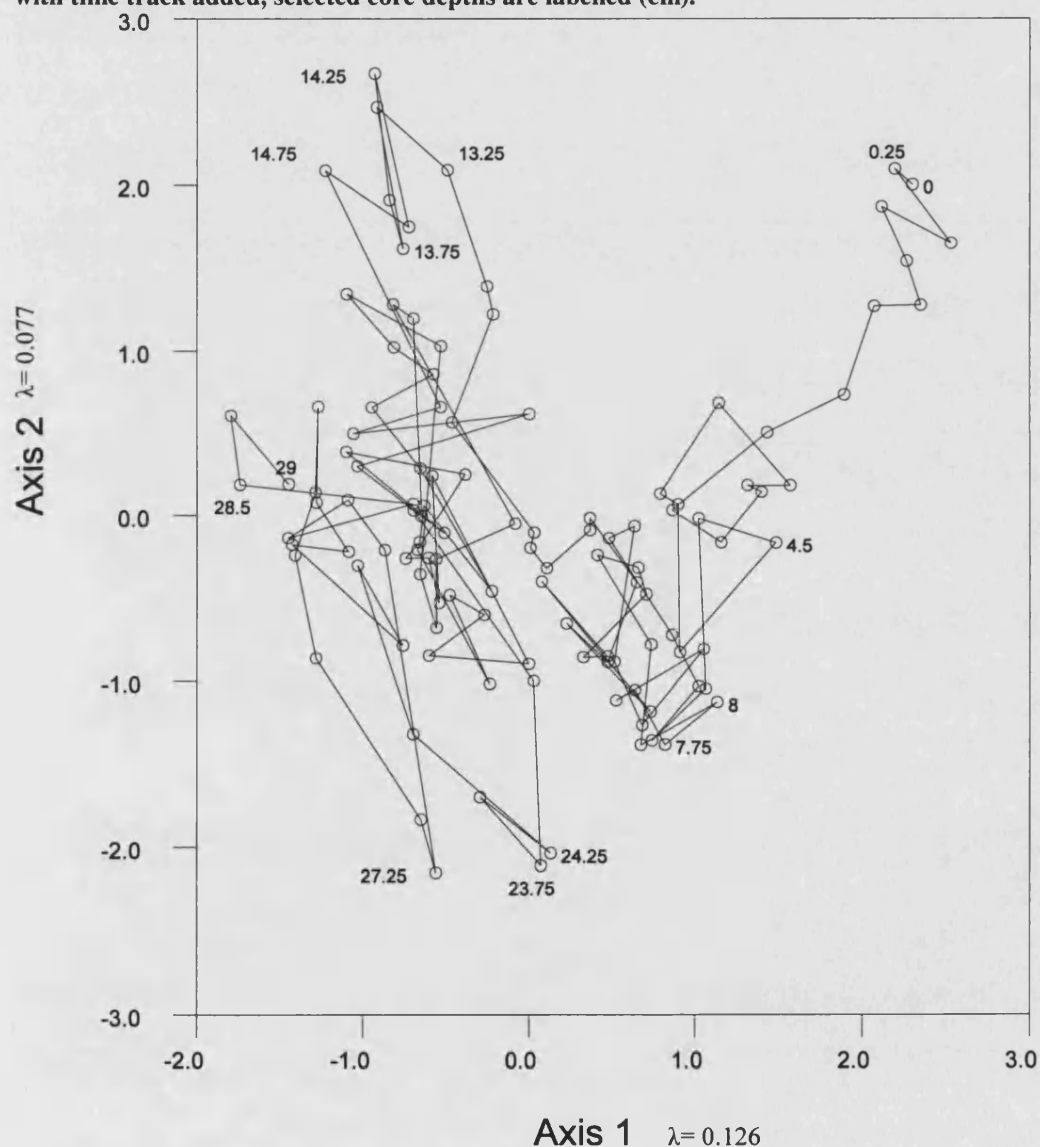
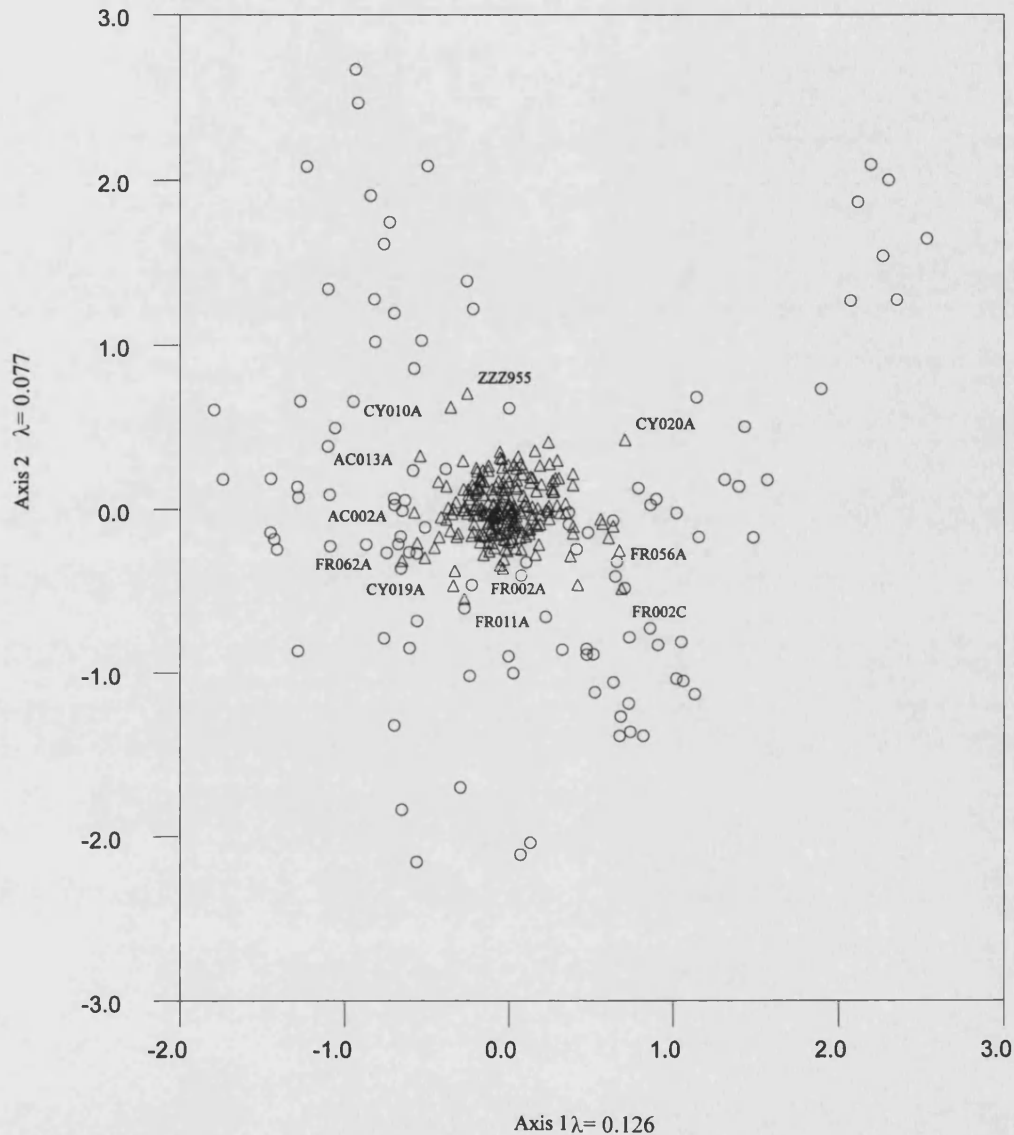


Figure 7.5: Biplot of 117 diatom samples (o) for Lake Gåvålivatnet and species (Δ - with selected taxa labelled) on PCA axis 1 and 2. Labelled taxa as follows: AC013A- *Achnanthes minutissima*, AC002A- *Achnanthes linearis*, ZZZ955- *Cyclotella* aff. *comensis* agg., CY010A- *Cyclotella comensis*, CY020A- *Cyclotella iris*, CY019A- *Cyclotella radiosa*, FR002A- *Fragilaria construens*, FR002C- *Fragilaria construens* var. *venter*, FR062A- *Fragilaria exigua*, FR011A - *Fragilaria lapponica*, FR056A- *Fragilaria pseudoconstruens*.



The PCA biplot of the diatom samples for Gåvålivatnet and associated species was plotted (Figure 7.5). The species are tightly clustered around the central part of the graph and only a limited number of species can be linked to the separate zones within the core. *Cyclotella iris* seems to be orientated towards the surficial sediments. The cluster of samples at ca. 7-8 cm (Figure 7.4) seem to be associated with changes in various *Fragilaria* species with *Fragilaria exigua*, *F. construens*, *F. construens* var. *venter* and *F. lapponica* all sharing similar positions on the biplot. In contrast the cluster of sites in the upper left corner of the biplot, representing the samples around

ca. 13-15cm in the core are associated with the planktonic species *Cyclotella comensis* and *Cyclotella* aff. *comensis* agg. The changes in these species, associated with the different zones within the core, can be seen in the down core diatom diagram (Figure 7.3).

7.1.5 The reconstruction of environmental variables

The diatom inferred reconstructed measurements for January temperature, TP, pH and ice-cover duration for Lake Gåvålivatnet are presented in this section. As with Lake Hornsjøen in order to assess whether it is appropriate to apply the transfer functions developed in Chapters 4 and 5 to the fossil assemblage, a DCA of the 79 surface sediments and the fossil diatoms were plotted with the fossil assemblages in conjunction (summary results of the DCA are shown in Table 5.8).

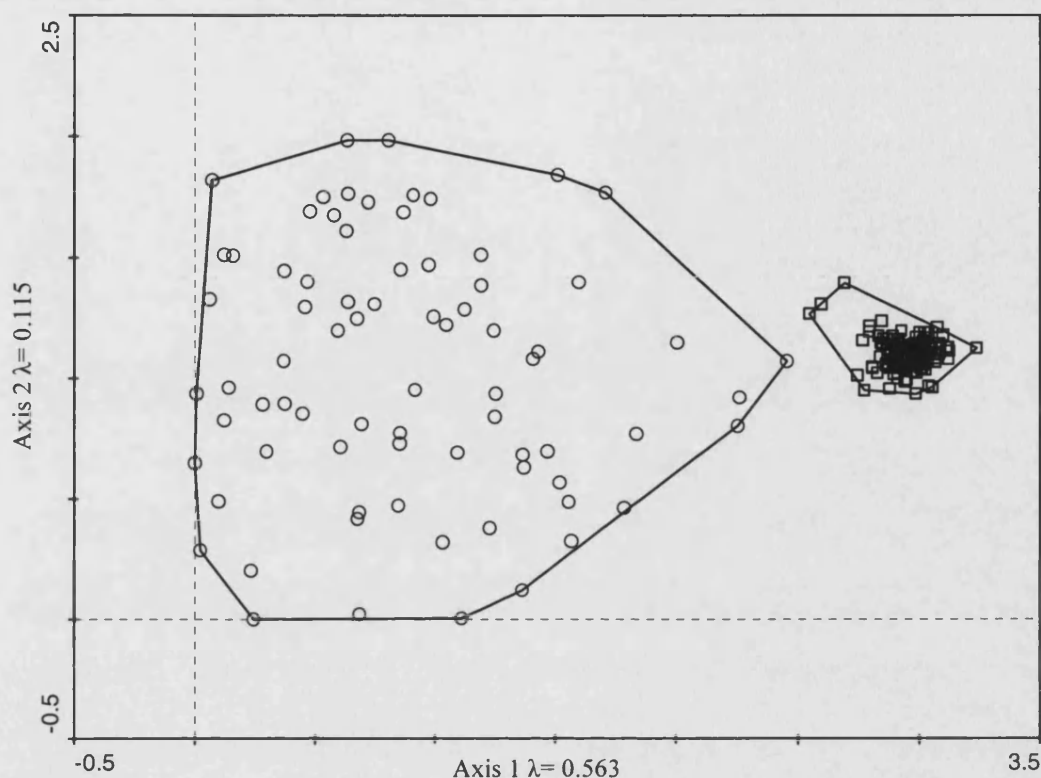
It can be seen that the fossil samples lie close to the ordination space of the training set samples (Figure 7.6). Therefore, the majority of the species that occur in the core will also be present within the training set making any environmental reconstructions using the 79 lake training set (i.e. January temperature and pH- discussed further later) more reliable. The reliability of the reconstructions of other variables (i.e. TP and ice-cover duration) using the other training sets is discussed later.

7.1.5.1 pH reconstruction

The pH transfer function was developed and discussed in Chapter 5. pH was reconstructed for this site using WA_(tol) developed from the 79 lake data set (using both inverse and classical regression co-efficients), and from the AL:PE training set using both MAT and WA techniques (See section 3.3.4 and 3.3.5). These reconstructions are presented in Figure 7.7.

The reliability of the reconstructions is good throughout the core, when using the 79 lake data, and the calibration sum never drops below 65%. The reliability of the reconstructions using the AL:PE data set are poorer at the top of the core for both the MAT and the WA methods, due primarily to the absence of *Cyclotella iris* in the AL:PE training set (Appendix 7.2). Also the reconstructions are not so reliable at ca. 14.5cm for both methods. For the rest of the core profile, however, they can be regarded as fairly trustworthy reconstructions.

Figure 7.6: DCA biplot of the 79 surface sample diatom assemblages (circles) and the fossil diatom assemblages (squares). Envelopes are drawn around the training set sites and the core samples.

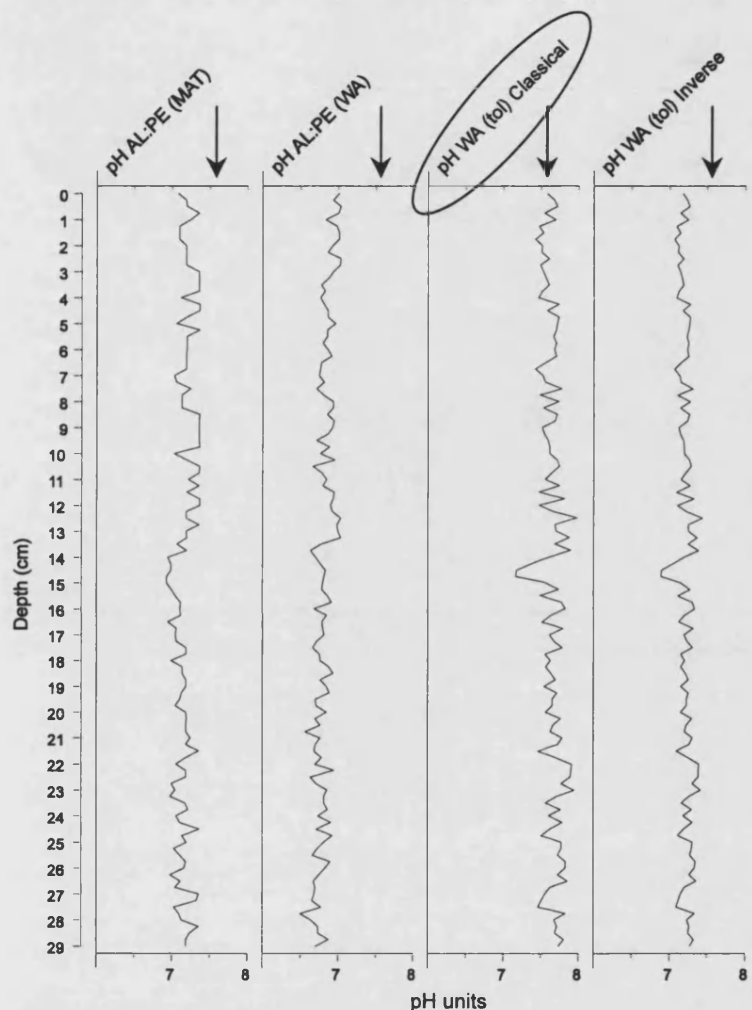


All the methods show pH variations throughout the core but overall the pH level does not change significantly. The diatom inferred pH from the 79 lake data set shows a distinct decrease in pH around 14cm which corresponds to the changes in the diatom profile outlined above. The AL:PE diatom inferred pH also has a slight lowering of pH for this section of the core but it is less pronounced using this data set.

Both the 'WA(tol) Inverse' and the 'WA(tol) Classical' derived from the 79 lake data set give slightly higher inferred pH values for the lake than those derived from the AL:PE data set. For WA inference methods it is recommended that, where the mean values of the parameter to be reconstructed lie close to the mean of the training set values inverse de-shrinking should be used (ref. Birks *et al.*, 1990). Current pH values for Lake Gåvålivatnet are 7.52 pH units. The mean pH for the 79 lake training set is 6.3 pH units, therefore, the classical de-shrinking coefficient is the most appropriate method for reconstruction as the pH of the site to be reconstructed lies at the extreme of the training set pH gradient. This reconstruction method compares extremely

favourably with the present day measured pH of 7.52 pH units. It is, therefore, this pH reconstruction method which is discussed further in section 7.3.

Figure 7.7: Diatom inferred pH for Lake Gåvålivatnet using the AL:PE data set (using both WA and MAT methods) and the 79 lake data set (using WA_(tol) with both inverse and classical de-shrinking coefficients). The current pH of 7.52 pH units is marked with an arrow. The circled method is the one adopted for further discussion.



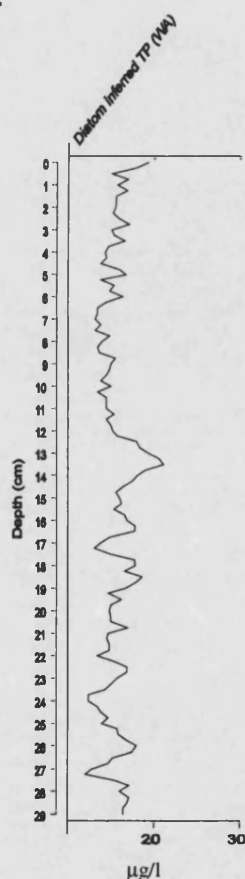
7.1.5.2 TP reconstruction

As with Lake Hornsjøen TP was reconstructed using the EDDI training set (Section 3.3.4 and Figure 7.8). TP is generally lowest between 7 to 11cm and varies little throughout the profile. The lower section of the core shows more variability in TP levels. The highest TP occurs between 12-14cm where TP reaches *ca.* 20µg/l. These correspond to changes in the *Cyclotella* sp. shown in Figure 7.3. Increases in *Cyclotella* species and TP also occur at the surface. The diatom inferred values for TP are generally between 12- 20µg/l. The TP for the lake was between 5 and 30µg/l (see

section 3.2.1.1 for problems with TP measurement discussion) suggesting that the reconstruction is quite close to the actual measured values.

The reliability of the TP reconstruction was evaluated by looking at the 'calibration set sum' for the WA analysis and the minimum dissimilarity co-efficient (min DC) for MAT (Appendix 7.2). As with pH, the TP reconstructions are not as good in the surficial samples and at *ca.*14cm, and generally have lower calibration sums and higher Min DC measures than pH. As with Lake Hornsjøen it may be more appropriate to use these reconstructions to look at general trends in TP rather than as accurate reconstructions of the parameter values.

Figure 7.8: Diatom inferred TP for Lake Gåvålivatnet using the EDDI data base and WA reconstruction methods.



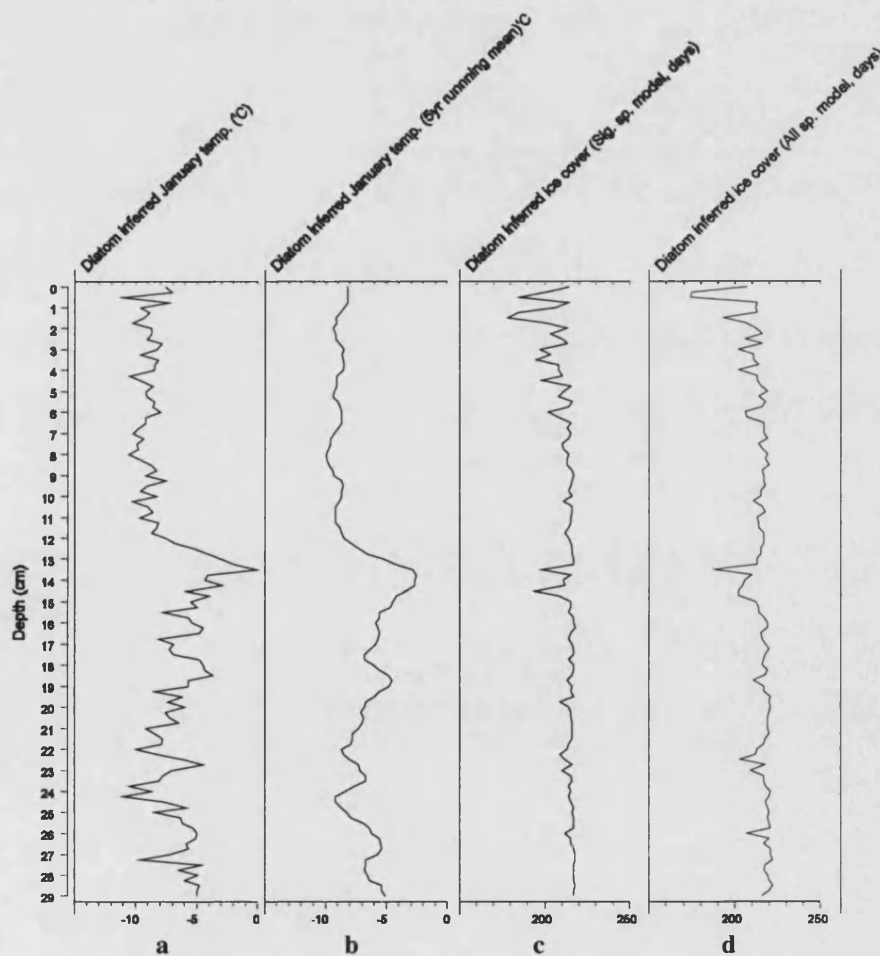
7.1.5.3 Ice-cover and January temperature reconstructions

Figure 7.9 illustrates the diatom inferred January temperature reconstructions and the diatom inferred ice-cover reconstruction. As with Lake Hornsjøen, the ice-cover duration for Gåvålivatnet shows few changes throughout the profile. There are, however, obvious changes in the ice-cover durations at 14cm and at the surface which most probably correspond with the changes in *Cyclotella* sp. abundance at these

levels. The reconstructions using either the model containing just the significant species, or that using all the species, are similar. Interestingly the January air temperatures show a rapid decrease above 13-14cm.

The calibration sum for the ice-cover reconstructions (78-54% for the all species model and 35-18% for the significant species model) demonstrates that the reliability of the reconstructions is poor. This poor calibration sum is probably due to the fact that many of the Norway 1 data set lakes did not have ice-cover duration measures and so were not included in the 40 lake ice-cover transfer function. This lake comes from a similar area to many of the lakes in the Norway 1 data set and may have many species in common. The number of species which have a significant relationship with ice-cover duration can be seen in the summary diagram in Figure 7.10. The species

Figure 7.9: Diatom inferred January temperature, using the 79 lake data set, a) with and b) without a running mean and diatom inferred ice-cover using the 40 lake data set c) using the significant species model d) using the all species model



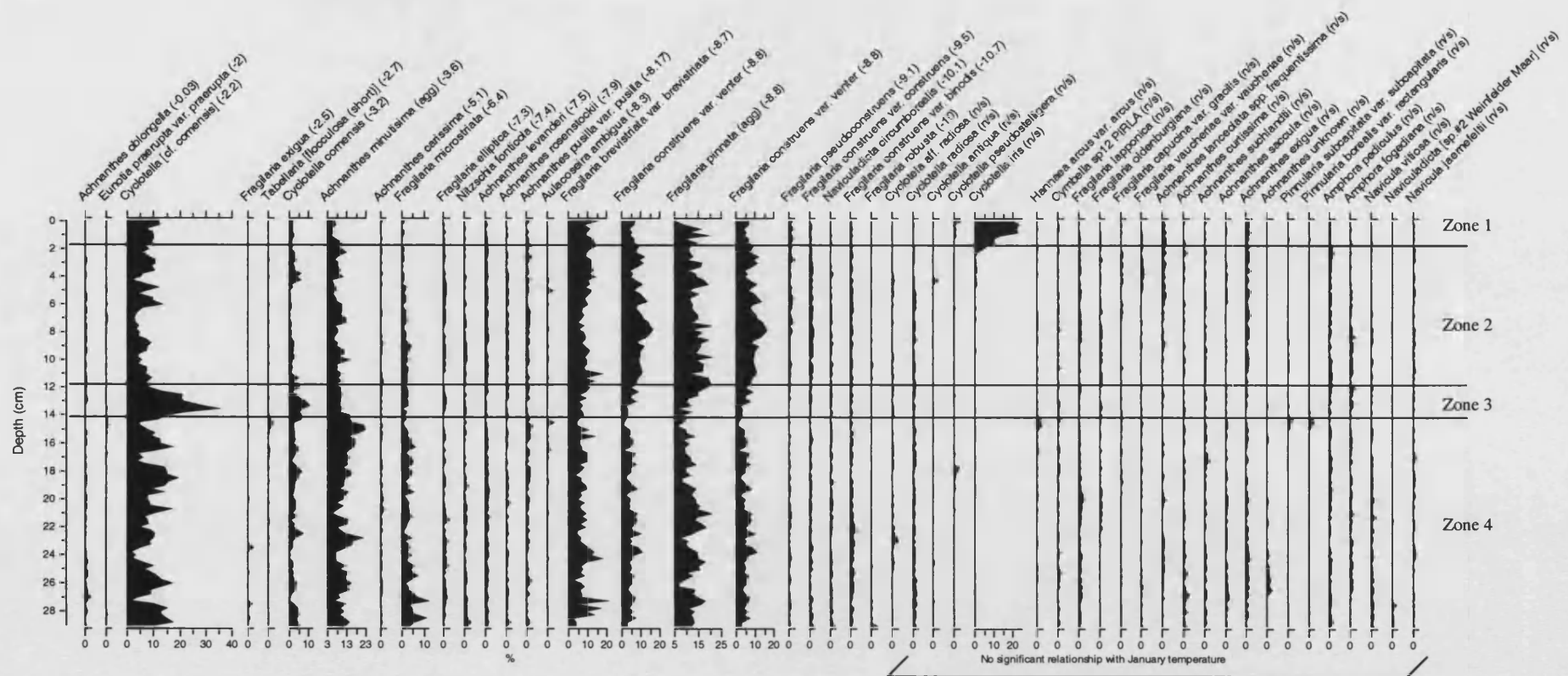


Figure 7.11: Summary diatom diagram for Lake Gåvålivatnet, with taxa <2% deleted and species arranged in order of January temperature optima (shown in brackets). Species with no significant relationship with January temperature, or those which were not present in the training set are also presented (n/s in brackets)

have been ordered in terms of ice-cover optima (in brackets) and no pattern can really be detected in terms of diatom abundance and the ice-cover duration preferences. The majority of the species in the core do not have a significant relationship with ice-cover. For these reasons, and the high errors involved in the ice-cover reconstructions, the reconstructed ice-cover durations are not discussed further within this chapter.

It would seem that the diatom inferred January temperatures show two quite distinct phases of temperature, divided by a distinct temperature shift at 11-13cm. The lower section of the core (14-29cm) represents slightly warmer temperatures overall, but with fluctuations ranging between -4 to -8°C but with a mean of -7.4°C. The upper part of the core (0-11cm) is represented by overall relatively cooler temperatures fluctuating around -7 to -9°C, with a mean of -9°C. These periods are separated by a very sharp change in diatom inferred January temperature at 11-13cm from -9 to -2.5°C. The changes in reconstructed January temperature seem to be driven by the fluctuations in *C. aff. comensis* (Figure 7.11). These changes are discussed further in comparison to the instrumental record in section 7.3.1.1. The reconstructed January temperature for the surface sediments, representing the year 2000, is -7.5°C which compares favourably with the actual measured value (-6.3°C).

7.2 Discussion

As with Lake Hornsjøen the main results from the discussion above have been synthesised in to a summary diagram (Figure 7.12) which contains the various diatom inferred reconstructions of TP, pH and January temperature, the results of the lithostratigraphic analyses and data which could be used to indicate changes in the proportions of lake habitat types down the core. This is discussed in the following section

The parameter changes evident in each zone of the core are then related to hypothesised changes in the lake system or the catchment in relation to changing lake productivity, chemical status and the lake's temperature regime (Sections 7.2.2 - 7.2.5).

Finally, as with Lake Hornsjøen, the lake parameters or diatom inferred values which have responded to recent climatic warming and can be used as climatic proxies are identified (section 7.3.1). It is then discussed whether these parameters also responded to climatic changes during the LIA (section 7.3.2).

7.2.1 Summary results and synthesis

As with the core at Lake Hornsjøen a summary diagram was produced in order to investigate the overall changes occurring at Gåvålivatnet with respect to the changes in the various chemical, environmental and physical conditions of the lake at different points over the last 500 years (Figure 7.12). The same parameters are including here as are included for Lake Hornsjøen (see section 6.2.1 for the rationale behind their inclusion).

7.2.2: Diatom zone four, covering the period from *ca.*1653 (29cm) to *ca.*1830 (14cm)

- Temperature changes and changes in the relative proportions of the lake habitats

The diatom inferred temperature reconstructions are highly variable for this lower section of the core but on average appear to be higher than within zones 1 and 2. The section between 18.5 to 24cm has a slightly lower inferred January air temperature than the rest of the zone but there is also a relatively high January inferred reconstruction at 22.5cm. It is hard to link the inferred temperatures with the other parameters within the profile due primarily to its inherent variability. It is apparent, however, that the PCA axis 2 scores closely follow the reconstructed January temperatures within this lower zone (discussed further in 7.3.2.1).

If the reconstructions are accepted this implies that the lake at this time should have a reduced ice-cover season, which should increase the proportion of the planktonic habitat availability. This should be reflected in the chrysophyte to diatom ratio, and non planktonic to planktonic diatom ratio. However, the zone is characterised by relatively high, but extremely variable, benthic diatom abundance.

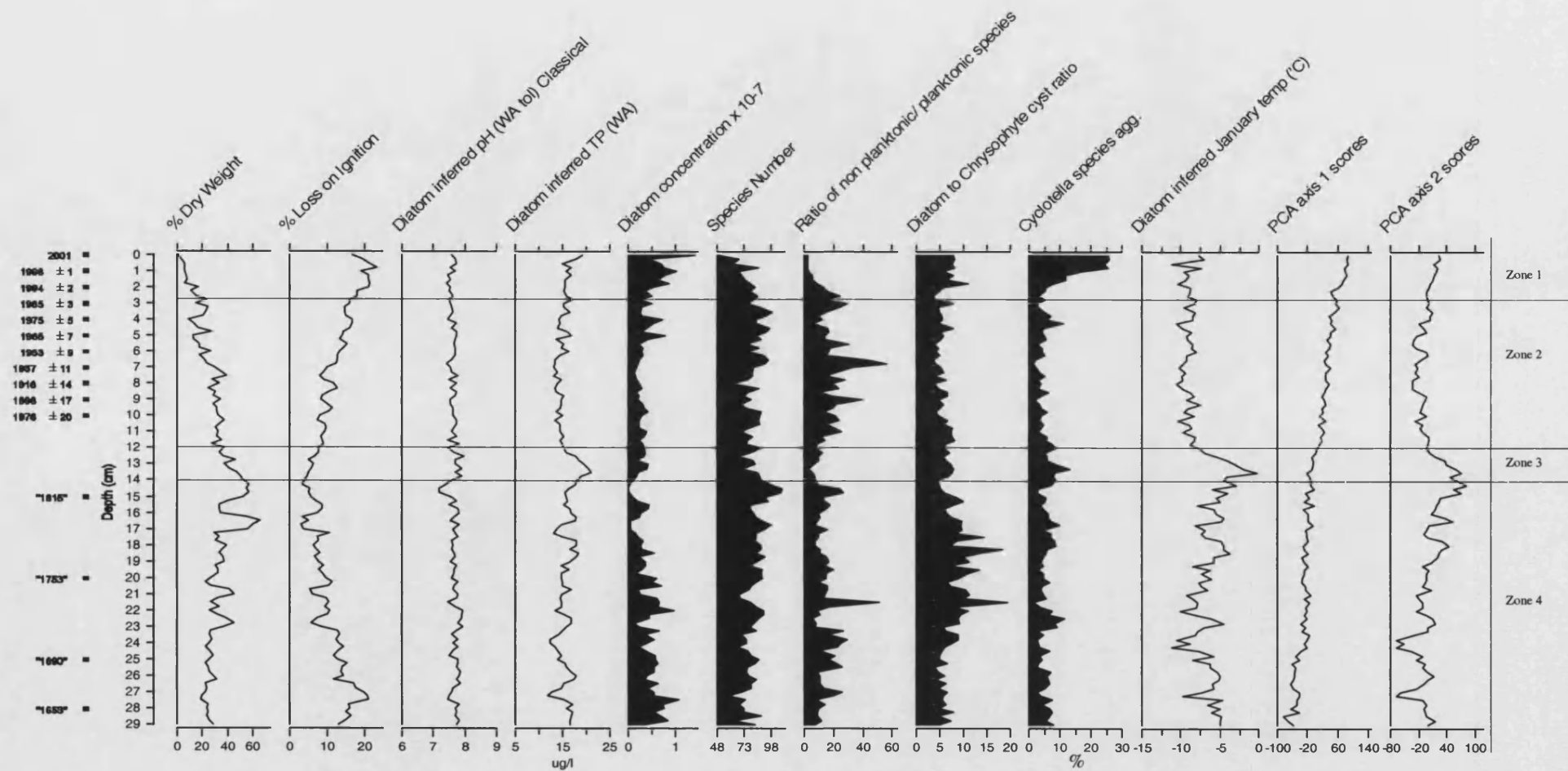


Figure 7.12: Summary diagram of reconstructed environmental variables, lithostratigraphic data, ordination results and diatom habitat ratios for Lake Gåvålivatnet

At the top of zone 4 from 14-15.5cm the abundance of benthic species increases. This corresponds to discrete increases in the abundance of several benthic diatom species, including *Pinnularia borealis*, *Pinnularia subcapitata*, *Tabellaria flocculosa*, *Eunotia praerupta* and *Hannaea arcus* (= *Fragilaria arcus*) (Figure 7.3). The increases of these species are, however, mainly short lived but may reflect a change towards warmer water temperatures possibly indicated by the January temperature profile which increases dramatically at 14.5cm (Figure 7.12). Most of these species are of benthic origin with the exception of *Tabellaria flocculosa* which is typically tychoplanktonic of epontic origin (i.e. it readily occurs in the plankton but is firmly attached to the substratum in origin, Denys 1991).

The pattern within the chrysophyte data is clearer with relatively high chrysophyte cyst abundances, suggesting reduced ice-cover, between 23-29cm representing ca.1700-1653. With a period of lower relative chrysophyte numbers above implying that the lake might have increased ice-cover for the time ca.1880-1700 (15-23cm). These do correspond to slightly reduced inferred January temperatures for this section.

- pH changes

The reconstructed pH varies throughout the zone and fluctuates around 7.5 pH units. There is a discrete but significant decrease in pH between 14 to 15cm. This is probably caused by the decrease in *Cyclotella* cf. *comensis* (pH optima of 6.9) and increases in *Achnanthes minutissima* (pH optima of 6.6), *Pinnularia subcapitata* (pH optima 6.1) and *Eunotia praerupta* (pH optima 5.9, optima all taken from Figure 5.31). A discrete lowering of pH such as this is hard to explain in terms of catchment or lake changes, as the pH rises again at 14cm. It could indicate some sort of catchment inwash of a more acidic nature, or it might be related to the planting of the trees within the catchment and the subsequent disruption of soil and possible increase of acidic vegetation deposits from the pine trees (see section 2.3.6). The pH, however, recovers quickly which suggests that the pine plantation is not responsible as this is likely to lower the pH of the soil for longer.

The lowering of the pH may be related to a period of decreased weathering within the catchment resulting in a reduction in the input of mineral nutrients to the lake, such as Ca^{2+} , lowering the lake water pH. Gåvålivatnet is located on calcareous sedimentary rock and changes in the weathering of this may affect the lake chemistry. Very cold conditions can lead to decreased mineral and chemical weathering in the catchment, reducing the input of base cations to the lake from weathering processes (White and Blum 1995). The episode is relatively discrete, however, (representing about 20 years) and changes in bedrock weathering may be unlikely. The reduced chrysophyte cyst numbers and increased benthic diatom abundance also both suggest this might be a cold phase for the lake, albeit short lived.

- Lake/ catchment productivity change

The theory outlined above concerning the possible in-flow of catchment material into the lake at the upper section of zone 4 is supported by the %LOI profile which shows a decline to minimum values at 14.5cm (Figure 7.12). This could suggest that the lake was very unproductive at this time, but may also indicate the increased input of catchment inorganic material due to the proposed catchment disturbance. In addition the diatom concentration is very low at 14 to 15cm, suggesting a possible concentration dilution effect for the diatom valves (a lowering of the diatom concentration per gram of sediment) due to the increase in catchment material. This theory would also correlate with the lithostratigraphy which documents a distinct, very compact grey layer at this point in the core (Section 2.3.6 and Figure 7.1).

The zone, however, shows a steady decrease in %LOI from the bottom to the top (Figure 7.1) of the section which is not as sudden as either the diatom concentration changes or the pH changes possibly suggesting that this is a longer term change, rather than a reflection of a discrete catchment disturbance event.

If the theory of catchment disturbance is dismissed the relatively low %LOI in this zone, could be associated with low organic production due to decreased temperatures within the lake or the catchment at this time. Diatom species numbers are also slightly increased for this period which might correspond to changes in competition patterns as lake productivity decreases. Theory suggests that species richness should be less in systems with higher levels of production (e.g. Goulden 1969; Margalef 1969). A

period of decreased temperatures for the lake at this time is not substantiated, however, by either the January temperature transfer function results or the chrysophyte cyst numbers throughout zone 4. The diatom inferred TP measurement for zone 4 also do not indicate a period of lower lake productivity at the top of the zone. The TP measures are variable throughout the core but are relatively high in zone 4 in comparison to zones 1 and 2.

It should be noted, however, that Gåvålivatnet is very base rich in comparison to Lake Hornsjøen (see tables 6.1 and 7.1) which can often complicate the link between %LOI and primary production (Battarbee *et al.*, 2002). The %LOI might not be driven by the primary production but more by the calcium carbonate amount within the lake, which suppresses the record of primary production in the lake (*c.f.* Battarbee *et al.*, 2002). The grey colour of the core in this middle section (13-15cm) might also substantiate this (Figure 7.1). Unfortunately, %LOI at 950°C was not conducted on this core which would have determined the relative importance of the carbonate component in the sediments.

7.2.3: Diatom zone three, covering the period from *ca.*1830 (14cm) to *ca.*1860 (12.5cm)

- Temperature changes and changes in the relative proportions of the lake habitats

The January temperature reconstructions in this zone indicate a large but discrete increase at 14.5cm to its maximum temperature of -1°C, with a rapid decrease back to -8°C at 12.5cm. This suggests a period in the lakes history characterised by longer ice-free seasons and a possible increase in wind induced mixing. These are both supported by the increased *Cyclotella* sp. agg. abundance and the decreased ratio of non planktonic to planktonic diatom species. There is also a decrease in the diatom species numbers which could be related to higher productivity at this time due to the longer growing season. The chrysophyte cyst numbers also increase in this zone in comparison to their levels in zone 4.

In terms of the species assemblage there is a large increase in *C. comensis* and *C. aff. comensis* within this zone and a corresponding decrease in the abundant benthic diatom species (e.g. *Fragilaria pinnata*, *F. construens* and *F. construens* var. *venter*, Figure 7.3) all indicating reductions in the ice-cover period (see section 1.3 and

1.4.1.2 and Lotter *et al.*, 2002; Smol and Douglas 1996; Douglas and Smol 1994; Lotter and Bigler 2000; Korhola and Weckstrom 2000; Korhola *et al.*, 1998). A similar inter-play was also seen between *C. comensis*, and the abundance of *F. pinnata* and *F. construens* var. *venter* in Hagelseewli in the Alps which was linked to increasing spring temperatures and reduced lake ice-cover durations (Goudsmit *et al.*, 2000; Lotter *et al.*, 2002; Lotter *et al.*, 2000).

In addition a reduced ice-cover period may increase the level of lake mixing, keeping fine sediment in suspension and reducing light penetration. Gåvålivatnet is a large lake with a long fetch and wind induced mixing, particularly in the littoral areas of the lake, may increase the sediment suspension resulting in shading for benthic communities. Furthermore, the increased temperatures may also cause an increase in spring runoff associated with snow melt and a smothering of the littoral communities from the increased minerogenic input (Anderson 2000). *F. pinnata* has been found to favour, low DOC conditions with high light intensity (Philibert and Prairie 2002) and *F. pinnata* var. *intercedens*, *F. pinnata* var. *acuminata* are particularly sensitive to reduced light levels (Smith 2002). The decreased light levels may, therefore, account for the decreases in *Fragilaria* species in this section of the core.

- pH changes

After the decline of the pH at 14.5cm the pH increases and remains relatively stable within this zone. The increase in the inferred pH values has been driven by the decrease in *Achnanthes minutissima* and the increases in *Cyclotella* species at this time.

- Lake/ catchment productivity change

The %LOI remains low within this zone. This could be correlated with increased calcium carbonate input to the lake system due to increased erosion or bedrock weathering linked to warmer temperatures and a thawing of the snow pack.

The low %LOI, however, may still indicate the influence of catchment disturbance or possibly the settling down of the sediment, and the lake system, after the disturbance in the upper section of zone 4, as diatom concentrations have risen again in this zone.

With the proposed increase in catchment erosion, levels of DOC in the lake may also have increased, due to higher suspended material and higher humic input from the catchment. Changes in DOC may again influence the littoral benthic diatom community by altering the penetration of solar ultraviolet radiation (UVR) and photosynthetically available radiation (PAR) (Laurion *et al.*, 1997).

The lower productivity of the lake reflected in the %LOI profile is not supported by the diatom inferred TP values which show a general increase in TP in this zone. This is driven by the relative increases in *Cyclotella* aff. *comensis* and *Cyclotella comensis* (SWAP optima 25.11µg/l) and the relatively low abundances of *Fragilaria pinnata* (SWAP optima 25.11µg/l and 7.9µg/l, Stevenson *et al.*, 1991). Jones and Juggins (1995) also demonstrated that *F. pinnata* has relatively low nutrient optima, and prospers at low chl *a* concentrations and low nutrient levels.

Many diatom species, however, although they have fairly narrow pH tolerances, have broader TP tolerances (Enache and Prairie 2002b). For example, *F. construens* is generally found in meso- eutrophic conditions (Agbeti and Dickman 1989; Hall and Smol 1992) but has also been associated with oligotrophic lakes (Enache and Prairie 2002b). Likewise, *F. brevistriata*, and its various morphotypes, is a species which is recorded in various trophic concentrations from oligotrophic to ultra- eutrophic environments (Whitmore 1989; Hall and Smol 1992; Enache and Prairie 2002a). Interpretation of TP related diatom change based on *Fragilaria* species should, often therefore, be treated with caution.

7.2.4: Diatom zone two, covering the period from *ca.*1860 (12.5cm) to *ca.*1997 (1.5cm)

- Temperature changes and changes in the relative proportions of the lake habitats

Cooler diatom inferred January temperatures in this zone suggest increases in lake ice-cover duration, with possible reductions in exposure, and subsequently a reduction in the level of wind induced mixing. The reduced annual ice-cover would also result in shorter annual open water, stratification and overturn periods, thereby reducing the abundance of the planktonic lake organisms.

Benthic diatom species are present in high abundances particularly within the lower section of the zone. This pattern is driven mainly by the decreases in *Cyclotella* aff. *comensis* and *Cyclotella comensis* and the higher relative abundance of the various *Fragilaria* species. The chrysophyte cyst abundance, however, seems to be relatively high and stable in this section of the core.

- pH changes

The diatom inferred pH changes are limited throughout this zone. The relatively stable level of pH before and after the episode of declining pH at 14-15cm may indicate that the pH changes were not related to changes in the vegetation of the catchment as suggested earlier.

- Lake/ catchment productivity change

Throughout this zone the %LOI profile increases steadily from the lower section to the top. This might represent the lake settling down after the proposed disturbance, evident within the middle of the core. The TP reconstructions do not mirror the increase in lake productivity, shown by the %LOI profile, and remain relatively stable throughout the zone.

7.2.5: Diatom zone one, covering the period from *ca.* 1997 (1.5cm) to *ca.* 2001 (surface sediments)

It is only really the significant increase in *Cyclotella iris* which has resulted in zone 1 being separated, in terms of diatom assemblage, from zone 2. This has significantly influenced the ratio of the planktonic to non planktonic diatom species. The sudden presence and increase in this species is very pronounced. This large *Cyclotella* species appears to be relatively rare in Scandinavian (Larsen *pers. com.*) or Scottish mountain lakes. It was not found within this training set, or the AL:PE and SWAP training sets (Cameron *et al.*, 1999; Stevenson *et al.*, 1991) despite the fact that Krammer and Lange Bertalot (1991) state that it is often abundant in modern sediments samples from clear acid lakes (Krammer and Lange-Bertalot 1991). The type found in this core is not illustrated here but is similar to that in Håkansson (1990, Figure 32, original material from the Brun & Héribaoud collection).

The species, and its varieties, have been found in sediments from: an oligotrophic cold water lake in Finland (Molder and Tynni 1968), within several alkaline, carbonate, and bicarbonate lakes in Ethiopia (Gasse *et al.*, 1982) and in several Algerian lakes from sediment dating from the Middle- Upper Pleistocene Epoch (Baudrimont 1973), and in Neogene continental deposits in the Sofia Basin Southern Bulgaria (Ognjanova-Rumenova 1996), amongst others.

Relatively little is known of its ecology and its sudden appearance within the surface sediment of this lake cannot readily be explained. There appears to be little change in the lake pH in this zone. There is a slight increase in the diatom inferred TP suggesting that it might be responding to a nutrient pulse within the lake. It is a relatively large, centric, planktonic species (typically between 15- 25µm) indicating that it may need an increased degree of water column mixing in order for it to remain suspended within the lakes' photic zone long enough for it to prosper. The increased mixing may result from the longer stratification periods due to a reduction in ice-cover in recent years. *Cyclotella* aff. *comensis* also achieves relatively high abundance within zone 1, suggesting that the rise in *C.iris* might be associated with a general rise in planktonic species associated with recent climate warming (see section 7.3.1).

7.2.6 Summary

Discussion of the changes in the diatom inferred variables, the lithostratigraphy of the core, and the analyses of the species assemblages, has indicated that the palaeolimnological record at Gåvålivatnet is hard to interpret in terms of consistent chemical, physical or environmental changes either within the catchment or the lake. The next sections assess which diatom inferred parameters and diatom species have responded to recent climate warming, evident within the instrumental record, and to LIA climate changes.

7.3 How faithfully are known climatic changes occurring over the last 500 years recorded by the palaeolimnological record at Gåvålivatnet

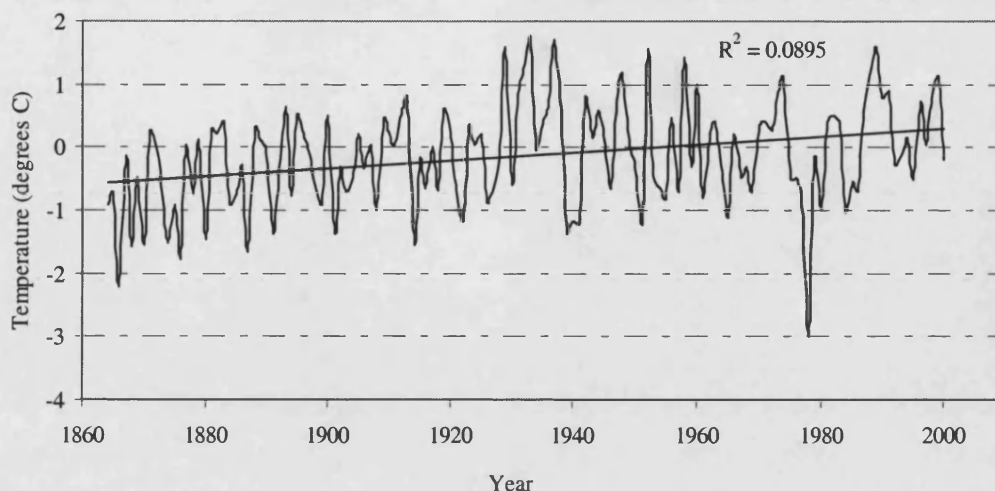
Gåvålivatnet is in a similar area to Lake Hornsjøen (Figure 2.9) and consequently both lakes will be subjected to similar changes in macro climate. It is assumed, therefore, that the LIA should also be recorded in the sediment record of Gåvålivatnet.

It should be noted, however, that the bathymetry of Gåvålivatnet is different to Lake Hornsjøen which may influence the way in which the lake responds to changes in climate. Gåvålivatnet is a double basin lake and is also larger and slightly deeper than Lake Hornsjøen (see section 2.3.6 and Figure 2.18b). The lake is slightly more exposed (Birks *pers. com.*), with a longer fetch and therefore will be affected by wind induced mixing to a higher degree than Lake Hornsjøen. It is thought, however, due to its similar altitude that the lake would stratify and show a similar thermal pattern throughout the year to Lake Hornsjøen.

The heat retention of an individual lake is influenced by differences in its size, mean depth, surface area, fetch and water clarity which are all major determinants of heat storage capacity (Gorham 1964; Timms 1975). Gåvålivatnet has a higher water volume than Lake Hornsjøen, therefore, taking longer to heat up, and it also has a larger heat capacity. Consequently, the lake's response to climatic change might be more gradual than at Lake Hornsjøen. In addition larger lakes also tend to have a longer spring circulation period (Wetzel 1983) having implications for the lakes diatom plankton growth, which tends to bloom in the spring (Lotter and Bigler 2000). The reduction of this spring circulation period, during times of colder climate, may, therefore have a more pronounced affect in these larger lakes.

7.3.1 The detection of recent climate change using the palaeolimnological record at Lake Gåvålivatnet

Average annual air temperatures at Gåvålivatnet have shown a varying but steady increase over the past 140 years (Figure 7.13). The higher R^2 value for Gåvålivatnet in comparison to Lake Hornsjøen (Figure 6.13, $R^2 = 0.0529$) is probably due to the inclusion of winter temperatures in this graph, and reflects the fact that winters have warmed more than summers recently in this area of Scandinavia (*c.f.* Nesje *et al.*, 2001; Nesje and Dahl 2003; Hansenn-Bauer and Nordli 2000). It can be seen that the measured January temperatures have been highly variable over the past 140 years with changes of as much as 4°C over the span of several years.

Figure 7.13: Instrumental record of average annual temperature (°C) for Lake Gåvålivatnet

7.3.1.1 Do the diatom inferred January temperatures reflect recent climate warming?

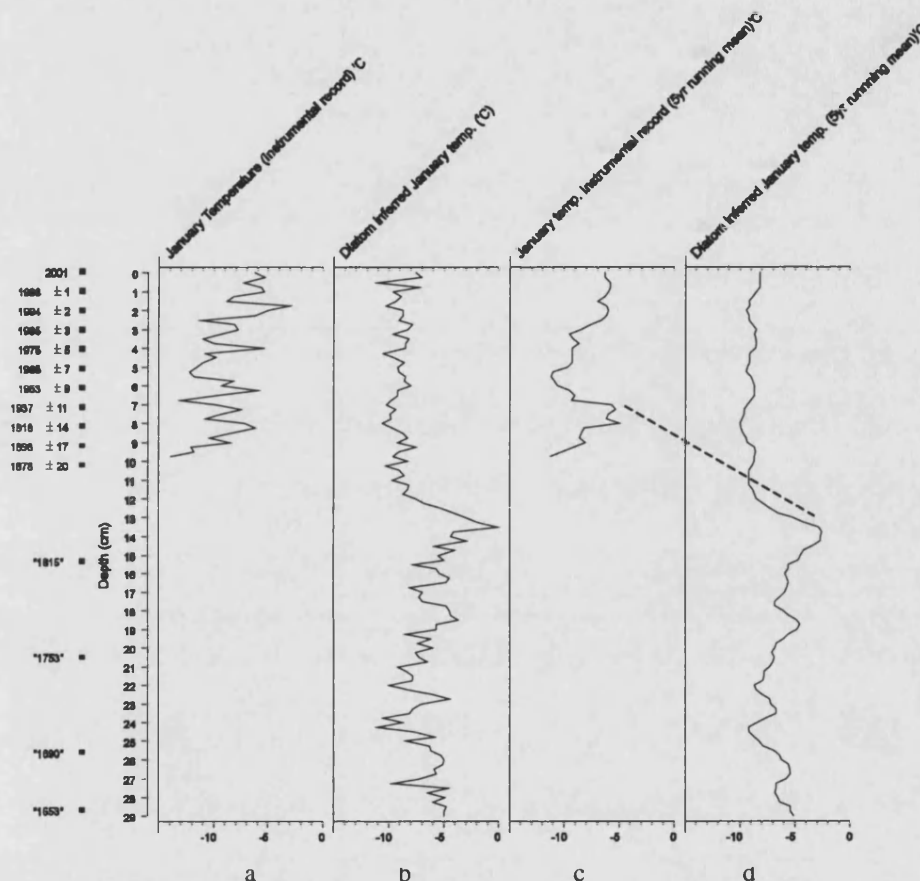
For Gåvålivatnet January air temperatures are available, which extend back to 1865, therefore, a direct comparison can be made between the diatom inferred January temperatures and the actual temperatures. The mean sedimentation rate was used to fit the measured temperature record to the core profile (Figure 7.14).

Due to the variability of the instrumental record a running mean of 5yrs was applied to the diatom inferred data and the instrumental record. It was, however, still difficult to detect similarities in the patterns of temperature change due to the different magnitudes of change, between the reconstructed values and the measured January temperature values.

It can be seen that although both the reconstructed values and the instrumental record waver around -10°C throughout, the reconstructed values fail to pick up the increase in temperature, evident within the instrumental record at 7-8cm. The diatom inferred temperature record, however, shows a similar increase at 12.5cm. There is a possibility that these might be connected, and due to a massive dating error, they could in fact represent the same event. However, there is little %LOI evidence for an in-wash event which may have caused such a dating error. Furthermore, the CRS and CIC dating models correlate well at the bottom of the core (Figure 7.2) again

suggesting an undisturbed sediment accumulation record. Without any independent way of verifying the ^{210}Pb dates this idea cannot therefore be investigated further.

Figure 7.14: Diatom inferred January temperature, using the 79 lake data set a) with and b) without a running mean, and January temperature from the instrumental record c) with and d) without a running mean. The dashed line indicates that these might be similar events due to a large dating error.



The relationship between the reconstructed January temperatures for the top 10cm of the core (i.e. the section covering the instrumental record) and the measured January temperatures were plotted against each other (Figure 7.15) to assess the accuracy of the reconstructed values. The resulting R^2 is low, indicating that the diatom inferred values either under or over estimate the actual January temperatures. There does not appear to be a systematic bias (Figure 7.16) in the reconstructed values, (i.e. a consistent over or under estimation at a particular point in the core), for most of the samples, but the temperatures at the top of the core do seem to be underestimated.

In order to investigate further the reason for the low R^2 value in Figure 7.15 the reconstructed and measured values were plotted again for just the upper 10cm of the

core (Figure 7.17). It can be seen that the reconstructed temperatures and the measured instrumental temperatures follow similar patterns of increase and decrease in the first 15 samples of the core, albeit at different magnitudes of change. This pattern breaks down after the *ca.*15th sample, as the sample increases and decreases are off set from one another. At this point in the core the errors associated with the dating technique also increase to a margin of ± 4 yrs. This means that because the actual measured January temperatures are so variable a date miscalculation of only a few years could cause the reconstructed values to look incorrect. This problem was also highlighted by Bigler and Hall (2002) who demonstrated that the relationship between reconstructed July temperatures and the instrumental record broke down in the 1960's as the dating errors increased.

Figure 7.15: Scatter plot of diatom inferred reconstructed January temperature against the January temperature from the instrumental record.

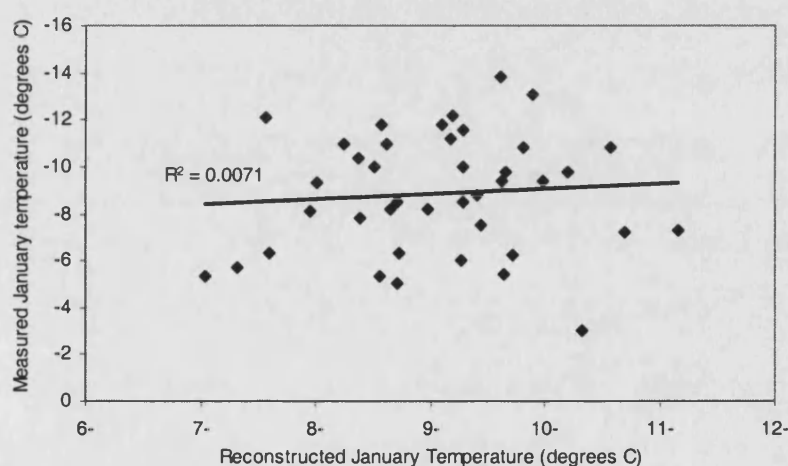


Figure 7.16: Predicted January temperatures- measured January temperatures against core depth for the samples 0-9.75cm in the Gåvålivatnet core.

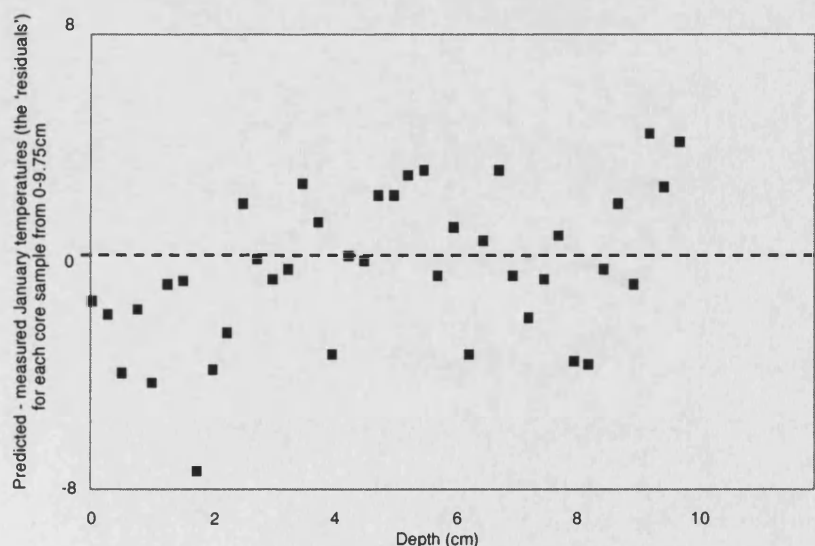


Figure 7.17: Diatom inferred January temperature (circles) and January temperature from the instrumental record (diamonds) plotted against core sample

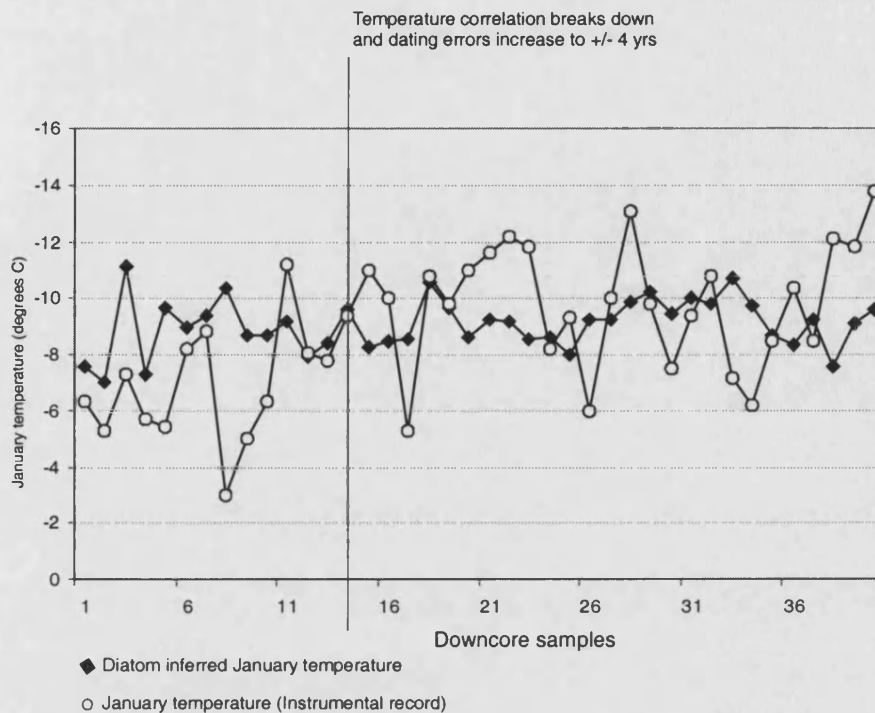
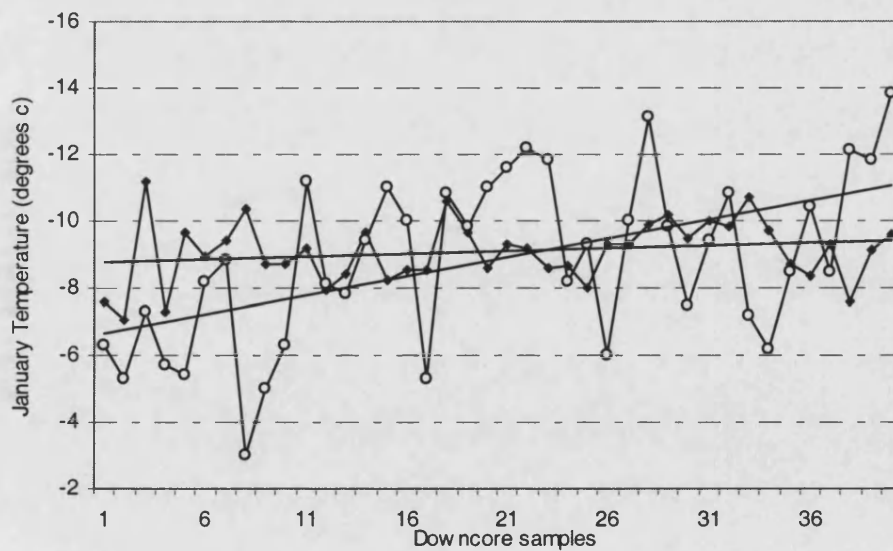


Figure 7.18: Diatom inferred January temperatures (diamonds) and January temperatures from the instrumental record (circles), both with linear regression lines plotted, against down core sample number.



In terms of an overall trend, however, Figure 7.18 illustrates that the measured January temperatures show a clear trend towards warmer winters over the past 140

years. The reconstructed values show a slight increasing trend but this is not as large an increase as the instrumental record, suggesting that the diatom inferred January temperatures do not accurately record recent climate warming significantly at this site.

This may be due to the fact that the diatom assemblage in the upper section of the core is dominated by *Fragilaria* species, (*Fragilaria construens* var. *venter*, *Fragilaria pinnata*, *Fragilaria pseudoconstruens* and *Fragilaria brevistriata*, Figure 7.3) and these have been shown to have low January temperature optima (all between -9.2 and -8.8°C, Figure 5.33) in effect suppressing the reconstructed values. *Fragilaria* species are, however, also very responsive to changes in light availability (see 6.16a *F. pinnata* and *F. pseudoconstruens* both prefer low temperatures, but also low TOC levels) and this may be a stronger driving variable influencing their growth in this upper section of the core.

7.3.1.2 Do changes in species abundance and within- lake habitat reflect recent climate warming?

The use of shifts in species assemblage, or abundances, to detect climate change at Gåvålivatnet is harder, than at Hornsjøen, because the species tend to increase and decrease in abundance rather than enter and the leave the assemblage profile. However, in the Gåvålivatnet core the percentage of *Cyclotella* species increases dramatically in the surficial sediments, mainly due to the influence of *Cyclotella iris* which is absent from the rest of the profile. *C. aff. comensis*, *C. comensis* and *C. pseudostelligera*, however, also rise in the top 6cm of the core (Figure 7.3). *Fragilaria* species correspondingly decrease slightly in the top sediments of the core. As noted for Lake Hornsjøen, increases in small *Cyclotella* sp. have often been linked to climate change in mountain lakes (Catalan *et al.*, 2002b; Sorvari and Korhola 1998) and their presence here may reflect the higher annual temperatures (See Figure 6.17 also) in the area over the last 100 years. As with Lake Hornsjøen the rise in the surface sediments of *Cyclotella pseudostelligera* may indicate longer ice-free periods as this species tends to grow in Autumn (See section 6.4.2.2 and Catalan *et al.*, 2002a).

In comparison to the smaller planktonic species, *Cyclotella iris* is a large diatom and increases in this species may have occurred due to the decreased ice-cover period

resulting from the recent mild winters. The subsequent increase in lake mixing would enable the species to remain suspended within the photic zone for longer periods.

Recent climate warming occurring over the last 20 years is reflected in the low ratio of non planktonic to planktonic diatoms due to the increases in *Cyclotella iris* and the other small *Cyclotella* species. Chrysophyte cyst production is relatively high in the upper sediments again suggesting that the 'chrysophyte cyst to diatom ratio' does not reflect recent climate warming.

7.3.1.3 Do changes in lake productivity reflect recent climate warming?

The %LOI does increase in the surface samples of Gåvålivatnet suggesting possible increases in primary production due to temperature rises and reduced ice-cover. The %LOI changes in the surface samples may, however, also be related to the delay in mineralisation of organic matter and not related to climate change.

The diatom inferred TP reconstructions also increase slightly in the surficial sediments suggesting greater in lake productivity. The higher levels of TP in this section of the core could, however, also possibly be due to changes in nutrient delivery, due to increased erosion levels, catchment thawing and changes to the various inputs to the lake (Nickus *et al.*, 1998; Catalan *et al.*, 2002c for similar discussions).

7.3.1.4 Summary of evidence reflecting recent climate warming

The discussion above has highlighted which diatom inferred parameters have adequately recorded the recent climate warming occurring at Gåvålivatnet. It would appear that the diatom inferred January temperatures did not reflect the true magnitude of the recent climate change, as shown by the instrumental record. Diatom inferred TP has changed slightly in accordance with recent climate warming but the increase is not substantial. In addition, several diatom species have responded to the recent climate warming probably due to changes in habitat availability, light penetration and water column mixing. %LOI has also increased in the surface sediments which might be related to higher within lake and catchment productivity due to the higher temperatures.

The discussion above has shown that some of the parameters in Figure 7.12 have changed in accordance with recent climate warming. These proxies are used in the following section to assess if they also adequately record changes in climate associated with the LIA.

7.3.2 The detection of climatic change associated with the LIA at Lake Gåvålivatnet

As with Hornsjøen, the LIA event was located within the sediment core by extrapolating the ^{210}Pb record. It is known that the LIA occurred in this area between 1650-1800, reaching its maxima at 1750 (section 1.5.1). This would be represented in the core by the sediments at 16-29cm (i.e. the majority of zone 4 in Figure 7.12) and the maxima should be represented by sediments at 19-21cm. The climatic changes occurring in the region have been discussed in sections 1.5.1 and 6.4.2.

7.3.2.1 Changes in diatom species and within lake habitat related to the LIA

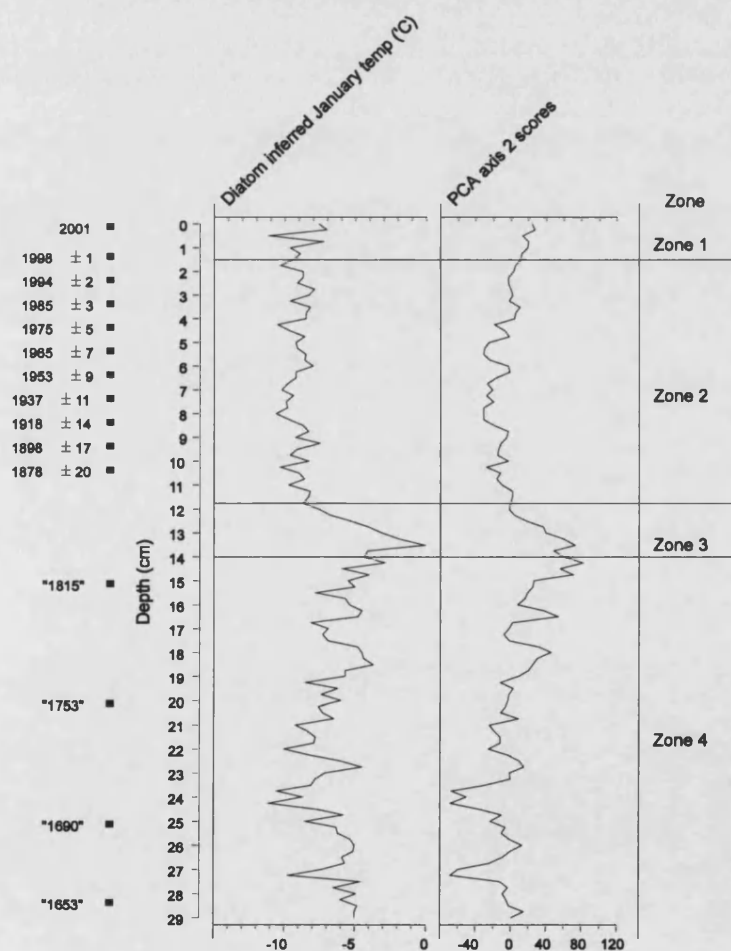
The high ratio of non planktonic to planktonic species (i.e. low relative planktonic species abundance) at the level associated with the LIA maxima in the core (19-21cm) may indicate periods of increased ice-cover duration. The ratio decreases substantially in zone 3 indicating a return to longer ice-free conditions after the termination of the LIA. The low relative abundance of chrysophyte cysts *ca.* 1800 and 1710 also supports these hypothesised longer ice-cover durations. With a longer ice-cover period the lake may only mix once having possible effects on the nutrient dynamics and the chrysophyte cyst population (Catalan *et al.*, 2002c). In addition the rise of *Cyclotella comensis* in zone 3 and its apparent preference for warmer climatic conditions (Figure 6.17 and section 6.4.2.1) would also support this. It should be noted, however, that the numbers of benthic diatom species are also high in zone 2 which should in theory represent higher temperatures after the LIA.

Figure 7.18 shows that there is a good relationship between the diatom inferred January temperatures and the PCA axis 2 scores, derived from the diatom assemblages, particularly evident in zones 3 and 4. Both of these parameters appear to be positively related to the abundances of *Cyclotella aff. comensis* and *Cyclotella comensis*. The species negatively associated with the PCA axis 2 scores are *Achnanthes levanderi*, *Cyclotella radiosa*, *Fragilaria construens* and *Fragilaria*

construens var. *venter*. These species have limited abundances within zones 1 and 3, (i.e. periods of relative warmth) suggesting that they are indeed related to the colder temperatures occurring during the LIA but their high abundances in zone 2 confuses this signal.

As with Hornsjøen analogue matching was attempted using both the 79 lake data set and the amalgamated EDDI training set (See section 6.4.2.1). For the 79 lake set the matches did not alter substantially in altitude and, therefore, few climatic interpretations could be made using this technique. The EDDI data set did not contain close enough analogues for reliable inferences to be made.

Figure 7.19: Diatom inferred January temperature and PCA axis 2 scores plotted stratigraphically for Lake Gåvålivatnet



7.3.2.2 Detecting the LIA using patterns of lake/catchment productivity

The palaeoclimatic %LOI signal at Gåvålivatnet is more complicated than at Lake Hornsjøen and the influence of catchment disturbance was discussed but dismissed

earlier. The %LOI signal is unusual for a high altitude lake in this region (See Chapter 2) but this may be related to its base rich geology.

Often sites on crystalline bedrock have %LOI signals that are driven by organic activity in the water column (Willemse and Tornqvist 1999; Nesje and Dahl 2001). For more base rich sites, such as this, the %LOI might be controlled by primary productivity but the signal is often more complex due to the production and preservation of authigenic calcite in the lake as well as the organic matter.

There is no obvious or discrete %LOI signal change for the time associated with the LIA in this core. There is a possibility that the relatively low %LOI from *ca.*1700-1800 (14-23cm) could be associated with the limited organic production within the lake during the LIA but the %LOI is also low in zone 3. In addition the TP reconstructions do not support this reduced productivity during the LIA.

7.3.2.3 Summary of the palaeolimnological evidence of the LIA

From the discussion above it is obvious that the recording of the LIA in the sediment record of Gåvålivatnet is not conclusive. There are changes in the ratio of non planktonic to planktonic species and chrysophyte cysts abundance, suggesting longer periods of ice-cover, but the trends are very variable. The January temperature transfer function, although it does suggest colder temperatures between 19 and 21cm (i.e. the LIA maxima), the signal is again variable and inconclusive, with equally large decreases in reconstructed temperatures at *ca.* 24cm . In addition it does not seem to reflect the scale of the recent climate warming and consequently its suitability for detecting LIA cooling is perhaps minimal.

7.4 Summary and conclusions

It can be concluded that some aspects of the diatom record at Gåvålivatnet and the reconstructed environmental variables can be related to changes in the Norwegian climate over the past 500 years. The record of these changes within the core and their interpretation is not, however, straight forward. In addition changes in %LOI and primary productivity may be suppressed due to the high calcium carbonate levels in the lake.

Recent climate warming in the lake area is evident in the diatom record, through a general increase in small *Cyclotella* species and a rapid increase in *Cyclotella iris*. These proxy temperature increases are not reflected in the diatom inferred reconstructed January temperatures, thought to be mainly due to the abundance of several *Fragilaria* species in the upper section of the core profile suppressing the reconstructed values.

Detection of changes in the various lithostrigraphic parameters, diatom species and diatom inferred variables associated with the LIA are harder to interpret. Many of the parameters are highly variable in the lower sections of the core, including the non planktonic to planktonic diatom species and chrysophyte cyst production in particular, making climatic interpretation difficult.

In addition, the influence of catchment disturbance cannot be ruled out completely at this site, because it is not in such a pristine catchment as Lake Hornsjøen. It should also be noted that Gåvålivatnet is a very different site in comparison to Lake Hornsjøen in its size, bathymetry, catchment size, bedrock and water chemistry. Although it might be subjected to the same macro climate changes, in terms of temperature and precipitation, the lake system might respond in a very different way to climatic change due to its different micro climate and limnological character. It remains, however, that with no obvious change in the lake's pH or TP, with the assumption that these reconstructed values are in fact correct; a change in another environmental variable must have produced the large shifts in diatom assemblage seen throughout the core.

This chapter has demonstrated that some changes in the palaeolimnological record of the lake can be related to climatic forcing in the lake region. The relationship between the changing climate and the lake system at Gåvålivatnet is, however, complex and climatic explanations are made tentatively. The following chapter discusses the results of the thesis and draws the conclusions together in a final discussion.

Chapter 8

Summary and Conclusions

8.1 Introduction

This chapter links the main findings from the study back to the objectives outlined in Chapter 1. There were two main aims of this thesis; firstly, to evaluate the relationship between diatom assemblages, and in particular planktonic diatom species, to lake ice-cover and secondly, to establish how diatoms can be used to detect climatic change within central Norway using the climatically well recorded Little Ice Age and recent climate warming as validation.

The apparent strength and nature of the relationship between diatom assemblages and lake ice-cover is summarised within this chapter. The problems relating to the creation, and application, of the ice-cover transfer function are also discussed. In addition the development of both the pH and January air temperature transfer functions are discussed briefly. Conclusions drawn from the analysis of the sedimentary sequences in both Hornsjøen and Gåvålivatnet are presented. Finally, the chapter concludes with an evaluation of the approach adopted within this research.

8.2 The relationship between ice-cover and diatom species, and the development of the ice-cover transfer function

One of the specific aims listed in Chapter 1 was to assess the relationship between planktonic diatom species and lake ice-cover and to attempt to reconstruct ice-cover using diatom assemblages through the development of a large high-mountain lake surface sediment training set. Due to unforeseen circumstances this training set had to be reduced to 40 lakes due to missing ice-cover data. This slightly jeopardised the investigation into the plankton/ice-cover relationship due to the reduction of the number of sites with planktonic diatoms present.

However, there was some indication that the planktonic species showed a preference for lower ice-cover durations (Figure 4.29). The exclusivity of this relationship could not be ascertained, however, because it was realised that the abundance of planktonic species might also be related to variables which were co-linear with ice-cover, such as lake depth and TOC. In addition the planktonic species were shown to have a strong

affinity with waters with higher pH and Ca^{2+} values, i.e. occurring in the 'base rich' lakes. The only real way to address this problem would be to design a training set where pH and Ca^{2+} were kept constant but with a strong ice-cover gradient. This, however, would not eliminate the problems of variables which are co-linear with ice-cover, because in order to maximise the ice-cover gradient many other variables will alter with altitude, such as TOC and lake nutrients (TP, TN etc).

Furthermore, the relative importance of lake nutrient levels for planktonic diatom growth could not satisfactorily be ascertained due to the problems with the accurate measurement of the TP gradient (Section 3.2.1.1). Variations in nutrient levels may be an important driving variable for diatom plankton growth, with many planktonic forms blooming in spring when lake nutrients are relatively high. This relationship, however, could not be explored fully within this thesis.

In addition it was difficult to identify significant trends in the planktonic species, and their relationship to different environmental variables, due to their relatively low abundance within the training set. This to some extent is unavoidable due to the very nature of these high-altitude, oligotrophic lake systems which tend to be dominated by benthic forms.

Ice-cover duration was shown, however, to be an important variable for influencing the diatom assemblages as a whole. Chapter 4 demonstrated that ice-cover was responsible for explaining a large proportion of the diatom variance (6.8%) and that this relationship was significant (Table 4.13). It should be remembered that some portion this variance may have been due to the effect of ice-cover acting with another variable/variables in conjunction, which was/were co-linear with ice-cover. Further variance partitioning might represent a way to investigate the independent influence of ice-cover duration.

The complex and multi-faceted nature of the relationship between lake ice-cover and the diatom species assemblages was highlighted in Chapter 4. The nature and duration of a lake's ice-cover will instigate numerous positive and negative feedback mechanisms, connected to the nutrient dynamics, habitat availability, light penetration and mixing regime of the lake (see Figure 1.1). In addition the nature of these

interactions are also dependent on the lake's size, water volume and exposure. At present many of these inter-linking mechanisms, and more importantly how they affect the biological community of a lake, are poorly understood. It may, therefore, have been naïve to try and relate diatom changes to 'ice-cover duration' *per se* using the traditional transfer function technique. It was also unfortunate that data from more thermistors were not available which would have provided valuable insights into the actual timing of ice-out and ice-on of the lake, rather than just the ice duration. Despite this the generation of an ice-cover transfer function was attempted (Chapter 4) and is discussed below.

It has been shown elsewhere that altitude is linearly related to air temperature, and that air temperatures have a direct influence on ice-cover formation and duration (Livingstone and Lotter 1998; Livingstone *et al.*, 1999; Livingstone 1997; Livingstone 1999). For this reason the training set was designed to cover a wide altitudinal range with few gaps within its gradient (Figure 2.8). Unfortunately, the lack of ice-cover data for the Norway 1 sites resulted in their exclusion from the 'ice-cover training set' and the ice-cover gradient displayed a bi-modal distribution (Figure 4.46). It is possible that this might have had implications for the generation and accuracy of the ice-cover transfer function and the generation of ice-cover optima for individual species.

Due to these problems, and the differences in the species ice-cover optima, in terms of both their rank position along the ice-cover gradient and their absolute optima, when using different techniques (WA and GLR) the ice-cover optima generated for individual species proved to be inconclusive. Furthermore, it should be remembered that an individual diatom will respond to a suite of driving variables and often the climatic influence is not strong enough, or is overridden by a potentially more influential variable such as pH. It is, therefore, difficult to estimate or quantify the true relationship of individual diatoms species to climate unless conducted as controlled culture experiments. Optima derived from laboratory experiments can in no way, however, mirror the results that might be obtained in the field, where diatoms will be responding to numerous variables of differing importance and also be affected by competition processes.

These problems may have subsequently influenced the accuracy of the diatom ice-cover transfer function. In addition, the predictive strength of the ice-cover transfer function might also have been increased if all 80 lakes could have been included in the analysis. Furthermore, as pointed out by Anderson (2000), problems may also occur using the transfer function technique if the variable to be reconstructed, in this case ice-cover, is not the *dominant* environmental signal explaining the diatom variance (see Table 4.13).

Despite the problems with the ice-cover transfer function it was applied to the two sediment cores in Chapters 7 and 8 to take the work to its logical conclusion. The reason for its poor reconstructions were not only related to the large errors involved in the actual model but also the fact that many of the species that did have a significant relationship with ice-cover duration were either not present or abundant within the core diatom assemblages.

It is believed, however, that qualitative judgements might be appropriate in terms of ice-cover preferences for each species and that the identification of shifts in diatom type categorised by habitat preference (e.g. planktonic to benthic) can directly be linked to ice-cover changes. This is discussed further in section 8.5

8.3 The January temperature transfer function

Due to the limited predictive power of the ice-cover transfer function the reconstruction of other environmental variables which might provide insights in to, or be related to, climatic change was attempted. Through the analysis of the 79 lake training set it was shown that January air temperature independently explained a large proportion of the diatom variance within the data set and for this reason it was thought feasible to create a January air temperature transfer function. Despite the fact that it is usually July temperature which is reconstructed using diatoms it was thought that January temperature might be important due to its control over ice thickness and therefore ice duration, and its links with the winter NAO index and levels of winter precipitation. January temperature may also simply indicate relatively warmer or colder years.

Although it was shown that it was feasible to create a January temperature transfer function, the reconstruction errors associated with the model were high (2.2°C) and probably beyond the scale of any climatic change which would have occurred during the Little Ice Age and/or evident over the instrumental record. It is interesting to note here, however, that many of the species that had high ice-cover optima also had low January temperature optima, suggesting that there is some degree of climatic control exerted on specific indicator species. The transfer function was applied to the sediment sequences in Chapters 6 and 7. From the outset, however, it was thought that this should be used in a more qualitative sense to look at climatic 'trends' due to the large errors involved in its application and in no way did it attempt to reconstruct actual temperature measurements. These reconstructions are compared and discussed further in section 8.5.

8.4 The pH transfer function

The link between pH and climate is evident in many other palaeoclimatic studies (Psenner and Schmidt 1992; Sommaruga-Wogarth *et al.*, 1997; Leira and Santos 2002; Wolfe 2002; Schmidt *et al.*, 1998) and, therefore, the 79 lake training set was used in the generation of a pH transfer function. It was thought that the creation of a training set from lakes which were in a similar location to the cored lakes (*c.f.* Cameron *et al.*, 1999) might be more accurate than using published pH training sets.

pH was shown to be the dominant explanatory environmental variable within the 79 lake training set (Figure 5.30). The errors associated with the resulting pH transfer function (RMSE 0.32 pH units) compared favourably with other pH transfer functions in the literature (Stevenson *et al.*, 1991; Cameron *et al.*, 1999; Enache and Prairie 2002). It was noted, however, that there were large discrepancies in the optima generated by different training sets for the same species (Table 5.26). Cameron *et al.*, (1999) also noted this discrepancy and suggested that it might be due to the still poorly understood, relationship between DOC, light, climate and pH in different lakes. It would appear that many variables exert a strong influence on the diatom variance and, therefore, the generation of optima for a single environmental variable is naturally problematic.

The hypothesised link between climate and pH was not evident within the sediment cores from Lake Hornsjøen or Lake Gåvålivatnet. The diatom inferred pH did not change significantly throughout either of the sediment profiles, demonstrating that the lakes were not sensitive to pH change, and consequently rendering them unsuitable for a climate pH investigation. For such a study the selection of lakes with lower concentrations of alkaline anions is necessary. Such 'soft water' sites may not, however, have been appropriate for this study due to the fact they may have limited abundances of planktonic diatoms present (see section 4.3.2 and Figure 4.30, planktonic forms tend to favour high Ca^{2+} and high alkalinity/pH waters), making an investigation in to the relationship between the planktonic diatoms and ice-cover problematic.

8.5 The detection of climate change over the past 500 years in Norway using the palaeolimnological record

An important aim of this study was to evaluate to what extent diatom assemblages reflected changes in climate and in particular changes associated with the LIA. Two sites were chosen in central Norway for detailed palaeolimnological analyses because it was known that the area was significantly affected by the LIA in the mid to late 18th century (see section 1.5.1). The sites chosen were, therefore, ideal for validation purposes due to the independent and multi proxy climatic evidence documenting the extent and duration of the LIA in the area and the independent reconstruction of the LIA maxima dates (section 1.5.1). An accurate chronology was developed for the cores using ^{210}Pb to ensure that the LIA could be 'located' within the sediment sequences of the two cores (see section 6.3.3 for discussion of the inherent dating caveats). By only focussing on this time period other factors which may have a major affect on the diatom variance (such as pH, TP through the Holocene) may have remained relatively stable.

At both lakes, pH and TP reconstructions, two variables often cited as strongly influencing diatom communities, remained relatively constant throughout the core profiles. However large shifts in diatom species abundance and assemblage were detected in both Gåvålivatnet and Hornsjøen. If the reliability of the transfer functions are to be believed and these two driving variables remained constant, it was tentatively suggested that climatic factors may have been responsible for the diatom

species changes. The influence of other unmeasured/ unknown environmental variables, however, can not and should not be excluded from consideration.

It is appreciated that the January temperature transfer function incurred large errors in its reconstructions but they do show trends in temperature which, according to the core chronologies, can be linked to lower temperatures during the LIA (See Figures 8.1 and 8.2). However, it must be realised that due to the large errors in the diatom inferred reconstructions that this could purely be coincidental. This evidence is, however, also substantiated by the decreases in chrysophyte cyst production and decreases in planktonic diatom abundances at similar times thought to be related to the longer ice-cover durations associated with the LIA (see section 6.3.2 and 7.3.2). Figures 8.1 and 8.2 also show that at both lakes substantial changes in the diatom composition and diatom inferred variables are evident which can be associated with the recent climatic warming evident within the instrumental record.

The recording of the LIA event and the recovery of the lake after the LIA appeared to be more apparent in the diatom record of Hornsjøen (Figure 8.1). The lake appeared to be most affected during and directly after the LIA maxima, with decreases in diatom inferred temperature and planktonic species between 1720 and 1800. This lake also showed a distinct increase in diatom inferred January temperature towards the top of the core profile, and a corresponding increase in small *Cyclotella* taxa, often associated with recent climate warming (Korhola and Weckstrom 2000; Sorvari and Korhola 1998; Lotter and Bigler 2000; Koinig *et al.*, 2002; Bigler and Hall 2003; Catalan *et al.*, 2002a), which both correlate with the increasing temperatures evident in the instrumental record over the last few decades.

This lake is situated in a very remote area with little anthropogenic catchment disturbance yet the palaeolimnological record also shows distinct changes in lithostratigraphy. It is suggested that the obvious changes in the lithostratigraphic pattern of the core sequence at Hornsjøen could be related, in a chronological sense, to the end of the LIA maxima (section 6.3). The %LOI, however, was fairly constant after the initial shift associated with the LIA, and showed no trends with the increases in temperatures over the past 140yrs. It was interesting to note that other lakes near Hornsjøen showed similar step-like patterns in their %LOI profiles (Chapter 2)

suggesting that the trend may be synchronous across the region and driven by the changing macro climatic conditions. It is, however, realised that these cores had not been dated and so these lithostratigraphic events may in fact be unrelated.

The detection of climatic change at Lake Gåvålivatnet was more problematic and the influence of catchment disturbance could not be ruled out at this site. In this way grain size and geochemical analyses of the cores might have been useful in order to determine the influence of any catchment disturbance. The January temperature reconstructions and the other biological proxy indicators (chrysophyte cyst production, planktonic diatom abundance) did seem to reflect climate changes linked to the LIA period. In addition distinct species shifts could be seen in the upper part of the core primarily evident in the rapid rise in abundance of *Cyclotella iris* which is absent from the rest of the core. However, the January temperature reconstructions in the upper part of the profile do not reflect the magnitude of the increasing temperatures shown by the instrumental record. This was attributed to the cosmopolitan nature of the abundant *Fragilaria* species within the core at this time, suppressing the diatom inferred temperatures.

The Central England Temperature Series (CETS) (Manley 1974, Parker *et al.*, 1992, updated by the Hadley centre) recorded back to 1659 is also plotted on Figures 8.1 and 8.2 in order to determine if this shows the shift in temperature associated with the LIA at the two sites and to compare it with the diatom inferred reconstructions. This temperature series was used because it has been shown that the winter air temperatures in Bergen, Norway, have a high correlation with the CET's record (Nesje and Dahl 2003 see Figure 1.2) and it also provides a extensive temperature record for validation purposes. The CETS temperature profile does record lower temperatures generally for the lower section of the two cores, with the coldest period being associated with 1690- 1720. This is slightly earlier than the recorded/ documented Norwegian LIA maxima (see section 1.5.1).

⑤

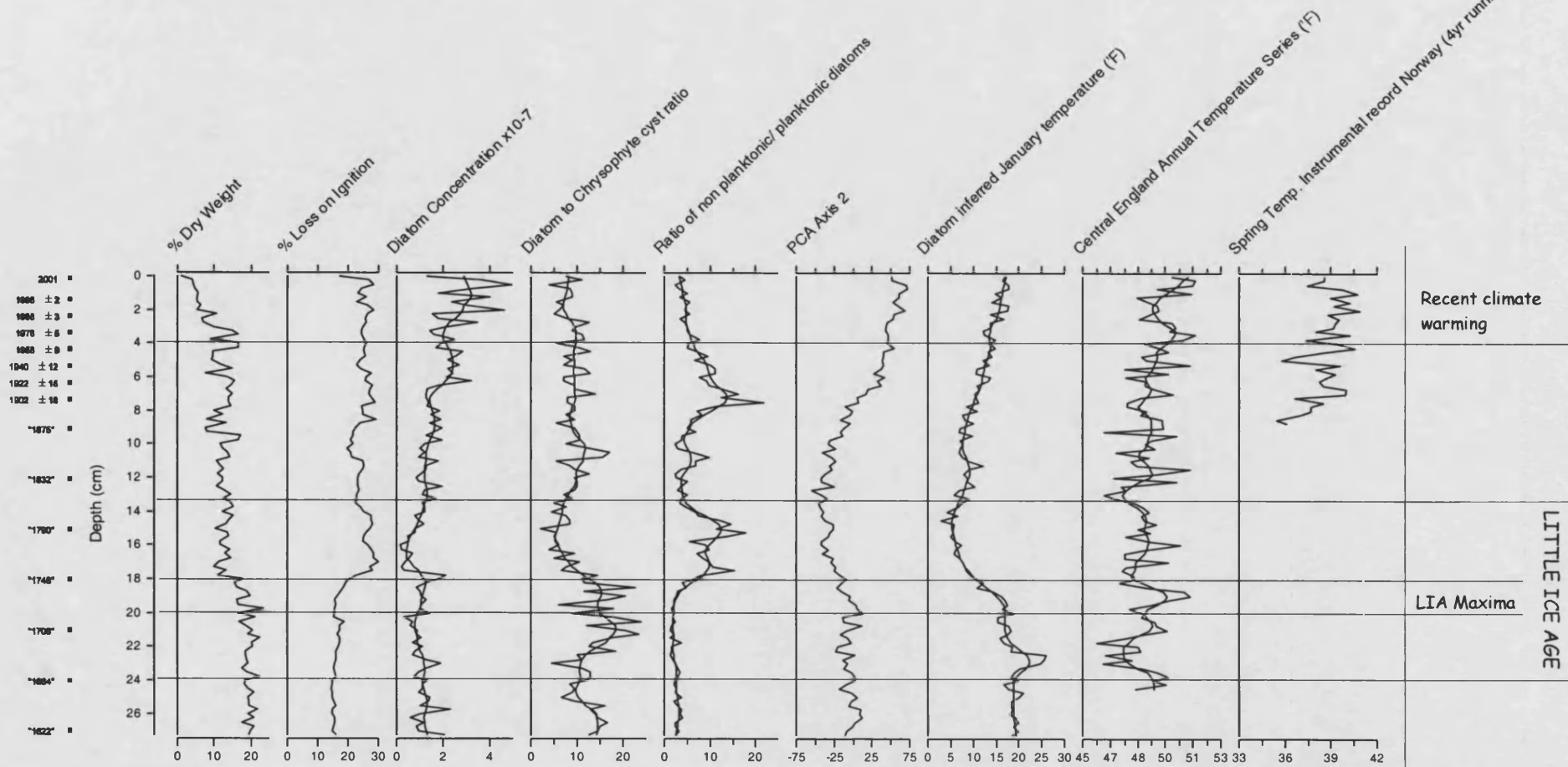


Figure 8.2: Summary diagram of various lithostratigraphic parameters, diatom composition data, diatom inferred temperature reconstruction and the Central England Temperature series (Average annual temperature, Manley 1974, updated by the Hadley Centre) applied to Lake Gåvålivatnet. The LIA zones are positioned according to the core chronology.

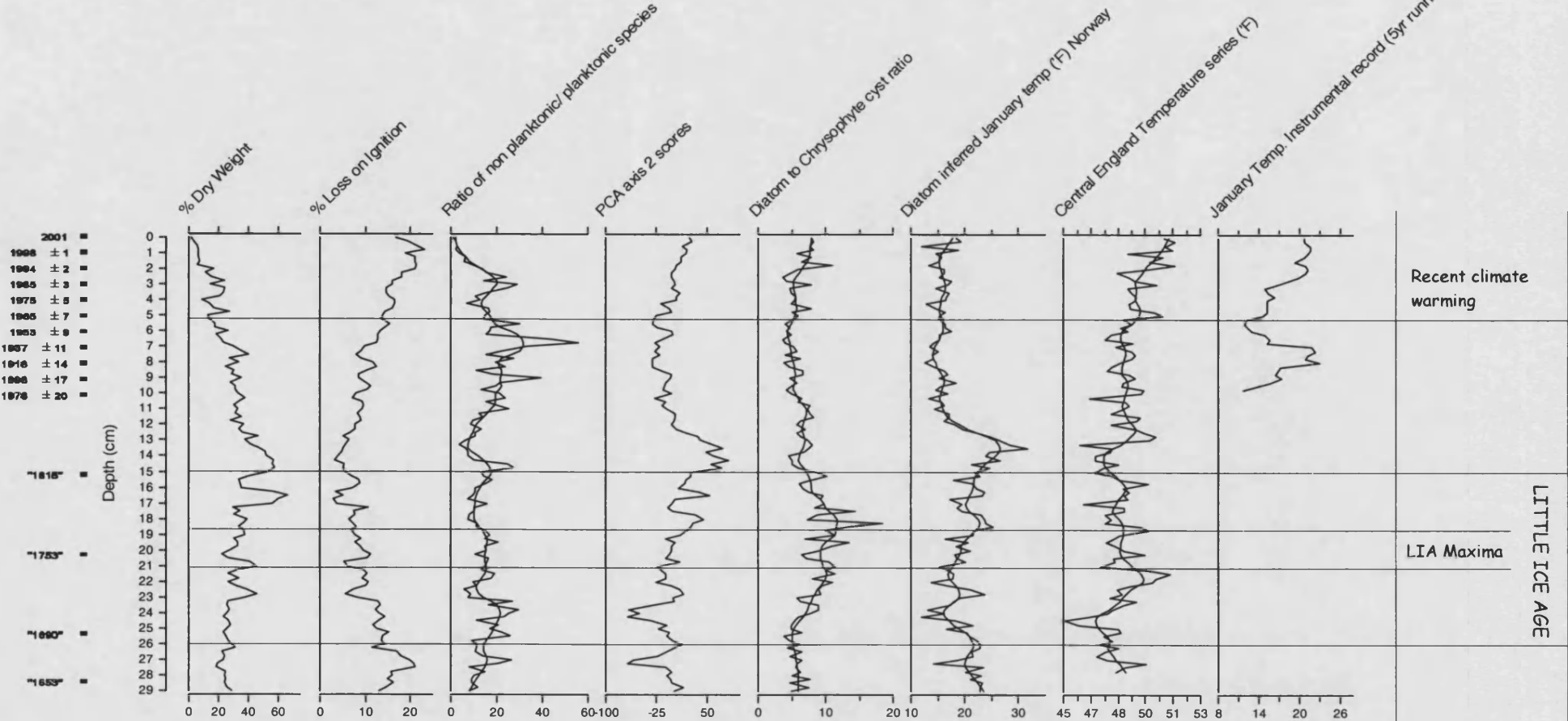
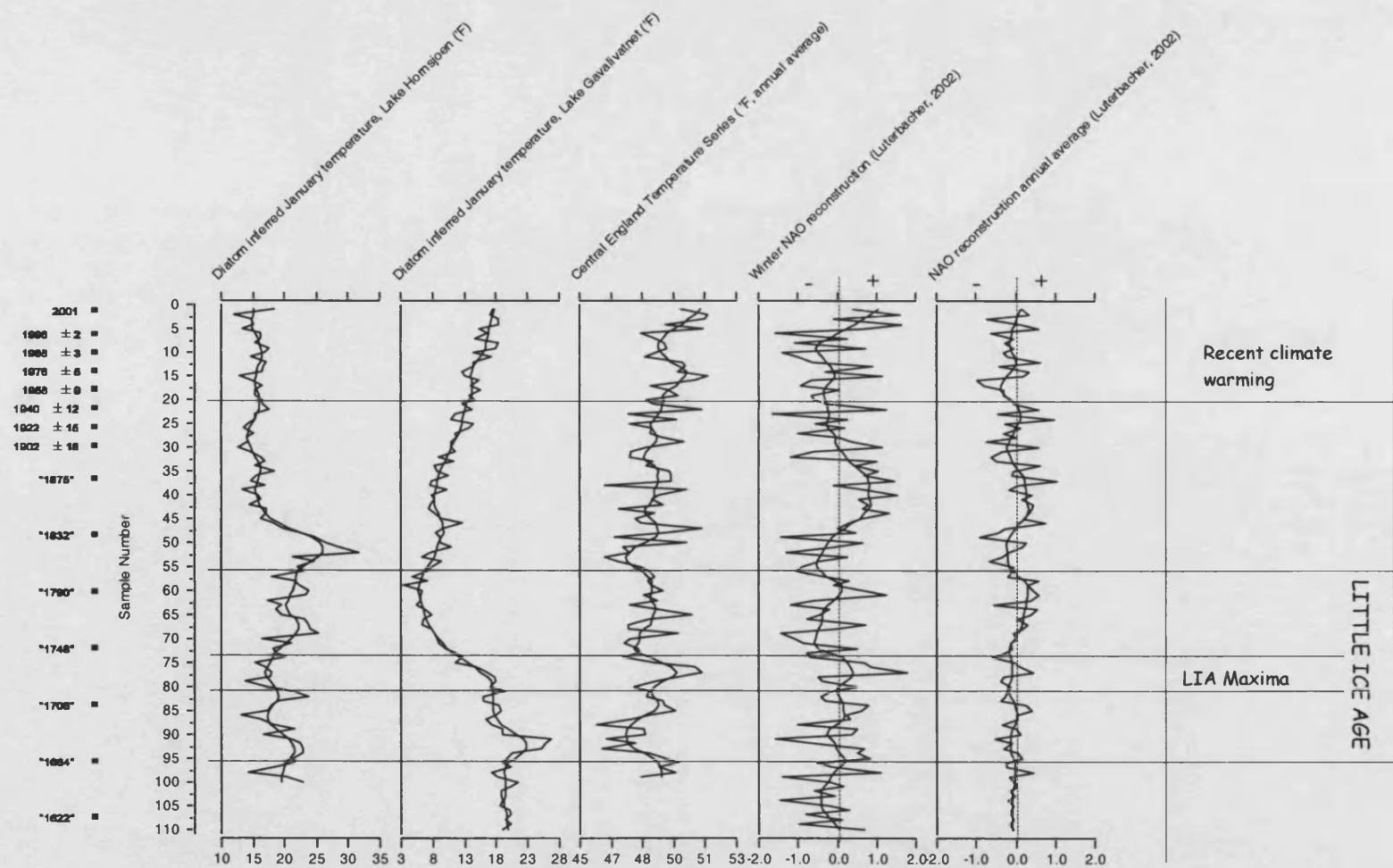


Figure 8.3: Diatom inferred temperature reconstructions for Lake Hornsjøen and Gåvålivatnet (°F), Central England Temperature series (°F, Manley 1974, Hadley Centre), Winter and annual NAO index reconstructions for the Northern Hemisphere (Luterbacher 2002). Each variable is constrained by the chronology for Lake Hornsjøen.



The CETS curve appears to agree particularly well with the diatom inferred January temperature for Lake Gåvålivatnet during the LIA period (Figure 8.2). The relationship breaks down in the upper section of the core as the diatom temperature reconstruction does not seem to reflect the increasing temperature occurring after the LIA period (Figure 8.2, 5-12cm)

The diatom inferred January temperature from the Lake Hornsjøen core, however, appears to mirror the CETS curve in the upper section of the profile (Figure 8.1 0-10cm). The discrete cold spell recorded by the diatoms at 1750 and 1800 is not evident within the CETS profile but the series does record slightly lower temperatures at this time. The main discrepancy between the two temperature curves for this lake occurs at the outset of the LIA (20-24cm Figure 8.1) where the diatom inferred temperatures are significantly higher than the recorded CETS temperatures.

Figure 8.3 compares the diatom temperature reconstructions from both cores with the CETS and the NAO index reconstructions (Luterbacher *et al.*, 1999, 2000 and 2001), all constrained using the chronology from Lake Hornsjøen. According to the chronology it can be seen that the LIA maxima was a period of predominantly positive winter NAO values causing increased winter precipitation in Norway, accounting for the large glacial advances. In a similar way the recent positive NAO values have again caused large glacial advance in Norway over recent years despite the increasing annual temperatures (see also Figure 1.2 and section 1.5.1).

The figure, however, demonstrates that it is difficult to identify a synchronous and discrete temperature response during the duration of the LIA using either the diatom inferred temperature record from Hornsjøen, Gåvålivatnet or the CETS curve. In fact the CETS curve shows relatively high temperatures for the period associated with the LIA maxima in Norway. The differences in the reconstructed temperatures between the study cores and the Central England temperature series may be related to the different geographical location of the two studies. It can be seen that the instrumental record from Norway does not mirror the CETS curve over recent years (Figure 8.1 and 8.2) confirming that differences should be expected in the temperature record of the two countries.

Furthermore, previous individual country based climatic investigations have shown that the timing of the LIA was not synchronous across the Northern Hemisphere (see section 1.5.1 and Six *et al.*, 2001; Nesje and Dahl 2003; Grove 2001; Grove 1988). Added to this, the inherent variability of the recorded temperature record, and the ranges of climatic conditions encompassed by the 'Little Ice Age' make comparison of reconstructed temperatures with the instrumental record extremely complex. This highlights a common problem in palaeoclimatological studies primarily concerning the chronic lack of country specific validation methods for the proxy temperature reconstructions and the absence of a precise chronological control (*c.f.* Bigler and Hall 2003) further complicates the validation process.

In conclusion, therefore, this study shows that the diatom record can to a certain extent be used to make qualitative inferences about the climate changes occurring at the two Norwegian lakes over the past 500 years. These are based primarily on the auto-ecology of the species and their habitat preferences, and in no way was it thought feasible to reconstruct actual temperature changes using these two lakes and the approaches developed in this thesis.

8.6 Key contributions of the current research and future work

The previous section and chapters 6 and 7 demonstrated how hard it is to compare the response of individual lake systems to the same climatic driving forces. The study also highlighted the difficulty of detecting a relatively short lived climatic event such as the LIA, which throughout its duration exhibited many climatically different phases. The thesis illustrates that although both the study lakes were within the same geographical area and at similar altitudes, the biological response to climatic change could not be predicted. Analysis of these two lakes highlighted the fact that individual lakes will respond differently to the same driving macroclimate changes, mainly due to their different chemistry, bathymetry and catchment characteristics (*c.f.* Catalan *et al.*; Battarbee *et al.*, 2002).

It would appear that although diatoms do seem to respond to climatic forcing, this response is not linearly related and is often not the dominate explanatory variable for the diatoms, making quantification of such a response problematic and fraught with technical difficulties. In addition further complications arise in palaeoclimatological

studies such as this, due to the necessity for accurate dating, the resolution of analysis, the inherent variability of the instrumental temperature record for validation, and the absence of individual lake microclimate and catchment data.

Increasingly, however, over the last few years much research has linked the growth of certain diatom species to changes in climate and specifically to changes in the nature and duration of lake ice-cover (*c.f.* Korhola and Weckstrom 2000; Sorvari and Korhola 1998; Smol 1988; Douglas and Smol 1994; Lotter and Bigler 2000; Ohlendorf *et al.*, 2000; Catalan *et al.*, 2002a; Koining *et al.*, 2000; Goudsmit *et al.*, 2000). The possibility of up scaling the relationship seen in these individual lakes in to an ice-cover transfer function has not, to date, been investigated or at least made widely available in the published literature. This thesis addressed this apparent gap in the research. It is, however, concluded that due to the complex nature of ice-cover, and its control over other inter linked and often unknown driving variables, the traditional transfer function approach is not appropriate. The relationship between lake ice-cover and diatom growth appears to be too complex to model, or summarise in a quantitative sense, using many different lakes and covering different geographical areas (i.e. through the generation of a training set).

Further intensive work on an individual lake basis is needed in order to truly understand the linking mechanisms between the water/air/ice-cover interface and the influence of lake bathymetry and catchment variables on the lake's ice-cover regime. To investigate the relationship between the individual diatom species and lake ice-cover; sediment trap data, continuous water sampling and lake water temperature measurements would be needed in order to relate the growth patterns of diatom species to the lake's seasonal, chemical and thermal regimes. This unfortunately is not possible in a study such as this due to time restrictions and the logistics of frequent visits to remote lakes.

The problems associated with the spot sampling of nutrients were highlighted in this work and it is likely that this also applies to other important chemical variables. In a similar way this intensive sampling should also be applied to the %LOI analysis because multi core studies have shown that the %LOI of one core collected from the deepest part of the basin may not reliably reflect a complete record of catchment

change (Snowball and Sandgren 1996). It might also be useful to explore in more detail the complex relationship between the diatoms, light levels and DOC concentrations and the potential links these variables might have with changing climate.

It is apparent that there is still a large proportion of the diatom variance that cannot be explained by the variables collected (Chapter 5). In this way the unmeasured influence of light availability, mixing regime, water temperature and the trophic cascade (i.e. involving the interaction between diatoms and other lake biota) amongst many other variables is not considered. Until these processes are accurately measured and the complex interactions between lake ice-cover, environmental parameters and the lake biota understood, the true influence of climate on diatoms assemblages can not be characterised.

References

- Adrian, R. & Deneke, R. (1996) Possible impact of mild winters on zooplankton succession in eutrophic lakes of the Atlantic European area. *Freshwater Biology*, 36, 757-770.
- Adrian, R., Walz, N., Hintze, T., Hoeg, S. & Rusche, R. (1999) Effects of ice duration on plankton succession during spring in a shallow polymictic lake. *Freshwater Biology*, 41, 1-12.
- Agbeti, M. & Dickman, M. (1989) Use of lake fossil diatom assemblages to determine historical changes in trophic status. *Canadian Journal of Fisheries and Aquatic Science*, 46, 1013-1021.
- Agbeti, M.D., Kinston, J.C., Smol, J.P. & Watters, C. (1997) Comparison of phytoplankton succession in two lakes of different mixing regimes. *Arch. Hydrobiol.*, 140, 37-69.
- Agusti- Panareda, A. & Thompson, R. (2002) Reconstructing air temperature at eleven remote alpine and arctic lakes in Europe from 1781 to 1997 AD. *Journal of Paleolimnology*, 28, 7-23.
- Allott, T.E.H., Golding, P.N.E. & Harriman, R. (1995) A palaeolimnological assessment of the impact of acid deposition on surface waters in North- West Scotland, a region of high sea-salt inputs. *Water, Air and Soil Pollution*, 85, 2425-2430.
- Anderson, N. J, Battarbee, R. W., Appleby, P. G, Stevenson, A. C., Oldfield, F, Darley, J, and Glover, G. (1986) Palaeolimnological evidence for the acidification of Loch Fleet. Palaeoecological Research Unit, Research Paper No. 17, -70pp. Department of Geography, University College London.
- Anderson, D.O. & Seip, H.M. (1999) Effects of a rainstorms high in sea-salts on labile inorganic aluminium in drainage from the acidified catchments of Lake Terjevann, southernmost Norway. *Journal of Hydrology*, 224, 64-79.
- Anderson, N.J. (2000) Diatoms, temperature and climatic change. *Eur. J. Phycol.*, 35, 307-314
- Anderson, N.J., Odgaard, B.V., Segerstrom, U. & Renberg, I. (1996) Climate-lake interactions recorded in varved sediments from a Swedish boreal forest lake. *Global Change Biology*, 2, 399-405.
- Anderson, W.L., Robertson, D.M. & Magnuson, J.J. (1996) Evidence of recent warming and El Nino- related variations in ice break up of Wisconsin lakes. *Limnology and Oceanography*, 41, 815-821.
- Appleby, P.G. & Oldfield, F. (1978) The calculation of ^{210}Pb dates assuming a constant rate of supply of unsupported ^{210}Pb to the sediment. *Catena*, 5, 1-8.

- Appleby, P.G. & Oldfield, F. (1983) The assessment of ^{210}Pb dates from sites with varying sediment accumulation rates. *Hydrobiologia*, 103, 29-35.
- Appleby, P.G. (2001) Chronostratigraphic techniques in recent sediments. *Tracking environmental change using lake sediments Volume 1: Basin Analysis, Coring and Chronological Techniques* (Eds. Last, W. M and Smol, J. P), pp. 171-203.
- Appleby, P.G., Nolan, P.J., Gifford, D.W., Godfrey, M.J., Oldfield, F., Anderson, N.J. & Battarbee, R.W. (1986) ^{210}Pb dating by low background gamma counting. *Hydrobiologia*, 141, 21-27.
- Appleby, P.G., Richardson, N. & Nolan, P.J. (1991) ^{241}Am dating of lake sediments. *Hydrobiologia*, 214, 35-42.
- Barber, H.G. & Haworth, E.Y. (1981) A guide to morphology of the diatom frustule. Freshwater Biological Association, Scientific Publications No.44, UK
- Barber, K.E., Battarbee, R.W., Brooks, S.J., Eglinton, G., Haworth, E.Y., Oldfield, F., Stevenson, A.C., Thompson, R., Appleby, P.G., Austin, W.E.N., Cameron, N.G., Ficken, K.J., Golding, P., Harkness, D.D., Holmes, J.A., Hutchinson, R., Lishman, J.P., Maddy, D., Pinder, L.C.V., Rose, N.L. & Stoneman, R.E. (1999) Proxy records of climate change in the UK over the last two millennia: documented change and sedimentary records from lakes and bogs. *Journal of the Geological Society, London*, 156, 369-380.
- Battarbee, R. W, Juggins, S, Gasse, F., Anderson, N. J, Bennion, H., Cameron, N. G, Ryves, D. B., Pailles, C., Chalieu, F., and Telford, R. (2001) European Diatom Database (EDDI). An information system for Palaeoenvironmental Reconstruction. 81, 1-94. London, ECRC Research Report.
- Battarbee, R.W. & Keen, M. (1982) The use of electronically counted microspheres in absolute diatom analysis. *Limnology and Oceanography*, 27, 182-188.
- Battarbee, R.W. & Renberg, I. (1990) The surface waters acidification project swap palaeolimnology programme. *Philosophical Transactions of the Royal Society of London B*, 327, 227-232.
- Battarbee, R.W. (1986) Diatom Analysis. *Handbook of Holocene Palaeohydrology and Palaeoecology* (Berglund, B. E.), pp. 527-570. John Wiley & Sons, Chichester.
- Battarbee, R.W., Cameron, N.C., Golding, P., Brooks, S.J., Switsur, R., Harkness, D., Appleby, P., Oldfield, F., Thompson, R., Monteith, D. & McGovern, A. (2001) Evidence for Holocene climate variability from the sediments of a Scottish remote mountain lake. *Journal of Quaternary Science*, 16, 339-346.
- Battarbee, R.W., Flower, R.J., Stevenson, A.C. & Rippey, B. (1985) Lake acidification in Galloway: A palaeoecological test of competing hypotheses. *Nature*, 314, 350-352.

- Battarbee, R.W., Grytnes, J.-A., Thompson, R., Appleby, P.G., Catalan, J., Korhola, A., Birks, H.J.B., Heegaard, E. & Lami, A. (2002) Comparing palaeolimnological and instrumental evidence of climate change for remote mountain lakes over the last 200 years. *Journal of Paleolimnology*, 28, 161-179.
- Battarbee, R.W., Thompson, R., Catalan, J., Grytnes, J.-A. & Birks, H.J.B. (2002b) Climate variability and ecosystem dynamics of remote alpine and arctic lakes: the MOLAR project. *Journal of Paleolimnology*, 28, 1-6
- Baudrimont, R. (1973) Recherches sur les Diatomacees des eaux continentales de l'Algerie ecologie et paleoecologie. *Mem.Soc.Hist.Nat.Afr.Nord*, 12, 150-266.
- Beare, A. H. (1995) AMPHORA database: an overview. Environmental Change Research Centre, UCL London.
- Belgrano, A., Lindhal, O. & Hernroth, B. (1999) North Atlantic Oscillation, primary productivity and toxic phytoplankton in the Gullmar Fjord, Sweden (1985-96). *Proceedings of the Royal Society of London, B*, 266, 425-430.
- Bennion, H. (1993) *A diatom phosphorous transfer function for eutrophic ponds in south-east England*. Unpublished Ph.D. thesis, University College London.
- Bigler, C. & Hall, R.I. (2002) Diatoms as indicators of climatic and limnological change in Swedish Lapland: a 100- lake calibration set and its validation for palaeoecological reconstructions. *Journal of Paleolimnology*, 27, 97-115.
- Bigler, C. & Hall, R.I. (2003) Diatoms as quantitative indicators of July temperature: a validation attempt at century- scale with meteorological data from northern Sweden. *Palaeogeography, Palaeoclimatology, Palaeoecology*, 189, 147-160.
- Birks, H.H., Battarbee, R.W. & Birks, H.J.B. (2000) The development of the aquatic ecosystem at Krakenes Lake , Western Norway, during the late-glacial and early Holocene- a synthesis. *Journal of Paleolimnology*, 23, 91-114.
- Birks, H.J.B. (1995) Quantitative palaeoenvironmental reconstructions. *Statistical modelling of Quaternary science data* (Eds. Maddy, D and Brew, J. S), pp. 161-254. Quaternary Research Associates.
- Birks, H.J.B., Line, J.M., Juggins, S., Stevenson, A.C. & ter Braak, C.J.F. (1990) Diatoms and pH reconstruction. *Philosophical Transactions of the Royal Society London B*, 327, 263-278.
- Birks, H.J.B., Jones, V.J. & Rose, N.L. (2004, in press) Recent environmental change and atmospheric contamination on Svalbard as recorded in lake sediments synthesis and general conclusions. *Journal of Palaeolimnology*
- Bothwell, M.L., Sherbopt, D. & Pollock, C.M. (1994) Ecosystem response to solar ultraviolet -B radiation: Influence of trophic-level interactions. *Science*, 265, 97-100.
- Bradbury, J.P. & Dieterich- Rurup, K.V. (1993) Holocene diatom paleolimnology of Elk Lake, Minnesota. *Elk Lake, Minnesota: Evidence for rapid climate change in the*

North- Central United States: Boulder, Colorado, Geological Society of America Special Paper, (Eds. Bradbury, J. P. and Dean, W. E.), pp. 215-237.

Bradley, R.S. & Jones, P.D. (1992) *Climate since A.D. 1500*. Routledge, London.

Briffa, K.R. & Schweingruber, F.H. (1992) Recent dendroclimate evidence of northern and central European summer temperatures. *Climate since A.D. 1500* (Eds. Bradley, R. S. and Jones P. D.), pp. 366-391. Routledge, New York.

Briffa, K.R. (2000) Annual climate variability in the Holocene: interpreting the message of ancient trees. *Quaternary Science reviews*, 19, 87-105.

Bronmark, C. & Hansson, L. (1998) *The Biology of lakes and ponds*. Oxford University Press, Oxford.

Camburn, K.E. & Charles, D.F. (2000) *Diatoms of Low-Alkalinity Lakes*. The Academy of Natural Sciences of Philadelphia, Philadelphia.

Camburn, K.E., Kingston, J.C. & Charles, D.F. (1984) *PIRLA diatom Iconograph*. Bloomington, USA.

Cameron, N. (1995) The representation of diatom communities by fossil assemblages in a small acid lake. *Journal of Paleolimnology*, 14, 185-223.

Cameron, N.G., Birks, H.J.B., Jones, V.J., Berge, F., Catalan, J., Flower, R.F., Garcia, J., Kawecka, B., Koining, K.A., Marchetto, A., Sanchez- Castillo, P., Schmidt, R., Sisko, N., Solovieva, E., Stefkova, E. & Toro, M. (1999a) Surface-sediment and epilithic diatom pH calibration sets for remote European mountain lakes (AL:PE project) and their comparison with the Surface Waters Acidification Programme (SWAP) calibration set. *Journal of Paleolimnology*, 22, 291-317.

Catalan, J. & Camarero, L. (1991) Ergoclines and biological processes in high mountain lakes: similarities between the summer stratification and the ice forming period in lake Redo (Pyrenees). *Verhandlungen Internationaler Verein für Limnologie*, 24, 1011-1015.

Catalan, J. (1992) Evolution of dissolved and particulate matter during the ice covered period in a deep high mountain lake. *Canadian Journal of Fisheries and Aquatic Science*, 49, 945-955.

Catalan, J., Pla, S., Rieradevall, M., Felip, M., Ventura, M., Buchaca, T., Camarero, L., Brancelj, A., Appleby, P.G., Grytnes, A., Agusti- Panareda, A. & Thompson, R. (2002a) Lake Redo ecosystem response to an increasing warming in the Pyrenees during the twentieth century. *Journal of Paleolimnology*, 28, 129-145.

Catalan, J., Ventura, M., Brancelj A., Granados, I., Theis, H., Nickus, U., Korhola, A., Lotter, A.F., Barbieri, A., Stuchlik, E., Lien, L., Bitusik, P., Buchaca, T., Camarero, L., Goudsmit, G.H., Kopacek, J., Lemcke, G., Livingstone, D.M., Muller, B., Rautio, M., Sisko, M., Sorvari, S., Struncky, O. & Toro, M. (2002b) Seasonal ecosystem variability in remote mountain lakes: implications for detecting climate signals in sediment records. *Journal of Paleolimnology*, 28, 25-46.

- Charles, D.F. (1985) Relationships between surface sediment diatom assemblages and lakewater characteristics in Adirondack lakes. *Ecology*, 66, 994-1011.
- Charles, D.F., Smol, J.P. & Engstrom, D.R. (1994) Paleolimnological approaches to biological monitoring. *Biological monitoring of aquatic systems* (Loeb, S. L. and Spacie, A.), CRC Press, Boca Raton, FL.
- Cole, G.A. (1975) *Textbook of limnology*. The C.V. Mosby Company, Saint Louis.
- Crowley, T.J., Lowery & T.S (2000) How warm was the medieval warm period? *Ambio*, 29, 54.
- Cullen, H.M., D'Arrigo, R.D., Cook, E.R. & Mann, M.E. (2001) Multiproxy reconstructions of the North Atlantic Oscillation. *Paleoceanography*, 16, 27-39.
- Cumming, B.F. & Smol, J.P. (1993) Development of diatom-based salinity models for paleoclimate research from lakes in British Columbia (Canada). *Hydrobiologia*, 269/270, 179-96.
- Cumming, B.F., Smol, J.P., Kingston, J.C., Charles, D.F., Birks, H.J.B., Camburn, K.E., Dixit, S.S., Uutala, A.J. & Selle, A.R. (1992) How much acidification has occurred in Adirondack Region Lakes (New York, USA) since Pre-industrial times? *Canadian Journal of Fisheries and Aquatic Science*, 49, 128-141.
- Dahl-Jensen, D., Mosegaard, K., Gundestrup, N., Clow, G.D.J.S.J., Hansen, A.W. & Balling, N. (1998) Past temperatures directly from the Greenland ice sheet. *Science*, 282, 268-271.
- Dean, W.E., Bradbury, J.P., Anderson, R.Y. & Barnosky, C.W. (1984) The variability of Holocene climate change: Evidence from varved lake sediments. *Science*, 226, 1191-1194.
- Denys, L. A check-list of the diatoms in the Holocene deposits of the Western Belgian coastal plain with a survey of their apparent ecological requirements. No. 246. 1991. Service Geologique de Belgique, Ministère des affaires économiques.
- Dillon, P.J. & Rigler, F.H. (1974) The phosphorus- chlorophyll relationship in lakes. *Limnology and Oceanography*, 19, 767-773.
- Dixit, S.S., Cumming, B.F., Birks, H.J.B., Smol, J.P., Kingston, J.C., Uutala, A.J., Charles, D.F. & Camburn, K.E. (1993) Diatom assemblages from Adirondack lakes (New York USA) and the development of inference models for retrospective environmental assessment. *Journal of Paleolimnology*, 8, 27-47.
- Donner, J.J. (1962) On the post-glacial history of the Grampian Highlands of Scotland. *Societas Scientiarum Fennica Commentationes Biologicae*, 24, 1-29.
- Douglas, M.S.V. & Smol, J.P. (1994) Limnology of high arctic ponds (Caper Herschel, Ellesmere Island, N.W.T). *Archiv für Hydrobiologie*, 131, 401-434.
- Douglas, M.S.V., Smol, J.P. & Blake Jr, W. (1994) Marked Post-18th Century Environmental Change in High- Arctic Ecosystems. *Science*, 266, 416-419.

- Enache, M. & Prairie, Y.T. (2002) WA-PLS diatom based pH, TP and DOC inference models from 42 lakes in the Abitibi clay belt area (Quebec, Canada). *Journal of Paleolimnology*, 27, 151-171.
- Evans, C.D., Monteith, D.T. & Harriman, R. (2001) Long-term variability in the deposition of marine ions at west coast sites in the UK Acid Waters Monitoring Network: impacts of surface water chemistry and significance for trend determination. *The Science of the Total Environment*, 265, 115-129.
- Felip, M., Bartumeus, F., Halca, S. & Catalan, J. (1999) Microbial plankton assemblages, composition and biomass, during two ice-free periods in a deep high mountain lake (Estany Redo, Pyrenees). *Journal of Limnology*, 58, 193-202.
- Flöder, S. & Sommer, U. (1999) Diversity in planktonic communities: An experimental test of the intermediate disturbance hypothesis. *Limnology and Oceanography*, 44, 1114-1119.
- Flower, R.J. & Battarbee, R.W. (1983) Diatom evidence for recent acidification of two Scottish lochs. *Nature*, 305, 130-133.
- Flower, R.J. & Battarbee, R.W. (1985) The morphology and biostratigraphy of *Tabellaria quadrisepata* (Bacillariophyceae) in acid waters and lake sediments in Galloway, Southwest Scotland. *British Phycological Society*, 20, 69-79.
- Flower, R.J. & Jones, V.J. (1989a) Taxonomic descriptions and occurrences of new *Achnanthes* taxa in acid lakes in the U.K. *Diatom Research*, 4, 227-239.
- Flower, R.J., Juggins, S. & Battarbee, R.W. (1997) Matching diatom assemblages in lake sediment cores and modern surface sediment samples: the implications for lake conservation and restoration with special reference to acidified systems. *Hydrobiologia*, 344, 27-40.
- Foy, R.H. & Gibson, C.E. (1993) The influence of irradiance, photoperiod and temperature on the growth kinetics of three planktonic diatoms. *European Journal of Phycology*, 28, 203-212.
- Fritsen, C.H. & Priscu, J.C. (1999) Seasonal change in the optical properties of the permanent ice-cover on Lake Bonney, Antarctica: Consequences for lake productivity and phytoplankton dynamics. *Limnology and Oceanography*, 44, 447-454.
- Fritz, S.C. (1996) Paleolimnological records of climate change in North America. *Limnology and Oceanography*, 41, 882-889.
- Fritz, S.C., Juggins, S., Battarbee, R.W. & Engstrom, D.R. (1991) Reconstruction of past changes in salinity and climate using a diatom-based transfer function. *Nature*, 352, 706-709.
- Fritz, S.C., Kingston, J.C. & Engstrom, D.R. (1993) Quantitative trophic reconstruction from sedimentary diatom assemblages: a cautionary tale. *Freshwater Biology*, 30, 1-23.

- Fritz, S.C., Kreiser, A.M., Appleby, P.G. & Battarbee, R.W. (1990) Recent acidification of upland lakes in North Wales: Palaeolimnological evidence. *Acid waters in Wales* (Edwards, R. W), pp. 27-37. Kluwer Academic Publishers, Netherlands.
- Gasse, F., Juggins, S. & Khelifa, L.B. (1995) Diatom-based transfer functions for inferring past hydrochemical characteristics of African lakes. *Palaeogeography, Palaeoclimatology, Palaeoecology*, 117, 31-54.
- Gasse, F., Talling, J.F. & Kilham, P. (1982) Diatom assemblages in East Africa: Classification, Distribution and Ecology. *Rev. Hydrobiologie Tropicale*, ORSTOM, Paris.
- Gauch, H.G. (1982) *Multivariate analysis in community ecology*. Cambridge University Press, New York.
- Geladi, P. & Kowalski, B.R. (1986) Partial least squares regression- a tutorial. *Analytica Chimica Acta*, 185, 1-17.
- Glew, J.R. (1988) A portable extruding device for close interval sectioning of unconsolidated core samples. *Journal of Paleolimnology*, 1, 235-239.
- Glueck, M.F. & Stockton, C.W. (2001) Reconstruction of the North Atlantic Oscillation. *International Journal of Climatology*, 21, 1453-1465.
- Goh, K.M. (1991) Carbon dating. *Carbon Isotope Techniques* (Eds. Goh, K. M), pp. 125-145. Cambridge Academic Press, Cambridge.
- Gordon, A.D. & Birks, H.J.B. (1985) *Numerical methods in Quaternary paleoecology I: zonation of pollen diagrams*. *New Phytologist*, 71, 961-979.
- Gorham, E. (1964) Morphometric control of annual heat budgets in temperate lakes. *Limnology and Oceanography*, 9, 525-529.
- Goudsmit, G.H., Lemcke, G., Livingstone, D.M., A.F.,L., Muller, B. & Strum, M. (2000) Hagelseewli: A fascinating high mountain lake- suitable for palaeoclimate studies? *Verhandlungen Internationaler Verein für Limnologie* 27, 1013-1022.
- Goulden (1969) Developmental phases of the biocenosis. *Proceedings of the Natural Academy of Science USA*, 62, 1066-1073.
- Gran, G. (1952) Determination of the equivalence point in potentiometric titration. Part II. *The Analyst*, 77, 661-671.
- Grim, E.C. (1987) A FORTRAN 77 program for stratigraphically constrained cluster analysis by the method of incremental sum of squares. *Computers and Geoscience*, 13, 13-15.
- Grove, J.M. & Battagel, A. (1983) Tax records from western Norway as an index of Little Ice Age environmental and economic deterioration. *Climatic Change*, 5, 265-82.

- Grove, J.M. (1988) Introduction. *The Little Ice Age* (Grove, J. M.), p. 498. Routledge, London.
- Grove, J.M. (1988) Scandinavia. *The Little Ice Age* (Grove, J. M), Routledge, London.
- Grove, J.M. (1988b) The glacial history of the Holocene. *The Little Ice Age* (Grove, J. M.), Routledge, London.
- Grove, J.M. (2001) The initiation of the little ice age in regions round the North Atlantic. *Climatic Change*, 48, 53-82.
- Håkansson, H. & Carter, J.R. (1990) An interpretation of Hustedt's terms 'Schattenlinie', 'Perlenreihe' and 'Hocker' using specimens of the *Cyclotella radiosa*-complex, *C. distinguenda* HUST., and *C. cyclopuncta* nov.sp. *Journal of Iowa Academic Science*, 97, 153-156.
- Håkansson, H. (1990) A comparison of *Cyclotella krammeri* sp. nov. and *C. schumanni* Håkansson stat. nov. with similar species. *Diatom Research*, 5, 261-271.
- Hall, R.I. & Smol, J.P. (1992) A weighted averaging regression and calibration model for inferring total phosphorous concentration from diatoms in British Columbia. *Freshwater Biology*, 27, 417-434.
- Hansenn-Bauer, I and Nordli, P. Ø. (2000) Annual and seasonal temperature variation in Norway 1876-1999. Hansenn-Bauer, I and Nordli, P. Ø. 25/98, 1-29. Det Norske meteorologiske institutt.
- Hanson, H.P., Hanson, C.S. & Yoo, B.H. (1992) Recent Great Lakes Ice Trends. *Bulletin American Meteorological Society*, 73, 577-584.
- Hanssen-Bauer, I, Nordli, Ø, and Forland, E. J. Principal component analysis of the NAACD temperature series. DNMI-report 7/97, 1-33. 1996. KLIMA.
- Hardin, G. (1960) The competitive exclusion principle. *Science*, 131, 1292-1297.
- Harriman, R. & Wells, D.E.W. (1985) Causes and effects of surface water acidification in Scotland. *Water Pollution Control*, 84, 215-224.
- Haworth, E.Y. & Hurley, M.A. (1984) Comparison of the stelligeroid taxa of the centric diatom genus *Cyclotella*. *Proceedings of the 8th International Diatom Symposium- Paris* (Richard, M), pp. 43-59. Koeltz Scientific Books, Koenigstein.
- Haworth, E.Y. (1980) Comparison of continuous phytoplankton records with the diatom stratigraphy in the recent sediments of Blelham Tarn. *Limnology and Oceanography*, 25, 1093-1103.
- Heathcote, J.A. & Lloyd, J.W. (1984) Groundwater chemistry in Southwest Suffolk (UK) and its relation to Quaternary geology. *Journal of Hydrology*, 75, 143-165.
- Hughes, M.K. & Diaz, H.F. (1994) Was there a medieval warm period and if so where and when? *Climatic Change*, 26, 109-142.

- Hughes, M.K. & Graumlich, L.J. (1996) Multimillennial dendroclimatic records from Western North America. *Climatic Variations and Forcing Mechanisms of the Last 2000 years* (Eds. Jones, P. D., Bradley, R. S, and Jouzel, J), pp. 109-124. Springer Verlag, Berlin.
- Huisman, J., Olff, H. & Fresco, L.F.M. (1993) A hierarchical set of models for species response analysis. *Journal of Vegetation Science*, 4, 37-46.
- Huntley, B. (1981) The past and present vegetation of the Caenlochan National Nature Reserve, Scotland II. Palaeological Investigations. *New Phytologist*, 87, 222.
- Hurrell, J.W. (1995) Decadal trends in the North Atlantic Oscillation regional temperatures and precipitation. *Science*, 269, 676-679.
- Hutchinson, G.E. (1961) The paradox of the plankton. *The American Naturalist*, 95, 137-145.
- Hutchinson, G.E. (1975) *A Treatise on Limnology*. Wiley, New York.
- Ingram, M.J., Underhill, D.J., & Wigley, T.M.L (1978) Historical climatology. *Nature*, 276, 329-334.
- Jones, P.D. & Bradley, R.S. (1992) Climatic variations over the last 500 years. editors. *Climate since AD 1500* (Eds. Jones, P. D. and Bradley, R. S), Routledge, London, New York.
- Jones, P.D., New, M., Parker, D.E., Martin, S. & Rigor, I.G. (1999) Surface air temperatures and its changes over the past 150 years. *Reviews of Geophysics*, 37, 173-199.
- Jones, V.J. & Flower, R.F. (1986) Spatial and temporal variability in periphytic diatom communities: Palaeoecological significance in an acidified lake. *Diatoms and Lake Acidity* (Eds. Smol, J. P, Battarbee, R. W, Davis, S, and Merilainen, J), pp. 87-94. Dr W. Junk, Dordrecht.
- Jones, V.J. & Juggins, S. (1995) The construction of a diatom-based chlorophyll a transfer function and its application at three lakes on Signy Island (maritime Antarctic) subject to differing degrees of nutrient enrichment. *Freshwater Biology*, 34, 433-445.
- Jones, V.J., Stevenson, A.C. & Battarbee, R.W. (1989) Acidification of lakes in Galloway, south-west Scotland: a diatom and pollen study of the post-glacial history of the Round Loch of Glenhead. *Journal of Ecology*, 81, 4-24.
- Jongman, R.H.G., ter Braak, C.J.F. & van Tongeren, O.F.R. (1987) *Data Analysis in Community and Landscape Ecology*. Pudoc, Washington.
- Juday, C.E.A. & Birge, E.A. (1933) The transparency, the colour and the specific conductance of the lake waters of northeastern Wisconsin. *Transactions of the Wisconsin Academy of Science Articles and Letters*, 23, 233-248.

- Juggins, S and ter Braak, C. J. F. (1993) CALIBRATE- a computer programme for species-environment calibration by [weighted averaging] partial least squares regression. Unpublished computer programme, Environmental Change Research Centre, 20pp. University College London.
- Juggins, S. (1997a) GLR Gaussian Logit Regression. Version 1.1 Unpublished Computer Programme.
- Juggins, S. (1994) MAT Modern Analog Technique Version 1.0. Unpublished Computer Programme.
- Juggins, S. (1997b) TRAN version 1.7 user manual. Unpublished Computer Programme, University of Newcastle upon Tyne.
- Juggins, S. (1991) ZONE version 1.2, Unpublished Computer Programme.
- Kalela-Brundin, M. (1999) Climatic information from tree rings of *Pinus sylvestris* L. and reconstruction of summer temperatures back to AD 1500 in Femundsmarka, eastern Norway, using partial least squares regression (PLS) analysis. *The Holocene*, 9, 59-77.
- Kent, M. & Coker, P. (1992) *Vegetation description and analysis*. John Wiley & Sons, UK.
- Kilham, S.S., Theriot, E.C. & Fritz, S.C. (1996) Linking planktonic diatoms and climate change in the large lakes of the Yellowstone ecosystem using resource theory. *Limnology and Oceanography*, 41, 1052-1062.
- Kilman, P., Kilman, S.S. & Hecky, R.E. (1986) Hypothesized resource relationships among African planktonic diatoms. *Limnology and Oceanography*, 31, 1169-1181.
- Kingston, J.C., Birks, H.J.B., Uutala, A.J., Cumming, B.F. & Smol, J.P. (1992) Assessing trends in fishery resources and lake water aluminium from paleolimnological analyses of siliceous algae. *Canadian Journal of Fish & Aquatic Science*, 49, 116-127.
- Koinig, K.A., Kamenik, C., Schmidt, R., Agusti-Panareda, A., Appleby, P., Lami, A., Prazakova, M., Rose, N., Schnell, O.A., Tessadri, R., Thompson, R. & Psenner, R. (2002) Environmental changes in an alpine lake (Gossenköllesee, Austria) over the last two centuries- the influence of air temperature on biological parameters. *Journal of Paleolimnology*, 28, 147-160.
- Koinig, K.A., Busing, N., Wille, A., Sattler, R., Schmidt, R. & Psenner, R. (2000) Diatom communities in the ice cover of an alpine lake- their influence on pH reconstruction from fossil diatom assemblages. *Verhandlungen Internationaler Verein für Limnologie*, 27.
- Korhola, A. & Weckström, J. (2000) A quantitative Holocene climate record from diatoms in Northern Fennoscandia. *Quaternary Research*, 54, 284-294.

- Korhola, A., Weckstrom, J., Olander, H. & Blom, T. (1998) Assessment of chironomid, cladoceran and diatom assemblages as markers of global change in subarctic Fennoscandian lakes. *Proceedings of the second international conference on climate and water Espoo, Finland 1-20th August* (Eds. R., Lemmela and Helenius, N.), pp. 562-575.
- Korsman, J.C. & Birks, H.J.B. (1990) Diatom-based water chemistry reconstructions from northern Sweden: a comparison of reconstruction techniques. *Journal of Paleolimnology*, 15, 65-77.
- Kowalski, B.R. & Seasholtz, M.B. (1991) Recent developments in multivariate calibration. *Journal of Chemometrics*, 5, 129-146.
- Kramer, J.R., Brassard, P., Collins, P., Clair, T.A. & Takats, P. (1990) Variability of organic acids in watersheds. *Organic Acids in Aquatic Ecosystems* (Eds. Perdue, E. M and Gjessing, E. T), pp. 127-139. John Wiley and Sons Ltd, UK.
- Krammer, K. & Lange-Bertalot, H. (1986) *Bacillariophyceae. 1. Teil: Naviculaceae. Süßwasserflora von Mitteleuropa*. Gustav Fisher Verlag, Stuttgart.
- Krammer, K. & Lange-Bertalot, H. (1988) *Bacillariophyceae. 2. Teil: Epithemiaceae. Süßwasserflora von Mitteleuropa*. Gustav Fisher Verlag, Stuttgart.
- Krammer, K. & Lange-Bertalot, H. (1991) *Bacillariophyceae. 3. Teil: Centrales, Fragilariaceae, Eunotiaceae. Süßwasserflora von Mitteleuropa*. Gustav Fisher Verlag, Stuttgart.
- Krammer, K. & Lange-Bertalot, H. (1991a) *Bacillariophyceae. 3. Teil: Centrales, Fragilariaceae, Eunotiaceae. Süßwasserflora von Mitteleuropa*. Gustav Fisher Verlag, Stuttgart.
- Krammer, K. & Lange-Bertalot, H. (1991b) *Bacillariophyceae. 4. Teil: Achnanthesaceae Kritische Ergänzungen zu Navicula (Lineolatae) und Gomphonema. Süßwasserflora von Mitteleuropa*. Gustav Fisher Verlag, Stuttgart.
- Kullberg, A., Bishop, K.H., Hargeby, A., Jansson, M. & Peterson, J.R.C. (1993) The ecological significance of dissolved organic carbon in acidified waters. *Ambio*, 22, 331-337.
- Laing, T.E., Ruhland, K.M. & Smol, J.P. (1999) Past environmental and climate changes related to tree-line shifts inferred from fossil diatoms from a lake near the Lena River Delta, Siberia. *The Holocene*, 9, 547-557.
- Lamb, H.H. (1966) *The Changing Climate*, Methuen, London.
- Lamb, H.H. (1979) Climatic variation and changes in the wind and ocean circulation: The Little Ice Age in the Northeast Atlantic. *Quaternary Research*, 11, 1-20.
- Laurion, I., Vincent, W.F. & Lean, D.R. (1997) Underwater ultraviolet radiation: development of spectral models for northern high latitude lakes. *Photochem. Photobiol.*, 65, 107-114.

- Leavitt, P.R., Findlay, D.L., Hall, R.I. & Smol, J.P. (1999) Algal responses to dissolved organic carbon loss and pH decline during whole lake acidification: Evidence from palaeolimnology. *Limnology and Oceanography*, 44, 757-773.
- Leira, M. & Santos, L. (2002) An early Holocene short climatic event in the northwest Iberian Peninsula inferred from pollen and diatoms. *Quaternary International*, 93-94, 3-12.
- Levesque, A.J., Mayle, F.E., Walker, I.R. & Cwynar, I.C. (1993) A previously unrecognised late glacial cold event in eastern North America. *Nature*, 361, 623-626.
- Lewin, J.C. (1962) Silicification. *Physiology and biochemistry of algae* (Eds. Lewin, R. A.), pp. 445-55. Academic, New York.
- Livingstone, D. & Lotter, A. (1998) The relationship between air and water temperatures in lakes of the Swiss Plateau: a case study with palaeolimnological implications. *Journal of Paleolimnology*, 19, 181-198.
- Livingstone, D.M. (1997) Break-up dates of alpine lakes as proxy data for local and regional mean surface air temperatures. *Climatic change*, 37, 407-439.
- Livingstone, D.M. (1999a) Ice break-up on southern Lake Baikal and its relationship to local and regional air temperatures in Siberia and to the North Atlantic Oscillation. *Limnology and Oceanography*, 44, 1486-1497.
- Livingstone, D.M., Lotter, A.F. & Walker, I.R. (1999) The decrease in summer surface water temperatures with altitude in Swiss Alpine lakes: a comparison with air temperature lapse rates. *Arctic, Antarctic and Alpine Research*, 31, 341-352.
- Livingstone, D.W. (1999) Ice break-up on southern Lake Baikal and its relationship to local and regional air temperatures in Siberia and to the North Atlantic Oscillation. *Limnology and Oceanography*, 44, 1486-1497.
- Livingstone, D.W. (1999) Large scale climatic forcing detected in historical observations of lake ice break-up. *Verhandlungen Internationaler Verein für Limnologie*, 27, 2775-2783.
- Lotter, A., Birks, J.H.B., Hofmann, W. & Marchetto, A. (1998) Modern diatoms, cladocera, chironomid, and chrysophyte cyst assemblages as quantitative indicators for the reconstruction of past environmental conditions in the Alps. I. Nutrients. *Journal of Paleolimnology*, 19, 443-463.
- Lotter, A., Hofmann, W., Kamenik, C., Lami, A., Ohlendorf, C., Strum, M., Van der Knapp, W. & Van Leeuwen, F.N. (2000) Sedimentological and biostratigraphical analyses of short sediment cores from Hagelseewli (2339 m a.s.l) in the Swiss Alps. *Journal of Limnology*, 59, 53-64.
- Lotter, A.F. & Bigler, C. (2000) Do diatoms in the Swiss Alps reflect the length of ice-cover? *Aquat. Science*, 62, 125-141.

- Lotter, A.F., Appleby, P.G., Bindler, R., Dearing, J.A. & Grytnes, J.A. (2002) The sediment record of the past 200 years in a Swiss high alpine lake: Hagelseewli (2339 m a.s.l). *Journal of Paleolimnology*, 28, 111-127.
- Lotter, A.F., Birks, J.H.B., Hofmann, W. & Marchetto, A. (1997) Modern diatoms, cladocera, chironomid, and chrysophyte cyst assemblages as quantitative indicators for the reconstruction of past environmental conditions in the Alps. I. Climate. *Journal of Paleolimnology*, 18, 395-420.
- Lotter, A., Hofmann, W., Kamenik, C., Lami, A., Ohlendorf, C., Strum, M., Van der Knapp, W. & Van Leeuwen, F.N. (2000) Sedimentological and biostratigraphical analyses of short sediment cores from Hagelseewli (2339 m a.s.l) in the Swiss Alps. *Journal of Limnology*, 59, 53-64.
- Lund, J.W.G. (1954) The seasonal cycle of the plankton diatom, *Melosira Italica* (EHR.) Kutz. Subsp. Subarctica O. Mull. *Journal of Ecology*, 42, 151-179.
- Luterbacher, J., Schmutz, C., Gyalistras, D., Jones, P.D., Davies, T.D., Wanner, H. & Xoplaki, E. (2000) Reconstruction of highly resolved NAO and EU indices back to AD 1500. *Geophysical Research Abstracts*, 2: 34.
- Luterbacher, J., Schmutz, C., Gyalistras, D., Xoplaki, E. & Wanner, H. (1999) Reconstruction of monthly NAO and EU indices back to AD 1675. *Geophysical Research Letters*, 26, 2745.
- Luterbacher, J., Xoplaki, E., Dietrich, D., Jones, P.D., Davies, T.D., Portis, D., Gonzalez-Rouco, J.F., von Storch, H., Gyalistras, D., Casty, C., and Wanner, H. (2002) Extending North Atlantic Oscillation reconstructions back to 1500. *Atmospheric Science Letters* 2 114-124
- MacDonald, G.M., Edwards, T.W.D., Moser, K.A., Pienitz, R. & Smol, J.P. (1993) Rapid response of treeline vegetation and lakes to past climate warming. *Nature*, 361, 243-246.
- Manley, G. (1974) Central England temperatures: monthly means 1659 to 1973. *Quarterly Journal of the Royal Meteorological Society*, 100, 389-405.
- Mann, M.E., Bradley, R.S. & Hughes, M.K. (1999) Northern Hemisphere Temperatures During the Past Millennium: Inferences, Uncertainties, and Limitations. *Geophysical Research Letters*, 26, 759.
- Margalef, R. Diversity and stability in ecological system (symposium report). 25-37. 1969. Upton N.Y., Brookhaven National Laboratory.
- Matthews, J.A. & Karlen, W. (1992) Asynchronous neoglaciation and Holocene climatic change reconstructed from Norwegian glaciolacustrine sedimentary sequences. *Geology*, 20, 991-994.
- Matthews, J.A. (1991) The late Neoglacial ('Little Ice Age') glacier maximum in southern Norway: new ¹⁴C dating evidence and climatic implication. *The Holocene*, 1, 219-233.

- Matthews, J.A., Dahl, S.-O., Nesje, A., Berrisford, M.S. & Anderson, C. (2000a) Holocene glacier variations in central Jotunheimen, southern Norway based on distal glaciolacustrine sediment cores. *Quaternary Science Reviews*, 19, 1625-1647.
- Miyajima, T., Nakanashi, M., Nakano, S. & Tezuka, Y. (1994) An autumnal bloom of the diatom *Meloseira granulata* in a shallow eutrophic lake; physical and chemical constraints on its population dynamics. *Arch. Hydrobiol.*, 130, 141-162.
- Moen, A. (1999) *National Atlas of Norway*. Norwegian Mapping Authority, Honefoss.
- MOLAR (2002), Work package 3: Climate variability and ecosystem dynamics at remote alpine and arctic lakes. MOLAR Work Package Outline.
- Molder, K. & Tynni, R. (1968) Über Finnlands rezente und subfossile Diatomeen II. *Bulletin Geological Society of Finland*, 40, 151-170.
- Moss, B. (1988) *Ecology of fresh waters, man and medium*. Blackwell Science Ltd, Oxford.
- Nesje, A. & Dahl, S.-O. (2001) The Greenland 8200 cal. yr BP event detected in loss-on-ignition profiles in Norwegian lacustrine sediment sequences. *Journal of Quaternary science*, 16, 155-166.
- Nesje, A. & Dahl, S.-O. (2003) The 'Little Ice Age' - only temperature? *The Holocene*, 13, 139-145.
- Nesje, A., Dahl, S.O. & Lovlie, R. (1995) Late Holocene glaciers and avalanche activity in the Alftobreen area, western Norway: evidence from a lacustrine sedimentary record. *Norsk Geologisk Tidsskrift*, 75, 120-126.
- Nesje, A., Dahl, S.-O., Lovlie, R. & Sulebak, J.R. (1994) Holocene glacier activity at the southernwestern part of Hardangerjokulen, central- southern Norway: evidence from lacustrine sediments. *The Holocene*, 4, 377-382.
- Nesje, A., Dahl, S.-O., Matthews, J.A. & Berrisford, M.S. (2001a) A ~4500 yr record of river floods obtained from a sediment core in Lake Atnsjoen, eastern Norway. *Journal of Paleolimnology*, 25, 329-342.
- Nesje, A., Johannessen, T. & Birks, H.J.B. (1995b) Briksdalsbreen, western Norway climatic effects on the terminal response of a temperate glacier between AD 1901 and 1994. *The Holocene*, 5, 343-347.
- Nesje, A., Kvamme, M., Rye, N. & Lovlie, R. (1991) Holocene glacial and climate history of the Josteldalsbreen region, Western Norway; evidence from lake sediments and terrestrial deposits. *Quaternary Science Reviews*,
- Nesje, A., Lie, Ø. & Dahl, S.-O. (2000) Is the North Atlantic Oscillation reflected in Scandinavian glacier mass balance records? *Journal of Quaternary science*, 15, 587-601.

- Nesje, A., Matthews, J.A., Dahl, S.O., Berrisford, M.S. & Anderson, C. (2001) Holocene glacier fluctuations of Flatebreen and winter- precipitation changes in the Jostedalsgreen region, western Norway, based on glaciolacustrine sediment records. *The Holocene*, 11, 267-280.
- Nicholls, N., Gruza, G.V., Jouzel, J., Karl, T.R., Ogallo, L.A. & Parker, D.E. (1996) Observed Climate Variability and Change. *Climate change* (Eds. Nicholls, N., Gruza, G. V., Jouzel, J., Karl, T. R., Ogallo, L. A., and Parker, D. E.), University Press, Cambridge.
- Nickus, U., Thies, H., Kuhn, M. & Psenner, R. (1998) The snow cover at a headwater site in the Tyrolean Alps: seasonal and local variability of atmospheric trace substances in the snow pack. *Head Water '98: Hydrology, Water Resources and Ecology of Mountain Areas*. (Eds. Tappeiner, U., Ruffini, F. V., and Fumai, M), pp. 39-42. IAHS Publication.
- Nordli, P. Ø. (2001) Reconstruction of nineteenth century summer temperatures in Norway by proxy data from farmers' diaries. *Climatic Change*, 48, 201-218.
- Nordli, P. Ø., Lie, Ø., Nesje, A. and Dahl, S.O. (2003 in press) Spring/ Summer Temperature Reconstruction in western Norway 1734-2003 a data-synthesis approach. *Climatic Change*
- Odland, A., Birks, H.J.B. & Line, J.M. (1995) Ecological optima and tolerances of *Thelypteris limbosperma*, *Athyrium distentifolium* and *Matteuccia struthiopteris* along environmental gradients in Western Norway. *Vegetatio*, 120, 115-129.
- OECD, (1982) Organisation for Economic Co-operation and Development. Eutrophication of waters: monitoring, assessment and control. Technical Report, Environmental Directorate, -154pp. Paris.
- Ognjanova-Rumenova, N.G. (1996) *Cyclotella iris* Brun & Heribaud- A group from the upper Miocene sediments of the Sofia Basin, Bulgaria. *Geologica Carpathica, Bulgaria*, 47, 301-310.
- Ohlendorf, C., Bigler, C., Goudsmit, G.H., Lemcke, G., Livingstone, D.M., Lotter, A.F. & Sturm, M. (2000) Causes and effects of long periods of ice-cover on a remote high Alpine Lake. *unpublished MOLAR report*.
- Oksanen, J. (2001) HOF: Ecological gradient analysis using Huisman-Olff_Fresco models.
- Oksanen, J and Minchin P. (2002) Continuum theory revisited; what shape are species response along ecological gradients *Ecological Modelling* 157, 119-129
- Oldfield, A. & Appleby, P. (1984) Empirical testing of ²¹⁰Pb-dating models for lake sediments. *Lake sediments and Environmental History* (Eds. Haworth, E. Y and Lund, J. W. G), pp. 93-124. Leicester University Press, UK, Leicester.

- Ormerod, S.J., Boole, P., McCahon, C.P., Weatherly, N.S., Pascoe, D. & Edwards, R.W. (1987) Short-term experimental acidification of a Welsh stream: comparing the biological effects of hydrogen ions and aluminium. *Freshwater Biology*, 17, 341-356.
- Ormerod, S.J., Wade, K.R. & Gee, A.S. (1987b) Macrofloral assemblages in upland Welsh stream in relation to acidity, and their importance to invertebrates. *Freshwater Biology*, 18, 545-557.
- Padisak, J., Krienitz, L., Scheffler, W., Koschel, R., Kristiansen, J. & Grigorszky, I. (1998) Phytoplankton succession in the oligotrophic Lake Stechline (Germany) in 1994 and 1995. *Hydrobiologia*, 369/370, 179-197.
- Parker, D.E., Jones, P.D., Bevan, A. & Folland, C.F. (1994) Interdecadal changes of surface temperatures since the 19th century. *Journal of Geophysical Research*, 99, 14373-14399.
- Parker, D.E., Legg, T.P. & Folland, C.K. (1992) A new daily Central England temperature series 1912-1991. *International Journal of Climatology*, 12, 317-342.
- Patrick, R. (1977) Ecology of freshwater diatoms and diatom communities. *The Biology of the Diatoms* (Ed. Werner, D), pp. 284-332. Blackwell, Oxford.
- Pears, N.V. (1968) Post-glacial tree lines of the Cairngorm Mountains, Scotland. *Transactions of the Botanical Society of Edinburgh*, 40, 394.
- Philibert, A. & Prairie, Y.T. (2002) Diatom-based transfer functions for western Quebec lakes (Abitibi and Haute Mauricie): the possible role of epilimnetic CO₂ concentration in influencing diatom assemblages. *Journal of Paleolimnology*, 27, 465-480.
- Pienitz, R. & Smol, J.P. (1993) Diatom assemblages and their relationship to environmental variables in lakes from the boreal forest-tundra ecotone near Yellowknife, Northwest Territories, Canada. *Hydrobiologia*, 269/270, 391-404.
- Pienitz, R., Smol, J.P. & Birks, H.J.B. (1995) Assessment of freshwater diatoms as quantitative indicators of past climatic change in the Yukon and Northwest Territories, Canada. *Journal of Paleolimnology*, 13, 21-49.
- Pla, S. (1999) *Chrysophycean cysts from the Pyrenees and their applicability as Palaeoenvironmental indicators*. PhD Thesis, University of Barcelona.
- Prairie, Y.T. (1996) Evaluating the predictive power of regression models. *Canadian Journal of Fish & Aquatic Sciences*, 53, 490-492.
- Psenner, R. & Schmidt, R. (1992) Climate-driven pH control of remote alpine lakes and effects of acid deposition. *Nature*, 356, 781-783.
- Rautio, M., Sorvari, S. & Korhola, A. (2000) Diatom and crustacean zooplankton communities, their seasonal variability and representation in the sediments of subarctic Lake Saanaajarvi. *Journal of Limnology*, 59, 81-96.

- Raven, J.A. & Geider, I.J. (1988) Temperature and algal growth. *New Phytol.*, 110, 441-461.
- Reid, P.C., Edwards, M., Hunt, H.G. & Warner, A.J. (1998) Phytoplankton change in the North Atlantic. *Nature*, 391, 546.
- Renberg, I. & Hultberg, H. (1992) A Paleolimnological Assessment of Acidification and Liming Effects on Diatom Assemblages in a Swedish Lake. *Canadian Journal of Fisheries and Aquatic Science*, 49, 65-73.
- Renberg, I. (1990) A procedure for preparing large sets of diatom slides from sediment cores. *Journal of Paleolimnology*, 4, 87-90.
- Renberg, I. (1991) The HON- Kajak sediment corer. *Journal of Paleolimnology*, 6, 167-170.
- Reynolds, C.S. (1984) *The ecology of freshwater phytoplankton*. Cambridge University Press, New York.
- Reynolds, C.S., Montecino, V., Graf, M.E. & Cabrera, S. (1986) Short- term dynamics of a *Melosira* population in the plankton of an impoundment in Central Chile. *Journal of plankton Research*, 8, 715-740.
- Richardson, P., Armstrong, R. & Goldman, C.R. (1970) Contemporaneous disequilibrium, a new hypothesis to explain the 'Paradox of the Plankton'. *Proc.Nat.Acad.Sci.*, 67, 1710-1714.
- Ritchie, J.C., McHenry, J.R. & Gill, A.C. (1973) Dating recent reservoir sediments. *Limnology and Oceanography*, 18, 254-263.
- Roberts, D. & McMinn, A. (1999) A diatom-based palaeosalinity history of Ace Lake, Vetsold Hils, Antarctica. *The Holocene*, 9, 401-408.
- Rodhe, W. (1948a) Environmental requirements of freshwater plankton algae. Experimental studies in the ecology of phytoplankton. *Symbol.Bot.Upsalien.*, 10, 149.
- Rosen, P., Dabakk, E., Renberg, I., Nilsson, M. & Hall, R. (2000a) Near-infrared spectrometry (NIRS): a new tool for inferring past climate changes from lake sediments. *The Holocene*, 10, 161-166.
- Rosen, P., Hall, R., Korsman, T. & Renberg, I. (2000) Diatom transfer functions for quantifying past air temperatures, pH and total organic carbon concentration from lakes in northern Sweden. *Journal of Paleolimnology*, 24, 109-123.
- Rosen, P., Segerstrom, U., Erikson, L., Renberg, I. & Birks, H.J.B. (2001a) Holocene climatic change reconstructed from diatoms, chironomids, pollen and near-infrared spectroscopy at an alpine lake (Sjuodjijaure) in northern Sweden. *The Holocene*, 11, 551-562.

- Round, F.E. & Brook, A.J. (1959) The phytoplankton of some Irish Loughs and an assessment of their trophic status. *Proceedings of the Royal Irish Academy*, 60, B, 167-191.
- Round, F.E., Crawford, M. & Mann, D.G. (1990) *Diatoms*. Cambridge University Press, Cambridge.
- Ruhland, K.M. & Smol, J.P. (2002) Freshwater diatoms from the Canadian Arctic treeline and development of paleolimnological inference models. *Journal of Phycology*, 38, 249-264.
- Ruttner, F. (1952) *Fundamentals of Limnology*. University of Toronto Press, Toronto.
- Ryves, D.B. (1994) *Diatom dissolution in saline lake sediments: an experimental study in the Great Plains of North America*. Unpublished Ph.D. thesis University College London.
- Sauberer, F. (1950) *Die spektrale Strahlungsdurchlässigkeit des Eises. 'Wetter und Leben' 2*
- Scheffler, W., Nicklisch, A. & Hepperle, D. (2000) Dimorphismus bei *Cyclotella pseudocomensis* (Bacillariophyceae Centrales). *Deutschsprachige Diatomogen Tagung, Bern*, Abstract 14.
- Schindler, E.A. (1990) Effects of climatic warming on lakes of the central boreal forest. *Science*, 250, 267-270.
- Schmidt, R., Koinig, K.A., Thompson, R. & Kamenik, C. (2002) A multi proxy core study of the last 7000 years of climate and alpine land-use impacts on an Austrian mountain lake (Uterer Landschitzsee, Niederee Tauern). *Palaeogeography, Palaeoclimatology, Palaeoecology*, 187, 101-120.
- Schmidt, R., Wunsam, S., Brosch, U., Fott, J., Lami, A., Löffler, H., Marchetto, A., Müller, H.W., Prazakova, M. & Schwaighofer, B. (1998) Late and post-glacial history of meromictic Langsee (Austria), in respect to climate change and anthropogenic impact. *Aquatic Sciences*, 60, 56-88.
- Seppä, H. & Birks, H.J.B. (2001) July mean temperature and annual precipitation trends during the Holocene in the Fennoscandian tree-line area: pollen- based climate reconstructions. *The Holocene*, 11, 527-539.
- Six, D., Reynaud, L. & Letreguilly, A. (2001) Alpine and Scandinavian glaciers mass balances, their relations with the North Atlantic Oscillation. *Earth and Planetary Sciences*, 333, 693-698.
- Skartveit, A. (1981) Relationships between precipitation chemistry, hydrology and runoff acidity. *Nordic Hydrology*, 12, 183-203.
- Sletten, K., Blikra, L.H., Ballantyne, C.K., Nesje, A. & Dahl, S.-O. (2002) Holocene debris flows recognised in a lacustrine sedimentary succession: sediment characteristics, chronostratigraphy and palaeoclimatic implications (In Sletten, K.

- 2002, *Holocene mass movement processes in Norway, and the development of a moraine complex on Svalbard* Geomorphology, sedimentology, chronostratigraphy and paleoclimate). Doctor Scientiarum thesis, Department of Geology, Bergen.
- Smith, I.R. (2002) Diatom-based Holocene paleoenvironmental records from continental sites on northeastern Ellesmere Island, high Arctic, *Canadian Journal of Paleolimnology*, 27, 9-28.
- Smol, J.P. & Douglas, M.S.V. (1996) Long-term environmental monitoring in arctic lakes and ponds using diatoms and other biological indicators. *Geoscience Canada*, 23, 225-230.
- Smol, J.P. (1983) Paleophycology of a high arctic lake near Cape Herschel, Ellesmere Island. *Canadian Journal Bot.*, 61, 2195-2204.
- Smol, J.P. (1988) Paleoclimate proxy data from freshwater arctic diatoms. *Verhandlungen Internationaler Verein für Limnologie.*, 23, 817-844.
- Smol, J.P., Walker, I.R. & Leavitt, R. (1991) Paleolimnology and hindcasting climate trends. *Verhandlungen Internationaler Verein für Limnologie*, 24, 1240-1246.
- Snowball, I. & Sandgren, P. (1996) Lake sediment studies of Holocene glacial activity in the Karsa valley, northern Sweden: contrasts in interpretation. *The Holocene*, 6, 367-372.
- Sommaruga-Wogarth, S., Koining, K., Schmidt, R., Sommaruga, R., Tessadri, R. & Psenner, R. (1997) Temperature effects on the acidity of remote alpine lakes. *Nature*, 387, 64-67.
- Sorvari, S. & Korhola, A. (1998) Recent diatom assemblage changes in subarctic Lake Saanajarvi, NW Finnish Lapland, and their palaeoenvironmental implications. *Journal of Paleolimnology*, 20, 205-215.
- Spaulding, S.A., Ward, J.V. & Baron, J. (1993) Winter phytoplankton dynamics in a subalpine lake, Colorado, USA. *Arch. Hydrobiol.*, 129, 179-198.
- Sporka, F., Stefkova, E., Bitusik, P., Thompson, R., Agusti- Panareda, A., Appleby, P.G., Grytnes, J.A., Kamenik, C., Krno, I., Lami, A., Rose, N. & Shilland, N.E. (2002) The paleolimnological analysis of sediments from high mountain lake Nizne Terianske pleso in the High Tatras (Slovakia). *Journal of Paleolimnology*, 28, 95-109.
- Stevenson, A.C., Juggins, S., Birks, H.J.B., Anderson, D.S., Anderson, N.J., Battarbee, R.W., Berge, F., Davis, R.B., Flower, R.J., Haworth, R.J., Jones, V.J., Kingston, J.C., Kreiser, A.M., Line, J.M., Munro, M.A.R. & Renberg, I. (1991) *The surface waters acidification project palaeolimnology programme: modern diatom/lake water chemistry data-set*. ENSIS Publishing Ltd., London.
- Stine, S. (1998) Medieval climate anomaly in the Americas. *Water, Environment and Society in Times of Climatic Change* (Issar, A. S and Brown, N), pp. 43-67. Kluwer, Dordrecht.

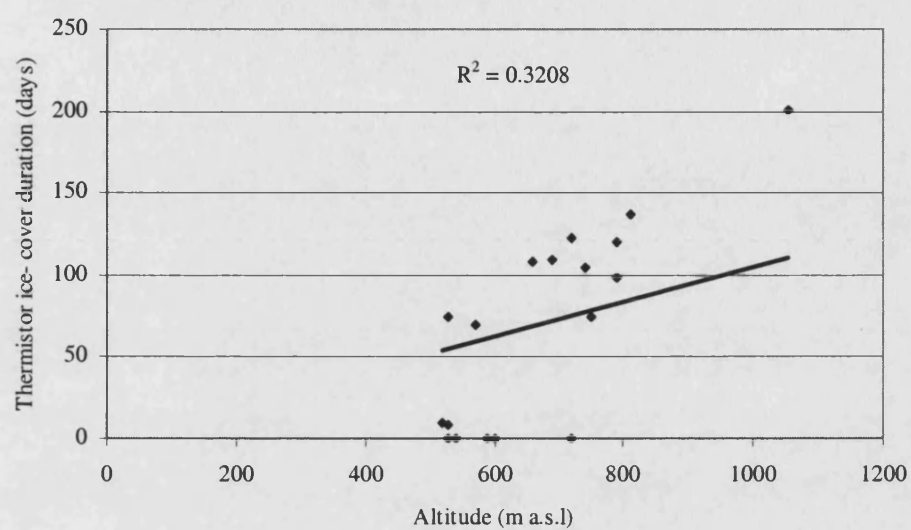
- Stoermer E.F. & Ladewski, T.B. (1976) *Apparent optimal temperatures for the occurrence of some common phytoplankton species in southern Lake Michigan*. Great Lakes Research Division Publ., 18 University of Michigan.
- Straile, D. & Adrian, R. (2000) The North Atlantic Oscillation and plankton dynamics in two European lakes- two variations on a general theme. *Global Change Biology*, 6, 663-670.
- Sze, P. (1994) *A biology of the algae (Second edition)*. W.M. C. Brown Publishers, Oxford.
- ter Braak, C. J. F. (1988) CANOCO- a FORTRAN program for canonical community ordination by [partial] [detrended] [canonical] correspondence analysis, principal components analysis and redundancy analysis (version 3.1) Agriculture Mathematics Group, Wageningen.
- ter Braak, C. J. F. (1990) Update notes. CANOCO version 3.1. Agriculture Mathematics Group, Wageningen.
- ter Braak, C.J.F. & Looman, C.W.N. (1986) Weighted averaging logistic regression and the Gaussian response model. *Vegetatio*, 65, 3-11.
- ter Braak, C.J.F. & Prentice, I.C. (1988) A theory of Gradient Analysis. *Advances in Ecological Research*, 18, 271-317.
- ter Braak, C.J.F. (1986) Canonical correspondence analysis: a new eigenvector technique for multivariate direct gradient analysis. *Ecology*, 67, 1167-1179.
- ter Braak, C.J.F. (1987) Calibration. *Data analysis in community and landscape ecology* (Eds. Jongman, R. H. G, ter Braak, C. J. F, and van Tongeren, O. R. F), pp. 78-90. Pudoc Wageningen.
- ter Braak, C.J.F., Juggins, S., Birks, H.J.B. & van der Voet, H. (1993) Weighted averaging partial least squares regression (WA-PLS): Definition and comparison with other methods for species- environment calibration. *Multivariate Environmental Statistics* (Patil, G. P and Rao, C. R), pp. 525-560. Elsevier.
- Teubner, K. (1995) A light microscopical investigation and multivariate statistical analyses of hetrovalvar cells of *Cyclotella* - species (Bacillariophyceae) from lakes of the Berlin- Brandenburg region. *Diatom Research*, 10, 191-205.
- Tilman, D. (1977) Resource competition between planktonic algae: an experimental and theoretical approach. *Ecology*, 58, 338-48.
- Timms, B.V. (1975) Morphometric control of variation in annual heat budgets. *Limnology and Oceanography*, 20, 110-112.
- Tvede, A.M. & Liestol, O. (1977) Blomsterskardbreen, Folgefonni, Mass balance ad recent fluctuations. *Norsk Polarinstitutt Arbok*, 1976, 225-233.
- Tvede, A.M. (1973) Folgefonni, en glasiologisk avviker. *Naturen*, 97, 11-15.

- van den Hoek, C., Mann, D.G. & Jahns, H.M. (1995) *Algae. An introduction to phycology*. Cambridge University Press, Cambridge.
- van den Wollenberg, A.L. (1977) Redundancy Analysis. An alternative for canonical correlation analysis. *Psychometrika*, 42, 207-219.
- van Loon, H. & Rogers, J.C. (1978) The Seesaw in winter temperature between Greenland and Northern Europe. Part I general description. *Monthly weather review*, 106, 296-310.
- Vavrus, S.J., Wynne, R.H. & Foley, J.A. (1996) Measuring the sensitivity of southern Wisconsin lake ice to climate variations and lake depth using a numerical model. *Limnology and Oceanography*, 41, 822-831.
- Vinebrooke, R.D. & Leavitt, P.R. (1996) Effects of ultraviolet radiation on periphyton in an alpine lake. *Limnology and Oceanography*, 41, 1035-1040.
- Walker, I.R., Levesque, A.J., Cwynar, L.C. & Lotter, A.F. (1997) An expanded surface -water paleotemperature inference model for use with fossil midges from eastern Canada. *Journal of paleolimnology*, 18, 165-178.
- Wathne, B. M, Patrick, S. T., Monteith, D., and Barth, H. (1993) (Eds). Ecosystems research report 9. AL:PE project part 1. EC report EUR161129 EN published by the EC. AL:PE, Acidification of mountain lakes: palaeolimnology and ecology AL:PE project part 1 April 1991-1993, European Union.
- Weckstrom, J., Korhola, A. & Blom, T. (1997) The relationship between diatoms and water temperature in thirty subarctic Fennoscandian lakes. *Arctic and Alpine Research*, 29, 75-92.
- Weckstrom, J., Korhola, A. & Bolm, T. (1997) Diatoms as quantitative indicators of pH and water temperature in subarctic Fennoscandian lakes. *Hydrobiologia*, 347, 171-184.
- Wetzel, R.G. & Likens, G.E. (1991) *Limnological Analysis*. Springer-Verlag, New York.
- Wetzel, R.G. (1983b) *Limnology*. W.B. Saunders Company, Philadelphia.
- Weyhenmeyer, G.A., Blenckner, T. & Pettersson, K. (1999) Changes in the plankton spring outburst related to the North Atlantic Oscillation. *Limnology and Oceanography*, 44, 1788-1792
- White, A.F. & Blum, A.E. (1995) Effects of climate on chemical weathering in watersheds. *Geochimica et Cosmochimica Acta*, 59, 1729-1747.
- Whitmore, T.J. (1989) Florida diatom assemblages as indicators of trophic state and pH. *Limnology and Oceanography*, 34, 882-895.
- Whittaker, J. (1984) Model Interpretation from the Additive Elements of the Likelihood Function. *Applied statistics*, 33, 52-64.

- Willemse, N.W. & Tornqvist, T.E. (1999) Holocene century scale temperature variability from West Greenland lake records. *Geology*, 30, 215-218.
- Willen, E. (1991) Planktonic diatoms- an ecological review. *Algological Studies (Archiv fur Hydrobiologie)*, 62, 69-106.
- Williams, L.D. & Wigley, T.M.L. (1983a) The initiation of the LIA in regions round the North Atlantic. *Climatic Change*, 48, 53-82.
- Williams, L.D. & Wigley, T.M.L. (1983b) A comparison of evidence for late Holocene Summer temperature variations in the Northern Hemisphere. *Quaternary Research*, 20, 286-307.
- Williamson, C.E., Stemberger, R.S., Morris, D.P., Frost, T.M. & Paulsen, S.G. (1996) Ultraviolet radiation in North American lakes: Attenuation estimates from DOC measurements and implications for plankton communities. *Limnology and Oceanography*, 41, 1024-1034.
- Winkler, S. (2003) A new interpretation of the date of the 'Little Ice Age' glacier maximum at Svartisen and Okstindan, northern Norway. *The Holocene*, 13, 83-95.
- Wolfe, A.P. (2002) Climate modulates the acidity of Arctic lakes on millennial time scales. *Geology*, 30, 215-218.
- Wright, R.F., Norton, S.A., Brakke, D.F. & Frogner, T. (1988) Experimental verification of episodic acidification of freshwaters by sea salts. *Nature*, 334, 422-424.
- Wunsam, S., Schmidt, R. & Klee, R. (1995) *Cyclotella*- taxa (Bacillariophyceae) in lakes of the Alpine region and their relationship to environmental variables. *Aquatic Sciences* 57, 4, 360-386.

Appendices

Appendix 3.1: Scatterplot of thermistor ice-cover duration (days) against altitude (m a.s.l) for 19 sites from the Scotland sub set of lakes with the R^2 value displayed.



Appendix 3.2: Summary of environmental data for the AL:PE training set used for the pH reconstruction in chapters 6 and 7. (Source Wathne *et al.*, 1993; Cameron *et al.*, 1999b). For more details of the training set see <http://craticula.ncl.ac.uk:8000/Eddi/jsp/index.jsp>.

Variable	Units	N	Min	Max	Mean
Alkalinity	µeq/l	104	-31.75	630	67.6
Aluminium (labile)	µeq/l	22	3.51	176	48.2
Aluminium (monomeric)	µg/l	24	3	147	42.5
Aluminium (total)	µg/l	43	10	256	61.9
Ammonium	µg/l	80	0	6120	1198
Calcium	µeq/l	118	6.17	519	88.8
Chloride	µeq/l	118	0	350	34.3
Conductivity	µs/cm	118	4.4	74.4	19.4
Iron	µg/l	20	5	471	75.2
Magnesium	µeq/l	118	4	222	24
Manganese	µg/l	15	1.5	17	7.2
Maximum depth of lake	m	118	1	73	15.5
Nitrate	µg/l	102	0.7	41000	8708
Nitrite	µg/l	28	40	190	95
pH	pH units	118	4.48	8.04	6.15
Potassium	µeq/l	118	0.89	48	6.09
Silica	mg/l	52	019	2.22	0.764
Sodium	µeq/l	118	4.57	309	39.8
Sulphate	µeq/l	118	13.8	198	50.3
Total nitrogen	µg/l	37	3.22	770	202
Total organic carbon	mg/l	50	0.2	4.87	1.32
Total phosphorus	µg/l	91	0.5	43	7.18
Water depth of diatom sample	m	118	1	73	15.5
Zinc	µg/l	21	0.36	14	6.75
Altitude	m a.s.l.	118	20	3050	1762

Appendix 3.3: Summary table of environmental data for the EDDI Swiss dataset used for the TP reconstruction in chapters 6 and 7. (Source Lotter *et al.* 1997; Lotter *et al.* 1998) For more information about the data set see <http://craticula.ncl.ac.uk:8000/Eddi/jsp/index.jsp>.

Variable	Units	N	Min	Max	Mean
Alkalinity	µeq/l	68	6.6	119	57.4
Calcium	µeq/l	68	178	6482	2747
Chlorophyll-a	µg/l	68	0.11	6.93	1.22
Conductivity	µS/cm	67	20.5	565	274
Magnesium	µeq/l	68	20.6	19.18	582
Maximum depth of lake	m	69	1.6	66	14.6
Nitrate	µg/l	68	30	5400	776
pH	pH units	68	7.65	8.9	8.21
Potassium	µeq/l	68	3.58	123	31.6
Sodium	µeq/l	68	10.4	874	131
Soluable reactive phosphorus	µg/l	68	1	61.5	6.44
Total nitrogen	µg/l	68	200	8360	1764
Total organic carbon	mg/l	68	0.45	10.5	3.31
Total phosphorus	µg/l	69	5.8	211	41.9
Water depth of diatom sample	m	69	1.6	66	14.6
Altitude	m a.s.l.	68	300	2350	N/a

Appendix 4.1: Table summarising the results of the water chemistry for the 40 lake data set.

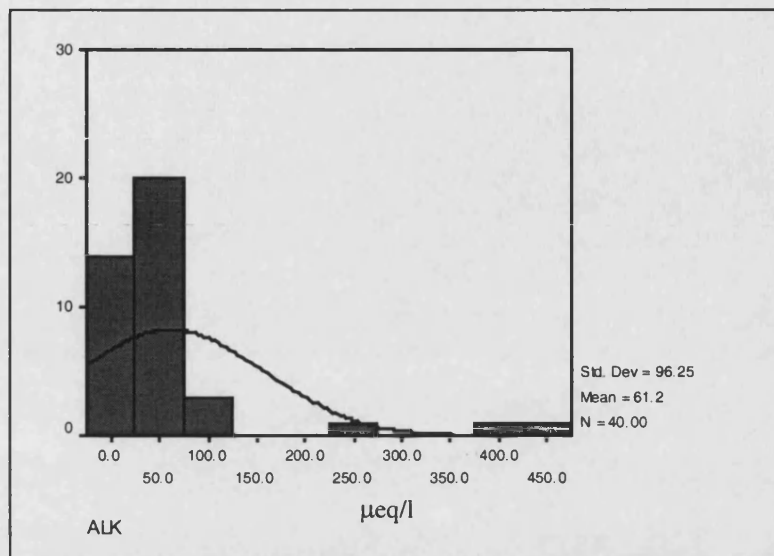
Code	Depth Max (m)	Precipitation (mm, annual)	pH	Alk $\mu\text{eq/l}$	Cond $\mu\text{S/cm}$	Na ⁺ $\mu\text{eq/l}$	K ⁺ $\mu\text{eq/l}$	Mg ²⁺ $\mu\text{eq/l}$	Ca ²⁺ $\mu\text{eq/l}$	Cl ⁻ $\mu\text{eq/l}$
CN0003	20.00	1150.00	5.94	6.00	4.95	16.96	3.07	5.84	14.97	14.11
CN0004	30.00	1334.00	6.64	52.00	11.08	22.17	6.40	12.34	71.86	22.57
CN0005	20.00	1492.00	6.79	55.00	11.80	16.52	1.02	17.27	82.34	14.11
CN0006	18.00	1431.00	6.47	31.00	15.68	23.04	2.30	6.83	114.77	19.75
CN0007	20.00	1159.00	6.25	20.00	5.86	14.35	5.12	7.81	27.45	8.46
CN0008	16.00	1039.00	6.43	27.00	8.02	22.61	3.33	9.05	44.91	11.28
CN0009	10.00	1034.00	6.75	56.00	14.05	21.31	2.05	13.16	101.30	14.11
CN0010	20.00	1088.00	6.14	10.00	4.14	8.26	4.35	6.33	16.47	5.64
CN0011	20.00	986.00	6.07	9.00	5.50	15.65	1.79	5.92	24.45	11.28
CN0012	30.00	880.00	6.45	27.00	6.76	16.52	3.84	9.05	33.43	14.11
CN0013	40.00	895.00	5.99	15.00	4.68	9.13	1.02	5.35	22.95	5.64
CN0014	20.00	775.00	6.29	23.00	4.68	8.70	2.05	6.41	25.45	2.82
CN0015	13.00	731.00	6.93	88.00	13.42	25.65	6.14	29.61	79.84	2.82
CN0016	18.00	1001.00	6.22	17.00	6.31	30.44	3.07	7.15	17.47	22.57
CN0017	12.00	1526.00	6.09	13.00	6.76	29.57	3.33	8.06	17.96	25.39
CN0018	15.00	583.00	6.79	55.00	11.08	20.00	6.40	23.03	67.37	5.64
CN0019	12.00	822.00	7.65	467.00	48.02	0.00	22.51	31.25	445.11	16.93
CN0020	9.00	840.00	6.48	47.00	11.17	0.00	6.40	23.03	51.40	19.46
CN0021	6.00	731.00	7.20	232.00	23.78	21.31	10.49	42.76	206.59	19.75
CN0022	10.00	971.00	7.65	413.00	48.38	0.00	27.11	119.25	347.30	42.32
SN0023	10.00	977.00	6.18	20.74	7.80	20.00	3.00	8.00	38.00	14.00
SC0002S	9.20	2590.00	6.08	26.00	30.00	153.00	5.00	61.00	36.00	162.00
SC0010S	4.30	2505.00	6.32	35.00	29.00	172.00	5.00	48.00	46.00	167.00
SC0029S	1.00	2161.00	6.13	28.00	19.00	120.00	3.00	33.00	33.00	109.00
SC0067S	5.10	2053.00	5.95	17.00	29.00	176.00	6.00	54.00	30.00	190.00
SC0068S	7.80	2000.00	6.47	52.00	37.00	213.00	6.00	54.00	78.00	225.00
SC0076S	24.00	2088.00	6.18	30.00	24.00	147.00	5.00	47.00	34.00	145.00
SC0108S	8.10	2107.00	5.92	18.00	17.00	99.00	5.00	28.00	30.00	102.00
SC0165S	46.00	1906.00	5.87	17.00	30.00	176.00	7.00	49.00	33.00	198.00
SC0172S	9.10	2699.00	6.58	57.00	22.00	101.00	4.00	30.00	75.00	115.00
SC0180S	14.00	1782.00	6.16	34.00	32.00	195.00	8.00	56.00	54.00	199.00
SC0191S	5.00	1792.00	6.20	34.00	28.00	152.00	4.00	45.00	67.00	168.00
SC0197S	11.50	1554.00	6.75	68.00	44.00	246.00	8.00	76.00	75.00	274.00
SC0204S	8.80	1513.00	6.45	43.00	19.00	110.00	4.00	29.00	51.00	94.00
SC0211S	3.50	1561.00	6.17	30.00	37.00	222.00	8.00	71.00	37.00	233.00
SC0330S	27.00	2095.00	6.66	55.00	19.00	92.00	7.00	31.00	63.00	89.00
SC0335S	6.00	1426.00	6.76	110.00	34.00	157.00	6.00	51.00	144.00	157.00
SC0349S	7.30	1087.00	5.97	22.00	41.00	250.00	9.00	58.00	50.00	268.00
SC0386S	10.00	1175.00	6.70	79.00	22.00	65.00	7.00	47.00	100.00	64.00
SC0399S	24.00	1213.00	5.42	9.00	18.00	77.00	4.00	32.00	32.00	73.00

Appendix 4.1: Continued

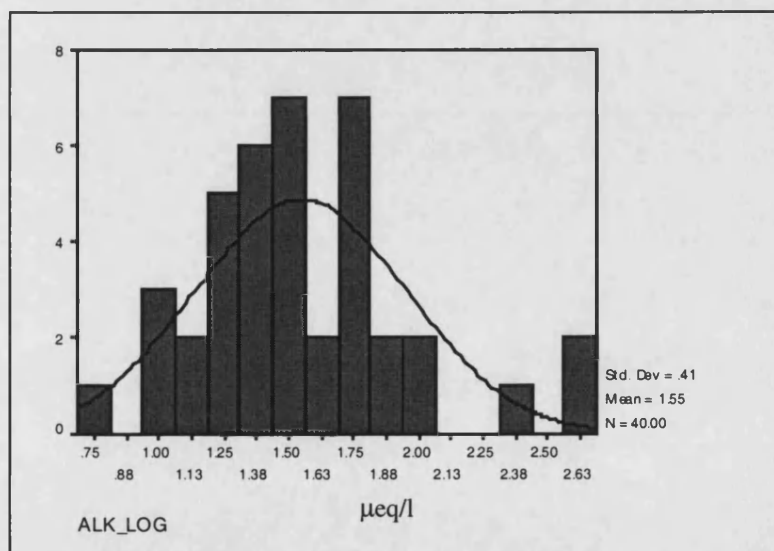
Code	NO ₃ ⁻ µeq/l	SO ₄ ²⁻ µeq/l	TN µg/l	TP µg/l	NH ₄ ⁺ µeq/l	Al-TM µg/l	Al-L µg/l	Al-NL µg/l	TOC mg/l	Ice days
CN0003	2.50	14.57	80.00	3.00	1.00	2.50	0.00	2.50	0.39	152.00
CN0004	1.50	20.82	117.00	2.00	1.00	11.00	0.00	11.00	2.00	159.00
CN0005	1.71	33.31	60.00	1.00	1.00	2.50	0.00	2.50	0.22	197.00
CN0006	2.78	83.28	72.00		1.00	2.50	0.00	2.50	0.28	211.00
CN0007	0.04	18.74	56.00	2.00	1.00	2.50	0.00	2.50	0.67	207.00
CN0008	0.29	22.90	83.00		1.00	6.00	1.00	5.00	0.84	206.00
CN0009	0.04	49.97	90.00	3.00	1.00	2.50	0.00	2.50	0.60	208.00
CN0010	0.50	14.57	74.00	2.00	1.00	2.50	0.00	2.50	0.34	228.00
CN0011	0.50	18.74	57.00		1.00	6.00	1.00	5.00	0.80	216.00
CN0012	0.71	14.57	75.00	2.00	1.00	2.50	0.00	2.50	0.32	208.00
CN0013	3.93	20.82	81.00	1.00	1.00	5.00	0.00	5.00	0.10	224.00
CN0014	2.28	16.66	71.00	1.00	1.00	2.50	0.00	2.50	0.22	225.00
CN0015	0.04	31.23	75.00	2.00	1.00	6.00	3.50	2.50	0.79	208.00
CN0016	0.29	10.41	62.00	1.00	1.00	12.00	2.00	10.00	0.71	165.00
CN0017	1.07	12.49	41.00	1.00	1.00	8.00	3.00	5.00	0.19	207.00
CN0018	0.86	27.07	62.00	0.00	1.00	5.00	0.00	5.00	1.20	215.00
CN0019	0.14	31.23	137.00	2.00	1.00	16.00	13.50	2.50	2.10	203.00
CN0020	0.29	24.15	155.00	4.00	1.00	29.00	0.00	31.00	4.60	196.00
CN0021	0.50	14.57	210.00	4.00	1.00	5.00	0.00	5.00	2.80	202.00
CN0022	0.29	56.21	105.00	3.00	1.00	16.00	13.50	2.50	1.60	199.00
SN0023	3.00	25.00	175.00	1.00	1.00	65.00	31.00	34.00	1.40	201.00
SC0002S	13.00	53.00	268.00	2.50	0.00	1.00	1.00	0.00	0.70	74.00
SC0010S	0.30	49.00	40.00	2.50	0.00	13.00	6.00	7.00	2.40	0.00
SC0029S	0.00	18.00	325.00	2.50	0.00	38.00	4.00	34.00	5.20	0.00
SC0067S	2.90	29.00	157.00	2.50	0.00	0.00	0.00	0.00	1.00	0.00
SC0068S	0.00	27.00	224.00	2.50	0.00	26.00	0.00	26.00	5.60	0.00
SC0076S	1.20	30.00	201.00	2.50	0.00	3.00	0.00	3.00	1.50	0.00
SC0108S	0.96	28.00	142.00	2.50	0.00	12.00	1.00	11.00	2.00	122.00
SC0165S	1.60	28.00	154.00	2.50	0.00	10.00	0.00	10.00	1.90	70.00
SC0172S	0.95	23.00	128.00	2.50	0.00	26.00	1.00	25.00	2.60	105.00
SC0180S	0.73	25.00	253.00	2.50	0.00	41.00	0.00	41.00	6.70	10.00
SC0191S	0.00	22.00	261.00	2.50	0.00	14.00	3.00	11.00	6.70	108.00
SC0197S	2.90	41.00	159.00	6.00	0.00	10.00	1.00	9.00	1.70	74.00
SC0204S	1.70	26.00	236.00	2.50	0.00	7.00	0.00	7.00	2.40	109.00
SC0211S	3.80	36.00	182.00	6.00	0.00	25.00	1.00	24.00	3.50	0.00
SC0330S	0.73	31.00	93.00	2.50	0.00	0.00	0.00	0.00	1.30	137.00
SC0335S	0.41	26.00	331.00	2.50	0.00	18.00	8.00	10.00	9.20	0.00
SC0349S	4.10	46.00	163.00	3.00	0.00	21.00	1.00	20.00	2.60	8.00
SC0386S	3.20	37.00	228.00	2.50	2.00	16.00	2.00	14.00	5.10	98.00
SC0399S	13.00	43.00	316.00	2.50	0.00	19.00	7.00	12.00	1.60	120.00

Appendix 4.2: Histograms with normal distribution curves plotted for a) Alkalinity and b) Alkalinity log transformed

a)



b)



Appendix 4.3: Species found within the 40 lake training set, species, codes and authorities are provided

AC001A	<i>Achnanthes lanceolata</i> (Breb. ex Kutz.) Grun. in Cleve & Grun. 1880
AC001T	<i>Achnanthes lanceolata robusta</i> (Hustedt) LB 1991
AC002A	<i>Achnanthes linearis</i> (W. Sm.) Grun. in Cleve & Grun. 1880
AC003A	<i>Achnanthes microcephala</i> (Kutz.) Cleve 1896
AC004A	<i>Achnanthes pseudoswazi</i> J.R. Carter 1963
AC005A	<i>Achnanthes calcar</i> Cleve 1891
AC007A	<i>Achnanthes oestrupii</i> (A. Cleve-Euler) Hust. 1930
AC013A	<i>Achnanthes minutissima minutissima</i> Kutz. 1833
AC018A	<i>Achnanthes laterostrata</i> Hust. 1933
AC019A	<i>Achnanthes nodosa</i> A. Cleve-Euler 1900
AC022A	<i>Achnanthes marginulata</i> Grun. in Cleve & Grun. 1880
AC024A	<i>Achnanthes depressa</i> (Cleve) Hust. 1933
AC025A	<i>Achnanthes flexella</i> (Kutz.) Brun 1880
AC027A	<i>Achnanthes holstii</i> Cleve 1881
AC029A	<i>Achnanthes sublaevis</i> Hust. 1936
AC034A	<i>Achnanthes suchlandtii</i> Hust. 1933
AC035A	<i>Achnanthes pusilla pusilla</i> Grun. in Cleve & Grun. 1880
AC039A	<i>Achnanthes didyma didyma</i> Hust. 1933
AC044A	<i>Achnanthes levanderi</i> Hust. 1933
AC046A	<i>Achnanthes altaica</i> (Poretzky) A. Cleve-Euler 1953
AC048A	<i>Achnanthes scotica</i> Jones & Flower
AC060A	<i>Achnanthes curtissima</i> J.R. Carter 1963
AC082A	<i>Achnanthes kriegeri</i> Krasske 1943
AC083A	<i>Achnanthes laevis</i> Ostr. 1910
AC105A	<i>Achnanthes petersenii</i> Hust. 1937
AC119A	<i>Achnanthes saccula</i> J.R. Carter in J.R. Carter & Watts 1981
AC134A	<i>Achnanthes helvetica</i> (Hustedt) Lange-Bertalot in LB & K 1989
AC134B	<i>Achnanthes helvetica alpina</i> Flower and Jones 1989
AC134C	<i>Achnanthes helvetica minor</i> Flower & Jones 1989
AC136A	<i>Achnanthes subatomoides</i> (Hust.) Lange-Bertalot & Archibald in K & LB 1985
AC142A	<i>Achnanthes kuelbsii</i> Lange-Bertalot 1989
AC143A	<i>Achnanthes oblongella</i> Ostr. 1902
AC146A	<i>Achnanthes lacus-vulcani</i> Lange-Bertalot & Krammer 1989
AC152A	<i>Achnanthes carissima</i> Lange-Bertalot 1990
AC153A	<i>Achnanthes impexa</i> Lange-Bertalot 1989
AC154A	<i>Achnanthes imperfecta</i> Schimanski 1978
AC161A	<i>Achnanthes ventralis</i> (Krasske) Lange-Bertalot 1989
AC173A	<i>Achnanthes stolidia</i> (Krasske) Krasske 1949
AC179A	<i>Achnanthes alteragracillima</i> Lange-Bertalot
AC182A	<i>Achnanthes rosenstockii</i> Lange-Bertalot 1989
AC9968	<i>Achnanthes</i> [marginulata] major Uaine (VJJ) 1988
AC9975	<i>Achnanthes</i> [altaica var. minor] L. Grannoch (RJF) 1988
AC9986	Unknown [<i>Achnanthes/Navicula</i> sp. 1] Low Tarn (EYH-SWAP) 1987
AC9999	<i>Achnanthes</i> sp.
AH001A	<i>Amphicampa hemicyclus</i> (Ehrenb.) Karsten 1928
AM001A	<i>Amphora ovalis ovalis</i> (Kutz.) Kutz. 1844
AM010A	<i>Amphora fogediana</i> Krammer 1985
AM011A	<i>Amphora libyca</i> Ehr.
AM012A	<i>Amphora pediculus</i> (Kutz.) Grun.
AM013A	<i>Amphora inariensis</i> Krammer
AM9999	<i>Amphora</i> sp.
AS001A	<i>Asterionella formosa formosa</i> Hassall 1850

Appendix 4.3 cont.

AU001C	<i>Aulacoseira italica</i> <i>valida</i> (Grun. in Van Heurck) Simonsen 1979
AU002A	<i>Aulacoseira ambigua</i> (Grun. in Van Heurck) Simonsen 1979
AU004A	<i>Aulacoseira lirata</i> <i>lirata</i> (Ehrenb.) R. Ross in Hartley 1986
AU005A	<i>Aulacoseira distans</i> <i>distans</i> (Ehrenb.) Simonsen 1979
AU005B	<i>Aulacoseira distans</i> <i>nivaloides</i> Camburn 1987
AU005D	<i>Aulacoseira distans</i> <i>tenella</i> (Nygaard) R. Ross in Hartley 1986
AU005E	<i>Aulacoseira distans</i> <i>nivalis</i>
AU005L	<i>Aulacoseira distans</i> <i>humilis</i> (A. Cleve-Euler) R. Ross in Hartley 1986
AU010A	<i>Aulacoseira perglabra</i>
AU010B	<i>Aulacoseira perglabra</i> <i>floriniae</i>
AU020A	<i>Aulacoseira subarctica</i> (O.Mull.) Haworth
AU022A	<i>Aulacoseira subborealis</i> SWAP 1989
AU023A	<i>Aulacoseira tethera</i> Haworth nov. sp. 1989
AU031A	<i>Aulacoseira alpigena</i> (Grunow) Krammer 1990
AU032A	<i>Aulacoseira lacustris</i> Krammer 1990
AU033A	<i>Aulacoseira pfaffiana</i> (Reinsch) Krammer 1990
AU9986	<i>Aulacoseira</i> [subarctica, Haworth 1989, type 2, fig 48] SWAP Sweden (IR & NJA) 1989
AU9999	<i>Aulacoseira</i> sp.
BR001A	<i>Brachysira vitrea</i> (Grun.) R. Ross in Hartley 1986
BR003A	<i>Brachysira serians</i> (Breb. ex Kutz.) Round & Mann 1981
BR004A	<i>Brachysira styriaca</i> (Grun. in Van Heurck) R. Ross in Hartley 1986
BR006A	<i>Brachysira brebissonii</i> <i>brebissonii</i> R. Ross in Hartley 1986
BR010A	<i>Brachysira neoexilis</i> Lange-Bertalot 1994
BR011A	<i>Brachysira procera</i> L-B & Moser 1994
BR9999	<i>Brachysira</i> sp.
CA002A	<i>Caloneis bacillum</i> <i>bacillum</i> (Grun.) Cleve 1894
CA003A	<i>Caloneis silicula</i> (Ehrenb.) Cleve 1894
CA048A	<i>Caloneis molaris</i> (Grunow) Krammer 1985
CA9999	<i>Caloneis</i> sp.
CM004A	<i>Cymbella microcephala</i> <i>microcephala</i> Grun. in Van Heurck 1880
CM006A	<i>Cymbella cistula</i> <i>cistula</i> (Ehrenb. in Hempr. & Ehrenb.) Kirchner 1878
CM009A	<i>Cymbella naviculiformis</i> Auersw. ex Heib. 1863
CM010A	<i>Cymbella perpusilla</i> A. Cleve 1895
CM013A	<i>Cymbella helvetica</i> <i>helvetica</i> Kutz. 1844
CM014A	<i>Cymbella aequalis</i> W. Sm. ex Grev. 1855
CM015A	<i>Cymbella cesatii</i> <i>cesatii</i> (Rabenh.) Grun. in A. Schmidt 1881
CM016A	<i>Cymbella amphicephala</i> <i>amphicephala</i> Naegeli ex Kutz. 1849
CM017A	<i>Cymbella hebridica</i> (Grun. ex Cleve) Cleve 1894
CM018A	<i>Cymbella gracilis</i> (Rabenh.) Cleve 1894
CM020A	<i>Cymbella gaeumannii</i> Meister 1934
CM022A	<i>Cymbella affinis</i> Kutz. 1844
CM031A	<i>Cymbella minuta</i> <i>minuta</i> Hilse ex Rabenh. 1862
CM047A	<i>Cymbella incerta</i> Grun. in Cleve & Moller 1878
CM049A	<i>Cymbella failaisensis</i> (Grun.) Krammer & Lange-Bertalot 1985
CM050A	<i>Cymbella subaequalis</i> Grun. in Van Heurck 1880
CM052A	<i>Cymbella descripta</i> (Hust.) Krammer & Lange-Bertalot 1985
CM085A	<i>Cymbella lapponica</i> Grun. ex Cleve 1894
CM101A	<i>Cymbella scotica</i> <i>naviculacea</i> (Grun. ex Cleve) R. Ross 1947
CM103A	<i>Cymbella silesiaca</i> Bleisch ex Rabenh. 1864
CM113A	<i>Cymbella reichardtii</i> Krammer 1985
CM9999	<i>Cymbella</i> sp.
CO001B	<i>Cocconeis placentula</i> <i>euglypta</i> (Ehrenb.) Grun. 1884

Appendix 4.3 cont.

CO067A	<i>Cocconeis neothumensis</i> Krammer 1991
CO9999	<i>Cocconeis</i> sp.
CY002A	<i>Cyclotella pseudostelligera</i> Hust. 1939
CY006A	<i>Cyclotella kuetzingiana kuetzingiana</i> Thwaites 1848
CY006B	<i>Cyclotella kuetzingiana planetophora</i> Fricke in A. Schmidt 1900
CY006C	<i>Cyclotella kuetzingiana radiosa</i> Fricke in A. Schmidt 1900
CY009A	<i>Cyclotella ocellata</i> Pant. 1902
CY010A	<i>Cyclotella comensis</i> Grun. in Van Heurck 1882
CY019A	<i>Cyclotella radiosa</i> (Grunow) Lemmerman 1900
CY020A	<i>Cyclotella iris</i> Brun
CY022B	<i>Cyclotella bodanica lemanica</i> (O.Muller ex Schroter) Bachmann 1903
CY028A	<i>Cyclotella distinguenda</i> Hust. 1927
CY028B	<i>Cyclotella distinguenda unipunctata</i> (Hustedt) Hakansson & Carter 1990
CY048A	<i>Cyclotella woltereckii</i> Hust. 1942
CY054A	<i>Cyclotella krammeri</i> Hakansson 1990
CY059A	<i>Cyclotella cyclopuncta</i> Hakansson & Carter 1990
CY061A	<i>Cyclotella gordonensis</i> Kling & Hakansson 1988
CY9984	<i>Cyclotella</i> [cf. <i>krammeri</i>] RIBA (P. Rioual) 1997
CY9987	<i>Cyclotella</i> [cf. <i>comensis</i>] Massif Central (PR) 1997
CY9999	<i>Cyclotella</i> sp.
DE001A	<i>Denticula tenuis tenuis</i> Kutz. 1844
DE002A	<i>Denticula elegans elegans</i> Kutz. 1844
DE003A	<i>Denticula kuetzingii</i> Grun.
DP001A	<i>Diploneis ovalis</i> (Hilse) Cleve 1894
DP065A	<i>Diploneis parma</i> Cleve 1891
DP9999	<i>Diploneis</i> sp.
DT021A	<i>Diatoma mesodon</i> (Ehrenber) Kutz. 1844
EU002A	<i>Eunotia pectinalis pectinalis</i> (O.F. Mull.) Rabenh. 1864
EU002D	<i>Eunotia pectinalis undulata</i> (Ralfs) Rabenh. 1864
EU002E	<i>Eunotia pectinalis minor impressa</i> (Ehr.) Hust.
EU003A	<i>Eunotia praerupta praerupta</i> Ehrenb. 1843
EU003B	<i>Eunotia praerupta bidens</i> (Ehrenb.) Grun. in Cleve & Grun. 1880
EU004A	<i>Eunotia tenella</i> (Grun. in Van Heurck) A. Cleve 1895
EU007A	<i>Eunotia bidentula</i> W. Sm. 1856
EU008A	<i>Eunotia monodon monodon</i> Ehrenb. 1843
EU009A	<i>Eunotia exigua exigua</i> (Breb. ex Kutz.) Rabenh. 1864
EU010A	<i>Eunotia faba</i> (Ehrenb.) Grun. in Van Heurck 1881
EU011A	<i>Eunotia rhomboidea</i> Hust. 1950
EU013A	<i>Eunotia arcus arcus</i> Ehrenb. 1837
EU014A	<i>Eunotia bactriana</i> Ehrenb. 1854
EU015A	<i>Eunotia denticulata denticulata</i> (Breb. ex Kutz.) Rabenh. 1864
EU016A	<i>Eunotia diodon</i> Ehrenb. 1837
EU017A	<i>Eunotia flexuosa flexuosa</i> Kutz. 1849
EU019A	<i>Eunotia iatriaensis</i> Foged 1970
EU020A	<i>Eunotia meisteri meisteri</i> Hust. 1930
EU020B	<i>Eunotia meisteri bidens</i> Hust. 1930
EU024A	<i>Eunotia glacialis</i> Meister 1912
EU025A	<i>Eunotia fallax</i> A. Cleve 1895
EU028A	<i>Eunotia microcephala</i> Krasske ex Hust. 1932
EU031A	<i>Eunotia septentrionalis septentrionalis</i> Ostr. 1898
EU032A	<i>Eunotia serra serra</i> Ehrenb. 1837
EU032B	<i>Eunotia serra diadema</i> (Ehrenb.) Patr. 1958

Appendix 4.3 cont.

EU032C	<i>Eunotia serra tetraodon</i> (Ehren) Norpel 1991
EU034A	<i>Eunotia parallela parallela</i> Ehrenb. 1843
EU039A	<i>Eunotia triodon</i> Ehrenb. 1837
EU040A	<i>Eunotia paludosa</i> Grun. 1862
EU040B	<i>Eunotia paludosa trinacria</i> (Krasske) Norpel 1991
EU043A	<i>Eunotia elegans</i> Ostr. 1910
EU047A	<i>Eunotia incisa</i> W. Sm. ex Greg. 1854
EU048A	<i>Eunotia naegeli</i> Migula 1907
EU049A	<i>Eunotia curvata curvata</i> (Kutz.) Lagerst. 1884
EU049B	<i>Eunotia curvata subarcuata</i> (Naegeli ex Kutz.) Woodhead & Tweed 1954
EU051A	<i>Eunotia vanheurckii vanheurckii</i> Patr. 1958
EU054A	<i>Eunotia hexaglyphis</i> Ehrenb. 1854
EU060A	<i>Eunotia pirla</i> Carter et Flower 1988
EU070A	<i>Eunotia bilunaris</i> (Ehrenb.) F.W. Mills 1934
EU070B	<i>Eunotia bilunaris mucophila</i> LB & Norpel 1991
EU105A	<i>Eunotia subarcuoides</i> Alles, Norpel, Lange-Bertalot 1991
EU106A	<i>Eunotia rhynchocephala</i> Hustedt 1936
EU107A	<i>Eunotia implicata</i> Norpel, Lange-Bertalot & Alles 1991
EU108A	<i>Eunotia intermedia</i> (Hust) Norpel, Lange-Bertalot & Alles 1991
EU110A	<i>Eunotia minor</i> (Kutz) Grunow in Van Heurck 1881
EU111A	<i>Eunotia soleirolii</i> (Kutz) Rabenhorst 1864
EU112A	<i>Eunotia arculus</i> (Grunow) LB & Norpel
EU9999	<i>Eunotia</i> sp.
FR001A	<i>Fragilaria pinnata pinnata</i> Ehrenb. 1843
FR001B	<i>Fragilaria pinnata lancettula</i> (Schum.) Hust. in A. Schmidt 1913
FR001B	<i>Fragilaria pinnata lancettula</i> (Schum.) Hust. in A. Schmidt 1913
FR001K	<i>Fragilaria pinnata acuminata</i> (A. Mayer) Regenbogen
FR002A	<i>Fragilaria construens construens</i> (Ehrenb.) Grun. 1862
FR002B	<i>Fragilaria construens binodis</i> (Ehrenb.) Grun. 1862
FR002C	<i>Fragilaria construens venter</i> (Ehrenb.) Grun. in Van Heurck 1881
FR002F	<i>Fragilaria construens pumila</i> Grun. in Van Heurck 1881
FR004B	<i>Fragilaria hungarica tumida</i> A. Cleve
FR005A	<i>Fragilaria virescens virescens</i> Ralfs 1843
FR005B	<i>Fragilaria virescens subsalina</i> Grun. in Van Heurck 1881
FR006A	<i>Fragilaria brevistriata brevistriata</i> Grun. in Van Heurck 1885
FR006E	<i>Fragilaria brevistriata capitata</i> (Herib.) Bass
FR007A	<i>Fragilaria vaucheriae vaucheriae</i> (Kutz.) J.B. Petersen 1938
FR009H	<i>Fragilaria capucina gracilis</i> (Oestrup) Hustedt 1950
FR009J	<i>Fragilaria capucina perminuta</i> (Grun.) L-B. 1991
FR010A	<i>Fragilaria constricta constricta</i> Ehrenb. 1843
FR010B	<i>Fragilaria constricta stricta</i> (A. Cleve) Hust. 1931
FR011A	<i>Fragilaria lapponica</i> Grun. in Van Heurck 1881
FR018A	<i>Fragilaria elliptica</i> Schum. 1867
FR056A	<i>Fragilaria pseudoconstruens</i> Marciniak 1982
FR062A	<i>Fragilaria microstriata</i> Marciniak in Metzeltin & Witkowski 1996
FR063A	<i>Fragilaria robusta</i> (Fusey) Manguin
FR064A	<i>Fragilaria exigua</i> Grun in Cleve & Moller 1878
FR9999	<i>Fragilaria</i> sp.
FU002A	<i>Frustulia rhomboides rhomboides</i> (Ehrenb.) De Toni 1891
FU002B	<i>Frustulia rhomboides saxonica</i> (Rabenh.) De Toni 1891
GO003A	<i>Gomphonema angustatum angustatum</i> (Kutz.) Rabenh. 1864
GO004A	<i>Gomphonema gracile</i> Ehrenb. 1838

Appendix 4.3 cont.

GO006A	Gomphonema acuminatum acuminatum Ehrenb. 1832
GO013A	Gomphonema parvulum parvulum (Kutz.) Kutz. 1849
GO050A	Gomphonema minutum (Ag.) Ag. 1831
GO072A	Gomphonema pseudotenellum Lange Bertalot 1985
GO079A	Gomphonema procerum Reichardt & L-B
GO9999	Gomphonema sp.
KR001A	Krasskella kriegnerana (Krasske) R. Ross & Sims 1978
MR001A	Meridion circulare circulare (Grev.) Ag. 1831
NA002A	Navicula jaernefeltii Hust. 1942
NA003A	Navicula radiosa radiosa Kutz. 1844
NA003B	Navicula radiosa tenella (Breb. ex Kutz.) Grun. ex Van Heurck 1885
NA003C	Navicula radiosa parva Wallace
NA005A	Navicula seminulum Grun. 1860
NA006A	Navicula mediocris Krasske 1932
NA007A	Navicula cryptocephala cryptocephala Kutz. 1844
NA013A	Navicula pseudoscutiformis Hust. 1930
NA014A	Navicula pupula pupula Kutz. 1844
NA016A	Navicula indifferens Hust. 1942
NA032A	Navicula cocconeiformis cocconeiformis Greg. ex Greville 1855
NA033A	Navicula subtilissima Cleve 1891
NA037A	Navicula angusta Grun. 1860
NA038A	Navicula arvensis Hust.
NA042A	Navicula minima minima Grun. in Van Heurck 1880
NA044A	Navicula krasskei Hust. 1930
NA045A	Navicula bryophila bryophila J.B. Petersen 1928
NA046A	Navicula contenta contenta Grun. in Van Heurck 1885
NA048A	Navicula soehrensensis soehrensensis Krasske 1923
NA048D	Navicula soehrensensis hassiaca (Krasske)Lange-Bertalot 1985
NA073A	Navicula placenta Ehrenb. 1854
NA090A	Navicula rotunda Hust. 1945
NA102A	Navicula laevisissima Kutz. 1844
NA112A	Navicula minuscula minuscula Grun. in Van Heurck 1880
NA114A	Navicula subrotundata Hust. 1945
NA133A	Navicula schassmannii Hust. 1937
NA134A	Navicula subminuscula Manguin
NA135A	Navicula tenuicephala Hust. 1942
NA149A	Navicula digitulus Hust. 1943
NA156A	Navicula leptostriata Jorgensen 1948
NA322A	Navicula detenta Hust. 1943
NA389B	Navicula gallica perpusilla (Grun) Lange-Bertalot 1985
NA669A	Navicula suchlandtii Hust. 1943
NA738A	Navicula vitiosa Schimanski 1978
NA751A	Navicula cryptotenella Lange-Bertalot 1985
NA779A	Navicula pseudoarvensis Hustedt 1942
NA9958	Navicula [PIRLA sp. 24] PIRLA 1985
NA9999	Navicula sp.
ND001A	Naviculadicta elorantana LB nov spec 1996
ND9997	Naviculadicta [sp.#2 Weinfelder Maar] LB & Metzeltin 1996
ND9998	Naviculadicta [sp.#1 Weinfelder Maar] LB & Metzeltin 1996
NE003A	Neidium affine affine (Ehrenb.) Pfitz. 1871
NE003B	Neidium affine longiceps (Greg.) Cleve 1896
NE003C	Neidium affine amphirhynchus (Ehrenb.) Cleve 1894

Appendix 4.3 cont.

NE004A	<i>Neidium bisulcatum bisulcatum</i> (Lagerst.) Cleve 1894
NE006A	<i>Neidium alpinum</i> Hust. 1943
NE036A	<i>Neidium ampliatus</i> (Ehren) Krammer 1985
NE9999	<i>Neidium</i> sp.
NI002A	<i>Nitzschia fonticola</i> Grun. in Van Heurck 1881
NI005A	<i>Nitzschia perminuta</i> (Grun. in Van Heurck) M. Perag. 1903
NI008A	<i>Nitzschia frustulum</i> (Kutz.) Grun. in Cleve & Grun. 1880
NI009A	<i>Nitzschia palea palea</i> (Kutz.) W. Sm. 1856
NI017A	<i>Nitzschia gracilis</i> Hantzsch 1860
NI025A	<i>Nitzschia recta</i> Hantzsch ex Rabenh. 1861
NI030A	<i>Nitzschia acidoclinata</i> Lange Bertalot
NI033A	<i>Nitzschia paleacea</i> (Grun. in Cleve & Grun.) Grun. in Van Heurck 1881
NI043A	<i>Nitzschia inconspicua</i> Grun. 1862
NI048A	<i>Nitzschia tubicola</i> Grun. in Cleve & Grun. 1880
NI9999	<i>Nitzschia</i> sp.
PE002A	<i>Peronia fibula</i> (Breb. ex Kutz.) R. Ross 1956
PI001A	<i>Pinnularia gibba</i> (Ehrenb.) Ehrenb. 1843
PI001B	<i>Pinnularia gibba linearis</i> Hust. 1930
PI004A	<i>Pinnularia interrupta</i> W. Smith
PI005A	<i>Pinnularia major major</i> (Kutz.) W. Sm. 1853
PI007A	<i>Pinnularia viridis viridis</i> (Nitzsch) Ehrenb. 1843
PI011A	<i>Pinnularia microstauron microstauron</i> (Ehrenb.) Cleve 1891
PI014A	<i>Pinnularia appendiculata</i> (Ag.) Cleve 1896
PI016A	<i>Pinnularia divergentissima divergentissima</i> (Grun. in Van Heurck) Cleve 1896
PI018A	<i>Pinnularia biceps biceps</i> Greg. 1856
PI022A	<i>Pinnularia subcapitata subcapitata</i> Greg. 1856
PI052A	<i>Pinnularia silvatica</i> J.B. Petersen 1935
PI056A	<i>Pinnularia rupestris</i> Hantzsch in Rabenh. 1861
PI9990	<i>Pinnularia</i> [cf. <i>pseudomicrostauron</i>] L. Hir (SF) 1986
PI9999	<i>Pinnularia</i> sp.
RH9999	<i>Rhopalodia</i> sp.
SA001A	<i>Stauroneis anceps anceps</i> Ehrenb. 1843
SA005A	<i>Stauroneis legumen</i> (Ehrenb.) Kutz. 1844
SA012A	<i>Stauroneis kriegeri</i> Patr. 1945
SA9999	<i>Stauroneis</i> sp.
SP005A	<i>Stenopterobia delicatissima</i> (Lewis) M. Perag. 1897
SP006A	<i>Stenopterobia curvula</i> (W Smith) Krammer 1987
SP9999	<i>Stenopterobia</i> sp.
ST014A	<i>Stephanodiscus medius</i> Hakansson 1986
SU001A	<i>Surirella angusta</i> Kutz. 1844
SU005A	<i>Surirella linearis linearis</i> W. Sm. 1853
SU005B	<i>Surirella linearis constricta</i> Grun. 1862
SU074A	<i>Surirella bifrons</i> Ehrenb. 1843
SU076A	<i>Surirella roba</i> Leclercq 1983
SU9999	<i>Surirella</i> sp.
SY002A	<i>Synedra rumpens rumpens</i> Kutz. 1844
SY003A	<i>Synedra acus acus</i> Kutz. 1844
SY004A	<i>Synedra parasitica parasitica</i> (W. Sm.) Hust. 1930
SY009A	<i>Synedra nana</i> Meister 1912
SY017A	<i>Synedra radians</i> Kutz. 1844
TA001A	<i>Tabellaria flocculosa flocculosa</i> (Roth) Kutz. 1844
TA003A	<i>Tabellaria binalis</i> (Ehrenb.) Grun. in Van Heurck 1881

Appendix 4.3 cont.

TA003B	<i>Tabellaria binalis elliptica</i> Flower (unpub) 1986
TA004A	<i>Tabellaria quadrisepata</i> Knudson 1952
TA006A	<i>Tabellaria ventricosa</i>
TA9997	<i>Tabellaria</i> [flocculosa (short)]
TA9998	<i>Tabellaria</i> [flocculosa (long)]
TA9999	<i>Tabellaria</i> sp.
TE001A	<i>Tetracyclus lacustris</i> Ralfs 1843
TH9999	<i>Thalassiosira</i> sp.
ZZZ974	Temporary sp. 26 <i>Cymbella</i> cf <i>microcephala</i>
ZZZ975	Temporary sp. 25 <i>Achnanthes minutissima</i> var. <i>macrocephala</i>
ZZZ977	Temporary sp. 23 <i>Eunotia seminulum</i>
ZZZ978	Temporary sp. 22 <i>Navicula</i> cf. <i>minuta</i>
ZZZ980	Temporary sp. 20 <i>Eunotia bilunaris</i> var. <i>linearis</i>
ZZZ981	Temporary sp. 19 <i>Brachysira</i> cf <i>procera</i>
ZZZ985	Temporary sp. 15 <i>Achnanthes minutissima</i> var. <i>jackii</i>
ZZZ986	Temporary sp. 14 <i>Aulacoseira distans</i> var. <i>septentrionalis</i>
ZZZ988	Temporary sp. 12 <i>Pinnularia biceps</i> var. <i>pusilla</i>
ZZZ989	Temporary sp. 11 <i>Achnanthes nitidiformis</i>
ZZZ991	Temporary sp. 9 <i>Achnanthes lanceolata</i> var. <i>frequentissima</i>
ZZZ992	Temporary sp. 8 <i>Pinnularia microstaurons</i> var. <i>adriondackensis</i>
ZZZ994	Temporary sp. 6 <i>Tabellaria flocculosa</i> var. <i>linearis</i>
ZZZ995	Temporary sp. 5 <i>Naviculadicta circumborealis</i>
ZZZ997	Temporary sp. 3 <i>Fragilaria suboldenburgiana</i>
ZZZ999	Temporary sp. 1 <i>Achnanthes minutissima</i> var. <i>inconspicua</i>

Appendix 4.4: GLR ice-cover (days) optima and tolerances for the 59 species which have a significant relationship with ice-cover. Those species marked in bold indicate species which either have optima outside the ice-cover range or where GLR failed to calculate optima measures.

Species Code	Optima	Tolerance	Species code	Optima	Tolerance
AH001A	0	0	NI017A	49	89
TA004A	-16	67	FR007A	74	69
BR011A	38	26	FR009H	79	74
EU070B	-102	136	NI002A	0	0
EU105A	-82	129	AC019A	86	115
EU106A	-1149	405	PI056A	102	85
AC004A	-4	81	AC044A	114	94
EU040A	9	90	AC002A	153	23
AC025A	28	74	AC048A	0	0
PE002A	7	96	AC034A	150	54
EU048A	4	105	AC035A	0	0
CM017A	-161	210	PI004A	3314	715
PI052A	12	93	NA149A	0	0
EU009A	-4	108	NA014A	0	0
EU019A	41	62	AU005A	0	0
EU004A	21	91	FR001A	0	0
BR010A	18	96	FR006A	0	0
SY002A	35	73	NA044A	0	0
NA156A	-106	193	AC134B	0	0
EU110A	1	115	AU020A	6507	590
BR001A	43	74	AC152A	188	17
CM010A	-25	144	FR001K	191	18
EU047A	9	119	AC082A	454	107
FR064A	-598	454	FR062A	0	0
TA9997	33	103	ZZZ986	0	0
CY006A	74	55	CY9984	0	0
EU003A	49	77	AU005B	223	15
NA032A	45	96	AU010B	0	0
EU043A	38	97			
CM018A	24	131			
CM014A	47	91			

Appendix 5.1: Table summarising the results of the water chemistry for the 80 lake data set

Code	Depth m Max	Ph	Alk µeq/l	Cond. µS/cm	Na ⁺ µeq/l	NH ₄ ⁺ µeq/l	K ⁺ µeq/l	Mg ²⁺ µeq/l	Ca ²⁺ µeq/l
96-10	3.5	5.82	18	4	7	0	2	7	33
96-12	2.1	6.73	127	18	27	4	12	56	101
96-36	6.6	6.43	57	19	26	2	4	15	95
96-37	12.5	5.47	11	9	18	0	4	9	38
96-54	5	6.23	35	14	22	3	6	19	81
96-71	8.2	5.55	13	8	18	0	7	16	24
96-78	15.5	5.42	10	6	12	0	3	12	32
96-9	8.5	5.72	17	12	11	1	5	7	46
98-1	3	6.27	42	9	12	1	0	21	68
98-10	14	5.76	20	5	13	0	4	8	33
98-13	2	7.53	731	113	39	0	45	167	977
98-14	1.6	7.22	377	50	39	0	18	75	425
98-15	6	7.17	277	49	34	0	23	54	399
98-16	1.1	7.57	598	90	44	3	54	92	786
98-17	2.8	7.41	489	58	25	0	11	42	572
98-2	12.5	6.15	37	7	14	0	3	13	52
98-20	4.5	6.15	41	8	18	0	8	14	50
98-21	3	6.62	74	11	22	0	6	34	74
98-22	1.9	6.64	85	12	22	0	4	43	72
98-23	6.5	6.41	60	10	24	1	3	23	67
98-3	4.8	6.22	39	8	15	0	0	24	54
98-5	10.5	6.4	48	8	12	0	2	24	57
98-6	15	6.01	25	6	12	0	3	11	41
98-7	18	5.88	22	5	10	1	4	7	38
98-8	11	5.79	21	5	12	2	4	7	34
98-9	16	5.69	17	4	9	0	3	7	25
99-43	1.6	5.99	135	22	30	0	3	16	201
99-44	1.3	6.36	339	47	28	0	3	23	439
99-50	2.1	6.78	1498	173	60	0	82	197	1585
CN0001	20	5.84	7	8.8	39	1	3	10	15
CN0002	40	5.95	7	7.4	30	1	3	7	18
CN0003	20	5.94	6	5	17	1	3	6	15
CN0004	30	6.64	52	11.1	22	1	6	12	72
CN0005	20	6.79	55	11.8	17	1	1	17	82
CN0006	18	6.47	31	15.7	23	1	2	7	115
CN0007	20	6.25	20	5.9	14	1	5	8	27
CN0008	16	6.43	27	8	23	1	3	9	45
CN0009	10	6.75	56	14.1	21	1	2	13	101
CN0010	20	6.14	10	4.1	8	1	4	6	16
CN0011	20	6.07	9	5.5	16	1	2	6	24
CN0012	30	6.45	27	6.8	17	1	4	9	33
CN0013	40	5.99	15	4.7	9	1	1	5	23
CN0014	20	6.29	23	4.7	9	1	2	6	25
CN0015	13	6.93	88	13.4	26	1	6	30	80
CN0016	18	6.22	17	6.3	30	1	3	7	17
CN0017	12	6.09	13	6.8	30	1	3	8	18
CN0018	15	6.79	55	11.1	20	1	6	23	67
CN0019	12	7.65	467	48	0	1	23	31	445
CN0020	9	6.48	47	11	0	1	6	23	51

Appendix 5.1 cont

Code	Depth	pH	Alk µeq/l	Cond. µS/cm	Na ⁺ µeq/l	NH ₄ ⁺ µeq/l	K ⁺ µeq/l	Mg ²⁺ µeq/l	Ca ²⁺ µeq/l
CN0021	6	7.2	232	23.8	21	1	10	43	207
CN0022	10	7.65	413	48	20	1	27	119	347
SN0023	10	6.18	20	7.8	20	0	3	8	38
SC0002	9.2	6.08	26	30	153	0	5	61	36
SC0010	4.3	6.32	35	29	172	0	5	48	46
SC0029	1	6.13	28	19	120	0	3	33	33
SC0067	5.1	5.95	17	29	176	0	6	54	30
SC0068	7.8	6.47	52	37	213	0	6	54	78
SC0076	24	6.18	30	24	147	0	5	47	34
SC0084	32	5.45	10	30	177	0	7	50	21
SC0101	1.7	6.88	94	30	148	0	5	41	92
SC0108	8.1	5.92	18	17	99	0	5	28	30
SC0124	6.2	6.58	53	22	118	0	6	38	51
SC0153	13	6.74	86	28	124	0	11	46	97
SC0165	46	5.87	17	30	176	0	7	49	33
SC0172	9.1	6.58	57	22	101	0	4	30	75
SC0180	14	6.16	34	32	195	0	8	56	54
SC0189	15	6.15	23	20	119	0	6	33	38
SC0190	47	6.15	28	34	205	0	7	54	58
SC0191	5	6.2	34	28	152	0	4	45	67
SC0197	11.5	6.75	68	44	246	0	8	76	75
SC0204	8.8	6.45	43	19	110	0	4	29	51
SC0211	3.5	6.17	30	37	222	0	8	71	37
SC0271	4.7	6.92	123	26	91	0	6	45	115
SC0330	27	6.66	55	19	92	0	7	31	63
SC0335	6	6.76	110	34	157	0	6	51	144
SC0349	7.3	5.97	22	41	250	0	9	58	50
SC0366	14	7.14	250	38	73	3	4	61	250
SC0382	21	5.94	18	13	58	0	2	15	37
SC0386	10	6.7	79	22	65	2	7	47	100
SC0399	24	5.42	9	18	77	0	4	32	32

Appendix 5.1 cont.

Code	Cl ⁻ μeq/l	NO ₃ ⁻ μeq/l	SO ₄ ²⁺ μeq/l	Al-TM μg/l	Al-NL μg/l	Al-L μg/l	TOC mg/l	ppt mm, annual	JanT °F	JulyT °F
96-10	8	0.52	9	4	4	0	0.8	600	13.2	43.26
96-12	14	1.2	36	7	5	2	2.1	540	10.68	48.12
96-36	25	2.1	39	6	5	1	2.4	1360	21.3	49.2
96-37	10	8.9	19	4	3	1	0.9	2000	22.02	48.48
96-54	17	0.69	54	1	0	1	2.8	900	19.68	48.48
96-71	13	0	16	6	2	4	2.6	900	20.22	47.76
96-78	9	6.1	12	6	5	1	1	900	18.6	45.78
96-9	8	0.35	15	5	4	1	0.9	860	14.28	43.8
98-1	7	0.35	35	29	0	29	0.9	700	18.6	46.68
98-10	4	0	18	3	3	0	1.5	860	14.64	44.34
98-13	26	0.38	376	5	2	3	1.9	430	12.3	49.02
98-14	10	0	105	9	5	4	3.3	900	13.2	50.1
98-15	7	0	187	6	5	1	1.5	450	7.08	48.48
98-16	23	0	270	4	4	0	3.1	450	7.8	49.38
98-17	6	0	89	8	6	2	2.7	500	12.84	49.74
98-2	8	1.1	17	0	0	0	0.9	700	18.6	46.68
98-20	4	0.34	24	5	5	0	0.7	540	11.04	47.22
98-21	3	0	28	6	5	1	1.1	540	11.76	47.94
98-22	2	0	27	12	8	4	1.9	540	12.12	48.48
98-23	7	0	22	9	9	0	2.3	540	14.28	51.36
98-3	6	0	28	0	0	0	0.7	700	18.96	47.04
98-5	6	3.8	22	0	0	0	0.8	1039	13.2	43.62
98-6	4	2.4	19	1	1	0	0.8	600	10.5	46.32
98-7	4	0	15	1	1	0	1.1	860	15.18	45.24
98-8	5	1.4	14	1	1	0	0.8	860	14.1	43.62
98-9	5	0	10	1	1	0	1.8	860	13.92	43.44
99-43	8	0	44	18	12	6	6.5	545	17.2	42.6
99-44	10	1	113	8	6	2	3.1	545	16.9	42.4
99-50	28	0	286	9	6	3	4.9	400	16.4	41.5
CN0001	42	2	15	19	14	5	1.1	1605	29.5	43.5
CN0002	31	3	17	2.5	2.5	0	0.036	1436	26.9	40.5
CN0003	14	2	15	2.5	2.5	0	0.39	1150	26.6	42.2
CN0004	23	1	21	11	11	0	2	1334	25.8	41.9
CN0005	14	2	33	2.5	2.5	0	0.22	1492	24.4	39.9
CN0006	20	3	83	2.5	2.5	0	0.28	1431	23.6	39
CN0007	8	0	19	2.5	2.5	0	0.67	1159	22.3	39.6
CN0008	11	0	23	6	5	1	0.84	1039	24.1	39.7
CN0009	14	0	50	2.5	2.5	0	0.6	1034	21.9	40.4
CN0010	6	0	15	2.5	2.5	0	0.34	1088	20.6	37.3
CN0011	11	0	19	6	5	1	0.8	986	24.5	39.2
CN0012	14	1	15	2.5	2.5	0	0.32	880	20.6	41
CN0013	6	4	21	5	5	0	0.1	895	20.1	40.2
CN0014	3	2	17	2.5	2.5	0	0.22	775	20.1	40.2
CN0015	3	0	31	6	2.5	3.5	0.79	731	21.5	42
CN0016	23	0	10	12	10	2	0.71	1001	25.5	42.3
CN0017	25	1	12	8	5	3	0.19	1526	24.2	40.5
CN0018	6	1	27	5	5	0	1.2	583	20.4	41
CN0019	16	0.14	31	16	13.5	2.5	2.1	822	22	41.2
CN0020	19	0.29	24	29	31	0	4.6	840	18.9	41
CN0021	20	0	15	5	5	0	2.8	731	20	42.4
CN0022	42	0.29	56	16	13	2.5	1.6	971	19.8	42.2

Appendix 5.1 cont.

Code	Cl ⁻ μeq/l	NO ₃ ⁻ μeq/l	SO ₄ ²⁺ μeq/l	Al-TM μg/l	Al-NL μg/l	Al-L μg/l	TOC mg/l	ppt mm, annual	JanT °F	JulyT °F
SN0023	14	3	25	65	34	31	1.4	977	25.7	40.8
SC0002	162	13	53	1	0	1	0.7	2590	33.2	47
SC0010	167	0.3	49	13	7	6	2.4	2505	35.26	51.01
SC0029	109	0	18	38	34	4	5.2	2161	32.7	47.02
SC0067	190	2.9	29	0	0	0	1	2053	34.6	49.6
SC0068	225	0	27	26	26	0	5.6	2053	34.24	49.62
SC0076	145	1.2	30	3	3	0	1.5	2000	33.8	48.78
SC0084	207	2.7	27	4	3	1	0.9	2093	31	48.75
SC0101	141	0	28	8	8	0	3	2049	30.3	48.12
SC0108	102	0.96	28	12	11	1	2	2107	32.3	47.79
SC0124	112	0	23	9	9	0	2.4	1972	31	49.4
SC0153	114	1.7	45	11	8	3	2.7	1912	30.75	49.8
SC0165	198	1.6	28	10	10	0	1.9	1906	33.2	50.1
SC0172	115	0.95	23	26	25	1	2.6	2699	34.6	49.9
SC0180	199	0.73	25	41	41	0	6.7	1782	33.6	51.08
SC0189	121	0.83	29	4	4	0	0.7	1880	29.2	48.8
SC0190	233	2.7	33	13	11	2	2	1830	31.2	51.5
SC0191	168	0	22	14	11	3	6.7	1792	32.4	49.5
SC0197	274	2.9	41	10	9	1	1.7	1554	33.8	48.8
SC0204	94	1.7	26	7	7	0	2.4	1513	31.6	48.45
SC0211	233	3.8	36	25	24	1	3.5	1561	32.89	48.92
SC0271	79	0.54	24	6	6	0	3.2	2461	30.5	50.2
SC0330	89	0.73	31	0	0	0	1.3	2095	30.7	48.1
SC0335	157	0.41	26	18	10	8	9.2	1426	32.98	51.2
SC0349	268	4.1	46	21	20	1	2.6	1087	33.26	48.4
SC0366	68	2	48	1	1	0	2.9	1900	30.9	49.9
SC0382	53	6.7	21	5	2	3	1.1	1169	27.6	47.4
SC0386	64	3.2	37	16	14	2	5.1	1175	30.69	47.96
SC0399	73	13	43	19	12	7	1.6	1213	30.8	47.9

Appendix 5.2: Species found within the 80 lake training set, species, codes and authorities are provided

AC001A	<i>Achnanthes lanceolata</i> (Breb. ex Kutz.) Grun. in Cleve & Grun. 1880
AC001T	<i>Achnanthes lanceolata robusta</i> (Hustedt) LB 1991
AC002A	<i>Achnanthes linearis</i> (W. Sm.) Grun. in Cleve & Grun. 1880
AC003A	<i>Achnanthes microcephala</i> (Kutz.) Cleve 1896
AC003A	<i>Achnanthes microcephala</i> (Kutz.) Cleve 1896
AC004A	<i>Achnanthes pseudoswazi</i> J.R. Carter 1963
AC005A	<i>Achnanthes calcar</i> Cleve 1891
AC007A	<i>Achnanthes oestrupii</i> (A. Cleve-Euler) Hust. 1930
AC008A	<i>Achnanthes exigua</i> Grun. in Cleve & Grun. 1880
AC013A	<i>Achnanthes minutissima minutissima</i> Kutz. 1833
AC018A	<i>Achnanthes laterostrata</i> Hust. 1933
AC019A	<i>Achnanthes nodosa</i> A. Cleve-Euler 1900
AC022A	<i>Achnanthes marginulata</i> Grun. in Cleve & Grun. 1880
AC024A	<i>Achnanthes depressa</i> (Cleve) Hust. 1933
AC025A	<i>Achnanthes flexella</i> (Kutz.) Brun 1880
AC027A	<i>Achnanthes holstii</i> Cleve 1881
AC029A	<i>Achnanthes sublaevis</i> Hust. 1936
AC034A	<i>Achnanthes suchlandtii</i> Hust. 1933
AC035A	<i>Achnanthes pusilla pusilla</i> Grun. in Cleve & Grun. 1880
AC037A	<i>Achnanthes biasoletiana</i> Grun. in Cleve & Grun. 1880
AC039A	<i>Achnanthes didyma didyma</i> Hust. 1933
AC044A	<i>Achnanthes levanderi</i> Hust. 1933
AC046A	<i>Achnanthes altaica</i> (Poretzky) A. Cleve-Euler 1953
AC048A	<i>Achnanthes scotica</i> Jones & Flower
AC049A	<i>Achnanthes ploenensis</i> Hust. 1930
AC060A	<i>Achnanthes curtissima</i> J.R. Carter 1963
AC082A	<i>Achnanthes kriegei</i> Krasske 1943
AC083A	<i>Achnanthes laevis</i> Ostr. 1910
AC105A	<i>Achnanthes petersenii</i> Hust. 1937
AC119A	<i>Achnanthes saccula</i> J.R. Carter in J.R. Carter & Watts 1981
AC134A	<i>Achnanthes helvetica</i> (Hustedt) Lange-Bertalot in LB & K 1989
AC134B	<i>Achnanthes helvetica alpina</i> Flower and Jones 1989
AC134C	<i>Achnanthes helvetica minor</i> Flower & Jones 1989
AC136A	<i>Achnanthes subatomoides</i> (Hust.) Lange-Bertalot & Archibald in K & LB 1985
AC142A	<i>Achnanthes kuelbsii</i> Lange-Bertalot 1989
AC143A	<i>Achnanthes oblongella</i> Ostr. 1902
AC146A	<i>Achnanthes lacus-vulcani</i> Lange-Bertalot & Krammer 1989
AC152A	<i>Achnanthes carissima</i> Lange-Bertalot 1990
AC153A	<i>Achnanthes impexa</i> Lange-Bertalot 1989
AC154A	<i>Achnanthes imperfecta</i> Schimanski 1978
AC161A	<i>Achnanthes ventralis</i> (Krasske) Lange-Bertalot 1989
AC169A	<i>Achnanthes grischuna</i> Wuthrich 1975
AC173A	<i>Achnanthes stolidia</i> (Krasske) Krasske 1949
AC178A	<i>Achnanthes straubiana</i> Lange-Bertalot 1996
AC179A	<i>Achnanthes alteragracillima</i> Lange-Bertalot
AC182A	<i>Achnanthes rosenstockii</i> Lange-Bertalot 1989
AC9968	<i>Achnanthes</i> [marginulata] major Uaine (VJJ) 1988
AC9975	<i>Achnanthes</i> [altaica var. minor] L. Grannoch (RJF) 1988
AC9999	<i>Achnanthes</i> sp.
AH001A	<i>Amphicampa hemicyclus</i> (Ehrenb.) Karsten 1928

Appendix 5.2 cont.

AM001A	<i>Amphora ovalis ovalis</i> (Kutz.) Kutz. 1844
AM001D	<i>Amphora ovalis affinis</i> (Kutz.) Van Heurck 1885
AM007A	<i>Amphora commutata</i> Grun. in Van Heurck 1880
AM010A	<i>Amphora fogediana</i> Krammer 1985
AM011A	<i>Amphora libyca</i> Ehr.
AM012A	<i>Amphora pediculus</i> (Kutz.) Grun.
AM013A	<i>Amphora inariensis</i> Krammer
AM9999	<i>Amphora</i> sp.
AM9999	<i>Amphora</i> sp.
AP001A	<i>Amphipecten pellucida</i> (Kutz.) Kutz. 1844
AS001A	<i>Asterionella formosa formosa</i> Hassall 1850
AU001C	<i>Aulacoseira italica valida</i> (Grun. in Van Heurck) Simonsen 1979
AU002A	<i>Aulacoseira ambigua</i> (Grun. in Van Heurck) Simonsen 1979
AU004A	<i>Aulacoseira lirata lirata</i> (Ehrenb.) R. Ross in Hartley 1986
AU004B	<i>Aulacoseira lirata lacustris</i> (Grun. in Van Heurck) R. Ross in Hartley 1986
AU005A	<i>Aulacoseira distans distans</i> (Ehrenb.) Simonsen 1979
AU005B	<i>Aulacoseira distans nivaloides</i> Camburn 1987
AU005D	<i>Aulacoseira distans tenella</i> (Nygaard) R. Ross in Hartley 1986
AU005E	<i>Aulacoseira distans nivalis</i>
AU005L	<i>Aulacoseira distans humilis</i> (A. Cleve-Euler) R. Ross in Hartley 1986
AU010A	<i>Aulacoseira perglabra</i>
AU010B	<i>Aulacoseira perglabra floriniae</i>
AU020A	<i>Aulacoseira subarctica</i> (O.Mull.) Haworth
AU022A	<i>Aulacoseira subborealis</i> SWAP 1989
AU023A	<i>Aulacoseira tethera</i> Haworth nov. sp. 1989
AU031A	<i>Aulacoseira alpigena</i> (Grunow) Krammer 1990
AU032A	<i>Aulacoseira lacustris</i> Krammer 1990
AU033A	<i>Aulacoseira pfaffiana</i> (Reinsch) Krammer 1990
AU9986	<i>Aulacoseira</i> [subarctica, Haworth 1989, type 2, fig 48] SWAP Sweden (IR & NJA) 1989
AU9999	<i>Aulacoseira</i> sp.
BR001A	<i>Brachysira vitrea</i> (Grun.) R. Ross in Hartley 1986
BR003A	<i>Brachysira serians</i> (Breb. ex Kutz.) Round & Mann 1981
BR004A	<i>Brachysira styriaca</i> (Grun. in Van Heurck) R. Ross in Hartley 1986
BR006A	<i>Brachysira brebissonii brebissonii</i> R. Ross in Hartley 1986
BR008A	<i>Brachysira minor</i> (Krasske 1939) nov. com.
BR010A	<i>Brachysira neoexilis</i> Lange-Bertalot 1994
BR011A	<i>Brachysira procera</i> L-B & Moser 1994
BR012A	<i>Brachysira garrensis</i> LB & (L.B)
BR9999	<i>Brachysira</i> sp.
CA002A	<i>Caloneis bacillum bacillum</i> (Grun.) Cleve 1894
CA003A	<i>Caloneis silicula</i> (Ehrenb.) Cleve 1894
CA018A	<i>Caloneis tenuis</i> Gregory (Krammer) 1985
CA048A	<i>Caloneis molaris</i> (Grunow) Krammer 1985
CA9999	<i>Caloneis</i> sp.
CM003A	<i>Cymbella sinuata sinuata</i> Greg. 1856
CM004A	<i>Cymbella microcephala microcephala</i> Grun. in Van Heurck 1880
CM006A	<i>Cymbella cistula cistula</i> (Ehrenb. in Hempr. & Ehrenb.) Kirchner 1878
CM008A	<i>Cymbella hybrida</i> Grun. ex Cleve 1894
CM009A	<i>Cymbella naviculiformis</i> Auerw. ex Heib. 1863
CM010A	<i>Cymbella perpusilla</i> A. Cleve 1895
CM013A	<i>Cymbella helvetica helvetica</i> Kutz. 1844
CM014A	<i>Cymbella aequalis</i> W. Sm. ex Grev. 1855

Appendix 5.2 cont.

- CM015A *Cymbella cesatii* *cesatii* (Rabenh.) Grun. in A. Schmidt 1881
CM016A *Cymbella amphicephala* *amphicephala* Naegeli ex Kutz. 1849
CM017A *Cymbella hebridica* (Grun. ex Cleve) Cleve 1894
CM018A *Cymbella gracilis* (Rabenh.) Cleve 1894
CM020A *Cymbella gaeumannii* Meister 1934
CM022A *Cymbella affinis* Kutz. 1844
CM026A *Cymbella cuspidata* Kutz. 1844
CM031A *Cymbella minuta* *minuta* Hilse ex Rabenh. 1862
CM033A *Cymbella hustedtii* Krasske 1923
CM036A *Cymbella obtusa* Greg. 1856
CM047A *Cymbella incerta* Grun. in Cleve & Moller 1878
CM049A *Cymbella failaisensis* (Grun.) Krammer & Lange-Bertalot 1985
CM050A *Cymbella subaequalis* Grun. in Van Heurck 1880
CM052A *Cymbella descripta* (Hust.) Krammer & Lange-Bertalot 1985
CM068A *Cymbella brehmii* Hust. 1912
CM085A *Cymbella lapponica* Grun. ex Cleve 1894
CM101A *Cymbella scotica* *naviculacea* (Grun. ex Cleve) R. Ross 1947
CM103A *Cymbella silesiaca* Bleisch ex Rabenh. 1864
CM109A *Cymbella tumidula* Grun. ex A. Schmidt 1875
CM113A *Cymbella reichardtii* Krammer 1985
CM9999 *Cymbella* sp.
CO001B *Cocconeis placentula* *euglypta* (Ehrenb.) Grun. 1884
CO067A *Cocconeis neothumensis* Krammer 1991
CO9999 *Cocconeis* sp.
CU001A *Chamaepinnularia* [sp. 2 *Julma Olkky*] L-B & Metzeltin 1996
CY002A *Cyclotella pseudostelligera* Hust. 1939
CY004A *Cyclotella stelligera* (Cleve & Grun. in Cleve) Van Heurck 1882
CY004B *Cyclotella stelligera* *glomerata* Haworth 1886
CY006A *Cyclotella kuetzingiana* *kuetzingiana* Thwaites 1848
CY006B *Cyclotella kuetzingiana* *planetophora* Fricke in A. Schmidt 1900
CY006C *Cyclotella kuetzingiana* *radiosa* Fricke in A. Schmidt 1900
CY009A *Cyclotella ocellata* Pant. 1902
CY010A *Cyclotella comensis* Grun. in Van Heurck 1882
CY013A *Cyclotella antiqua* W. Sm. 1853
CY019A *Cyclotella radiosa* (Grunow) Lemmerman 1900
CY020A *Cyclotella iris* Brun
CY022B *Cyclotella bodanica* *lemanica* (O.Muller ex Schroter) Bachmann 1903
CY028A *Cyclotella distinguenda* Hust. 1927
CY028B *Cyclotella distinguenda* *unipunctata* (Hustedt) Hakansson & Carter 1990
CY036A *Cyclotella praetermissa* J.W.G. Lund 1951
CY048A *Cyclotella woltereckii* Hust. 1942
CY052A *Cyclotella rossii* Hakansson 1990
CY054A *Cyclotella krammeri* Hakansson 1990
CY059A *Cyclotella cyclopuncta* Hakansson & Carter 1990
CY061A *Cyclotella gordonensis* Kling & Hakansson 1988
CY9984 *Cyclotella* [cf. *krammeri*] RIBA (P. Rioual) 1997
CY9987 *Cyclotella* [cf. *comensis*] Massif Central (PR) 1997
CY9999 *Cyclotella* sp.
DE001A *Denticula tenuis* *tenuis* Kutz. 1844
DE002A *Denticula elegans* *elegans* Kutz. 1844
DE003A *Denticula kuetzingii* Grun.
DP001A *Diploneis ovalis* (Hilse) Cleve 1894

Appendix 5.2 cont.

DP065A	<i>Diploneis parma</i>	Cleve 1891
DP9999	<i>Diploneis</i> sp.	
DT021A	<i>Diatoma mesodon</i>	(Ehrenber) Kutz. 1844
EP001A	<i>Epithemia sorex</i>	<i>sorex</i> Kutz. 1844
EP9999	<i>Epithemia</i> sp.	
EU002A	<i>Eunotia pectinalis</i>	<i>pectinalis</i> (O.F. Mull.) Rabenh. 1864
EU002D	<i>Eunotia pectinalis</i>	<i>undulata</i> (Ralfs) Rabenh. 1864
EU002E	<i>Eunotia pectinalis</i>	<i>minor impressa</i> (Ehr.) Hust.
EU003A	<i>Eunotia praerupta</i>	<i>praerupta</i> Ehrenb. 1843
EU003B	<i>Eunotia praerupta</i>	<i>bidens</i> (Ehrenb.) Grun. in Cleve & Grun. 1880
EU004A	<i>Eunotia tenella</i>	(Grun. in Van Heurck) A. Cleve 1895
EU007A	<i>Eunotia bidentula</i>	W. Sm. 1856
EU008A	<i>Eunotia monodon</i>	<i>monodon</i> Ehrenb. 1843
EU009A	<i>Eunotia exigua</i>	<i>exigua</i> (Breb. ex Kutz.) Rabenh. 1864
EU010A	<i>Eunotia faba</i>	(Ehrenb.) Grun. in Van Heurck 1881
EU011A	<i>Eunotia rhomboidea</i>	Hust. 1950
EU013A	<i>Eunotia arcus</i>	<i>arcus</i> Ehrenb. 1837
EU014A	<i>Eunotia bactriana</i>	Ehrenb. 1854
EU015A	<i>Eunotia denticulata</i>	<i>denticulata</i> (Breb. ex Kutz.) Rabenh. 1864
EU016A	<i>Eunotia diodon</i>	Ehrenb. 1837
EU017A	<i>Eunotia flexuosa</i>	<i>flexuosa</i> Kutz. 1849
EU019A	<i>Eunotia iatriaensis</i>	Foged 1970
EU020A	<i>Eunotia meisteri</i>	<i>meisteri</i> Hust. 1930
EU020B	<i>Eunotia meisteri</i>	<i>bidens</i> Hust. 1930
EU024A	<i>Eunotia glacialis</i>	Meister 1912
EU025A	<i>Eunotia fallax</i>	A. Cleve 1895
EU026A	<i>Eunotia praerupta-nana</i>	Berg
EU028A	<i>Eunotia microcephala</i>	Krasske ex Hust. 1932
EU029A	<i>Eunotia valida</i>	Hust. 1930
EU031A	<i>Eunotia septentrionalis</i>	<i>septentrionalis</i> Ostr. 1898
EU032A	<i>Eunotia serra</i>	<i>serra</i> Ehrenb. 1837
EU032B	<i>Eunotia serra</i>	<i>diadema</i> (Ehrenb.) Patr. 1958
EU032C	<i>Eunotia serra</i>	<i>tetraodon</i> (Ehren) Norpel 1991
EU034A	<i>Eunotia parallela</i>	<i>parallela</i> Ehrenb. 1843
EU039A	<i>Eunotia triodon</i>	Ehrenb. 1837
EU040A	<i>Eunotia paludosa</i>	Grun. 1862
EU040B	<i>Eunotia paludosa</i>	<i>trinacria</i> (Krasske) Norpel 1991
EU043A	<i>Eunotia elegans</i>	Ostr. 1910
EU044A	<i>Eunotia acmocephala</i>	Fusey 1953
EU046B	<i>Eunotia perpusilla</i>	<i>tridentata</i> (May.) A Berg
EU047A	<i>Eunotia incisa</i>	W. Sm. ex Greg. 1854
EU048A	<i>Eunotia naegeli</i>	Migula 1907
EU049A	<i>Eunotia curvata</i>	<i>curvata</i> (Kutz.) Lagerst. 1884
EU049B	<i>Eunotia curvata</i>	<i>subarcuata</i> (Naegeli ex Kutz.) Woodhead & Tweed 1954
EU049C	<i>Eunotia curvata</i>	<i>capitata</i> (Grun.) Woodhead & Tweed 1954
EU051A	<i>Eunotia vanheurckii</i>	<i>vanheurckii</i> Patr. 1958
EU054A	<i>Eunotia hexaglyphis</i>	Ehrenb. 1854
EU060A	<i>Eunotia pirla</i>	Carter et Flower 1988
EU070A	<i>Eunotia bilunaris</i>	(Ehrenb.) F.W. Mills 1934
EU070B	<i>Eunotia bilunaris</i>	<i>mucophila</i> LB & Norpel 1991
EU105A	<i>Eunotia subarcuoides</i>	Alles, Norpel, Lange-Bertalot 1991
EU106A	<i>Eunotia rhynchocephala</i>	Hustedt 1936

Appendix 5.2 cont.

EU107A	<i>Eunotia implicata</i>	Norpel, Lange-Bertalot & Alles 1991
EU108A	<i>Eunotia intermedia</i>	(Hust) Norpel, Lange-Bertalot & Alles 1991
EU110A	<i>Eunotia minor</i>	(Kutz) Grunow in Van Heurck 1881
EU111A	<i>Eunotia soleirolii</i>	(Kutz) Rabenhorst 1864
EU112A	<i>Eunotia arculus</i>	(Grunow) LB & Norpel
EU9999	<i>Eunotia</i> sp.	
FR001A	<i>Fragilaria pinnata</i>	<i>pinnata</i> Ehrenb. 1843
FR001B	<i>Fragilaria pinnata</i>	<i>lancettula</i> (Schum.) Hust. in A. Schmidt 1913
FR001E	<i>Fragilaria pinnata</i>	<i>intercedens</i> (Grun. in Van Heurck) Hust. 1931
FR001K	<i>Fragilaria pinnata</i>	<i>acuminata</i> (A. Mayer) Regenbogen
FR002A	<i>Fragilaria construens</i>	<i>construens</i> (Ehrenb.) Grun. 1862
FR002B	<i>Fragilaria construens</i>	<i>binodis</i> (Ehrenb.) Grun. 1862
FR002B	<i>Fragilaria construens</i>	<i>binodis</i> (Ehrenb.) Grun. 1862
FR002C	<i>Fragilaria construens</i>	<i>venter</i> (Ehrenb.) Grun. in Van Heurck 1881
FR002F	<i>Fragilaria construens</i>	<i>pumila</i> Grun. in Van Heurck 1881
FR004B	<i>Fragilaria hungarica</i>	<i>tumida</i> A. Cleve
FR005A	<i>Fragilaria virescens</i>	<i>virescens</i> Ralfs 1843
FR005B	<i>Fragilaria virescens</i>	<i>subsalina</i> Grun. in Van Heurck 1881
FR006A	<i>Fragilaria brevistriata</i>	<i>brevistriata</i> Grun. in Van Heurck 1885
FR006E	<i>Fragilaria brevistriata</i>	<i>capitata</i> (Herib.) Bass
FR007A	<i>Fragilaria vaucheriae</i>	<i>vaucheriae</i> (Kutz.) J.B. Petersen 1938
FR009H	<i>Fragilaria capucina</i>	<i>gracilis</i> (Oestrup) Hustedt 1950
FR009I	<i>Fragilaria capucina</i>	<i>austriaca</i> (Grun) Lange-Bertalot 1980
FR009J	<i>Fragilaria capucina</i>	<i>perminuta</i> (Grun.) L-B. 1991
FR010A	<i>Fragilaria constricta</i>	<i>constricta</i> Ehrenb. 1843
FR010B	<i>Fragilaria constricta</i>	<i>stricta</i> (A. Cleve) Hust. 1931
FR011A	<i>Fragilaria lapponica</i>	Grun. in Van Heurck 1881
FR015A	<i>Fragilaria lata</i>	(Cleve-Euler) Renberg 1977
FR018A	<i>Fragilaria elliptica</i>	Schum. 1867
FR056A	<i>Fragilaria pseudoconstruens</i>	Marciniak 1982
FR062A	<i>Fragilaria microstriata</i>	Marciniak in Metzeltin & Witkowski 1996
FR063A	<i>Fragilaria robusta</i>	(Fusey) Manguin
FR064A	<i>Fragilaria exigua</i>	Grun in Cleve & Moller 1878
FR9999	<i>Fragilaria</i> sp.	
FU002A	<i>Frustulia rhomboides</i>	<i>rhomboides</i> (Ehrenb.) De Toni 1891
FU002B	<i>Frustulia rhomboides</i>	<i>saxonica</i> (Rabenh.) De Toni 1891
FU002E	<i>Frustulia rhomboides</i>	<i>saxonica undulata</i> Hust.
GO003A	<i>Gomphonema angustatum</i>	<i>angustatum</i> (Kutz.) Rabenh. 1864
GO004A	<i>Gomphonema gracile</i>	Ehrenb. 1838
GO006A	<i>Gomphonema acuminatum</i>	<i>acuminatum</i> Ehrenb. 1832
GO013A	<i>Gomphonema parvulum</i>	<i>parvulum</i> (Kutz.) Kutz. 1849
GO013C	<i>Gomphonema parvulum</i>	<i>exilissimum</i> Grun. in Van Heurck 1880
GO050A	<i>Gomphonema minutum</i>	(Ag.) Ag. 1831
GO072A	<i>Gomphonema pseudotenellum</i>	Lange Bertalot 1985
GO075A	<i>Gomphonema anoenum</i>	Lange-Bertalot 1985
GO077A	<i>Gomphonema lacus-vulcani</i>	Reichardt & L.B.
GO079A	<i>Gomphonema procerum</i>	Reichardt & L-B
GO9999	<i>Gomphonema</i> sp.	
KR001A	<i>Krasskella kriegeana</i>	(Krasske) R. Ross & Sims 1978
MR001A	<i>Meridion circulare</i>	<i>circulare</i> (Grev.) Ag. 1831
NA002A	<i>Navicula jaernefeltii</i>	Hust. 1942
NA003A	<i>Navicula radiosa</i>	<i>radiosa</i> Kutz. 1844

Appendix 5.2 cont.

NA003B	<i>Navicula radiosa tenella</i> (Breb. ex Kutz.) Grun. ex Van Heurck 1885
NA003C	<i>Navicula radiosa parva</i> Wallace
NA005A	<i>Navicula seminulum</i> Grun. 1860
NA006A	<i>Navicula mediocris</i> Krasske 1932
NA007A	<i>Navicula cryptocephala cryptocephala</i> Kutz. 1844
NA008A	<i>Navicula rhynchocephala rhynchocephala</i> Kutz. 1844
NA010A	<i>Navicula pygmaea</i> Kutz. 1849
NA012A	<i>Navicula aboensis</i> (Cleve) Hust. 1952
NA013A	<i>Navicula pseudoscutiformis</i> Hust. 1930
NA014A	<i>Navicula pupula pupula</i> Kutz. 1844
NA014C	<i>Navicula pupula capitata</i> Skvortz. & Meyer 1928
NA014E	<i>Navicula pupula rostrata</i> Hust. 1911
NA016A	<i>Navicula indifferens</i> Hust. 1942
NA017A	<i>Navicula ventralis</i> Krasske 1923
NA032A	<i>Navicula cocconeiformis cocconeiformis</i> Greg. ex Greville 1855
NA032A	<i>Navicula cocconeiformis cocconeiformis</i> Greg. ex Greville 1855
NA033A	<i>Navicula subtilissima</i> Cleve 1891
NA033A	<i>Navicula subtilissima</i> Cleve 1891
NA037A	<i>Navicula angusta</i> Grun. 1860
NA038A	<i>Navicula arvensis</i> Hust.
NA042A	<i>Navicula minima minima</i> Grun. in Van Heurck 1880
NA044A	<i>Navicula krasskei</i> Hust. 1930
NA045A	<i>Navicula bryophila bryophila</i> J.B. Petersen 1928
NA046A	<i>Navicula contenta contenta</i> Grun. in Van Heurck 1885
NA048A	<i>Navicula soehrensensis soehrensensis</i> Krasske 1923
NA048D	<i>Navicula soehrensensis hassiaca</i> (Krasske)Lange-Bertalot 1985
NA073A	<i>Navicula placenta</i> Ehrenb. 1854
NA090A	<i>Navicula rotunda</i> Hust. 1945
NA099A	<i>Navicula bremensis</i> Hust. 1957
NA100A	<i>Navicula explanata</i> Hust. 1948
NA101A	<i>Navicula jaagii</i> Meister 1934
NA102A	<i>Navicula laevisissima</i> Kutz. 1844
NA112A	<i>Navicula minuscula minuscula</i> Grun. in Van Heurck 1880
NA114A	<i>Navicula subrotundata</i> Hust. 1945
NA124A	<i>Navicula molestiformis</i> Hust.
NA129A	<i>Navicula seminuloides</i> Hust. 1937
NA133A	<i>Navicula schassmannii</i> Hust. 1937
NA134A	<i>Navicula subminuscula</i> Manguin
NA135A	<i>Navicula tenuicephala</i> Hust. 1942
NA141A	<i>Navicula disjuncta</i> Hust. 1930
NA149A	<i>Navicula digitulus</i> Hust. 1943
NA156A	<i>Navicula leptostriata</i> Jorgensen 1948
NA160A	<i>Navicula submolesta</i> Hust. 1949
NA166A	<i>Navicula submuralis</i> Hust.
NA168A	<i>Navicula vitabunda</i> Hust. 1930
NA322A	<i>Navicula detenta</i> Hust. 1943
NA389B	<i>Navicula gallica perpusilla</i> (Grun) Lange-Bertalot 1985
NA402A	<i>Navicula gottlandica</i> Grun. in Van Heurck 1880
NA462A	<i>Navicula joubaudii</i> Germain 1982
NA650A	<i>Navicula stroemii</i> Hust. 1931
NA669A	<i>Navicula suchlandtii</i> Hust. 1943
NA738A	<i>Navicula vitiosa</i> Schimanski 1978

Appendix 5.2 cont.

NA751A	<i>Navicula cryptotenella</i>	Lange-Bertalot 1985
NA755A	<i>Navicula kuelbsii</i>	Lange-Bertalot 1985
NA779A	<i>Navicula pseudoarvensis</i>	Hustedt 1942
NA9958	<i>Navicula</i> [PIRLA sp. 24]	PIRLA 1985
NA9997	<i>Navicula</i> [cf. <i>wuestii</i>]	
NA9999	<i>Navicula</i> sp.	
ND001A	<i>Naviculadicta elorantana</i>	LB nov spec 1996
ND9997	<i>Naviculadicta</i> [sp.#2 Weinfelder Maar]	LB & Metzeltin 1996
ND9998	<i>Naviculadicta</i> [sp.#1 Weinfelder Maar]	LB & Metzeltin 1996
NE001A	<i>Neidium iridis iridis</i> (Ehrenb.)	Cleve 1894
NE003A	<i>Neidium affine affine</i> (Ehrenb.)	Pfitz. 1871
NE003B	<i>Neidium affine longiceps</i> (Greg.)	Cleve 1896
NE003C	<i>Neidium affine amphirhynchus</i> (Ehrenb.)	Cleve 1894
NE004A	<i>Neidium bisulcatum bisulcatum</i> (Lagerst.)	Cleve 1894
NE006A	<i>Neidium alpinum</i>	Hust. 1943
NE007A	<i>Neidium dubium dubium</i> (Ehrenb.)	Cleve 1894
NE014A	<i>Neidium septentrionale</i>	Cleve-Euler 1939
NE036A	<i>Neidium ampliatus</i> (Ehren)	Krammer 1985
NE9999	<i>Neidium</i> sp.	
NI002A	<i>Nitzschia fonticola</i>	Grun. in Van Heurck 1881
NI005A	<i>Nitzschia perminuta</i> (Grun. in Van Heurck)	M. Perag. 1903
NI008A	<i>Nitzschia frustulum</i> (Kutz.)	Grun. in Cleve & Grun. 1880
NI009A	<i>Nitzschia palea palea</i> (Kutz.)	W. Sm. 1856
NI017A	<i>Nitzschia gracilis</i>	Hantzsch 1860
NI025A	<i>Nitzschia recta</i>	Hantzsch ex Rabenh. 1861
NI030A	<i>Nitzschia acidoclinata</i>	Lange Bertalot
NI033A	<i>Nitzschia paleacea</i> (Grun. in Cleve & Grun.)	Grun. in Van Heurck 1881
NI043A	<i>Nitzschia inconspicua</i>	Grun. 1862
NI048A	<i>Nitzschia tubicola</i>	Grun. in Cleve & Grun. 1880
NI065A	<i>Nitzschia archibaldii</i>	Lange-Bertalot 1980
NI195A	<i>Nitzschia supralitorea</i>	Lange-Bertalot 1979
NI198A	<i>Nitzschia lacuum</i>	Lange-Bertalot 1980
NI206A	<i>Nitzschia solita</i>	Hustedt 1953
NI216A	<i>Nitzschia pura</i>	Hustedt 1954
NI9999	<i>Nitzschia</i> sp.	
PE001A	<i>Peronia heribaudii</i>	Brun & M. Perag. in Herib. 1893
PE002A	<i>Peronia fibula</i> (Breb. ex Kutz.)	R. Ross 1956
PI001A	<i>Pinnularia gibba</i> (Ehrenb.)	Ehrenb. 1843
PI001B	<i>Pinnularia gibba linearis</i>	Hust. 1930
PI004A	<i>Pinnularia interrupta</i>	W. Smith
PI005A	<i>Pinnularia major major</i> (Kutz.)	W. Sm. 1853
PI007A	<i>Pinnularia viridis viridis</i> (Nitzsch)	Ehrenb. 1843
PI011A	<i>Pinnularia microstauron microstauron</i> (Ehrenb.)	Cleve 1891
PI014A	<i>Pinnularia appendiculata</i> (Ag.)	Cleve 1896
PI015A	<i>Pinnularia abaujensis abaujensis</i> (Pant.)	R. Ross in Hartley 1986
PI016A	<i>Pinnularia divergentissima divergentissima</i> (Grun. in Van Heurck)	Cleve 1896
PI018A	<i>Pinnularia biceps biceps</i>	Greg. 1856
PI020A	<i>Pinnularia undulata</i>	Greg. 1854
PI022A	<i>Pinnularia subcapitata subcapitata</i>	Greg. 1856
PI042A	<i>Pinnularia nodosa nodosa</i> (Ehrenb.)	W. Sm. 1856
PI048A	<i>Pinnularia brebissonii brebissonii</i> (Kutz.)	Rabenh. 1864
PI051A	<i>Pinnularia lata lata</i> (Breb.)	W. Sm. 1853

Appendix 5.2 cont.

PI052A	<i>Pinnularia silvatica</i> J.B. Petersen 1935
PI055A	<i>Pinnularia balfouriana</i> Grun. ex Cleve 1896
PI056A	<i>Pinnularia rupestris</i> Hantzsch in Rabenh. 1861
PI132A	<i>Pinnularia lundii</i> Hust. 1954
PI161A	<i>Pinnularia subrostrata</i> (A. Cleve) A. Cleve-Euler 1955
PI9990	<i>Pinnularia</i> [cf. <i>pseudomicrostauron</i>] L. Hir (SF) 1986
PI9999	<i>Pinnularia</i> sp.
RH9999	<i>Rhopalodia</i> sp.
SA001A	<i>Stauroneis anceps</i> <i>anceps</i> Ehrenb. 1843
SA005A	<i>Stauroneis legumen</i> (Ehrenb.) Kutz. 1844
SA006A	<i>Stauroneis phoenicenteron</i> <i>phoenicenteron</i> (Nitzsch) Ehrenb. 1943
SA012A	<i>Stauroneis kriegeri</i> Patr. 1945
SA014A	<i>Stauroneis gracilis</i> Ehrenb. 1843
SA9999	<i>Stauroneis</i> sp.
SP005A	<i>Stenopterobia delicatissima</i> (Lewis) M. Perag. 1897
SP006A	<i>Stenopterobia curvula</i> (W Smith) Krammer 1987
SP9999	<i>Stenopterobia</i> sp.
ST014A	<i>Stephanodiscus medius</i> Hakansson 1986
SU001A	<i>Surirella angusta</i> Kutz. 1844
SU005A	<i>Surirella linearis</i> <i>linearis</i> W. Sm. 1853
SU005B	<i>Surirella linearis</i> <i>constricta</i> Grun. 1862
SU074A	<i>Surirella bifrons</i> Ehrenb. 1843
SU076A	<i>Surirella roba</i> Leclercq 1983
SU9999	<i>Surirella</i> sp.
SY002A	<i>Synedra rumpens</i> <i>rumpens</i> Kutz. 1844
SY003A	<i>Synedra acus</i> <i>acus</i> Kutz. 1844
SY004A	<i>Synedra parasitica</i> <i>parasitica</i> (W. Sm.) Hust. 1930
SY009A	<i>Synedra nana</i> Meister 1912
SY017A	<i>Synedra radians</i> Kutz. 1844
TA001A	<i>Tabellaria flocculosa</i> <i>flocculosa</i> (Roth) Kutz. 1844
TA003A	<i>Tabellaria binalis</i> (Ehrenb.) Grun. in Van Heurck 1881
TA003B	<i>Tabellaria binalis</i> <i>elliptica</i> Flower (unpub) 1986
TA004A	<i>Tabellaria quadrisepata</i> Knudson 1952
TA006A	<i>Tabellaria ventricosa</i>
TA9997	<i>Tabellaria</i> [<i>flocculosa</i> (short)]
TA9998	<i>Tabellaria</i> [<i>flocculosa</i> (long)]
TA9999	<i>Tabellaria</i> sp.
TE001A	<i>Tetracyclus lacustris</i> Ralfs 1843
TH9999	<i>Thalassiosira</i> sp.
ZZZ974	Temporary sp. 26 <i>Cymbella</i> cf <i>microcephala</i>
ZZZ975	Temporary sp. 25 <i>Achnanthes minutissima</i> var. <i>macrocephala</i>
ZZZ977	Temporary sp. 23 <i>Eunotia seminulum</i>
ZZZ978	Temporary sp. 22 <i>Navicula</i> cf. <i>minuta</i>
ZZZ980	Temporary sp. 20 <i>Eunotia bilunaris</i> var. <i>linearis</i>
ZZZ981	Temporary sp. 19 <i>Brachysira</i> cf <i>procera</i>
ZZZ985	Temporary sp. 15 <i>Achnanthes minutissima</i> var. <i>jackii</i>
ZZZ986	Temporary sp. 14 <i>Aulacoseira distans</i> var. <i>septentrionalis</i>
ZZZ988	Temporary sp. 12 <i>Pinnularia biceps</i> var. <i>pusilla</i>
ZZZ989	Temporary sp. 11 <i>Achnanthes nitidiformis</i>
ZZZ990	Temporary sp. 10 <i>Achnanthes pusilla</i> (fat)
ZZZ991	Temporary sp. 9 <i>Achnanthes lanceolata</i> var. <i>frequentissima</i>
ZZZ992	Temporary sp. 8 <i>Pinnularia microstaurons</i> var. <i>adriondackensis</i>

Appendix 5.2 cont.

- ZZZ994 Temporary sp. 6 *Tabellaria flocculosa* var. *linearis*
ZZZ995 Temporary sp. 5 *Naviculadicta circumborealis*
ZZZ997 Temporary sp. 3 *Fragilaria suboldenburgiana*
ZZZ999 Temporary sp. 1 *Achnanthes minutissima* var. *inconspicua*

Appendix 6.1: Full list of species, authorities and species codes found within core 98-18

AC046A	<i>Achnanthes altaica</i> (Poretzky) A. Cleve-Euler 1953
AC156A	<i>Achnanthes amoena</i> Hustedt 1952
AC037A	<i>Achnanthes biasolettiana</i> Grun. in Cleve & Grun. 1880
AC005A	<i>Achnanthes calcar</i> Cleve 1891
AC152A	<i>Achnanthes carissima</i> Lange-Bertalot 1990
AC060A	<i>Achnanthes curtissima</i> J.R. Carter 1963
AC039A	<i>Achnanthes didyma</i> didyma Hust. 1933
AC025A	<i>Achnanthes flexella</i> (Kutz.) Brun 1880
AC134A	<i>Achnanthes helvetica</i> (Hustedt) Lange-Bertalot in LB & K 1989
AC134B	<i>Achnanthes helvetica alpina</i> Flower and Jones 1989
AC027A	<i>Achnanthes holstii</i> Cleve 1881
AC153A	<i>Achnanthes impexa</i> Lange-Bertalot 1989
AC082A	<i>Achnanthes kriegeri</i> Krasske 1943
AC142A	<i>Achnanthes kuelbsii</i> Lange-Bertalot 1989
AC146A	<i>Achnanthes lacus-vulcani</i> Lange-Bertalot & Krammer 1989
AC083A	<i>Achnanthes laevis</i> Ostr. 1910
AC001A	<i>Achnanthes lanceolata</i> (Breb. ex Kutz.) Grun. in Cleve & Grun. 1880
AC001C	<i>Achnanthes lanceolata elliptica</i> Cleve 1891
AC018A	<i>Achnanthes laterostrata</i> Hust. 1933
AC044A	<i>Achnanthes levanderi</i> Hust. 1933
AC002A	<i>Achnanthes linearis</i> (W. Sm.) Grun. in Cleve & Grun. 1880
AC022A	<i>Achnanthes marginulata</i> Grun. in Cleve & Grun. 1880
AC003A	<i>Achnanthes microcephala</i> (Kutz.) Cleve 1896
AC013A	<i>Achnanthes minutissima</i> minutissima Kutz. 1833
AC019A	<i>Achnanthes nodosa</i> A. Cleve-Euler 1900
AC105A	<i>Achnanthes petersenii</i> Hust. 1937
AC004A	<i>Achnanthes pseudoswazi</i> J.R. Carter 1963
AC035A	<i>Achnanthes pusilla</i> pusilla Grun. in Cleve & Grun. 1880
AC116A	<i>Achnanthes rossii</i> Hust. 1954
AC119A	<i>Achnanthes saccula</i> J.R. Carter in J.R. Carter & Watts 1981
AC048A	<i>Achnanthes scotica</i> Jones & Flower
AC9999	<i>Achnanthes</i> sp.
AC173A	<i>Achnanthes stolidia</i> (Krasske) Krasske 1949
AC178A	<i>Achnanthes straubiana</i> Lange-Bertalot 1996
AC136A	<i>Achnanthes subatomoides</i> (Hust.) Lange-Bertalot & Archibald in Krammer & Lange-Bertalot 1985
AC034A	<i>Achnanthes suchlandtii</i> Hust. 1933
AC161A	<i>Achnanthes ventralis</i> (Krasske) Lange-Bertalot 1989
AM010A	<i>Amphora fogediana</i> Krammer 1985
AM011A	<i>Amphora libyca</i> Ehr.
AM001A	<i>Amphora ovalis</i> ovalis (Kutz.) Kutz. 1844
AM012A	<i>Amphora pediculus</i> (Kutz.) Grun.
AM008A	<i>Amphora thumensis</i> (Mayer) A. Cleve
AS001A	<i>Asterionella formosa</i> formosa Hassall 1850
AU002A	<i>Aulacoseira ambigua</i> (Grun. in Van Heurck) Simonsen 1979
AU005A	<i>Aulacoseira distans</i> distans (Ehrenb.) Simonsen 1979
AU005B	<i>Aulacoseira distans nivaloides</i> Camburn 1987
AU001C	<i>Aulacoseira italica</i> valida (Grun. in Van Heurck) Simonsen 1979
AU032A	<i>Aulacoseira lacustris</i> Krammer 1990
AU004A	<i>Aulacoseira lirata</i> lirata (Ehrenb.) R. Ross in Hartley 1986
AU010A	<i>Aulacoseira perglabra</i>
AU010B	<i>Aulacoseira perglabra floriniae</i>
AU9999	<i>Aulacoseira</i> sp.
AU020A	<i>Aulacoseira subarctica</i> (O.Mull.) Haworth
BR006A	<i>Brachysira brebissonii</i> brebissonii R. Ross in Hartley 1986

Appendix 6.1 cont.

BR010A	<i>Brachysira neoexilis</i>	Lange-Bertalot 1994
BR9999	<i>Brachysira</i> sp.	
BR004A	<i>Brachysira styriaca</i>	(Grun. in Van Heurck) R. Ross in Hartley 1986
BR001A	<i>Brachysira vitrea</i>	(Grun.) R. Ross in Hartley 1986
BR005A	<i>Brachysira zellensis</i>	(Grun.) Round & Mann 1981
CA002A	<i>Caloneis bacillum bacillum</i>	(Grun.) Cleve 1894
CA9999	<i>Caloneis</i> sp.	
CO001B	<i>Cocconeis placentula euglypta</i>	(Ehrenb.) Grun. 1884
CO001C	<i>Cocconeis placentula lineata</i>	(Ehrenb.) Van Heurck 1885
CY9987	<i>Cyclotella</i> [cf. <i>comensis</i>]	Massif Central (PR) 1997
CY9984	<i>Cyclotella</i> [cf. <i>krammeri</i>]	RIBA (P. Rioual) 1997
CY013A	<i>Cyclotella antiqua</i>	W. Sm. 1853
CY010A	<i>Cyclotella comensis</i>	Grun. in Van Heurck 1882
CY061A	<i>Cyclotella gordonensis</i>	Kling & Hakansson 1988
CY054A	<i>Cyclotella krammeri</i>	Hakansson 1990
CY006A	<i>Cyclotella kuetzingiana kuetzingiana</i>	Thwaites 1848
CY006B	<i>Cyclotella kuetzingiana planetophora</i>	Fricke in A. Schmidt 1900
CY006C	<i>Cyclotella kuetzingiana radiosa</i>	Fricke in A. Schmidt 1900
CY009A	<i>Cyclotella ocellata</i>	Pant. 1902
CY002A	<i>Cyclotella pseudostelligera</i>	Hust. 1939
CY9999	<i>Cyclotella</i> sp.	
CM022A	<i>Cymbella affinis</i>	Kutz. 1844
CM015A	<i>Cymbella cesatii cesatii</i>	(Rabenh.) Grun. in A. Schmidt 1881
CM006A	<i>Cymbella cistula cistula</i>	(Ehrenb. in Hempr. & Ehrenb.) Kirchner 1878
CM038A	<i>Cymbella delicatula</i>	Kutz. 1849
CM052A	<i>Cymbella descripta</i>	(Hust.) Krammer & Lange-Bertalot 1985
CM051A	<i>Cymbella elginensis</i>	Krammer 1981
CM049A	<i>Cymbella failaisensis</i>	(Grun.) Krammer & Lange-Bertalot 1985
CM020A	<i>Cymbella gaeumannii</i>	Meister 1934
CM018A	<i>Cymbella gracilis</i>	(Rabenh.) Cleve 1894
CM013A	<i>Cymbella helvetica helvetica</i>	Kutz. 1844
CM085A	<i>Cymbella lapponica</i>	Grun. ex Cleve 1894
CM004A	<i>Cymbella microcephala microcephala</i>	Grun. in Van Heurck 1880
CM031A	<i>Cymbella minuta minuta</i>	Hilse ex Rabenh. 1862
CM009A	<i>Cymbella naviculiformis</i>	Auersw. ex Heib. 1863
CM010A	<i>Cymbella perpusilla</i>	A. Cleve 1895
CM103A	<i>Cymbella silesiaca</i>	Bleisch ex Rabenh. 1864
CM003A	<i>Cymbella sinuata sinuata</i>	Greg. 1856
CM9999	<i>Cymbella</i> sp.	
CM050A	<i>Cymbella subaequalis</i>	Grun. in Van Heurck 1880
DE003A	<i>Denticula kuetzingii</i>	Grun.
DE001A	<i>Denticula tenuis tenuis</i>	Kutz. 1844
DP001A	<i>Diploneis ovalis</i>	(Hilse) Cleve 1894
DP061A	<i>Diploneis subovalis</i>	Cleve 1894
EP001A	<i>Epithemia sorex sorex</i>	Kutz. 1844
EU013A	<i>Eunotia arcus arcus</i>	Ehrenb. 1837
EU049A	<i>Eunotia curvata curvata</i>	(Kutz.) Lagerst. 1884
EU009A	<i>Eunotia exigua exigua</i>	(Breb. ex Kutz.) Rabenh. 1864
EU010A	<i>Eunotia faba</i>	(Ehrenb.) Grun. in Van Heurck 1881
EU017A	<i>Eunotia flexuosa flexuosa</i>	Kutz. 1849
EU054A	<i>Eunotia hexaglyphis</i>	Ehrenb. 1854
EU107A	<i>Eunotia implicata</i>	Norpel, Lange-Bertalot & Alles 1991
EU047A	<i>Eunotia incisa</i>	W. Sm. ex Greg. 1854
EU042A	<i>Eunotia lapponica</i>	Grun. ex A. Cleve 1895

Appendix 6.1 cont.

EU020B	<i>Eunotia meisteri bidens</i> Hust. 1930
EU020A	<i>Eunotia meisteri meisteri</i> Hust. 1930
EU110A	<i>Eunotia minor</i> (Kutz) Grunow in Van Heurck 1881
EU003A	<i>Eunotia praerupta praerupta</i> Ehrenb. 1843
EU106A	<i>Eunotia rhynchocephala</i> Hustedt 1936
EU9999	<i>Eunotia</i> sp.
EU105A	<i>Eunotia subarcuoides</i> Alles, Norpel, Lange-Bertalot 1991
EU004A	<i>Eunotia tenella</i> (Grun. in Van Heurck) A. Cleve 1895
FR006A	<i>Fragilaria brevistriata brevistriata</i> Grun. in Van Heurck 1885
FR009H	<i>Fragilaria capucina gracilis</i> (Oestrup) Hustedt 1950
FR010A	<i>Fragilaria constricta constricta</i> Ehrenb. 1843
FR002B	<i>Fragilaria construens binodis</i> (Ehrenb.) Grun. 1862
FR002A	<i>Fragilaria construens construens</i> (Ehrenb.) Grun. 1862
FR002D	<i>Fragilaria construens exigua</i> (W. Sm.) Schulz 1922
FR002F	<i>Fragilaria construens pumila</i> Grun. in Van Heurck 1881
FR002C	<i>Fragilaria construens venter</i> (Ehrenb.) Grun. in Van Heurck 1881
FR018A	<i>Fragilaria elliptica</i> Schum. 1867
FR064A	<i>Fragilaria exigua</i> Grun in Cleve & Moller 1878
FR011A	<i>Fragilaria lapponica</i> Grun. in Van Heurck 1881
FR014A	<i>Fragilaria leptostauron leptostauron</i> (Ehrenb.) Hust. 1931
FR062A	<i>Fragilaria microstriata</i> Marciniak in Metzeltin & Witkowski 1996
FR001E	<i>Fragilaria pinnata intercedens</i> (Grun. in Van Heurck) Hust. 1931
FR001B	<i>Fragilaria pinnata lancettula</i> (Schum.) Hust. in A. Schmidt 1913
FR001A	<i>Fragilaria pinnata pinnata</i> Ehrenb. 1843
FR056A	<i>Fragilaria pseudoconstruens</i> Marciniak 1982
FR063A	<i>Fragilaria robusta</i> (Fusey) Manguin
FR9999	<i>Fragilaria</i> sp.
FR007A	<i>Fragilaria vaucheriae vaucheriae</i> (Kutz.) J.B. Petersen 1938
FR005A	<i>Fragilaria virescens virescens</i> Ralfs 1843
FU002A	<i>Frustulia rhomboides rhomboides</i> (Ehrenb.) De Toni 1891
FU002B	<i>Frustulia rhomboides saxonica</i> (Rabenh.) De Toni 1891
GO006A	<i>Gomphonema acuminatum acuminatum</i> Ehrenb. 1832
GO004A	<i>Gomphonema gracile</i> Ehrenb. 1838
GO013A	<i>Gomphonema parvulum parvulum</i> (Kutz.) Kutz. 1849
GO9999	<i>Gomphonema</i> sp.
KR001A	<i>Krasskella kriegnerana</i> (Krasske) R. Ross & Sims 1978
MR001A	<i>Meridion circulare circulare</i> (Grev.) Ag. 1831
MR001B	<i>Meridion circulare constrictum</i> (Ralfs) Van Heurck 1885
NA012A	<i>Navicula aboensis</i> (Cleve) Hust. 1952
NA038A	<i>Navicula arvensis</i> Hust.
NA099A	<i>Navicula bremensis</i> Hust. 1957
NA032A	<i>Navicula cocconeiformis cocconeiformis</i> Greg. ex Greville 1855
NA046A	<i>Navicula contenta contenta</i> Grun. in Van Heurck 1885
NA751A	<i>Navicula cryptotenella</i> Lange-Bertalot 1985
NA115A	<i>Navicula difficillima</i> Hust. 1950
NA149A	<i>Navicula digitulus</i> Hust. 1943
NA141A	<i>Navicula disjuncta</i> Hust. 1930
NA039A	<i>Navicula festiva</i> Krasske 1925
NA389A	<i>Navicula gallica</i> (W. Sm.) Lagerst. 1873
NA389B	<i>Navicula gallica perpusilla</i> (Grun) Lange-Bertalot 1985
NA002A	<i>Navicula jaernefeltii</i> Hust. 1942
NA466A	<i>Navicula kriegeri</i> Krasske 1943
NA156A	<i>Navicula leptostriata</i> Jorgensen 1948
NA006A	<i>Navicula mediocris</i> Krasske 1932

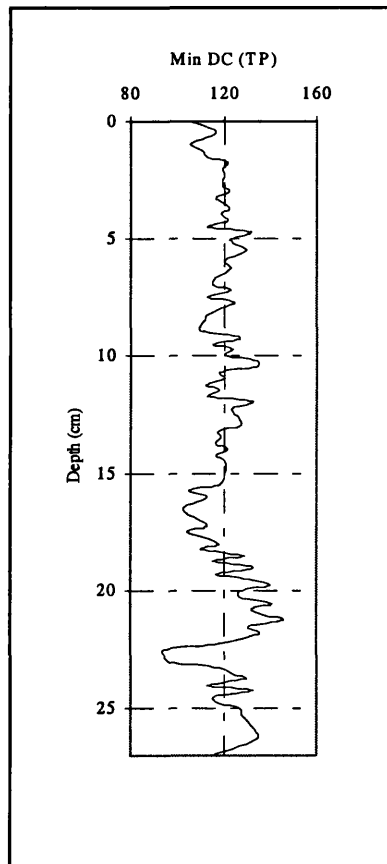
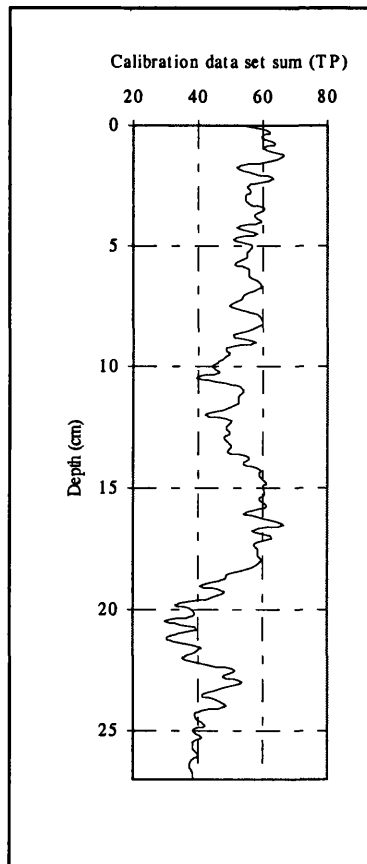
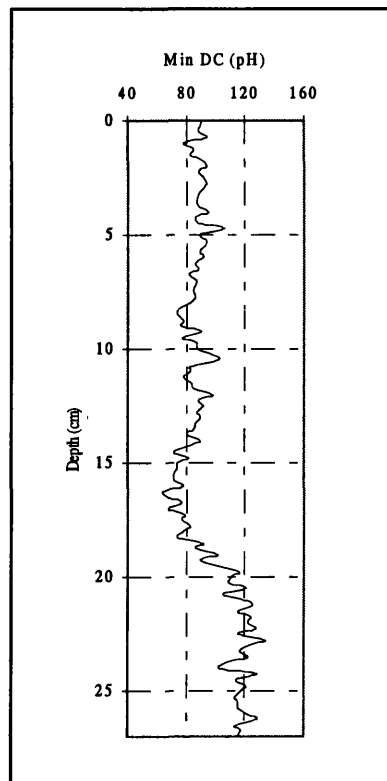
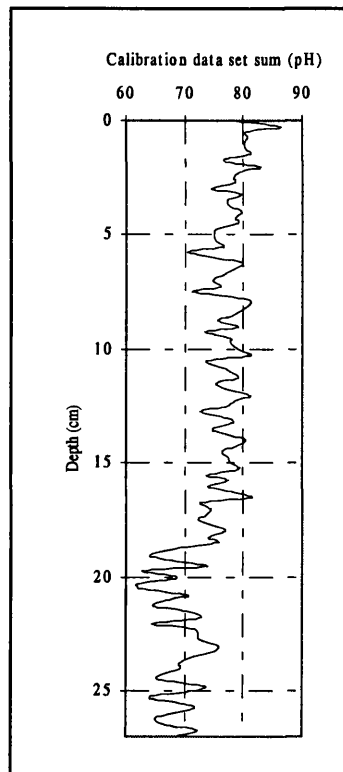
Appendix 6.1 cont.

NA042A	<i>Navicula minima minima</i> Grun. in Van Heurck 1880
NA112D	<i>Navicula minuscula muralis</i> (Grun. in Van Heurck) Lange-Beralot in Lange-Bertalot & Rumrich 1981
NA123A	<i>Navicula modica</i> Hust. 1945
NA779A	<i>Navicula pseudoarvensis</i> Hustedt 1942
NA013A	<i>Navicula pseudoscutiformis</i> Hust. 1930
NA014A	<i>Navicula pupula pupula</i> Kutz. 1844
NA003C	<i>Navicula radiosa parva</i> Wallace
NA003A	<i>Navicula radiosa radiosa</i> Kutz. 1844
NA133A	<i>Navicula schassmannii</i> Hust. 1937
NA129A	<i>Navicula seminuloides</i> Hust. 1937
NA005A	<i>Navicula seminulum</i> Grun. 1860
NA048A	<i>Navicula soehrensensis soehrensensis</i> Krasske 1923
NA9999	<i>Navicula</i> sp.
NA134A	<i>Navicula subminuscula</i> Manguin
NA741A	<i>Navicula subplacentula</i> Hust. in A. Schmidt et. al. 1930
NA033A	<i>Navicula subtilissima</i> Cleve 1891
NA135A	<i>Navicula tenuicephala</i> Hust. 1942
NA738A	<i>Navicula vitiosa</i> Schimanski 1978
ND9998	<i>Naviculadicta</i> [sp.#1 Weinfelder Maar] LB & Metzeltin 1996
ND9997	<i>Naviculadicta</i> [sp.#2 Weinfelder Maar] LB & Metzeltin 1996
NE003A	<i>Neidium affine affine</i> (Ehrenb.) Pfitz. 1871
NE006A	<i>Neidium alpinum</i> Hust. 1943
NE036A	<i>Neidium ampliatus</i> (Ehren) Krammer 1985
NE9999	<i>Neidium</i> sp.
NI028A	<i>Nitzschia capitellata</i> Hust. 1930
NI003A	<i>Nitzschia denticula</i> Grun. in Cleve & Grun. 1880
NI002A	<i>Nitzschia fonticola</i> Grun. in Van Heurck 1881
NI008A	<i>Nitzschia frustulum</i> (Kutz.) Grun. in Cleve & Grun. 1880
NI017A	<i>Nitzschia gracilis</i> Hantzsch 1860
NI043A	<i>Nitzschia inconspicua</i> Grun. 1862
NI009A	<i>Nitzschia palea palea</i> (Kutz.) W. Sm. 1856
NI033A	<i>Nitzschia paleacea</i> (Grun. in Cleve & Grun.) Grun. in Van Heurck 1881
NI005A	<i>Nitzschia perminuta</i> (Grun. in Van Heurck) M. Perag. 1903
NI216A	<i>Nitzschia pura</i> Hustedt 1954
NI9999	<i>Nitzschia</i> sp.
PE002A	<i>Peronia fibula</i> (Breb. ex Kutz.) R. Ross 1956
PI055A	<i>Pinnularia balfouriana</i> Grun. ex Cleve 1896
PI012D	<i>Pinnularia borealis rectangularis</i> Carlson 1913
PI048A	<i>Pinnularia brebissonii brebissonii</i> (Kutz.) Rabenh. 1864
PI016A	<i>Pinnularia divergentissima divergentissima</i> (Grun. in Van Heurck) Cleve 1896
PI001A	<i>Pinnularia gibba</i> (Ehrenb.) Ehrenb. 1843
PI004A	<i>Pinnularia interrupta</i> W. Smith
PI005A	<i>Pinnularia major major</i> (Kutz.) W. Sm. 1853
PI011A	<i>Pinnularia microstauron microstauron</i> (Ehrenb.) Cleve 1891
PI042A	<i>Pinnularia nodosa nodosa</i> (Ehrenb.) W. Sm. 1856
PI056A	<i>Pinnularia rupestris</i> Hantzsch in Rabenh. 1861
PI052A	<i>Pinnularia silvatica</i> J.B. Petersen 1935
PI9999	<i>Pinnularia</i> sp.
PI022A	<i>Pinnularia subcapitata subcapitata</i> Greg. 1856
RH001A	<i>Rhopalodia gibba gibba</i> (Ehrenb.) O. Mull. 1895
SL004A	<i>Sellaphora verecundiae</i> Lange-Bertalot 1994
SA001A	<i>Stauroneis anceps anceps</i> Ehrenb. 1843
SA002A	<i>Stauroneis parvula</i> Grun.

Appendix 6.1 cont.

SA003A	<i>Stauroneis smithii smithii</i> Grun. 1860
SP005A	<i>Stenopterobia delicatissima</i> (Lewis) M. Perag. 1897
SU005A	<i>Surirella linearis linearis</i> W. Sm. 1853
SY003A	<i>Synedra acus acus</i> Kutz. 1844
SY009A	<i>Synedra nana</i> Meister 1912
SY004A	<i>Synedra parasitica parasitica</i> (W. Sm.) Hust. 1930
SY004B	<i>Synedra parasitica subconstricta</i> (Grun. in Van Heurck) Hust. 1930
SY002A	<i>Synedra rumpens rumpens</i> Kutz. 1844
TA9998	<i>Tabellaria [flocculosa (long)]</i>
TA9997	<i>Tabellaria [flocculosa (short)]</i>
TA001A	<i>Tabellaria flocculosa flocculosa</i> (Roth) Kutz. 1844
ZZZ999	Temporary sp. 1 <i>Achnanthes minutissima</i> var. <i>inconspicua</i>
ZZZ989	Temporary sp. 11 <i>Achnanthes nitidiformis</i>
ZZZ986	Temporary sp. 14 <i>Aulacoseira distans</i> var. <i>septentrionalis</i>
ZZZ975	Temporary sp. 25 <i>Achnanthes minutissima</i> var. <i>macrocephala</i>
ZZZ997	Temporary sp. 3 <i>Fragilaria suboldenburgiana</i>
ZZZ965	Temporary sp. 35 <i>Cymbella</i> PIRLA sp 12
ZZZ995	Temporary sp. 5 <i>Naviculadicta circumborealis</i>
ZZZ991	Temporary sp. 9 <i>Achnanthes lanceolata</i> var. <i>frequentissima</i>
TE001A	<i>Tetracyclus lacustris</i> Ralfs 1843

Appendix 6.2: Graphs showing the reliability of the pH and TP transfer functions for Lake Hornsjøen (Calibration set sum refers to WA methods and Min DC refers to MAT methods)



Appendix 7.1: Species names, codes and authorities for species found in Lake Gåvålivatnet

AC001R	<i>Achnanthes lanceolata</i> ssp. <i>frequentissima</i> Lange-Bertalot
AC002A	<i>Achnanthes linearis</i> (W. Sm.) Grun. in Cleve & Grun. 1880
AC003A	<i>Achnanthes microcephala</i> (Kutz.) Cleve 1896
AC004A	<i>Achnanthes pseudoswazi</i> J.R. Carter 1963
AC005A	<i>Achnanthes calcar</i> Cleve 1891
AC006A	<i>Achnanthes clevei</i> Grunow 1880 AC006A
AC007A	<i>Achnanthes oestrupii</i> (A. Cleve-Euler) Hust. 1930
AC008A	<i>Achnanthes exigua</i>
AC013A	<i>Achnanthes minutissima</i> <i>minutissima</i> Kutz. 1833
AC013C	<i>Achnanthes minutissima</i> var. <i>jackii</i>
AC018A	<i>Achnanthes laterostrata</i> Hust. 1933
AC019A	<i>Achnanthes nodosa</i> A. Cleve-Euler 1900
AC022A	<i>Achnanthes marginulata</i> Grun. in Cleve & Grun. 1880
AC023A	<i>Achnanthes conspicua</i> A.MAYER
AC025A	<i>Achnanthes flexella</i> (Kutz.) Brun 1880
AC027A	<i>Achnanthes holstii</i> Cleve 1881
AC034A	<i>Achnanthes suchlandtii</i> Hust. 1933
AC035A	<i>Achnanthes pusilla</i> <i>pusilla</i> Grun. in Cleve & Grun. 1880
AC037A	<i>Achnanthes biasoletiana</i> Grun. in Cleve & Grun. 1880
AC039A	<i>Achnanthes didyma</i> <i>didyma</i> Hust. 1933
AC044A	<i>Achnanthes levanderi</i> Hust. 1933
AC046A	<i>Achnanthes altaica</i> (Poretzky) A. Cleve-Euler 1953
AC048A	<i>Achnanthes scotica</i> Jones & Flower
AC060A	<i>Achnanthes curtissima</i> J.R. Carter 1963
AC065A	<i>Achnanthes exilis</i>
AC082A	<i>Achnanthes kriegeri</i> Krasske 1943
AC083A	<i>Achnanthes laevis</i> Ostr. 1910
AC098A	<i>Achnanthes montana</i> Krasske 1943
AC105A	<i>Achnanthes petersenii</i> Hust. 1937
AC116A	<i>Achnanthes rossii</i>
AC119A	<i>Achnanthes saccula</i> J.R. Carter in J.R. Carter & Watts 1981
AC134A	<i>Achnanthes helvetica</i> (Hustedt) Lange-Bertalot in LB & K 1989
AC134B	<i>Achnanthes helvetica</i> <i>alpina</i> Flower and Jones 1989
AC136A	<i>Achnanthes subatomoides</i> (Hustedt.) Lange-Bertalot & Archibald in K & L-B 1985
AC142A	<i>Achnanthes kuelbsii</i> Lange-Bertalot 1989
AC143A	<i>Achnanthes oblongella</i>
AC146A	<i>Achnanthes lacus-vulcani</i> Lange-Bertalot & Krammer 1989
AC152A	<i>Achnanthes carissima</i> Lange-Bertalot 1990
AC153A	<i>Achnanthes impexa</i> Lange-Bertalot 1989
AC156A	<i>Achnanthes amoena</i> Hustedt 1952
AC161A	<i>Achnanthes ventralis</i> (Krasske) Lange-Bertalot 1989
AC167A	<i>Achnanthes daonensis</i> Lange-Bertalot 1989
AC170A	<i>Achnanthes joursacense</i>
AC173A	<i>Achnanthes stolidia</i> (Krasske) Krasske 1949
AC178A	<i>Achnanthes straubiana</i> Lange-Bertalot 1996
AC179A	<i>Achnanthes minutissima</i> var. <i>gracillima</i> / <i>A. alteragracillima</i>
AC182A	<i>Achnanthes rosenstockii</i>
AC972	<i>Achnanthes minnutissima</i> var. <i>macrocephala</i>
AC9968	<i>Achnanthes helvetica</i> var. <i>major</i>
AC9999	<i>Achnanthes</i> species
AM001A	<i>Amphora ovalis</i> <i>ovalis</i> (Kutz.) Kutz. 1844
AM004A	<i>Amphora veneta</i>

Appendix 7.1 cont.

AM008A	<i>Amphora thumensis</i> (Mayer) A. Cleve
AM010A	<i>Amphora fogediana</i> Krammer 1985
AM011B	<i>Amphora libyca</i> Ehr.
AM012A	<i>Amphora pediculus</i> (Kutz.) Grun.
AM013A	<i>Amphora inariensis</i> Krammer
AM9999	<i>Amphora</i> species
AP001A	<i>Amphipleura pellucida</i>
AU001A	<i>Aulacoseira italica</i> (Ehrenberg) Simonsen 1979
AU002A	<i>Aulacoseira ambigua</i> (Grun. in Van Heurck) Simonsen 1979
AU004A	<i>Aulacoseira lirata</i> <i>lirata</i> (Ehrenb.) R. Ross in Hartley 1986
AU9999	<i>Aulacoseira</i> sp.
BR001A	<i>Brachysira vitrea</i> (Grun.) R. Ross in Hartley 1986
BR003A	<i>Brachysira serians</i>
BR004A	<i>Brachysira styriaca</i> (Grun. in Van Heurck) R. Ross in Hartley 1986
BR005A	<i>Brachysira zellensis</i>
BR006A	<i>Brachysira brebissonii</i> <i>brebissonii</i> R. Ross in Hartley 1986
BR010A	<i>Brachysira neoexilis</i> Lange-Bertalot 1994
CA002A	<i>Caloneis bacillum</i> <i>bacillum</i> (Grun.) Cleve 1894
CA003A	<i>Caloneis silicula</i> (Ehrenb.) Cleve 1894
CA018A	<i>Caloneis tenuis</i> Gregory (Krammer) 1985
CA9999	<i>Caloneis</i> sp
CE002A	<i>Fragilaria arcus</i> (Ehr.)Cleve 1898
CM003A	<i>Cymbella sinuata</i> <i>sinuata</i> Greg. 1856
CM004A	<i>Cymbella microcephala</i> <i>microcephala</i> Grun. in Van Heurck 1880
CM005A	<i>Cymbella aspera</i> (Her.)Peragallo 1849
CM006A	<i>Cymbella cistula</i> <i>cistula</i> (Ehrenb. in Hempr. & Ehrenb.) Kirchner 1878
CM007A	<i>Cymbella delicatula</i> Kutz. 1849
CM009A	<i>Cymbella naviculiformis</i> Auersw. ex Heib. 1863
CM010A	<i>Cymbella perpusilla</i> A. Cleve 1895
CM012A	<i>Cymbella leavis</i>
CM013A	<i>Cymbella helvetica</i> <i>helvetica</i> Kutz. 1844
CM014A	<i>Cymbella aequalis</i> W.Smith 1953
CM015A	<i>Cymbella cesatii</i> <i>cesatii</i> (Rabenh.) Grun. in A. Schmidt 1881
CM016A	<i>Cymbella amphicephala</i> var. <i>amphicephala</i> Naegeli ex Kutz. 1849
CM017A	<i>Cymbella hebridica</i> (Grun. Ex Cleve) Cleve 1894
CM018A	<i>Cymbella gracilis</i> (Rabenh.) Cleve 1894
CM020A	<i>Cymbella gaeumannii</i> Meister 1934
CM022A	<i>Cymbella affinis</i> Kutz. 1844
CM026A	<i>Cymbella cuspidata</i> Kutzing 1844
CM031A	<i>Cymbella minuta</i> <i>minuta</i> Hilse ex Rabenh. 1862
CM049A	<i>Cymbella failaisensis</i> (Grun.) Krammer & Lange-Bertalot 1985
CM050A	<i>Cymbella subaequalis</i> Grun. in Van Heurck 1880
CM052A	<i>Cymbella descripta</i> (Hust.) Krammer & Lange-Bertalot 1985
CM093A	<i>Cymbella obscura</i>
CM103A	<i>Cymbella silesiaca</i> Bleisch ex Rabenh. 1864
CM9999	<i>Cymbella</i> sp
CO001A	<i>Cocconeis placentula</i> Ehrenberg
CO001C	<i>Cocconeis placentula</i> <i>lineate</i> (Ehrenb.) Van Heurck 1885
CO067A	<i>Cocconeis neothumensis</i>
CO9999	<i>Cocconeis</i> sp
CY002A	<i>Cyclotella pseudostelligera</i> Hust. 1939

Appendix 7.1 cont.

CY004B	<i>Cyclotella stelligera</i> var <i>glomerata</i>
CY009A	<i>Cyclotella ocellata</i> Pantocsek
CY010A	<i>Cyclotella comensis</i> Grun. in Van Heurck 1882
CY013A	<i>Cyclotella antiqua</i> W. Sm. 1853
CY019A	<i>Cyclotella radiosa</i> Grunow
CY020A	<i>Cyclotella iris</i>
CY028A	<i>Cyclotella distinguenda</i> var. <i>unipunctata</i>
CY052A	<i>Cyclotella rossii</i> Hakansson 1990
CY055A	<i>Cyclotella schumannii</i> (Grunow) Hakansson 1990
CY059A	<i>Cyclotella cyclopuncta</i> Hakansson & Carter
CY061A	<i>Cyclotella gordonensis</i> Kling & Hakansson 1988
CY9987	<i>Cyclotella</i> [cf. <i>comensis</i>] Massif Central (PR) 1997
CY9999	<i>Cyclotella</i> sp.
DE001A	<i>Denticula tenuis</i> <i>tenuis</i> Kutz. 1844
DE002A	<i>Denticula elegans</i> var. <i>elegans</i> Kutz. 1844
DE003A	<i>Denticula kuetzingii</i> Grun.
DP001A	<i>Diploneis ovalis</i> (Hilse) Cleve 1894
DP007A	<i>Diploneis oblongella</i> var. <i>oblongella</i> (Naegeli ex Kutz.) R. Ross 1947
DP009A	<i>Diploneis elliptica</i> var. <i>elliptica</i> (Kutz.) Cleve 1894
DP065A	<i>Diploneis parma</i> Cleve 1891
DP9999	<i>Diploneis</i> sp
DT021A	<i>Diatoma mesodon</i> (Ehrenberg) Kuetzing 1844
EP001A	<i>Epithemia sorex</i> <i>sorex</i> Kutz. 1844
EP004A	<i>Epithemia turgida</i>
EP007A	<i>Epithemia adnata</i> (Kützing) Brébisson
EP9999	<i>Epithemia</i> sp
EU003A	<i>Eunotia praerupta</i> <i>praerupta</i> Ehrenb. 1843
EU004A	<i>Eunotia tenella</i> (Grun. in Van Heurck) A. Cleve 1895
EU013A	<i>Eunotia arcus</i> <i>arcus</i> Ehrenb. 1837
EU017A	<i>Eunotia flexuosa</i> <i>flexuosa</i> Kutz. 1849
EU045A	<i>Eunotia nymanniana</i>
EU047A	<i>Eunotia incisa</i> W. Sm. ex Greg. 1854
EU048A	<i>Eunotia nagelii</i>
EU070B	<i>Eunotia bilunaris</i> var. <i>mucophila</i> Lange- Bertalot & Noerpel
EU107A	<i>Eunotia implicata</i> Norpel, Lange-Bertalot & Alles 1991
EU110A	<i>Eunotia minor</i> (Kuetzing) Grunow
EU114B	<i>Eunotia muscicola</i> var <i>tridentula</i>
EU9999	<i>Eunotia</i> sp
FR001A	<i>Fragilaria pinnata</i> <i>pinnata</i> Ehrenb. 1843
FR001B	<i>Fragilaria pinnata</i> <i>lancettula</i> (Schum.) Hust. in A. Schmidt 1913
FR001E	<i>Fragilaria pinnata</i> <i>intercedens</i> (Grun. in Van Heurck) Hust. 1931
FR001K	<i>Fragilaria pinnata</i> var <i>acuminatum</i>
FR002A	<i>Fragilaria construens</i> <i>construens</i> (Ehrenb.) Grun. 1862
FR002B	<i>Fragilaria construens</i> <i>binodis</i> (Ehrenb.) Grun. 1862
FR002C	<i>Fragilaria construens</i> <i>venter</i> (Ehrenb.) Grun. in Van Heurck 1881
FR002CL	<i>Fragilaria construens</i> <i>venter</i> (Long)
FR002F	<i>Fragilaria construens</i> var <i>pumilla</i>
FR004B	<i>Fragilaria hungaria</i> var <i>tumida</i>
FR005A	<i>Fragilaria virescens</i>
FR006A	<i>Fragilaria brevistriata</i> <i>brevistriata</i> Grun. in Van Heurck 1885
FR006E	<i>Fragilaria brevistriata</i> var <i>capitata</i> Grun. in Van Heurck 1885

Appendix 7.1 cont.

FR007A	<i>Fragilaria vaucheriae</i> var. <i>vaucheriae</i>
FR009A	<i>Fragilaria capucina</i> (Grunow) Lange-Bertalot
FR009H	<i>Fragilaria capucina gracilis</i> (Oestrup) Hustedt 1950
FR009I	<i>Fragilaria capucina</i> var. <i>austriaca</i> (Grunow) Lange-Bertalot
FR009J	<i>Fragilaria capucina</i> var. <i>perminuta</i>
FR011A	<i>Fragilaria lapponica</i> Grun. in Van Heurck 1881
FR013A	<i>Fragilaria oldenburgiana</i> Hust.
FR014A	<i>Fragilaria leptostauron leptostauron</i> (Ehrenb.) Hust. 1931
FR014B	<i>Fragilaria leptostauron</i> var. <i>dubia</i>
FR015A	<i>Fragilaria lata</i>
FR018A	<i>Fragilaria elliptica</i> Schum. 1867
FR056A	<i>Fragilaria pseudoconstruens</i> Marciniak 1982
FR062A	<i>Fragilaria microstriata</i> Marciniak in Metzeltin & Witkowski 1996
FR063A	<i>Fragilaria robusta</i> (Fusey) Manguin
FR064A	<i>Fragilaria exigua</i> Grun in Cleve & Moller 1878
FR9999	<i>Fragilaria</i> sp
GO003A	<i>Gomphonema angustatum</i> (Kutz.) Rabenh. 1864
GO004A	<i>Gomphonema gracile</i> Ehrenb. 1838
GO006A	<i>Gomphonema acuminatum acuminatum</i> Ehrenb. 1832
GO008A	<i>Gomphonema subtile</i> Ehrenberg 1843
GO013A	<i>Gomphonema parvulum parvulum</i> (Kutz.) Kutz. 1849
GO050A	<i>Gomphonema minutum</i>
GO072A	<i>Gomphonema pseudotenellum</i>
GO080A	<i>Gomphonema pumilum</i> (Grunow) Lange-Bertalot & Reichardt
GO9999	<i>Gomphonema</i> sp
KR001A	<i>Krasskella kriegeana</i> (Krasske) R. Ross & Sims 1978
MR001A	<i>Meridion circulare circulare</i> (Grev.) Ag. 1831
NA 043A	<i>Navicula subatamoides</i>
NA002A	<i>Navicula jaernefeltii</i> Hust. 1942
NA003A	<i>Navicula radiosa</i> Kutz. 1844
NA005A	<i>Navicula seminulum</i> Grun. 1860
NA006A	<i>Navicula mediocris</i> Krasske 1932
NA007A	<i>Navicula cryptocephala</i> var. <i>cryptocephala</i> Kutz. 1844
NA008A	<i>Navicula rhynchocephala</i> var. <i>rhynchocephala</i> Kutz. 1844
NA013A	<i>Navicula pseudoscutiformis</i> Hust. 1930
NA014A	<i>Navicula pupula pupula</i> Kutz. 1844
NA016A	<i>Navicula indifferens</i> Hust. 1942
NA017A	<i>Navicula ventralis</i>
NA032A	<i>Navicula cocconeiformis cocconeiformis</i> Greg. ex Greville 1855
NA033A	<i>Navicula subtilissima</i> Cleve 1891
NA042A	<i>Navicula minima</i> var. <i>minima</i> Grun. in Van Heurck 1880
NA044A	<i>Navicula krasskei</i> HUSTEDT
NA045A	<i>Navicula bryophila</i> var. <i>bryophila</i> J.B. Petersen 1928
NA046A	<i>Navicula contenta contenta</i> Grun. in Van Heurck 1885
NA048A	<i>Navicula soehrensii</i> var. <i>hassica</i>
NA050A	<i>Navicula clementis</i> Grunow
NA057A	<i>Navicula elginensis</i>
NA057A	<i>Navicula elginensis</i> (Greg.) Ralfs 1861
NA066B	<i>Navicula capitata</i> var. <i>hungarica</i> (Grun.) R. Ross 1947
NA076A	<i>Navicula variostrata</i>
NA084A	<i>Navicula arvensis</i> Hust.
NA090A	<i>Navicula rotunda</i>

Appendix 7.1 cont.

NA102A	<i>Navicula laevis</i> Kutz. 1844
NA112A	<i>Navicula minuscula</i> var. <i>minuscula</i> Grun. in Van Heurck 1880
NA112D	<i>Navicula muralis</i> var. <i>miniscula</i>
NA114A	<i>Navicula subrotundata</i> Hust. 1945
NA115A	<i>Navicula difficillima</i> Hust. 1950
NA123A	<i>Navicula modica</i> Hust. 1945
NA128A	<i>Navicula schoenfeldii</i> Hust.
NA129A	<i>Navicula seminuloides</i> Hust. 1937
NA133A	<i>Navicula schassmannii</i> Hust. 1937
NA135A	<i>Navicula tenuicephala</i> Hust. 1942
NA141A	<i>Navicula disjuncta</i> Hust. 1930
NA149A	<i>Navicula digitulus</i> Hust. 1943
NA152A	<i>Navicula lapidosa</i> Krasske
NA156A	<i>Navicula leptostriata</i> Jorgensen 1948
NA166A	<i>Navicula submuralis</i>
NA322A	<i>Navicula detenta</i> Hustedt 1942
NA389B	<i>Navicula gallica perpusilla</i> (Grun) Lange-Bertalot 1985
NA433D	<i>Navicula ignota</i> var. <i>acceptata</i> (Hustedt) Lange-Bertalot 1985
NA590A	<i>Navicula pseudoarvensis</i> Hustedt 1942
NA593A	<i>Navicula pusio</i> Cleve 1896
NA650A	<i>Navicula stroemi</i>
NA738A	<i>Navicula vitiosa</i> Schimanski 1978
NA751A	<i>Navicula cryptotenella</i> Lange-Bertalot 1985
NA755A	<i>Navicula kuelbsii</i>
NA761A	<i>Navicula lenzii</i> Hust in Schmidt et al 1936
NA779A	<i>Navicula pseudoarvensis</i>
NA9958	<i>Navicula PIRLA</i> sp24
NA9999	<i>Navicula</i> sp
NAO99A	<i>Navicula bremensis</i> Hust. 1957
ND9997	<i>Naviculadicta</i> [sp.#2 Weinfelder Maar] LB & Metzeltin 1996
ND9998	<i>Naviculadicta</i> [sp.#1 Weinfelder Maar] LB & Metzeltin 1996
NE003A	<i>Neidium affine</i> <i>affine</i> (Ehrenb.) Pfitz. 1871
NE003B	<i>Neidium affine</i> var. <i>longiceps</i> (Gregory) Cleve
NE006A	<i>Neidium alpinum</i> Hust. 1943
NE007A	<i>Neidium dubium</i> var. <i>dubium</i> (Ehrenb.) Cleve 1894
NE036A	<i>Neidium ampliaticum</i> (Ehr.) Krammer 1985
NE9999	<i>Neidium</i> sp
NI002A	<i>Nitzschia fonticola</i> Grun. in Van Heurck 1881
NI005A	<i>Nitzschia perminuta</i> (Grun. in Van Heurck) M. Perag. 1903
NI008A	<i>Nitzschia frustulum</i> (Kutz.) Grun. in Cleve & Grun. 1880
NI009A	<i>Nitzschia palea</i> <i>palea</i> (Kutz.) W. Sm. 1856
NI017A	<i>Nitzschia gracilis</i> Hantzsch 1860
NI024A	<i>Nitzschia sublinearis</i>
NI033A	<i>Nitzschia paleacea</i> (Grun. in Cleve & Grun.) Grun. in Van Heurck 1881
NI043A	<i>Nitzschia inconspicua</i> Grun. 1862
NI216A	<i>Nitzschia pura</i>
NI9999	<i>Nitzschia</i> sp
PI001A	<i>Pinnularia gibba</i> (Ehrenb.) Ehrenb. 1843
PI004A	<i>Pinnularia interrupta</i> W. Smith
PI007A	<i>Pinnularia viridis</i> var. <i>viridis</i> (Nitzsch) Ehrenb. 1843
PI011A	<i>Pinnularia microstauron</i> <i>microstauron</i> (Ehrenb.) Cleve 1891

Appendix 7.1 cont.

PI012D	<i>Pinnularia borealis</i> var <i>rectangularis</i>
PI016A	<i>Pinnularia divergentissima</i> <i>divergentissima</i> (Grun.in Van Heurck) Cleve 1896
PI018A	<i>Pinnularia biceps</i> Gregory 1856
PI022A	<i>Pinnularia subcapitata</i> <i>subcapitata</i> Greg. 1856
PI9999	<i>Pinnularia</i> sp
RH001A	<i>Rhapalodia gibba</i>
SA001A	<i>Stauroneis anceps</i> <i>anceps</i> Ehrenb. 1843
SA003A	<i>Stauroneis smithii</i> <i>smithii</i> Grun. 1860
ST9999	<i>Stephanodiscus</i> sp
SU005A	<i>Surirella linearis</i> <i>linearis</i> W. Sm. 1853
SU073A	<i>Surirella bifrons</i> Ehrenberg
SU9999	<i>Surirella</i> sp
SY001A	<i>Synedra ulna</i> (Nitzsch) Ehrenb.
SY002A	<i>Synedra rumpens</i> <i>rumpens</i> Kutz. 1844
SY003A	<i>Synedra acus</i> <i>acus</i> Kutz. 1844
SY004A	<i>Synedra parasitica</i> <i>parasitica</i> (W. Sm.) Hust. 1930
SY011A	<i>Synedra delicatissima</i> var. <i>delicatissima</i>
SY013A	<i>Synedra tenera</i>
SY081A	<i>Synedra cyclopum</i> Brutschy 1922
SY9999	<i>Synedra</i> sp
TA9997	<i>Tabellaria</i> [<i>flocculosa</i> (short)]
TA9998	<i>Tabellaria</i> [<i>flocculosa</i> (long)]
ZZZ962	<i>Diatomella balfouriana</i>
ZZZ964	<i>Fragilaria capucina</i> var <i>alpestris</i>
ZZZ965	<i>Cymbella</i> sp12 PIRLA
ZZZ966	<i>Cyclotella</i> aff <i>radiosa</i>
ZZZ970	<i>Br acysira</i> cf. <i>procera</i>
ZZZ971	<i>Achnanthes</i> unknown
ZZZ974	<i>Cymbella</i> cf <i>microcephala</i>
ZZZ986	<i>Aulacoseira distans</i> var <i>septentrionalis</i>
ZZZ989	<i>Achnanthes nitidiformis</i>
ZZZ995	<i>Naviculadicta circumborealis</i>
ZZZ997	<i>Fragilaria suboldenburgiana</i>
ZZZ999	<i>Achnanthes minnutissima</i> var <i>inconspicua</i>

Appendix 7.2: Graphs showing the reliability of the pH and TP transfer functions for Lake Gåvålivatnet (Calibration set sum refers to WA methods and Min DC refers to MAT methods)

